Haematopoietic Stem/Progenitor Cell Interactions with the Bone Marrow Vascular Niche

Chao-Hui Chang

Wolfson College

Supervisor Prof. Suzanne Watt

Co-supervisor Dr. Sarah Hale

Thesis submitted for the degree of Doctor of Philosophy
at the University of Oxford
Trinity term 2013

Nuffield Division of Clinical Laboratory Sciences,
Radcliffe Department of Medicine, University of Oxford
and NHS Blood and Transplant, Oxford

ABSTRACT

Umbilical cord blood (UCB) is used as a source of haematopoietic stem cells (HSCs) for transplantation but shows defective homing to the bone marrow niche and delayed haematological reconstitution. Following transplantation, HSCs will home to the bone marrow in response to the CXCL12 chemokine, adhere to the bone marrow sinusoidal endothelial cells and then migrate into and lodge in bone marrow niches. In addition to CXCR4, a variety of molecules have been described as being important in these processes. In this laboratory, junctional adhesion molecule-A (JAM-A) was shown to be expressed on human UCB $CD133^+/CD34^+$ cells and regulated by hypoxia. In this thesis, further phenotypic studies show that this molecule is most highly expressed on human $CD41a^+$ megakaryocytes and $CD14^+$ monocytes/macrophages in UCB. JAM-A was also found to be expressed on all human UCB $CD133^+$ cells, which have been shown by others to encompass the HSCs and early myeloid-lymphoid precursors and on the majority of $CD34^+$ haematopoietic progenitor cells (HPCs). While it is also present on bone marrow sinusoidal endothelium (BMEC), JAM-A is not detected on cultured bone marrow mesenchymal stromal cells (MSCs). JAM-A blockade, silencing and overexpression experiments showed that JAM-A contributes to, but is not solely responsible for, the adhesion of $CD34^+$ haematopoietic progenitor cells to IL-1β activated BMEC-60 cells and fibronectin. Lack of significance in cell migration suggested that JAM-A is more likely to act as an adhesion molecule or a regulator of adhesion rather than as a migratory molecule in such cells. Further functional studies using the proximity ligation assay highlight a potential association of JAM-A with CXCR4 and the adhesion molecules, tetraspanin CD82 and integrin β1. Mechanistic studies were commenced to establish if JAM-A could modulate CXCR4 signalling following CXCL12 stimulation, but time constraints prevented these from being completed. These preliminary experiments which were carried out first in the Jurkat cell line lacking JAM-A or transduced to express JAM-A, however, suggest that JAM-A may modulate CXCL12-induced Rap1 phosphorylation and ERK1/2 phosphorylation. The former pathway is important for integrin function and the latter pathway is important in cell adhesion. The results described here, although requiring finalisation, support the hypothesis that JAM-A acts as an adhesion molecule and also may fine tune CXCR4 and integrin mediated functions on human $CD34^+$ cells, thereby potentially regulating engraftment of these cells to the bone marrow niche.

PUBLICATIONS

Publications

- Zhou B, Tsaknakis G, Coldwell KE, Khoo CP, Roubelakis MG, Chang CH, Pepperell E, Watt, SM. A novel function for the haemopoietic supportive murine bone marrow MS-5 mesenchymal stromal cell line in promoting human vasculogenesis and angiogenesis. Br J Haematol 2012 May; 157(3):299-311.

Manuscripts in preparation

- Chang CH, Hale SJ, Zhang Y, Gabrowska R, Martin-Rendon E, Watt SM. JAM-A interacts with CXCR4 to modulate human $CD34^+$ haematopoietic stem/progenitor cell adhesion to bone marrow endothelium.
- Hale SJ, Chang CH, Zhang Y, Fisher N, Martin-Rendon E, Watt SM. Development of an *in vitro* model of the human bone marrow endothelial niche reveals factors important in angiogenic modulation.

Published meeting abstracts

- Chang CH, Hale SJ, Zhang Y, Martin-Rendon E, Watt SM (2013). Improving cord blood engraftment: a role for JAM-A in regulating $CD34^+$ haematopoietic stem/progenitor cell adhesion to the bone marrow vascular niche. NHS Blood and Transplant UK R&D conference, Oxford University, Oxford, UK.
- Hale SJ, Chang CH, Zhang Y, Fisher N, Martin-Rendon E, Watt SM (2013). Targeting bone marrow angiogenesis to improve haematopoietic engraftment. NHS Blood and Transplant UK R&D conference, Oxford University, Oxford, UK.
- Zhou B, Tsaknakis G, Coldwell KE, Khoo CP, Roubelakis MG, Chang CH, Pepperell E, Watt, SM (2013). A novel function for the marrow MS-5 mesenchymal stem/stromal cell line in promoting human vasculogenesis, angiogenesis and haemopoiesis. 7^{th} Mesenchymal Stem Cell Conference, Birmingham,UK.
- Chang CH, Hale SJ, Zhang Y, Martin-Rendon E, Watt SM (2012). Junctional adhesion molecule-A (JAM-A) is involved in human $CD34^+$ haematopoietic stem/progenitor cell interactions with the bone marrow stem cell niche. MSD Dphil Day, Oxford University, Oxford, UK.
- Chang CH, Hale SJ, Zhang Y, Martin-Rendon E, Watt SM (2012). Junctional adhesion molecule-A (JAM-A) is involved in human $CD34^+$ haematopoietic stem/progenitor cell

interactions with the bone marrow stem cell niche. NHS Blood and Transplant UK R&D conference, Oxford University, Oxford, UK.

- Khoo CP, Roubelakis MG, Tsaknakis G, Zhou B, Coldwell KE, Mistry A, Chang CH, Pepperell E, Watt, SM (2012). CXCL12 produced within the haemopoietic stem cell niche regulates human blood vessel formation. NHS Blood and Transplant UK R&D conference, Oxford University, Oxford, UK.
- Zhou B, Tsaknakis G, Coldwell KE, Khoo CP, Roubelakis MG, Chang CH, Pepperell E, Watt, SM (2012). A novel function for the haemopoietic supportive murine bone marrow MS-5 mesenchymal stromal cell line in promoting human vasculogenesis and angiogenesis. ISSCR conference, Yokohama, Japan.
- Chang CH, Hale SJ, Martin-Rendon E, Watt SM (2011). Leukaemic Stem-like Cell Interactions in the Bone Marrow Niche. NDCLS Dphil Open Day, Oxford University, Oxford, UK.

Awards

- Conference and Fieldwork Grants for the 6th UK Cancer Stem Cell Symposium from Wolfson College, University of Oxford, Oxford, UK (2011).
- College Fee Bursaries from Wolfson College, University of Oxford, Oxford, UK (2010-2012).

ACKNOWLEDGMENTS AND DECLARATION

I sincerely thank Prof. Suzanne Watt and Dr. Sarah Hale for giving this opportunity to study in this laboratory at the University of Oxford and for their supervision and co-supervision throughout my doctoral research. I also thank Dr. Enca Martin-Rendon for her advice and her guidance with the cloning studies in this thesis. Thanks to Dr. Youyi Zhang for imparting her expertise in bone marrow section staining in this research. Without their supervision I could not have achieved this thesis.

I would also like to thank my laboratory colleagues who provide such a pleasant environment to work in. Thanks to Prof. Suzanne Watt and Dr. Enca Martin-Rendon for good laboratory management as well as to Mr. Hoi Pat Tsang for ensuring orders processed and stores replenished in this laboratory, both of which enabled me to carry out my research efficiently. Thanks to Dr. Lee Carpenter for providing constructive advice in my early study. Thanks to Ms. Sandy Britt and Ms. Janice Walton for managing all the cord blood collection and those who kindly offered their cord blood samples for this research. In addition, I sincerely appreciate all the kind support and advice in science and on life as well as every social break from Dr. Cheen Khoo and Mr. Dominic Sweeney. Furthermore, thanks to Miss Anna French, Miss Laura Newton, Dr. Daniel Markson, Ms. Suranahi Buglass, Ms. Nita Fisher, Dr. Kate Coldwell, Dr. Lisa McRae and Ms. Jennifer Kean for their presence, advice and social breaks over the duration of my study. Finally, I would like to thank all my new colleagues, Mark, Rosalba, Francesca, David, Rita and Shiji for providing a happy and intelligent atmosphere in this laboratory at my last stage of research.

I must also thank Cheng-Tao Yang for being a wonderful, patient and supportive husband whilst I was conducting the research or writing this thesis. Equally, I could not have achieved this thesis without the support from my parents Mr. Ching-Chung Chang and Ms. Hsiu-Yueh Ko foremost, my family and Cheng-Tao's family. I equally deeply appreciate families and friends in Taiwan who have been looking after my parents and dogs and cats that have been accompanying to my parents while I was aboard. Finally, I am grateful having all the friends in Oxford and Taiwan for their presence and support over the period of my research. Special thanks also to Wolfson College for conference travelling grants, financial support, and as well as friendly staff whenever I came to them, for which I am deeply grateful.

I certify that I carried out over 98% of research in this thesis. Collaborative work is acknowledged in the text where Dr. Allison Blair and Dr. Charlotte Cox of the University of Bristol provided sources of human acute lymphoid leukaemia bone marrow cells and helped phenotype JAM-A on these patient samples, for which I am greatly appreciative.

TABLE OF CONTENTS

Abbreviations

ALL	Acute lymphoid leukaemia
AML	Acute myloid leukaemia
BM	Bone marrow
BMEC	Bone marrow endothelial cells
BMSC	Bone marrow stromal cell
CD	Cluster of Differentiation
CXCL12	C-X-C motif chemokine 12
CXCR4	Chemokine receptor type 4
DNA	Deoxyribonucleic acid
ESC	Embryonic stem cells
Flt-3L	Fms-like tyrosine kinase 3 ligand
G-SCF	Granulocyte-colony stimulating factor
GVHD	Graft versus host disease
HS/PC	Haematopoietic stem/progenitor cell
HST	Haematopoietic stem cell transplantaion
HUVEC	Human umbilical vein endothelial cell
IL	Interleukin
iPSC	Induced pluripotent stem cell
LSC/LIC	Leukaemic stem cell/ Leukaemic initiating cell
MNC	Mononuclear cell
NOG	NOD/Shi-scid IL2rgamma(null)
NSG	NOD *scid* IL2 receptor gamma chain knockout
PCR	Polymerase chain reaction
Rap1	Ras-proximate-1 or Ras-related protein 1
RNA	Ribonucleic acid
SCF	Stem cell factor
SCID	Severe combined immunodeficiency
TPO	Thrombopoietin
UCB	Umbilical cord blood
UCBT	Umbilical cord blood transplantation

CHAPTER 1

INTRODUCTION

1.1. Umbilical Cord Blood Transplantation (UCBT)

Stem cell therapy is a promising option for a number of diseases. The first of these has successfully used haematopoietic stem cell transplantation (HST) to treat malignant and non-malignant conditions of the blood in humans. Therapies used may be autologous or allogeneic, may use bone marrow, mobilised peripheral blood or umbilical cord blood (UCB) as a source of stem cells, and the selection of donor cells is based on the type of disease and if appropriate donor cells are available for treatment. Nowadays, up to 55,000-60,000 HST are performed worldwide annually (1, 2). Sixty percent of HSTs will be autologous and most use G-SCF mobilised peripheral blood as the transplant source. However, for allogeneic donations, 3 out of 10 patients who require allogeneic HST will have a matched sibling donor (3, 4).

Umbilical cord blood transplantation (UCBT) is one source of haematopoietic stem cell (HSCs) for patients without matched siblings. Since the first UCBT was reported by Gluckman *et al.* in a child with Fanconi's anemia (5), approximately >30,000 UCBT have been performed globally over the last 25 years (4). UCBT is beneficial not only because it can be collected and banked for immediate usage, but also because of a reduced rate of acute and chronic graft versus host disease (GVDH) despite an enhanced degree of disparity with human leucocyte antigen (HLA) matching between donor and recipient as reviewed in (6, 7) and shown in Figure 1.1. Nevertheless, a primary limitation of UCBT is the limited haematopoietic stem cell (HSC) number in one UCB unit, particularly where this is used to transplant an adult. Low cell dose correlates with decreased short term engraftment of

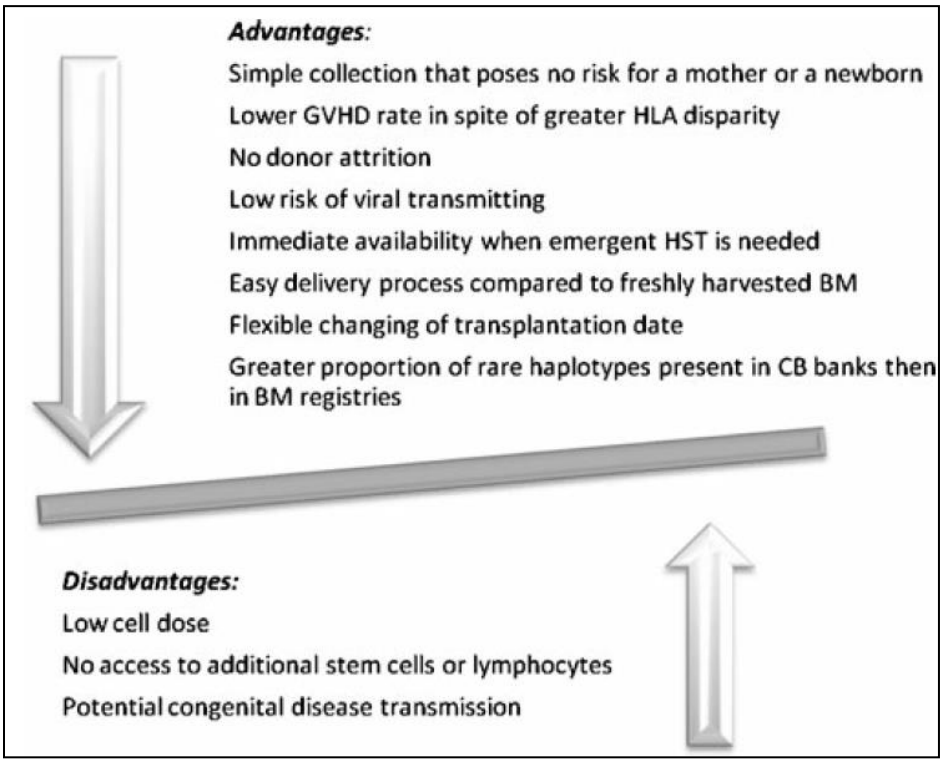

Figure 1.1. Advantages and disadvantages of using umbilical cord blood transplantation (UCBT).
Although multiple benefits have been observed from using UCBT, a few weaknesses remained unsolved due to current technology limitation. Stanevsky *et al.* summarised both sides of using UCBT in clinical treatments. Abbreviations: GVDH: graft versus host disease; HLA: human leucocyte antigen; HST: haematopoietic stem cell transplantation; BM: bone marrow; CB: cord blood. The figure is taken from Stanevsky *et al.* (6). Springer and the Stem Cell Reviews 7, 2010, 425-33, Cord Blood Stem Cells for Hematopoietic Transplantation, Stanevsky A, Figure 1, original copyright notice is given to the publication in which the material was originally published with kind permission from Springer Science and Business Media.

neutrophils and platelets and delayed longer term immune reconstitution (4). Some findings have shown that $CD34^+$ cell dosage is important for a faster neutrophil recovery post-transplant (8-10). To improve the success rate of UCBT, several strategies have been proposed. Multiple donors have been suggested (11), although in some clinical trials it was found that one donor from a double transplantation predominantly engrafted (12). Another strategy is to expand the stem cells *ex vivo* for transplantation, such as by co-culturing UCB-derived haematopoietic stem/progenitor cells (HS/PCs) with mesenchymal stem/stromal cells (MSCs) and/or with cytokines or growth factors (13). Despite this, the effect of co-

transplantation of MSCs is still controversial (14, 15). Lately, several studies have illustrated that intra-bone marrow injection may improve haematopoietic recovery (16-18). Other studies on the cross-talk between HS/PCs and the bone marrow niche highlight their potential importance in haematopoietic recovery after transplantation (19). First, Robinson *et al*. (20) showed that UCB $CD34^+$ cells have a defect in their ability to interact with bone marrow sinusoidal endothelium compared to bone marrow and mobilised peripheral blood. Secondly, a study by Gold *et al.* depicted the expression profiling of a number of adhesion molecules on $CD34^+$ cells and showed that various adhesion molecules correlated with neutrophil, platelet or red blood cell reconstitution (21). Thus, functional adhesion and homing molecules also play an important role in the success of UCBT.

1.2. Stem Cells- A General Introduction

The term stem cell was first used in 1909 by a Russian histologist, Alexander A. Maximow, who postulated a cellular hierarchy in haematopoiesis from a common precursor (review in (22)). Similar stem cell populations are thought to be responsible for the regeneration of tissues, such as intestine, skin etc. and for normal maintenance. Lorenz *et al.* (23) showed that spleen or bone marrow (BM) cells from healthy donors were able to restore bone marrow function following its failure in irradiation exposed recipients, yet this still left open the question as to whether the recovery from BM failure originated from multiple progenitors or from a single stem cell (reviewed in (22)). Haematopoietic stem cell research started to bloom when McCulloch and Till showed colony formation in irradiated mouse spleens followed a single viable BM cell infusion (24). Subsequent studies indicated that a multipotent stem cell contained in the injected marrow cells could differentiate into the colony, and a single viable cell was sufficient to give rise to the colony formation (25, 26). The initial definition of these colony-forming cells later was applied to the definition of stem

cells, which are a population of undifferentiated cells characterised by their self-renewal ability and multiple lineage potency. Moreover, stem cells are capable of dividing symmetrically or asymmetrically so as to maintain their numbers, with asymmetric division also being able to generate a family of differentiated daughter cells over a lifetime. It is known that both intrinsic mechanisms and extrinsic mechanisms (e.g. contact with the microenvironment (niche)) can regulating stem cell division (as reviewed in (27)). The details of the microenvironment in regulating stem cell fate will be discussed in the following sections.

There have been two primary groups of stem cells postulated. These are embryonic stem cells and non-embryonic stem cells, the latter being more commonly known as adult stem cells or somatic stem cells. Embryonic stem cells are pluripotent, while adult stem cells are located in various organs and thought to be multipotent or give rise to at least two lineages of differentiated cells. Embryonic stem cells (ESCs) were first isolated by Professors Martin Evans and Matthew Kaufman as pluripotential cells derived from inner cell mass of the murine blastocyst (28). Martin postulated that ESCs existed in this cell population (29). The currently available human ESCs (hESCs) lines have been derived with informed consent from donors undergoing *in vitro* fertilisation treatment. In 2007, the Human Fertilisation and Embryology Authority (HFEA) in the UK allowed women to donate their eggs for research. Although their usage in research still causes much ethical debate, hESCs have been shown to differentiate into three germ layers, ectoderm, mesoderm and endoderm, with mesoderm for example giving rise to HSCs and all blood lineages (reviewed in (30)).

More recently, the production of induced pluripotent stem cells (iPSCs) from mouse (31) and human somatic cells (32, 33) has generated a new wave of stem cell research. Despite the differences in factors used to produce these cells, iPS cells can be pluripotent and

generate different lineages. Genetic analysis including gene expression profiling and postmodification (methylation) profiling and tetratoma formation indicates that iPSCs do not result from genetic mutations (32). Despite being generated reproducibly, a typical issue for iPSC production is its low efficiency, with a mere 0.02% transfected fibroblasts becoming iPSCs after reprogrammimg. Several induction strategies, such as viral vectors, miRNAs and epidermal plasmids, are used. Another interesting question is whether iPSCs are similar to ESCs. Genetic profiling has been used to assess this but a conclusion has not been reached on this point. At least two factors lead to the different results; one is the induction systems that are used and the second is the heterogeneous gene profiling in iPSCs from different sources (reviewed in (34)). Even though there is need to understand the reprogramming mechanisms, iPSCs demonstrate less controversial ethical issues when being applied to clinical applications, such as tissue engineering, disease modelling and drug discovery (reviewed in (34)).

1.3. Haematopoietic Stem/Progenitor Cells (HS/PCs)

Haematopoietic stem/progenitor cells (HS/PCs) were the first defined and are the best-characterised adult stem cells in the field. HS/PCs are now defined as a population capable of long-term haematopoietic repopulation after transplantation, with self-renewal ability and with the ability to give rise to all blood cell lineages (as reviewed in (22)). In 1978, haematopoietic progenitor cells (HPCs) were found in human UCB and these progenitor cells gave rise to myelocytic colonies (35). Moreover, Prindull *et al.* worked out the ratio of colony formation was 1 in 1678 UCB cells and this was significantly higher than such cells in adult peripheral blood (35). Much of our understanding of haematopoiesis is based on the studies in the mouse. Luis *et al.* have summarised the development of murine and human haematopoiesis and the timeline is shown in Figure 1.2 (36).

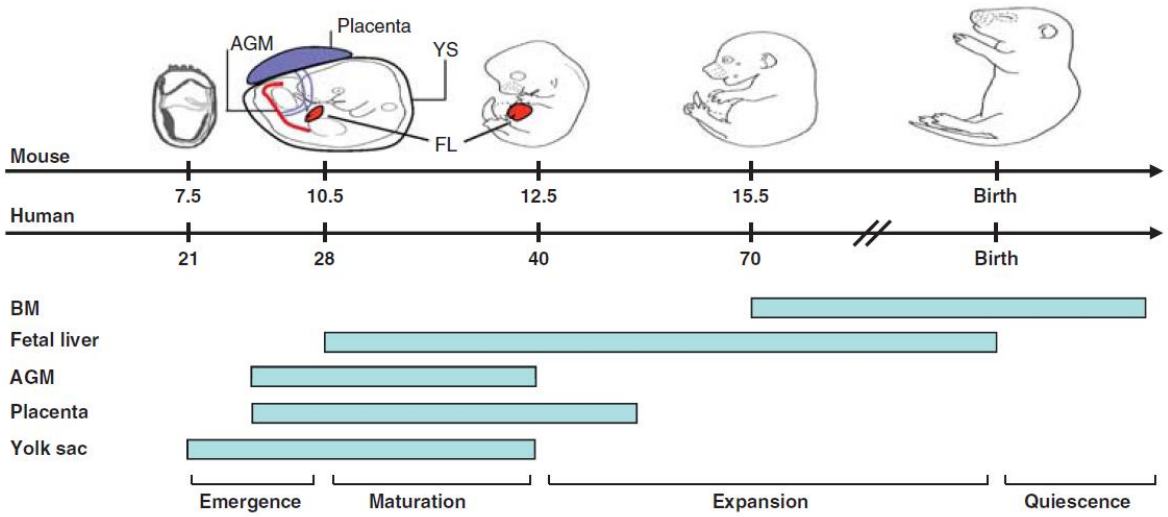

Figure 1.2. Establishment of haematopoiesis during embryonic development.
Bars represent the major active haematopoietic sites at different stages of embryonic development in mouse and human. The primitive haematopoietic progenitor is firstly detected in yolk sac before the circulation is established. The definitive haematopoietic stem cell (HSC) is then detectable in aorta gonad mesonephros (AGM) region and placenta, and then in the fetal liver (FL). The FL subsequently becomes the major haematopoietic region until the HSCs migrate into bone marrow (BM) where they reside after birth. The figure is taken from Luis *et al.* (36). Reprinted by permission from Macmillan Publishers Ltd: Leukemia (36), Copyright (2012).

The development of the haematopoiesis system begins in the yolk sac (YS) in mammalian embryo when the circulation system is not established. This transient haematopoietic tissue mainly generates red blood cells, although a minor population of myeloid progenitors is also detectable at this stage. This stage is referred to primitive haematopoiesis as erythrocytes produced in this stage do not enucleate and as HSCs are not produced. The wave of primitive haematopoiesis is followed by definitive haematopoiesis which is first established in the aota-gonad-mesonephros (AGM) region. Shortly after this, the definitive HSCs can be detected in the placenta and fetal liver (FL), which subsequently becomes the major haematopoietic organ until bone marrow (BM) haematopoiesis system is established at birth. In the last stage of gestation, HSCs migrate to the BM, the main region for haematopoietic cell generation after birth. Several differences exist between fetal and adult

HSCs. The fetal HSCs are more actively cycling and have higher self-renewal capacity than adult HSCs, while adult HSCs are mostly quiescent or slowly cycling. In mice, the HSCs in liver expand rapidly up to 38 fold prior to exit to the spleen or BM. In addition, there is increasing evidence for differences between the two HSC sources in terms of their functions and gene expression profiles (reviewed in (36)).

To purify human HSCs, a number of surface expression markers are used. CD34 was first identified as an HS/PC surface antigen using the early human myeloblastic cell line KG-1a as an immunogen and to screen for antibodies (reviewed in (37)). The monoclonal anti-My-10 antibody was generated in hybridising SP-2 plasmacytoma cells with splenocytes from BALB/c mice, followed by repeated immunisation with viable KG-1a cells (38). Civin *et al.* showed that the CD34 (My-10) antigen was able to identify human HS/PCs (38). Multiple antibodies have been generated against human CD34 and the antigen was also initially termed HPCA-1 (39, 40). In addition, the LTC-ICs from the BM cells were found enriched in $CD34^+$ populations (41). Combined with fluorescence-activated cell sorting (FACS), it then became possible to isolate this particular HS/PC population. Furthermore, Berenson *et al.* provided *in vivo* evidence that the $CD34^+$ cell population could engraft into and repopulate haematopoiesis in irradiated baboons (42). A number of functional studies on the CD34 antigen suggested it had a role as an adhesion molecule on endothelial cells and this depended on its glycosylation state (reviewed in (43)). As a variety of studies led to the concept that human HS/PCs are positive for CD34 antigen expression, the QBend10 CD34 antibody is now used with magnetic activated cell sorting to isolate these cells from human UCB, BM and mobilised peripheral blood (44).

Osawa *et al*., on the other hand, showed that $CD34^-$ HS/PC from murine bone marrow generated multilineage repopulation after transplantation (45). A series of subsequent

reports further supported the concept that murine $CD34^-$ HS/PC exist (defined as a side population (SP) cells; reviewed in (37)). Goodell *et al.* reported that human $CD34^-$ HS/PC had LTC-IC capability and developed into $CD34^+$ cells (46). These studies suggested that $CD34^-$ HSCs were more quiescent than $CD34^+$ HSCs in the mouse and that CD34 was an activation marker on these cells. It is also worth noting that CD34 is expressed outside the haematopoietic cell population, such as on vascular endothelial cells (47) and fibroblasts or pericytes (48). A few reports have suggested that murine $CD34^+$ HSCs are in an activated or cycling state, and that these $CD34^+$ HSCs are able to revert to quiescent $CD34^-$ state (reviewed in (49)). Bhatia *et al.* described a $CD34^-$ cell population from UCB, displayed abilities of engraftment, differentiation and reconstitution of haematopoietic lineages in NOD/SCID mice (50). CD34 can however be detected internally in human HS/PCs before it is expressed on the cell surface (51). Since CD34 antigen expression is likely to be variable on the surface of HS/PCs, other makers have been considered.

AC133 or CD133 antigen is another common HSC marker that has been described since 1990s. It is also called Prominin-1 (52, 53). Yin *et al.* first showed that CD133 was selectively expressed on $CD34^+$ human HS/PC and this double positive cell population from fetal bone marrow possessed engraftment ability (54). Miraglia *et al.* (55) characterised the CD133 antigen as a five-transmembrane glycoprotein that is expressed (though not exclusively) on HS/PCs (56, 57).

Varied proportions of CD133-postive cells have been observed by de Wynter *et al.* in human UCB, but still these authors confirmed that UCB-derived $CD34^+CD133^+$ cells engrafted more than $CD34^+CD133^-$ cells (58). On the other hand, other groups have proposed that the $CD34^-$ $CD133^+$ population contains HS/PC capacity and can also differentiate into $CD34^+$ cells, suggesting that it is more primitive than $CD34^+$ cells in human haematopoiesis (reviewed in

(59)). Recent reports show that CD133 is expressed not only by human UCB HSCs but also granulocyte-monocyte progenitors (GMP), although it is lacking on megakaryocyte-erythroid progenitors (MEP) (60). Indeed, based on CD133 expression, Gorgens *et al.* (60) have proposed a new model of haematopoietic development that is illustrated in Figure 1.3. These other models are described in more detail below.

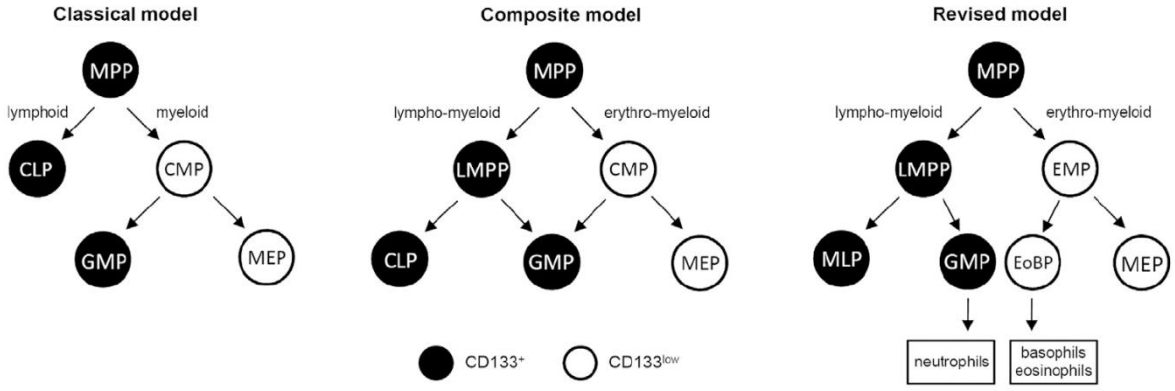

Figure 1.3. Overview of different models of haematopoietic differentiation based on CD133 expression. The figure from Gorgens et al. (60) shows the expression of CD133 (black circles) on the classical (61), composite (62), and revised (60) models of haematopoiesis. MMP: multipotent progenitor cells; LMPP: lymphoid-primed multipotent progenitor cells; CLP: common lymphoid progenitor cells; CMP: common myeloid progenitor cells; GMP: granulocyte-monocyte progenitor; MEP: megakaryocyte-erythroid progenitor; EoBP: eosinophil-basophil progenitor. Reprinted from Cell Report 3, Gorgens A, Radtke S, Mollmann M, Cross M, Durig J, Horn PA, Giebel B., Revision of the human hematopoietic tree: granulocyte subtypes derive from distinct hematopoietic lineages, 1539-52, Copyright (2013), with permission from Elsevier.

The function of murine and human CD133 in HS/PCs is not entirely clear as there appear to be species differences in its expression and function (63). It is however known that it is not required for homing or colony formation, although it has been proposed that CD133/prominin-1 localises in the uropod of migration HS/PCs (64, 65) (Figure 1.4).

However, CD133 has been shown to be involved in human HSC fate decisions and as an important physiological regulator of HSC maintenance and expansion. More specifically, it has been shown that human HS/PCs contain an intracellular pool of CD133 within

membrane vesicles and has been proposed by Bauer *et al.* (66) and Fargeas *et al.* (67) that CD133/prominin-1-containing lipid rafts hold key determinants that maintain stem cell properties and that their loss results in lineage differentiation. In the mouse, CD133 appears not to have this function, but to modify the development of MEPs under steady state conditions and of erythroid cells under physiological stress (63). Additional cell surface markers have been proposed to identify HS/PCs in combination of CD34 or CD133 antigens.

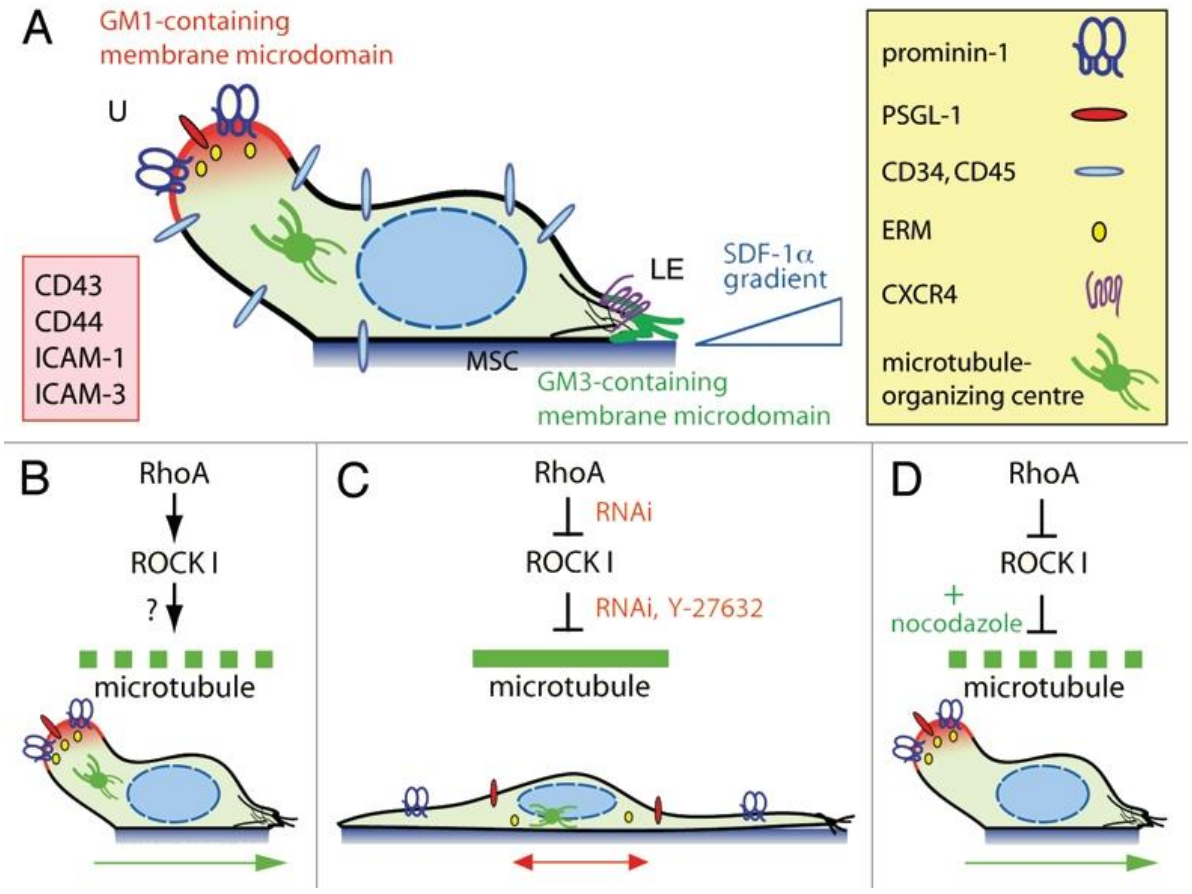

Figure 1.4. CD133/prominin-1 does not polarise with CXCR4 upon CXCL12/SDF-1 presentation.
With permission from the corresponding author the cartoon is taken from Fonseca and Corbeil (65) which shows the leading edge (LE) of a haematopoietic stem/progenitor cell (HS/PC) migrating on MSC (mesenchymal stromal cells) where CXCR4 is recognising CXCL12 or SDF-1. The uropod (U), which exists at the rear pole of the HS/PC, contains CD133/prominin-1 as well as other molecules such as ICAM-3 and PSGL-1. Polarisation is inhibited in RhoA/ROCKI-deficient HS/PCs and restored by the addition (+) of nocodazole. Republished with permission of Communicative & integrative biology from The hematopoietic stem cell polarization and migration: A dynamic link between RhoA signaling pathway, microtubule network and ganglioside-based membrane microdomains, Fonseca AV, Corbeil D, 4: 201-4, 2011; permission conveyed through Copyright Clearance Center, Inc.

Lineage markers exclusion, for example, alone with CD34-positive selection has been used to isolate mouse or human HS/PCs. However, the lack of congruence of other surface markers between mice and humans has raised a concern in analysing murine results for estimation in humans. Take for example, the $Lin^{-}Sca\text{-}1^{+}c\text{-}kit^{+}$ (LSK) population, which has been used for mice HS/PC isolation (reviewed in (22)). By coordinating these markers with $CD150^{+}CD48^{-}$ cell surface phenotype and other markers, murine HSCs have been categorised into long-term (LT), intermediate-term (IT), short-term (ST) and multipotent progenitors (MPPs) as shown in Figure 1.5. Mouse HSCs express CD150, while human HSCs do not (68). Hence, subsequent studies in human HSC isolation introduced CD90 (Thy1), CD45RA and CD38 as markers, of which $CD34^{+}CD90^{+}$ cells contain multilineage HSCs and the latter two are makers for more differentiated progenitors. These markers together with lineage negative (Lin^{-}) markers led to a picture of this cell population as $Lin^{-}CD34^{+}CD90^{+}CD45RA^{-}CD38^{-}$ (Figure 1.5; reviewed in (22)). Integrins are another set of surface expressing molecules that recently has been proposed for HSCs characterisation. In the human, HSCs express integrin $\alpha 6$ (CD47f) (reviewed in (22)). In the mouse, integrin $\alpha 2$ (CD49b) is differentially expressed on LT and IT-HSCs, while integrin $\alpha 6$ (CD47f) is expressed on normal mammary stem cells (Figure 1.5.B; reviewed in (22)). A model for determine mouse and human HSC differentiation into committed progenitor cells using a combination of markers is shown in Figure 1.5.

Mouse HSCs are defined as long-term HSCs (LT-HSCs), intermediate-term HSCs (IT-HSCs) and short-term HSCs (ST-HSCs) or multipotent progenitors (MPPs) dependent on the duration of repopulation after *in vivo* transplantation. The MPPs lose self-renewal capacity by showing only transient repopulation capacity while they still preserve the ability to commit into further downstream lineages. An initial model, the classical model of haematopoiesis,

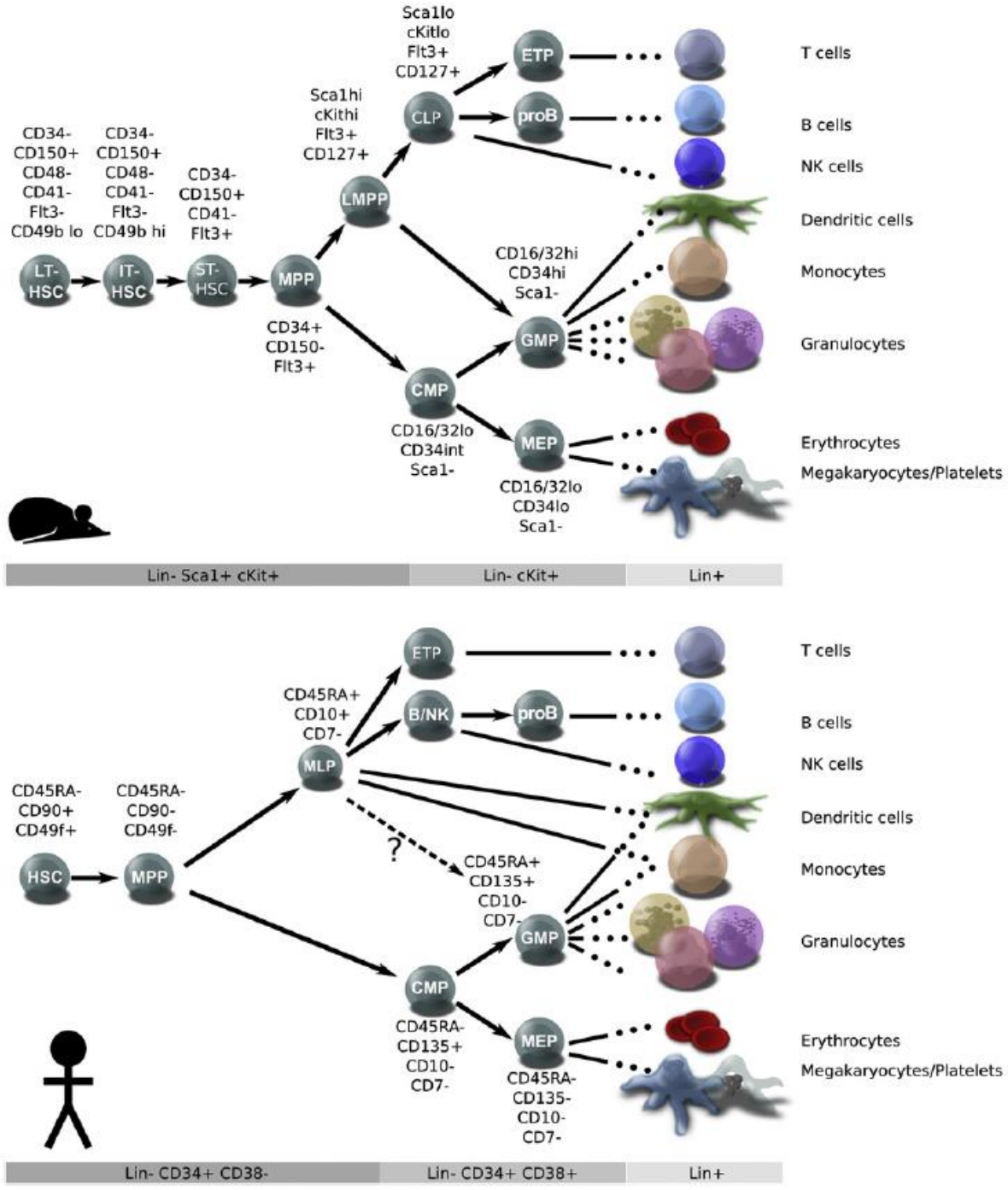

Figure 1.5. The Doulatov models of haematopoiesis in the adult mouse and human.
The upper and lower figures show the recent lineage maps for the phenotypic identification of mouse and human haematopoietic lineages as described by Doulatov *et al.* (22). Such studies are based on epigenetic and transcriptional differences between closely related progenitor cell subsets. To the right are the terminally differentiated cells. Doulatov *et al.* (22) have segregated haematopoietic stem cells (HSCs) into long-term (LT), intermediate-term (IT), and short-term (ST) subsets which are based on the extent of their repopulation potential. Immature lymphoid progenitors are described as multipotent lymphoid progenitors (MLPs) and, in this model, these not only generate the earliest thymic progenitors (ETP) but also generate dendritic cells and monocytes, and possibly granulocyte-monocyte progenitors (GMP). MPP: multipotent progenitor; MEP: megakaryocyte-erythroid progenitor; CMP: common myeloid progenitor; CLP: common lymphoid progenitor. Taken from Doulatov *et al.* (22). Reprinted from Cell Stem Cell 10, Doulatov S, Notta F, Laurenti E, Dick JE., 120-36, Hematopoiesis: a human perspective, Copyright (2012) with permission from Elsevier.

suggested that MPPs segregated into lymphoid and myeloid lineages, referred as common lymphoid progenitors (CLP) and common myeloid progenitors (CMP) respectively. In this classical model, the CLPs gave rise to B cell precursors and earliest thymic progenitors (ETPs) which further committed into T cell and nature killer (NK) cell lineages. On the myeloid side, CMPs gave rise to granulocyte-monocyte progenitors (GMPs) and megakaryocyte-erythroid progenitors (MEPs). Later on, however, Kawamoto *et al.* [68] found that a progenitor with lymphoid lineage potential always coupled with partial myeloid potential, while CLPs proposed in the classical model were never observed. This introduced the idea of the existence of lymphoid-primed multipotent progenitor (LMPP) cells, where lymphoid and myeloid fates are still coupled (reviewed in (22, 69)). LMPPs appear to be a transient lympho-myeloid population with a predilection to lymphoid differentiation. Some studies have shown an asymmetry of differentiation, with rapid myeloid and gradual lymphoid differentiation from such progenitors (70). Moreover, epigenetic analysis has indicated that myeloid promoter silencing contributes to this lymphoid development (reviewed in (22)). Together these studies support the existence of LMPPs and explain its preference for lymphoid commitment. Given the uncertainties in human cells, a multilymphoid progenitor (MLP) was proposed by Doulatov *et al.* (71) to describe a progenitor that gave rise to all but was not limited to lymphoid lineages (Figure 1.5). In their study, Doulatov *et al.* showed an MLP population, losing self-renewal, displayed potentials to give rise to B cells, T cells, natural killer (NK) cells, dendritic cells (DC), monocytes and macrophages (71). Recently, Gorgens *et al.* (60) have suggested that CD133 can discrimate between these progenitor cells and that $CD133^{+}$ MPPs generate $CD133^{+}$ LMPPs and $CD133^{-}$ EMP (erythro-myeloid progenitors), the latter being the precursors for an eosinophil-basophil progenitor and an MEP (Figure 1.3).

1.4. Leukaemic Initiating Cells (LICs) or Stem-like Cells (LSCs)

Johannes Muller in the 1840s led a group of German pathologists to examine tissue sections under high magnification and initiated the investigation of origin of tumours. Julius Cohnheim in 1867 postulated that tumours were derived from “embryonic cell nests”, residual embryonic cells left behind in the adult organism (reviewed in (72)). The idea of malignant stem cells developed further until in 1974 Pierce (73) proposed malignant stem cells exist in a tumour and could contribute to tumour progression while investigating a mice teratocarcinoma (reviewed in (72)). The term of cancer stem cells (CSCs) or cancer-initiating cells was therefore introduced by distinguishing such cells from the bulk of the tumour and demonstrating that these cells are responsible for long-term tumour growth and maintenance of cancer phenotype in recipients. In the CSC field, there is longest and strongest evidence supporting a CSC for acute leukaemia, while recent studies have also identified the existence of CSCs in other solid tumours (reviewed in (74)).

Leukaemia is a blood cancer characterised by an abnormal increase of immature blood cells in the bone marrow (BM) and associated with suppression of normal haematopoiesis. Although around 70-80% of young patients with acute lymphoid leukaemia and approximately 50% of older patients with acute leukaemia can achieve complete remissions with current standard treatment, a significant proportion of patients relapse and in some cases the 5-year survival rate without transplantation drops to <30% (reviewed in (75)). Building on HSC knowledge and the relevant techniques, research into leukaemic stem-like cells (LSCs) or leukaemic initiating cells (LICs) has grown rapidly compared to research on other cancer stem cells. A series of investigations have demonstrated that an LIC population, initially defined by a $CD34^{+}CD38^{-}$ HS/PC phenotype, was capable of establishing human acute myeloid leukaemia (AML) in a recipient mouse and passing on this disease from

animal to animal (reviewed in (75)). LICs were first identified by Bonnet *et al.* from AML blasts using a xenogeneic transplantation model (76). Before this, Lapidot *et al.* provided evidence that stem-like cells occurred in the $CD34^{+}CD38^{-}$ cell fraction from human acute myeloid leukaemia (AML) but not in $CD34^{+}CD38^{+}$ or $CD34^{-}$ cell fractions (77). However, current studies using NSG (NOD *scid* IL2 receptor gamma chain knockout mice) rather than NOD/SCID (NOD/Shi-scid IL2rgamma null) mice, have shown that LICs also exist in the $CD34^{-}$ cell population, suggesting heterogeneity in LICs and that more makers are needed for their identification (reviewed in (75)). With more markers used to identify normal HS/PCs, Goardon *et al.* more recently showed LICs co-exist in the LMPP-like and GMP-like populations from AML (78). Furthermore, in acute lymphoid leukaemia (ALL), Cox. *et al.* found that $CD34^{+}CD7^{-}$ LSCs exist in the pro-T cell population of T-cell acute lymphoid leukaemia (T-ALL) (79) and in the $CD34^{+}CD10^{-}CD19^{-}$ or $CD133^{+}CD38^{-}CD19^{-}$ LICs or pro-B cell and pre-B cell populations of B-cell ALL (B-ALL) (80, 81). In these latter studies, the LICs could pass on the disease in secondary and tertiary murine recipients and hence these LICs demonstrated self-renewal ability [78]. In addition, these authors observed resistance of their characterised LICs to treatment with dexamethasone and vincristine, standard drugs in childhood ALL therapy (81). LICs are believed to display slow cycling and be able to survive in mouse transplant models from weeks to months (reviewed in (74)). Increasing evidence indicates that the interaction between LICs and niche cells is responsible for chemoresistance and relapse in patients as reviewed in (74, 82). The interaction between BM niches and HS/PCs and LICs will be discussed in the following sections.

Some authors report the aberrant expression of the specific markers and use these for isolation LICs from HS/PCs in patients. These include the absence of CD90, the upregulation of CD123, CLL-1, CD96, CD47, CD200 and Tim3, and abnormal expression of lineage markers

(Dr A Blair, personal communication). Among these markers, CD47 and Tim3 have been used for the separation of HS/PCs from LICs in leukaemic bone marrow samples. The functions of the above antigens are poorly understood, except of CD47, which mediates survival signals in host phagocytes (reviewed in (75)). Very recently, Bonardi *et al.* (83) detected differences in membrane protein expression on normal and acute myeloid leukaemia (AML) $CD34^+$ cells using proteomic and transcriptomic approaches. The increased expression was found for previously identified candidate markers, such as CD44, CD47, CD135, CD96 and VLA5, as well as for novel markers, such as CD82, CD97, CD99, PTH2R, MET and CD49f, suggesting new potential markers for LIC detection (83).

1.5. The Bone Marrow Niches

1.5.1. Cellular components of the bone marrow niches

The concept of the niche, a specialised microenvironment in body, was first described by Schofield in 1978 (84). Schofield proposed that the microenvironment surrounding the cells was responsible for directing cell fate (84). Lord *et al.* showed that the HS/PCs reside disproportionately in the bone marrow (BM) cavity, suggesting cell components in the BM, in particular near the endosteum or the bone, could regulate HS/PCs (85). Additionally, Shackney *et al.* showed that the proliferation of the precursors was slower in the centre of the BM (86). In 1992, Naito *et al.* illustrated the BM compartment with a computer-assisted three-dimensional reconstruction of the BM from eight clinical surgical specimens (87). They were able to visualise the networks of arteries, sinusoids and a vein and the distribution of different lineages of cells in the BM, providing an image of the architecture of this functional unit, the niche, in bone (Figure 1.6).

It has been proposed that HS/PCs can only maintain their stemness inside a specific niche, but then proliferate or differentiate when they relocate out of this specific stem cell niche. Three anatomical HS/PC niches are described in the bone marrow. These are 1) the endosteal niche (88-90), which is located adjacent to the bone surface, and is thought to keep HSC/HPCs quiescent; 2) the vascular niche (91, 92), which is thought to support the proliferation and maturation of HSC/HPCs, and therefore there are also more committed HPCs harboured within this niche; and 3) the bone marrow proper (93, 94). Some researchers argue that these niches are not distinct but form a continuum within the bone marrow compartment (reviewed in (95)).

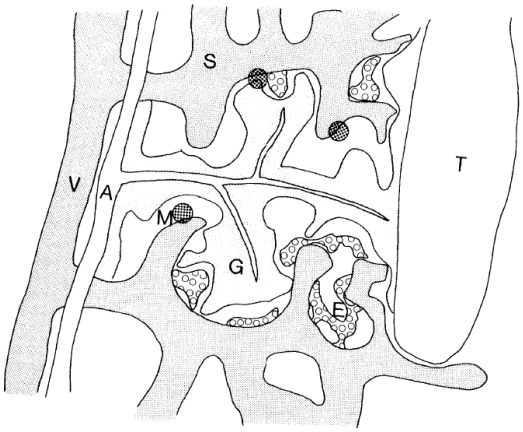

Figure 1.6. The functional unit of the bone marrow.
A functional unit of bone marrow is composed of a central arteriole (A) and sinuses (S). The parallel arrangement of the afferent and efferent vessels ensures a uniform, arterio-sinal distance. G: granulocytes; E: erythroblastic cords; M: megakaryocytes; T: bone trabecula; V: vein. The figure is taken from Naito *et al.* (87). Reprinted from Naito K, Tamahashi N, Chiba T, Kaneda K, Okuda M, Endo K, Yoshinaga K, Takahashi T., The microvasculature of the human bone marrow correlated with the distribution of hematopoietic cells. A computer-assisted three-dimensional reconstruction study, 166: 439-50, 1992 with permission from Tohoku University Medical Press.

The endosteal niche or osteoblastic niche has been defined as the microenvironment along endosteum of the bone, which is rich in osteblasts and hypoxic. It is estimated that oxygen tensions in this region can be as low as 1.3% oxygen (96). This region is also associated with high concentrations of calcium coming from the bone (97). One hypothesis is the existence of a gradient of cell development in bone marrow where relatively quiescent cells locate along the endosteal region and are able to mobilise to vascular zones where proliferation,

differentiation and maturation occurs (86). The regulation of haematopoiesis by osteoblasts was first proposed by Taichman and Emerson (88). Two earlier landmark reports had demonstrated that osteogenic cells in the endosteal niche maintained the pool of HS/PCs in the body through bone morphogenetic protein (BMP) signalling (89) and parathyroid hormone (PTH)/PTH-related protein (PTHrP) receptor (PPR) signalling-mediated Notch signalling (90). These authors provided molecular evidence by showing osteogenic cells directly regulated HS/PC numbers and survival in the BM after transplantation. Other molecules, such as osteopontin (OPN) (98, 99), leucocyte cell adhesion molecule (ALCAM; also known as CD166) (100, 101), Angiopoietin 1 and Tie2 receptor (102), have been shown play a role in HS/PC regulation in the endosteal niche. Furthermore, Gillette *et al.* using live cell image illustrated physical contacts between HS/PCs and osteoblasts (103). Two groups around the same time reported successful detection of HS/PCs in the BM of live animals using real-time imaging technology. Lo Celso *et al.* suggested that HS/PC subsets localised distinct distance from the endoseal niche according to their stage of differentiation, suggesting this niche may maintain the HS/PC pool in the BM (104). Xie *et al.* indicated that HS/PCs attempted to home to the endoseal niche in irradiated mouse BM for their expansion (105). This contact led to redistribution of adhesion molecules on and polarity of HS/PCs, followed by an exchange of lipid or membrane components between the two cell types, eventually turning on signalling inside the osteoblasts, with CXCL12 secretion for example, a well-known HS/PC homing factor (reviewed in (106)).

In contrast to these studies, a large number of $CD150^{+}$ HS/PCs were observed adjacent to the vascular niche (also known as the endothelial niche), in particular being close to sinusoidal vasculature (91) (reviewed in (107)). Previous studies showed that vascular endothelial cells from non-haematopoietic organs did not support haematopoiesis *in vitro*.

This implies that phenotypically and functionally distinguished bone marrow sinusoidal endothelial cells (BMECs) display different and specific functions (108). Indeed, BMECs are distinguished from other vessels by constantly expressing endothelial-selectin (E-Selectin) (109), VACM-1 (109, 110) and platelet selectin (P-Selectin) (109) and as well as CXC-chemokine ligand 12 (CXCL12; reviewed in (107)). These molecules are known to play important roles in HS/PC homing, mobilisation and engraftment. A growing body of research has implicated the sinusoidal endothelium or vasculature in the bone marrow in supporting such HS/PCs functions as survival, proliferation and differentiation of myeloid lineages (reviewed in (107)). Earlier investigations suggested that the endosteal niche maintains HS/PCs in quiescence, while the endothelial niche is associated with their expansion (reviewed in (111)). More recently, it was shown that endothelial niche also regulates HS/PC dormancy, self-renewal and resistance to chemotherapy through E-Selectin interaction (112) and SCF signalling (113).

Apart from osteoblasts and endothelial cells, CXCL12-abundant reticular (CAR) cells (114), Nestin$^+$ or Leptin Receptor$^+$ (LepR$^+$) mesenchymal stem cells (Nest or LepR$^+$ MSC) (115) and human ARCs (MCAM/CD146-expressing subendothelial cells) (116) in the bone marrow were found to be involved in HS/PC regulation. Adipocytes have been shown to negatively regulate HS/PC engraftment (117). Katayama *et al.* showed that the sympathetic nervous system regulates HS/PC attraction to their niche (118). Osteomacs (119), a subpopulation of bone marrow macrophages, and regulatory T cells (120) are the two very recent cell populations that have been demonstrated to support HS/PCs engraftment in the niche.

However, whether if these are distinct or a continuum of niches is a matter for some debate (91-93). More and more evidence lately demonstrates that the vascular network as being adjacent to the endosteal niche, suggesting an overlap in the regulation of HS/PCs by the

vascular and endosteal niches. Lo Celso *et al.* showed that osteoblasts and vessels were in close proximity, of which >90% were observed within 20 μm, and this was where HS/PC engrafted (104). An updated integrated overview was described by Lo Celso and Scadden to provide a hypothesis for niche elements and a dynamic model of the niche without dissecting it into small units (Figure 1.7) (95).

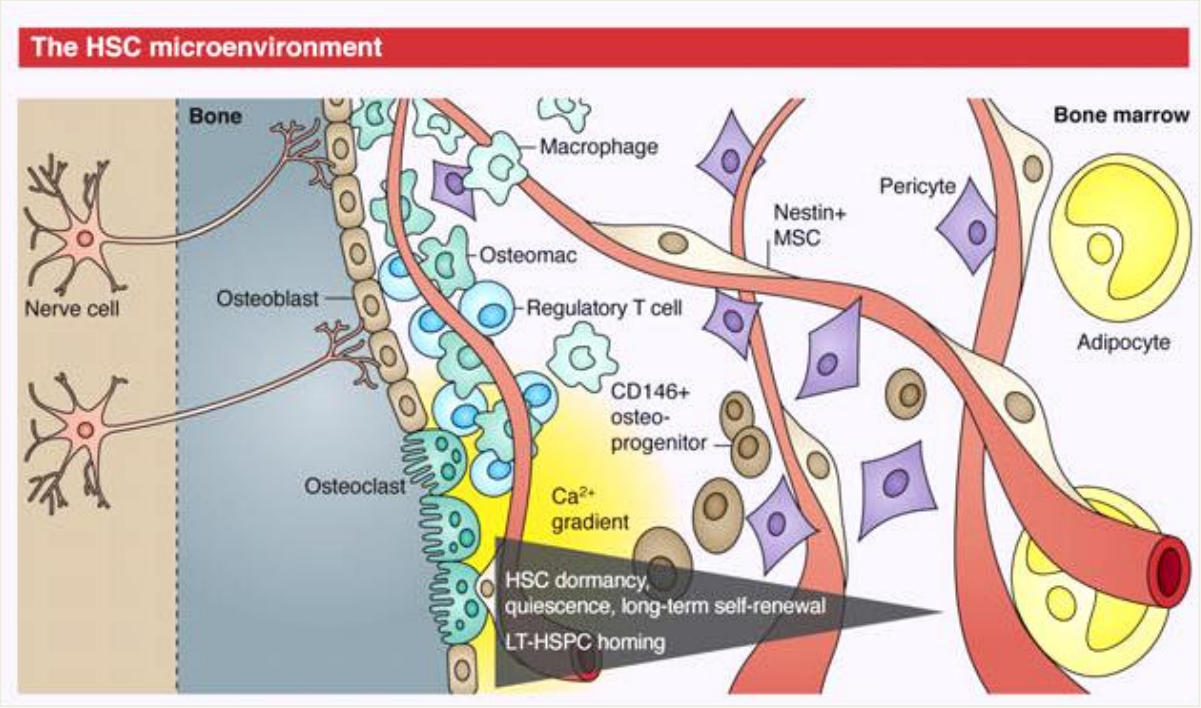

Figure 1.7. A model of the bone marrow niche.
An recent view of the bone marrow niche mainly containing the endosteal niche built by osteoblasts, osteoclasts and osteoprogenitors ($CD146^+$ osteoprogenitor), and $Nestin^+$ mesenchymal stem cells ($Nestin^+$MSCs) and pericytes lining the sinusoids (the vascular niche). Other recently identified HS/PC regulators, autonomous nervous system, bone marrow macrophages (osteomac), regulatory T cells and adipocytes are also shown. Calcium is the main chemical element that has been studied in the niche as well shown in the figure. The figure is taken from Lo Celso and Scadden (95). Republished with permission of The Company of Biologists Ltd. from The haematopoietic stem cell niche at a glance, Lo Celso C, Scadden DT, J Cell Sci 124: 3529-35, and 2011 of copyright; permission conveyed through Copyright Clearance Center, Inc.

1.5.2. Molecular regulators between the niche and HS/PCs

A number of factors have been identified on niche cells that generate signals for HS/PCs that direct their cell fate (95, 121) which have been summarised by Lo Celso and Scadden (Figure 1.8; (95)) and in Table 1.1. It has been reported that a soluble calcium ion gradient spreads out from the endosteal surface (97). Deletion of the calcium sensing receptor (CASR) on HS/PCs resulted in a defect in the ability of HS/PCs to reside in the endosteal niche, suggesting its function is involved inretaining HS/PCs in the niche (122).

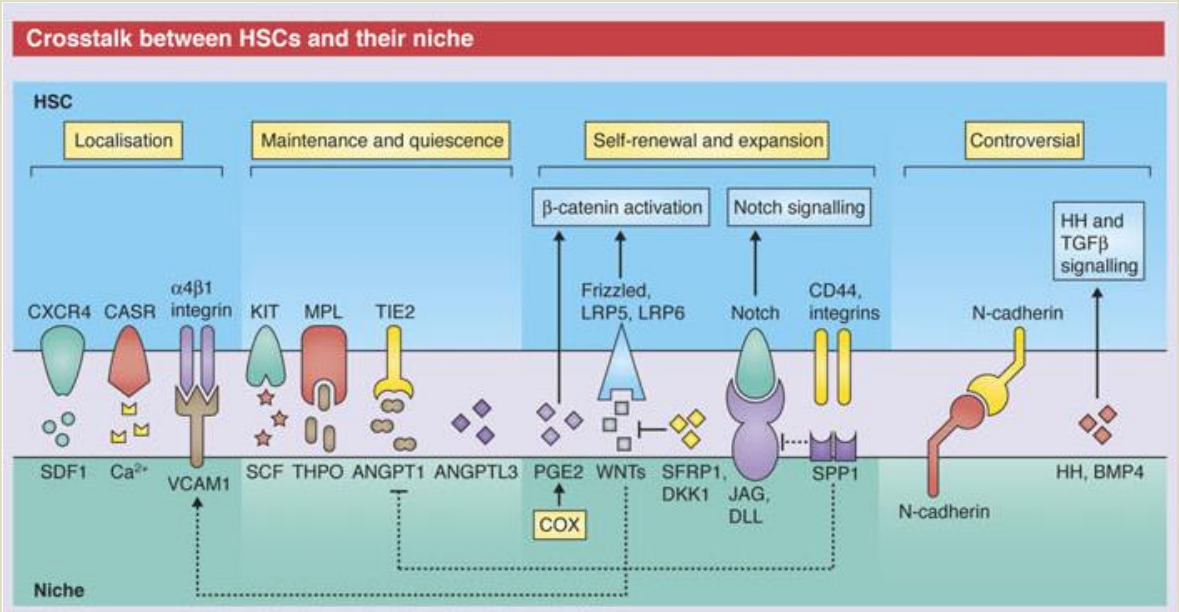

Figure 1.8. A summary of the interaction between HSCs and their niche.
The figure depicts an updated view of potential crosstalk between HSCs and their niche in the bone marrow. The blue panel on the top indicates the molecules that are expressed on HSC and their interacting partners on niche cells are shown in green panel at the bottom. Moreover, the known biological functions by which the interactions of each pair of molecules occur are also highlighted in the yellow boxes at the top. The figure is taken from Lo Celso and Scadden (95). Republished with permission of The Company of Biologists Ltd. from The haematopoietic stem cell niche at a glance, Lo Celso C, Scadden DT, J Cell Sci 124: 3529-35, and 2011 of copyright; permission conveyed through Copyright Clearance Center, Inc.

The CX chemokine ligand 12 (CXCL12) and CX chemokine receptor 4 (CXCR4) axis is the best defined signalling complex in HS/PCs and CXCL12 is expressed on perivascular cells

throughout the bone marrow (114). More recently, two studies by Greenbaum *et al.* and Ding *et al.* demonstrated that CXCL12 is expressed not only on perivascular cells but on other niche cell types (123, 124). Greenbaum *et al.* observed the majority of CXCL12 expression by CXCL12 adventitial reticular cells (CAR cells) and a minority by mature osteoblasts and endothelial cells (123). Ding *et al.* showed that the highest CXCL12 expression occurred in perivascular mesenchymal stromal cells, followed by endothelial cells, osteoblasts and haematopoietic cells in a decreasing order (124). Conditional deletion of *Cxcl12* in various niche cells in murine models caused differential depletion of HS/PCs subsets. Greenbaum *et al.* concluded that the osteoblastic niche, including CAR cells and osteoblasts, support lymphoid progenitor and HPCs maintenance while endothelial niche, consisting of endothelial cells and specific mesenchymal progenitors, supported HSCs in the bone marrow (123). Ding *et al.* on the other hand, suggested that osteoblastic niche supports lymphoid progenitors, while endothelial niche regulates HS/PC maintenance in the bone marrow (124). In addition, Calvi *et al.* showed that constitutively activated jagged 1 by osteoblasts increased the frequency of HS/PCs in mice (90). Although Duncan *et al.* showed that Notch signalling was required to maintain the HSC pool after birth (125), this function remains controversial as it could not be confirmed in other *in vivo* studies reviewed in (95, 150). Bone morphogenetic protein (BMP) signalling pathways regulate HS/PC numbers through intrinsically activated hedgehog signalling (89, 126) or through cross-talk with stromal cells in the niche (127). Wnt signalling is another interesting regulator of HS/PCs. Studies that overexpressed WNT negative regulators, such as DKK1 (dickkopf homolog 1) or WIF (WNT inhibitor factor 1), led to impairment of HSC self-renewal (128, 129).

Likewise, knocking out another the WNT negative regulator, SERP1 (secreted frizzled-related protein 1), or a WNT synergetic transcription factor, EBF2 (early B-cell factor 2), resulted in

impaired HSC homeostasis (130) and HPC maintenance (131). Osteopontin (OPN) is another main regulator enriched in the endosteal niche, which negatively regulates HS/PC numbers and their cell sensitivity to stimuli in the microenvironment (98, 99). Angiopoietin 1 and its Tie2 receptor have been identified in the endosteal niche (102), while angiopoietin-like proteins have also been identified in the vascular niche and these support HS/PC survival and *ex vivo* expansion (132, 133). A model proposed by Kobayashi *et al.* have suggested that stress in the bone marrow can activate BMECs which in turn modulates the balance of HS/PC self-renewal and differentiation through angiocrine factors secreted by Akt-activated BMECs (151). Other signalling pathways, such as via the myeloproliferative leukaemia virus oncogene (Mpl) receptor and thrombopoietin (TPO) (134), c-kit receptor and stem cell factor (SCF) (113, 135, 136), and Insulin-like growth factor 1 (IGF-1) (137) are thought to be involved in the interactions between niche cells and HS/PCs.

Table 1.1. Molecular pathways implicated in HSC-niche interactions.

Secreted factors and receptors	
	Calcium censing receptor (CASR)-calsium (122)
	CX chemokine receptor 4 (CXCR4)- CX chemokine ligand 12 (CXCL12) interactions (114, 123, 124)
	Parathyroid hormone (PTH) signalling (90)
	Notch signalling (90, 125)
	Bone morphogentic protein (BMP) signalling (89, 126, 127)
	Hedgehog signalling (126)
	Canonical Wnt signalling (128-131)
	Osteopontin (OPN) (98, 99)
	Angiopoietin and angiopoietin-like proteins (102, 132, 133)
	Myeloproliferative leukaemia virus oncogene (Mpl) receptor and thrombopoietin (TPO) (134)
	c-Kit receptor and stem cell factor (SCF) (113, 135, 136)
	Insulin-like growth factor 1 (IGF-1) (137)
Adhesion related molecules	
	Integrin interactions: Integrin $\alpha 4\beta 1$ (Very late antigen-4,VLA-4) (138, 139), Integrin $\alpha 5\beta 1$ (Very late antigen-5,VLA-5) (140)
	CD44 and hyaluronan (141, 142)
	E-selectin ligand (ESL) and E-selectin (112)
	N-cadherin (89, 143, 144)
	Cdc42 and Rac proteins (145-147)
	Junctional adhesion molecules: JAM-B and JAM-C (148), ESAM (149)

The table is modified from Lane *et al.* who summarised the published signalling pathways that regulate HSC functions by niche cells in 2009 (121). The table is extended with more candidates and relevant references are included based on current reviews and more recent findings.

The interaction between HS/PCs and niche cells through adhesion molecules is of interest. Two integrins are particularly well studied. These are integrin $\alpha4\beta1$, also called Very late antigen-4 (VLA-4), which mediates HS/PC retention in the bone marrow niche by binding to fibronectin (138) or vascular cell adhesion molecule-1 (VCAM-1) on bone marrow endothelium (139). Integrin $\alpha5\beta1$, also known as Very late antigen-5 (VLA-5), also mediates HS/PC adhesion to fibronectin in the bone marrow. These integrins correlate with CXCL12-dependent functions (140). Other integrins including integrin $\alpha1\beta1$, $\alpha2$, $\beta1$ and $\beta7$ have been proposed to take part in HSC homeostasis as reviewed in (95). CD44 and its binding partner, hyaluronan, mediate the homing to and engraftment in the bone marrow of both HS/PCs and their malignant counterparts (141, 142). Additionally, E-selectin in the bone marrow vascular niche has been found to not only mediate HS/PC attachment to the niche, but also regulate HS/PC homeostasis in response to chemotherapy or irradiation (112). The role of N-cadherin in HS/PC regulation by the niche is controversial (89, 143, 144). Previous studies have shown that GTPases, such as Cdc42 and Rac proteins, regulate HS/PC mobilisation and adhesion (145). Recent findings suggest that loss of Cdc42 in aging HSCs results in impairment of HSC polarity and consequently a loss of the HSCs in the bone marrow (146, 147). The junctional adhesion molecule (JAM) family is another subset of candidates of interest and the studies related to these molecules have largely been done while this thesis work was being conducted. JAM-A is now known to be expressed on murine long-term repopulating HSCs (152). The interaction of JAM-B and JAM-C regulates HS/PC maintenance in the bone marrow (148). Moreover, JAM-B and JAM-C also regulate CXCL12 secretion by the bone marrow stromal cells (148) and by lymph node cells (153), suggesting another potential role in regulating haematopoiesis. Furthermore, endothelial-cell-selective adhesion molecule (ESAM), a non-classical JAM molecule, recently has been

shown on HS/PCs (154, 155), and its homophilic interaction between HS/PCs and the niche contributes to a balance in HS/PC homeostasis (149). The details about JAM family are in section 1.9.

1.5.3. Leukaemic initiating (LIC) or stem cell (LSC) niche

It has been proposed that cancer cells are able to take the advantages of the signals provided by the surrounding cells to support their survival and proliferation. Solid evidence by Ninomiya *et al.* demonstrated that transplanted human leukaemic cells, like normal HS/PCs, homed to the BM and initially localised on the endosteum in the epiphysis region of the bone and subsequently expanded to the inner vascular and diaphysis of the bone (156). The cells mainly proliferated in epiphysis of the bone. After treatment with Ara-C, the residual leukaemic cells adhered to endothelium and endosteum, suggesting anti-apoptotic signals are provided from both osteoblasts and endothelium (156). Colmone *et al.* and Sipkins *et al.* using dynamic *in vivo* confocal imaging illustrated that leukaemic cells not only engrafted into CXCL12-abundant niches, but also created their own niches in bone marrow in a delayed manner, and these also recruited transplanted normal $CD34^+$ cells to the tumour blasts (157, 158). Three pairs of interaction between normal HS/PCs and niche cells, CXCR4-CXCL12, VLA-4 and VCAM-1, and CD44 and hyaluronan, have been well studied in the relationship between leukaemic cells and niches (reviewed in (159)). Osteopontin, WNT signalling and a number of angiogenic factors, including basic fibroblast growth factor (bFGF), insulin-like growth factor (IGF), interleukin-6 (IL-6) and vascular endothelial growth factor (VEGF), are involved in the crosstalk as well (159). Additionally, the hypoxic conditions throughout the bone marrow are unique for leukaemia. It has been proposed that leukaemic cells are able to adapt to this condition to support their survival. Hypoxia-

inducible transcription factor 1 alpha (HIF-1α) expression was observed in leukaemic cell clusters from the bone marrow (160) and correlates to poor survival in leukaemia (161). It is also worth noting that CXCR4, CXCL12 and VEGF are upregulated by HIF-1 α in leukaemic cells under hypoxic condition, and this may highlight the importance of these molecules in the crosstalk of leukaemic cells and their niche (reviewed in (159)). Indeed, Colmone *et al.* found that LICs hijacked the normal niche in the bone marrow and created a CXCL12-rich niche which affected the homing of transplanted normal $CD34^+$ cells (157). Currently anti-CXCR4 and anti-CD44 are being used in clinical trials for AML (reviewed in (162)). Targeting LICs though blocking these and other molecular interactions in the niche may therefore provide insights into new therapies for leukaemia (162, 163).

1.6. Cell-cell Contact in the Bone Marrow Vascular Niche

Gold *et al.* demonstrated that the expression of different adhesion receptors correlated with haematopoietic reconstitution after transplantation, suggesting that different cell-cell contacts in the niche may direct HS/PC fates (21). In their study, they showed increasing expression of ICAM-1 and a number of integrins, namely integrin α2, α3, α4, α6, and β1, positively correlated with shorter time to platelet recovery. In addition, increasing integrin αL and P-Selectin receptor expression contributed to neutrophil recovery. Robinson *et al.* further showed that human UCB $CD34^+$ HS/PCs were poorly fucosylated and that fucosylation of these cells most likely of PSGL-1 enhanced human HS/PC engraftment in immunodeficient mice (20). Interestingly, CD44 enhanced red blood cell recovery (21). Over the last decade, a number of secreted factors or cytokines have been identified in bone marrow niche cells and these regulate HS/PC quiescence, self-renewal, proliferation or differentiation. However, studies on direct contact between niche cells and HS/PC are

comparatively fewer. More evidence nowadays emphasises the importance of the direct contact as many of the secreted factors appear to function at close range. Hence, direct contact retains stem cells in the niche, where they can respond. Previously the major body of studies on the cell-cell contact in the BM focused on interactions with bone marrow derived MSCs (164-169) and only a few drew attention to the interactions with endothelium (170, 171). Prevention of direct contact between HS/PCs and stromal cells resulted in an increase in HS/PC proliferation (as reviewed in (172)). This is still debated as some studies show integrin-mediated interactions inhibit progenitor cell proliferation and others have proposed that integrin engagement prevents $CD34^+$ cell apoptosis (as reviewed in (172)).

Endothelium also regulates the biological functions of HS/PC. Cheng *et al.* showed that direct contact with human brain endothelium supports HS/PC *ex vivo* expansion through Wnt signalling (171). However, differential effects on HSC by endothelium were observed when co-cultured with various types of endothelial cells. Li *et al.* observed that co-culture with brain, liver and heart endothelial cells preferentially supported transplanted HS/PC maintenance in the BM compared to those from kidney and lung (173). In 2005, Kiel *et al.* showed that $CD150^+$ HSCs localised near sinusoids in the bone marrow, indicating the existence of a vascular niche (174). This raised attention to the importance of bone marrow endothelial cells (BMECs), which are functionally and phenotypically distinct from other types of endothelium (108). Rafii's group (175) and van der Schoot's group (176) were amongst the first to investigate the role of bone marrow endothelial cells in regulating HS/PC fate. Rafii *et al.* demonstrated that bone marrow endothelium could support the proliferation and differentiation of myeloid progenitors, and megakaryopoiesis in particular, yet the detailed mechanism was unclear (170). In order to set up an *in vitro* model for study, they generated stable cell lines from human primary BMECs using different strategies.

Candal *et al.* immortalised their isolated BMECs by transfection with large T antigen of SV40 (177), and Rood *et al.* introduced human papilloma virus 16 E6/E7 DNA into their BMEC line (178). However, both groups found that resting BMEC lines only express weak E-selectin and VCAM-1, which are normally constitutively expressed by primary BMECs (177, 178). The expression of these adhesion molecules can be overcome by interleukin-1 beta (IL-1β) or tumour necrosis factor-alpha (TNF-α) stimulation, whereas long-term *in vitro* culture requiring additional cytokines or serum gradually resulted in the loss of their angiogenic potential (179). Rafii's group showed that the transformed BMEC lines support *ex vivo* HS/PC expansion (180) and haematopoietic cell transendothelial migration towards CXCL12 (181, 182), the latter in an E-Selectin-dependent manner (183). As indicated above, Winkler *et al.* also described a role for E-selectin on endothelial cells of the vascular niche, indicating that E-selectin is a regulator of HS/PC proliferation and chemoresistance (112).

1.7. Haematopoietic Stem/Progenitor Cell (HS/PC) Homing

HS/PC homing is a multi-step process where cells pass from the circulation into the bone marrow via sinusoidal endothelial cells. A model of transendothelial migration was proposed in 1994 showing how circulating cells adhere onto the endothelial cells and then transmigrate across the vessel wall into the tissue (184, 185). In principle, the cells in the circulation first attach to and roll on the endothelial cells primarily by interactions between selectins and their ligands. P-selectin and L-selectin are both involved. This leads to the cell motility slowing down and provides increased opportunities for them to sense local chemoattractants. Following stimulation by the chemoattractants, principally CXCL12, a number of membrane proteins, and in particular the integrin VLA-4, are activated on both cell types and this contributes to firm interaction between the rolling HS/PCs and sinusoidal

endothelial cells. The rolling cells arrest and firmly adhere onto the endothelium. Subsequently, the cells crawl on the endothelium in response to the gradient of chemokines on the luminal face of endothelium in a similar manner to that depicted in Figure 1.9 and in order to find preferential sites for transmigration (184, 185). To date, two methods of

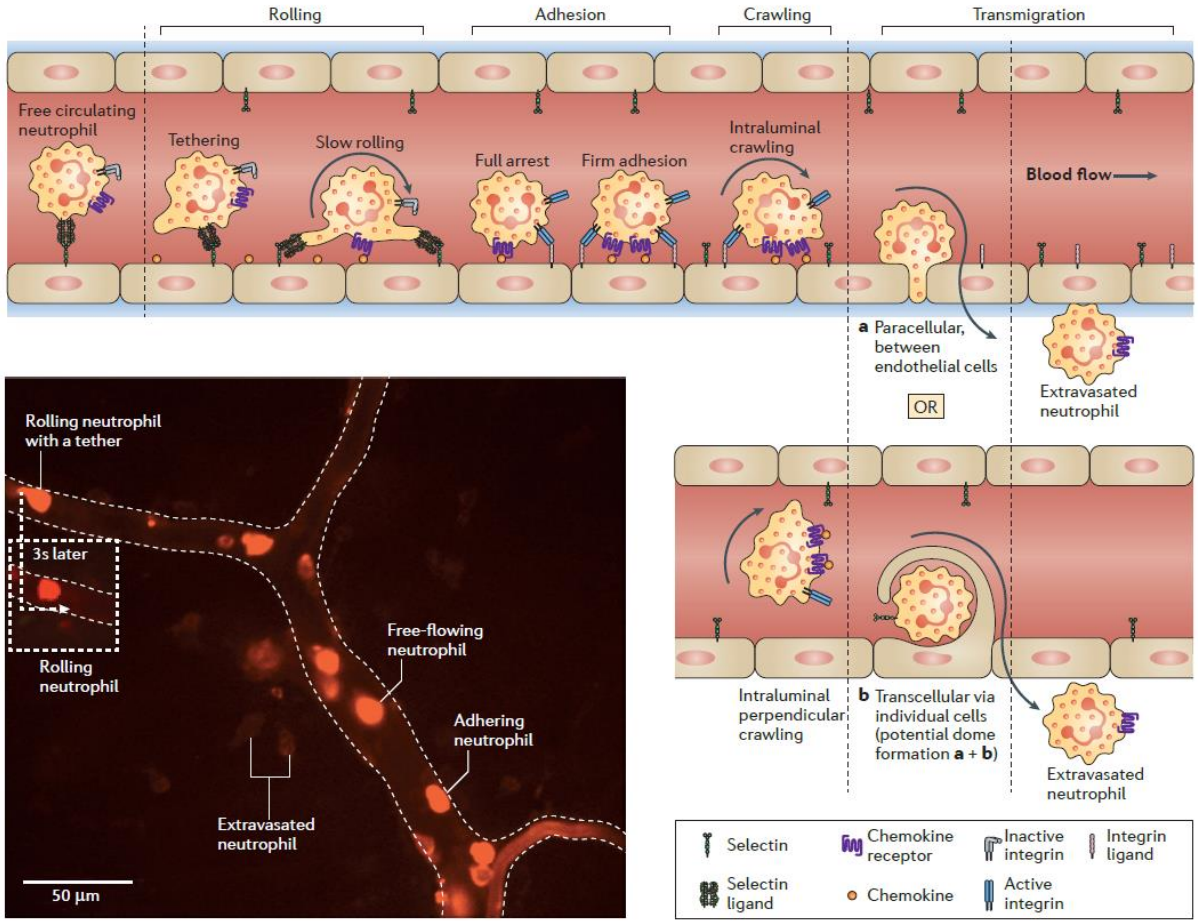

Figure 1.9. The multi-step model of transendothelial migration.
The PE-conjugated antibody against LY6G$^+$ neutrophils represents the current understanding of transendothelial migration from the blood stream to the tissue, which has also been applied to HS/PCs. The figure on the top shows a series of steps where circulating cells first contact the endothelial cells. These include a rolling step, when the cells tether and slowly roll, followed by adhesion which results in cell arrest and firm adhesion, and intraluminal crawling before transmigration. Two possible methods of transmigration have been proposed: (a) paracellular transmigration, when the cells pass between endothelial cells; and (b) transcellular transmigration, when the cells pass through endothelial cells. Rolling is mainly selectin-mediated, whereas adhesion, crawling and transmigration depend on integrin interactions. The model suggests that chemokines or factors lining the luminal surface of the endothelium activate cell rolling and then the integrins by changing their conformation on the circulating cells. By doing this, it allows subsequent events to happen. Crawling cells may follow the gradient of the chemokines on the endothelium to find the preferential site for transmigration. An intravital microscopy image shows a skin capillary with PE-conjugated LY6G$^+$ neutrophils (red) that were induced to migrate. Different stages of migration are indicated in the image. The figure is taken from Kolaczkowaska *et al.* (186). Abbreviations: PE, phycoerythrin. Reprinted by permission from Macmillan Publishers Ltd: Nature Reviews Immunology (186), Copyright (2013).

transmigration have been demonstrated, paracellular migration where the cells pass between the endothelial cells and transcellular migration where the cells pass through the endothelial cells (reviewed in (186); Figure 1.9).

Regarding the transendothelial migration that occurs in HS/PC homing, a few cellular compartments have been identified as being involved in different steps of this process. A chemotactic cytokine, CXCL12, also known as SDF-1 (stromal cell-derived factor-1), is the main signal for $CXCR4^+$ HS/PC homing. CXCL12 is presented on the lumen of the bone marrow endothelial cells (BMECs) (187) by proteoglycans on the BMECs (188). This CXCL12 presentation on BMECs causes CXCR4 polarisation on $CXCR4^+$ cells, which is an initial step for cell transmigration (Figure 1.9) (189). In the transmigration that follows, $\beta1$ and $\beta2$ integrins and the addressin CD44 on HS/PCs are responsible for their interactions with specific extracellular matrix molecules such as fibronectin and hyaluronic acid, while adhesion receptors expressed on endothelial cells, such as vascular cell adhesion molecule-1 (VCAM-1), play a role. Other immunoglobulin-like proteins, CD31 and junctional adhesion molecules (JAMs) for example, and the sialomucin, CD164, have been also identified to play a part in this process (reviewed in (172)). CD31 in particular is likely to be involved in the transmigration of HS/PCs between endothelium (190), while CD164 enhances CXCR4 responses (140) and also acts as an adhesion molecule for HS/PC adhesion to BM MSCs.

Interestingly, malfunction of these adhesion molecules is witnessed on leukaemia. Take for example. $\alpha4\beta1$ integrin (also known as vary-late antigen (VLA)-4) and $\alpha5\beta1$ integrin (also known as VLA-5), which are present in chronic myelogenous leukaemic (CML) cells. However, their cell adhesion capacity is less than their normal counterparts and, as CML progresses, this loss of capacity provides a possible explanation for a massive expansion of CML cells in the bone marrow and premature release of immature leukaemic cells into the circulation

(172). Furthermore, higher functional VLA-4 expression in acute myeloid leukaemia (AML) cells correlates with better survival (191).

1.8. The CXCR4 and CXCL12 Axis

1.8.1. CXCL12 and its cognate receptors in haematopoiesis

CXCL12, also known as SDF-1 (stromal cell-derived factor-1) (192), is a chemotactic cytokine, which is 8-14 kD in size and contains four conserved cysteine residues (193). CXCL12 was initially found to be secreted by bone marrow mesenchymal stromal cells and this was shown to promote B-cell progenitor proliferation and growth (194). Not exclusively produced by bone marrow mesenchymal stromal cells (114), CXCL12 is also expressed by other bone marrow niche cells, such as endothelial cells (187, 195, 196), adventitial reticular cells (114) and osteoblasts (197) as reviewed in (198). As described earlier, two independent groups selectively deleted *Cxcl12* from various bone marrow niche cells and showed different effects on HS/PCs in these conditional knockout mice. Ding and Morrison observed that deletion of *Cxcl12* from endothelial cells caused a depletion of HSCs but not myelo-erythroid or lymphoid progenitors, whereas deletion from osteoblasts resulted in partial depletion of lymphoid progenitors but not the other two cell subsets, suggesting two distinct niches occupied by HSCs and lymphoid progenitors (124). Greenbaum *et al.*, however, found a modest loss of long-term repopulating activity caused by *Cxcl12* deletion from endothelial cells, and no effect on HSCs or lymphoid progenitors in its deletion from osteoblasts (123). Apart from the regulation on HS/PC development, previous studies on CXCL12 have illustrated its chemoattractic effect on human mononuclear cells (199) and HS/PCs (200). Moreover, CXCL12 also increases HS/PC adhesion to numerous extracellular matrices, and adhesion molecules through activating integrins (as reviewed in (201)). Two

receptors have been characterised that bind CXCL12, CXCR4 (199) and CXCR7/RDC1 (202) (Table 1.2). Initial studies on CXCR4 focused on its role in the pathogenesis of HIV infection. This finding revealed that CXCR4 serves as a co-receptor for T-tropic (X4) HIV viruses to enter into $CD4^+$ T cells (203). The CXCR4 and CXCL12 axis is widely believed to be a crucial regulator of haematopoietic stem/progenitor cells (HS/PCs) and leukaemic stem-like cells (LSCs) homing and engraftment in the bone marrow. Bone marrow mesenchymal stromal cell highly express CXCL12 and this acts to retain $CXCR4^+$ HS/PCs in the bone marrow. By disrupting the interaction of CXCL12 and CXCR4, the retaining force is lost and this caused HS/PC mobilisation (204). More evidence illustrated reduced HS/PCs number in the bone marrow of CXCR4 deficient mice (114). In addition, both *cxcl12* or *cxcr4* knockout mice show impaired haematopoietic precursor cell migration to the bone marrow during embryonic development, suggesting an important role of CXCL12/CXCR4 axis in the homing of HS/PCs to the bone marrow (205-207). Previous findings in our laboratory indicated that CD164 (endolyn) is a co-receptor of CXCR4 on human umbilical cord blood (UCB) $CD133^+$ cells. CD164 in this manner co-regulates CXCR4-dependent cell migration (140, 208) and cell adhesion (188).

CXCR7 is a relatively newly identified CXCL12 receptor. It shows greater binding affinity to CXCL12 than to its other ligand CXCL11. In addition, the interaction of CXCL12 with CXCR7 is stronger than that with CXCR4, while this binding affinity can compete by CXCR4 expression on the membrane. CXCR7 expression is tightly regulated in various types of circulating cells (reviewed in (209)). Lymphocytes and granulocytes from the bone marrow and peripheral blood express CXCR7, yet those from the umbilical cord blood fail to express this receptor (210). Moreover, CXCR7 expression on HS/PCs is not observed (210, 211), but the expression was observed in their malignant counterparts (210).

Table 1.2. Chemokine and chemokine receptor binding affinities.

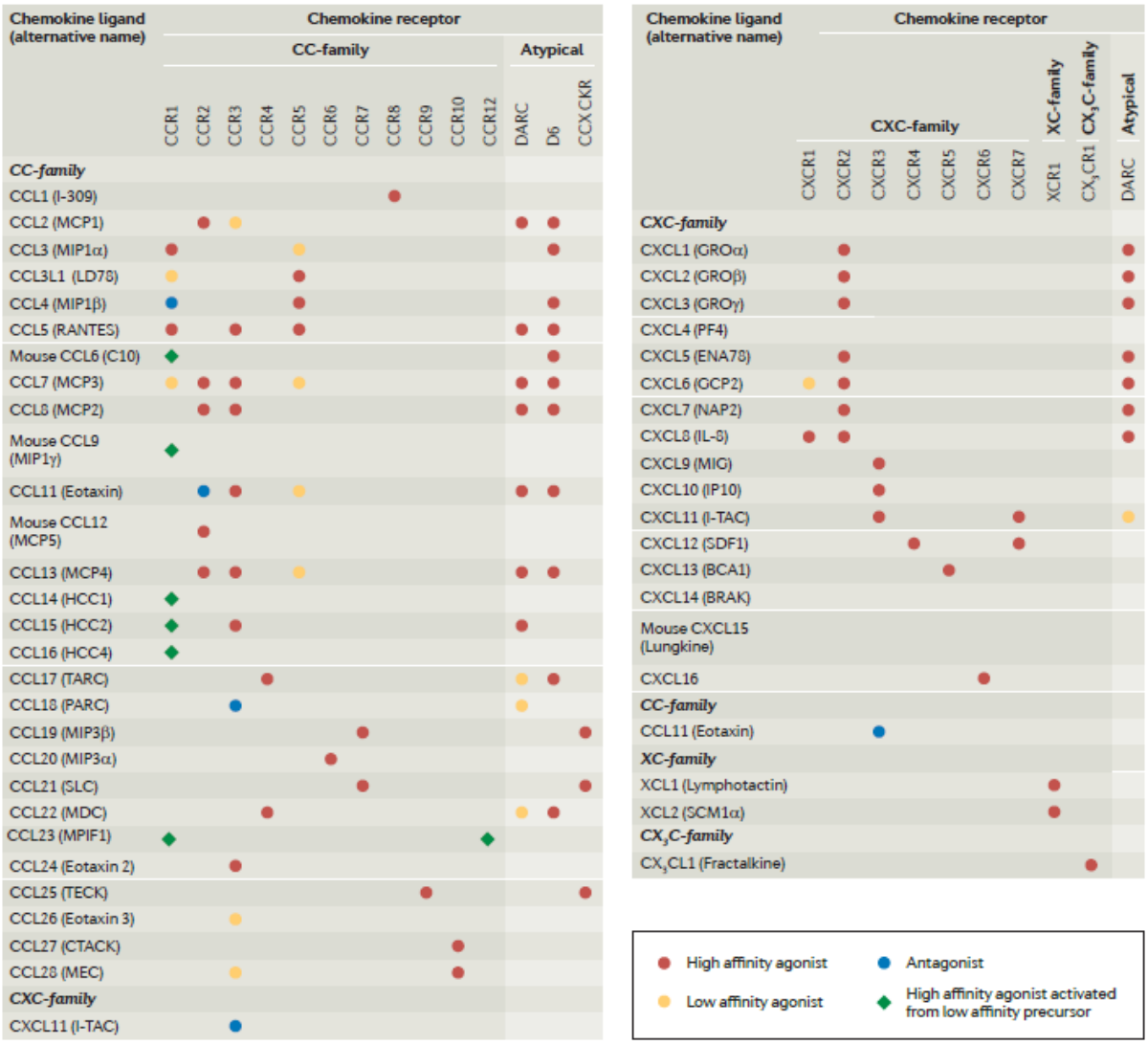

The table summarises known interactions between chemokines and their receptors, which were assessed by their potential downstream cellular effects, such as migration, signal induction and binding analyses in several studies. Chemokine receptors are listed at the top and 'Atypical' receptors are those that are only known to bind chemokine ligands but their downstream signalling pathways are not well defined. Chemokines are listed in the systematic nomenclature with one of the most common synonyms for each chemokine. Ligand affinities for the same receptor can vary and these are indicated in different colours. High affinity ligands (red): the dissociation constants range from the picomolar to the low nanomolar range; Low affinity ligands (yellow) range over several hundred nanomolar concentrations. Several ligands need to be activated by proteolysis before they can bind to a receptor (green); and some chemokine ligands bind but function as receptor antagonists (blue). The table is taken from Schall *et al.* (212). Reprinted by permission from Macmillan Publishers Ltd: Nature Reviews Immunology (212), Copyright (2011).

1.8.2. The CXCL12 and CXCR4 signalling cascade

It has been suggested that the CXCR4 and CXCL12 axis through various signalling pathways can support HS/PC or tumour cell proliferation, survival, cytokine production, chemotaxis and adhesion (213). CXCR4 is a 7 transmembrane G-protein coupled receptor (Figure 1.10).

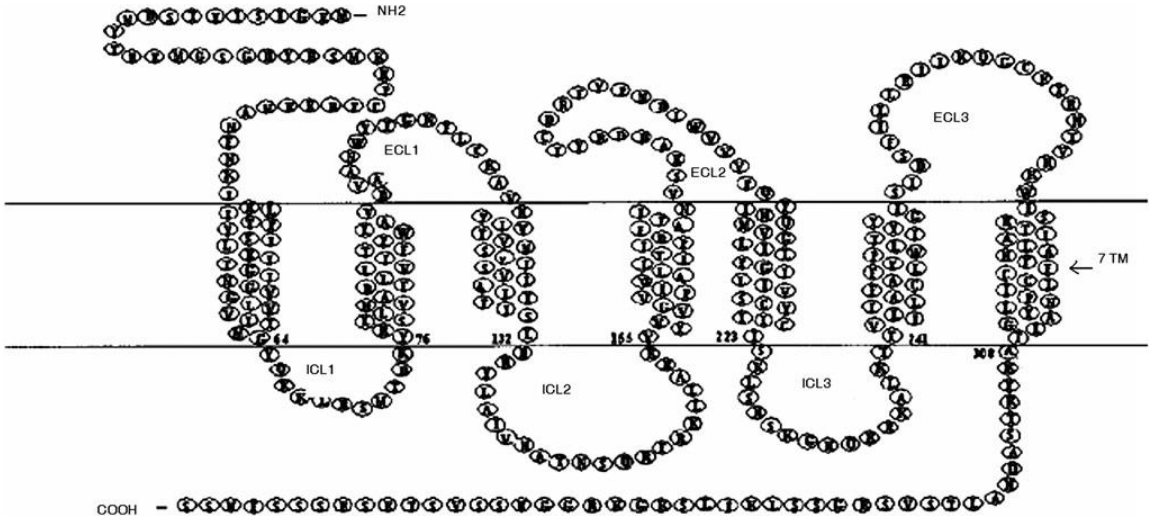

Figure 1.10. CXCR4 structure.
CXCR4 is a transmembrane protein with 3 extracellular loops (ECL), 7 transmembrane domains, and 3 intracytoplasmic loops (ICLs) along with extracellular N and intracellular C terminals. The figure is taken from Sharma *et. al* (214). Reprinted with permission from STEM CELLS & DEVELOPMENT, Volume 20, published by Mary Ann Liebert, Inc., New Rochelle, NY.

Its extracellular domain allows chemokine binding, such as CXCL12, and is dependent on the secondary intracytoplasmic loop structure where the interacting G-protein lodges. The G-protein contains three subunits, the Gα, Gβ and Gγ proteins. When CXCL12 binds to its receptor, it releases the Gα protein in order to activate the downstream kinases, PI3K for example, while Gβ and Gγ proteins form a dimer which activates different signalling cascades, including the Ras/MAPK and PKC pathways (Figure 1.11) (214). It has been proposed that the CXCL12/CXCR4 axis may also modulate leukaemic cell egress from the

bone marrow into the peripheral blood as peripheral blood (PB) $CD34^+$ cells and leukaemic cells were able to transmigrate towards CXCL12 *in vitro* (215) and towards the conditioned medium from MS-5, a mouse cxcl12-producing stromal cell line (216). CXCR4 expression levels on the acute myeloid leukaemia cell surface positively correlated with their cell mobility. On the other hand, CXCR4 may also be highly expressed on acute lymphoid leukaemia (ALL) cells, yet the correlation between CXCR4 expression and ALL cell mobility

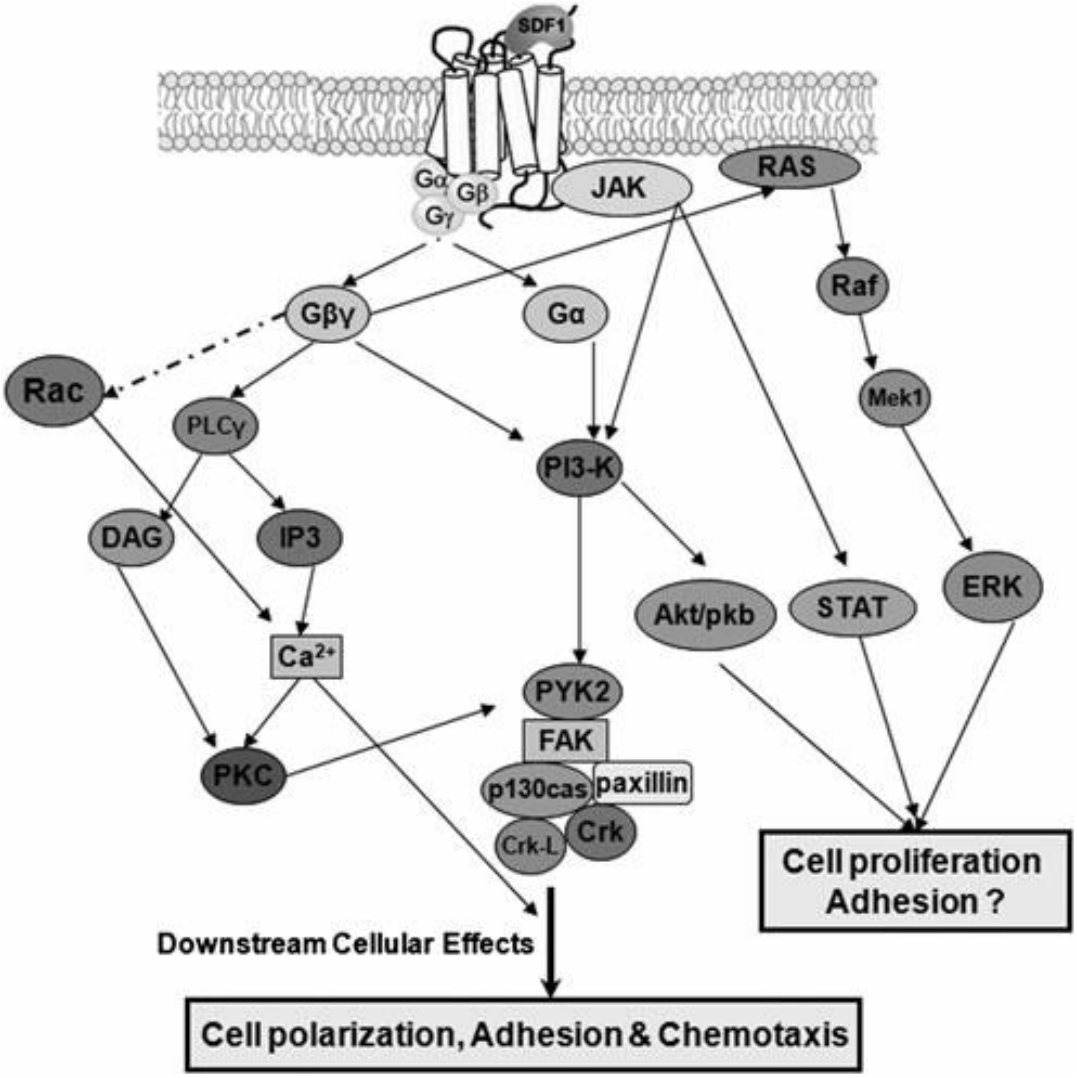

Figure 1.11. Downstream signalling cascade and cellular effects from CXCR4 binding to CXCL12.
In this cascade, CXCL12 binding to CXCR4 triggers the Gα-protein-dependent PI3K/Akt pathway, Gβγ-protein-dependent Ras/MAPK, PKC pathways and a Gi-protein-independent JAK/STAT pathway. The downstream cellular effects included cell polarisation, adhesion, chemotaxis and cell proliferation. The figure is taken from Sharma *et. al* (214). Reprinted with permission from STEM CELLS & DEVELOPMENT, Volume 20, published by Mary Ann Liebert, Inc., New Rochelle, NY.

was inconclusive (217). Therefore, it has been suggested that CXCR4 internalisation is important rather than their surface expression (216, 218). Alternatively, CXCR4 expression may not reflect the function of the CXCR4 molecule in transmitting signals.

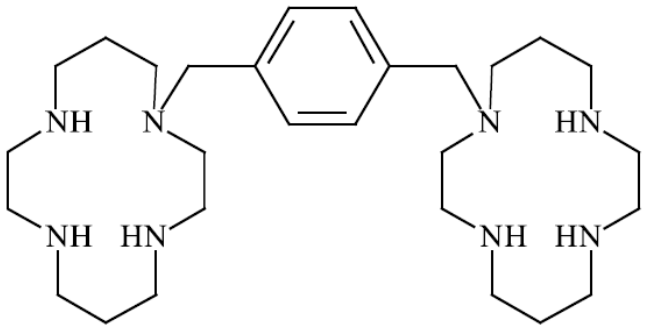

Figure 1.12. Chemical structure of AMD3100.
Chemical structure of the bicyclam AMD3100 (1, 1P-[1,4-phenylenebis (methylene)]-bis-1,4,8,11-azatetra decane). The figure is taken from Hatse *et al.* (219). Reprinted from FEBS Letters 527, Hatse S, Princen K, Bridger G, De Clercq E, Schols D, Chemokine receptor inhibition by AMD3100 is strictly confined to CXCR4, 255-62, Copyright (2002) with permission from Elsevier.

AMD3100 (Figure 1.12) was initially developed as an anti-HIV drug and it was shown to directly bind to CXCR4, a co-receptor for HIV entry and infection. AMD3100 inhibits HIV binding to cells at a 10 nM concentration but shows no toxicity to the host cells up to a concentration of 500 μM. However, an unexpected side effect was observed when AMD3100 was first used in clinical trials. This was a rapid increase of white blood cell count in the peripheral blood at 6 hours post AMD3100 infusion into patients ((220) and reviewed in (221)). With further analysis, the majority of cells mobilised by AMD3100 appeared to in carry the CD34 marker, suggesting that AMD3100 serves as a mobiliser for HS/PCs from the bone marrow into the circulation ((222) and reviewed in (221)). Currently, AMD3100 (Mozobil™) is used in combination with granulocyte colony-stimulating factor (G-CSF) for mobilising HS/PCs into the peripheral blood of patients as a source of cells for autologous transplantation where these patients are refractory to G-CSF mobilisation reviewed by De Clercq (223). Interestingly, AMD3100 not only binds to CXCR4 but also to CXCR7, while it

appears to have opposite effects on the two receptors (224). This may raise concerns pharmacology when using this compound as a tool to dissect CXCL12 biological functions *in vivo* particularly if the receptors are expressed on the same cell type (224). AMD3100 is also being used in acute leukaemic patients to prevent the adhesion of AML cells to the niche and thus to make the AML cells more susceptible to chemotherapeutic agents (225) as well as in some other haematological malignancies (226). Timelines for these developments are shown in Figure 1.13.

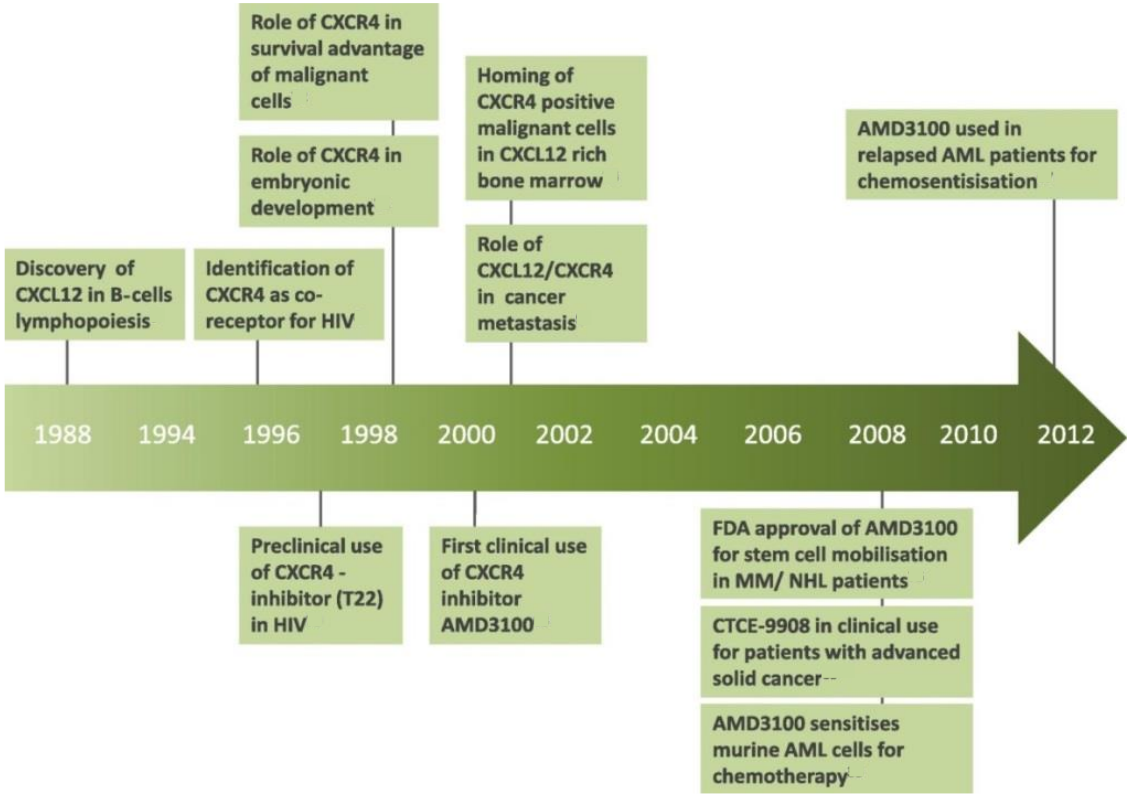

Figure 1.13. A timeline summarising important studies on chemokine receptor 4 (CXCR4) and chemokine ligand (CXCL12) in oncology.
CXCL12 was firstly found to regulate B-cell development (205) prior to its receptor, CXCR4, being identified. CXCR4 was also found to act as a cofactor for HIV infection in T cells (203). A study using the CXCR4 inhibitor (T22) as a therapy for HIV infection soon followed (227). The role of CXCR4 in haematopoiesis development (207) and in malignant cells were established (228). AMD3100 was next used in clinical trials in human volunteers (220). Two studies illustrated that CXCL12/CXCR4 played a role in the engraftment of circulating malignant haematological cells (226) and in solid tumour cell metastasis (229). AMD 3100 was approved to be used in multiple myeloma and non-Hodgkin's lymphoma (MM/NHL) patients, solid tumours or acute myeloid leukaemia (AML) patients. The figure is taken from Domanska *et al.* (221). Reprinted from Eur J Cancer 49, Domanska UM, Kruizinga RC, Nagengast WB, Timmer-Bosscha H, Huls G, de Vries EG, Walenkamp AM, A review on CXCR4/CXCL12 axis in oncology: no place to hide, 219-30, Copyright (2013) with permission from Elsevier.

1.9. The Junctional Adhesion Molecule (JAM) Family

1.9.1. Classification

JAM-A (Junctional Adhesion Molecule-A), known also as the F11 receptor (F11R), was the first identified JAM protein and was found to be expressed on platelets by Naik *et al.* using the F11 antibody (230, 231). Martin-Padura *et al.* later reported Jam proteins in tight junction and showed that these modulated monocyte transendothelial migration in murine models (232). Williams *et al.* from the same group further characterised JAMs in the human and established that human JAM protein was the F11 antigen that Naik *et al.* had described previously (233). To avoid confusion, the nomenclature was revised. To date, there are seven members of the JAM family in mammals, namely JAM-A, JAM-B, JAM-C, the coxsackie virus and adenovirus receptor (CAR), JAML, endothelial cell-selective adhesion molecule-1 (ESAM-1) and JAM-4 (Table 1.3; (234)).

Table 1.3. Summary of JAM family member expression patterns, putative functions and ligands.

Molecule	Expression pattern	Function	Ligands
JAM-A	Epithelial cells, endothelial cells, neutrophils, monocytes, DC, lymphocytes, platelets, hematopoietic progenitors	Leucocyte transmigration, tight junction maintenance, polarization, regulation of DC migration into LNs	JAM-A LFA-1 $\alpha_V\beta_3$
JAM-B	Endothelial cells, fibroblasts, MSC	Leucocytes transmigration, tight junction maintenance,	JAM-C $\alpha_4\beta_1$
JAM-C	Endothelial cells, fibroblasts, epithelial cells, hematopoietic progenitors	Leucocytes transmigration, tight junction maintenance, regulation of naïve T cell homeostasis	JAM-C JAM-B CAR $\alpha_M\beta_2$ $\alpha_X\beta_2$
ESAM-1	Endothelial cells, hematopoietic progenitors	Leucocytes transmigration	ESAM-1
CAR	Epithelial cells, cardiomyocytes	Transepithelial migration of neutrophils, costimulation	JAML JAM-C
JAML	Neutrophils TCRγδ T cells	Transepithelial migration of neutrophils, costimulation	CAR
JAM-4	Epithelial cells, hematopoietic cells	Unknown	Unknown

The table is taken from Arcangeli *et al.* (234). Springer and Archivum Immunologiae et Therapiae Experimentalis 61, 2012, 15-23, Function of Junctional Adhesion Molecules (JAMs) in Leukocyte Migration and Homeostasis, Arcangeli ML, Frontera V, Aurrand-Lions M., Table 1, original copyright notice is given to the publication in which the material was originally published with kind permission from Springer Science and Business Media.

1.9.2. JAM-A expression and structural features

Independent studies have confirmed Jam expression profiles in the murine embryo and in the adult mouse. During embryogenesis, jam-a was expressed in endotherm and ectoderm as early as E8.5 days post-coitum and the expression was continuously significant in epithelial and endothelial regions during organogenesis (235). In human, JAM-A is encoded by 13 exons in the F11R gene (236). There are two isoforms of mRNAs encoded by this gene (236). The type 1 isoform is expressed in endothelium, platelets, white blood cells and several cancer cell lines, whereas the type 2 isoform is limited to endothelium (236). These isoforms have not been shown to be translated into different proteins. JAM-A has been shown to be widely expressed in a variety of cell types, including endothelial cells (232, 233), epithelial cells (232) and most of immune cells, such as neutrophils (233), monocytes (233, 237), platelets (230), dendritic cells (238), lymphocytes (233, 238) and haematopoietic progenitors (152, 239). With the exception of JAML, which has only been observed in neutrophils and T cells (240), other members of the JAM family have been predominantly found on endothelial cells, epithelial cells or fibroblasts. Apart from their expression on endothelial and epithelial cells, JAM-C (148), ESAM-1 (149) and JAM-4 (241) are also expressed on haematopoietic progenitors. By contrast, JAM-B is not expressed on haematopoietic progenitors but on endothelial cells, fibroblasts and mesenchymal stromal cells (MSCs) as reviewed in (234).

JAM protein structure was firstly defined for JAM-A and showed to be an integral membrane protein containing two extracellular Ig-like domains and one intracellular PDZ-binding domain (Figure 1.14; (242)). The outer extracellular domain interacts with another JAM unit and the inner domain can interact with integrins either in cis (the complex formed on the same cell) or trans (between cells). The cytosolic PDZ-binding domain transmits an

outside-in signal after binding to its cognate ligand. It has been shown that JAM proteins play a role not only in cell-cell junction formation, but also mediate cell adhesion and transendothelial migration.

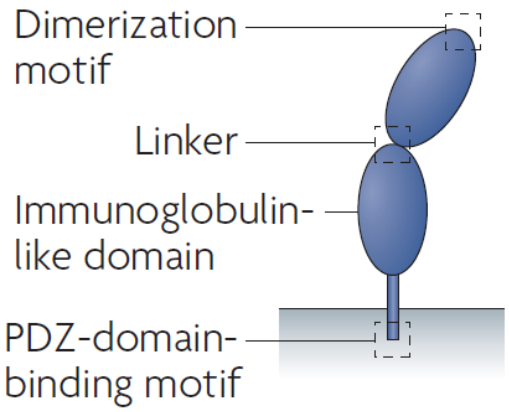

Figure 1.14. The structure of junctional adhesion molecure (JAM).
JAM is a transmembrane protein with 2 immunoglobulin-like (Ig-like) domains (oval shape) in the extracellular membrane region and one PDZ-binding motif in its cytosolic tail. The outer Ig-like domain is mainly used for homodimerisation, and the inner Ig-like domain is for heterodimer formation. The figure is taken from Weber *et al.* (243). Reprinted by permission from Macmillan Publishers Ltd: Nature Reviews Immunology (243), Copyright (2007).

1.9.3. The interactions and the functions of JAM-A on endothelium and epithelium

It has been shown that JAM-A interacts with itself (244) and other integrins, such as LFA-1 ($\alpha L\beta 2$ integrin) (245, 246) and $\alpha v\beta 3$ integrin (247, 248). JAM-A homodimers are predominantly found in tight junctions, but are also observed between platelets or between platelet and endothelium and this promotes platelet aggregation and activation (242). More recently, the interactions observed between platelets or injured vascular endothelium and peripheral blood $CD34^+$ cells suggest that JAM-A may regulate further biological functions (239). So far JAM-A has not been shown to form heterodimers with other JAMs, while JAM-B and JAM-C have been shown to form heterodimers with each other (249, 250) (Figure 1.15).

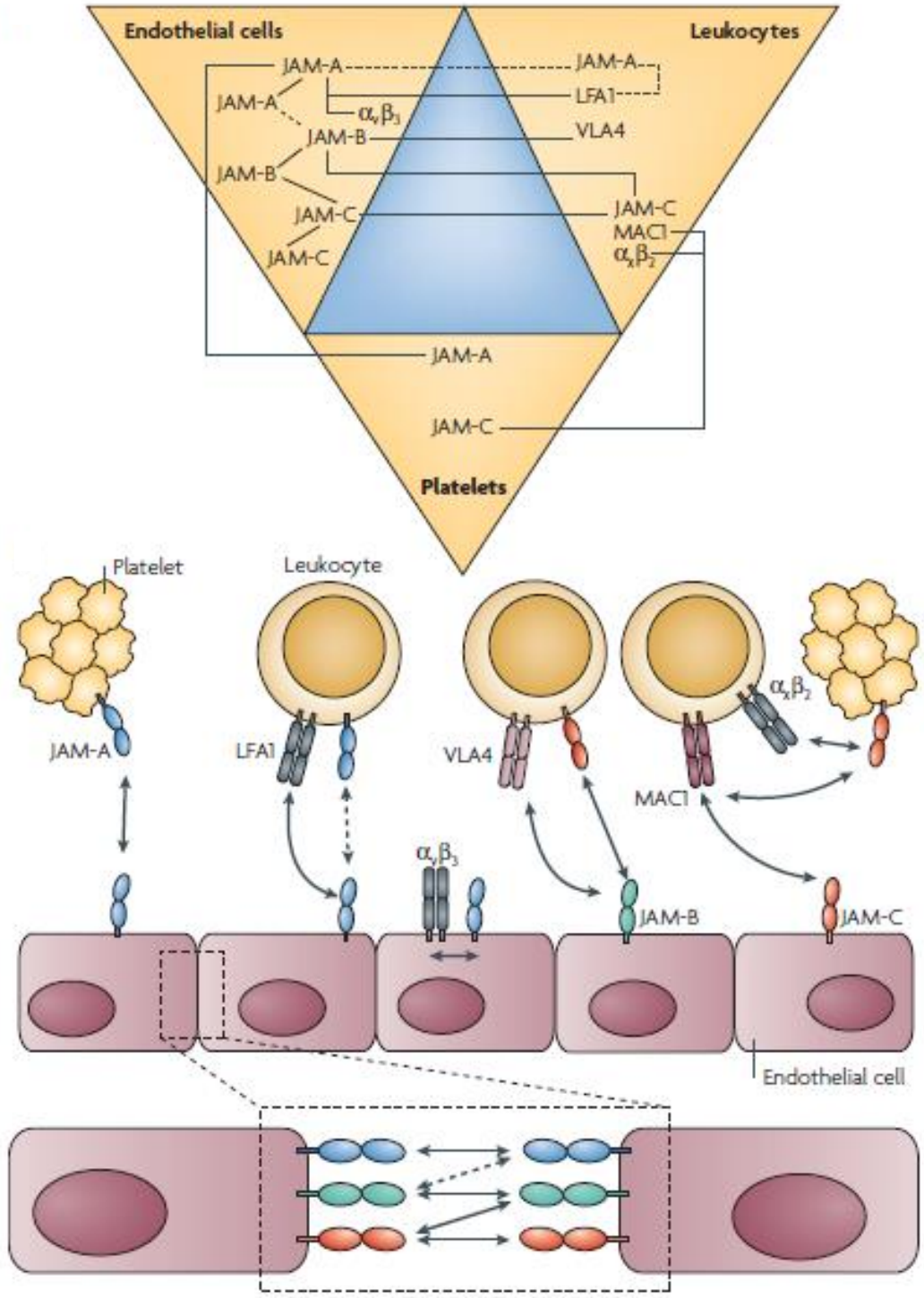

Figure 1.15. Cellular expression and extracellular ligands of junctional adhesion molecules (JAMs).
Junctional adhesion molecule A (JAM-A), JAM-B and JAM-C are expressed on endothelial cells, leucocytes and platelets forming various homophilic and heterophilic interactions. The interactions are shown in solid lines and predicted interactions are in dashed lines. JAMs on endothelial cells form both homophilc and heterphilic dimers at junctions. In addition, they bind integrins expressed on leucocytes. The integrin $\alpha L\beta 2$ (also known as lymphocyte function-associated antigen 1; LFA1) interacts with JAM-A, integrin $\alpha 4\beta 1$ (also known as very late antigen 4; VLA4) interacts with JAM-B, and integrin MAC1 interacts with JAM-C. On platelets, JAM-A homophilic interaction in trans and JAM-C heterophilic interaction occur between platelets and endothelial cells or leucocytes, respectively. The figure is taken from Weber *et al.* (243). Reprinted by permission from Macmillan Publishers Ltd: Nature Reviews Immunology (243), Copyright (2007).

Heterophilic interactions of JAM-A have been shown to occur for transendothelial migration of immune cells, leucocytes (232), neutrophils (251) and dendritic cells (238), as well as in endothelial (248, 252), vascular smooth muscle (253) and certain types cancer cells, such as breast cancer (254, 255) and melanoma (256). In an earlier study, JAM-A-deficient mice impaired basic (b)-FGF induced endothelial proliferation and migration (247) and prevented b-FGF induced angiogenesis (248). Lately, the tetraspanin CD9 has been shown to link JAM-A to this b-FGF specific induction of angiogenesis (257). Jam-a knock-out mouse studies have shown an impairment in immune cell transmigration (258, 259) and infiltration (260, 261), increased vascular permeability and the mobility of endothelial (252) or epithelial cells (254). JAM-A has also been observed in the apical region of inflammatory brain endothelium and functions in immune cell infiltration, suggesting that contact of endothelial-JAM-A is not limited to endothelial junctions (262). The studies on circulating cells will be discussed more in the following section.

In terms of secondary messages transmitted by JAM-A, cis-dimerisation of JAM-A mediates neutrophil or lymphocyte migration by regulating integrin β1 expression/function through Rap1 signalling (248, 263-265) or MAPK signalling (266). JAM-A precipitated with PDZ-GEF, a Rap 1 activator, and other scaffold proteins at the junctions (255). JAM-A dimerisation has also been shown to modulate epithelial cell proliferation through the PI3K/Akt/β-catenin pathway (267).

1.9.4. The interactions and the functions of JAM-A on leucocytes

As circulating cells do not normally adhere to the vascular endothelium, the function of JAMs on leucocytes could be different to those on endothelium and epithelium. The functions of JAM-A on leucocytes has also been less studied, for example LFA-1, a putative

JAM-A interacting integrin, has been shown in some experiments to redistribute on polarised leucocyte, leading to their migration by binding to ICAM1 or JAM-A on endothelium (Figure 1.16).

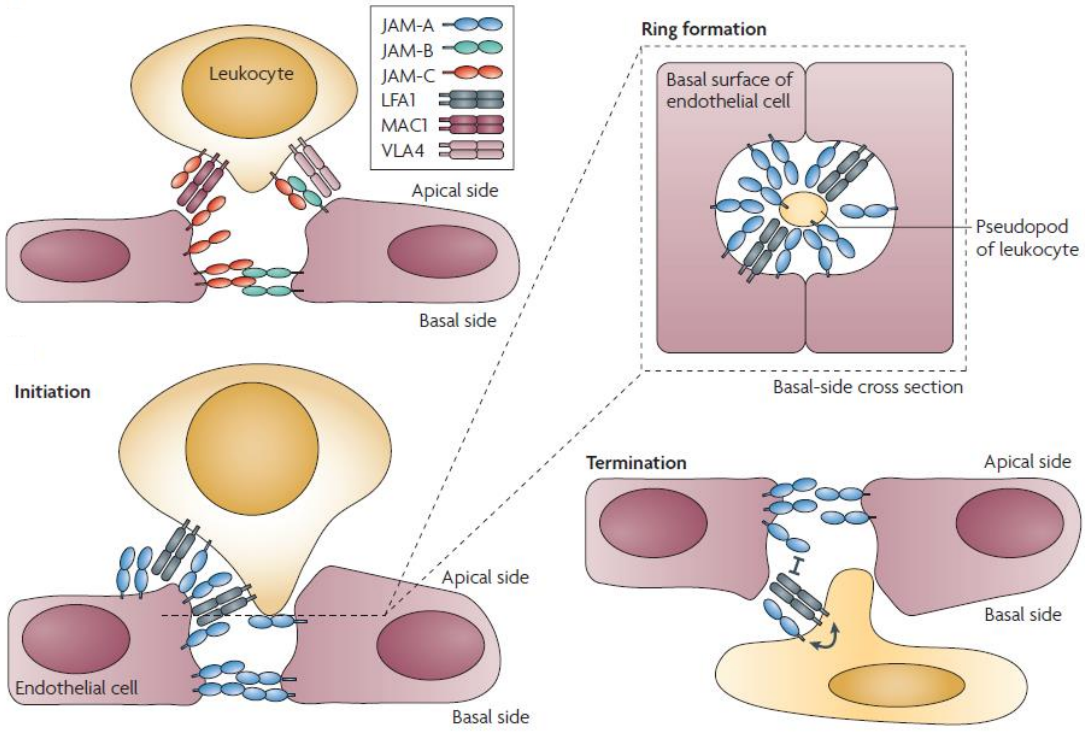

Figure 1.16. Molecular models of junctional adhesion molecule-A (JAM-A) in leucocyte adhesion and transmigration.
Endothelial cell junctions are rich in junctional adhesion molecules (JAMs). For leucocyte adhesion, endothelial JAM-C supports the adhesion and diapedesis of leucocytes by interacting with leucocyte MAC1, followed by the interaction between endothelial JAM-B and very late antigen 4 (VLA4) on leucocytes. During leucocyte transendothelial migration, the endothelial junctional complex is temporarily opened. Endothelial JAM-A is redistributed to the apical surface, and this possibly provides directional cues to leucocytes to move towards the enothelial junction. The interaction between leucocyte lymphocyte function-associated antigen 1 (LFA1) and endothelial JAM-A interrupts JAM-A homophilic interactions at the junctions and this facilitates cell transmigration. Endothelial-cell JAM-A concentrates in a central ring-like structure during leucocyte transmigration, whereas leucocyte JAM-A may confer signals that are important for de-adhesion and polarity at the terminal stage of transmigration. The figure is taken from Weber *et al.* (243). Reprinted by permission from Macmillan Publishers Ltd: Nature Reviews Immunology (243), Copyright (2007).

On neutrophils, LFA-1 has been demonstrated to form heterophilic interactions to compete with and destabilise the JAM-A-JAM-A homophilic interactions at the endothelial junctions

(where trimerisation of JAM-A may temporarily occur) so as to promote their transendothelial migration (268). In contrast, Cera *et al.* showed JAM-A at the leading edge of activated neutrophils mediating internalisation and recycling of integrins via Rap1 signalling while undergoing transmigration (251). In addition, in the same study, an enhancement in neutrophil random motility was observed by reducing JAM-A expression on leucocytes (251).

In 2008 Sugano *et al.* demonstrated that the enriched murine HSC fraction highly expressed Jam-a, and showed that JAM-A was as a novel marker to enrich long-term repopulating HSCs (152). More recently, JAM-A expression was defined on human peripheral blood $CD34^+$ cells (239). In the same study, JAM-A was shown to promote cell adhesion onto injured vascular walls and to mediate $CD34^+$ cell differentiation into endothelial progenitor cells (239).

1.9.5. Other JAMs

JAM-B and JAM-C

In contrast to JAM-A, JAM-B and JAM-C have been investigated more on leucocytes. Heterophilic interactions of JAM-C with JAM-B were not only observed at inter-endothelial junctions, but also between leucocytes and endothelium. *jam-B* mutant murine embryonic stem (ES) cells were shown to have normal morphology and pluripotency, and mice were fertile with no overt developmental defects and ES cells had no impaired self-renewal and differentiation abilities (269). In comparison to *jam-b*, two-thirds of *jam-c*-deficient mice died within 48 hours after birth. Among the survivors, loss of jam-c led to an increase in myeloid progenitors and granulocytes in the bone marrow (270). In adults, the binding of HSCs through JAM-C to JAM-B on bone marrow stromal cells mediated HSC maintenance (148). In addition, JAM-C binding was suggested to be involved in certain immune responses.

JAM-C transcription was up-regulated in activated T cells (271). JAM-C deficiency affected the adaptive immune response against pathogens in addition to the innate immune system (272). Using JAM-C antibody to block JAM-C on endothelial cells resulted in JAM-B moving to the apical region of endothelial cells for leucocyte adhesion (250). Interruption of JAM-C reduced monocyte recruitment to inflamed endothelial areas by interfering their directional migration (273). JAM-C also plays a role in *in vivo* neutrophil transendothelial migration (274) and leucocyte infiltration in knock-out mouse models (275), despite only minimal effects being observed in leucocyte adhesion and transmigration on HUVEC in a shear stress conditions in another study (276). It is also worth noting that JAM-C is not the only heterophilic partner of JAM-B. Integrin, VLA4, on lymphocytes has been shown to bind to endothelial-JAM-B for rolling and adhesion (271). Likewise, Mac-1 integrin is another heterophilic binding partner for JAM-C. This heterophilic binding has been shown to exist between neutrophils and endothelium (277, 278) or epithelium (279, 280) and to contribute to transmigration. Similarly, Mac-1-JAM-C interactions modulate CD34 cell adhesion onto platelets (281).

In endothelium, JAM-C positively regulates cell permeability through Rap1b and integrin β1 but not Rap1a signalling (282). A soluble form of JAM-C, which is cleaved by disintegrin and metalloproteinases 10 and 17, can regulate human microvascular endothelial cell (HMVEC) and immortalized human dermal microvascular endothelial cell tubule formation and chemotaxis (283). In endothelial or epithelial cancers, JAM-C binding is involved in cancer cell invasion. JAM-C homophilic interactions have also been observed between lung carcinoma cell line (NCI-H522) and endothelium (Chinese hamster ovary (CHO) cells) (284). In addition, JAM-C on murine B16 melanoma cell binds to JAM-C and JAM-B of lung

microvascular endothelium for their adhesion and metastasis (285). It was believed that JAM-C controls epithelial tumour cell polarity and migration (286).

More recently, it has been found that JAM-B and JAM-C modulate CXCR4 and CXCL12 as reviewed in (234). Inhibition of JAM-C increases CXCL12 in lymph node stromal cells (153), while JAM-B deletion increases CXCL12 secretion by stromal cells and reduces CXCR4 expression on HSCs (148).

ESAM-1

ESAM-1 is another JAM member that has been studied in haematopoietic cells. As it is selectively expressed on endothelial cells and HS/PCs, it has been proposed as a haematopoietic cell marker for mice (154, 155). In addition, it has been suggested that ESAM-1 binding controls HSC quiescence versus self-renewal (149).

1.10. Rap1 Signalling in Haematopoietic Cells

Rap1 (Ras-proximate-1 or Ras-related protein 1) is a small G protein that belongs to Rap family, a Ras superfamily. To date, there are five members of the Rap family, namely Rap1A, Rap1B, Rap2A, Rap2B and Rap2C. Rap1 was first discovered by Kitayama et al. in 1989 as a product of K-rev gene named as a transformation suppressor of K-Ras (287). Like other small G protein, Rap1 exists in an inactivate form in cells when bound to guanine nucleotide diphosphate (GDP) and is activated when GDP is exchanged with guanine nucleotide triphosphate (GTP) by nucleotide exchange factors (GEF) (reviewed in (288-290)). The Rap1-GTP active form can be switched back to Rap1-GDP by GTPase-activating proteins (GAP) (reviewed in (288-290)).

Several GEFs have been discovered and these can activate Rap1 when they are activated by distinct stimuli. C3G was the first Rap1-GEF identified on the cell membrane by associating

with Crk adaptor proteins (291). Calcium and diacylglycerol (CalDAG)-GEFs is another Rap1-GEF family member that responds to calcium and diacylglycerol for its activation (reviewed in (288-290)). Four isoforms of CalDAG-GEFs have been identified. Each displays varied expression patterns in different cell types and shows different preferential activation of Rap family members. Cyclic adenosine monophosphate (cAMP)-GEFs or EPAC (exchange proteins directly activated by cAMP) constitutes another group of Rap1-GEFs. As its name implies, this class of Rap1-GEFs directly binds to cAMP for its activation (reviewed in (288-290)). PDZ-GEF, another Rap1-GEF family member, is named for its protein structure since it contains a PDZ domain and a Rap1-binding domain (reviewed in (288-290)). A study has shown that junctional adhesion molecule, JAM-A, interacts with PDZ-GEFs and mediates Rap1 activation in mammalian breast cancer cells enhancing cell migration (255). It is also worth noting that PDZ-GEF/Rap1-mediated signals not only exist at the junctions of identical cell types but also between different cell lineages. Wang *et al.* for example demonstrated that PDZ-GEFs are involved in the germ line stem cell survival by interacting with their somatic niche in testis (292).

Only two families of Rap1-GAPs have been identified. They are Rap1-GAPs (293) and signal-induced proliferation associated gene-1 (SPA-1) (294). Rap1-GAP1 was the first isolated Rap1-specific GAP that was initially discovered on the membrane of HL-60 cells (295). SPA-1 expression is limited to haematopoietic tissues, and is particularly high in lymphoid tissues (294, 296). SPA-1 is predominantly expressed in immature bone marrow cells, whereas Rap1-GAP is found predominantly expressed in mature cells (297). Spa-1 deficiency in the bone marrow has been implicated in an array of myeloid disorders, such as chronic myelogenous leukaemia (CML) and myelodysplastic syndrome (MDS) through Rap1-GTP accumulation and constitutive ERK activation (297). It has thus been proposed that

disorders in haematopoietic cell and niche cell interaction due to abnormal Rap1 activation may deregulate biological functions of haematopoietic cells.

Rap1-mediated cell adhesion has been well-studied. Rap1 has been implicated in various cellular processes in mammalian cells mainly through ERK activation and integrin-mediated cellular functions. The Rap1 downstream effectors comprise c-Raf, B-Raf, RalGEFs, AF-6, PI3K, RapL, Rap1-GTP-interacting adaptor molecule (RISM) and Rap1/Krev1 interaction trapped 1 (KRIT-1/CCM1) as reviewed in (289, 298). They are selectively activated by Rap1 depending on cell context. Take haematopoietic cells for instance, Rap1 positively regulates integrin-mediated cell adhesion of all examined haematopoietic cells to date. With Rap1 activation, terminal differentiation of megakaryocyte is initiated and enhanced myelocyte proliferation occurs through the same Rap1 effector, B-Raf, and ERK activation (299). On the other hand, modulation of T lymphocyte adhesion by Rap1 is accompanied by T cell activation through antagonising Ras/Raf/ERK signalling pathway (299).

1.11. Key Aims and Objectives of This Thesis

The overall objective of this research was to investigate mechanisms which regulate the interaction between HS/PCs or LICs and the bone marrow vascular niche, and specifically to:

- Investigate JAM-A expression on normal and malignant haematopoietic cells and bone marrow vascular niche cell components.
- Determine the role of JAM-A in regulating UCB $CD34^+$ cell and leukaemic cell line *in vitro* adhesion to and migration across bone marrow endothelial cells.
- Investigate the downstream signalling mediated through JAM-A in response to CXCL12 stimulation.

CHAPTER 2

MATERIALS AND METHODS

2.1. Reagent Suppliers

The chemical reagents that were used for this study and their manufactures are summarised in the following table.

Table 2.1. The list of reagents used with their suppliers.

Reagent	Company
2-Mercaptoethanol	Sigma-Aldrich Ltd., Gillingham, UK
Accuspin System-Histopaque-1077	Sigma-Aldrich Ltd., Gillingham, UK
Acetic acid	Sigma-Aldrich Ltd., Gillingham, UK
Active Rap1 Pull-Down and Detection Kit	Thermo Fisher Scientific Inc., Loughborough, UK
Advanced protein concentration assay reagent (5X)	Cytoskeleton, Inc., Denver, USA,
Agar	Sigma-Aldrich Ltd., Gillingham, UK
Agarose	Sigma-Aldrich Ltd., Gillingham, UK
Amaxa Cell Line Nucleofection Kit V (for HL-60)	Lonza Biologics, Tewkesbury, UK
Amaxa Human $CD34^+$ Cell Nucleofector Kit	Lonza Biologics, Tewkesbury, UK
Ammonium chloride	Sigma-Aldrich Ltd., Gillingham, UK
Ampicillin	Sigma-Aldrich Ltd., Gillingham, UK
Aquamount	VWR International Ltd., Lutterworth, UK
BCECF-AM (3',6'-*bis*(Acetyloxy)-5(or 6)-[[(acetyloxy)methoxy]carbonyl]-3-oxo-spiro[isobenzofuran-1(3*H*),9'-[9*H*]xanthene]-2',7'-dipropanoic acid 2',7'-*bis*[(acetyloxy)methyl] ester)	Invitrogen Ltd., Paisley, UK
Beta-mercaptoethanol (β-mercaptoethanol)	VWR International Ltd., Lutterworth, UK
BSA (Bovine Serum Albumin)	Sigma-Aldrich Ltd., Gillingham, UK
CD34 or CD133 MicroBead kits	Miltenyi Biotec GmbH, Bergisch Gladbach, Germany
Citric acid	Sigma-Aldrich Ltd., Gillingham, UK
Citroclear solution	TCS Biosciences Ltd., Botolph Claydon, Buckingham, UK
Collagen, bovine, Type I	Sigma-Aldrich Ltd., Gillingham, UK
CXCL12 (Recombinant Human SDF-1α)	Peprotech, Hamburg, Germany,
DAB Substrate Kit for Peroxidase	Vector Laboratories, Inc., CA, USA
DAPI (4', 6-Diamidino-2-pyenylindole)	Sigma-Aldrich Ltd., Gillingham, UK
DEPC-water (nuclease free water)	Invitrogen Ltd., Paisley, UK
DMEM (Dulbecco's Modified Eagle's Medium)	PAA Laboratories GmbH, Pasching, Austria
DMSO (Dimethyl sulphoxide)	Sigma-Aldrich Ltd., Gillingham, UK
DNA Ligation Kit	TaKaRa Bio Inc., Japan,
DTT (Dithiothreitol)	Invitrogen Ltd., Paisley, UK
Duolink® *in situ* PLA proximity ligation assay kit	Cambridge Bioscience Ltd., Cambridge, UK
EBM-2 (Endothelial Basal Medium)	Lonza Biologics plc., Slough, UK
EDTA (Ethylenediaminetetraacetic acid)	Sigma-Aldrich Ltd., Gillingham, UK
EGM-2 bullet kits (Lonza Walkersville Endothelial Growth Medium)	Lonza Biologics, Tewkesbury, UK
Ethanol	VWR International Ltd., Lutterworth, UK
FBS (Fetal bovine serum)	PAA Laboratories GmbH, Pasching, Austria
FcR Blocking Reagent	Miltenyi Biotec GmbH, Bergisch Gladbach,

Reagent	Company
	Germany
Fibronectin	Sigma-Aldrich Ltd., Gillingham, UK
Flt-3 (Recombinant Human Fms-like tyrosine kinase 3) ligand	R&D Systems, Inc., Minneapolis, USA
Fluorescent mounting medium	DakoCytomation Ltd., Cambridge, UK
Full-Range Rainbow Molecular Weight Markers	PAA Laboratories GmbH, Pasching, Austria
GelRed Nucleic Acid Stain	Biotium Inc., Cambridge, UK
Glycine	Sigma-Aldrich Ltd., Gillingham, UK
GM-CSF (Human Granulocyte-Macrophage Colony-Stimulating Factor)	Miltenyi Biotec GmbH, Bergisch Gladbach, Germany
Goat serum	Sigma-Aldrich Ltd., Gillingham, UK
Haematoxylin solution	Sigma-Aldrich Ltd., Gillingham, UK
HBSS (Hank's Balanced Salt Solution)	PAA Laboratories GmbH, Pasching, Austria
Hydrocortisone sodium succinate	StemCell Technologies, Grenoble, France
Hydrogen peroxide (H_2O_2)	Sigma-Aldrich Ltd., Gillingham, UK
iBlot®Transfer Stack, nitrocellulose Mini	Invitrogen Ltd., Paisley, UK
iBlot®Transfer Stack, PVDF Mini	Invitrogen Ltd., Paisley, UK
IL-1β (Recombinant Human Interleukin-1β)	Invitrogen Ltd., Paisley, UK
IL-6 (Recombinant Human Interleukin-6)	R&D Systems, Inc., Minneapolis, USA
IMDM (Iscove's Modified Dulbecco's Medium)	Invitrogen Ltd., Paisley, UK
IMMOLASE™ DNA Polymerase	Gentaur GmbH, Aachen, Germany
ImmunoPure goat anti-mouse peroxidase conjugated secondary antibody	Thermo Fisher Scientific Inc., Loughborough, UK
ImmunoPure goat anti-rabbit peroxidase conjugated secondary antibody	Thermo Fisher Scientific Inc., Loughborough, UK
Isopropanol	VWR International Ltd., Lutterworth, UK
JM109 Competent Cells	Stratagene Ltd., Cambridge, UK
Kanamycin	Sigma-Aldrich Ltd., Gillingham, UK
Kb DNA Ladder	Agilent Technologies Inc.
LB (Luria-Bertani medium)	Sigma-Aldrich Ltd., Gillingham, UK
Lipofectamine™2000	Invitrogen Ltd., Paisley, UK
Magnesium chloride ($MgCl_2$)	Sigma-Aldrich Ltd., Gillingham, UK
Methanol	VWR International Ltd., Lutterworth, UK
MTT (Methylthiazolyldiphenyl-tetrazolium bromide)	Sigma-Aldrich Ltd., Gillingham, UK
MyeloCult H5100	StemCell Technologies, Grenoble, France
NuPAGE ® Novex Bis-Tris Gels	Invitrogen Ltd., Paisley, UK
NuPAGE® LDS Sample Buffer (4X)	Invitrogen Ltd., Paisley, UK
NuPAGE® MES Running Buffer (20X)	Invitrogen Ltd., Paisley, UK
NuPAGE® Reducing Agent	Invitrogen Ltd., Paisley, UK
NuPAGE®Antioxidant	Invitrogen Ltd., Paisley, UK
One Shot® TOP 10 Chemically Competent Cells	Invitrogen Ltd., Paisley, UK
Opti-MEM	Invitrogen Ltd., Paisley, UK
Paraformaldehyde	Sigma-Aldrich Ltd., Gillingham, UK
PBS solution (Phosphate buffered saline)	PAA Laboratories GmbH, Pasching, Austria
PBS tablet (Phosphate-Buffered Saline)	Sigma-Aldrich Ltd., Gillingham, UK
pCR® II-TOPO® vector (TOPO TA Cloning)	Invitrogen Ltd., Paisley, UK
PfuTurbo® DNA Polymerase	Stratagene Ltd., Cambridge, UK
PLA (Olink in situ Proximity Ligation Assay)	Olink Bioscience, Uppsala, Sweden
PMSF (phenylmethanesulphonylfluoride or phenylmethylsulphonyl fluoride)	Sigma-Aldrich Ltd., Gillingham, UK
Proteinase inhibitors cocktail	Sigma-Aldrich Ltd., Gillingham, UK
PureLink™ HiPure Plasmid Filter Purification Kits (Midi preparation of Plasmid DNA)	Invitrogen Ltd., Paisley, UK
PureLink™ Quick Gel Extraction and PCR Purification	Invitrogen Ltd., Paisley, UK

Reagent	Company
Combo Kit	
RPMI-1640 medium	PAA Laboratories GmbH, Pasching, Austria
S.O.C. medium	Invitrogen Ltd., Paisley, UK
SCF (Recombinant Human Stem Cell Factor)	R&D Systems, Inc., Minneapolis, USA
Skim Milk powder	Fluka Biochemika, Buchs, Switzerland
Sodium Acetate (CH_3COONa)	Sigma-Aldrich Ltd., Gillingham, UK
Sodium Azide (NaN_3)	Sigma-Aldrich Ltd., Gillingham, UK
Sodium Bicarbonate ($NaHCO_3$)	Sigma-Aldrich Ltd., Gillingham, UK
Sodium Chloride (NaCl)	Sigma-Aldrich Ltd., Gillingham, UK
Sodium Citrate	VWR International Ltd., Lutterworth, UK
Sodium Fluoride (NaF)	Sigma-Aldrich Ltd., Gillingham, UK
Sodium Vanadate (Na_3VO_4)	Sigma-Aldrich Ltd., Gillingham, UK
StemSpan medium	StemCell Technologies, Grenoble, France
Super Signal® West Pico Chemiluminescent Substrate Kits	Thermo Fisher Scientific Inc., Loughborough, UK
TAE Buffer (10X) (Tris-Acetate-EDTA)	Invitrogen Ltd., Paisley, UK
TPO (Recombinant Human Thrombopoietin)	R&D Systems, Inc., Minneapolis, USA
Tris-HCl	Sigma-Aldrich Ltd., Gillingham, UK
Trisodium Citrate	VWR International Ltd., Lutterworth, UK
Triton X-100	Sigma-Aldrich Ltd., Gillingham, UK
Trypan Blue Solution	Sigma-Aldrich Ltd., Gillingham, UK
Trypan Blue stain	Invitrogen Ltd., Paisley, UK
Trypsin-EDTA	PAA Laboratories GmbH, Pasching, Austria
TSAP (Thermosensitive Alkine Phosphatase)	Promega Co., Madison, USA
Tween-20	Sigma-Aldrich Ltd., Gillingham, UK
Vectastain Elite ABC Kit	Vector Laboratories, Inc., CA, USA

2.2. Cell Culture

2.2.1. Cell lines

The HL60 cell line is human promyelocytic leukaemia cell line originally derived from cells obtained from a 36-year-old woman with acute promyelocytic leukaemia (300). The cells were cultured in IMDM medium (Invitrogen Ltd.) with 20% (v/v) fetal bovine serum (FBS; PAA Laboratories GmbH) in T25 tissue culture grade flasks (Appleton Woods Ltd., Birmingham, UK) in a 37°C CO_2 air-jacked incubator (MCO-20AIC, Triple Red Ltd., Buckinghamshire, UK). Cells were cultured at 0.5-1x10^5 cells/ml and passaged when cells (every two to three days) reached 6-9x10^5cells/ml. The cells were passaged by maintaining 0.5-1 ml of the original cell suspension at the concentration indicated and topping up the fresh medium to 10 mls. This cell line was obtained from LGC Promochem (Middlesex, UK).

The KG-1 cell line was derived by Dr. H.P. Koeffler and Dr. D.W. Golde from a bone marrow aspirate of a 59-year-old caucasian male with erythroleukaemia after this evolved into acute myeloid leukaemia (301) and was obtained from LGC Promochem (Middlesex, UK). This cell line was cultured in IMDM medium (Invitrogen Ltd.) with 20% (v/v) FBS (PAA Laboratories GmbH) at an initial concentration of $2x10^5$ cells/ml in T25 tissue culture grade flasks (Appleton Woods Ltd.) in a 37°C 5% CO_2 in air water-jacketed incubator (MCO-20AIC, Triple Red Ltd.). Medium was changed every two or three days and the cells were passaged every week by maintaining 1 ml of original cell suspension and topping up the fresh medium to 10 mls, i.e. splitting the cells to $2x10^5$ cells/ml.

The TF-1 cell line was established by Dr. T. Kitamura *et al.* in 1987 from a heparinised bone marrow aspirate from a 35 year old Japanese male with severe pancytopaenia (302) and was obtained from LGC Promochem (Middlesex, UK). The cells were cultured in RPMI-1640 medium (PAA Laboratories GmbH) with 10% or 20% (v/v) FBS (PAA Laboratories GmbH) and 2 ngs/ml GM-CSF (Miltenyi Biotec GmbH), with the cells initiated at a concentration of 2-$5x10^4$ cells/ml in T25 tissue culture grade flasks (Appleton Woods Ltd.) in a 37°C 5% CO_2 in air water-jacketed incubator (MCO-20AIC, Triple Red Ltd.). Every two to three days the cells were passaged by maintaining 0.5-1 ml of the original cell suspension and topping up the fresh medium to 10 ml, i.e. splitting the cells to 2-$5x10^4$cells/ml.

The Jurkat cell line was established from the peripheral blood of a 14-year-old boy with T cell acute lymphocytic leukaemia (T-ALL) by Schneider *et al.* (303) and was obtained from LGC Promochem (Middlesex, UK). This cell line was maintained in RPMI-1640 medium (PAA Laboratories GmbH) with 10% (v/v) FBS (PAA Laboratories GmbH) in T25 tissue culture grade flasks (Appleton Woods Ltd.) in a 37°C 5% CO_2 in air water-jacketed incubator (MCO-20AIC, Triple Red Ltd.) for two or three days before passage. Approximate 0.5-1 ml of

original cell suspension was remained during passage and topped up with the fresh medium to 10 mls. Cell cultures were initiated with 1-3x10^5cells/ml and diluted to this concentration on passage.

The CEM cell line was established in 1964 from peripheral blood of a 3-year-old female T-ALL patient (304). This cell line was maintained in RPMI-1640 medium (PAA Laboratories GmbH) with 10% (v/v) FBS (PAA Laboratories GmbH) in T25 tissue culture grade flasks (Appleton Woods Ltd.) in a 37°C 5% CO_2 in air water-jacketed incubator (MCO-20AIC, Triple Red Ltd.) for two or three days before passage. Approximately 0.5-1 ml of old cell suspension was used during passage and topped up with the fresh medium to 10 mls. The doubling time was approximately 24-30 hours. Cell cultures were initiated with 1-3x10^5 cells/ml and diluted to this concentration on passage. This cell line was kindly provided by Dr. Allison Banham, University of Oxford.

The MOLT-4 cell line was established in 1971 from peripheral blood of a 19-year-old male T-ALL patient (305). This cell line was maintained in RPMI-1640 medium (PAA Laboratories GmbH) with 10% (v/v) FBS (PAA Laboratories GmbH) in T25 tissue culture grade flasks (Appleton Woods Ltd.) in a 37°C 5% CO_2 in air water-jacketed incubator (MCO-20AIC, Triple Red Ltd.) for two or three days before passage. Approximately 0.5-1 ml of old cell suspension was used during passage and topped up with the fresh medium to 10 mls. The doubling time was approximately 40 hours. Cell cultures were initiated at 1-3x10^5 cells/ml and diluted to this concentration on passage. This cell line was kindly provided by Dr. Allison Banham, University of Oxford.

The Reh cell line was established in 1974 from peripheral blood of a 15-year-old North African female ALL patient (306). This cell line was maintained in RPMI-1640 medium (PAA Laboratories GmbH) with 20% (v/v) FBS (PAA Laboratories GmbH) in T25 tissue culture

grade flasks (Appleton Woods Ltd.) in a 37°C 5% CO_2 in air water-jacketed incubator (MCO-20AIC, Triple Red Ltd.) for three to four days before passage. Approximately 1-2 mls of the cell suspension was used during passage and topped up with the fresh medium to 10 mls. The doubling time was approximately 50-70 hours. Cells cultures were initiated at 2-4x10^5 cells/ml and diluted to this concentration on passage. This cell line was kindly provided by Dr. Allison Banham, University of Oxford.

The NALM-1 cell line was established in 1975 from peripheral blood of a 3-year-old CML female patient (307). This cell line was grown in RPMI-1640 medium (PAA Laboratories GmbH) with 10% (v/v) FBS (PAA Laboratories GmbH) in T25 tissue culture grade flasks (Appleton Woods Ltd.) in a 37°C 5% CO_2 in air water-jacketed incubator (MCO-20AIC, Triple Red Ltd.) for two to three days before passage. Approximately 0.5-1 ml of original cell suspension was used during passage and topped up with the fresh medium to 10 mls. The doubling time was approximately 48-72 hours. Cell cultures were initiated at 2-3x10^5 cells/ml and diluted to this concentration on passage. This cell line was kindly provided by Dr. Allison Banham, University of Oxford.

The BMEC-60 cell line was generated by Professor E. van der Schoot's group (178) and was obtained from LGC Promochem (Middlesex, UK). The primary bone marrow endothelial cells were isolated from a consented patient undergoing cardiac surgery and transformed cell lines were established by immortalising with the amphotrophic helper-free retroviral pLXSN16E6/E7 vector (308). The BMEC-60 cells were one of these series of immortalised cell lines. This cell line was grown in complete EGM-2 medium (EBM-2 basic medium containing EGM-2 bullet kit; Lonza Biologics plc.) in T75 tissue culture grade flasks (Appleton Woods Ltd.) in a 37°C 5% CO_2 in air water-jacketed incubator (MCO-20AIC, Triple Red Ltd.), and the complete EGM-2 medium was replaced every 2-3 days till the cells reached confluence.

When passaged, the culture medium was firstly removed from cells and the cells were washed with HBSS (PAA Laboratories GmbH). After removing the washing buffer, the cells were briefly rinsed with 1 ml trypsin-EDTA solution (170,000 Us/L trypsin and 200 mgs/L EDTA; PAA Laboratories GmbH) and incubated with the same amount at 37°C in a 5% CO_2 in air water-jacketed incubator (MCO-20AIC, Triple Red Ltd.). The dispersed cells were observed under an inverted Eclipse TS100 microscope (Nikon UK Ltd., Surry, UK). Ten mls of fresh culture (complete EGM-2) medium was subsequently added to neutralise the trysin. Three to four ml of the neutralised cell suspension was used during passage and topped up with fresh culture medium to 30 mls.

The HEK 293T cell line was generated from human embryonic kidney fibroblasts, as a highly transfectable derivative of the HEK 293 cell line, into which the temperature sensitive gene for SV40 T-antigen was inserted. The basal medium for this cell line was DMEM medium (PAA Laboratories GmbH) containing FBS (PAA Laboratories GmbH) at a final concentration of 10% (v/v). The cells were passaged using trypsin-EDTA when the cells reached the over 90% confluence. For trypsinisation, the culture medium was removed and discarded and the cells then washed with HBSS (PAA Laboratories GmbH). One ml trypsin-EDTA solution (170,000 Us/L trypsin and 200 mgs/L EDTA; PAA Laboratories GmbH) was subsequently added to and the cells rinsed and reincubated with 1ml of trypsin-EDTA. The dispersed cells were observed under an inverted microscope before 10 mls of fresh culture medium was added to neutralise the trypsin. A subcultivation ratio of 1:8-1:10 was used during passage. This cell line was obtained from LGC Promochem (Middlesex, UK).

2.2.2. Primary Cells

Bone marrow stomal cells (BMSCs) and human mesenchymal stem/stromal cells (MSCs) were purchased from Lonza Biologics. BMSC had been characterised as supporting cells for

long-term culture initiating cells by the manufacturer (LTC-IC; Lonza Walkersville, Inc., Walkersville, US). MSC had been cultured from normal human bone marrow and characterised as $CD105^+$, $CD166^+$, $CD29^+$, $CD44^+$ and CD14, CD34 and CD45 negative and for trilineage (osteogenic, adipogenic, chrondrogenic) potential by the manufacturer. These cells were cultured in MyeloCult H5100 medium (Stem Cell Technologies) with 10^{-6} M hydrocortisone sodium succinate (Stem Cell Technologies) and the culture initiated with $2x10^4$ cells/cm^2. The culture medium was changed every three days and cells were passaged once a week when they reached over 90% confluence by washing with HBSS twice followed by incubation with 1 ml trypsin-EDTA (170,000 Us/L trypsin and 200 mgs/L EDTA (PAA Laboratories GmbH) in a 37°C 5% CO_2 in air water-jacketed incubator (MCO-20AIC, Triple Red Ltd.) for 5 minutes. The trypsin-EDTA (PAA Laboratories GmbH) was neutralised by adding 10ml fresh culture medium and $2x10^4$ cells/cm^2 replated in T75 tissue culture grade flasks (Appleton Woods Ltd.). Three different batches of BMSCs and MSCs were used for the studies described in this thesis.

Primary acute lymphoblastic leukaemic cells. B-cell acute lymphoblastic leukaemic cells (B-ALL) and two T-cell acute lymphoblastic leukaemic cells (T-ALL) were sourced by Dr. Allison Blair, University of Bristol, and then stored in liquid nitrogen before being used in assays or in collaborative studies to assess JAM-A expression by flow cytometry.

2.3. $CD34^+$ or $CD133^+$ Cell Isolation from Human Umbilical Cord Blood

Human umbilical cord blood (UCB) was collected from healthy births from the John Radcliffe Hospital, Oxford, with informed, written pre-consent and ethical approval from the Oxford Radcliffe Research Ethical Committee for the use of umbilical cord blood following delivery as a source of stem cells for study of cell differentiation in normal and disease conditions (CO2.313). The UCB samples were used as anonymised linked donations either under an

HTA licence or with ethical permission from the Berkshire Research Ethics Committee (10/H0505/34). The UCB was diluted in HBSS (PAA Laboratories GmbH) containing 0.3% (w/v) sodium citrate (VWR International Ltd.) and 0.5% (w/v) Bovine Serum Albumin (BSA; Sigma-Aldrich Ltd.). Mononuclear cells (MNCs) were separated using Accuspin™-Histopaque®-1077 tubes (Sigma-Aldrich Ltd.) as described and detailed in section 2.3.1 (140). MNCs were cryopreserved before CD34 or CD133 positive cell isolation using MicroBead kits (Miltenyi Biotec GmbH) as described in section 2.3.2. The isolated cells were then cultured in StemSpan medium (Stem Cell Technologies) with 100 ngs/ml of recombinant human Fms-like tyrosine kinase 3 ligand (Flt-3 ligand; R&D Systems, Inc.), recombinant human interleukin-6 (IL-6; R&D Systems, Inc.), recombinant human stem cell factor (SCF; R&D Systems, Inc.) and 20 ngs/ml of recombinant human thrombopoietin (TPO; R&D Systems, Inc.) in a 37°C 5% CO_2 in air water-jacketed incubator (MCO-20AIC, Triple Red Ltd.) overnight prior to using in assays.

2.3.1. Mononuclear cell (MNC) isolation

Before the separation, UCB was diluted with MACS buffer (HBSS solution containing 0.3% (w/v) sodium citrate and 0.5% (w/v) BSA) at a ratio 1:1 when the white blood cell (WBC) count less than $7x10^6$ cells/ml or at 1:20 when the WBC count over $7x10^6$ cells/ml. The diluted UCB was layered on Accuspin™-Histopaque®-1077 tubes (Sigma-Aldrich Ltd.) at 30-35ml/tube and centrifuged at 800g in an Heraeus Multifuge 4KR centrifuge (DJB Labcare Ltd., Buckinghamshire, UK) at room temperature for 30 minutes with the brake off. The MNC layer was collected and washed three times in 50mls Falcon centrifuge tubes (Appleton Woods Ltd.) in MACS buffer (0.3% (w/v) sodium citrate and 0.5% (w/v) BSA in HBSS solution without Ca^{2+} and Mg^{2+}) at the speed of 400g once and then 200g twice, for 10 minutes each

at 4°C. After the last wash, around 50 μls of cell solution was used for cell counting and cells were cryopreserved at $1x10^8$ cells per vial (section 2.4) before CD34 or CD133 positive cell isolation. Alternatively, for the studies on screening surface molecule expression on haemopoietic lineages, UCB MNCs were collected as described in section 2.9.1.3.

2.3.2. CD34 or CD133 magnetic selection and culture

The $CD34^+$ or $CD133^+$ cells were isolated from the thawed MNCs (isolated in section 2.3.1.) using magnetic beads. The MNCs were resuspended gradually in MACS buffer at the density of $1x10^8$ cells per 300 μls. One hundred μl of FcR blocking solution (Miltenyi Biotec GmbH) and 100 μl of CD34 or CD133 microbeads (Miltenyi Biotec GmbH) were added per $1x10^8$ cells and the cells were incubated at 4°C for 30 minutes. Next, 5 mls of MACS buffer was added and cells centrifuged at 350 xg at 4°C in an Heraeus Multifuge 4KR centrifuge (DJB Labcare Ltd.) for 5 minutes, followed by resuspending cells in 5 mls of fresh MACS buffer at 4°C. MACS separation columns (Miltenyi Biotec GmbH) were equilibrated and rinsed with 5 mls of ice cold MACS buffer before applying the cells to the column. The column was washed with 4 mls of ice cold MACS buffer three times and the labelled cells were eluted in 5 mls of ice cold MACS buffer. The eluted cells were then applied to a second pre-rinsed column and all the washing and elution repeated. The $CD34^+$ or $CD133^+$ cells were centrifuged at 350 xg at 4°C in an Heraeus Multifuge 4KR centrifuge (DJB Labcare Ltd.) for 5 minutes to remove the supernatants and then placed at $1x10^6$ cells/ml of StemSpan medium (Stem Cell Technologies) with 100 ngs/ml of Flt-3 ligand (R&D Systems, Inc.), IL-6 (R&D Systems, Inc.) and SCF (R&D Systems, Inc.), and 20 ngs/ml of TPO (R&D Systems, Inc.) in a 37°C 5% CO_2 in air water jacketed incubator (MCO-20AIC, Triple Red Ltd.) overnight prior to use in assays.

2.4. Cell Cryopreservation and Thawing

The medium or buffer was removed from the cells by centrifuging at 350 xg at 4°C in an Heraeus Multifuge 4KR centrifuge (DJB Labcare Ltd.) for 5 minutes and the cell pellet was placed in cryopreservation medium comprising 90% (v/v) FBS (PAA Laboratories GmbH) and 10% (v/v) DMSO (Sigma-Aldrich Ltd.). Cells were transferred to 2 mls cryovials (Alpha Laboratories Ltd.) using 1ml per vial. The vials were kept in freezing containers (Mr Frosty) at -80°C overnight before being transferred to the liquid nitrogen for long-term preservation at -196°C. For thawing, the cells were quickly defrosted in a 37°C water bath (Grant Instruments Ltd., Cambridge, UK) and then transferred to a fresh 15ml Falcon tube (Appleton Woods Ltd.). Nine ml of 100% (v/v) FBS (PAA Laboratories GmbH) or cell culture medium was slowly dropped into the thawed cells, followed by centrifugation at 350 xg at 4°C in an Heraeus Multifuge 4KR centrifuge (DJB Labcare Ltd.) for 5 minutes. The supernatants were removed and discarded and cell pellets were the resuspended in fresh culture medium and incubated in a 37°C 5% CO_2 in air-water jacketed incubator (Triple Red Ltd.).

2.5. JAM-A cDNA Preparation and Ligation into the pCR®II-TOPO® Vector and Sequencing

2.5.1. Principle

In order to clone JAM-A full-length sequence into a lentiviral vector efficiently for generating JAM-A-expressing lentiviral vector particles described in the next section, two-step cloning was applied. In brief, the JAM-A-pENTR221 clone was purchased from I.M.A.G.E. clone in order to obtain JAM-A sequence. JAM-A sequence was added two specific restriction enzyme cutting sites in front and at the end of the sequence by PCR amplification

programme using designed primers. The JAM-A amplicons containing *Bam* HI and *Xho* I cutting sites were cloned into a pCR®II-TOPO® vector (Invitrogen Ltd.) for full-length sequencing by Source BioScience UK Ltd. (Nottingham, UK). After the JAM-A sequence was confirmed, it was cleaved at the designed cutting sites from the pCR®II-TOPO® vector

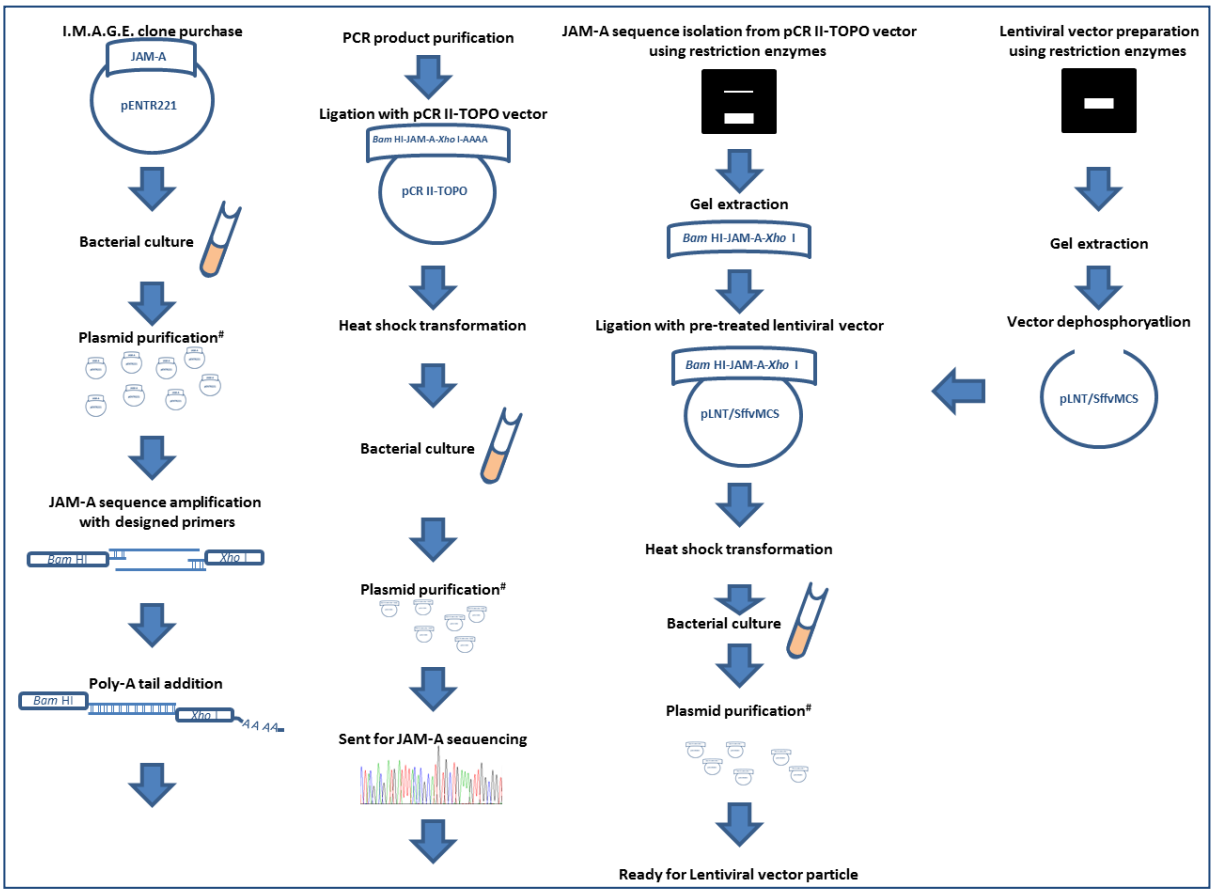

Figure 2.1. The flowchart of JAM-A containing lentiviral vector particle preparation.
The procedure of JAM-A expression lentiviral vector particle construction is shown schematically. The JAM-A containing vector was purchased from I.M.A.G.E. clone (top left-hand corner). The JAM-A sequence was amplified by PCR using designed primers to add two restriction digestion sites at each end of the JAM-A sequence. After adding a poly-A tail, the purified PCR product was cloned into the pCR II-TOPO vector and transformed into competent cells. The plasmid was purified and sent to Source BioScience UK Ltd. (Nottingham, UK) for sequencing. The validated sequence was restriction digestion from DNA isolated from the relevant clone and ligated into the prepared pLNT/SffvMCS lentiviral vector. After heat shock transformation, bacterial culture and plasmid purification, the JAM-A containing pLNT/SffvMCS lentiviral vector was ready for lentiviral vector particle preparation. #At each purification step, DNA was used for restriction enzyme digestion for sequence validation.

(Invitrogen Ltd.) by *Bam* HI and *Xho* I restriction enzymes and cloned into a pLNT/SffvMCS lentiviral vector for lentiviral vector particle production (Figure 2.1). The detailed cloning techniques that were used for JAM-A- pCR®II-TOPO® construct preparation was described in this section.

2.5.2. The JAM-A cDNA sequence and the pENTR221 vector

The JAM-A cDNA clone in the pENTR221 vector (Figure 2.3.A) was first purchased from I.M.A.G.E. clone (Clone #100066761, EU831732; Geneservice (http://www.lifesciences.sourcebioscience.com/). The sequence was based on EU831732 from PubMed and the JAM-A CDS (coding DNA sequence) region was at bps 23 to 919 as shown in gray in Figure 2.2. The restriction enzyme map of the JAM-A containing pENTR221 construct was predicted by NEB Cutter v2.0 (http://tools.neb.com/NEBcutter2/) and is shown in Figure 2.3.B.

JAM-A sequence (EU831732)

GTACAAAAAAGCAGGCTCCACCATGGGGACAAAGGCGCAAGTCGAGAGGAAACTGTTGTGCCTCTTCATATTGGCGATC
CTGTTGTGCTCCCTGGCATTGGGCAGTGTTACAGTGCACTCTTCTGAACCTGAAGTCAGAATTCCTGAGAATAATCCTGTG
AAGTTGTCCTGTGCCTACTCGGGCTTTTCTTCTCCCCGTGTGGAGTGGAAGTTTGACCAAGGAGACACCACCAGACTCGTT
TGCTATAATAACAAGATCACAGCTTCCTATGAGGACCGGGTGACCTTCTTGCCAACTGGTATCACCTTCAAGTCCGTGACA
CGGGAAGACACTGGGACATACACTTGTATGGTCTCTGAGGAAGGCGGCAACAGCTATGGGGAGGTCAAGGTCAAGCTCA
TCGTGCTTGTGCCTCCATCCAAGCCTACAGTTAACATCCCCTCCTCTGCCACCATTGGGAACCGGGCAGTGCTGACATGCT
CAGAACAAGATGGTTCCCCACCTTCTGAATACACCTGGTTCAAAGATGGGATAGTGATGCCTACGAATCCCAAAAGCACC
CGTGCCTTCAGCAACTCTTCCTATGTCCTGAATCCCACAACAGGAGAGCTGGTCTTTGATCCCCTGTCAGCCTCTGATACTG
GAGAATACAGCTGTGAGGCACGGAATGGGTATGGGACACCCATGACTTCAAATGCTGTGCGCATGGAAGCTGTGGAGCG
GAGTGTGGGGGTCATCGTGGCAGCCGTCCTTGTAACCCTGATTCTCCTGGGAATCTTGGTTTTTGGCATCTGGTTTGCCTA
TAGCCGAGGCCACTTTGACAGAACAAAGAAAGGGACTTCGAGTAAGAAGGTGATTTACAGCCAGCCTAGTGCCCGAAGT
GAAGGAGAATTCAAACAGACCTCGTCATTCCTGGTGAAGCTTGACCCAGCTTTCTTGTAC

Figure 2.2. The sequence of JAM-A cDNA (EU831732).
The sequence contains 943 nucleotides and the open reading frame start from 23 nt to end at 919 nt (gray). The information was obtained from NCBI (http://www.ncbi.nlm.nih.gov/nuccore).

The purchased JAM-A sequence-containing clone was firstly confirmed using restriction enzyme digestion based on the map in Figure 2.3.B. and the results are shown in Figure 4.15.

A

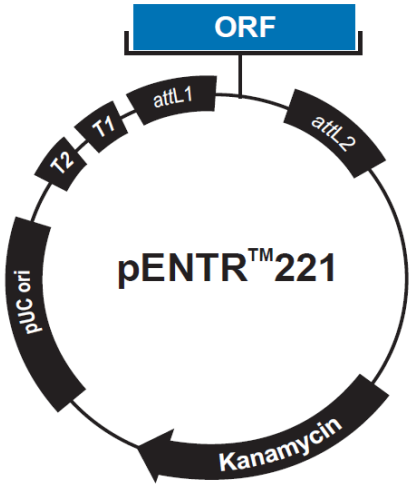

B

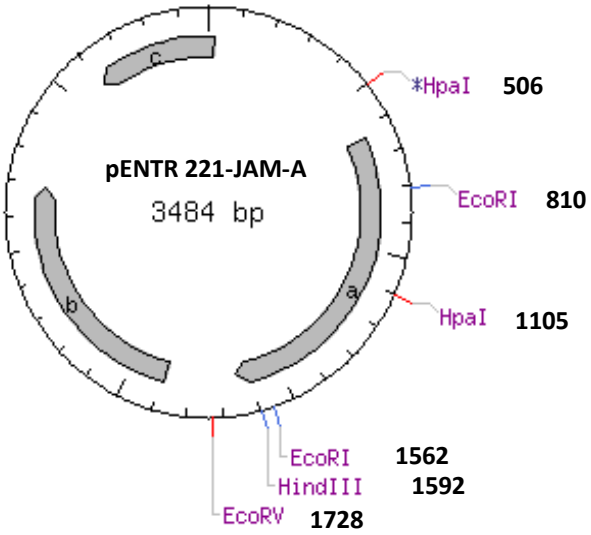

a:JAM-A, 338aa
b: Kanamycin resistance, 269aa
c: Origin of replication (ori)

Figure 2.3. Maps of original pENTR™221 vector and the JAM-A I.M.A.G.E. clone.
(A) The figure was taken from Invitrogen Ltd., and shows the elements of the pENTR™221 vector, including *rrn*B T2 transcription termination sequence (bps 268-295), *rrn*B T1 transcription termination sequence (bps 427-470), M13 forward (-20) priming site (bps 537-552), *att*L1 (bps 569-667, complementary strand), open reading frame insertion site (ORF, bps 668-669), *att*L2 (bps 617-770), M13 reverse priming site (bps 811-827), Kanamycin resistance gene (bps 940-1749) and pUC origin (bps 1870-2543). The construct for pENTR™221 without insert contained 2546 nucleotides. (B) The restriction enzyme restriction map of the JAM-A clone (Clone #100066761) was predicted using NEB Cutter v2.0 (http://tools.neb.com/NEBcutter2/).

2.5.3. Bacterial culture

The JAM-A-pENTR221 bacterial colony (purchased from I.M.A.G.E. clone (section 2.5.1)) was spread on LB (Luria-Bertani, 1 tablet in 50 mls sterile water containing 2 gs/L inert binder; Sigma-Aldrich Ltd.) agar plates (1.5% (w/v) of agar in LB solution; Sigma-Aldrich Ltd.) containing antibiotics, either 25 μgs/ml kanamycin (Sigma-Aldrich Ltd.) or 100 μgs/ml ampicillin (Sigma-Aldrich Ltd.) based on the DNA plasmid used.

The plates were incubated at 37°C in an Innova 4230 shaking incubator (New Brunswick Scientific Ltd., Hertfordshire, UK) for 12-16 hours until colonies appeared. Individual colonies were selected and initially inoculated in 2 mls of LB medium (Sigma-Aldrich Ltd.) containing appropriate antibiotics for 8 hour incubation in an Innova 4230 shaking incubator (250 r.p.m.; New Brunswick Scientific Ltd.) at 37°C. The mini bacterial culture was then inoculated into 200 mls of fresh LB medium with appropriate antibiotics and cultured in the same incubator at 37°C with 250 r.p.m. shaking overnight.

2.5.4. Plasmid DNA purification

Each bacterial culture was transferred to a 50 ml Falcon tube (Appleton Woods Ltd.) and harvested by centrifuging at 4,000 xg in Hettich Rotina 46R centrifuge (DJB Labcare Ltd.) for 10 minutes at room temperature and the supernatant medium was discarded. Plasmids were then purified using Midi PureLink™ HiPure Plasmid Filter Purification Kit (Invitrogen Ltd.) according to the manufacturer's instructions. In brief, the bacteria were resuspended in Resuspension Buffer with RNase A (20 mgs/ml in Resuspension buffer (R3), provided in the kit; Invitrogen Ltd.) at the ratio of 100 mls of bacterial culture in 10 mls of R3 Buffer (50 mM Tris-HCl pH 8.0, 10 mM EDTA) until the suspension was homogeneous. Next, an equal volume of L7 Lysis Buffer (0.2 M NaOH and 1% (w/v) SDS) was added for bacterial lysis by gently mixing and incubating for 5 minutes at room temperature followed by adding the

same volume of N3 Precipitation Buffer (3.1 M Potassium acetate pH 5.5). The Filter Midi Column was equilibrated with EQ1 equilibration Buffer (0.1 M Sodium acetate, pH 5.0, 0.6 M NaCl and 0.15% (v/v) Triton X-100) according to the instruction and the cell lysate was applied and allowed to run through by gravity flow. The Filter Midi Column was removed once the flow had stopped and washed with 20 mls of W8 Wash Buffer (0.1 M Sodium acetate pH 5.0, 825 mM NaCl) three times. The column was then placed in a 15 ml Falcon tube (Appleton Woods Ltd.) containing 3.5 mls of isopropanol (VWR International Ltd.) and 5 mls of E4 Elution Buffer (100 mM Trish-HCl pH 8.5 and 1.25 M NaCl) was added to the column for plasmid elusion. The supernatants were removed by centrifuging at 12,000 xg for 30 minutes at 4°C in a Hettich Rotina 46R centrifuge (DJB Labcare Ltd.). Following this, a 3 ml aliquot of 70% (v/v) ethanol (VWR International Ltd.) was added and then the DNA pellet was centrifuged at the highest speed for 5 minutes at 4°C in a Hettich Rotina 46R centrifuge (DJB Labcare Ltd.) prior to let air-dry. Finally, the DNA pellet was resuspended in 50 µls DEPC-water (Invitrogen Ltd.) and 2 µls of the solution was used for DNA concentration determination on the Thermo Scientific NanoDrop™ Spectrophotometer (Thermo Fisher Scientific Inc.). DNA was then diluted with DEPC-water (Invitrogen Ltd.) to a concentration of 1 µg/µl for use.

2.5.5. Restriction enzyme digestion

The restriction enzyme map of the plasmid was predicted on NEB Cutter v2.0 (http://tools.neb.com/NEBcutter2/) and a number of enzymes were selected for plasmid digestion and verification (Table 2.2). Five hundred ngs of DNA per condition was used for each enzyme digestion in the appropriate 1x NEB Buffer (Table 2.2; New England Biolab Ltd.) at 25°C in a water bath for 1 hour and the half of the product was subsequently separated

by agarose gel electrophoresis (section 2.5.6). Different combinations of restriction enzyme digest or digest solely were used for JAM-A sequence checking, while the combination of Bam HI and Xho I was used to cleave full-length of designed JAM-A sequence from pCR®II-TOPO® vector.

Table 2.2. Selected restriction enzymes and their working buffers.

Restriction Enzyme	# NEB Restriction enzyme Working buffer (Ingredients)	% Activity
Hpa I	NEB Buffer 4 (50 mM Potassium Acetate, 20 mM Tris-acetate, 10 mM Magnesium Acetate, 1 mM DTT, pH 7.9)	100%
Eco RI	NEB Buffer EcoRI (50 mM NaCl, 100 mM Tris-HCl, 10 mM $MgCl_2$, 0.025% Triton X-100, pH 7.9)	100%
Hpa I and *Eco* RI	NEB Buffer 4 (50 mM Potassium Acetate, 20 mM Tris-acetate, 10 mM Magnesium Acetate, 1 mM DTT, pH 7.9)	100% and 100%
Eco RV	NEB Buffer 3 (100 mM NaCl, 50 mM Tris-HCl, 10 mM $MgCl_2$, 1 mM DTT, pH 7.9)	100%
Hind III	NEB Buffer 2 (50 mM NaCl, 10 mM Tris-HCl, 10 mM $MgCl_2$, 1 mM DTT, pH 7.9)	100%
Eco RV and *Hind* III	NEB Buffer 2 (50 mM NaCl, 10 mM Tris-HCl, 10 mM $MgCl_2$, 1 mM DTT, pH 7.9)	75% and 100%
Bam HI and *Xho* I	NEB Buffer 3 (100 mM NaCl, 50 mM Tris-HCl, 10 mM $MgCl_2$, 1 mM DTT, pH 7.9)	100%

2.5.6. DNA gel electrophoresis

Purified or restriction enzyme digested DNA plasmids or PCR fragments were subjected to agarose gel electrophoresis for their molecule size verification. DNA (250 ngs) was mixed with 10X BlueJuice Gel Loading Buffer (65% (w/v) Sucrose, 10 mM Tris-HCl pH 7.5, 10 mM EDTA and 0.3% (w/v) Bromophenol Blue; Invitrogen Ltd.) and topped up with DEPC-water (Invitrogen Ltd.) to give 250 ng of DNA in 10µl of 1X gel loading buffer. Agarose gels (0.7% (w/v)) were made by dissolving agarose (Sigma-Aldrich Ltd.) in 1X TAE buffer diluted from 10X TAE buffer (400 mM Tris-acetate and 10 mM EDTA; Invitrogen Ltd.) containing 1X

GelRed™ (1: 10,000 dilution from the stock; Biotium Inc.) in a HU6 Mini Horizontal Gel Unit (Camlab Ltd., Cambridge, UK). After the gel solidified, the gel was transferred to a gel running tray (Camlab Ltd.) and fresh prepared 1X TAE buffer was added until it covered the gel. Two hundred and fifty ngs of DNA sample was used for size checking. Two μls DNA Ladder (Agilent Technologies Inc.) were then applied in a separate well on the gel in each experiment and the gel electrophoresed at 80-120 volts for 30-60 minutes. The gel was placed under a UV light (UVitech Ltd., Cambridge, UK) for DNA detection.

2.5.7. JAM-A primer design

The JAM-A PCR primers were designed based on the first 22-24 nucleotides of EU831732 sequence from the indicated start or stop codons (Figure 2.2) and were synthesised by Eurofins MWG Operon (Ebersberg, Germany). The forward primer (5'-CGGGATCCGCCACCATGGGGACAAAGGCGCAAGTCG-3') included, starting from the 5'-end, two random nucleotides (5'-CG-3'), a *Bam* HI restriction cutting site (5'-GGATCC-3') and a Kozak sequence (5'-GCCACC-3') (309-311), and the reverse primer (5'-CGCTCGAGCTACACCAGGAATGACGAGGTCTG-3') included, starting from the 5'-end, two random nucleotides (5'-CG-3'), an *Xho* I restriction site (5'-CTCGAG-3') and a stop codon (5'-CTA-3') at the 5'-end.

2.5.8. 2-step polymerase chain reaction (2-step PCR)

The extracted JAM-A-pENTRA221 plasmid after restriction enzyme digestion verification was used as template to amplify the JAM-A sequence using designed primers and *Pfu*Turbo® DNA polymerase (Stratagene Ltd.). Fifty ngs of DNA template was mixed with 1 mM dNTP mixture (Promega Co.), 0.2 μM forward and reverse primers and 2.5 units of *Pfu*Turbo® DNA polymerase in 1X of *Pfu*Turbo® DNA PCR buffer that was diluted from 10X buffer (200 mM

Tris-HCl pH 8.8, 20 mM $MgSO_4$, 100 mM KCl, 100 mM $(NH_4)SO_4$, 1% Triton X-100 and 1 mg/ml nuclease-free BSA, supplied with the kit; Stratagene Ltd.). The reaction was performed using a 2-step PCR programme. This included heating to 95°C for 2 minutes, followed by 10 cycles of 95°C for 45 seconds, 56°C for 45 seconds and 72°C for 1.5 minutes, and another 25 cycles of 95°C for 45 seconds, tested annealing temperature from 62-69°C (Figure 4.16) for 45 seconds and 72°C for 1.5 minutes, and a final elongation at 72°C for 10 minutes using a T3000 ThermoCycler PCR machine (Biometra GmbH).

2.5.9. Poly-A tail addition to PCR fragments for vector cloning

In order to ligate the JAM-A PCR amplicons into the TOPO TA cloning® vector (Invitrogen Ltd.), a poly-A tail was added to the PCR products using Immolase™ DNA polymerase (Gentaur GmbH). For this, 15 µls of PCR product was mixed with 5mM dATP (Promega Co.), 5 units of DNA polymerase and 5mM $MgCl_2$ in 1X ImmoBuffer that was diluted from 10X buffer (160 mM $(NH_4)_2SO_4$, 1 M Tris-HCl pH 8.3, and 0.1% Tween-20, supplied with the kit; Gentaur GmbH) at 70°C for 45 minutes using a T3000 ThermoCycler PCR machine (Biometra GmbH).

2.5.10. PCR product purification

The PCR product was added to 5 times the gel volume of the Buffer QG (Qiagen Ltd., Manchester, UK) and mixed well before the whole mixture was transferred to an elution column. The column was centrifuged at 12,000 xg in a Hettich Mikro 46R centrifuge (DJB Labcare Ltd.) for 1 minute at room temperature prior to washing the column with 750 µls Wash Buffer PE (Qiagen Ltd.) containing ethanol (VWR International Ltd.) at 12,000 xg in an Hettich Mikro 46R centrifuge (DJB Labcare Ltd.) for 1 minute. All the eluant was discarded. The column was centrifuged at 12,000 xg in a Hettich Mikro 46R centrifuge (DJB Labcare

Ltd.) for additional 2 minutes before placing it in a clean 1.5 ml eppendorf tube (Appleton Woods Ltd.) for elution of the DNA. 30 µls of pre-heated DEPC-water (Invitrogen Ltd.) was added to the column and incubated at room temperature for 5 minutes before centrifuging the column at 12,000 xg in an Hettich Mikro 46R centrifuge (DJB Labcare Ltd.) for 2 minutes at room temperature. The DNA concentration was determined using a Thermo Scientific NanoDrop™ Spectrophotometer (Thermo Fisher Scientific Inc.).

2.5.11. DNA ligation

After purification, the poly-A tail containing JAM-A DNA fragment was cloned into pre-digested pCR® II-TOPO® vector (Figure 2.4; Invitrogen Ltd.) using a DNA ligation kit (TaKaRa Bio Inc.) at various ratios of vector to insert (1:0.5, 1:1, and 1:2; Table 4.2). One µl of vector was mixed with 0.5-2 µls insert and topped up to 6 µl with DEPC-water (Invitrogen Ltd.). An equal volume of ligation Mix (TaKaRa Bio Inc.) was then added and the mixture incubated at 16°C in a water bath for 30 minutes according to the manufacturer's instructions. Three to five µls of the ligation product was used for transformation.

2.5.12. Heat shock transformation

One shot® TOP10 (Invitrogen Ltd.) or JM109 (Stratagene Ltd.) competent bacteria were used for heat shock transformation using the manufacturer's instructions. Three to five µls of the JAM-A- pCR® II-TOPO® ligation product were mixed with 50 µls of TOP 10 competent bacteria (Invitrogen Ltd.) on ice for 30 minutes and the mixture was heat shocked at 42°C for 30 seconds in a water bath. Two hundred and fifty µls of S.O.C. medium (2% tryptone, 0.5% yeast extract, 10 mM NaCl, 2.5 mM KCl, 10 mM $MgCl_2$, 10 mM $MgSO_4$, and 20 mM glucose; Invitrogen Ltd.) were then added to the mixture and incubated in an Innova 4230 shaking incubator (New Brunswick Scientific) at 37°C for 1 hour. Approximately 80-100 µls of

resulting bacteriawers streaked out on LB agar plates containing 100 µgs/ml ampicillin (Sigma-Aldrich Ltd.) as described in section 2.5.3.

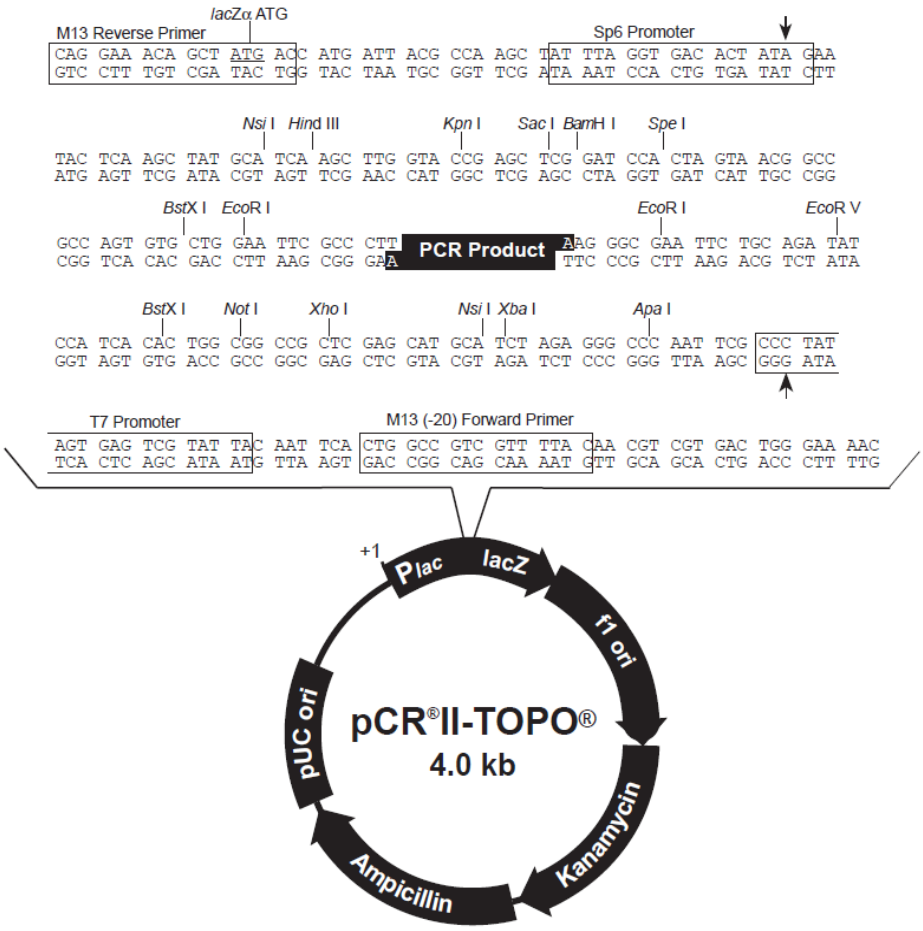

Figure 2.4. pCR®II-TOPO® vector map.
The figure was taken from Invitrogen Ltd. and shows the elements on the pCR®II-TOPO® vector, including the *Lac*Z gene (bps 1-589), M13 Reverse priming site (bps 205-221), Sp6 promoter (bps 239-256), Multiple Cloning Site (bps 269-383), T7 promoter (bps 406-425), M13 (-20) Forward priming site (bps 433-448), f1 origin (bps 590-1027), Kanamycin resistance ORF (bps 1361-2155), Ampicillin resistance ORF (bps 2173-3033) and pUC origin (bps 3178-3851). The pCR®II-TOPO® without insert comprised 3974 nucleotides.

2.5.13. JAM-A cDNA sequencing

Nine JAM-A-pCR®II-TOPO® clones were identified as having the full-length JAM-A sequence by *Bam* HI and *Xho* I digestion (Chapter 4, Figure 4.18) and three (clone #3, #4 and #8) were then selected for sequencing by Source BioScience UK Ltd. (Nottingham, UK) using M13

forward and reverse primers supplied by the company. Clone #8 contained the correct sequence (Chapter 4, Figure 4.17) and was used for lentiviral vector production (section 2.6).

2.6. Lentiviral Vector Production, Storage and Transduction of Target Cells

2.6.1. Principle

Once the JAM-A sequence was inserted into the pCR®II-TOPO® vector (section 2.5) it was then cloned into a lentiviral vector in order to generate JAM-A-expressing lentiviral vector particles. The full-length JAM-A sequence was cleaved from pCR®II-TOPO® vector using a combination of *Bam* HI and *Xho* I restriction enzymes and ligated into a pre-digested lentiviral genome vector, pLNT/SffvMCS lentiviral vector (Figure 2.5). The ligated JAM-A-pLNT/SffvMCS lentiviral genome vector, along with packaging vector pΔ8.91 (Figure 2.6) and envelope vector pVSV-G (Figure 2.7) were then transfected into HEK293T cells for producing lentiviral vector particle. As the pLNT/SffvMCS lentiviral genome vector did not contain any reporter gene for subsequent titrations (section 2.6.10.) and M.O.I. determinations (section 2.6.11.), an eGFP-containing lentiviral genome vector, pHR'SINcPPT-SEW vector (Figure 2.8), was used to make eGFP-containing lentiviral vector particles in parallel with the JAM-A-containing lentiviral vector particle production. The M.O.I. of JAM-A-containing lentiviral vector particles were then estimated from the tirtrationof eGFP-containing lentiviral vector particles.

2.6.2. Lentiviral vector maps

The lentiviral genome vectors, the pLNT/SffvMCS lentiviral vector (Figure 2.5), the eGFP containing genome vector, pHR'SINcPPT-SEW vector (Figure 2.8), the packaging vector pΔ8.91 (Figure 2.6) and the envelope vector pVSV-G (Figure 2.7) were individually transformed into JM109 competent bacteria (Stratagene Ltd.) and streaked out on LB agar

plates (Sigma-Aldrich Ltd.) containing 100 μgs/ml ampicillin (Sigma-Aldrich Ltd.) followed by incubation overnight at 37°C in an Innova 4230 shaking incubator (New Brunswick Scientific). Individual colonies were picked up and inoculated into LB containing 100 μgs/ml ampicillin (Sigma-Aldrich Ltd.) for plasmid purification. The details are similar to those described in section 2.5.

2.6.2.1. pLNT/SffvMCS lentiviral vector

This vector was kindly provided by Professor Adrian Thrasher, Institute of Child Heath, London, and was used for overexpression of JAM-A. The JAM-A sequence was cloned into the multiple *Bam*HI, *Xho*I, *Kpn*I and *Mul*I restriction enzyme cloning site of this vector(shown in the top left region of the vector; Figure 2.5).

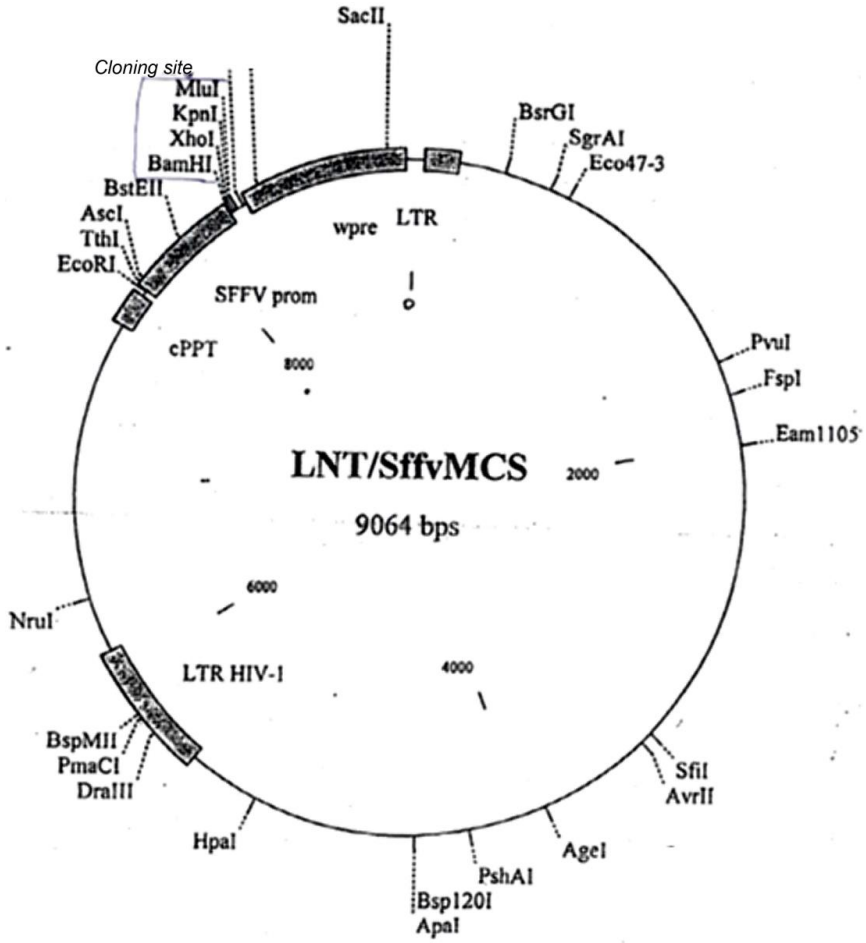

Figure 2.5. The pLNT/SffvMCS lentiviral vector map.
The figure shows the main elements on the vector, including the LTR HIV-1, the cPPT (central polypurine tract) and the SFFV (spleen focus-forming virus) promoter region in front of the multiple *Bam*HI, *Xho*I, *Kpn*I and *Mul*I cloning site, followed by the woodchuck hepatitis virus posttranscriptional regulatory element (wpre) and long terminal repeats (LTR). The pLNT/SffvMCS lentiviral vector without insert comprised 9064 nucleotides. (kindly provided by Dr. Enca Rendon-Martin).

2.6.2.2. pΔ8.91 vector

The pΔ8.91 vector(Figure 2.6) was kindly provided by by Professor Adrian Thrasher, Institute of Child Heath, London. This vector was used for co-transfection with the pLNT/SffvMCS lentiviral vector and the pVSV-G vector into HEK 293T cells to form lentiviral particles. The pΔ8.91 vector is a packaging vector able to recognise the packaging sequence (ψ) in the pLNT/SffvMCS lentiviral vector and packaged the transcribed RAN (Ribonucleic acid) from the pLNT/SffvMCS lentiviral vector into newly made viral particles.

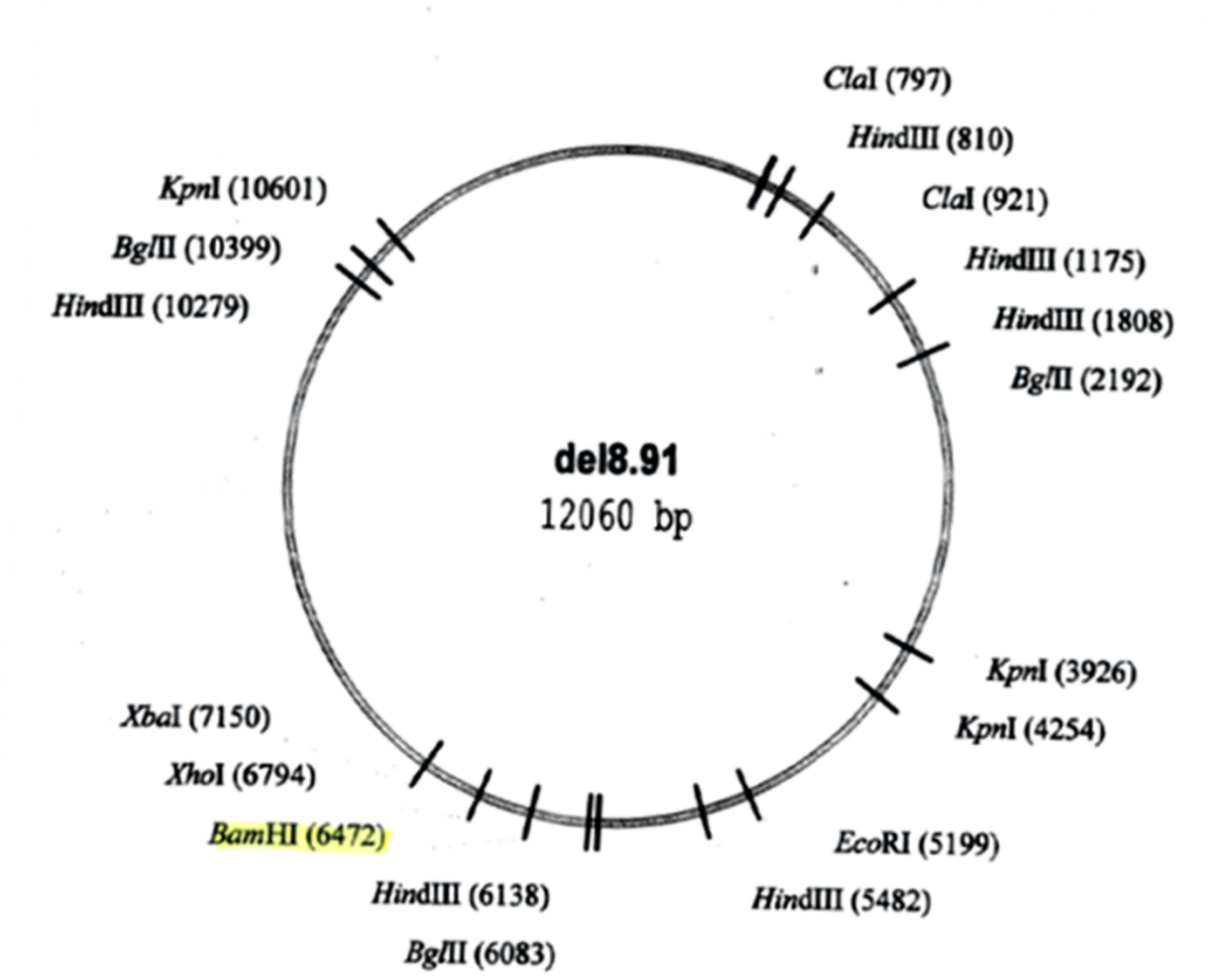

Figure 2.6. The pΔ8.91 vector restriction map.
The shows the restriction enzyme sites on the vector. The pΔ8.91 vector comprised 12060 nucleotides. (kindly provided by Dr. Enca Rendon-Martin).

2.6.2.3. pVSV-G vector

This pVSV-G vector (Figure 2.7) was kindly provided by Professor Adrian Thrasher, Institute of Child Heath, London. This vector contains the viral envelope gene and was co-transfected with the pLNT/SffvMCS lentiviral vector and packaging vector (pΔ8.91) into the HEK 293T cell line to produce lentiviral particles.

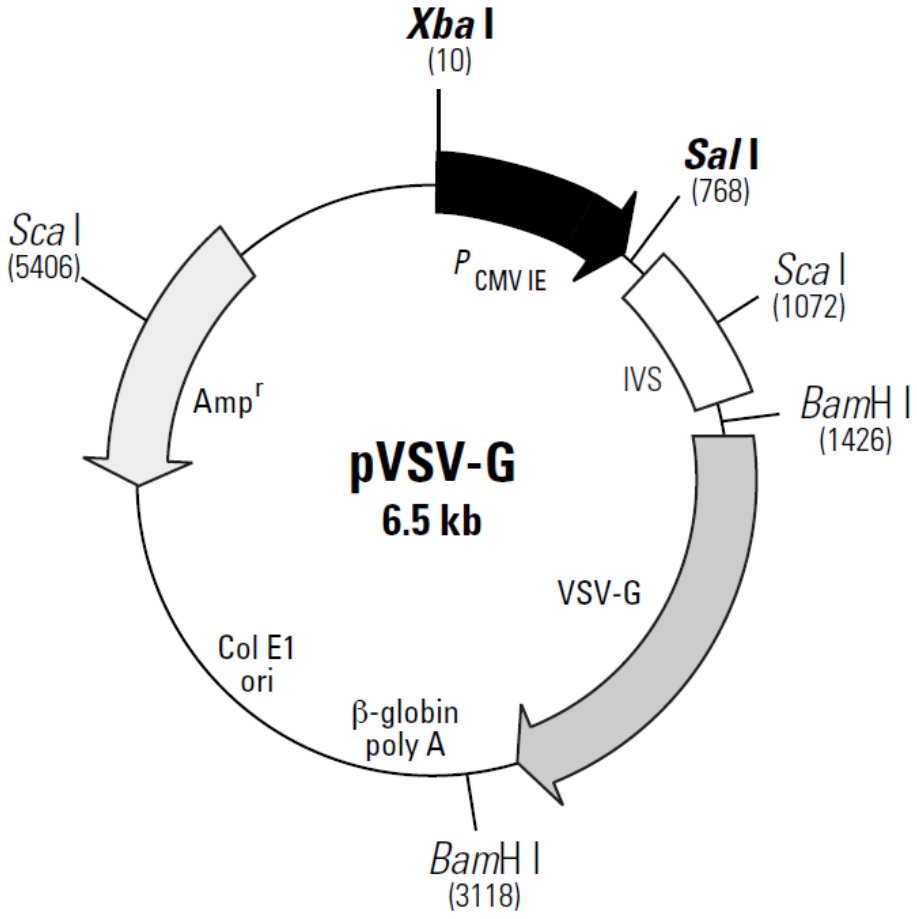

Figure 2.7. The pVSV-G vector map.
The figure was taken from Clontech Laboratories, Inc. and shows the elements on the pVSV-G vector, including the CMV promoter (bps 1–768), Rabbit β-globin IVS (intervening sequence; bps 768–1432), VSV-G envelope gene start codon (bps 1450–1452) and stop codon (bps 2983–2985), β-globin poly A sequence (bps 3288–3293), Col E1 origin of replication, site of replication initiation (bps 4087), and ampicillin resistance gene (β-lactamase) start codon (bps 5712–5710) and stop codon (bps 4853–4851). The pVSV-G vector comprised 6500 nucleotides. This figure was taken from http://old.takara.co.kr/pds/shop/product/reffile/PT3343-5W.pdf (Clontech Laboratories, Inc.).

2.6.2.4. The pHR'SINcPPT-SEW vector

This vector (Figure 2.8) was kindly provided by Professor Adrian Thrasher, Institute of Child Heath, London. This viral vector contained enhanced green fluorescent protein cDNS (eGFP) and when co-transfected with the pΔ8.91 lentiviral vector and pVSV-G vector into HEK 293T cells to form lentiviral particles.

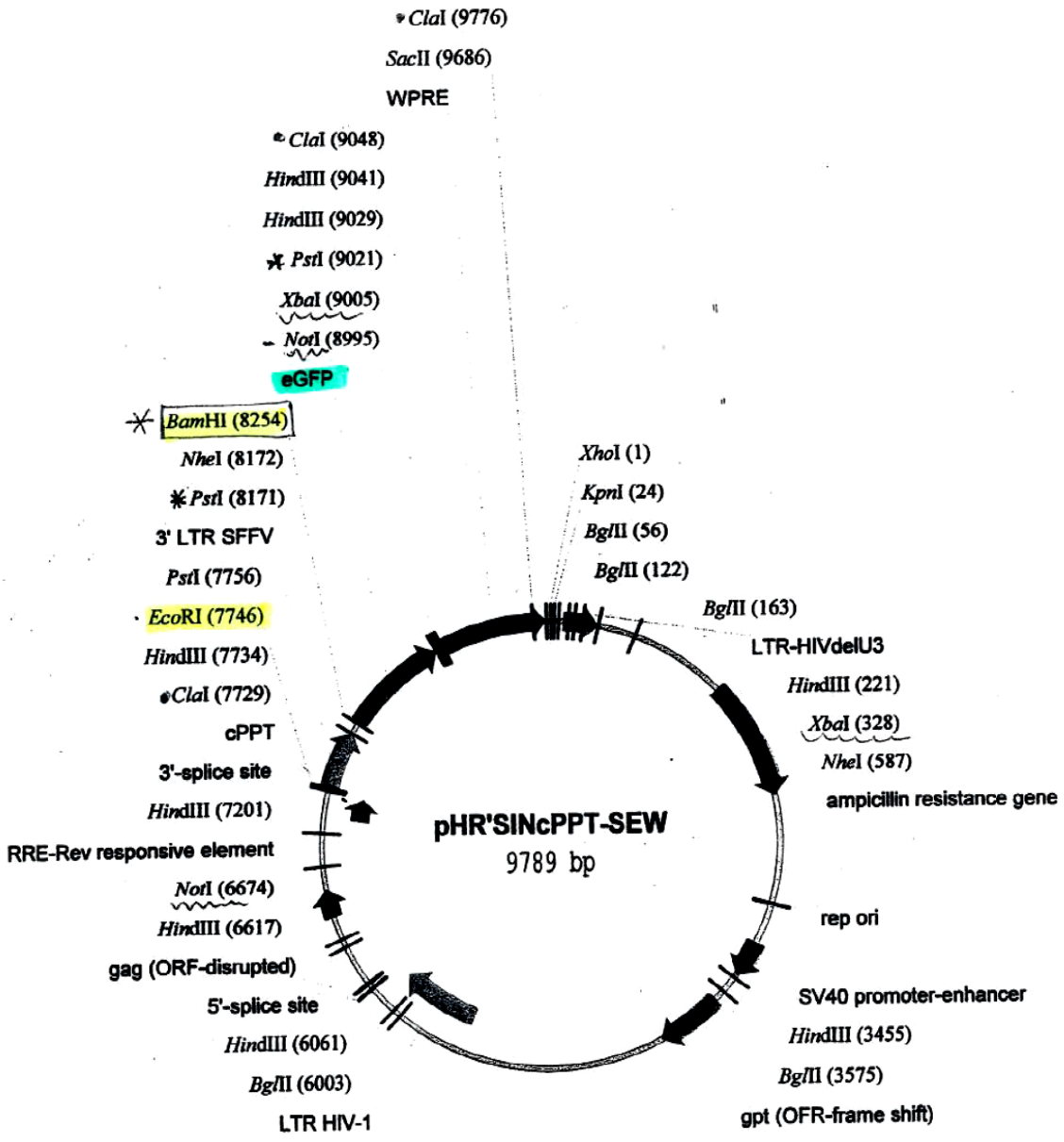

Figure 2.8. pHR'SINcPPT-SEW vector restriction map.
The figure shows the main elements on the vector. The comments for pHR'SINcPPT-SEW vector were 9789 nucleotides. (kindly provided by Dr. Enca Rendon-Martin).

2.6.3. JAM-A sequence and pLNT/SffvMCS lentiviral vector preparation

After the JAM-A sequence from JAM-A-pCR®II-TOPO® clone #8 was confirmed (section 2.5.13), the plasmid, as well as the purified pLNT/SffvMCS lentiviral vector (Figure 2.5), were digested using a combination of *Bam* HI and *Xho* I (section 2.5.5) to generate aJAM-A full-length sequence and an open pLNT/SffvMCS lentiviral vector, respectively. The digested products were subjected to DNA agarose gel for separation and purification as described below.

2.6.4. Gel extraction

The digested DNA fragment or the lentiviral vector was separated by gel electrophoresis (section 2.5.6) and the predicted band was excised under UV light in a minimal area of gel using a clean, sharp razor blade. The excised gel was weighed and then 3 times the gel volume of the Buffer QG (Qiagen Ltd.) was added. The gel was then incubated at 50°C for 10 minutes until the gel slice dissolved. One gel volume of 100% isopropanol (VWR International Ltd.) was then added and mixed well before the whole mixture was transferred to an elution column. The column was centrifuged at 12,000 xg in an Hettich Mikro 46R centrifuge (DJB Labcare Ltd.) for 2 minutes at room temperature prior to washing the column with 750 µls Wash Buffer PE (Qiagen Ltd.) containing ethanol (VWR International Ltd.) at 12,000 xg in a Hettich Mikro 46R centrifuge (DJB Labcare Ltd.) for 2 minutes. All the eluant was discarded. The column was centrifuged at 12,000 xg in a Hettich Mikro 46R centrifuge (DJB Labcare Ltd.) for additional 3 minutes before placing it in a clean 1.5 mls eppendorf tube (Appleton Woods Ltd.) for elution of the DNA. 30 µls of pre-heated DEPC-water (Invitrogen Ltd.) were added to the column and incubated at room temperature for 5 minutes before centrifuging the column at 12,000 xg in a Hettich Mikro 46R centrifuge (DJB Labcare Ltd.) for 2 minutes at room temperature. The DNA concentration was

determined using a Thermo Scientific NanoDrop™ Spectrophotometer (Thermo Fisher Scientific Inc.).

2.6.5. pLNT/SffvMCS lentiviral vector dephosphorylation

The purified pLNT/SffvMCS lentiviral vector was firstly digested using a combination of *Bam* HI and *Xho* I restriction enzymes (section 2.5.5) and then the TSAP (Thermosensitive Alkaline Phosphatase) kit (Promega Co.) was used to dephosphorylate the digestion site. Five μgs of purified pLNT/SffvMCS lentiviral vector (Figure 2.5) were dephosphorylated using 5 units of TSAP phosphatase in 10 μls of the kit supplied working buffer (250 mM Tris-acetate, pH 7.5, 1 M potassium acetate, 100 mM magnesium acetate and 10 mM DTT) at 37°C for 15 minutes. The reaction was then inactivated at 74°C for 15 minutes.

2.6.6. JAM-A- pLNT/SffvMCS lentiviral vector construction

The purified JAM-A sequence from section 2.6.4 and dephosphorylated pLNT/SffvMCS lentiviral vector from section 2.6.5 were subsequently ligated and transformed into JM109 competent bacteria (Stratagene Ltd.), followed by colony amplification and plasmid purification. The procedures followed the description in section 2.5. The JAM-A-pLNT/SffvMCS lentiviral vector construct was used to generate lentiviral vector particle in HEK293T cells as described in the following sections.

2.6.7. Culture of HEK239T cells for lentiviral vector particle production

HEK293T cells were defrosted from liquid nitrogen at 37°C as described in section 2.4 and cultured as described in section 2.2.1. The cells were cultured in T75 tissue culture grade flasks (Appleton Woods Ltd.) until they reached 70-80% confluence. The HEK293T culture medium was replaced with 30 mls of fresh DMEM medium (PAA Laboratories GmbH) containing 10% FBS (PAA Laboratories GmbH) on the day of transfection.

2.6.8. Transfection of HEK293T cells using Lipofectamine 2000

eGPF containing lentiviral vector particles (LV-eGFP viral particles) were made using the pHR'SINcPPT-SEW vector in parallel to the other non-eGPF lentiviral vector particles. Two 15ml Falcon tubes (Appleton Woods Ltd.) were used and 3.75 mls Opti-Mem medium (Invitrogen Ltd.) added to each tube. The three lentiviral vectors, namely 50 μgs of the lentiviral vector (either JAM-A containing pLNT/SffvMCS vector or pHR'SINcPPT-SEW vector), 17.5 μgs of the pΔ8.91 vector and 17.5 μgs of the pVSV-G vector, were added together in one tube, while 200 μl of Lipofectamine 2000 (Invitrogen Ltd.) was added into the other tube. The contents of the two tubes were then gently mixed together by inversion five times and this was followed by incubation at room temperature for 20 minutes. The transfection mixture was then added to the HEK293T cells containing the freshly prepared 30 mls of culture medium and incubated in a 37°C 5% CO_2 in air in a water-jacketed incubator (MCO-20AIC, Triple Red Ltd.) overnight. The incubation medium was removed on the next day and replaced with 15 mls of fresh culture medium.

2.6.9. Lentiviral particle harvest and storage

At 48 hours post transfection, the HEK293T culture medium was collected in 15ml Falcon tubes (Appleton Woods Ltd.) and centrifuged at 350 xg at room temperature in an Heraeus Multifuge 4KR centrifuge (DJB Labcare Ltd.) for 5 minutes. The supernatants were aliquoted into 2 ml cryovials (Alpha Laboratories Ltd., Hampshire, UK) and frozen at -80°C.

2.6.10. Titration of eGFP lentiviral vector particles

The eGPF containing lentiviral particles (LV-eGFP viral particles) made using pHR'SINcPPT-SEW vector were used in this titration. $5x10^4$ HEK 293T cells per well were plated into a 24-well plate (flat clear bottom; Appleton Woods Ltd.) the day before assaying and incubated in

a 37°C 5% CO_2 in air water-jacketed incubator (MCO-20AIC, Triple Red Ltd.). The medium was removed prior to adding the LV-eGFP viral particles at different dilutions from $1:10^{-3}$ to $1:10^{-6}$. The LV-eGFP viral particle stock was serially diluted with fresh HEK 293T culture medium and 1 ml of the diluted viral vector applied to wells containing HEK 293T cells. The assay was performed in triplicate for each dilution. The infected green cells were monitored at 24 hours post transduction under an Eclipse TE2000-U inverted microscope (Nikon UK Ltd.) as shown in Figure 2.9. The transduction units per ml (T.U. /ml) were calculated according to the equation:

$$\text{Titre} = \frac{\text{Average of green colonies}}{\text{Dilution factor}} = \text{T.U. /ml}$$

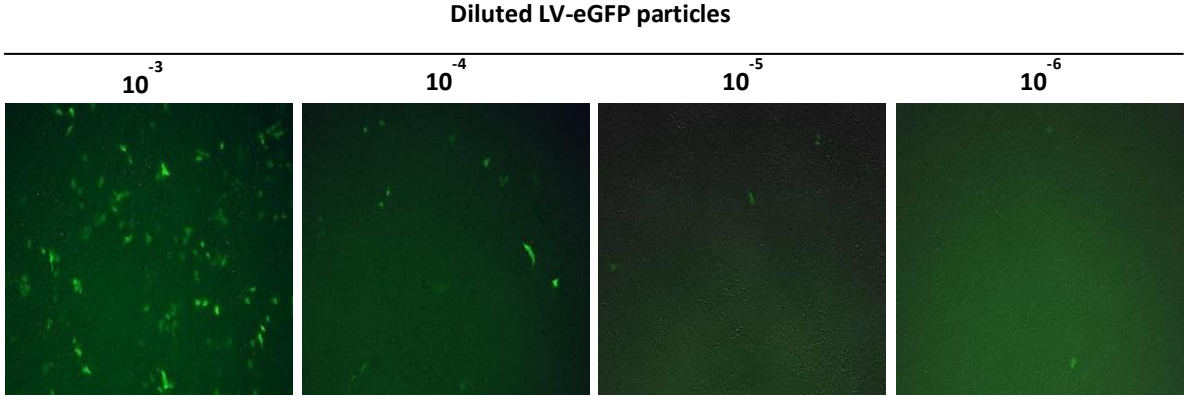

Figure 2.9. Titration in HEK 293T cells of LV-eGFP viral particles.
The LV-eGFP lentiviral particles at various dilutions were titrated in HEK 293T cells. The images represent the numbers of green colonies observed with viral stock dilutions ranging from 10^{-3} to 10^{-6}. Magnification: X4.

As the JAM-A containing pLNT/SffvMCS vector does not incorporate any reporter genes, such as eGFP, for titration detection, the result of the LV-eGFP viral particles was used as estimation for the JAM-A-pLNT/SffvMCS vector. For more accurate determinations of viral titres in future, eGFP should be substituted for JAM-A in the JAM-A-pLNT/SffvMvc vector so

that transduction efficiency can then be measured by flow cytometry. To measure the accuracy of viral titre estimations in the eGFP or JAM-A transduced cells, PCR analyses would also need to be applied using primers specific for the JAM-A or eGFP constructs to measure the viral vector copy numbers in the cells.

2.6.11. Multiplicity of Infection (M.O.I.) determination

The multiplicity of infection (M.O.I.) in target cells was assessed using the eGFP-containing viral vector particles as the JAM-A-pLNT/SffvMCS vector did not contain a reporter gene. The eGFP-containing lentiviral vector was made in parallel and used to estimate the M.O.I. of the JAM-A overexpression lentiviral vector. When transducing suspension cells, $2x10^5$ Jurkat cells were seeded into a 24-well plate (flat clear bottom; Appleton Woods Ltd.) containing 0.5 mls culture medium, and 0.5 mls of diluted eGFP-containing lentiviral vector particles was applied to measure the optimal M.O.I. for the cells (M.O.I.=0 to M.O.I.=40 in Figure 4.22). The transduced cells were incubated in a 37°C 5% CO_2 in air water-jacketed incubator (MCO-20AIC, Triple Red Ltd.) and examined at 48 hours post transduction under an Eclipse TE2000-U inverted microscope (Nikon UK Ltd.). The percentage of transduced cells was also measured by FACS analysis using a BD LSR II flow cytometer (section 2.9). The optimal M.O.I. was determined of using the lentiviral vector particles with the highest transduction efficiency while maintaining cell viability.

2.7. RNA Interference Using siRNA and Nucleofection

An Inventoried Silencer® Select Pre-designed JAM-A siRNA set was synthesised by and purchased from Ambion® (Invitrogen Ltd.), and contained one non-silencing control and three different siRNA fragments targeting the 3'UTR of human JAM-A mRNA (Table 2.3). To optimise the working concentration of siRNAs using the nucleofection system, a

fluorescence-labelled siRNA (Tye563 Fluorescent-labelled siRNA duplex; OriGene Technologies, Inc.) was applied to HL-60 cells prior to JAM-A siRNAs being applied. One siRNA concentration was selected to verify JAM-A knock-down efficiency in HL-60 cells. Once the knock-down efficiency was determined, the siRNAs at these concentrations were applied to UCB $CD34^+$ cells. The knock-down efficiency and cell viability post nucleofection were measured by FACS (section 2.9).

Table 2.3. JAM-A siRNAs

Description	siRNA ID	Sense Sequence (5'-3')	Antisense Sequence (5'-3')
Non-Silencing control		N.A.	N.A.
JAM-A siRNA-150	s27150	GCCUAGUGCCCGAAGUGAAtt	UUCACUUCGGGCACUAGGCtg
JAM-A siRNA-151	s27151	CCAUCCAAGCCUACAGUUAtt	UAACUGUAGGCUUGGAUGGag
JAM-A siRNA-152	s27152	GGAUAGUGAUGCCUACGAAtt	UUCGUAGGCAUCACUAUCCca
Tye563 Fluorescent-labelled siRNA duplex	SR30002	N.A.	N.A.

N.A.: Not available.

HL-60 cells were harvested after culture in IMDM medium (Invitrogen Ltd.) with 20% (v/v) FBS (PAA Laboratories GmbH) in a 37°C 5% CO_2 in air water-jacketed incubator (MCO-20AIC, Triple Red Ltd.) when they reached a density of 6-9x10^5 cells/ml. The culture medium was removed by transferring the cells to a 15 ml Falcon tube (Appleton Woods Ltd.) and centrifugation at 90g in an Heraeus Multifuge 4KR centrifuge (DJB Labcare Ltd.) at room temperature for 10 minutes. 2x10^6 cells were resuspended in 100 µls of the Nucleofector® Solution that was pre-mixed with supplement (Lonza Biologics). Twenty nM, 100 nM and 200 nM of the Tye563 Fluorescent-labelled siRNA duplex were added separately to the 100 µls of cell suspension and mixed well before the cell/siRNA mixtures were transferred to cuvettes. The HL-60 cells were nucleofected using the Amaxa Cell line nucleofector Kit V (Lonza Biologics) and programme T-019 (Amaxa Nucleofector® I Device) following the

manufacturer's instructions. Once the programme had finished, 0.5 mls of cell culture medium was then added and the total samplewas transferred to 12-well plate (flat clear bottom; Appleton Woods Ltd.) containing 1 ml/well of pre-warmed HL-60 cell culture medium. The nucleofected cells were then incubated in a 37°C 5% CO_2 in air water-jacketed incubator (MCO-20AIC, Triple Red Ltd.) and tested at the indicated time points.

As for UCB $CD34^+$ cells, $1x10^6$ cells per reaction were used according to the manufacturer's instructions. The UCB MNCs were thawed for CD34 positive cell isolation the day before nucleofection. The isolated UCB $CD34^+$ cells were then placed at $1x10^6$ cells/ml in StemSpan medium (Stem Cell Technologies) with 100 ngs/ml of Flt-3 ligand (R&D Systems, Inc.), IL-6 (R&D Systems, Inc.) and SCF (R&D Systems, Inc.) and 20 ngs/ml of TPO (R&D Systems, Inc.) in a 37°C 5% CO_2 in air water-jacketed incubator (MCO-20AIC, Triple Red Ltd.) overnight. On the day of nucleofection, UCB $CD34^+$ cells were harvested by centrifuging at 200g in a Heraeus Multifuge 4KR centrifuge (DJB Labcare Ltd.) at room temperature for 10 minutes. $1x10^6$ cells were resuspended in 100 µls of the Nucleofector® Solution from the Amaxa Human $CD34^+$ cell Nucleofector Kit (Lonza Biologics) which had been pre-mixed with the kit provided supplement at the ratio of 4.5:1 (Lonza Biologics). Following this, 100 nM of the functionally validated siRNAs was applied separately to the 100 µls of cells and mixed well before the cell/siRNA mixtures were transferred to cuvettes. The programme U-008 (Amaxa NucleofectorR® I Device) was used for nucleofection according to the manufacturer's instructions. Once the programme was finished, 0.5 mls of the StemSpan cell culture medium was then added and the total sample was transferred to 12-well plate (flat clear bottom; Appleton Woods Ltd.) containing 1 ml/well of pre-warmed StemSpan medium with cytokines as described above. The nucleofected cells were then incubated in a 37°C CO_2 air-jacked incubator (Triple Red Ltd.) and analysed at the indicated time points.

2.8. Immunofluorescence Analysis

Eight-well glass culture slides (BD Falcon™; Becton Dickinson Ltd.) were coated with 150 μls of 10 μgs/ml fibronectin (Sigma-Aldrich Ltd.) in HBSS (PAA Laboratories GmbH) at 4°C overnight. After the fibronectin solution was removed, the slides were allowed to air dry before 150 μls of 200 ngs/ml CXCL12 (Peprotech) in HBSS (PAA Laboratories GmbH) were added. The slides were then incubated at 37°C for 30 minutes prior to cells being added. The cells were harvested and resuspended in their basic medium with 0.5% (w/v) BSA (Sigma-Aldrich Ltd.) at a density of 1-2x10^5 cells per 100 μls. One hundred μls of cells were added per well and incubated for the indicated times, before being fixed in 4% (w/v) paraformaldehyde (Sigma-Aldrich Ltd.) for 15 minutes at room temperature. The fixed cells were then blocked in 150 μls of the blocking solution (4% (w/v) BSA in HBSS) for 30 minutes at 4°C. The primary antibodies and secondary antibodies (Table 2.4) were diluted in 2% (w/v) BSA in HBSS to the working concentrations (Table 2.5) and 100 μls applied to the wells at 4°C overnight.

Table 2.4. The list of antibodies used in immunofluorescence assay.

Antibody (Clone)	Isotype	Working Condition	Company	Catalogue number
JAM-A (M.Ab.F11)	Mouse IgG1	10 ugs/ml	BD Pharmingen™	BD552147
JAM-A	Rabbit IgG	10 ugs/ml	Invitrogen Ltd.	36-1700
CXCR4	Rabbit IgG	10 ugs/ml	Abcam plc.	Ab2074
CD164 (N6B6)	Mouse IgG2a	10 ugs/ml	BD Pharmingen™	BD551296
ICAM-3 (ICAM-3.3)	Mouse IgG1	10 ugs/ml	R&D Systems, Inc.,	BBA15
CD82 (B-L2)	Mouse IgG1	10 ugs/ml	Abcam plc.	Ab47153
CXCL12 (79018)	Mouse IgG1	10 ugs/ml	R&D Systems, Inc.	MAB350
CD29 (Mab13)	Rat IgG1	10 ugs/ml	BD Pharmingen™	BD552828
CD29 (18/CD29)	Mouse IgG1	10 ugs/ml	BD Pharmingen™	BD610468
Alexa Fluor®488 goat anti-mouse	Not available	2 ugs/ml	Invitrogen Ltd.	A-11001
Alexa Fluor®555 goat anti-mouse	Not available	2 ugs/ml	Invitrogen Ltd.	A-12424
Alexa Fluor®555 goat anti-rabbit	Not available	2 ugs/ml	Invitrogen Ltd.	A-21428
Alexa Fluor®488 goat anti-rat	Not available	2 ugs/ml	Invitrogen Ltd.	A-11006

N.A.: not assayed.

The cells were then gently washed with the blocking solution three times between each incubation step. Finally, the chambers on the slides were removed. Becton Dickinson Fluorescent mounting medium (DakoCytomation Ltd.) containing 5 □gs/ml DAPI nucleic acid dye (Sigma-Aldrich Ltd.) was added dropwise onto the slides, and covered with 22 X 64 mm glass cover slips (VWR LabShop) before being sealed around the edges with transparent nail polish. The labelled cells were examined under an Eclipse TE600 microscope (Nikon UK Ltd.). The protocol is summarised in Figure 2.10.

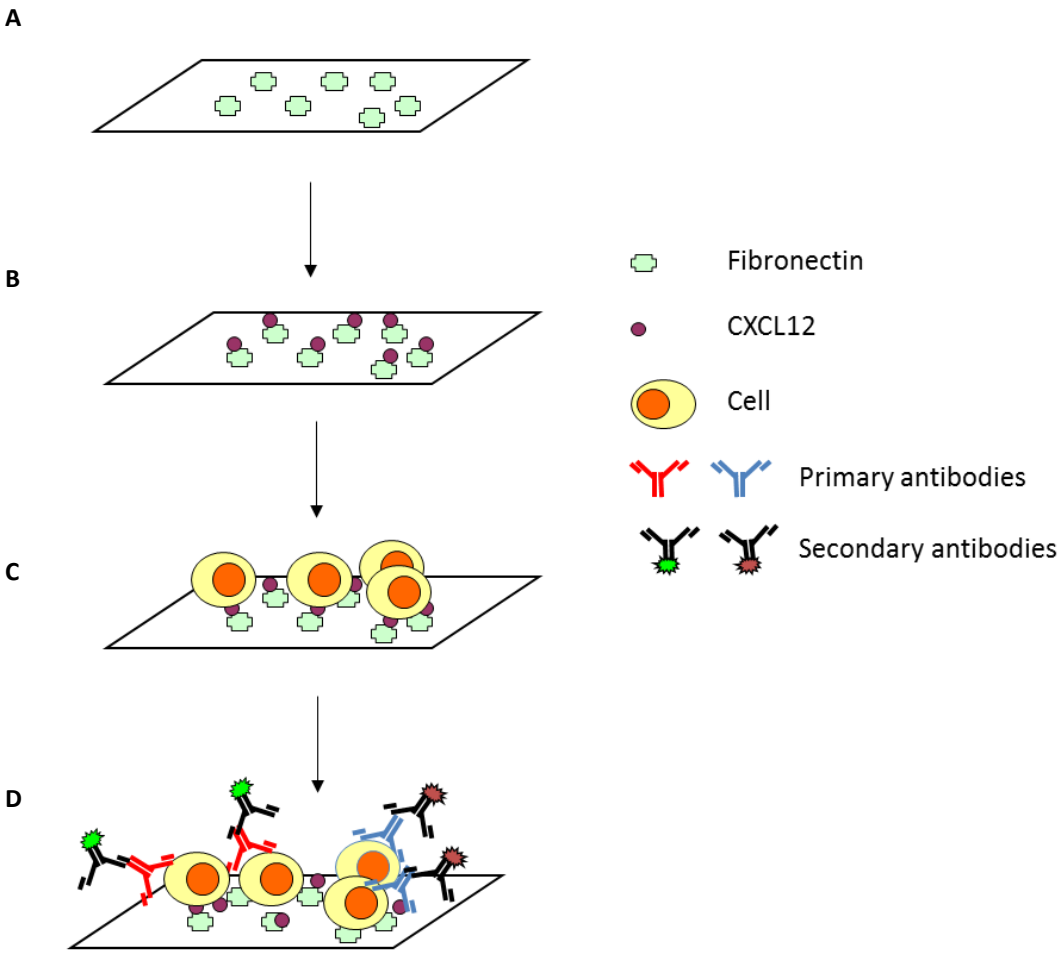

Figure 2.10. An illustration of the immunofluorescence staining protocol.
(A) The slides were coated with fibronectin (green cross) at 4°C overnight followed by (B) CXCL12 (purple circle) and placed in a 37°C incubator for 30 minutes. (C) 1-2X10^5 cells (yellow circle) were added at 37°C for 0-30 minutes. (D) The proteins of interest were labelled with appropriate primary (red and blue shapes) and fluorescently tagged secondary antibodies (black shapes) and visualised on the fluorescence microscope.

2.9. Flow Cytometry

2.9.1. Cell preparation

2.9.1.1. Suspension cell harvesting from culture

Cultured suspension cells were harvested by transferring the cells to Falcon tubes (Appleton Woods Ltd.) and centrifuging at 350 xg in an Heraeus Multifuge 4KR centrifuge (DJB Labcare Ltd.) at room temperature for 5 minutes. The supernatants were removed and discarded. The cells were then resuspended in FACS buffer, comprising HBSS (PAA Laboratories GmbH) containing 1% (w/v) BSA (Sigma-Aldrich Ltd.) prior to labelling.

2.9.1.2. Adherent cell harvesting from culture

The cells were treated 1 ml of trypsin-EDTA (170,000 Us/L trypsin and 200 mgs/L EDTA; PAA Laboratories GmbH) in a 37°C 5% CO_2 in air water-jacketed incubator (MCO-20AIC, Triple Red Ltd.) for around 5 minutes after the culture medium was removed and the cells were washed with HBSS (PAA Laboratories GmbH). 10mls of fresh culture medium containing FBS were subsequently added to neutralise the trysin. The cells were then transferred to Falcon tubes (Appleton Woods Ltd.) and centrifuged at 350 xg in a Heraeus Multifuge 4KR centrifuge (DJB Labcare Ltd.) at room temperature for 5 minutes. The supernatants were removed and discarded. The cells were then resuspended in FACS buffer (1% (w/v) BSA (Sigma-Aldrich Ltd.) in HBSS (PAA Laboratories GmbH)) ready for labelling.

2.9.1.3. Isolation of mononuclear cells (MNCs) from umbilical cord blood (UCB) for flow cytometry

To screen cell surface molecule expression on different haemopoietic lineages from umbilical cord blood (UCB), the nucleated cells were collected after the erythrocytes had been lysed by diluting 1 ml of UCB in 10 mls of ammonium chloride solution (150 mM

ammonium chloride, 10 mM sodium bicarbonate and 1 mM EDTA in distilled H_2O; all from Sigma-Aldrich Ltd.) at the room temperature for 10 minutes in 15ml Falcon tubes (Appleton Woods Ltd.). The cells were then centrifuged at 350 xg in a Hettich Rotina 46R centrifuge (DJB Labcare Ltd.) at the room temperature for 10 minutes. The supernatants were removed and discarded and the cell pellets were resuspended in FACS buffer (1% (w/v) BSA (Sigma-Aldrich Ltd.) in HBSS (PAA Laboratories GmbH)) ready for labelling.

2.9.2. Antibodies and antibody labelling for flow cytometry

The cells were resuspended in FACS buffer (1% (w/v) BSA (Sigma-Aldrich Ltd.) in HBSS solution (PAA Laboratories GmbH) at the density of $2x10^6$ cells per ml and then incubated with 2 µls of the Fc receptor blocking solution (Miltenyi Biotec GmbH) at 4°C for 30 minutes. Each 1-$2x10^5$ cell aliquot in 100 µls of the FACS buffer was stained with the antibodies against the molecules of interest at 4°C for 30 minutes. Ten uls of the antibodies that were used for the FACS analysis are listed in Table 2.5. The labelled cells were then washed in 5 mls of FACS buffer and centrifuged at 350 xg in a Hettich Rotina 46R centrifuge (DJB Labcare Ltd.) at 4°C for 5 minutes. The supernatants were removed and discarded. The cells were then resuspended in 500 µls of the FACS buffer and transferred to FACS tubes (BD Falcon™, Becton Dickinson Ltd.) for analysis on a BD LSR II flow cytometer using FACSDiva software (Becton Dickinson Ltd.).

Before flow cytometric analysis, 1 µl of the pre-made 0.5 mgs/ml DAPI stock solution (Sigma-Aldrich Ltd.) was added for viability staining. In general, the expression analysis was only carried out on live cells of the samples. The strategy for gating live cells is illustrated using plots of one isolated UCB $CD34^+$ cells as an example in Figure 2.11. Most experiments were carried out on a BD LSR II flow cytometer (Becton Dickinson Ltd.) using the BD

FACSDiva 6 software program (Becton Dickinson Ltd.) by collecting at least 10,000 viable cells per samples.

Table 2.5. The list of antibodies used in FACS analysis.

Antibody (Clone)	Conjugate	Isotype	Company	Catalogue number
CD3 (UCHT1)	FITC	mouse IgG1	BD Pharmingen™	BD555332
CD7 (M-T701)	APC	mouse IgG1	BD Pharmingen™	BD561604
CD10 (HI10a)	APC	mouse IgG1	BD Pharmingen™	BD332777
CD11a (HI111)	APC	mouse IgG1	BD Pharmingen™	BD559875
CD11b/Mac-1 (ICRF44)	APC	mouse IgG1	BD Pharmingen™	BD561015
CD14 (M5E2)	FITC	mouse IgG2a	BD Pharmingen™	BD555397
CD18 (6.7)	FITC	mouse IgG1	BD Pharmingen™	BD555923
CD19 (HIB19)	FITC	mouse IgG1	BD Pharmingen™	BD555412
CD29	FITC	mouse IgG1	Immunotec Inc.	
CD34 (AC136)	APC	mouse IgG2a	Miltenyi Biotec GmbH,	130-090-954
CD34 (8G12)	PerCP	mouse IgG1	BD Pharmingen™	BD345803
CD38 (HIT2)	FITC	mouse IgG1	BD Pharmingen™	BD555459
CD41a (HIP8)	FITC	mouse IgG1	BD Pharmingen™	BD555466
CD45 (2D1)	PerCP	mouse IgG1	BD Pharmingen™	BD345809
CD45RA (HI100)	APC-H7	mouse IgG2b	BD Pharmingen™	BD560674
CD49d	APC	mouse IgG1	R&D Systems®, Inc.	FAB1354A
CD49e	APC	mouse IgG1	R&D Systems®, Inc.	FAB1644A
CD54 (HA58)	APC	mouse IgG1	BD Pharmingen™	BD559771
CD51/CD61 (23C6)	N/C	mouse IgG1	BD Pharmingen™	BD555504
CD56 (B159)	APC	mouse IgG1	BD Pharmingen™	BD555518
CD62E (68-5H11)	APC	mouse IgG1	BD Pharmingen™	BD551144
CD66 (B1.1/CD66)	FITC	mouse IgG2a	BD Pharmingen™	BD551479
CD123 (7G3)	PE-Cy7	mouse IgG2a	BD Pharmingen™	BD560826
CD133 (293C3)	APC	mouse IgG2b	Miltenyi Biotec GmbH,	130-090-854
CD164 (N6B6)	PE	mouse IgG2a	BD Pharmingen™	BD551298
CD164 (N6B6)	FITC	mouse IgG2a	BD Pharmingen™	BD551297
CD235a (HIR2)	APC	mouse IgG2b	BD Pharmingen™	BD551336
CXCR4 (12G5)	APC	mouse IgG2a	BD Pharmingen™	BD555976
JAM-A (M.Ab.F11)	PE	mouse IgG1	BD Pharmingen™	BD552556
	N/C	mouse IgG1	BD Pharmingen™	BD552147
Human HSC lineage cocktail containing:			eBioscience Inc.	22-7776
CD2 (RPA-2.10)	APC	mouse IgG1		
CD3 (OKT3)	APC	mouse IgG2a		
CD14 (61D3)	APC	mouse IgG1		
CD16 (CB16)	APC	mouse IgG1		
CD19 (HIB19)	APC	mouse IgG1		
CD56 (CB56)	APC	mouse IgG1		
CD235a (HIR2)	APC	mouse IgG2b		
Goat Anti–Mouse IgGs	APC	IgG	Invitrogen Ltd.	A865

HSC: Haematopoietic stem cell. N/C: non-conjugated. FITC: fluorescein isothiocyanate, APC: allophycocyanin, PE: phycoerythrin, PerCP: peridinin-chlorophyll-protein complex.

Bone marrow samples were analysed in collaboration with Dr Allison Blair and staff at the University of Bristol. The results were analysed using FlowJo v10.0.6 software (Miltenyi Biotec. GmbH) in both Bristol and Oxford.

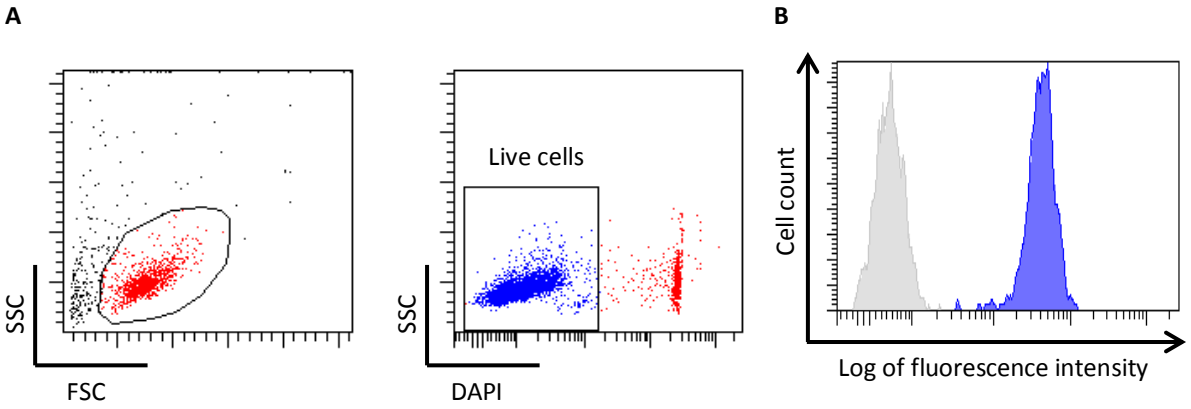

Figure 2.11. General gating strategy for FACS analysis of purified CD34$^+$ cells.
(A) The representative FACS dotplots (in red) show the gating of live cells base on forward scatter channel (FSC) and side scatter channel (SSC) followed by (B) DAPI staining (blue for viable cells; red for non-viable cells). The live cells were determined as DAPI-negative (blue). (C) The median fluorescence intensity (M.F.I.) of antibody (blue) or isotype (gray) stained viable cells was determined using FACSDiva software (Becton Dickinson Ltd.).

2.9.3. Fluorescence compensation

In some cases when performing dual- or multi-colour fluorescence studies, spectral overlap may happen and fluorescence compensation was carried out as follows. FACS tubes (BD Falcon™, Becton Dickinson Ltd.) were set up containing 100 µls of FACS buffer (1% (w/v) BSA in HBSS; Sigma-Aldrich Ltd.) and one drop of BD™ CompBead anti-mouse Ig, κ (Becton Dickinson Ltd.) per tube before separately adding to each tube 10 µls of antibody conjugated with different fluorochromes, and the mixture incubated in a dark carbinet at room temperature for 30 minutes. A negative control was set up in parallel using BD™ CompBead negative controls (Becton Dickinson Ltd.) under the same conditions but without

adding antibody. At the end of incubation, the beads were washed in FACS buffer and resuspended in 500 µls of fresh FACS buffer for analysis on a BD LSR II flow cytometer using compensation settings in the FACSDiva software (Becton Dickinson Ltd.).

2.10. Western Blotting

2.10.1. Principle

Western blotting was used to analyse protein expression in crude total cell lysates. To do this, cells were lysed and the total protein was quantified. Equal amounts of protein from the lysates were heated in buffer containing DTT to cleave disulphide bonds. Following this, samples were subjected to polyacrylamide gel electrophoresis (SDS-PAGE electrophoresis) for separation based on their molecular weight, before being transferred to PVDF membranes. The proteins of interest were detected by blotting with appropriate primary and secondary antibodies. The blots were developed using the ECL system. For quantification, the intensities of the bands were determined using Quantity One software.

2.10.2. Protein extraction

The total protein from 0.5-2x10^6 cells was extracted using 50 µls of PY lysis buffer (50 mM Tris-HCl pH8.0, 150 mM NaCl, 1% (v/v) Triton X-100, 5 mM EDTA and 50 mM NaF, adding fresh prepared 5 mM DTT, 0.1 M PMSF, 100 mM Na_3VO_4 and proteinase inhibitors cocktails (AEBSF–[4-(2-aminoethyl)benzenesulphonyl fluoride hydrochloride], aprotinin, bestatin hydrochloride, E-64–[N-(trans-Epoxysuccinyl)-L-leucine 4-guanidinobutylamide], Leupeptin hemisulphate salt and pepstatin A ; Sigma-Aldrich Ltd.) on ice for 30 minutes, followed by centrifuging at 12,000 xg in a Hettich Mikro 46R centrifuge (DJB Labcare Ltd.) at 4°C for 30 minutes. The protein supernatants were then transferred to new vials for storage at -80°C or for protein concentration analysis.

2.10.3. Protein concentration determination

The protein lysate was ten-times diluted in PY lysis buffer from the manufacturer for determining the protein concentration. The 5X concentrated advanced protein concentration assay reagent (Cytoskeleton Inc.) was freshly diluted fivefold with distilled water before use. Three µls of diluted protein lysate and 300 µls of x1 protein concentration assay reagent from the manufacturer were added to a transparent 96-well flat bottom plate (Appleton Woods Ltd.) and mixed well. The plate was then placed in a Bio-Rad Model 680 microplate reader (Bio-Rad Laboratories, Inc.) to measure the absorbance at 595nm. The protein concentration was calculated based on 1.0 OD_{595} = 37.5 µg protein per ml as described by the manufacturer.

2.10.4. SDS-polyacrylamide gel electrophoresis (SDS-PAGE)

Twenty µgs of each protein lysate was mixed with 4X NuPAGE® LDS Sample Buffer (Invitrogen Ltd.), 5% (v/v) 2-Mercaptoethanol (Sigma-Aldrich Ltd.) and 10X NuPAGE® Reducing Agent (Invitrogen Ltd.). The mixture was topped up with DEPC-water (Invitrogen Ltd.) to 20 µl and heated at 95°C on a block heater (SBH 130D, Stuart®, Staffordshire, UK) for 10 minutes. The samples were briefly centrifuged in a Hettich Mikro 46R centrifuge (DJB Labcare Ltd.) for 1 minute before being applied to pre-equilibrated 12-15% (w/v) NuPAGE® Novex Bis-Tris Gels (Invitrogen Ltd.) and subjected to electrophoresis according to the manufacturer's instructions. In addition, 4 µls of Full-Range Rainbow Molecular Weight Markers (PAA Laboratories GmbH), a mixture of individually coloured proteins of defined size, were loaded in parallel. The gel was electrophoresed in 1X NuPAGE® MES Running Buffer containing NuPAGE® Antioxidant (Invitrogen Ltd.) in a XCell SureLock™ Mini-Cell Electrophoresis System (Invitrogen Ltd.) at 200 volts for 30-40 minutes until the Full-Range

Rainbow Molecular Weight Markers were separated clearly. The separated proteins were then transferred from the gel to PVDF or NC membranes with the iBlot®Transfer Stack (Invitrogen Ltd.) using iBlot programme 2 for 6-7 minutes (Invitrogen Ltd.).

2.10.5. Immunoblotting

The membrane was blocked using a blocking buffer of 5% (w/v) skim milk (Sigma-Aldrich Ltd.) in 0.1% PBST wash buffer (0.1% (v/v) Tween-20 (Sigma-Aldrich Ltd.) in PBS (PAA Laboratories GmbH)) on a shaker at room temperature for 1 hour. After blocking, the blot was probed with mouse anti-human JAM-A primary antibody (BD 612120, BD Pharmingen™) at 1:800 dilution, rabbit anti-human phosphor-p44/42 MAPK (Thr202/Tyr204) primary antibody (#9101, Cell Signaling Technology) at 1:1000 dilution, rabbit-anti human p44/42 MAPK (#9102, Cell Signaling Technoloty) primary antibody at 1:1000 dilution, rabbit anti-human phosphor-PKC-ζ primary antibody (0.2 mgs/ml, sc-12894-R, Santa Cruz Biotechnology) at 1:500 dilution, rabbit anti-human PKC-ζ primary antibody (0.2 mgs/ml, sc-216, Santa Cruz Biothechnology) at 1:500 dilution, rabbit anti-human phosphor-Akt (Ser473) primary antibody (#9271, Cell Signaling Technoloty) at 1:1000 dilution, or rabbit anti-human Akt primary antibody (#9272, Cell Signaling Technoloty) at 1:1000 dilution in blocking buffer as described above. For loading controls, the blot was probed with mouse anti-human α-tubulin (T5168, Sigma-Aldrich Ltd.) or with mouse anti-human GAPDH (ab37187, Abcam plc.) at 1:2000 dilutions in blocking buffer on a shaker at the room temperature for 1 hour. The membrane was then washed three times in wash buffer as described above on a shaker at the room temperature for 10 minutes each time. Next, the membrane was incubated with ImmunoPure goat anti-mouse or goat anti-rabbit peroxidase conjugated secondary antibody (Thermo Fisher Scientific Inc.) at a dilution of 1:7000 on a shaker at the room

temperature for 1 hour. The membrane was washed three times with wash buffer on a shaker at the room temperature for 10 minutes each time prior to signal detection.

2.10.6. Protein signal development

SuperSignal West Pico Chemiluminescent Substrate kits (Thermo Fisher Scientific Inc.) were used for signal detection. The kits contained the luminal/enhancer solution and the peroxidase stable solution. The two solutions were freshly mixed together at a 1:1 ratio and allowed to react for 5 minutes to give the working solution. The blots were then placed in the working solution for 5 minutes at room temperature. After the incubation, the blot was drained and exposed to Amersham Hyperfilm™ ECL Higher performance chemiluminescence film (GE Healthcare Ltd.) for 1 to 10 minutes. The films were developed in a Kodak X-OMAT1000 processor (Eastman Kodak Ltd.).

2.10.7. Densitometry analysis

The protein on the blots was quantified using densitometry software. The films were first scanned into Adobe Photoshop software (Adobe Systems Inc.) and the images were subsequently imported into Quantity One 4.6.3 basic software (Bio-Rad Laboratories Inc.). The minimal area of signal was gated and the density/mm^2 was determined. The signal density was then normalised to the total amount of protein in each well as determined by densitometry analysis of α-tubulin or GAPDH.

2.11. ctive Rap1 Pull-Down and Detection

2.11.1. Principle

An active Rap1 pull-down and detection kit was purchased from Thermo Scientific (Thermo Fisher Scientific Inc.) to monitor Rap1 small GTPase activation. The kit contained a GST-fusion protein of the Rap1-binding domain (RBD) from human RalGDS along with

glutathione agarose resin to specifically pull down active Rap1 and an anti-Rap1 antibody for Western blot detection. In addition, two control nucleotides, GTPγS and GDP, were provided to generate positive and negative controls respectively for the experiments.

2.11.2. Cell stimulation and protein extraction

Ten million cell aliquots were resuspended in 0.5 mls of serum free basal medium for the cell type and placed in an Innova 4230 shaking incubator (New Brunswick Scientific) at 37°C for 10 minutes before the stimulation of 100 nM CXCL12 (Peprotech) for 0, 30 seconds and 1 minute. The cells were then centrifuged at 900g in a Hettich Mikro 46R centrifuge (DJB Labcare Ltd.) at 4°C for 30 seconds. After disposing of the supernatants, the cell pellets were lysed in 0.5 ml of ice-cold kit-provided cell lysis buffer (25 mM Tris-HCl pH 7.2, 150 mM NaCl, 5 mM $MgCl_2$, 1% NP-40 and 5% glycerol; Thermo Fisher Scientific Inc.) containing freshly added protease inhibitor cocktail (AEBSF–[4-(2-aminoethyl)benzenesulphonyl fluoride hydrochloride], aprotinin, bestatin hydrochloride, E-64–[N-(trans-epoxysuccinyl)-L-leucine 4-guanidinobutylamide], leupeptin hemisulphate salt and pepstatin A; Sigma-Aldrich Ltd.) and 1 mM PMSF (Sigma-Aldrich Ltd.) on ice for 5 minutes. To collect cleared protein lysates, the samples were centrifuged at 16,000 g in a Hettich Mikro 46R (DJB Labcare Ltd.) at 4°C for 10 minutes and the supernatants were then transferred to new eppendorfs (Appleton Woods Ltd.) for protein concentration determination as described in section 2.10.3.

2.11.3. *In vitro* GTPγS and GDP treatment

Five hundred μgs of protein lysate was diluted in 500 μls of the kit-provided lysis buffer buffer (25 mM Tris-HCl pH 7.2, 150 mM NaCl, 5mM $MgCl_2$, 1% v/v) NP-40 and 5% (v/v) glycerol; Thermo Fisher Scientific Inc.) for each treatment. Ten μls of 0.5 M EDTA pH 8.0 (final concentration 10 mM; Sigma-Aldrich Ltd.) were added to the protein lysate and this

was followed by 5 μls of 10 mM GTPγS (final concentration 0.1mM) or 5 μls of 100mM GDP (final concentration 1mM) (Thermo Fisher Scientific Inc.). The mixture was then incubated at 30°C in an Innova 4230 incubator (New Brunswick Scientific) for 30 minutes with constant agitation. Thirty-two μls of 1 M $MgCl_2$ (final concentration 60mM; Sigma-Aldrich Ltd.) were added and the samples were placed on ice to stop the reaction.

2.11.4. Active Rap1 pull down for Western blot detection

Before pulling down active Rap1, 50 μgs of the protein lysates were set aside for total Rap1 detection by immunoblotting. One hundred μls of the 50% (v/v) glutathione resin slurry was added to a collection tube with a spin cup and centrifuged at 6000g in a Hettich Mikro 46R centrifuge (DJB Labcare Ltd.) for 40 seconds at 4°C. The flow-through was discarded and the binding resin was washed by gently inverting the tube after the addition of 400 μls of the lysis buffer (25 mM Tris-HCl pH 7.2, 150 mM NaCl, 5mM $MgCl_2$, 1% (v/v) NP-40 and 5% (v/v) glycerol; Thermo Fisher Scientific Inc.) and then centrifuging the tube at 6000g in a Hettich Mikro 46R centrifuge (DJB Labcare Ltd.) for 40 seconds at 4°C. One mg of protein lysate was transferred to 700 μls of the lysis buffer immediately after adding 20 μgs of GST-RalGDS-RBD to the spin cup containing the glutathione resin. The cap of the collection tube was sealed and the sample mixed by gentle inversion. The tubes were placed in a 4°C cold room for 1 hour with gentle rocking. To remove non-binding protein lysate, the tubes were centrifuged in a Hettich Mikro 46R microcentrifuge (DJB Labcare Ltd.) at 6000g at 4°C for 40 seconds. The resin-bound protein lysate was washed three times in 400 μls of the lysis buffer buffer (25 mM Tris-HCl pH 7.2, 150 mM NaCl, 5mM $MgCl_2$, 1% (v/v) NP-40 and 5% (v/v) glycerol; Thermo Fisher Scientific Inc.) and centrifuged under the same conditions. The flow-through was discarded after each wash. To obtain the resin-bound protein lysate, the

spin cup was transferred to a new collection tube, and the resin resuspended in 50 µls of 2x SDS sample buffer (125 mM Tris-HCl pH 6.8, 2% (v/v) glycerol, 4% (w/v) SDS and 0.05% (w/v) bromophenol blue; Thermo Fisher Scientific Inc.) containing freshly added 0.05% (v/v) β-mercaptoethanol (VWR International Ltd.) at room temperature for 3 minutes. The tubes were centrifuged in an Hettich Mikro 46R microcentrifuge (DJB Labcare Ltd.) at 6000g at 4°C for 2.5 minutes and the eluted samples were heated at 95°C for 5 minutes before being subjected to electrophoresis and immunoblot transfer exactly as described in section 2.10.4. Twenty-five µls of pull-down protein lysate were applied to each lane and in 12-15% (w/v) NuPAGE® Novex Bis-Tris gels. Immunoblotting of Rap1 was performed as described in section 2.10.5 using a blocking buffer of 3% (w/v) BSA in Tris-buffered saline (TBS; 25 mM Tris-HCl, pH 7.5, 150 mM NaCl; Sigma-Aldrich Ltd.) on a shaker at the room temperature for 2 hours. A 1:1000 dilution of rabbit anti-human Rap1 primary antibody (5 units/50µls; Thermo Fisher Scientific Inc.) in TBST (TBS containing 0.05% (v/v) Tween-20, 5% (w/v) BSA, and 0.1% (w/v) NaN_3; all from Sigma-Aldrich Ltd.) was added for Rap1 labelling and placed on a shaker at 4°C overnight. This was followed by incubating with goat anti-rabbit peroxidase conjugated secondary antibody (Thermo Fisher Scientific Inc.) at a dilution of 1:7000 on a shaker at the room temperature for 1 hour. The membrane was washed in TBST buffer for 5 minutes and five times each. The Rap1 protein signal was then detected as described in section 2.10.6.

2.12. Functional Assays

2.12.1. JAM-A protein Blockade for functional studies

In some functional studies, JAM-A was blocked using the recombinant human JAM-A/Fc chimaeric proteins (1103-JM, R&D Systems Inc.), anti-human JAM-A antibody (AF1103; R&D

Systems, Inc.), recombinant human IgG1/Fc (110-HG, R&D Systems Inc.) and normal goat IgG (AB-108-C, R&D Systems, Inc.), the latter as controls. The blockade protocol was described by Stellos *et al.* (239) and carried out as follow. TF-1, HL-60 or purified UCB $CD34^+$ cells were harvested and washed in HBSS (PAA Laboratories GmbH) once by centrifuging at 350 xg in an Heraeus Multifuge 4KR centrifuge (DJB Labcare Ltd.) at room temperature for 5 minutes. The supernatants were discarded and the cell pellets were subsequently resuspended in the assay medium (0.5% (w/v) BSA in their basic culture medium without FBS) at a density of 1-2x10^6 cells/ ml and containing 2 μls of FcR blocking solution (Miltenyi Biotec GmbH). The antibodies or chimaeric proteins were then added to the cells at a final concentration at 10 μgs/ml and incubated at 37°C incubator for 30 minutes.

2.12.2. Migration assays

2.12.2.1. Fibronectin coating

The 3μm transwell inserts (BD Falcon™, Becton Dickinson Ltd.) were placed in a 24-well plate (Appleton Woods Ltd.) coated with 100 μls of 10 μgs/ml human plasma fibronectin (Sigma-Aldrich Ltd.) in HBSS (PAA Laboratories GmbH) at 4°C overnight or 2 hour at room temperature before use (312). The fibronectin solution was then removed and the inserts allowed to air dry before cell seeding.

2.12.2.2. BMEC-60 cell seeding and stimulation with IL-1β

For the transendothelial migration assay, 2x10^4 BMEC-60 cells per insert was plated in 100 μl EGM-2 medium (Lonza Biologics) in the upper chamber and 600 μls EGM-2 medium (Lonza Biologics) was added into the bottom chamber and incubated in a 37°C 5% CO_2 in air water-jacketed incubator (MCO-20AIC, Triple Red Ltd.) overnight. Non-adherent BMEC-60 cells were removed from the inserts and the adherent cells were then stimulated with 10 ngs/ml

of Recombinant Human Interleukin-1β (IL-1β; Invitrogen Ltd.) in EGM-2 medium in a 37°C 5% CO_2 in air water-jacketed incubator (Triple Red Ltd.) for four hours. The IL-1β containing medium was removed and the activated BMEC-60 cells were washed twice with the basal medium of migration assayed cells but containing 0.5% (w/v) BSA (Sigma-Aldrich Ltd.).

2.12.2.3. Cell migration assays

Haematopoietic cell lines (section 2.2.1) and $CD34^+$ cells isolated from UCB (section 2.3) were harvested from their separate culture media as described previously by transferring them to a 15 ml Falcon tube (Appleton Woods Ltd.) and centrifuging at 350 xg at 4°C in a Heraeus Multifuge 4KR centrifuge (DJB Labcare Ltd.) for 5 minutes. The supernatants were removed and discarded and cell pellets were then resuspended in the separate assay media, comprising their basal medium with 0.5% (w/v) BSA (Sigma-Aldrich Ltd.) at the density of 1-$2x10^6$ cells/ ml. One hundred μls of cells was then applied to inserts that had been pre-coated with either fibronectin only or activated BMEC-60 cells (sections 2.12.2.2), with various concentrations of CXCL12 (Peprotech) ranging from 100 to 1600 ng/ml in the assay medium in the lower chamber. The cells were allowed to migrate from upper to lower chamber after incubation in a 37°C 5% CO_2 in air water-jacked incubator (MCO-20AIC, Triple Red Ltd.) for 5 hours.

2.12.2.4. BCECF-AM solution preparation and cell staining

To make BECEF-AM stock, 50 μgs of BCECF-AM dye (Invitrogen Ltd.) were disssolved in 100% (v/v) DMSO (Sigma-Aldrich Ltd.) and aliquoted for storage at -20°C. For staining, cells were harvested and resuspended in HBSS with Ca^{2+} and Mg^{2+} at the density of $2x10^6$ cells/ml. 5μls of BCECF-AM stock were added to $2x10^6$ cells/ml and incubated in a 37°C 5% CO_2 in air water-jacked incubator (Triple Red Ltd.) for 30 minutes. Cells were washed by centrifuging

at 350 xg in a Heraeus Multifuge 4KR centrifuge (DJB Labcare Ltd.) at room temperature for 5 minutes. The supernatants were removed and discarded. Cells were resuspended in FACS buffer (1% (w/v) BSA (Sigma-Aldrich Ltd.) in HBSS (PAA Laboratories GmbH)) at the density of $2x10^6$ cells/ ml.

2.12.2.5. Detection of migrating cells

The migrating cells were harvested from the lower chamber into collection tubes. To remove the migrating cells from the bottom of the insert, the insert was washed in 500 µls of trypsin-EDTA (PAA Laboratories GmbH) followed by 1 ml of HBSS (PAA Laboratories GmbH) and the cells were then moved into the collection tube. The migrating cells were centrifuged at 350 xg in a Heraeus Multifuge 4KR centrifuge (DJB Labcare Ltd.) at room temperature for 5 minutes and resuspended in 300 µls of FACS buffer (1% (w/v) BSA in HBSS; Sigma-Aldrich Ltd.) in HBSS (PAA Laboratories GmbH)). BCECF-AM stained cells were added in an equal amount to the initiating cell number ($1\text{-}2x10^5$ cells per tube). The mixed migrating and stained cells were transferred to a FACS tube (BD Falcon™, Becton Dickinson Ltd.) for FACS analysis (Figure 2.12). The percentage of migrating cells was measured using FACSDiva software (Becton Dickinson Ltd.) and calculated using the following equation:

$$\text{Migrating cell percentage \%} = \frac{\text{FACS measured migrating cell number (red)}}{\text{FACS measured labelled cell number (green)}} \text{ X } 100\%$$

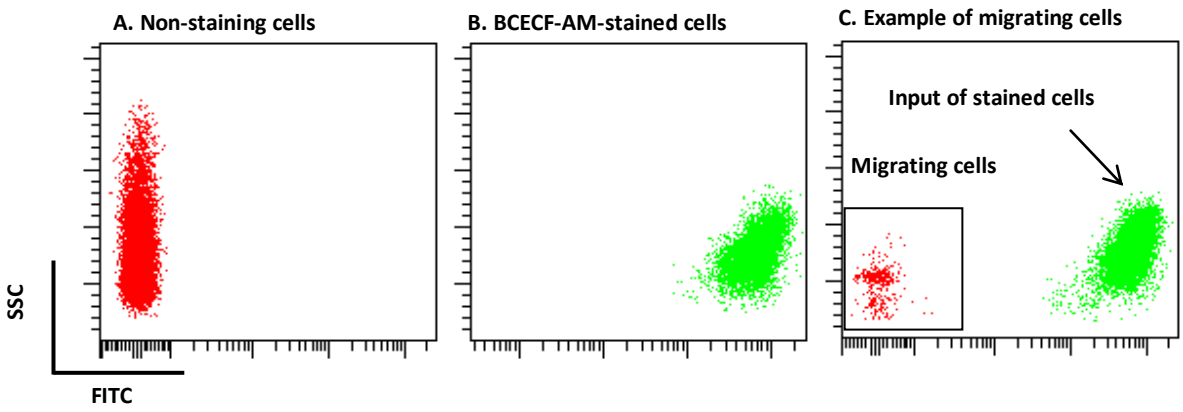

Figure 2.12. An example of FACS analysis for the transwell migration assay.
Representative FACS plots of (A) non-staining cells (red) and (B) BCECF-AM stained cells (green) that were detected by FACS. (C) An aliquot of stained cells (green) equal to the initiating input number in the migration assay was added to the migrating cells which were harvested from the bottom of the transwell (red). The percentage of migrating cells was determined using FACSDiva software (Becton Dickinson Ltd.).

2.12.3. Adhesion assays

2.12.3.1. Extracellular matrix or activated BMEC-60 cells coating

Black 96-well flat bottomed plates (BD Falcon™, Becton Dickinson Ltd.) were coated with 10 μgs/ml of human plasma fibronectin (Sigma-Aldrich Ltd.) in PBS (PAA Laboratories GmbH), or 50 μgs/ml of bovine collagen I (BD Pharmingen™, Becton Dickinson Ltd.) in 0.02N acetic acid (Sigma-Aldrich Ltd.), or sterile 50 μgs/ml BSA (Sigma-Aldrich Ltd.) in PBS (PAA Laboratories GmbH) at 100 μl per well at 4°C overnight (sections 2.12.2.1). The solutions were then removed and discarded before target cells were plated. For the studies on adhesion to BMEC-60 cells, $2x10^4$ cells per well of BMEC-60 cells were seeded and incubated in 100 μls per well of EGM-2 medium (Lonza Biologics) in a 37°C 5% CO_2 in air water-jacketed incubator (MCO-20AIC, Triple Red Ltd.) overnight the day before the assay. The medium was then removed and 100 μls/well of EGM-2 medium containing 10 ngs/ml IL-1β (Invitrogen Ltd.) were added for BMEC-60 cell stimulation and cells incubated in a 37°C 5%

CO_2 in air water-jacketed incubator (MCO-20AIC, Triple Red Ltd.) for 4 hours (sections 2.12.2.2). The cytokine containing medium was removed and washed twice with assay medium (sterile 0.5% (w/v) BSA (Sigma-Aldrich Ltd.) in basal medium) before the target cells were added.

2.12.3.2. Cell staining and adhesion assays

Cells were harvested from normal culture medium by transferring to a 15 ml Falcon tube (Appleton Woods Ltd.) and centrifuging at 350 xg at 4°C in a Heraeus Multifuge 4KR centrifuge (DJB Labcare Ltd.) for 5 minutes. The supernatants were removed and the cell pellets were then resuspended in HBSS (PAA Laboratories GmbH) with calcium and magnesium at a density of $2x10^6$ cells per ml. Five µls of BCECF-AM stock aliquot (section 2.12.2.4) were added to $2x10^6$ cells/ml and incubated in a 37°C 5% CO_2 in air water-jacketed incubator (MCO-20AIC, Triple Red Ltd.) for 30 minutes. Cells were centrifuged at 350 xg in a Heraeus Multifuge 4KR centrifuge (DJB Labcare Ltd.) at room temperature for 5 minutes. The supernatants were removed and discarded. Cells were resuspended in assay medium at a density of $2x10^6$ cells/ml and 100 µls of the cells added to the wells pre-coated with extracellular matrix or activated BMEC-60 cells The cells were allowed to adhere in a 37°C 5% CO_2 in air water-jacked incubator (MCO-20AIC, Triple Red Ltd.) for 1 hour.

2.12.3.3. Detection of adhering cells

To determine the percentage of adhering cells, the absorbance was read before washing as an input baseline using a VICTOR™ X5 Multilabel Plate Reader at 488nm wavelength (Perkin Elmer Inc., Waltham, USA). Following this, the medium was removed from the wells and the non-adherent cells were removed by gently pipetting twice with 100 µls/well of PBS (PAA Laboratories GmbH). The adherent cells were then placed in 100 µls of PBS for detection in

the plate reader. The values were normalised to the input values for each well using the following equation:

$$\text{Relative adhesion percentage} = \frac{\text{Measured adhering cell absorption}}{\text{Input cell absorption}} \text{ X } 100\%$$

2.13. Duolink™ *in situ* PLA Proximity Ligation Assays

2.13.1. Principle

The Duolink® *in situ* PLA proximity ligation assay kit (PLA assay; Cambridge Bioscience Ltd.) was used for detecting *in situ* protein-protein interaction. In this assay, cells were plated on glass slide for primary antibody and PLA probe labelling. PLA probes were secondary antibodies that specifically recognised primary antibodies of various species and were conjugated with short DNA fragments onto their Fc fragments. Two types of the short DNA compensating fragments, MINUS and PLUS, were designed by the company so that different antibodies and different molecular interactions could be detected on a single cell. Following PLA probe labelling of secondary antibodies, a short PCR procedure was carried out to hybridise and amplify the compensating DNA fragments, providing their conjugated antibodies were targeting a pair of interacting proteins. TaxRed DNA dye was then applied to visualise the amplified DNA fragments under a microscope (313). The process is illustrated in Figure 2.13.

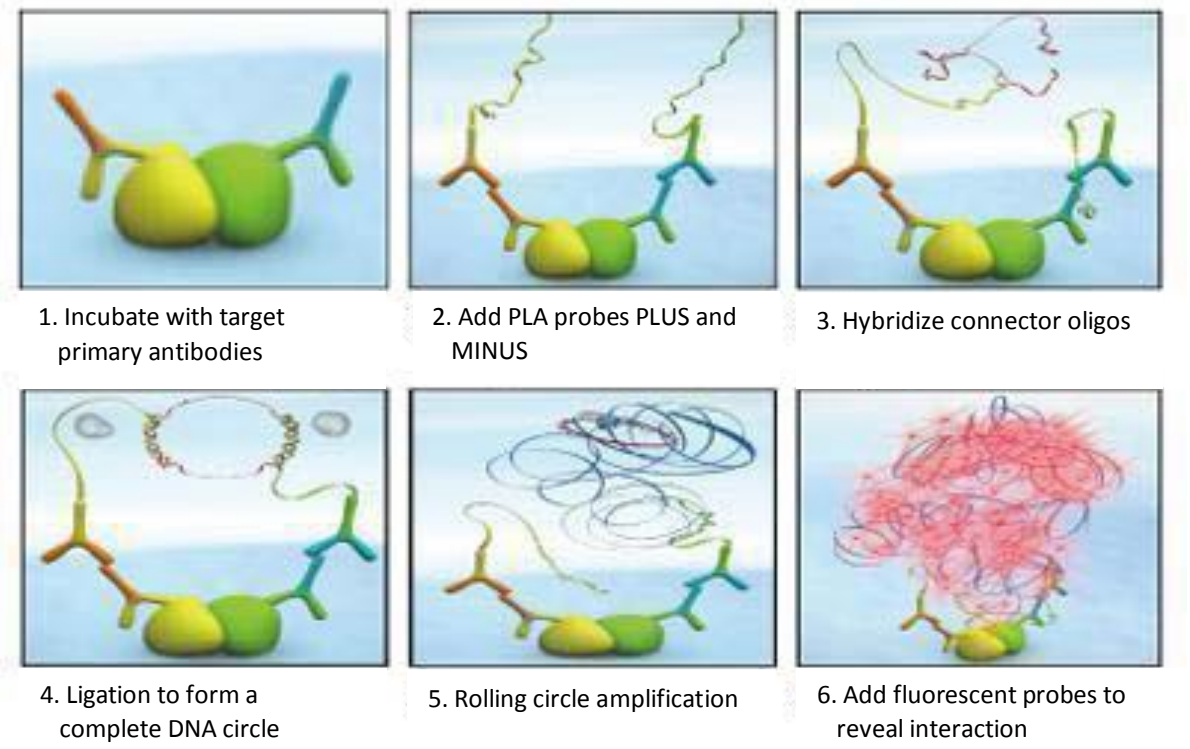

Figure.2.13. Duolink™ *in situ* PLA proximity ligation assay.
The series of pictures briefly illustrates how the proximity ligation assay works to identify the protein-protein interaction. The image was taken and modified from *Abnova* (http://www.abnova.com.) with permission from Abnova Corporation.

2.13.2. Sample preparation

Eight-well glass culture slides (Becton Dickinson Ltd.) were coated with 150 µls of 10 µgs/ml human plasma fibronectin (Sigma-Aldrich Ltd.) in HBSS (PAA Laboratories GmbH) at 4°C overnight. Next, 200 ngs/ml CXCL12 (Peprotech) in HBSS (PAA Laboratories GmbH) or HBSS only was added and incubated at 37°C for 30 minutes. Approximately 1-2x10^5 cells in 100 µls of their basal media containing 0.5% (w/v) BSA (Sigma-Aldrich Ltd.) were plated onto these slides and allowed to react in a 37°C 5% CO_2 in air water-jacketed incubator (MCO-20AIC, Triple Red Ltd.) for the indicated times, and then the cells were fixed by adding 100 µls of 4% (w/v) paraformaldehyde (Sigma-Aldrich Ltd.) for 15 minutes at room temperature.

2.13.3. Blocking and antibody labelling

The fixed cells were then blocked in 150 µls of the Duolink® blocking stock (Cambridge Bioscience Ltd.) at a 1:5 dilution in sterile distilled water for 30 minutes at 37°C. The primary antibodies were diluted in 1X Duolink® antibody diluent (Cambridge Bioscience Ltd.) to their working concentration as shown in Table 2.5 and 100 µls per well added for labelling at 4°C overnight. The cells were gently washed with the Duolink® Wash buffer (TBST; Cambridge Bioscience Ltd.) three times at room temperature. For example, 16 µls of anti-mouse PLA probe MINUS and 16 µls of anti-rabbit PLA probe PLUS were mixed in 68 µls of 1X Duolink® antibody diluent (Cambridge Bioscience Ltd.) and added for labelling at 37°C for 1 hour. The blocking solution was removed and the cells were gently washed with the Duolink® Wash buffer (TBST; Cambridge Bioscience Ltd.) twice for 5 minutes each wash.

2.13.4. Detection

2.13.4.1. Hybridisation

One-times Duolink® hybridisation solution was made from the 5X Duolink® hybridisation stock (Cambridge Bioscience Ltd.) by adding sterile distilled water. After removing the Duolink® Wash buffer (TBST; Cambridge Bioscience Ltd.) from the cells, 100 µls per well of the diluted Duolink® hybridisation solution was applied and incubated at 37°C in a pre-heated humidified chamber for 15 minutes. The hybridisation solution was then removed and the cells were gently washed with the Duolink® wash buffer (TBST; Cambridge Bioscience Ltd.) once for 1 minute.

2.13.4.2. Ligation

One-times Duolink® Ligation solution was made from the 5X Duolink® Ligation stock (Cambridge Bioscience Ltd.) with 1 unit per reaction of Duolink® *in situ* PLA Ligase in sterile

distilled water. One hundred µls per well of the diluted Duolink® Ligation solution were then added at 37°C in a pre-heated humidified chamber for 15 minutes. The ligation solution was removed and the cells were gently washed with the Duolink® wash buffer (TBST; Cambridge Bioscience Ltd.) twice for 2 minutes each.

2.13.4.3. Amplification

One-times Duolink® amplification solution was made from the 5X Duolink® amplification stock (Cambridge Bioscience Ltd.) with 5 units per reaction of Duolink® *in situ* PLA Polymerase in sterile distilled water. One hundred µls per well of the diluted Duolink® amplification solution were then added in a 37°C pre-heated humidified chamber for 90 minutes. The Amplification solution was removed and the cells were gently washed with the Duolink® Wash buffer (TBST; Cambridge Bioscience Ltd.) twice for 2 minutes each.

2.13.4.4. Detection

One-times Duolink® detection solution was made from the 5X Duolink® detection 613 stock (Cambridge Bioscience Ltd.) in sterile distilled water. One hundred µls per well of the diluted Duolink® detection solution were then applied for the reaction in a 37°C pre-heated humidity chamber for 60 minutes.

2.13.4.5. Final wash and mounting

After removing the detection solution, the slides were washed with 2X Duolink® wash buffer SSC (Cambridge Bioscience Ltd.) for 2 minutes, 1X Duolink® wash buffer SSC for 2 minutes, 0.2X Duolink® wash buffer SSC for 2 minutes, 0.02X Duolink® wash buffer SSC for 2 minutes, 70% (v/v) ethanol (VWR International Ltd.) in distilled water for 1 minute, and then allowed to dry in a dark cabinet for light protection. Finally, the chambers on the slides were removed. The Duolink® mounting medium (Cambridge Bioscience Ltd.) was applied to the

slides, which were then covered with 22 X 64 mm glass coverslips (VWR LabShop) and the edges sealed with transparent nail polish. The fluorescence was analysed under an Eclipse TE600 microscope (Nikon UK Ltd.).

2.14. Immunohistochemical Staining of Sections

Immunohistochemistry staining was performed on formalin-fixed, paraffin-embedded tissue sections obtained from the John Radcliffe Hospital, Oxford. The tissue sections were kindly provided by Prof. Kevin Gatter of Nuffield Division of Clinical Laboratory Sciences, University of Oxford. The sections were deparaffinised in Citroclear (TCS Biosciences Ltd.) for 10 minutes twice, followed by immersing in 100% (v/v) ethanol (VWR International Ltd.) for 5 minutes twice, 95% (v/v) ethanol (VWR International Ltd.) for 5 minutes twice and in 75% ethanol (VWR International Ltd.) for 5 minutes before rinsing in deionised water. To enhance immunostaining, the antigen was pre-retrieved in 10 mM citrate buffer pH 6.0 (10X Citrate buffer: 9.5 ml of solution A (2.1 gs citric acid in 100 mls distilled water) plus 41.5 mls of solution B (2.94 gs sodium citrate in 100 mls distilled water and topped up to 100 mls with distilled water) by microwaving slides in a glass Coplin staining jar at 100 watts for 5 minutes three times, with 5 minute cooling-down intervals inbetween. After the third cool down, the sections were washed in PBS for 5 minutes. The sections were next treated with freshly made 3% (v/v) H_2O_2 (Sigma-Aldrich Ltd.) in 100% (v/v) methanol (VWR International Ltd.) for 30 minutes to inactivate the endogenous peroxidase in the tissues and this was followed by washing in PBS (Sigma-Aldrich Ltd.) for 5 minutes twice. The sections were blocked with blocking buffer (10% (v/v) normal goat serum (Sigma-Aldrich Ltd.) in PBS (Sigma-Aldrich Ltd.)) at the room temperature for 30 minutes before staining with the anti–JAM-A antibody at 1:1000 dilutions (Novus Biologicals, Ltd., Cambridge, clone 2E3-1C8) in blocking buffer as described previously at 4°C overnight. The sections were washed with PBS solution (Sigma-

Aldrich Ltd.) for 10 minutes three times before incubating with biotinylated goat anti-mouse IgG antibody (Sigma-Aldrich Ltd.) at the dilution of 1:200 in blocking buffer at the room temperature for 30 minutes. The sections were subsequently washed in PBS (Sigma-Aldrich Ltd.) for 6 minutes three times, and labelled using the VECTASTAIN Elite® ABC Kit (Vector Laboratories, Inc.) at the room temperature for 40 minutes, followed by washing in the PBS solution (Sigma-Aldrich Ltd.) for 10 minutes, three times. The sections were then stained using the DAB (3,3'-diaminobenzidine) substrate kit for peroxidase detection (comprising Buffer Stock Solution, DAB Stock Solution, Hydrogen Peroxide Stock Solution and Nickel Solution; Vector Laboratories, Inc.) for 3 minutes and counterstained with haematoxylin solution (2g/l; Sigma-Aldrich Ltd.) for 10 seconds at room temperature. The slides were washed in running water before being mounted using Aquamount (VWR International Ltd.) for observation under bright field of an Eclipse TE600 microscope (Nikon UK Ltd.).

2.15. Immunofluorescence Internalisation Assay

The immunofluorescence internalisation assay was performed by collecting and incubating the HL-60 cells (1-2X10^5 in 100 μls pre-chilled IMDM with 0.1% (w/v) BSA) and adding 15 μg/ml anti-JAM-A antibody or anti-integrin β1 (CD29) at 4°C for 30 minutes as listed in Table 2.4. The cells were washed with pre-cooled medium (IMDM with 0.1% (w/v) BSA) to remove unbound antibody and seeded onto the 10 μgs/ml human plasma fibronectin (Sigma-Aldrich Ltd.) coated slides with or without 200 μgs/ml CXCL12 (Peprotech; Section 2.8) for the indicated times. Before fixation, the cells were placed on ice and acid washed (ice-cold 50 mM glycine in Ca^{2+}/Mg^{2+} containing HBSS, pH 2.5, for three washes and Ca^{2+}/Mg^{2+} containing HBSS, pH 7.5, twice) to remove the antibodies from the cell surface. Cells were fixed in 4% (w/v) paraformaldehyde (Sigma-Aldrich Ltd.) in PBS (PAA Laboratories GmbH) for

15 minutes at room temperature and blocked in blocking solution (2% (w/v) BSA in HBSS) for 30 minutes at 4°C before permeabilisation in 0.1% (v/v) Triton X-100 in blocking solution as described previously for 5 minutes at room temperature. The cells were then stained with the secondary antibody, washed, mounted and analysed as described in Section 2.8. 100 cells were counted per condition using DAPI (Sigma-Aldrich Ltd.) counterstain.

2.16. Human Phospho-Kinase Antibody Array

A pilot study was carried out using a Human Phospho-Kinase Array Kit (R&D systems) to detect relative levels of phosphorylation of 46 kinase phosphorylation sites. To prepare samples, cells were rinsed with PBS (PAA Laboratories GmbH) and the supernatants removed by centrifuging the cells at 350 xg in a Heraeus Multifuge 4KR centrifuge (DJB Labcare Ltd.) at room temperature for 5 minutes. 1x 10^7 cells were lysed in Lysis Buffer 6 (R&D systems) on ice for 30 minutes, followed by centrifuging at 14,000 xg in a Hettich Mikro 46R centrifuge (DJB Labcare Ltd.) at 4°C for 5 minutes. The protein lysate was then transferred to clean tubes for protein concentration determination as described in section 2.10.3. Five hundred µgs of protein lysate were used per membrane. The protein assay membranes were transferred into separate wells of an 8-well multi-dish (R&D systems) and 1 ml of Buffer 1 (R&D systems) applied to each membrane, incubating for 1 hour on a rocking platform. Five hundred µgs of protein lysate were topped up to 334 µls with Lysis Buffer 6 (R&D systems) plus 1666 µls with Lysis Buffer 1 (R&D systems). Next, after removing Buffer 1 from the membranes, 1 ml of adjusted protein lysate was added to the membranes and incubated overnight at 4°C on a rocking platform. Each membrane was moved into individual plastic containers containing 10 mls of 1X washing buffer (R&D systems) for 10 minutes on a rocking platform, and washed three times. For one membrane,

20 µls of reconstituted Detection Antibody Cocktail A (R&D systems) in 1 ml of 1X Array Buffer 2/3 (R&D systems) were applied and incubated at room temperature for 2 hours on a rocking platform. Likewise, for the second membrane, 20 µls of reconstituted Detection Antibody Cocktail B (R&D systems) in 1 ml of 1X Array Buffer 2/3 (R&D systems) was applied and incubated under the same conditions as membrane one. The membranes were washed three times by removing the membranes to individual containers and adding 10 mls of 1X Washing buffer (R&D systems) for 10 minutes on a rocking platform. Following this, 1 ml of Streptavidin-HRP that was diluted in 1X Array Buffer 2/3 (R&D systems) was added to each membrane and these were incubated at room temperature for 30 minutes on a rocking platform, followed by washing three times as previously described. The signal development and densitometry analyses were performed as described in section 2.10.6 and section 2.10.7.

CHAPTER 3

JAM-A EXPRESSION ON HUMAN CD34$^+$ AND CD133$^+$ CORD BLOOD CELLS, LEUKAEMIC CELLS AND BONE MARROW NICHE CELLS

3.1. Introduction

Bone marrow niches control haematopoietic stem/progenitor cell (HS/PC) fate and play an important role in supporting their malignant cell counterparts, yet the regulation of these processes is still not fully understood. The chemokine, CXCL12, and its receptor, CXCR4, are critical for HS/PC and leukaemic initiating cell (LIC) engraftment and retention in these bone marrow niches (reviewed in (114, 158, 213)). It is now well recognised that the functions of this chemokine receptor and CXCL12 can be modulated by co-receptors, co-associating molecules and small molecules. Our laboratory and others have, for example, shown that endolyn (CD164) can function as a co-receptor for CXCR4, both co-localising with this chemokine receptor and modulating CXCR4 signalling in response to CXCL12 stimulation (140, 208, 314). Others have demonstrated that syndecan-4 co-associates with CXCR4 on lymphocytes and macrophages and facilitates CXCL12 binding to these cells, although this has not been demonstrated on HS/PCs (315). Further studies by Leung et al. have reported that CXCL12 stimulation for 4h can upregulate genes involved in adhesion and homing in human umbilical cord blood (UCB) CD34$^+$ cells, one of these being the tetraspanin CD9 (316). In other cases, a variety of molecules can alter CXCR4 or CXCL12 expression or function, affecting the cell's response to CXCL12. For example, CD26 (DPP4 or dipeptidyl peptidase 4) can cleave CXCL12 reducing the chemotactic response (317), caspase and calpain 1 inhibitors upregulate CXCR4 on UCB CD34$^+$ cells (318), and PGE2 (prostatglandin E2) can upregulate CXCR4 on HS/PC and modulate in vivo homing in both human and murine cells

(319, 320). Molecules, such as UTP, have also been shown to enhance human CD34$^+$ cell homing/migration towards CXCL12 by preventing the down-regulation of cell surface CXCR4 and hence acting synergistically with the CXCR4-CXCL12 axis (321). Interestingly, in these latter studies, which are summarised in Figure 3.1, Rossi *et al.* compared the transcriptomes of rhG-CSF mobilised peripheral blood CD34$^+$ cells 24 h after stimulation with CXCL12, UTP or UTP plus CXCL12 or without stimulation and found that UTP treatment without or with CXCL12 also up-regulated many genes involved in cell motility or homing, including endolyn or CD164 and F11R or JAM-A (321).

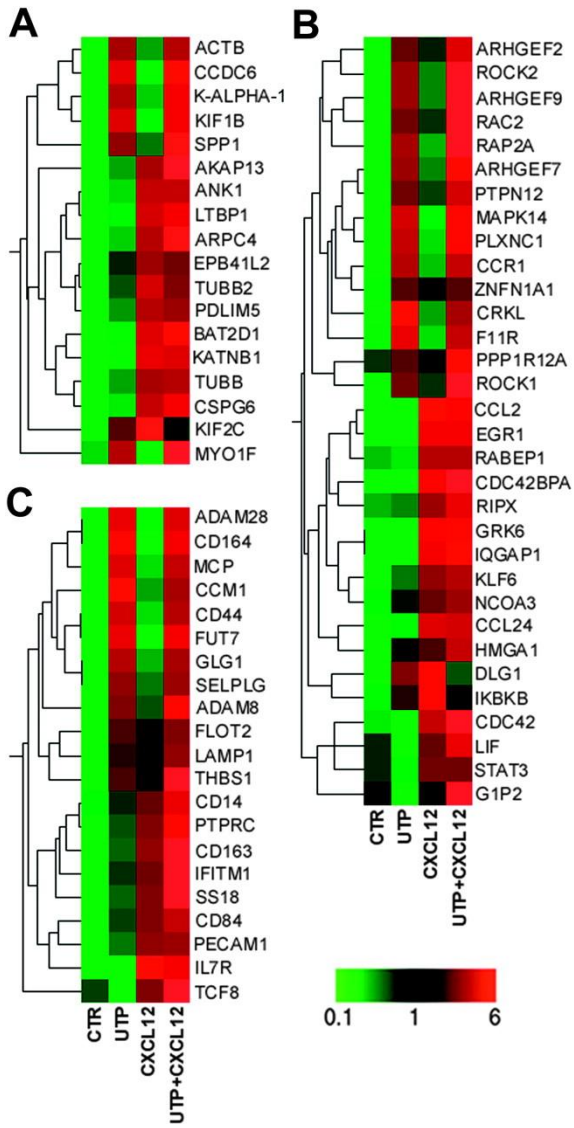

Figure 3.1. Microarray analysis of human CD34$^+$ cells from rhG-CSF molbilised peripheral blood.
Studies described by Rossi et al. (2007) which demonstrate an Eisen tree map of molecules from rhG-CSF mobilised peripheral blood CD34$^+$ cells regulated by 24 h stimulation with UTP, CXCL12 or UTP plus CXCL12 versus untreated control (CTR) cells and categorised as belonging to (A) cytoskeleton organisation and biogenesis, (B) cell motility, small GTPase mediated signal transduction and RHO protein signal transduction and (C) cell adhesion. (Figure taken from Rossi et al. (321)). Republished with permission of American Society of Hematology, from The extracellular nucleotide UTP is a potent inducer of hematopoietic stem cell migration, Rossi L, Manfredini R, Bertolini F, Ferrari D, Fogli M, Zini R, Salati S, Salvestrini V, Gulinelli S, Adinolfi E, Ferrari S, Di Virgilio F, Baccarani M, Lemoli RM., Blood 109: 533-42,2007; permission conveyed through Copyright Clearance Center, Inc.

Both CXCR4 in normal human $CD133^+$ or $CD34^+$ HS/PCs and CXCL12 are regulated by hypoxia (322-324) and hypoxic microenvironments have been identified within the bone marrow, both under normal homeostatic conditions and following and during the progression of acute leukaemias and myelomas (160, 161, 325, 326). Transcriptome analysis of UCB $CD133^+$ HS/PCs conducted in our laboratory confirmed that *CXCR4* gene expression was upregulated by exposure of these cells to hypoxia for 24 hours (324). Interestingly, other cell surface receptors involved in cell adhesion and motility were also upregulated. These included *CRKL* (327), *AVIL* (328), *PLXNC1* (329) and *JAM-A* (251). Given that JAM-A was identified in at least two of the studies presented above, we hypothesised that JAM-A may have an important role in the homing and migration or adhesion of human HS/PCs to niche elements in the bone marrow, and may also act as a co-receptor for CXCR4 or in concert with CXCR4 and CXCL12 to enhance these functions.

JAM-A (junctional adhesion molecule-A), initially known as the F11 receptor (F11R), was identified by Naik *et al.* on human platelets using the F11 antibody (230, 231). Williams *et al.* identified human JAM-A as equivalent to the F11R antigen (233). JAM-A is an integral type I transmembrane protein containing two extracellular Ig-like domains and a cytoplasmic PDZ-binding domain for signal transduction (242). Two proteins, with molecular masses of 32 and 35kD, have been identified on platelet membranes with F11 antibodies to JAM-A (230, 330). To date, as well as studies by our group and others showing JAM-A expression in human $CD133^+$ or $CD34^+$ human HS/PCs (321, 324), JAM-A has been found to be highly expressed on human epithelial cells and endothelial cells, and is also expressed on mature human haematopoietic cells such as platelets (230, 231), lymphocytes (233), monocytes (233), neutrophils (251) and dendritic cells (331, 332). It has been reported that JAM-A interacts homophilically (244), as well as heterophilically with intergrins, such as LFA-1

(αLβ2) (245, 246) and αvβ3 (247, 333) on the same cell (cis-interaction) or between two cells (trans-interaction), at least in neutrophils and endothelial cells. The JAM-A homodimer has been predominantly found in epithelial and endothelial tight junctions, and also observed between platelets or between platelets and endothelial cells (242).

3.2. Aims and Objectives

The aim of this chapter was to carry out a more detailed investigation of the expression of the JAM-A protein on normal human UCB haematopoietic subsets and human leukaemic cell lines using the M.Ab.F11 JAM-A antibody and flow cytometry, ahead of examining its role in haematopoiesis. The expression of JAM-A was further examined on human bone marrow derived cells and leukaemic sections. This was extended to collaboration with Dr. Allison Blair of University of Bristol, where JAM-A expression was also tested on primary human bone marrow acute lymphocytic leukaemic (ALL) samples using flow cytometry. As JAM-A is a homophilic adhesion molecule expressed on endothelium, a further aim was to examine its expression on human bone marrow niche cells.

3.3. Results

3.3.1. JAM-A is expressed on the majority of human haematopoietic progenitor cells from human umbilical cord blood.

In this chapter, cell surface JAM-A protein expression was firstly examined on UCB $CD133^+$ or $CD34^+$ progenitor cells and the results are shown in Figure 3.2. The mononuclear cell fraction (MNC) was prepared and labelled with CD133-APC (293C3) or CD34-APC (AC136) and JAM-A-PE (M.Ab.F11) antibodies as described in Chapter 2, Section 2.9 of the Materials and Methods. Mouse-IgG2b-APC or mouse-IgG2a-APC and mouse-IgG1-PE served as respective isotype controls (Figure 3.2.).

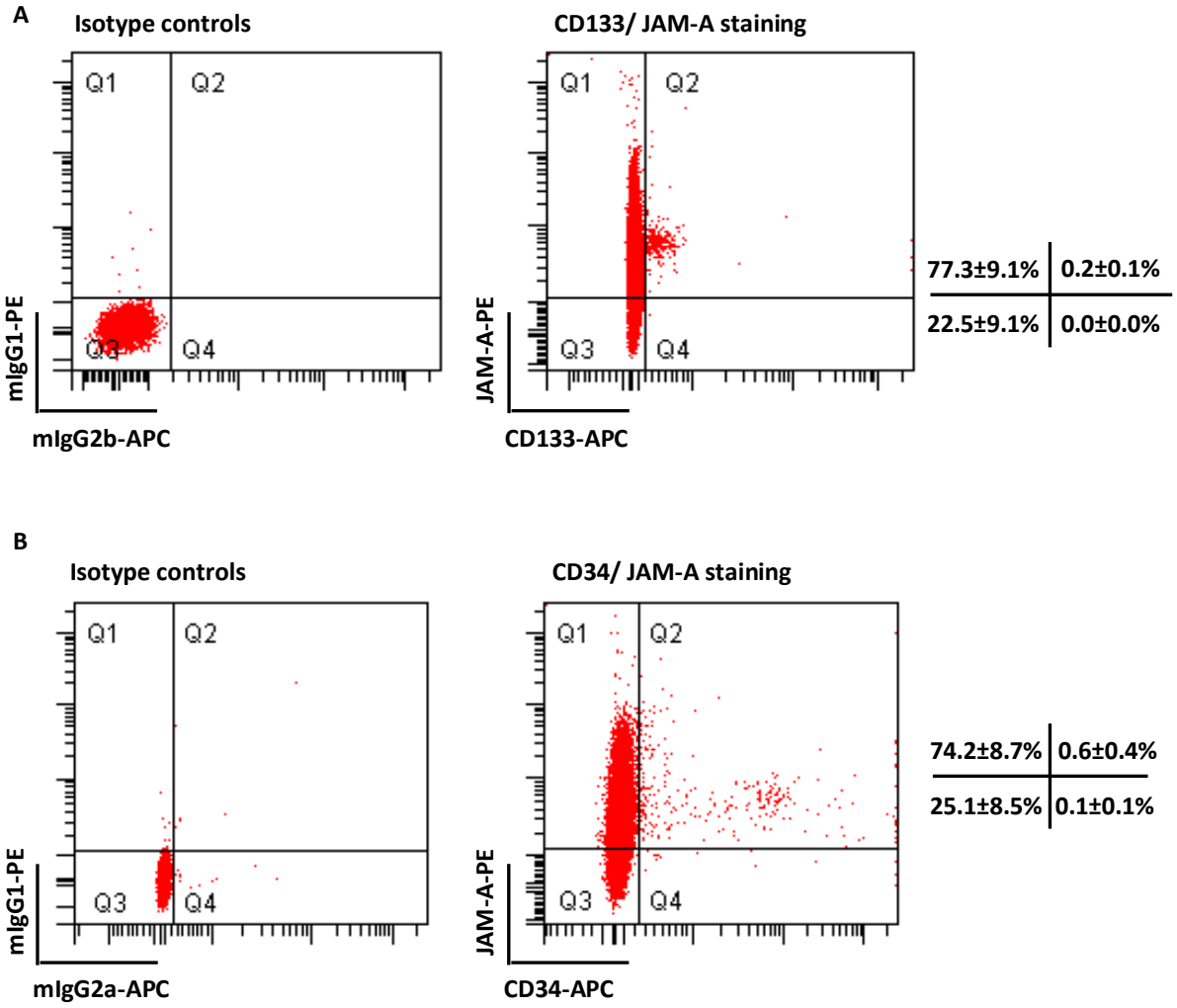

Figure 3.2. Expression of JAM-A on CD133 or CD34-positive human umbilical cord blood cells.
Cells were labelled with relevant PE- or APC- isotype controls (left dotplots) or with JAM-A-PE (M.Ab.F11) together with (A) CD133-APC (293C3) or (B) CD34-APC (AC136) antibodies (right dotplots) as described in section 2.11. Representive dotplots show dual-colour FACS analysis of (A) isotype controls or JAM-A and CD133 for N=4 independent human UCB MNCs or (B) isotype controls or JAM-A and CD34 for N=6 independent human UCB MNCs. The percentage of cells stained with JAM-A and CD133 or CD34 antibodies in each quadrant is indicated for individual experiments and as the mean ± S.E.M for N= 4-6 independent experiments.

When the UCB MNC fraction was examined by dual surface staining with CD133 and JAM-A antibodies by flow cytometry, 0.2±0.1% of the MNC population was CD133 and JAM-A double positive with the Median Fluorescence Intensity (M.F.I.) for JAM-A being 481±41. This incorporated all the $CD133^+$ cells (Figure 3.2.A). The expression on $CD34^+$ cells was similarly examined and 0.6±0.4% of MNC were found to co-express $CD34^+$ and JAM-A (M.F.I.

for JAM-A = 414±31), while 0.1±0.1% were CD34-positive and JAM-A-low/negative (Figure 3.2.B). Thus, 100% of $CD133^+$ cells and 90.4±6.5% of $CD34^+$ cells from UCB co-expressed JAM-A on their cell surfaces. Interestingly, these experiments also showed that between 74.2±8.7% and 77.3±9.1% of the other MNCs in UCB expressed the JAM-A protein above background levels set for the isotype control antibodies (Figure 3.2).

To enrich the primitive cell pools for this study, UCB $CD133^+$ and $CD34^+$ cells were isolated using magnetic anti-CD133 and anti-CD34 Microbeads from Miltenyi Biotec GmbH and MNCs from three different batches of UCB units. The purified cells were cultured in serum free Stemspan medium with cytokines including stem cell factor (SCF), *Interleukin-6* (IL-6), thrombopoietin (TPO) and Fms-like Tyrosine Kinase-3 ligand (Flt-3L) at 37°C overnight (See Materials and Methods, Chapter 2 Section 2.3.2) before analysing these cells by flow cytometry. The purity of the $CD133^+$ cells as determined by flow cytometry using the CD133 antibody (293C3) averaged 87.5±2.4% (Figure 3.3.A). Of these, all the viable $CD133^+$ cells expressed JAM-A, showing an average M.F.I. for JAM-A of 5017±378 (Figure 3.3.B). The purity of the $CD34^+$ cells was determined by flow cytometry using the class III CD34 antibody (AC136) and averaged 95.3±2.3% positive (Figure 3.4.A). Of these cells, 94.9±2.1% of the viable $CD34^+$ cells expressed JAM-A, showing an average M.F.I. for JAM-A of 1381±196 (Figure 3.4.B).

A

Experiments	CD133 Purity (%)	$CD34^+$ population (%)	JAM-A co-expression (%)
#1	92.1	95.8	98.9
#2	84.4	94.1	97.4
#3	85.9	98.5	98.7

B

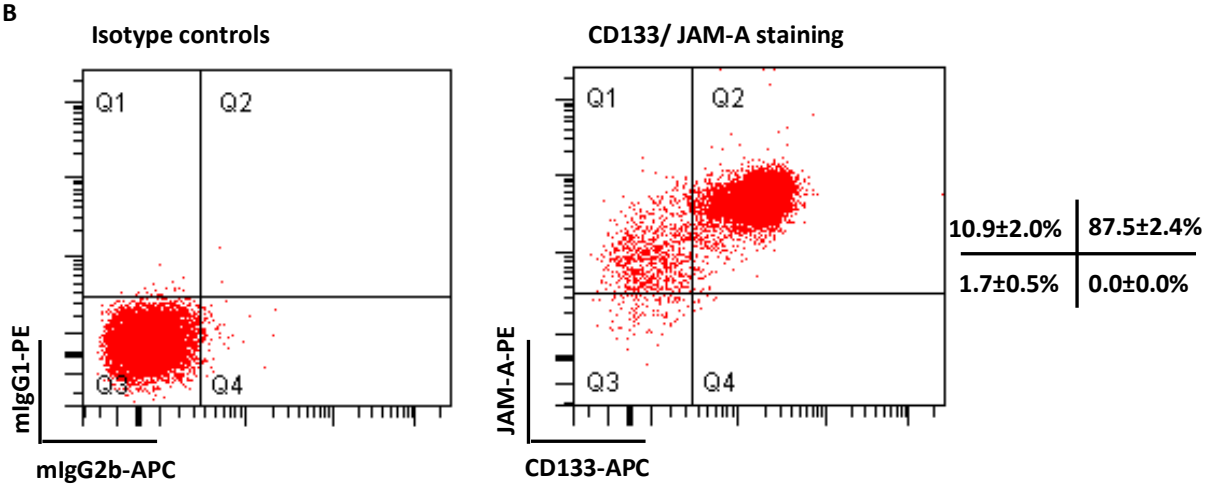

Figure 3.3. Expression of JAM-A on purified CD133-positive human umbilical cord blood cells.
Cells were labelled with relevant PE-, APC- or PerCP- isotype controls or with JAM-A-PE (M.Ab.F11) , CD133-APC (293C3), CD34-PerCP (8G12) antibodies as described in section 2.9. DAPI was used to exclude non-viable cells, before cells were analysed by flow cytometry. (A) A summary of the percent purity of each cell subset. (B) Representive dotplots showing dual-colour FACS analysis of isotype controls (left) or CD133 and JAM-A expression (right) on purified human UCB $CD133^+$ cells. The percentage of cells in each quadrant is indicated for individual experiments in (A) and as the mean ± S.E.M for N= 3 independent experiments in (B).

A

Experiments	CD34 Purity (%)	JAM-A co-expression (%)
#1	98.5	98.1
#2	97.6	95.8
#3	97.3	90.9

B

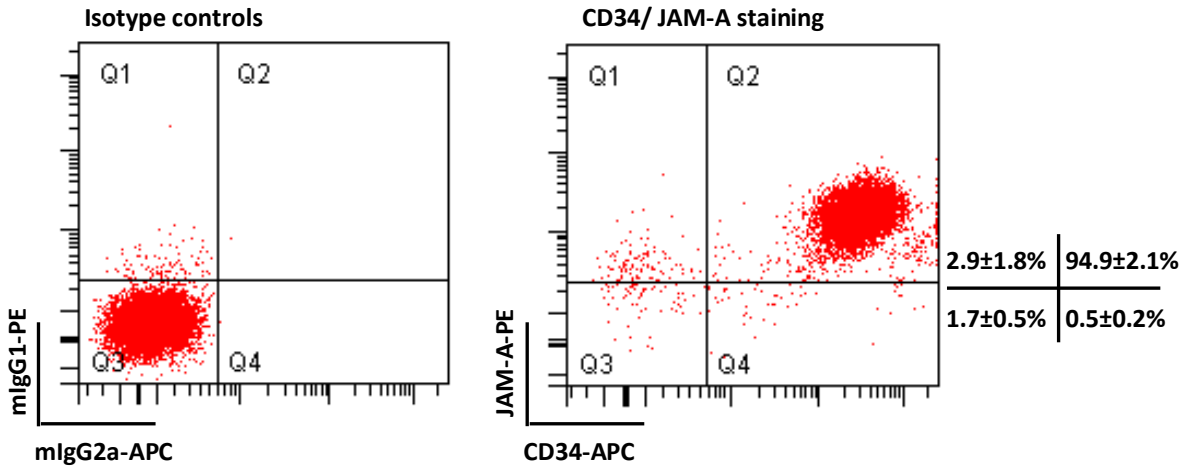

Figure 3.4. Expression of JAM-A on purified CD34 -positive human umbilical cord blood cells.
Cells were labelled with relevant PE- or APC- isotype controls or with JAM-A-PE (M.Ab.F11) and CD34-APC (AC136) antibodies, as described in section 2.9. DAPI was used to exclude non-viable cells, before cells were analysed by flow cytometry. (A) A summary of the percent purity of each cell subset. (B) Representive dotplots showing dual-colour FACS analysis of isotype controls (left) or CD34 and JAM-A expression (right) on purified human UCB $CD34^+$ cells. The percentage of cells in each quadrant is indicated for individual experiments (A) and as the mean ± S.E.M for N= 3 independent experiments (B).

Differential expression of JAM-A was noted on the purified $CD34^+$ cell population and the M.F.I. of subpopulations were further examined. The cells with the highest CD34 positive staining were observed to have slightly lower JAM-A staining (695.0±78.0 M.F.I.) than the bulk of the $CD34^+$ cell population (1220.0±187.7 M.F.I.) and the CD34-dim cells expressed even lower JAM-A (270.3±47.2 M.F.I.; Figure 3.5). As a consequence of these studies, the next analysis was to define the expression of JAM-A on the common human myeloid and lymphoid subsets from UCB by flow cytometry.

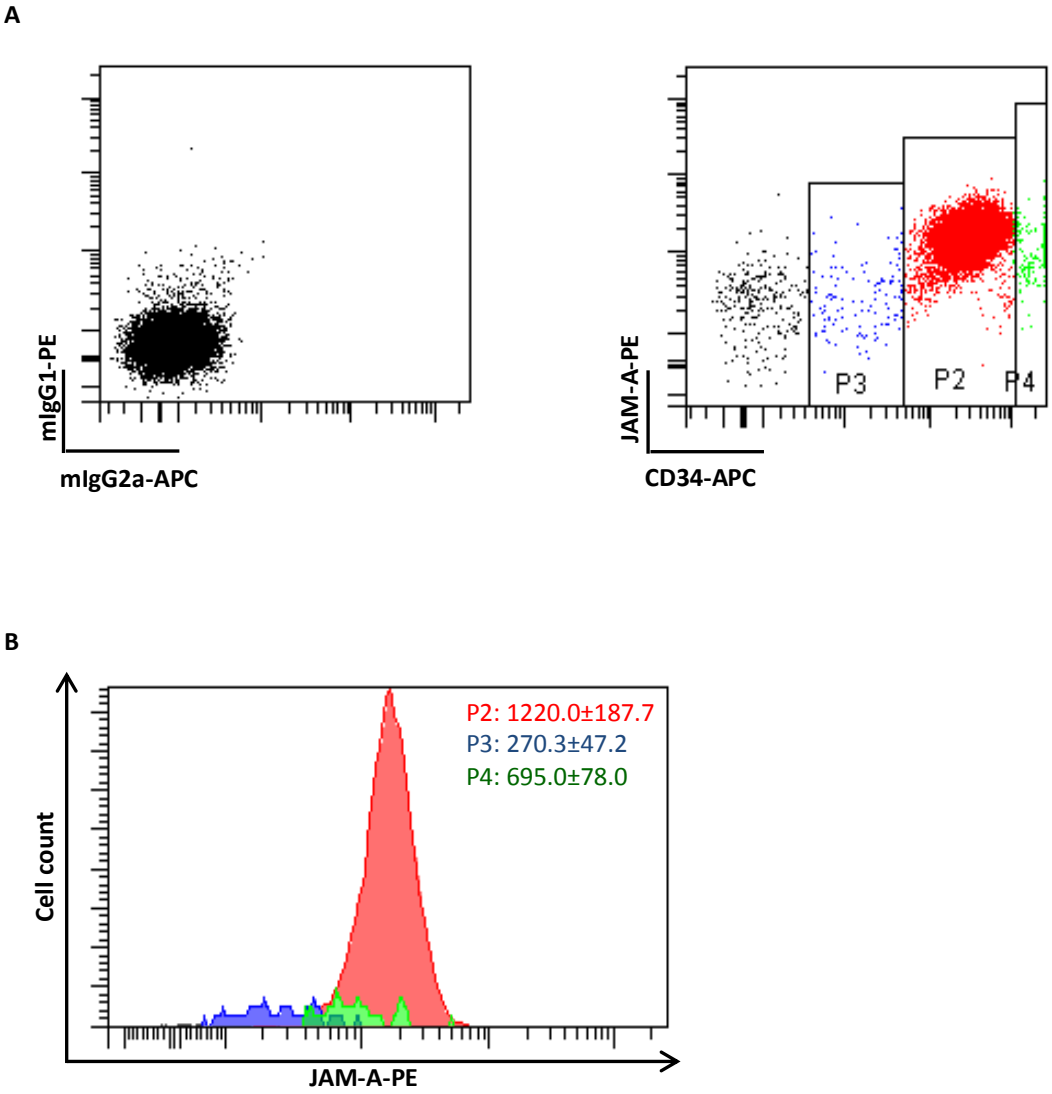

Figure 3.5. Differential expression of JAM-A on purified UCB CD34 positive cells.
Cells were labelled with relevant PE- or APC- isotype controls or with PE -JAM-A (M.Ab.F11) or APC-CD34 (AC136) antibodies for dual-colour FACS analysis of CD34 and JAM-A expression on purified human UCB $CD34^+$ cells (N=3). (A) Representitive FACS dotplot of purified UCB $CD34^+$ cells stained with CD34-APC and JAM-A-PE (right) and their isotype controls (left). Different levels of CD34-expressing cells were gated as shown. (B) The relative level of JAM-A-PE fluorescence in each group is shown in the histograms (B) according to the colour in the histogram in (A). Median fluorescence intensity (M.F.I.) ± S.E.M are shown in (B) for N= 3 independent experiments. The M.F.I.s of JAM-A fluorescence were for the isotype control 43.2±6.5, for $CD34^+$ total cells 1220.0±187.7 (P2, red), for CD34-dim cells 270.3±47.2 (P3, blue) and for CD34-high cells 695.0±78.0 (P4, green).

3.3.2. JAM-A expression on myeloid progenitor cells

As JAM-A expression was evident on immature haematopoietic progenitor cells, its expression on common myeloid progenitors (CMP) and common lymphoid progenitors (CLP) was examined further. The strategies to identify CMP and CLP from UCB units were a modification of published protocols using different combinations of cell surface phenotypes and commencing with enriched UCB $CD34^+$ cells. Studies by Goardon *et al*. (78) have demonstrated that it is possible to identify CMP and other enriched myeloid progenitor cells in human bone marrow as illustrated in Figure 3.6.

For these published studies, $CD34^+$ human bone marrow cells were enriched using MACS technologies, cryopreserved and then thawed and cultured overnight in SCF, Flt-3L and TPO (See Materials and Methods, Chapter 2 Section 2.3.2) before being subjected to flow cytometric analyses. Viable cells were selected as Hoechst 33258 negative (Figure 3.6, top left dotplot), then as Lin^- cells based of negative staining for CD2, CD3, CD4, CD7, CD8, CD10, CD11b, CD14, CD19, CD20, CD56 and CD235a (Figure 3.6, top middle dotplot), before being gated on $CD34^+CD38^+$ cells (Figure 3.6., top right dotplot). The latter cells were then gated based on CD123 and CD45RA markers (Figure 3.6., lower middle dotplot). The $CD123^{+/low}CD45RA^-$, $CD123^{low/-}CD45RA^-$ and $CD123^+CD45RA^+$ cells contained the following myeloid progenitor cells, CMP (common myeloid progenitors), MEP (megakaryocyte-erythroid progenitors) and GMP (granulocyte/monocyte progenitors). These could then be segregated again on the basis of CD110 and CD45RA expression. As shown in Figure 3.6 (lower right dotplot), CMP were $CD110^-CD45RA^-$, MEP were $CD110^+CD45RA^-$ and GMP were $CD110^-CD45RA^+$. The $CD34^+CD38^-$ cells (Figure 3.6., upper right dotplot) could be segregated into MMP (multipotential progenitor cells), HSC (haematopoietic stem cells) and $CD38^-CD45RA^+$cells.

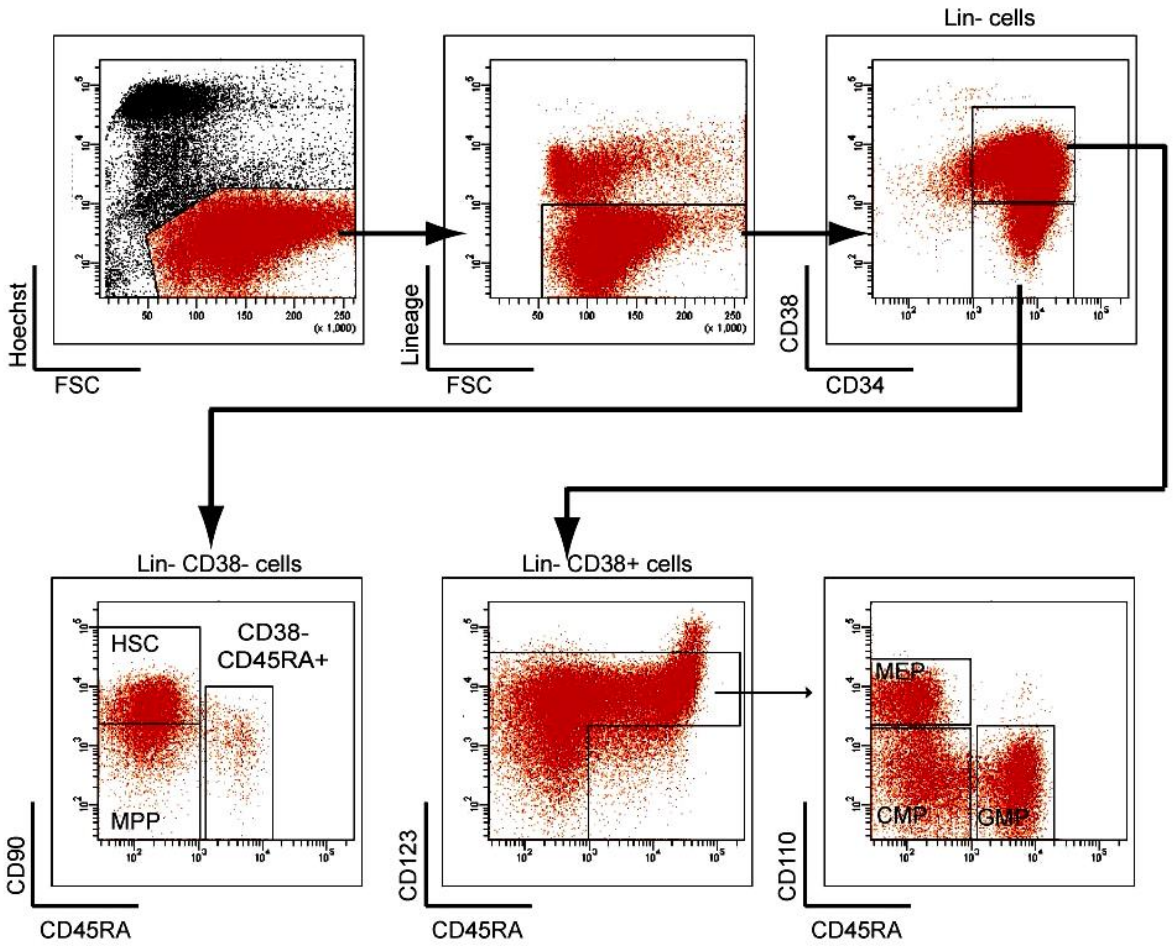

Figure 3.6. Goardon et al. gating strategy for immunophenotyping and FACS-sorting human bone marrow stem/progenitor compartments.
Normal $CD34^+$ haematopoietic progenitor cells from human bone marrow analysed for expression of lineage markers, CD34, CD38, CD45RA, CD90, CD110 and CD123 were categorised as HSCs: $Lin^-CD34^+CD38^-CD90^+CD45RA^-$; MPPs: $Lin^-CD34^+CD38^-CD90^-CD45RA^-$; $CD38^-CD45RA^+$cells: $Lin^-CD34^+CD38^-CD90^-CD45RA^+$; CMPs: $Lin^-CD34^+CD38^+CD123^{low/+}D45RA^-CD110^-$; GMPs: $Lin^-CD34^+CD38^+CD123^+CD45RA^+CD110^-$ and MEPs: $Lin^-CD34^+CD38^+CD123^{-/low}CD45RA^-CD110^+$. Taken from Goardon *et al.* (78). Reprinted from Cancer Cell 19, Goardon N, Marchi E, Atzberger A, Quek L, Schuh A, Soneji S, Woll P, Mead A, Alford KA, Rout R, Chaudhury S, Gilkes A, Knapper S, Beldjord K, Begum S, Rose S, Geddes N, Griffiths M, Standen G, Sternberg A, Cavenagh J, Hunter H, Bowen D, Killick S, Robinson L, Price A, Macintyre E, Virgo P, Burnett A, Craddock C, Enver T, Jacobsen SE, Porcher C, Vyas P., Coexistence of LMPP-like and GMP-like leukemia stem cells in acute myeloid leukemia, 138-52, Copyright (2011), with permission from Elsevier.

Using these and related methods, Goardon *et al.* (78) were able to subdivide and sort for enriched subsets of hHSCs, hMPPs, $hCD38^-CD45RA^+$ cells, hCMPs, hGMPs and hMEPs as

i) $Lin^-CD34^+CD38^-CD90^+CD45RA^+$,

ii) $Lin^-CD34^+CD38^-CD90^-CD45RA^-$,

iii) $Lin^-CD34^+CD38^-CD90^-CD45RA^+$,

iv) $Lin^-CD34^+CD38^+CD123^{low/+}CD45RA^-CD110^-$,

v) $Lin^-CD34^+CD38^+CD123^+CD45RA^+CD110^-$ and

vi) $Lin^-CD34^+CD38^+CD123^{-/low}CD45RA^-CD110^-$ respectively.

In the experiments presented in this chapter, UCB $CD34^+$ cells were enriched using MACS technologies, cryopreserved and then thawed and cultured overnight in SCF, Flt-3L, TPO and IL-6 (See Materials and Methods, Chapter 2 Section 2.3.2) before being subjected to flow cytometric analyses. The strategy described above to analyse rare progenitor cells by flow cytometry was modified to take into account the flow cytometer available for use. DAPI was used as the viability stain in place of Hoechst 33258, and the lineage marker mix contained CD2 (RPA-2.10), CD3 (OKT3), CD7 (M-T701), CD10 (HI10a), CD11b (ICRF44), CD14 (HIB19), CD16 (CB16), CD19 (HIB19), CD56 (CB56) and CD235a (HIR2) antibodies. CD16 was present in the purchased cocktail of lineage markers although it was not present in the original protocol by Goardon *et al*. (78), and CD4, CD8 and CD20 were not included in the protocol described here.

Each set of markers was first assessed on the MACS enriched human UCB $CD34^+$ cell population as shown in the Figure 3.7. The percent positive, when determined as cells above the gate set for the isotype controls, was as follows. 92.4±4.0% of the MACS enriched viable cells were CD34 positive (Figure 3.7.A), 39.5±7.8% were lineage-positive (Figure 3.7.B), 26.3±7.8% were CD38 positive (Figure 3.7.C), 34.1±12.5% were CD45RA positive (Figure 3.7.D), 6.0±3.0% were CD123 positive (Figure 3.7.E) and 9.5±6.3% CD7 positive (Figure 3.5.F). It is evident that cells with weaker, dim or negative staining were located in the negative gate.

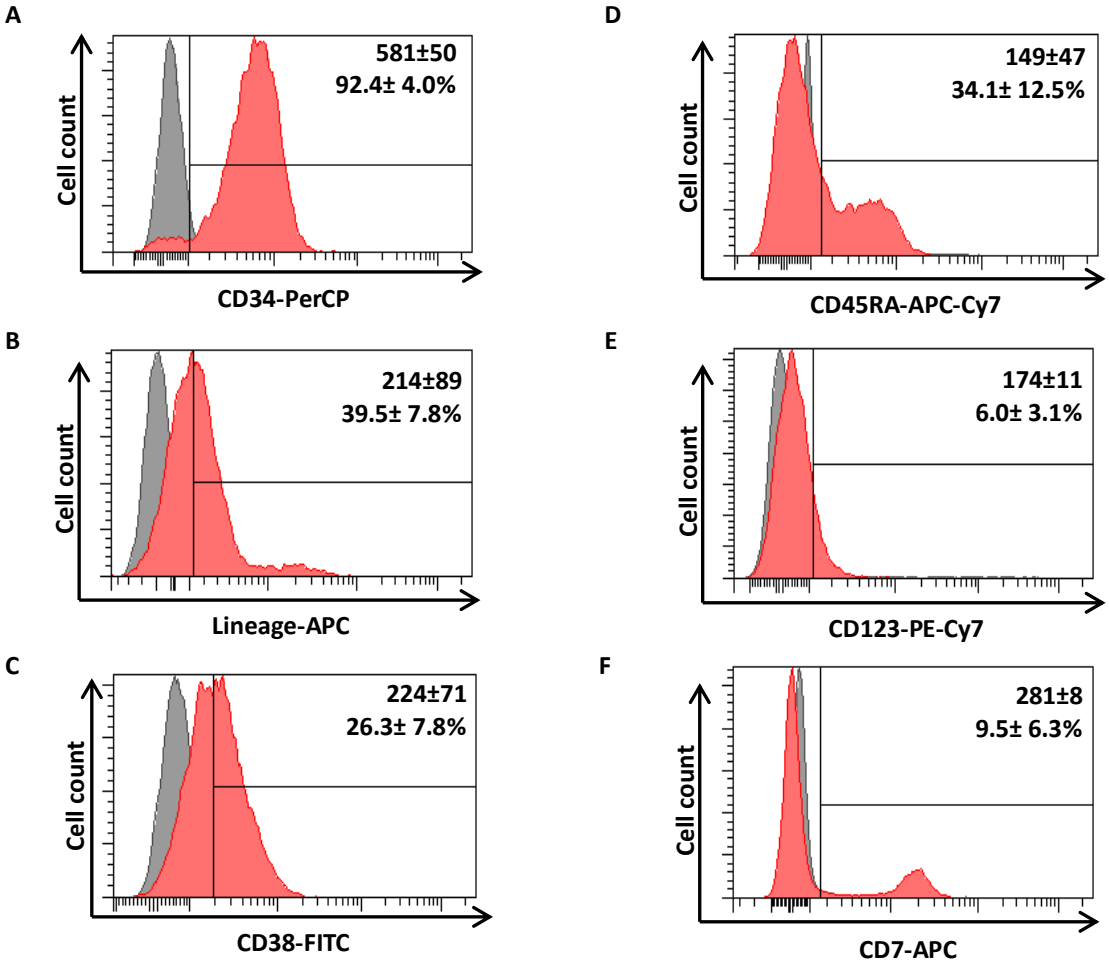

Figure 3.7. Proportion of the expression of selective markers on UCB CD34$^+$ cells.
Representative FACS histograms of purified UCB CD34$^+$ cells stained with the (A) PerCP-CD34 (8G12), (B) APC-Lineage marker mix, (C) FITC-CD38 (HIT2), (D) APC-Cy7- CD45RA (HI100), (E) PE-Cy7-CD123 (7G3) and (F) APC-CD7(M-T701) shown in red in comparision to their isotype controls (gray). Values are M.F.I.± S.E.M and the % positive± S.E.M for cells above of the gate set for the isotype control. In these experiments of N=3, the purity of CD34 positive population was 92.4±4.0%.

The pool of CD34$^+$ cells isolated from the same UCB unit was divided into two, one for myeloid progenitor cell analysis and the other for lymphoid progenitor cell analysis. The myeloid progenitor cell gating strategy and staining protocols, which as indicated above were a modification of the published protocol described in Figure 3.6 (78), are outlined in Figure 3.8 and described in Chapter 2 Section 2.9.

Figure 3.8. A flowchart showing the flow cytometric gating strategy for CMP, GMP and MEP.

Using DAPI staining, 87.6±5.7% (Figure 3.8.B, top left dotplot) of the enriched and overnight cultured UCB $CD34^+$ cells were viable (DAPI negative). Among these viable cells and as gated, lineage-negative (Lin^-) cells constituted 60.9±4.2% of the cells (Figure 3.9.B, top middle dotplot) and 53.2±6.2% of these were further identified as CD34 and CD38 double positive ($CD34^+CD38^+$ in Figure 3.9.B, top right dotplot). The myeloid progenitor population was subsequently gated from the $lin^-CD34^+CD38^+$ population using CD123 (7G3) and CD45RA (HI100) antibodies. Here, the myeloid progenitor cells, which were $CD45RA^-CD123^{+/low}$, $CD45RA^-CD123^{low/-}$ and $CD45RA^+CD123^+$, included the CMP, MEP and GMP fractions respectively (Figure 3.9.B, middle and lower left dotplot). Of these and based on phenotype, the GMPs would be located in the $CD45RA^+$ gate and the MEPs and CMPs in the $CD45RA^-$ gate. Our flow cytometer did not allow us to further subdivide these cells into CD110 positive and negative subfractions if JAM-A expression were to be analysed, and hence CMP and MEP populations could not be distinguished and are referred to as the CMP/MEP mixed cell population. From our results, CMP/MEP comprised 69.3±1.8% of the $lin^-CD34^+CD38^+CD45RA^-CD123^{+/-}$ population, while GMP made up to 18.7±2.3% of these cells.

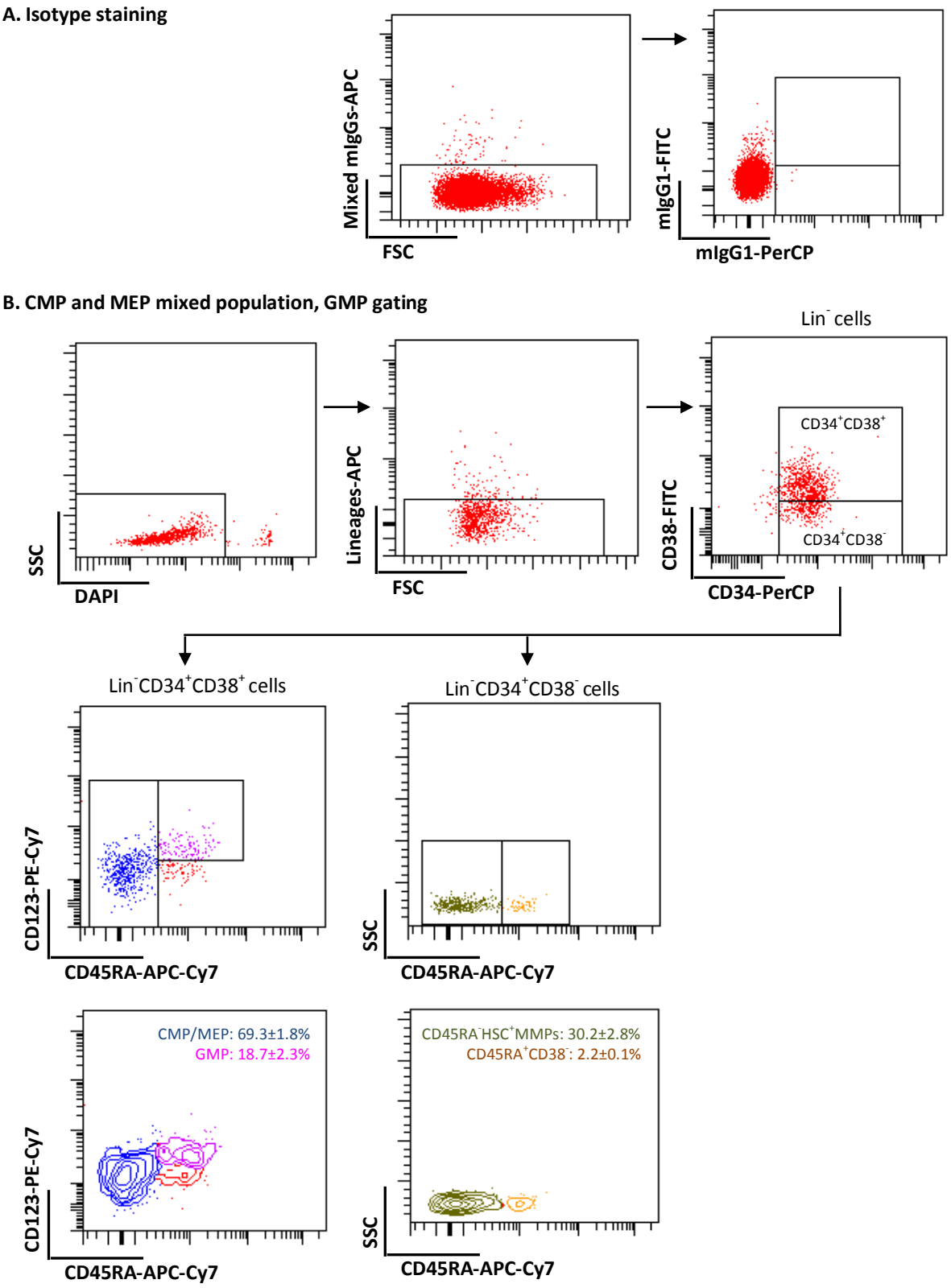

Figure 3.9. Phenotypically defined common granulocyte/monocyte progenitors (GMP), common myeloid progenitors (CMP), megakaryocyte/erythroid progenitors (MEP), haematopoietic stem cells (HSC) and multipotential progenitors (MPP) in human umbilical cord blood.
Purified UCB $CD34^+$ cells were analysed for expression of lineage markers, CD38, CD34, CD123 and CD45RA (B; top box) by comparison to their isotype controls (A). The colour codes show the difference subsets. Values are M.F.I.± S.D. and the % positive± S.E.M for In these experiments of N=3, the purity of CD34 positive population was 92.4±4.0%.

Essentially all the early myeloid progenitor cells expressed JAM-A (Figure 3.10, left histogram). GMPs showed relatively higher levels of JAM-A expression (M.F.I. 1834±278) compared to CMP/MEP (M.F.I. 1594±228) but these differences did not reach statistical significance using Student's *t-test* (CMP/MEP v.s. GMP: p=0.54).

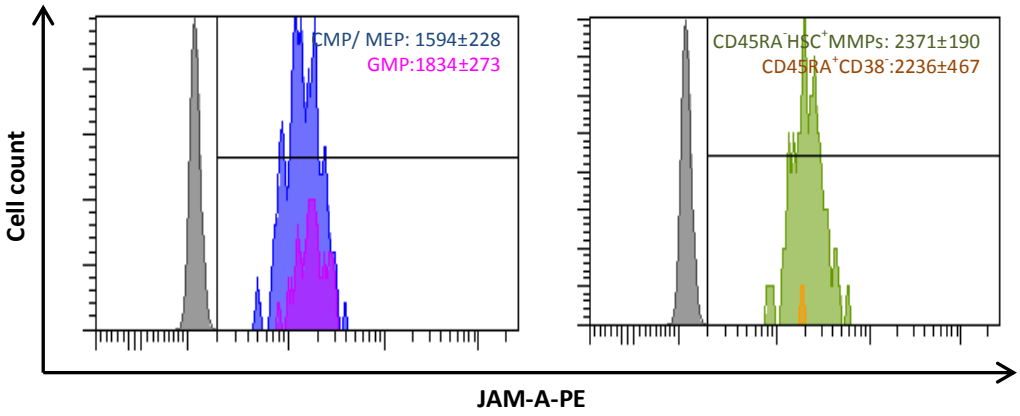

Figure 3.10. Expression of JAM-A on phenotypically defined common granulocyte/monocyte progenitors (GMP), common myeloid progenitors (CMP), megakaryocyte/erythroid progenitors (MEP), haematopoietic stem cells (HSC) and multipotential progenitors (MPP).
JAM-A expression on the cell populations defined in Figure 3.9.B is shown in correlative colours in comparision to isotype staining (gray). The proportion and JAM-A M.F.I. of CMP/MEP (blue)**:** lin$^-$CD34$^+$CD38$^+$CD123$^{+/-}$ CD45RA$^-$, GMP (purple): lin$^-$CD34$^+$CD38$^+$CD123$^+$CD45RA$^+$, HSC and MMP containing population (green): lin$^-$ CD34$^+$CD38$^-$CD45RA$^-$ and CD45RA$^+$CD38$^-$ population (yellow): lin$^-$CD34$^+$CD38$^-$CD45RA$^-$ are shown accordingly. Values are M.F.I.± S.D. and the % positive± S.E.M for In these experiments of N=3, the purity of CD34 positive population was 92.4±4.0%.

In addition to myeloid progenitor cells, phenotypically defined HSC and MPP containing populations (lin$^-$CD34$^+$CD38$^-$CD45RA$^-$, referred to as CD45RA$^-$HSC/MPP) and the CD45RA$^+$CD38$^-$ population (lin$^-$CD34$^+$CD38$^-$CD45RA$^+$) were examined for their JAM-A expression in parallel experiments (Figure 3.10, right histogram). Our flow cytometer did not allow us to further subdivide these cells into HSC and MPP subfractions using the CD90 marker. CD45RA$^-$HSC/MPPs made up to 30.2±2.8% of lin$^-$CD34$^+$CD38$^-$ cells, while the CD45RA$^+$CD38$^-$ population accounted for 2.2±0.1% of these cells. Both CD45RA$^-$HSC/MPPs

(M.F.I. 2371±190) and the $CD45RA^{+}CD38^{-}$ population (M.F.I. 2237±467) showed relatively higher levels of JAM-A expression compared to myeloid progenitors, although this was not statistically significant using Student's *t*-test ($CD45RA^{-}$HSC/MPPs v.s. CMP/MEPs: p=0.059; $CD45RA^{-}$HSC/MPPs v.s. GMPs: p=0.18; $CD45RA^{+}CD38^{-}$ population v.s. CMP/MEPs: p=0.28; $CD45RA^{+}CD38^{-}$ population v.s. GMPs: p=0.50; $CD45RA^{-}$HSC/MPPs v.s. $CD45RA^{+}CD38^{-}$ population: p=0.80).

3.3.3. JAM-A expression on lymphoid progenitor cells

Studies by Hoebeke *et al.* (334) and Hao *et al.* (335) have identified lymphoid progenitor cells as being $CD34^{+}CD38^{-}CD7^{+}$ in UCB as illustrated in Figures 3.11. This research demonstrated that such cells could give rise to B and T lymphoid cells, NK cells and dentritic cells. In other recent studies, these cells have been termed multi-lymphoid progenitors (MLP) and are considered in the Discussion in more detail.

For the experiments described in this Chapter, a flowchart of the gating strategy for these phenotypically defined CLP and their JAM-A expression is given in Figure 3.12.A. Viable purified UCB $CD34^{+}$ cells were gated as DAPI negative cells and were found to be 87.6±5.7% viable (Figure 3.12.C, left dotplot). This was followed by dual-staining with CD34 and CD38 (Figure 3.12.C, middle dotplot). $CD34^{+}CD38^{-}$ population accounted for 50.5±7.5%. Among them, CLP ($CD34^{+}CD38^{dim/-}CD7^{+}$) accounted for 3.5±0.7% with JAM-A M.F.I. being 2126 ±229 (Figure 3.12.D). This was not statisticaly significantly different from the JAM-A staining on UCB $CD34^{+}$ early myeloid progenitor cells (p>0.1).

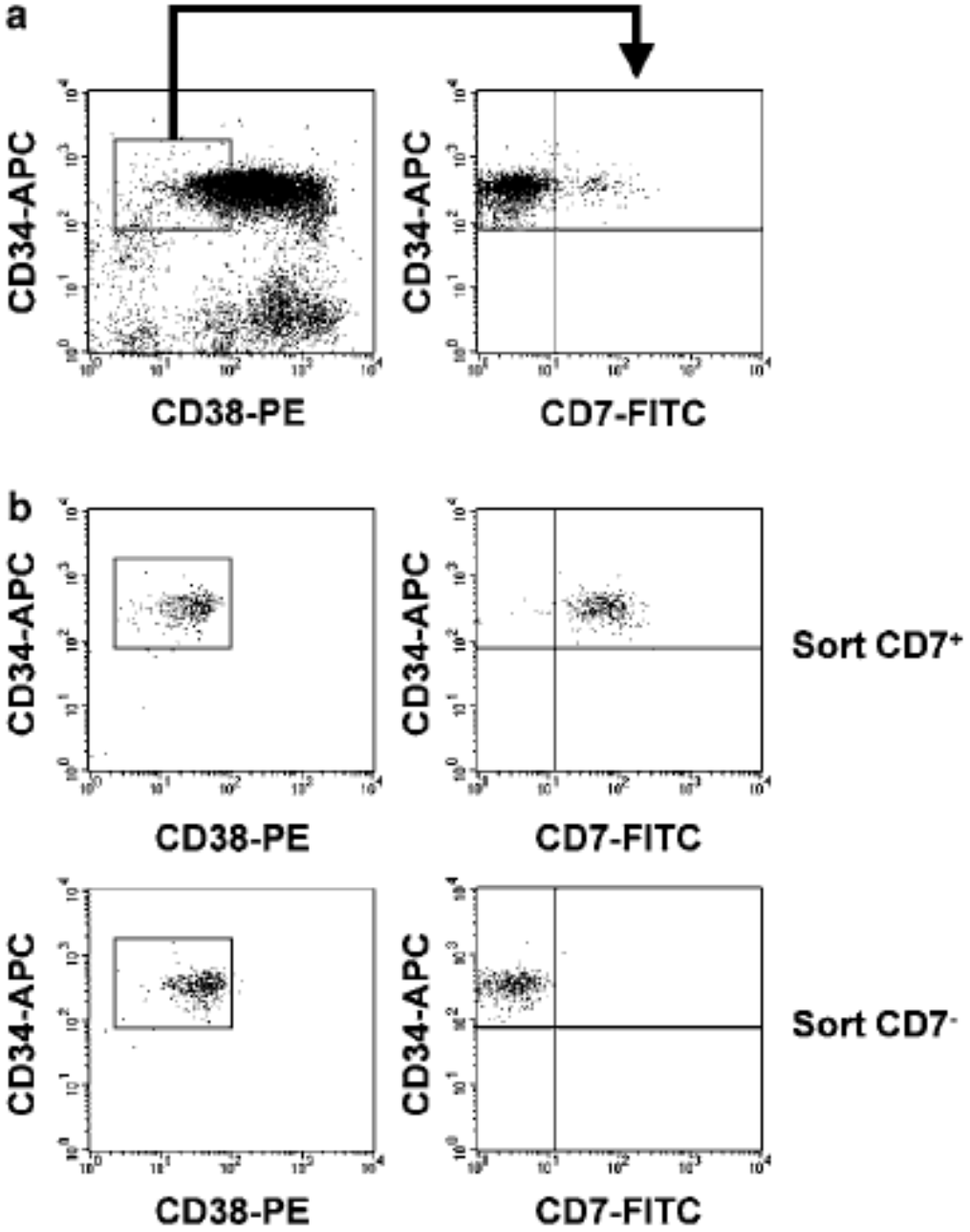

Figure 3.11. Gating strategy developed by Hoebeke et al. for immunophenotyping and flow sorting human umbilical cord blood common lymphoid progenitor cells (CLP).
Normal $CD34^+$ haematopoietic progenitor cells from human umbilical cord blood analysed for expression of CD34, CD38 and CD7 were categorised as $CD34^+CD38^-CD7^+$ CLP or $CD34^+CD38^-CD7^-$ CLP. (A) Example of sorting strategy. (B) Reanalysis of sorted cells. Taken from Hoebeke *et al.* (334). Reprinted by permission from Macmillan Publishers Ltd: Leukaemia (334), Copyright (2007).

A

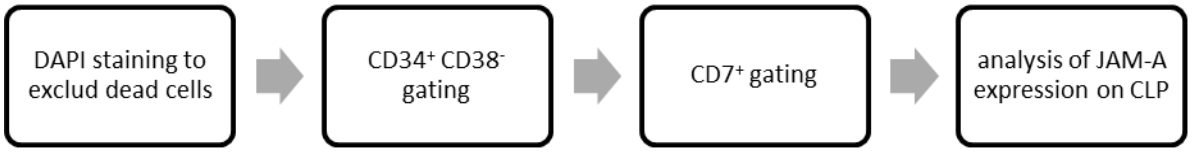

B. Isotype staining

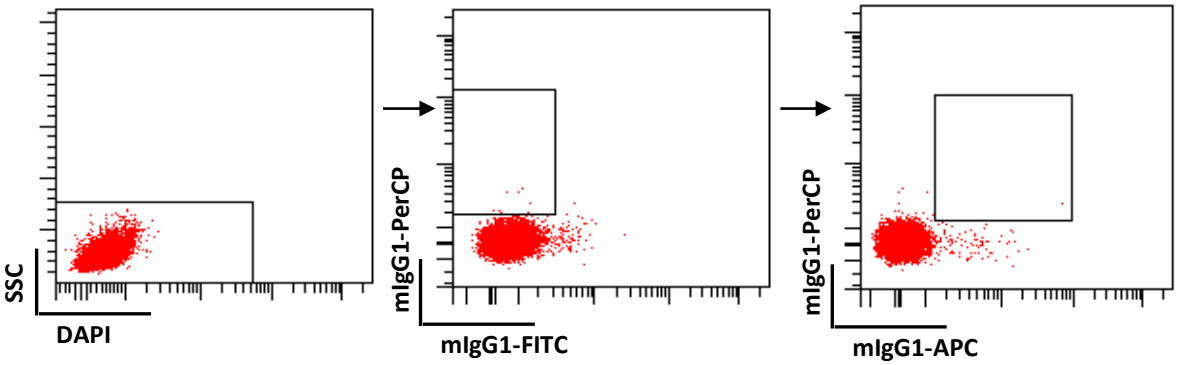

C. CLP gating

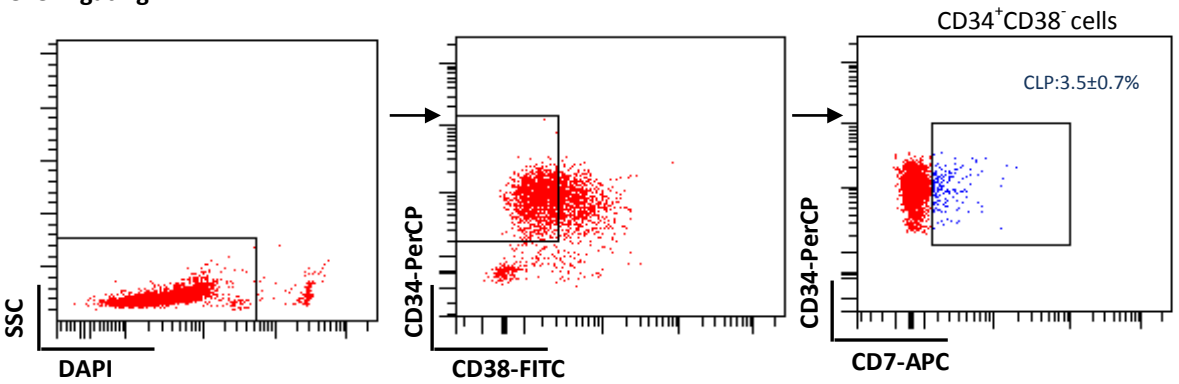

D

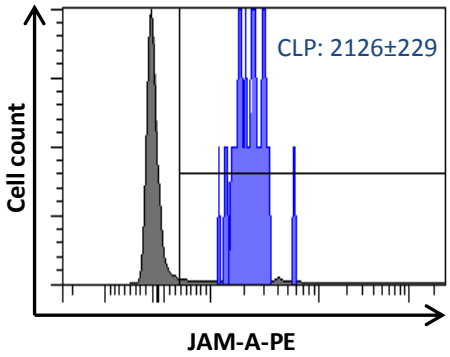

Figure 3.12. Expression of JAM-A on common lymphoid progenitors (CLP).
(A) A flowchart of gating strategy for CLP is shown. Purified UCB $CD34^+$ cells were analysed for viability and expression of CD38, CD34 and CD7 (C) by comparison to their isotype controls (B). CLP (blue): $CD34^+CD38^-CD7^+$. (D) JAM-A expression on CLP (blue) was shown in comparision to its isotype staining (gray). Values are mean M.F.I.± S.E.M. and the % positive±S.E.M for In these experiments of N=3, the purity of CD34 positive population was 92.4±4.0%.

Multi-colour staining of JAM-A on $CD34^+$ cells expressing CD19 or CD7 was also conducted to investigate if JAM-A expression differed on the $CD34^+/CD19^+$ and the $CD34^+/CD7^+$ subpopulations. This was based on the classification used by Dr. Alison Blair's group (79, 81, 336). In the purified UCB $CD34^+$ cell population, 1.3±0.3% were $CD19^+$ ($CD34^+/CD19^+$), and the majority (1.2±0.3%) of these were JAM-A positive (Figure 3.13).

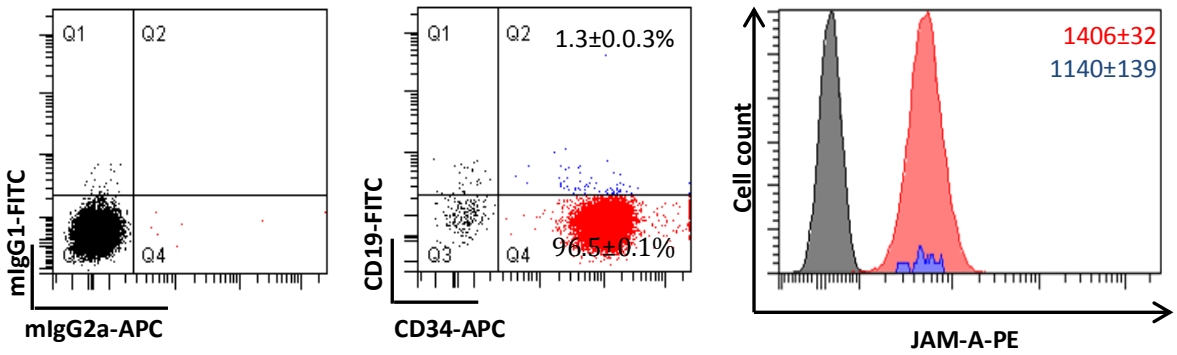

Figure 3.13. Expression of JAM-A and CD19 on purified UCB $CD34^+$ cells.
Representive dotplots showing dual-colour FACS analysis of purified UCB $CD34^+$ cells using PerCP-CD34 (8G12) against FITC-CD19 (HIB19) (middle dotplots) or their isotype controls (left dotplots). The histogram plots show JAM-A expression (M.Ab.F11) on the double positive population (blue) or single $CD34^+$ cells (red) in comparison to the isotype control (black). Values are mean M.F.I.± S.E.M. for the positive histograms and the mean % positive± S.E.M for the CD34/CD7 quadrants for N=3 independent experiments. The purity of CD34 positive population was 95.7±0.4%.

Additionally, 3.9±0.6% of the UCB cells coexpressed CD34 and CD7, all of which were JAM-A positive (Figure 3.14). In both cases, the double positive cells showed slightly lower JAM-A M.F.I.s compared to the $CD34^+$ cells which were $CD19^-$ or $CD7^-$ (1140±139 v.s. 1406±32 for the CD19 analyses and 1884±304 v.s. 1992±360 for the CD7 analyses).

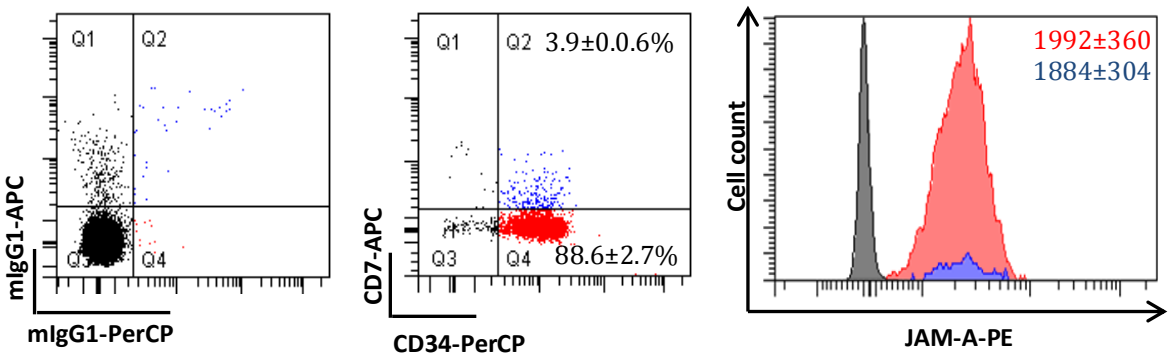

Figure 3.14. Expression of JAM-A and CD7 on purified UCB CD34 cells.
Representive dotplots showing dual-colour FACS analysis of purified UCB $CD34^+$ cells using PerCP-CD34 (8G12) against APC-CD7 (M-T701) and JAM-A expression level (M.Ab.F11) on the double $CD34^+CD7^+$ (blue) or single $CD34^+$ cells (red) were shown in comparison to the isotype control (black) in the right panels. Values are mean M.F.I.± S.E.M. for the CD34/CD7 quadrants and the mean % positive± S.E.M. for the positive histograms for N=3 independent experiments. The purity of CD34 positive population was 86.9±6.4%.

3.3.4. JAM-A is more highly expressed on monocytes and megakaryocyte progenitor cells than on other myeloid and lymphoid cells from human umbilical cord blood.

It was noted that JAM-A expression was not limited to human UCB $CD34^+$ or $CD133^+$ cells, but was also present on more mature haematopoietic cells. In order to investigate this, dual-colour FACS analysis was applied to the UCB MNC populations using different lineage markers combined with JAM-A staining. In the FACS analyses presented here (See Materials and Methods, Chapter 2 Section 2.9), 92.9±1.3% of MNCs was $CD45^+$ and 10.1±3.7% was $CD45^-CD235a^+$ (Table 3.1). This is consistent with other studies where the UCB $CD45^-$ cell population has been shown to contain nucleated erythroid cells (nRBCs) and where the upper limit of nucleated red blood cell counts has been estimated as 22 nRBCs per 100 white blood cells (337). Among the $CD45^+$ cells, 76.6±5.1% of $CD45^+$ MNCs expressed JAM-A above isotype control levels, while $CD235a^+$ red cells varied in their positivity, ranging from

16.9% to 93.8% and averaging 55% (Figure 3.15). Table 3.1 summarises the percentage of each subpopulation in UCB MNCs and the JAM-A-positive proportion (above the isotype control) in each subset among tested UCB units.

Table 3.1. JAM-A expression on umbilical cord blood mononuclear cells.

Biomarker	% Cells positive (Mean ± SEM)	% of Cell subset expressing JAM-A (Mean ± SEM)
CD45 - Common leucocyte antigen marker	92.9±1.3%	76.7±5.1%
CD235a (Glycophorin A) - Erythroid marker	10.1±3.7%	4.1±1.5%
Myeloid lineages		
CD66 - Neutrophil marker	54.4±3.5%	48.0±2.2%
CD14 - Monocyte marker	9.7±1.1%	9.6±1.1%
CD41a - Megakaryocyte and early HPC marker*	10.6±3.6%	10.6±3.6%
Lymphoid lineages		
CD19 - B lymphoid marker	5.2±1.1%	3.8±0.9%
CD3 - T lymphoid marker	22.8±2.8%	17.3±4.0%
CD56 - NK cell marker	4.2±0.8%	3.2±0.6%

*HPC: haematopoietic progenitor cell.
Values are the means± S.E.M. for N=7 UCB samples.

JAM-A was expressed on the surface of most myeloid lineage cells, being present on 90% of $CD66^+$ neutrophils, 99% of $CD14^+$ monocytes, and on 100% of $CD41a^+$ megakaryocyte precursors (Figure 3.16).

For the lymphoid lineages, almost three quarters of CD19, CD3 or CD56 positive cells co-expressed JAM-A when gated against the negative isotype control. These included 74% of $CD19^+$ B lymphocytes , 70% of $CD3^+$ T lymphocytes and 73% of $CD56^+$ natural killer (NK) cells being JAM-A positive (Figure 3.17).

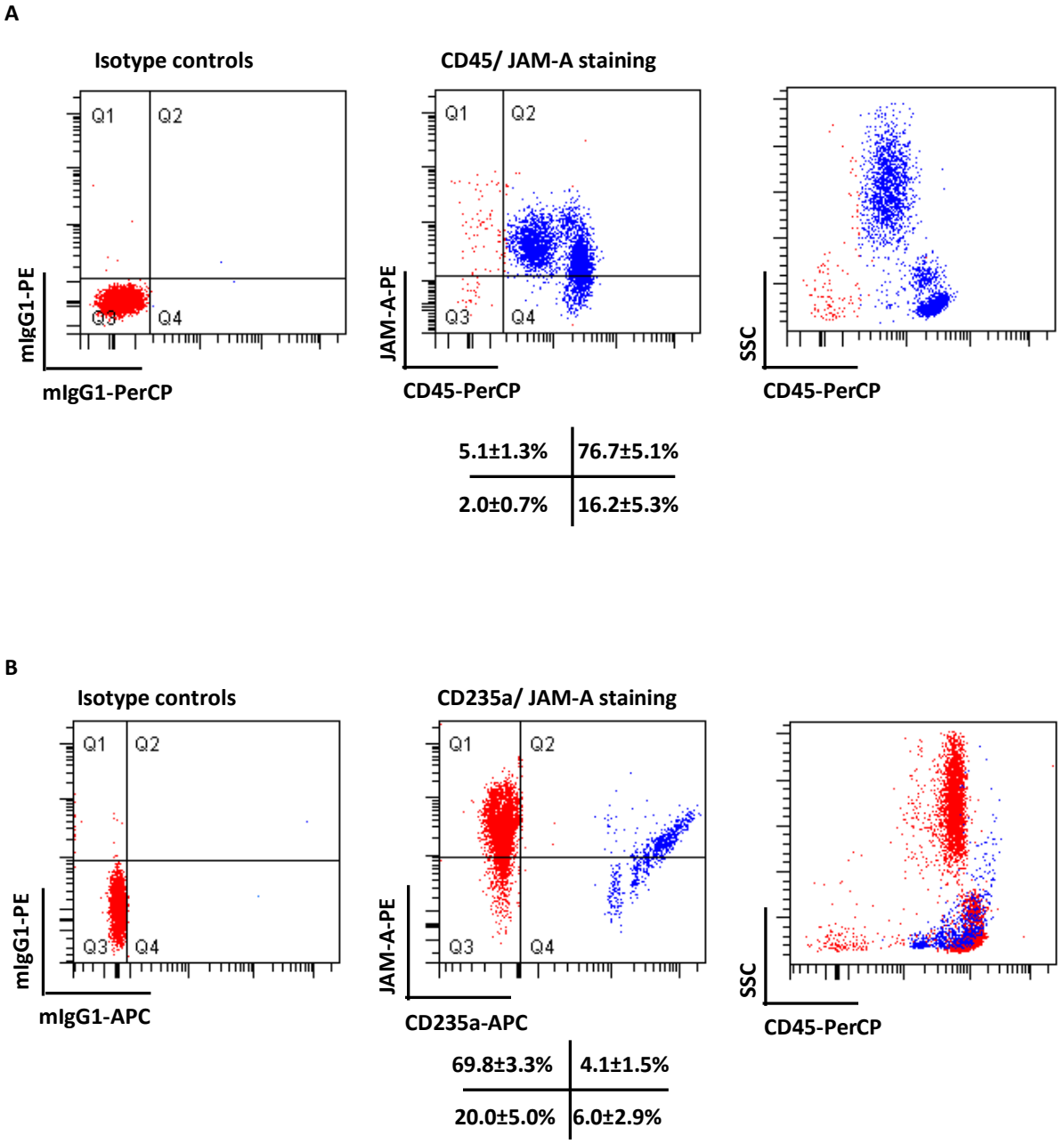

Figure 3.15. Expression of JAM-A on CD45 and CD235a positive cells.
Representative dotplots of human UCB MNCs stained for isotype controls (left dotplots in A and B) or (A) PE-JAM-A (M.Ab.F11) with PerCP-CD45 (2D1) (top middle dotplot) or (B) PE-JAM-A (M.Ab.F11) with APC-CD235a (HIR2) (lower middle dotplot). In the JAM-A and CD45 or CD235a dot plots, the percentage of cells in each quadrant is given as the mean ± S.E.M. for N= 3 independent experiments. The right hand panel of dotplots refers to the distribution of the CD45 and CD235a positive cells backgated onto MNCs analysed for CD45 versus side-scatter (blue).

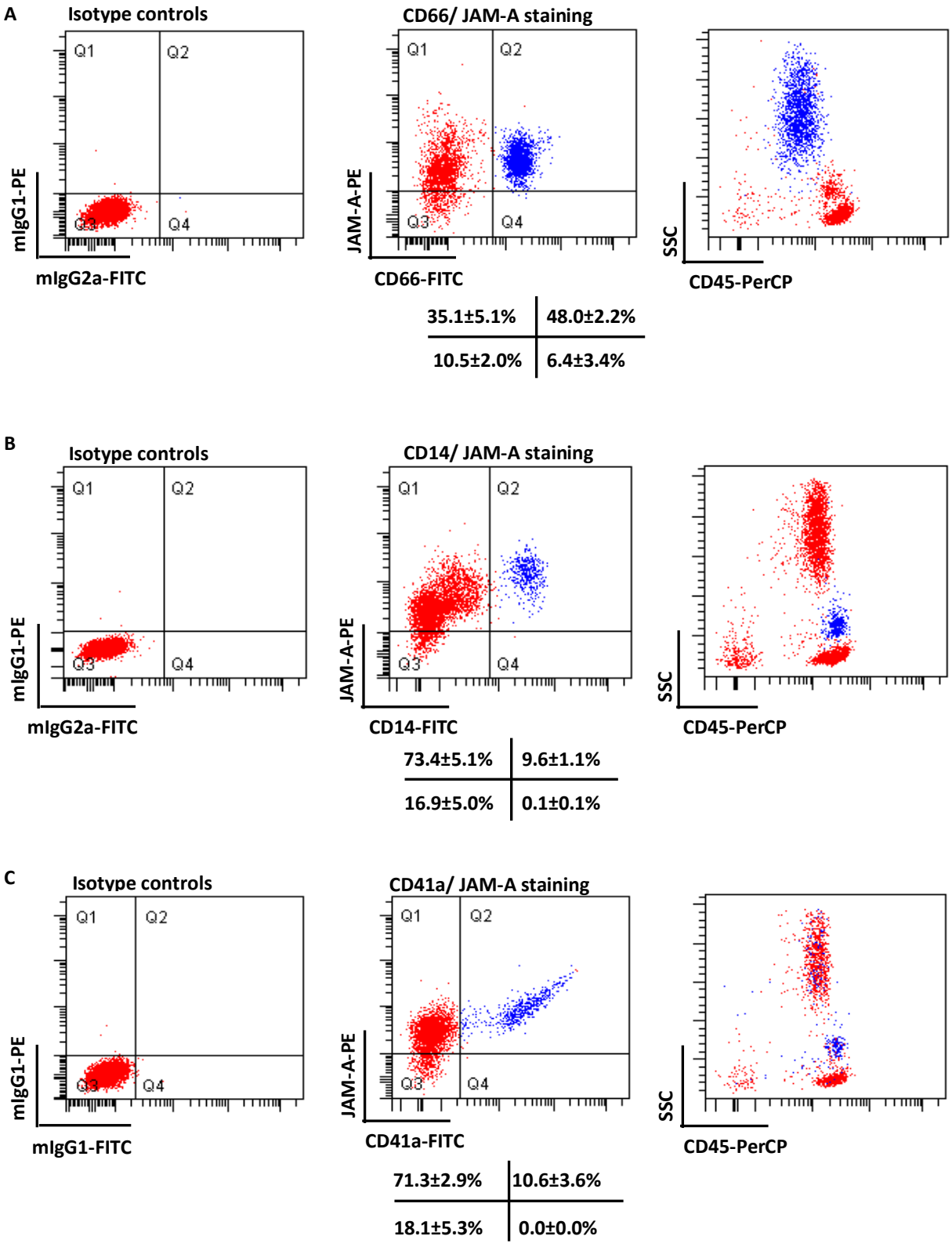

Figure 3.16. Expression of JAM-A on myeloid lineage cells.
Representitive dotplots of dual-colour FACS analysis of isotype controls (left dotplots in A to C) or human UCB MNCs stained with (A) PE-JAM-A (M.Ab.F11) and FITC-CD66 (B1.1/CD66), (B) PE-JAM-A (M.Ab.F11) and FITC-CD14 (M5E2) or (C) PE-JAM-A (M.Ab.F11) and FITC-CD41a (HIP8) (middle dotplots). The percentage of cells in each quadrant of cells as means ± S.E.M. for N= 3 independent experiments is shown underneath each of the respective dot plots. The right hand panel of dotplots refers to the distribution of the CD66, CD14 or CD41a positive cells backgated on to the MNCs analysed for CD45 versus side-scatter (blue).

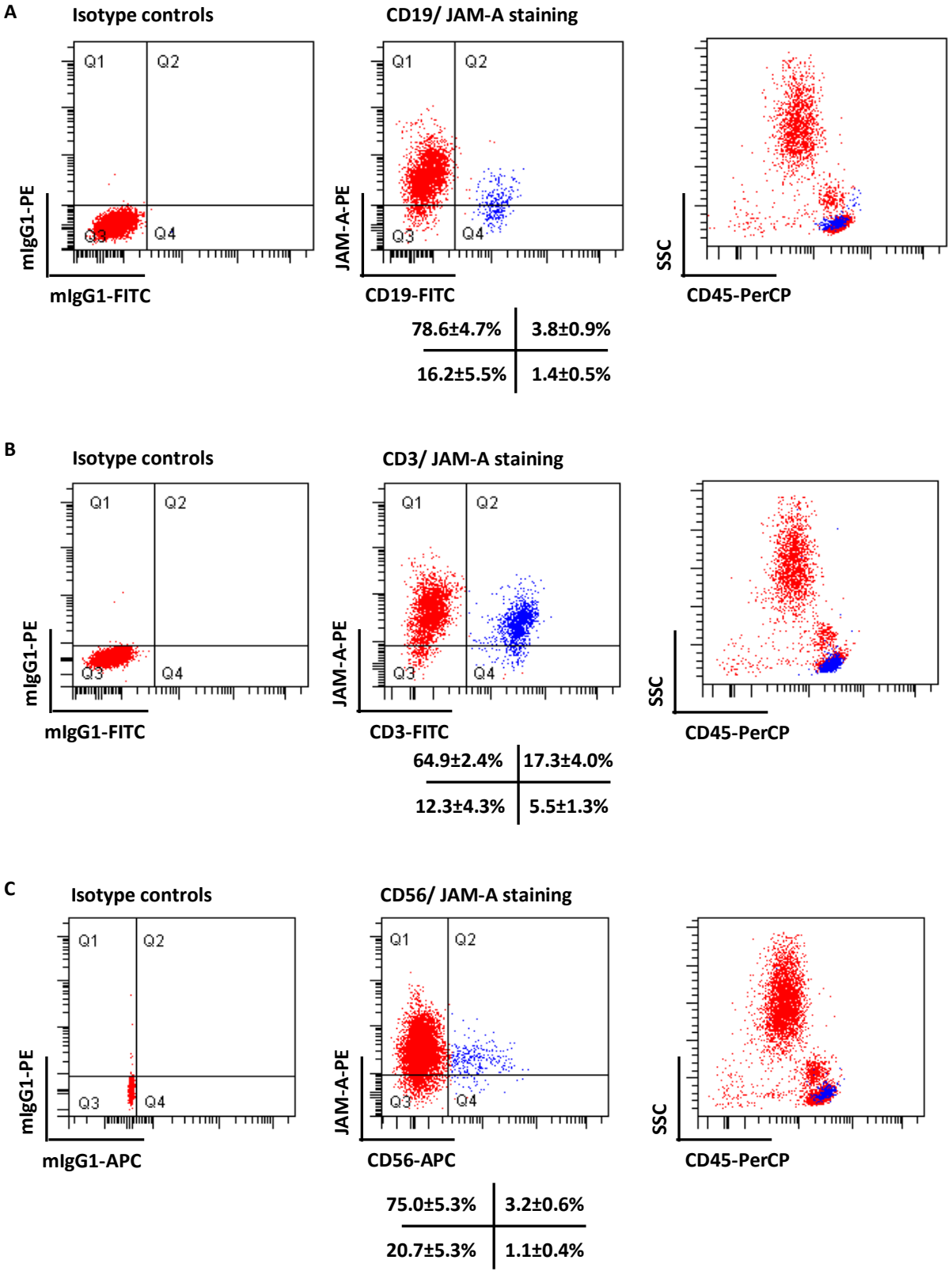

Figure 3.17. Expression of JAM-A on lymphoid lineage cells.
Representitive dotplots of dual-colour FACS analysis for isotype controls (left dotplots in A to C) and human UCB MNCs stained for (A) PE-JAM-A (M.Ab.F11) and FITC-CD19 (HIB19), (B) PE-JAM-A (M.Ab.F11) and FITC-CD3 (UCHT1) or (C) PE-JAM-A (M.Ab.F11) and APC-CD56 (B159) (middle dotplots). The percentage of cells in each quadrant of cells as means ± S.E.M. for N= 3 independent experiments is shown underneath each of the respective dot plots. The right hand panel of dotplots refers to the distribution of the CD19, CD3 or CD56 positive cells backgated on to the MNCs analysed for CD45 versus side-scatter (blue).

Although the expression levels of JAM-A on cell subsets by flow cytometry as described here is semi-quantitative, the M.F.I. values for 3 individually stained UCB units provided an indication of variability in JAM-A expression within a single subset of cells and between cell subsets, and this is shown in Figure 3.18. This suggests that JAM-A is more highly expressed on $CD14^+$ monocytes and $CD41a^+$ megakaryocyte precursors, although further studies are required to confirm the number of molecules of JAM-A expressed by these cells.

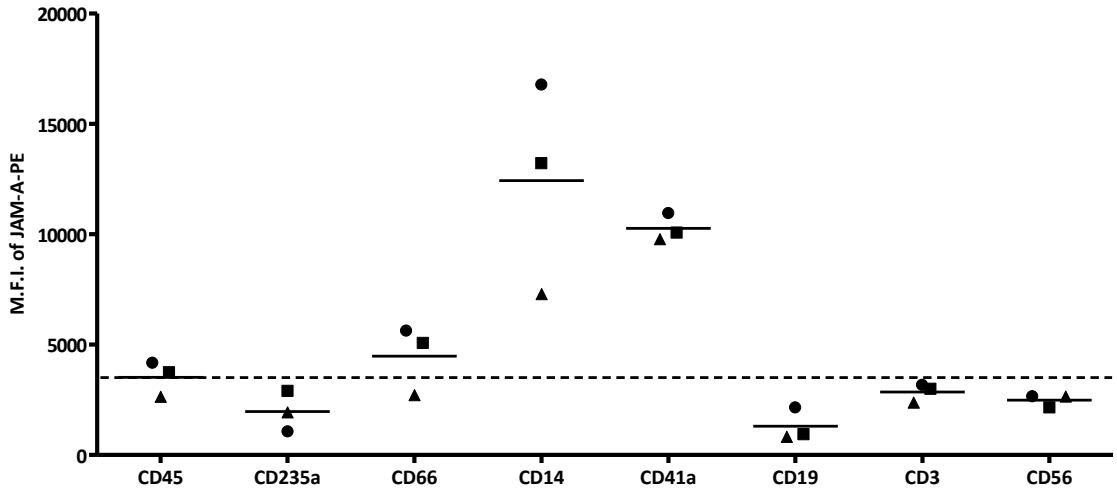

Figure 3.18. Comparison of PE-JAM-A fluorescence intensity on individual UCB myeloid and lymphoid lineage cell subsets.
The plot depicts PE-JAM-A (M.Ab.F.11) fluorescence intensity on each human UCB MNC subset indicated from three umbilical cord blood units. The bar represents the mean for N= 3 independent experiment.

3.3.5. JAM-A expression on human leukaemic cell lines.

To begin to assess JAM-A expression on acute leukaemic cells, its surface expression was tested on 4 acute myeloid leukaemic (AML) cell lines and 5 acute lymphoid leukaemic (ALL) cell lines, including 3 of T-ALL cell lines and 2 of B-ALL cell lines. JAM-A was expressed relatively more highly on the selected B-ALL cell lines, NALM-1 and Reh, and on the AML cell

lines, KG-1, HL-60 and TF-1, when compared to the T-ALL cell lines, CEM and MOLT-4 as defined by the MFI value. There was no expression observed on Jurkat cells (Figure 3.19).

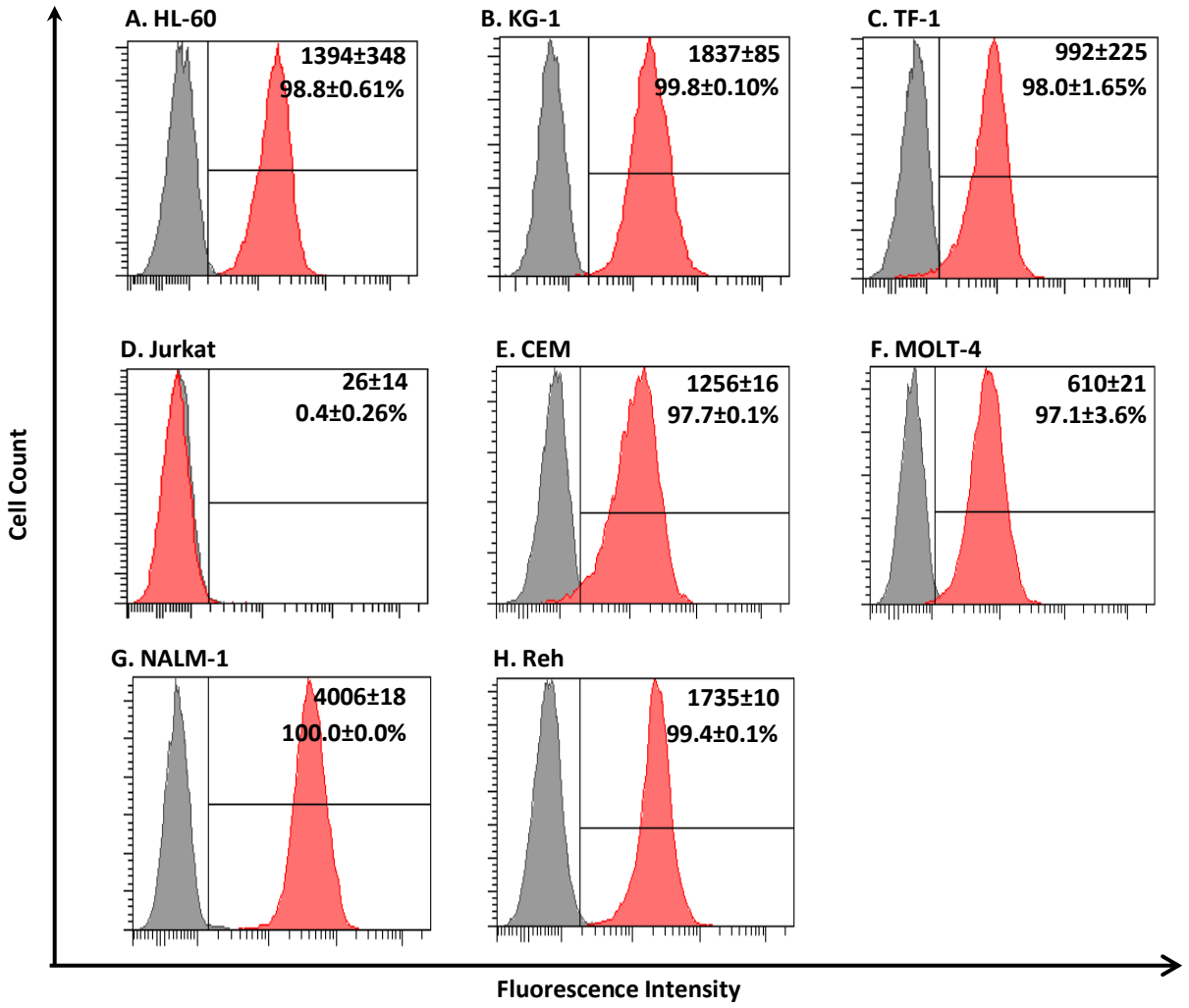

Figure 3.19. Expression of JAM-A on acute leukaemic cell lines.
Representative FACS histograms of acute leukaemic cell lines, including (A-C) acute myeloid leukaemia (HL-60, KG-1 and TF-1 cells) and (D-H) acute lymphoid leukaemia (Jurkat, CEM and MOLT-4 cells of T-ALL, and NAML-1 and Reh cells of B-ALL), stained with the PE-JAM-A antibody (M.Ab.F11; red) and its isotype control (gray). Values are mean M.F.I.± S.E.M. and the mean % positive± S.E.M for N= 3 independent experiments above the gate set for the isotype controls.

3.3.6. JAM-A expression on bone marrow niche cells.

As JAM-A is an adhesion molecule and able to form homophilic and heterophilic interactions between contacting cells, surface JAM-A expression on three bone marrow niche elements was analysed. Those analysed were primary human bone marrow stromal cells (BMSCs) which support LTC-IC (long term culture-initiating cell), human mesenchymal stem/stromal cells (MSCs) which support both haematopoiesis and vasculogenesis (338), and an amphotrophic helper-free retroviral pLXSN16E6/E7 vector transformed bone marrow endothelial cell line (BMEC-60) (308) which represented bone marrow endothelium. BMSCs were isolated from non-irradiated human bone marrow and grown in long-term culture medium. These cells form an adherent monolayer and were produced and characterised for their ability to support haematopoietic progenitor cells by Lonza Biologics (Lonza Group Ltd.). MSC were harvested from normal bone marrow, cultured and tested for CD105, CD166, CD29, CD44 positivity and CD14, CD34 and CD45 negativity by the Lonza Biologics (Lonza Group Ltd.). Only BMEC-60 cells expressed JAM-A (Figure 3.20).

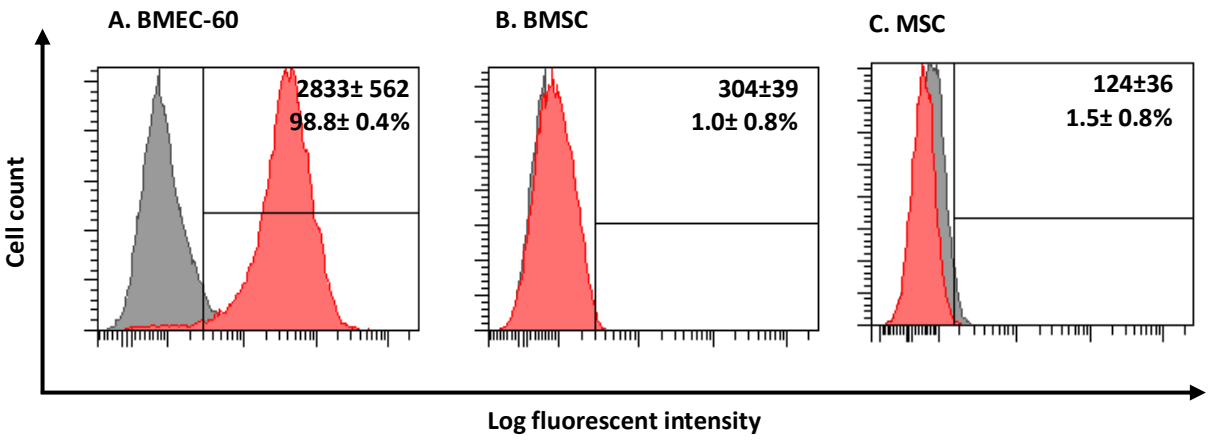

Figure 3.20. JAM-A expression on bone marrow endothelial niche cells.
Representative FACS histograms of (A) BMEC-60, (B) BMSC and (C) MSC stained with the PE-JAM-A antibodies (M.Ab.F11; red) and their isotype controls (gray). M.F.I.± S.E.M. and the % positive± S.E.M above the gates set for the isotype controls are shown for the primary antibody stain in the top right corner of the plot. N=3 independent experiments.

BMEC-60 cells were also analysed for selected adhesion molecules, including E-selectin (CD62E), ICAM-1 (CD54) and the integrins, CD29, CD18, CD11a and CD51/61 before and after IL-1β stimulation. Figure 3.21 shows the absence of E-selectin, β2-integrin and αL-integrin on cultured BMEC-60 cells before IL-1β stimulation (Figure 3.21.A, D and E). Upon 4 hour IL-1β stimulation, E-selectin expression was induced on the BMEC-60 with 51.5±9.8% of BMEC-60 population having higher expression levels above the gate set for the isotype control. This was associated with an increase in median fluorescence intensity to 384.3±124.5 from 90.3±3.6 for the unstimulated cells (Figure 3.21.A). ICAM-1 expression was enhanced also from an M.F.I. of 11034±626.6 to 37687±958 on the whole BMEC-60 population (Figure 3.21.B). CD29 (β1-integrin) was essentially unchanged, while D51/CD61 (αVβ3 integrin) was decreased. Both CD18 (β2-integrin) and CD11a (αL-integrin) were consistently absent from BMEC-60 cells with or without IL-1β stimulation (Figure 3.21.D and E). These findings were reminiscent of those for primary bone marrow endothelial cells and other transformed bone marrow endothelial cell lines (177, 178, 181). Surface and total JAM-A expression remained essentially unchanged with IL-1β stimulation as determined using Student's *t*-test (p=0.697 and p =0.278 respectively; Figure 3.22).

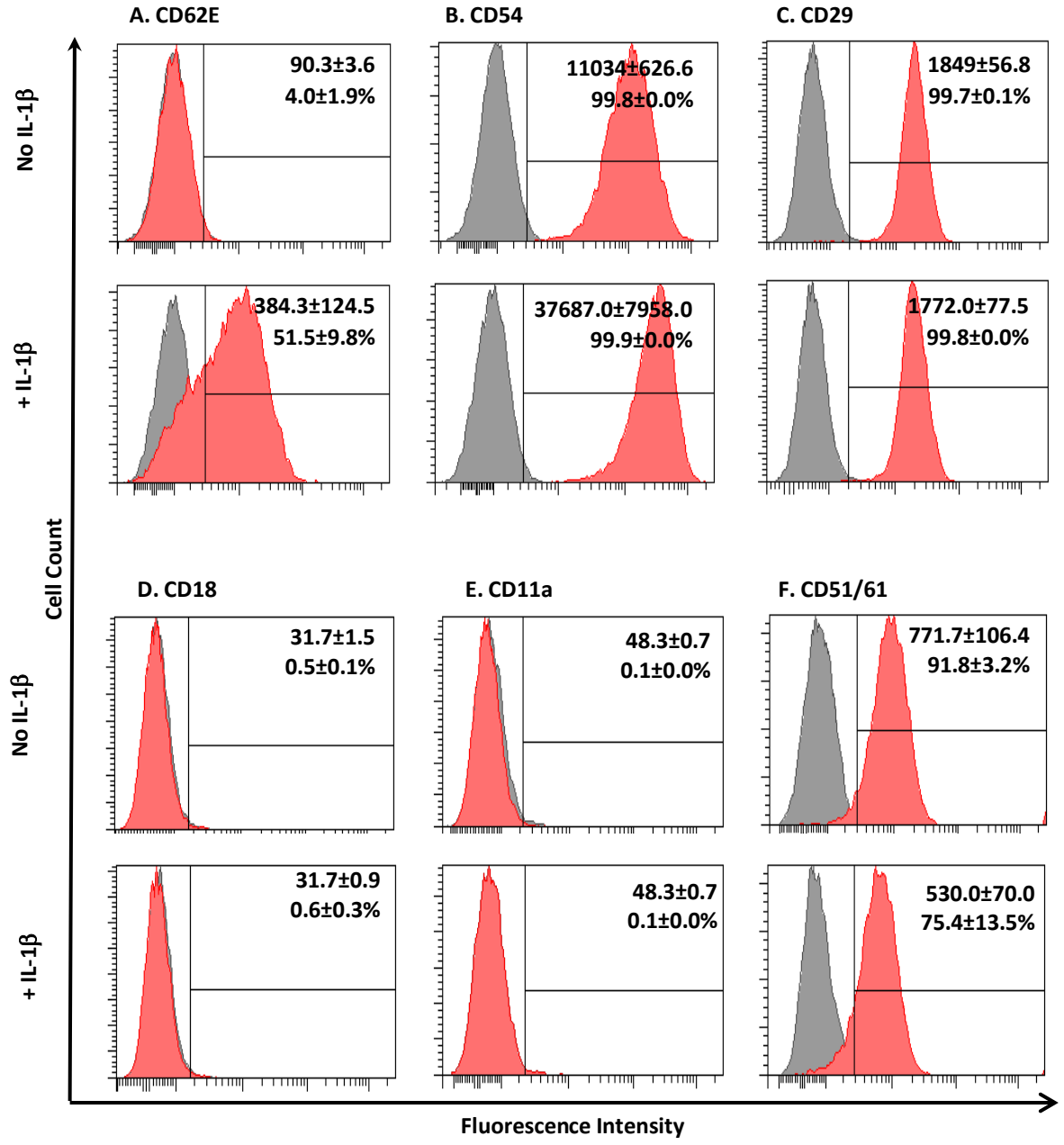

Figure 3.21. Phenotype of BMEC-60 cells before and after IL-1β stimulation.
Representative FACS histograms of BMEC-60 stained with the (A) APC-CD62E (68-5H11; E-selectin), (B) APC-CD54 (HA58; ICAM-1), (C) FITC-CD29 (β1-integrin), (D) FITC-CD18 (6.7; β2-integrin), (E) APC-CD11a (HI11; αL-integrin) and (F) APC-CD51/CD61 (23C6; αVβ3 integrin) antibodies (red) and their isotype controls (gray). M.F.I.± S.E.M. and the % positive± S.E.M. above the gate set for the isotype controls are shown for the primary antibody stain in the top right corner of the plot. N=3 independent experiments.

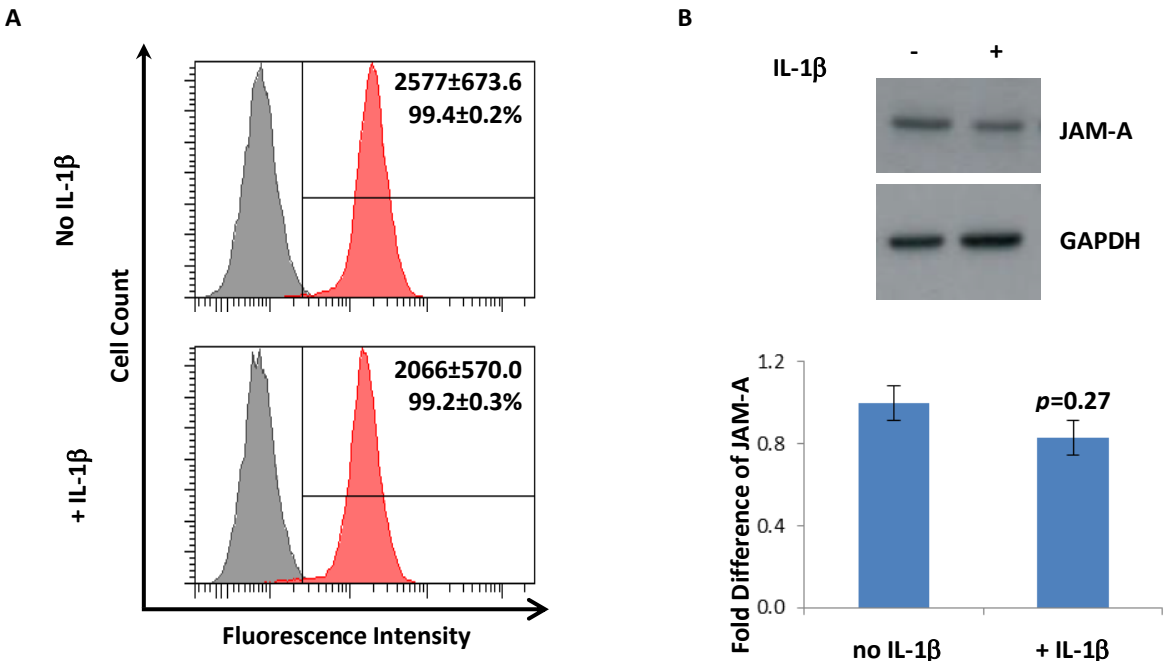

Figure 3.22. JAM-A expression on BMEC-60 cells before and after IL-1β stimulation.
(A) Representative FACS histograms of BMEC-60 stained with the PE-JAM-A antibodies (M.Ab.F11; red) and their isotype controls (gray). M.F.I.± S.E.M. and the % positive± S.E.M. are shown for the primary JAM-A antibody stain in the top right corner of the plot. (B) Total JAM-A expression level in BMEC-60 cells was examined by Western blotting withd GAPDH representing the loading control. The densometry of the normalised JAM-A expression level was shown in the bottom. The intensity values were measured using Quantity One software (Bio-Rad Lab Inc.) and normalised to GAPDH. The relative values of controls (no IL-1β) were set as 1.00. N=3 independent experiment. The statistical analysis was done using Student's *t*-test and values < 0.05 are considered significant.

3.3.7. JAM-A expression on bone marrow sections.

In order to examine JAM-A expression in human bone marrows *in situ*, 6 normal bone marrow sections, 5 B-ALL bone marrow sections, 3 T-ALL bone marrow sections, and 22 AML bone marrow sections were stained with JAM-A (see Materials and Methods Chapter 2, Section 2.14). As shown in Figure 3.23, the majority of bone marrow haematopoietic cells were JAM-A positive, although this varied from weaker to very strong staining both for cells within the section and between sections. Variable staining was noted on cells with the morphology of nRBCs, lymphoid cells or neutrophils. Of particular note was the strong

staining of megakaryocytes. These findings are consistent with the FACS analyses on $CD41a^+$ megakaryocytic precursors and more mature lineage restricted UCB cells. Where blood vessels were observed in these sections, the endothelial cells stained weakly positive for JAM-A (Figure 3.23).

Leukaemic bone marrow sections were obtained from adult and paediatric patients on presentation, and the demographics are summarised in Table 3.2. The AML bone marrows were obtained from these patients who had AML which was classified as minimally differentiated, with differentiation, megarkaryocytic, myelomonocytic, or monoblastic and monocytic. There was consistent JAM-A positivity on most cells in the AML sections categorised as megarkaryocytic, myelomonocytic, or monoblastic and monocytic (Figures 3.24 to 3.28). This reflects in part the high levels on JAM-A on megakaryocytes and monocytes in UCB or in normal bone marrow sections. In AML sections, JAM-A positive cells were generally observed, although some variability was noted (Figures 3.24-28). In the B-ALL and T-ALL sections, some variability in JAM-A positivity of the cells was noted (Figures 3.29 and 3.30). For this reason, collaboration was established with Dr Allison Blair to assess the different B and T cell subsets in ALL bone marrow samples on presentation. The results of these experiments are shown in the next section. Of particular note again was the strong staining of megakaryocytes, where these were present, in all the bone marrow sections whether leukaemic or normal. Where blood vessels were observed in the leukaemic sections, the endothelial cells were positive for JAM-A, and appeared to demonstrate stronger staining than observed in normal bone marrow.

Table 3.2. Anonymised patient information at presentation

Donor	Age	Sex	Diagnosis	WHO type	Karyotype
D01	38	Male	Normal	NT	NT
D02	84	Female	Normal	NT	NT
D03	55	Male	Normal	NT	NT
D04	76	Female	Normal	NT	NT
D05	81	Male	Normal	NT	NT
D06	81	Male	Normal	NT	NT
AML01	61	Female	AML	9867	46,XX
AML02	42	Male	AML M1-M2	9867	46,XY
AML03	73	Male	AML	9867	45,XY,t(3;9)(p21;q32),-6, t(7;21)(p21;q22),del(15)(q15q24),der(17)t(17;19)(p1?3;p13),der(?)t(?;19)(?;q?),der(21)t(6;?;21)(q11;?;p1)inc[3]
AML04	39	Male	AML M4/M5	9867	46,XY
AML05	73	Male	AML	9867	44,XY,add(4)(q2?),-5,-7,+der(11)(?), +der(13)(?),-14,-14,-15,add(21)(q22),
AML06	43	Male	AML M4	9867	47~49,Y,-X, del(8)(p?11p?21)[5], idic(8)(p1?)[5],+idic(8)(p1?)[2],idic(?13)(q13-14)[5],+idic(?13)(q13-q14)[5], ?del(16)(q1?)[5],-18[5],-20[5], +mar1[5],+mar2[5][cp5].
AML07	79	Female	AML	9872	43,XX,-2,add(5)(q?15),-7, i(8)(q10),+i(8)(q10),add(12)(p11),add(14)(p10), -15, der(16;21)(p10;q10), der(17)t(17;?;15)(p1?;?;q21),inc[3]/46,XX, +1,add(2)(p1?),-4,add(5)(q?15),-8,-12, +der(?14)t(14;?13)(q2?;?q?14), add(21)(p10),+add(21)(p10)inc[2]
AML08	80	Male	AML	9872	46,XY
AML09	66	Male	AML	9872	47,XY,+11[3]/46,XY[57]
AML11	54	Female	AML	9872	46,XX,t(8;21)(q22;q22)
AML12	48	Female	AML	9872	46, XX
AML13	49	Female	AML	9874	46,XX
AML14	66	Male	AML M5	9874	46,XY
AML15	44	Male	AML	9874	46,XY
AML16	46	Female	AML M2	9874	46,XX
AML17	64	Male	AML	9874	46,XY
AML18	66	Male	AML	9891	46,XY
AML19	51	Female	AML	9891	46,XX,t(11;19)(q23;p13.?1)
AML21	29	Male	AML M5	9891	49,XY,+21,+21,+21[7]/49,idem,der(10)(?)[5]
AML22	82	Male	AML M5	9891	N./A.
AML23	46	Male	AML M5	9891	46,XY,inv ins(10;11)(p13;q23q13)
AML24	3	Female	AML M7	9910	47,XX,add(1)(p36),der(7)t(7;11)(p14~15;q12~13),+21c[3]/48,XX,der(5)t(1;5)(q25;q35), der(7)t(7;11)(p14~15;q12~13),+13,+21c[5]/47,XX,+21c[4]
ALL02	35	Male	T-ALL	N./A.	45,X,-Y, t(3;10)(p2?3;p1?5),del(5)(q3?1.3;q3?5), t(7;14)(p?15;q32)[7]/46,XY[1]
ALL03	3	Female	B-ALL	N./A.	45,X,-X,t(4;15)(q21;q?14)[9]/46,XX[1]
ALL04	45	Male	B-ALL	N./A.	46,XY,t(11;19)(q23;p13)
ALL05	15	Male	B-ALL	N./A.	35~38,XY,-2[6],-3[6],-4[6],-7[6],-9[4],-12[6],-15[6],-16[6],-17[5][cp6]/46,XY[4]
ALL06	2	Female	B-ALL	N./A.	52,XX,+X,+6,+14,+17,+21,+21

ALL07	1	Female	Pre B-ALL	N./A.	46,XX
ALL08	7	Female	ALL Relapsed	N./A.	43~44,X,-X[7], add(5)(q?3)[6], del(9)(p1)[5],add(12)(p1)[7],+13[4],-17[7],-18[7],+1~3mar[4], inc[cp7]/46, XX[23]
ALL09	9	Male	T-ALL	N./A.	46,XY,del(16)(q13q22 or q22q24)[2]/ 46,XY[28] Unstimulated culture 46,XY [18] B/T cell stimulated culture

N./A.: The information is not available. NT: Not tested or not relevant. Eight French-American-British (FAB) AML subtypes were proposed in 1976 (339). It based on the type of cell from which leukaemia developed and its degree of maturity, AML was divided from M0 through M7. M0: Undifferentiated acute myeloblastic leukaemia; M1: Acute myeloblastic leukaemia with minimal maturation; M2: Acute myeloblastic leukaemia with maturation; M3: Acute promyelocytic leukaemia; M4: Acute myelomonocytic leukaemia; M4eos: Acute myelomonocytic leukaemia with eosinophilia; M5: Acute monocytic leukaemia; M6: Acute erythroid leukaemia; M7: Acute megakaryocytic leukaemia; M8: acute basophilic leukaemia. In 2008, WHO updated the classification system in tumours of haematopoietic and lymphoid tissues (340) and the relative codes for AML substypes are shown in the table, which are 9867: Acute myelomonocytic leukaemia, 9872: Acute myeloid leukaemia with minimal differentiation, 9874: Acute myeloid leukaemia with maturation, 9891: Acute monoblastic and monocytic leukaemia, and 9910 Acute megakaryoblastic leukaemia.

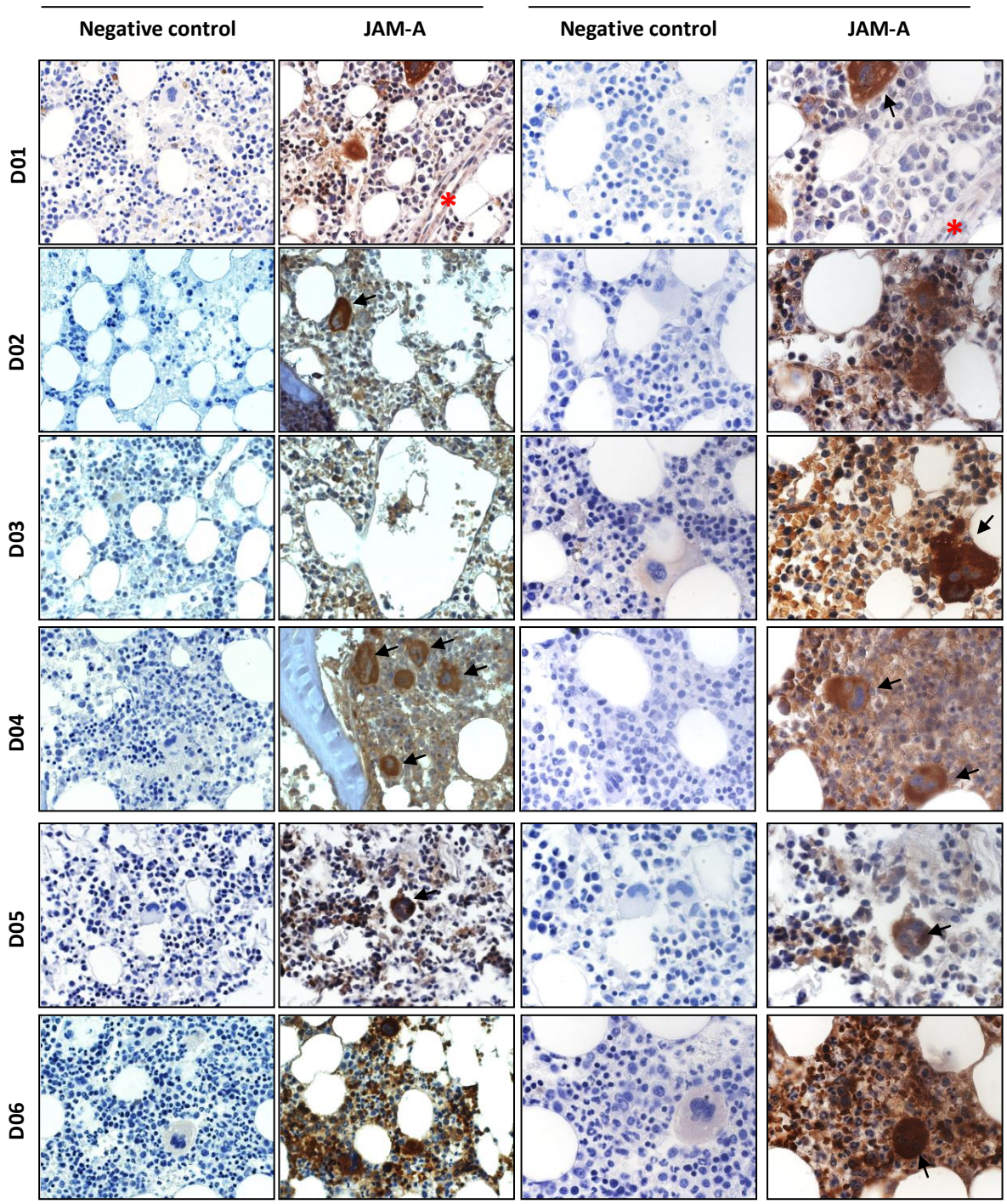

Figure 3.23. JAM-A expression on normal human bone marrow sections.
Paraffin sections of human bone marrow trephines obtained from patients without evidence of malignant disease were stained for isotype negative control or for JAM-A (2E3-1C8) and developed using immuno-histochemical techniques described in Chapter 2, Section 2.14, before being examined by light microscopy. Arrows show strong megakaryocyte and stars represent blood vessel endothelial cell staining (donor D01) for JAM-A respectively. Magnification X60 (left) and X100 (right).

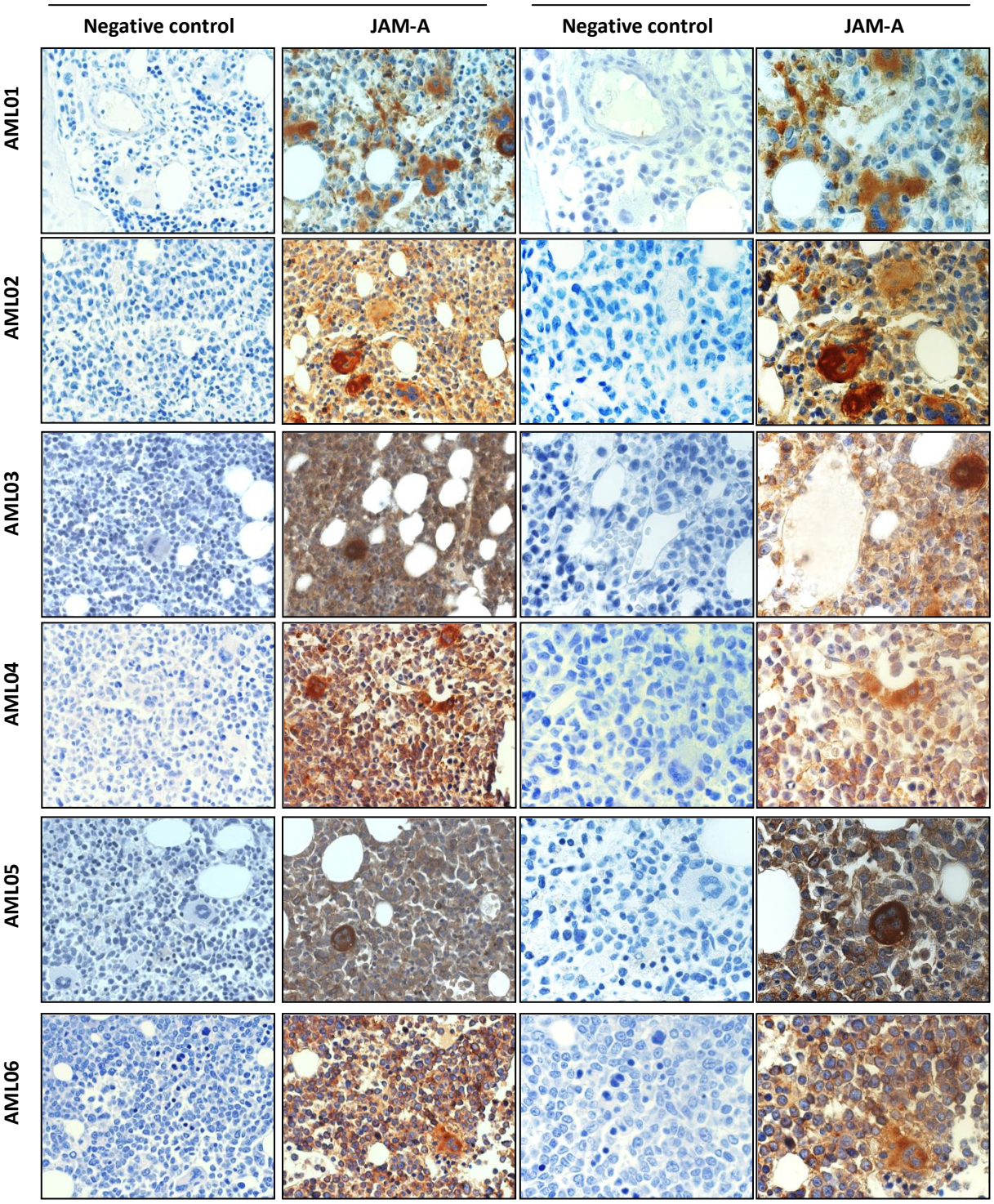

Figure 3.24. JAM-A expression on human acute myelomonocytic leukaemia bone marrow sections.
Paraffin sections of human bone marrow trephines obtained from patients with AML categorised as acute myelomonocytic leukaemia were stained for isotype negative control or for JAM-A (2E3-1C8) and developed using immunohistochemical techniques described in Chapter 2, Section 2.14, before being examined by light microscopy. Magnification X60 (left) and X100 (right).

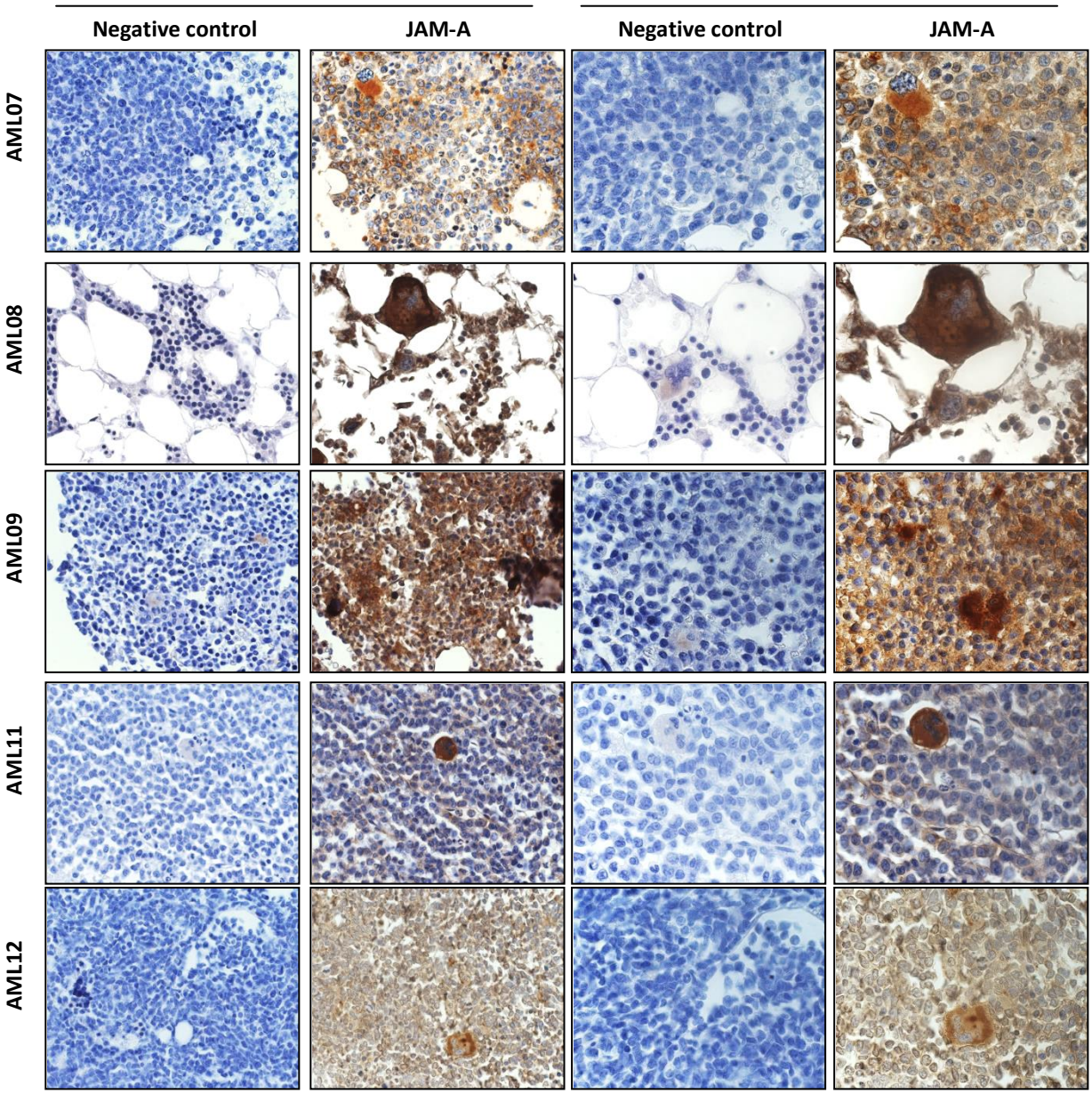

Figure 3.25. JAM-A expression on human acute myeloid leukaemia with minimal differentiation bone marrow sections.
Paraffin sections of human bone marrow trephines obtained from patients with AML categorised as acute myeloid leukaemia with minimal differentiation were stained for isotype negative control or for JAM-A (2E3-1C8) and developed using immunohistochemical techniques described in Chapter 2, Section 2.14, before being examined by light microscopy. Magnification X60 (left) and X100 (right).

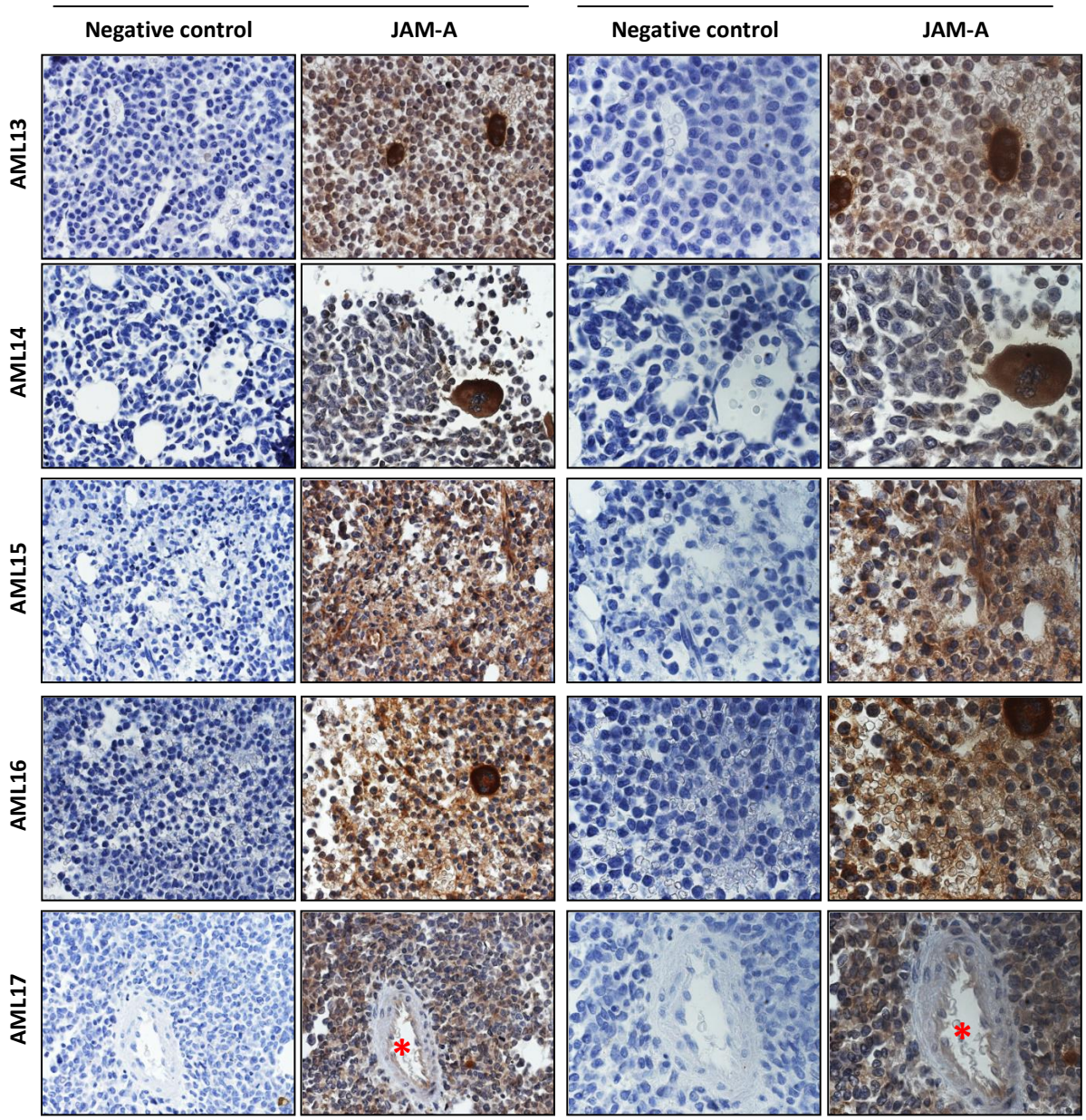

Figure 3.26. JAM-A expression on human acute myeloid leukaemia with maturation bone marrow sections. Paraffin sections of human bone marrow trephines obtained from patients with AML categorised as acute myeloid leukaemia with maturation were stained for isotype negative control or for JAM-A (2E3-1C8) and developed using immunohistochemical techniques described in Chapter 2, Section 2.14, before being examined by light microscopy. Stars represent blood vessel endothelial cell staining (AML17) for JAM-A. Magnification X60 (left) and X100 (right).

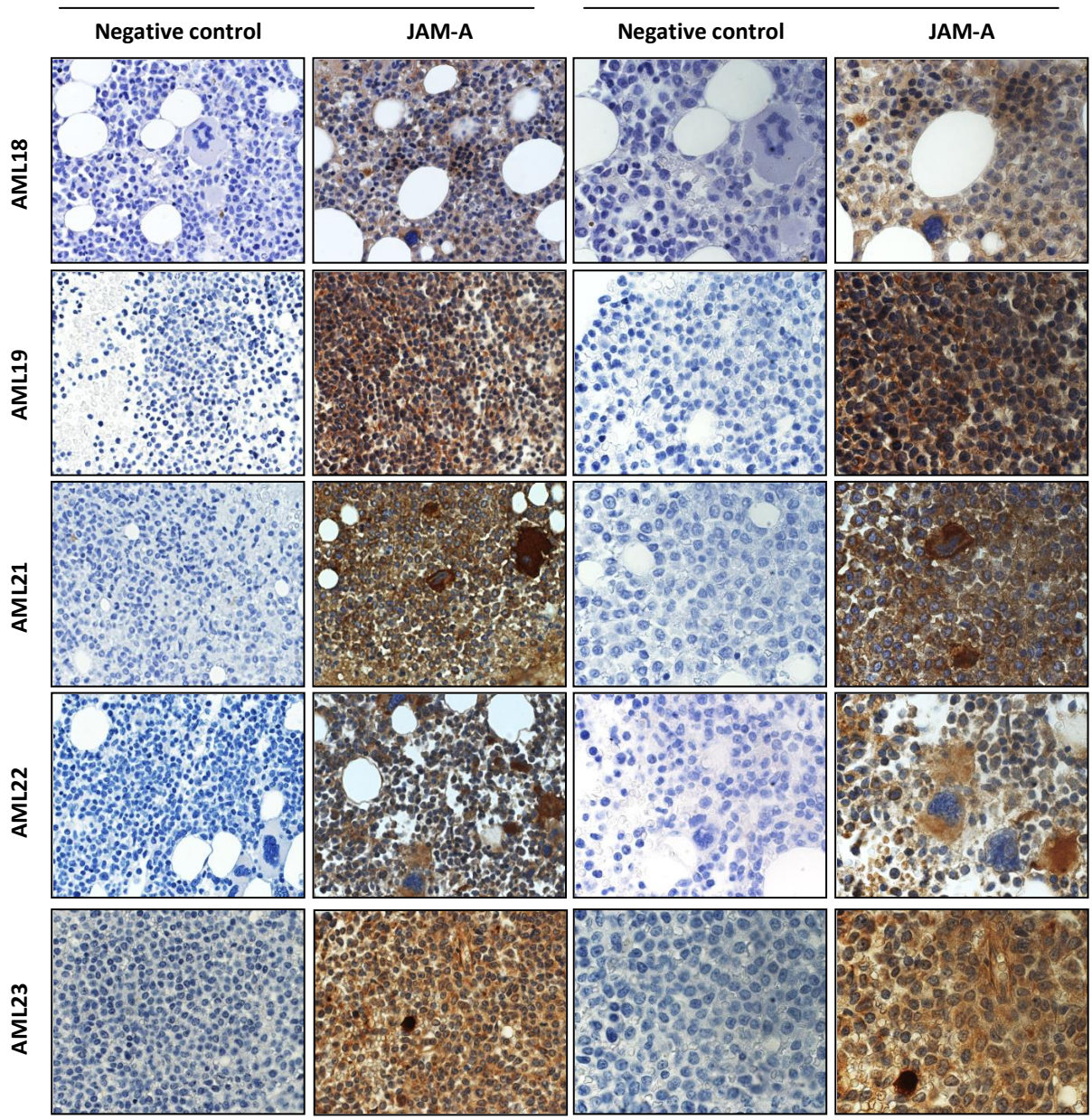

Figure 3.27. JAM-A expression on human acute monoblastic and monocytic leukaemia bone marrow sections.

Paraffin sections of human bone marrow trephines obtained from patients with AML categorised as acute monoblastic and monocytic leukaemia were stained for isotype negative control or for JAM-A (2E3-1C8) and developed using immunohistochemical techniques described in Chapter 2, Section 2.14, before being examined by light microscopy. Magnification X60 (left) and X100 (right).

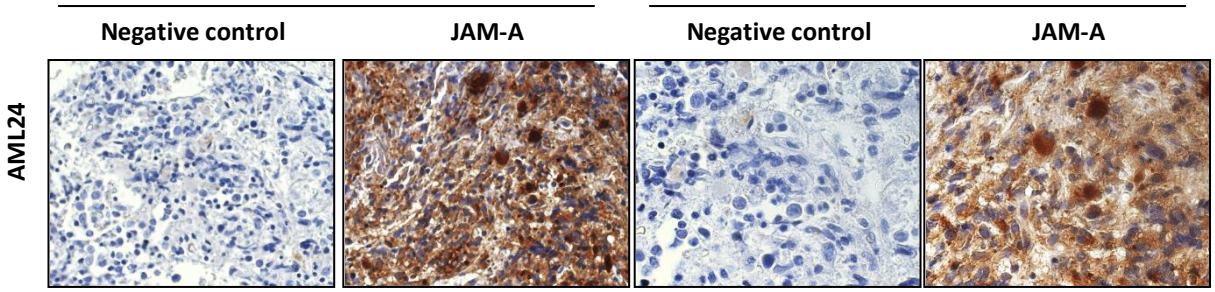

Figure 3.28. JAM-A expression on human acute megakaryoblastic leukaemia bone marrow sections.
Paraffin sections of human bone marrow trephines obtained from patients with AML categorised as acute megakaryoblastic leukaemia were stained for isotype negative control or for JAM-A (2E3-1C8) and developed using immunohistochemical techniques described in Chapter 2, Section 2.14, before being examined by light microscopy. Magnification X60 (left) and X100 (right).

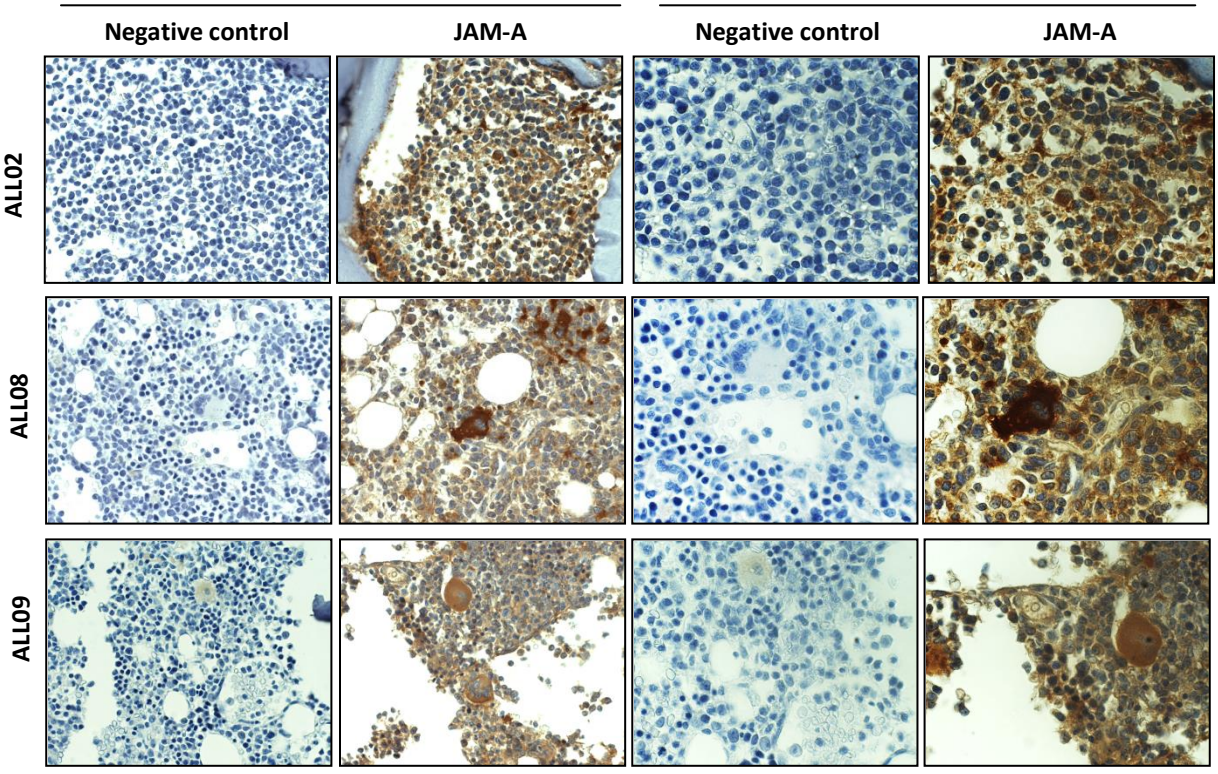

Figure 3.29. JAM-A expression on human T-ALL bone marrow sections.
Paraffin sections of human bone marrow trephines obtained from patients with T-ALL were stained for isotype negative control or for JAM-A (2E3-1C8) and developed using immunohistochemical techniques described in Chapter 2, Section 2.14, before being examined by light microscopy. Magnification X60 (left) and X100 (right).

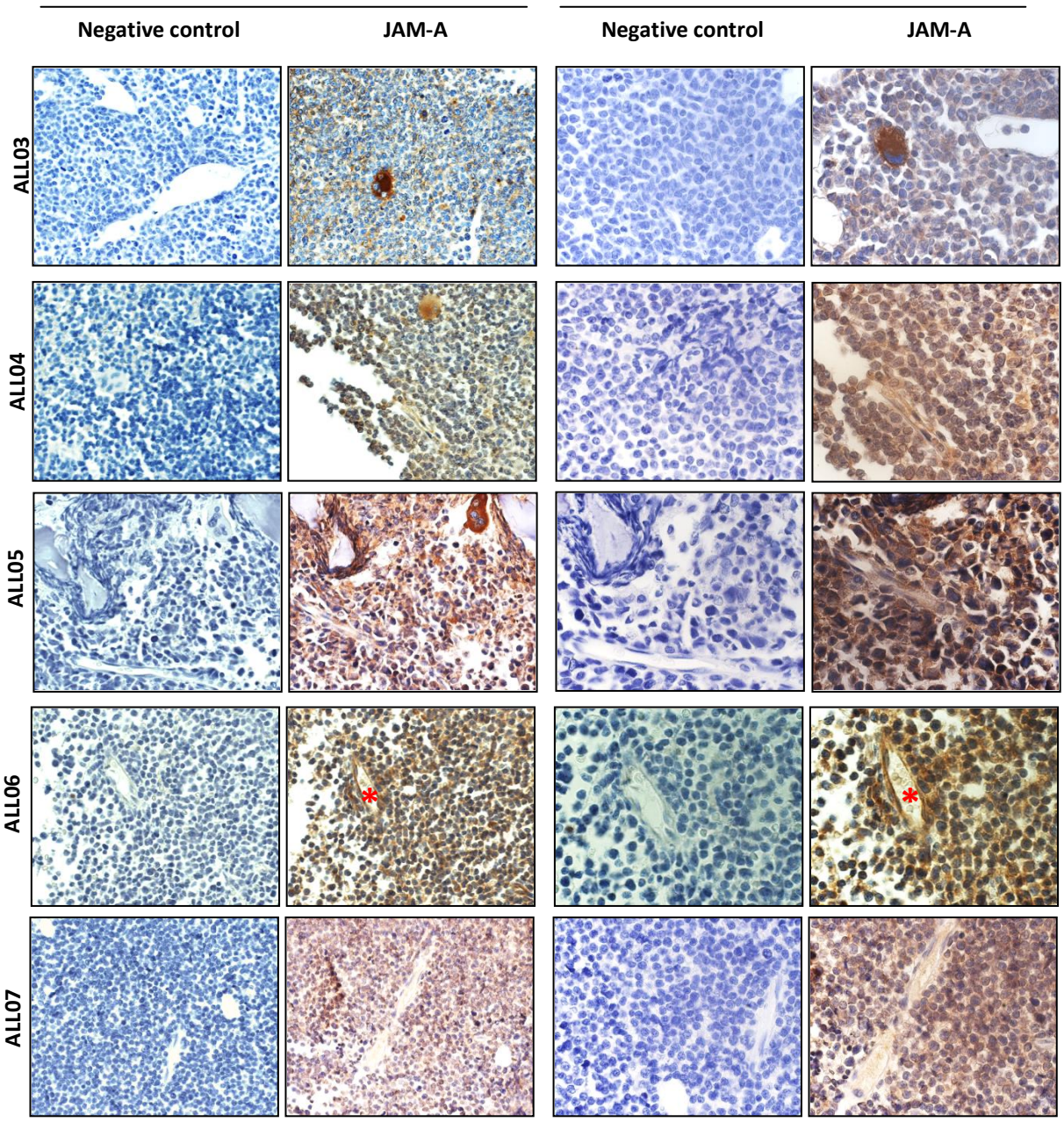

Figure 3.30. JAM-A expression on human B-ALL bone marrow sections.
Paraffin sections of human bone marrow trephines obtained from patients with B-ALL were stained for isotype negative control or for JAM-A (2E3-1C8) and developed using immunohistochemical techniques described in Chapter 2, Section 2.14, before being examined by light microscopy. The stars for patient ALL06 show blood vessel endothelial cell staining for JAM-A. Magnification X60 (left) and X100 (right).

3.3.8. JAM-A expression on acute lymphoblastic leukaemic bone marrow cell fractions by flow cytometry

Because it was difficult to determine the precise numbers and expression levels of JAM-A^+ cells in the leukaemic bone marrow sections and as stated, a collaboration was established with Dr. Allison Blair to examine B-ALL and T-ALL bone marrow samples collected from children presenting to the Bristol Children's Hospital for their JAM-A expression by flow cytometry. Nine B-ALL and 2 T-ALL bone marrow samples were available. These were tested for cell surface markers and cultured in Bristol and the results analysed in Oxford. *In vitro* and *in vivo* studies by Dr Blair's group previously had defined the phenotypic characteristics of B-ALL and T-ALL leukaemic stem-like cells or leukaemia initiating cells. These are illustrated diagrammatically for B-ALL or T-ALL cells in Figure 3.31. In lineage tree diagrams, the haematopoietic stem cell compartment can be divided into self-renewing stem cell and pluripotent stem/progenitor cells which are $CD133^+CD34^-$ and/or $CD133^+CD34^+$ and are believed to generate lymphoid progenitors and myeloid progenitors. The lymphoid progenitors can give rise to T cell or B cell lineages, although not exclusively. In the B cell lineage, the cells are segregated into Pro-B ($CD34^+CD10^-CD19^+$), Pre Pre-B ($CD34^+CD10^+CD19^+$), Pre-B ($CD34^+CD10^{+/-}CD19^+C\mu^+$) and mature B cells. Blair and colleagues have suggested that human leukaemic initiating cells may come from the Pro-B to Pre-B cells stages, all of which express CD19, when assayed in NSG mice (79, 81). They have also shown that the $CD133^+CD19^-$ B-ALL cells, that may represent $CD34^-$ cells prior to B lymphoid lineage commitment, also contain leukaemia initiating cells when transplanted into NOD/SCID mice (81).

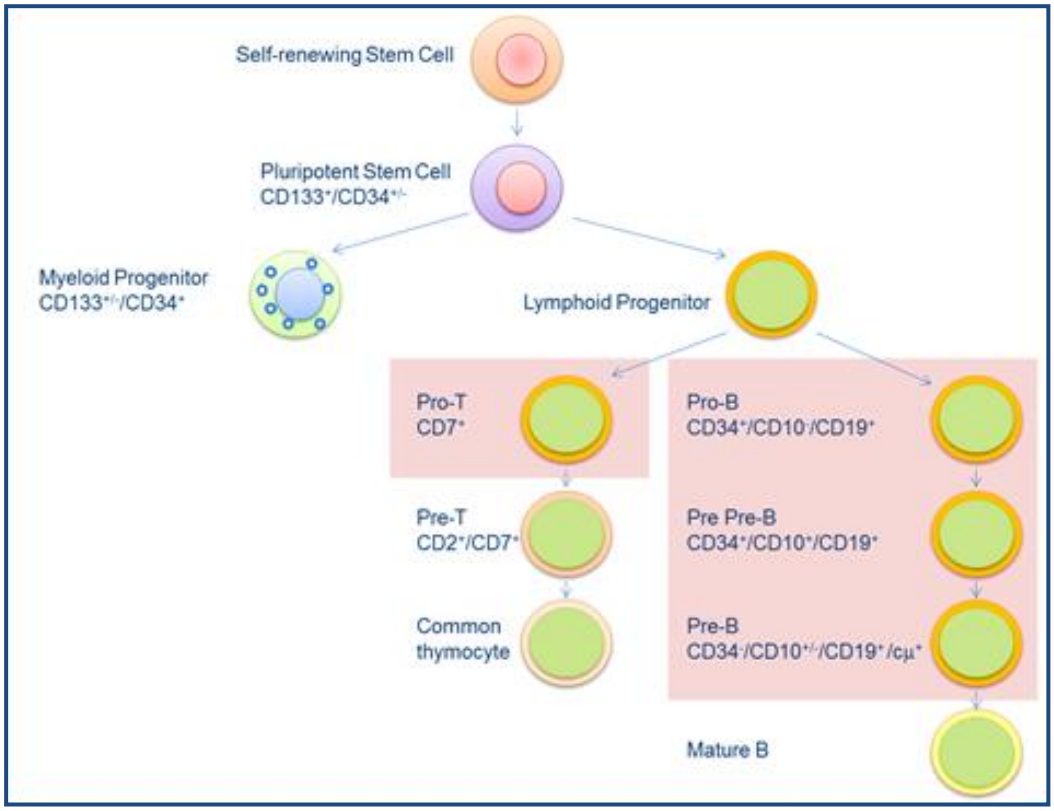

Figure 3.31. Phenotypically defined B-ALL and T-ALL leukaemic initiating cell subsets.
The figure shows a lineage map for the phenotypic identification human leukaemic stem-like cells from the haematopoietic lineages as described by Dr. Allison Blair. At the bottom are the terminally differentiated cells. The haematopoietic stem cells are divided into self-renewing stem cells and pluripotent stem cells which are believed to generate lymphoid progenitor and myeloid progenitor as shown. The lymphoid progenitors give rise to B cell and T cell lineages which are segregated into Pro-B, Pre-Pre B, Pre-B and mature B cells or Pro-T, Pre-T and common thymocyte respectively based on their phenotypic expression of cell surface markers. Cox *et al.* have suggested that human leukaemia initiating cells may come from the stages of Pro-T cells or Pro-B to Pre-B cells once committed to these lineages (79, 81). (Figure kindly provided by Dr. Allison Blair).

3.3.8.1. Analysis of JAM-A on B cell acute lymphoblastic leukaemia (B-ALL) bone marrow cell fractions

The bone marrow B-ALL cells were first subdivided into different phenotypic subsets based on their expression of CD34 and CD19 cell surface makers. In the patients tested, the proportions of the different cell subsets were variable as illustrated in Figure 3.32. Of particular note in these 9 patients' bone marrow samples was the variation in the CD34 and CD19 expression. In 4 of 9 cases, over 60% of the bone marrow B-ALL samples were

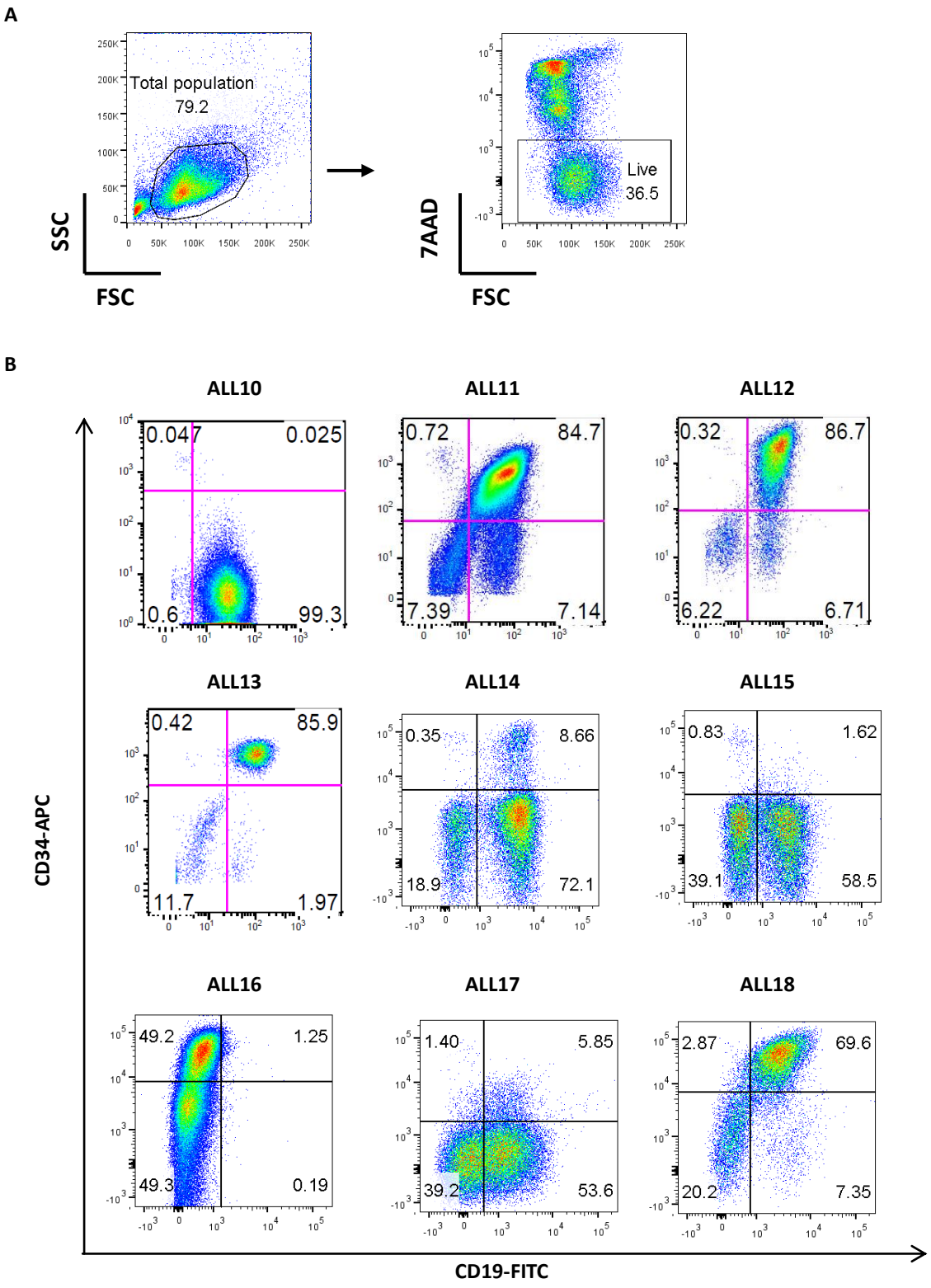

Figure 3.32. Expression of CD34 and CD19 on human bone marrow B-ALL cells.
Multiple colour FACS analysis of viable CD34 and CD19 expression on 9 human B-ALL bone marrow cells at presentation. (A) depicts the gating strategy for live cells before CD34 or CD19 expression analysis. The cell population was gated first according to FSC against SSC filter, followed by 7AAD -negative gating (live cells). The expression of CD34 and CD19 on live cells is shown in (B) after Flojo analysis. The percentage of cells in each quadrant is shown in the corners of the plots. The colour of the dots indicates the cell density in the population, with decreasing cell numbers occurring from red to yellow to green to blue.

$CD34^+CD19^+$, while patients ALL10 and ALL14 had almost exclusively $CD34^-CD19^+$ cells. Two patients, ALL15 and ALL17, had almost exclusively $CD34^-$ cells with a slightly higher proportion in $CD34^-CD19^+$ cells. Patient ALL16, on the other hand, showed predominantly equal cell populations with either $CD34^+CD19^-$ and $CD34^-CD19^-$ cells.

These subsets of cells were further examined for JAM-A expression using multi-colour FACS analysis. The results are shown in Figure 3.33 for the whole B-ALL population and for the CD34 and CD19 defined subsets. Eight of the 9 bone marrow samples were mostly JAM-A positive, ranging from 75.9% to 99.4%. Patient ALL13, on the other hand, had lower cell numbers expressing JAM-A. The percentage of $JAM\text{-}A^+$ cells in each bone marrow sample was further examined within defined CD34 and CD19 subsets and the results are shown in Figure 3.33 and Figure 3.34. JAM-A expression varied for $CD34^+CD19^-$ (range 48.6 to 100%), $CD34^+CD19^+$ (range 30.9 to 100%), $CD34^-CD19^+$ (range 18.4 to 99.1%) and $CD34^-CD19^-$ (range 49.3 to 85.3%) cells. JAM-A expression on $CD34^+CD19^-$ and $CD34^+CD19^+$ cell subpopulations was significantly higher than on the $CD34^-CD19^-$ cell subpopulation ($p<0.01$ and $p<0.05$ respectively ; Figure 3.33).

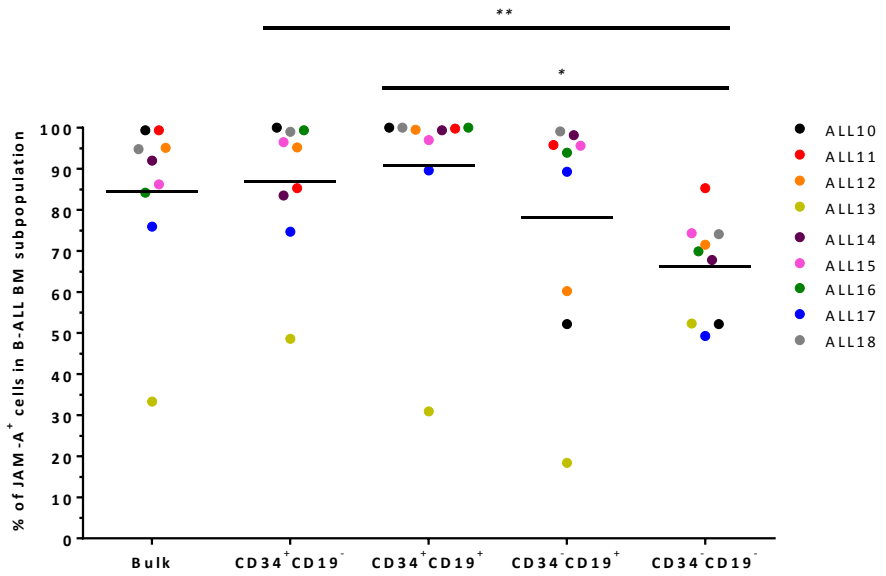

Figure 3.33. Expression of JAM-A on subsets of B-ALL cells.
The individual data from Figure 3.34 for the percent JAM-A positive cells are summarised in this figure and the bar in each group represents the median. The statistical analysis was done using Student's *t*-test and values < 0.05 (*) or <0.01 (**) are considered significant.

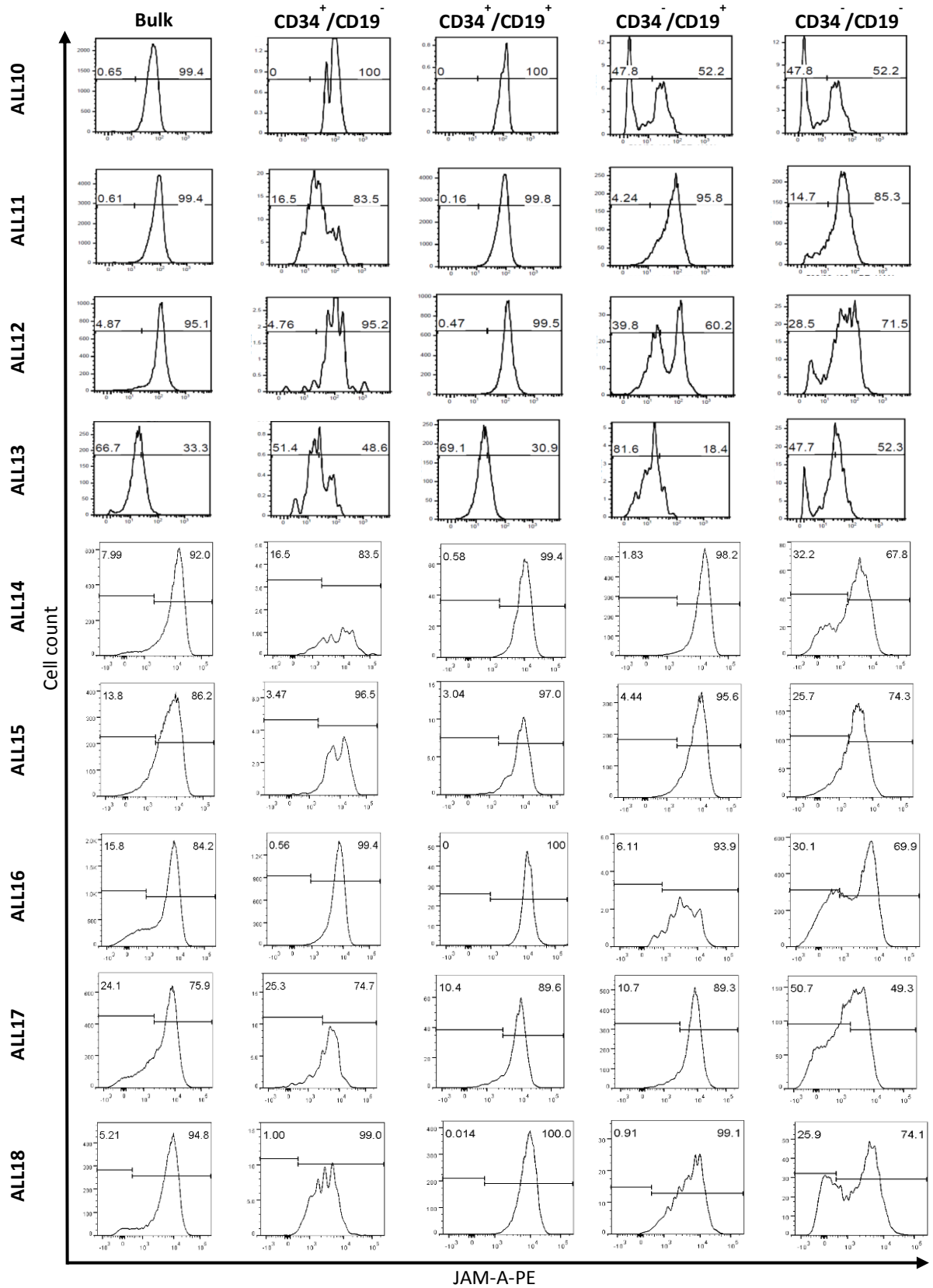

Figure 3.34. Expression of JAM-A on subsets of B-ALL cells.
Multi-colour FACS analysis was used to determine cell surface CD34, JAM-A and CD19 expression on 9 human B-ALL bone marrow leukaemic samples at presentation. The cells were gated for $CD34^{+}CD19^{-}$, $CD34^{+}CD19^{+}$, $CD34^{-}CD19^{+}$ and $CD34^{-}CD19^{-}$ as in Figure 3.32.B. The bar represents the percentage of JAM-A positive cells versus negative cells in the whole sample and four subfractions.

In pilot experiments, two leukaemic bone marrows (ALL10 and ALL11) were sorted into $CD34^{+}JAM\text{-}A^{+}$, $CD34^{-}JAM\text{-}A^{-}$, $CD34^{+}JAM\text{-}A^{-}$ and $CD34^{-}JAM\text{-}A^{+}$ and then cultured *in vitro* in 20% HIT medium (5X human insulin transferrin, Stemcell Technologies) with 20ng/ml of IL-3, 20ng/ml of IL-7, 50ng/ml SCF, 10μM 2-mercaptoethanol and 1% penicillin/ streptavidin antibodies (10,000 U/ml) for 6 weeks. For these 2 leukaemic samples, the unsorted nucleated cell number increased approximately 10 fold over this period (data not shown). Even though the starting populations varied in their CD34 positivity and were mostly JAM-A positive (respectively for ALL10 : less than 0.1 and 99.4% ; ALL11 : 85.4 and 99.4%), by week 6, 37-42% of the cultured bone marrow leukaemic cells were $CD34^{-}JAM\text{-}A^{+}$ and 25-27% $CD34^{+}JAM\text{-}A^{+}$ (Figure 3.35). In these 2 samples (ALL10 and ALL11), 30% of the cells at week 6 were $CD34^{-}JAM\text{-}A^{-}$ (Figure 3.35).Time constraints did not allow these studies to be taken further. However, while it is evident that these studies are preliminary, it would be of interest to determine if those cells which lack CD34 and have also lost JAM-A are more aggressive leukaemia initiating cells.

To summarise the observations obtained here, in 4 of the B-ALL bone marrow samples examined, the majority of cells were $CD34^{+}CD19^{+}$ and would therefore represent the pro B or pre pre-B cell stage, while in another 4 between 40 to 99% of cells were $CD34^{-}CD19^{+}$ and would therefore represent the pre-B cell stage. Two of the latter contained significant numbers of pro-B or pre pre-B cells. One sample contained around 50% $CD34^{+}CD19^{-}$ cells and were likely equivalent to either CLP or pluripotent cells. With the exception of one donor, most of the cells in these three categories were JAM-A positive. It is of interest to note that all leukaemic bone marrow samples contained a $CD34^{-}CD19^{-}$ subset which made up between approximately 1 to 50% of the bone marrow mononuclear cells. These cells may have lost either or both of these markers as the leukaemia developed or they may represent

A

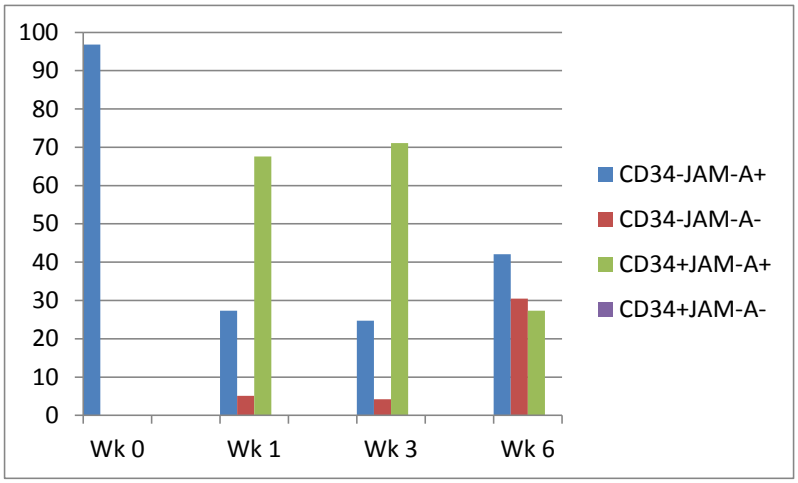

B

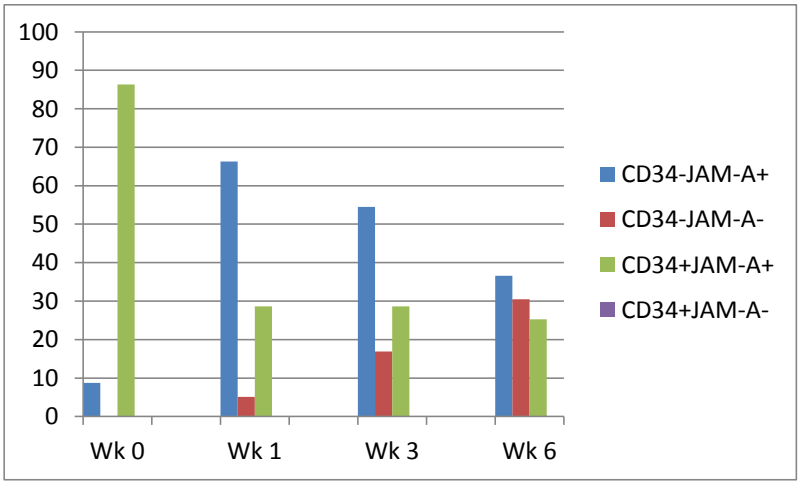

Figure 3.35. Changes in CD34 and JAM-A leukaemic cell subsets during 6 weeks of culture.
(A) ALL10 and (B) ALL11 samples were sorted using CD34 and JAM-A dual-colour staining and cultured *in vitro* in 20% HIT medium (5X human insulin transferin, Stemcell Technologies) with 20ng/ml of IL-3, 20ng/ml of IL-7, 50ng/ml SCF, 10μM 2-mercaptoethanol and 1% penicillin/ streptividin antibodies (10,000 U/ml) for 6 weeks. The percentage of each subset is shown for each ALL sample in the starting population (wk0) and at weeks 1, 3 and 6 of culture. (Data kindly provided by Dr. Allison Blair).

the most primitive of cells in the bone marrow which express CD133 but are CD34 and CD19 negative (341). These $CD34^{-}CD19^{-}$ cells expressed lower levels of JAM-A overall, but could often be divided into two subsets, one being $JAM\text{-}A^{+}$ and one being $JAM\text{-}A^{lo/-}$. Interestingly as indicated above, Cox *et al.* showed that $CD133^{+}CD19^{-}$ B-ALL cells could proliferate *in vitro*

and engraft NOD/SCID mice *in vivo* (81). Although these JAM-A$^{lo/-}$ cell subsets have not as yet been tested for CD133 expression, Dr. Blair's group has shown that CD34^{+}CD19^{+}, CD34^{+}CD19^{-} and CD34^{-} B-ALL cell subsets all contain leukaemic initiating cells following transplantation into NSG mice (342). One might speculate that these CD34^{-}CD19^{-} cells, particularly those lacking JAM-A, may contribute substantially to the metastatic spread of this disease if they are not held within the bone marrow and thus also contribute significantly to relapse from this disease. Further studies to assess this are however required. Pilot sorting experiments carried out in Bristol indeed demonstrated that at least *in vitro* both JAM-A^{+} and JAM-A^{-} cells could proliferate over a 6 week period of culture.

3.3.8.2. T cell-acute lymphoblastic leukaemia (T-ALL) bone marrow cell fractions

The phenotypic characteristics of T-ALL leukaemia initiating cells are illustrated diagrammatically in Figure 3.31. One suggested mechanism of T cell development is that the lymphoid progenitors differentiate into Pro-T cells (CD7^{+}) and then become Pre-T cells (CD2^{+}CD7^{+}) and then common thymocyte progenitors.

Table 3.2. T-ALL primary cell staining for CD34, CD7 and JAM-A.

T-ALL samples (% of positive staining)	ALL19	ALL20
JAM-A	99.6	99.57
CD34	0.14	50.76
CD7	99.21	0.25
CD34^{+}/CD7^{+} (/JAM-A^{+})	0.03 (0.03)	0.03 (0.03)
CD34^{+}/CD7^{-} (/JAM-A^{+})	0.11 (0.09)	50.73 (50.58)
CD34^{-}/CD7^{+} (/JAM-A^{+})	99.18 (98.85)	0.22 (0.20)
CD34^{-}/CD7^{-} (/JAM-A^{+})	0.68 (0.62)	49.02 (48.76)

Two T-ALL primary cell samples were stained with antibodies against JAM-A, CD34 and CD7. The cells were gated firstly live cells with 7AAD dye and the percentages of each single, dual, or multiple-staining were shown in the tables. (Data kindly provided by Dr. Charlotte Cox).

Only two T-ALL primary bone marrow samples were available for analysis and these were carried out by Dr Charlotte Cox in Dr Blair's laboratory. The FACS analyses of these bone marrows for expression of CD34, CD7 and JAM-A are summarised in Table 3.2. Over 99% of the two examined bone marrow samples expressed JAM-A. In bone marrow ALL19, 99.21% were CD7 positive and only 0.14% were CD34 positive. The cells were thus almost exclusively $CD34^{-}CD7^{+}$ and 98.18% of these expressed JAM-A. In bone marrow ALL20, approximately half the cells were either $CD34^{+}CD7^{-}$ or $CD34^{-}CD7^{-}$ and over 99% of these expressed JAM-A. Only 0.25% of ALL20 bone marrow cells expressed CD7. Previously Cox *et al.* have shown that the cells which grow *in vitro* mainly existed in $CD34^{+}CD7^{-}$ and $CD34^{+}CD7^{+}$ cell subfractions, but only the former showed engraftment ability and underwent differentiation *in vivo* (79). The two patients' samples examined contained the same proportion of $CD34^{+}CD7^{+}$ cells which was <1% and these were all JAM-A positive. $CD34^{+}CD7^{-}$ cell fractions were also observed but the percentages ranged from 0.11 to 50.73% and most but not all cells were JAM-A positive. No conclusions could be drawn because of the small cohort of patients. However, there was essentially no $JAM\text{-}A^{-}$ cells in these two samples.

3.4. Discussion

In this chapter, a comprehensive analysis was carried out of the differential expression of JAM-A protein on phenotypically defined UCB haematopoietic progenitor subsets, various more mature UCB lineage cells, leukaemic cell lines, three types of bone marrow vascular niche cells, and to a lesser extent on primary leukaemias. JAM-A protein was co-expressed on 74 to 77% of UCB MNCs and 82.6±5.6% of $CD45^{+}$ UCB MNCs. Of these, the majority of UCB $CD66^{+}$ neutrophils, $CD14^{+}$ monocytes and $CD41a^{+}$ megakaryocyte progenitors expressed

JAM-A on their surface. For more mature lymphoid cells, 70 to 74% of $CD3^+$ T cells, $CD56^+$ NK cells and $CD19^+$ B cells from UCB expressed JAM-A. The expression of JAM-A on $CD235a^+$ erythroid cells varied widely amongst donors, ranging from as low as 16.9% to as high as 93.8%. The highest level of JAM-A expression was found on UCB $CD14^+$ monocytic cells and $CD41a^+$ megakaryocyte precursors. These studies are consistent with a less extensive study by Willams *et al.,* who showed that 100% of $CD14^+$ cells expressed JAM-A compared to 50-70% of $CD3^+$ or $CD19^+$ cells expressing JAM-A (233). Although described on platelets (239), the high level of expression of JAM-A on $CD41a^+$ megakaryocyte precursors has not previously been reported, nor has such an extensive analysis been carried out on human UCB.

The expression of JAM-A on phenotypically defined haematopoietic progenitor cells was also examined. This is much more challenging than examining more lineage restricted cells because of the rarity of the progenitor cells. Classically, haematopoiesis maps identify very rare HSCs which differentiate into committed progenitor cells at defined branch points, with HSCs generating lymphoid (T, B, NK cells) and myeloid (neutrophils, eosinophils, mast cells, basophils, monocytes, erythrocytes and megakaryocytes) as well as dendritic cell lineages via a series of intermediate progenitor cells. The earliest defined restricted progenitors were, at the time the experiments were done in this thesis, reported as CMP and CLP. The former were cited as being able to generate GMPs and MEPs, while the latter generated B lymphoid progenitor cells as well as ETPs or the earliest thymic progenitor cells which could give rise to T and NK lineage cells. They were also reported to generate dendritic cells (334, 335). It was originally reported that approximately 1 in 10^6 cells in UCB, 1 in $3x10^6$ in bone marrow and 1 in $6x10^6$ in mobilised peripheral blood (PB) represented the transplantatble HSC, at least as measured by their scid repopulating ability in NOD/SCID mice (343). This is about 5

times higher when cells are tansplanted into improved murine models such as into NSG mice (22).

In UCB, our studies showed that ≤ 1% of the MNCs were $CD133^+$ or $CD34^+$, markers found on human HSCs and their immediate progeny (140). Essentially all these human UCB $CD133^+$ and the majority of $CD34^+$ progenitor cells expressed JAM-A. The detection of JAM-A protein on these cells extended the earlier transcriptome study from our laboratory (324) and that of Rossi *et al.* (321), which identified JAM-A gene expression in $CD133^+$ and $CD34^+$ cells respectively. While our experiments were being conducted, Stellos *et al*. (239) reported that JAM-A protein was expressed on human PB $CD34^+$ cells and that these included endothelial progenitor cells. While purified $CD133^+$ cells showed relatively homogeneous expression of JAM-A in our studies, JAM-A expression on UCB $CD34^+$ cells fell into three subgroups. The highest JAM-A expression was found on majority of intermediate to high $CD34^+$ cells. The cells expressing the lowest levels of CD34, in contrast, expressed lower JAM-A levels on their cell surface, perhaps suggesting that the most primitive and most mature $CD34^+$ UCB progenitors express slightly less JAM-A than the majority of haematopoietic progenitor cells in UCB. This observation led us to examine the expression of JAM-A on the more primitive progenitor cell subsets in more detail. First, a modified protocol from Goarden *et al*. (78) for detecting phenotypically defined HSC and myeloid progenitor cell subsets was followed. This modification was made because of the restricted number of detection channels in our flow cytometer. Using this multi-colour flow cytometry method to study JAM-A expression on CMPs, GMPs, MEPs, HSCs and MMPs, all these enriched subsets were found to express JAM-A at relatively high levels. Thus, the phenotypically defined CMP/MEP $lin^-CD34^+CD38^+CD123^{+/-}CD45RA^-$ cells, the GMP $lin^-CD34^+CD38^+CD123^+CD45RA^+$ cells, the HSC and MMP containing $lin^-CD34^+CD38^{dim/-}CD45RA^-$ cells all expressed JAM-A on their cell

surface. The definitive proof that these subsets express JAM-A would come from further *in vitro* and *in vivo* functional analyses of sorted cell subsets expressing the multiple markers described above or with newer marker sets added. For example, Notta *et al*. (344, 345) have more recently defined the human long term repopulating HSC as being $CD34^{+}CD38^{dim/-}CD45RA^{-}CD90^{+}CD49f^{+}$, while the $CD34^{+}CD38^{dim/-}CD45RA^{-}CD90^{-}CD49f^{-}$ cells only provide transient multilineage haematopoietic reconstitution and are considered to be MPPs (Figure 1.5). They also defined the human CMP as $CD45RA^{-}CD135^{+}CD10^{-}CD7^{-}$, the MEP as $CD45RA^{-}CD135^{-}CD10^{-}CD7^{-}$ and the GMP as $CD45RA^{+}CD135^{+}CD10^{-}CD7^{-}$ (22), while Goarden *et al.* (78) segregated these cells on the basis of CD110 expression rather than CD135 expression. In the latter protocol and in our studies, we excluded CD10 and CD7 positive cells in the lineage depletion step. Hence, the two protocols differ on the basis of the expression of CD110, the thrombopoietin receptor, versus the expression of CD135, the Flt3 receptor. Unfortunately, it was not possible for us to segregate our HSC and MPP cell subsets based on CD90 and CD49f expression, nor our CMP, MEP and GMP subsets based on CD110 or CD135 expression, and then to analyse these for JAM-A because of flow cytometry channel constraints. Interestingly, while we were conducting our experiments, Sugano *et al.* (152) demonstrated that JAM-A was present on murine long term repopulating HSC from murine adult bone marrow, but, unlike our human bone marrow sections and UCB studies, only 2% of murine bone marrow cells expressed JAM-A and this molecule was gradually lost as the haematopoietic progenitor cells became more lineage restricted. Thus, the expression of JAM-A on haematopoietic cells appears to differ significantly between mouse and human. This discrepancy between mouse and human has also been demonstrated with other markers. These include CD34, with >99% of human HSC activity predicted in the human

$CD34^+$ cells fraction, while, in mice, $CD34^-$ cells possess significant HSC potential (Figure 1.5; reviewed in (22)).

We next used the protocol described by Hoebeke *et al.* (334) for the phenotypic detection of CLPs from human UCB. These authors reported that the CLP candidate cell from human UCB could be defined by their $CD34^+CD38^{dim/-}CD7^+$ phenotype with such cells generating T, B and NK cells. Using this protocol, we demonstrated that over 94% of human UCB phenotypically identified as such CLP by this definition co-expressed JAM-A. More recent studies have redefined models for human haematopoiesis (22, 345) and these revised lineage maps for human and mouse haematopoiesis are shown in Figure 1.5. The changes to these lineage maps compared to the classical lineage pathways have principally been for the lymphoid pathway.

In their studies, Hoebeke *et al.* (334) also described human UCB $CD34^+CD38^{dim/-}CD7^-$ cells with both lymphoid and myeloid potential. More recently, Doulatov *et al.* (71) reported that Multi-Lymphoid Progenitors (MLP for B, T and NK cells) were present in 1% of $CD34^+$ cells characterised as $CD34^+CD38^{dim/-}CD90^{lo/-}CD45RA^+$ and could also give rise to myeloid cells but not erythroid or megakaryocytic cells. However, in their model, they propose that MLP in the human are defined as $CD10^+$ and $CD7^-$ and that $CD34^+CD38^+$ with $CD7^+$ or $CD10^+$ cells are already committed to the T and B lymphoid lineages respectively. They however do not exclude UCB $CD34^+CD38^{dim/-}CD7^+$ cells being a transient population of CLP, which may not exist in the adult (22).

In the studies presented in this chapter, JAM-A expression on both human UCB $CD34^+CD19^+$ B lymphoid and $CD34^+CD7^+$ T lymphoid cells was also analysed. Our results indicated that the JAM-A expressing cells accounted for 94.4±4.2% in UCB $CD19^+CD34^+$ cells population and 98.8±2.1% in UCB $CD7^+CD34^+$ populations. Moreover, their JAM-A expression level showed

no difference to their CD34 single positive populations. The studies presented in this chapter thus suggest that JAM-A is expressed on the majority of HS/PCs from human UCB, and its expression showed no statistically significant differences amongst examined progenitor cells.

In order to investigate the difference of JAM-A expression in normal and malignant haematopoietic cells, JAM-A expression was examined on 6 normal bone marrow sections, 22 acute myeloid leukaemic bone marrow sections and 8 acute lymphoblastic leukaemic bone marrow sections using immunohistochemistry staining. JAM-A expression varied among bone marrow sections stained particularly if they were ALL samples or miminally differentiated AML samples, and less so for other AML subgroups. In general, JAM-A was always highly expressed on megakaryocytes in each section, and was weak on endothelium from normal bone marrow and when observed in leukaemic sections appeared to be substantially higher on the endothelium. It would be of interest to follow this up further as JAM-A expression on leukaemic bone marrow endothelium may be altered by the leukaemic cells and this may affect the leukaemic niche.

In order to quantify JAM-A positive cells in ALL subpopulations, 9 primary bone marrow acute B-lymphoblastic leukaemia (B-ALL) and two acute T-lymphoblastic leukaemia (T-ALL) were examined in a collaboration with Dr. Allison Blair at the University of Bristol. In the B-ALL bone marrow samples, the majority of bone marrow cells expressed JAM-A on their surface, with the exception of the $CD34^{-}CD19^{-}$ cells. In general, JAM-A expression on $CD34^{+}$ cells, whether CD19 positive or negative, was consistently higher than on $CD34^{-}$ cells, especially when $CD34^{+}CD19^{-}$ cells were compared to $CD34^{-}CD19^{+}$ cells ($p<0.05$). Two T-ALL patients showed similar JAM-A profiles with over 99% of the cells being JAM-A positive but with variable CD34 and CD7 staining. Whether JAM-A expression correlates with any

particular primary T-ALL cell subpopulation could not be determined because of the small number of samples available. Interestingly, both JAM-A$^+$ and JAM-A$^-$ cells expanded in culture and it will be important to determine if the loss of JAM-A is associated with poorer outcomes for patients with B-ALL. During this thesis research, Bornardi *et al.* reported that JAM-A expression on human AML CD34$^+$ cells was higher than their CD34$^-$ AML counterparts in proteomic study (83). When compared with normal bone marrow, they found no difference between the transcriptional levels of JAM-A in AML and normal bone marrow CD34$^+$ cells, but there was an upregulation of another JAM family member, ESAM (83). These data were not subsequently confirmed at the protein level.

Acute leukaemic cell lines were also assessed in this thesis for their surface JAM-A so that they could be used in future experiments. Strong JAM-A expression was detected in the early myeloid cell line, KG-1, and moderate levels in the other two myeloid cell lines, HL-60 and TF-1, that were tested. Weak expression was observed on T-ALL cell lines, CEM, MOLT-4 and JAM-A was not detectable on Jurkat cells. In contrast, the two tested primary T-ALL cell lines showed strong JAM-A expression.

JAM-A expression was further assessed on the three selected bone marrow niche cell types and only BMEC-60 bone marrow endothelial cells expressed JAM-A. It has been suggested that JAM-A redistributes from tight endothelial junctions to the apical area of human brain endothelial cells for leucocyte transmigration (262) and perhaps a similar mechanism exists for migrating HSCs across bone marrow endothelium. JAM-A-αVβ3-integrin cis-heterophilic binding has been demonstrated on HUVECs *in vitro* and this regulates HUVEC migration on vitronectin (333). JAM-A can also interact with LFA-1 and αVβ3 integrins although the studies here show an absence of LFA-1 and a presence of αVβ3 integrin on BMEC-60 cells. A point worth considering is that bone marrow endothelium may lose a number of adhesion

molecules from their surface during *in vitro* culture, and they can be regained by adding certain cytokines, such as interleukin-1β (IL-1 β) or tumour necrosis factor-α (TNF-α). In this study, IL-1β was used to activate BMEC-60 cells and this rescued the expression of E-selectin and VCAM-1 on BMEC-60 cells in agreement with previous publications (175, 178, 181), while the levels of JAM-A, CD29 (β1-integrin) and CD51/CD61 (αVβ3-integrin) remained unchanged. In addition, LFA-1 (CD11a/CD18, αLβ2-integrin) remained absent on BMEC-60 cells with this stimulation. Other studies have suggested that inflammatory cytokines are able to cause JAM-A to redistribute on endothelium from cell-cell junctions to the apical region to support immune cell attachment and then infiltration (262, 346). Since bone marrow endothelial cells have the phenotypic characteristics of inflamed endothelium and are fenestrated, JAM-A may exist more on the endothelial surface facing the blood flow than between endothelial cells in bone marrow and may thus play a more specialised role in HSPC migration.

In conclusion, the results in this chapter show that JAM-A is expressed on haematopoietic progenitor cells and particularly highly on monocytes and megakaryocytes in human UCB. Its expression on bone marrow endothelium might suggest a role for JAM-A in the interaction of these cell types with the the bone marrow endothelium or the vascular niche and this may be modulated in the leukaemic environment. Studies to address the biological functions of JAM-A are discussed in the following chapters.

CHAPTER 4

DOES JAM-A REGULATE HAEMATOPOIETIC PROGENITOR CELL ADHESION TO AND MIGRATION ACROSS BONE MARROW NICHE ELEMENTS?

4.1. Introduction

Following transplant, haematopoietic stem/progenitor cells (HS/PCs) will home to the bone marrow in response to CXCL12 chemokine, adhere to the bone marrow sinusoidal endothelial cells and then migrate into and lodge in the bone marrow niches. However, the mechanisms leading up to cell lodgement in bone marrow niches, especially in bone marrow sinusoidal niche, are not fully revealed. There are three bone marrow niches described for HS/PCs, the endosteal or osteoblastic niche, the vascular niche and the bone marrow compartment (93). There still remains considerable controversy as to whether the bone marrow stem cell niches are distinct and have specific functions. Some studies suggest that the more immature HSC lodges in the endosteal niche where its quiescence is maintained (94, 99, 347), although recent studies in mice suggest that HSCs may be preferentially located in the vascular/sinusoidal niche and lymphoid progenitors may reside in the endosteal niche (123, 124). Others suggest no distinction between niches (93, 94, 115, 348).

In addition to CXCR4, a variety of molecules has been described as being important for the homing, transendothelial migration and retention of HS/PCs in bone marrow niches. These include selectins and their ligands, integrins (e.g. VLA-4 and VLA-5), sialomucins such as CD164, and addressins (e.g. CD44) (314, 348, 349).

Although Chapter 3 describes junctional adhesion molecule-A (JAM-A) as being relatively highly expressed on human UCB $CD133^+$ and $CD34^+$ HS/PCs and on BMEC-60 cells, but not

BM MSCs, its roles in HS/PC cell adhesion and migration to bone marrow vascular niche elements have not been examined. JAM-A is also expressed in high amounts on $CD14^+$ monocytes and $CD41a^+$ megakaryocyte precursors (Chapter 3) and platelets (231), and to a lesser and more variable extent on such lineage restricted cells as neutrophils, erythroid cells, and T and B cells (Chapter 3) (233). As JAM-A showed expression on a panel of haematopoietic cells and cell lines and as well as on bone marrow endothelial cells but no other vascular niche cells, its roles in HS/PC cell adhesion and migration to the bone marrow vascular niche was examined in this chapter.

On platelets, JAM-A-JAM-A homophilic interactions have been reported to occur between platelets or between platelets and endothelium (230, 237, 242, 350). A series of JAM-A studies by Dejana's group has also shown that loss of JAM-A caused impaired neutrophil cell adhesion and mobility. Firstly, impaired directional movement was observed in murine JAM-$A^{-/-}$ polymorphonuclear leucocytes (PMN) accompanied by an increase in adherent cells in the lumen of vessels and a decreasing infiltration to the site of injured vessel *in vivo* (351). Moreover, on murine JAM-$A^{-/-}$ neutrophils, higher levels of $\beta1$ and $\beta2$ integrin expression were observed on the cell surface and this was believed to contribute to an enhancement of integrin-mediated adhesion and a reduction in neutrophil migration (251).

4.2. Aims and Objectives

The overall aims of this chapter were to investigate whether JAM-A on normal and malignant human HS/PCs was involved in their cell adhesion onto and migration across bone marrow niche elements. The objectives of this chapter were twofold:

Objective 1: To examine the role of JAM-A in the adhesion of UCB $CD34^+$ and leukaemic cell lines to bone marrow niche elements *in vitro*.

Objective 2: To examine the role of JAM-A in regulating migration of UCB $CD34^+$ and leukaemic cell lines to CXCL12 *in vitro*.

4.3. Results

4.3.1. JAM-A contributes to the in vitro adhesion of acute myeloid leukaemic cell lines to BMEC-60 cells.

Since JAM-A was shown in Chapter 3 to be expressed on selective haematopoietic cell lines representing myeloid, and T and B lymphoid progenitor cells, the initial adhesion studies were carried out on the myeloid leukaemic cell lines, TF-1 and HL-60, using collagen I, fibronectin and BMEC-60 cells as substrates.

4.3.1.1. Acute myeloid leukaemic TF-1 cells

TF-1 cell adhesion was assayed on two extracellular matrix substrates that are present in bone marrow, collagen I and fibronectin (352) and then on BMEC-60 cells after IL-1β stimulation for 4 hours (Chapter 2, Materials and Methods, section 2.12). The results demonstrated that TF-1 cells adhered to fibronectin (20.9±1.0%; $p<0.01$) and onto IL-1β pre-treated BMEC-60 cells at a similar level (19.6±1.1%; $p<0.01$), and to a lesser extent to collagen I (7.4±1.5%, $p=0.61$), the latter being similar to their adhesion to BSA (8.8±2.3% adherent cells), which was used as a negative control (Figure 4.1).

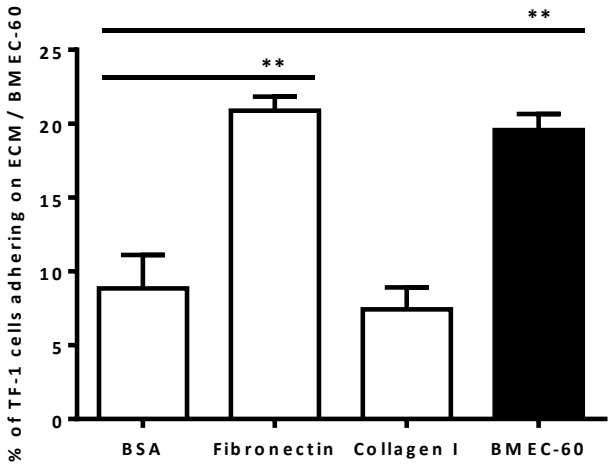

Figure 4.1. TF-1 cell adhesion to different extracellular matrices and IL-1β-pretreated BMEC-60 cells.
TF-1 cells were allowed to adhere to BSA, a negative control, fibronectin or collagen I, two different extracellular matrices (ECM), or IL-1β-pretreated BMEC-60 cell (BMEC-60) at 37°C for 1 hour. Values are means ± S.E.M. for n=3-4 independent experiments. The statistical analysis was done using Student's *t*-test and p values < 0.05 or < 0.01 (**) are considered significant or very significant respectively.

To block JAM-A binding, the TF-1 cells were pre-incubated with JAM-A chimaeric proteins or anti-JAM-A antibody (purified goat polyclonal antibody, AF1103, R&D systems) (239) before allowing them to adhere to IL-1β activated BMEC-60 cells or to fibronectin (Chapter 2, Materials and Methods, section 2.12). In these experiments, 20.2± 1.1% of cells in the chimaeric protein control (Fc) and 18.8±2.3% of cells in the antibody control (goat IgG) adhered onto BMEC-60 cells, showing no statistical difference in adhesion to the untreated group (21.7±0.6%; p=0.28 and p=0.30, respectively; Figure 4.2). With JAM-A blockade, TF-1 cell adhesion was reduced to 14.7±0.4% in the presence of the JAM-A-Fc chimaeric protein (p<0.01) and to 13.0±1.1% in the presence of the anti-JAM-A antibody (p=0.09; Figure 4.2), when compared to the non-blocking control Fc protein or to control antibody respectively.

Since TF-1 cells also adhered to fibronectin, the effects of blocking JAM-A with soluble chimaeric proteins or antibodies were also examined with this substrate. The adhering TF-1 cells decreased from 25.4±1.3% to 19.7±1.4% with JAM-A-Fc chimaeric protein addition and

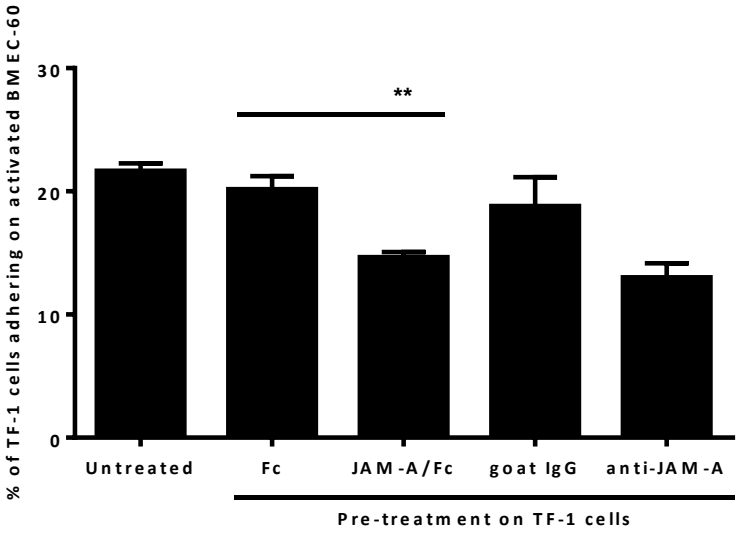

Figure 4.2. JAM-A blockade of TF-1 cell adhesion onto IL-1β-pretreated BMEC-60 cells.
TF-1 cells were incubated with or without (untreated) the indicated chimaeric proteins (10 μg/ml) or antibody (10 μg/ml, AF1103, R&D systems) and allowed to adhere to IL-1β-pretreated BMEC-60 cells at 37°C for 1 hours. Values are means ± S.E.M. for n=3 independent experiments. The statistical analysis was done using Student's *t*-test and p values < 0.05 or < 0.01 (**) are considered significant or very significant respectively.

from 25.9±2.7% to 14.7±2.3% with JAM-A antibody (Figure 4.3), but this could not be analysed statistically with any accuracy as only 2 assays were done.

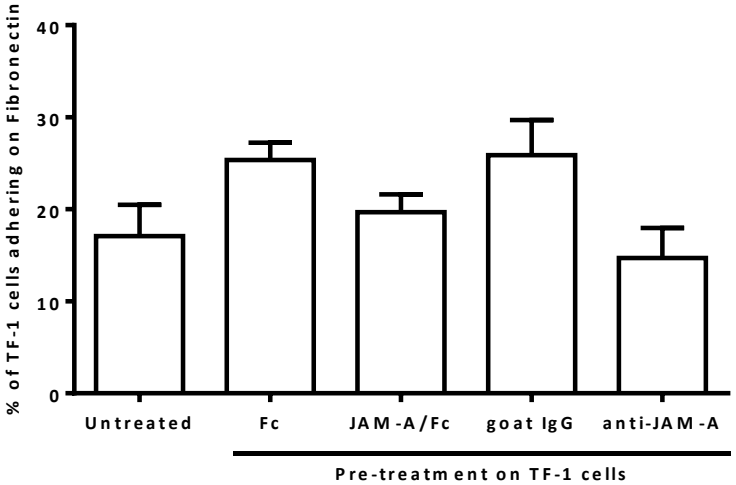

Figure 4.3. Effects of JAM-A blockade on TF-1 cell adhesion to fibronectin.
TF-1 cells were incubated with or without (untreated) the indicated chimaeric proteins (10 μg/ml) or antibody (10 μg/ml, AF1103, R&D systems) and allowed to adhere to IL-1β-pretreated BMEC-60 cells at 37°C for 1 hours. Values are means ± SD for n=2 independent experiments.

In order to specifically validate this JAM-A-dependent adhesion, TF-1 cells, which had been selected after stable JAM-A knockdown with two JAM-A shRNAs, were tested for adhesion to fibronectin or BMEC-60 cells. The selected transduced TF-1 cells containing JAM-A shRNA were kindly provided by Drs Sarah Hale and Youyi Zhang from our laboratory. The level of JAM-A expression was firstly examined by FACS. This showed that TF-1 cells stably transduced with the J2 shRNA-containing viral vector particles and J3 shRNA-containing viral vector particles or a non-silencing control shRNA expressed significantly lower levels of JAM-A on their cell surface than did the untreated TF-1 cells or TF-1 cells stably transduced with non-silencing shRNAs.

This was reflected in the M.F.I. values, which were reduced by 38.1% (M.F.I. at 1432±8.3 v.s. 3757±23.6) for J1 shRNA TF-1 cells and 44.7% (M.F.I. at 1338±16.6 v.s. 2991±39.2) for J2 shRNA cells compared to the non-silencing (NS) control (Figure 4.4.A). The TF-1 cells were then allowed to adhere to IL-1β-pretreated BMEC-60 cells (Figure 4.4.B). TF-1 cells with reduced JAM-A expression were less adherent to IL-1β-pretreated BMEC-60 than the original TF-1 cells or those TF-1 cells that had been transduced with a non-silencing shRNA. This decrease was from 18.2±1.5% to 11.4±2.3% with J2 shRNA transduced TF-1 cells (p<0.05) and from 19.6±2.7% and 14.2±2.5% with J3 shRNA transduced TF-1 cells (p=0.19; Figure 4.4.B) compared to the non-silencing control cells.

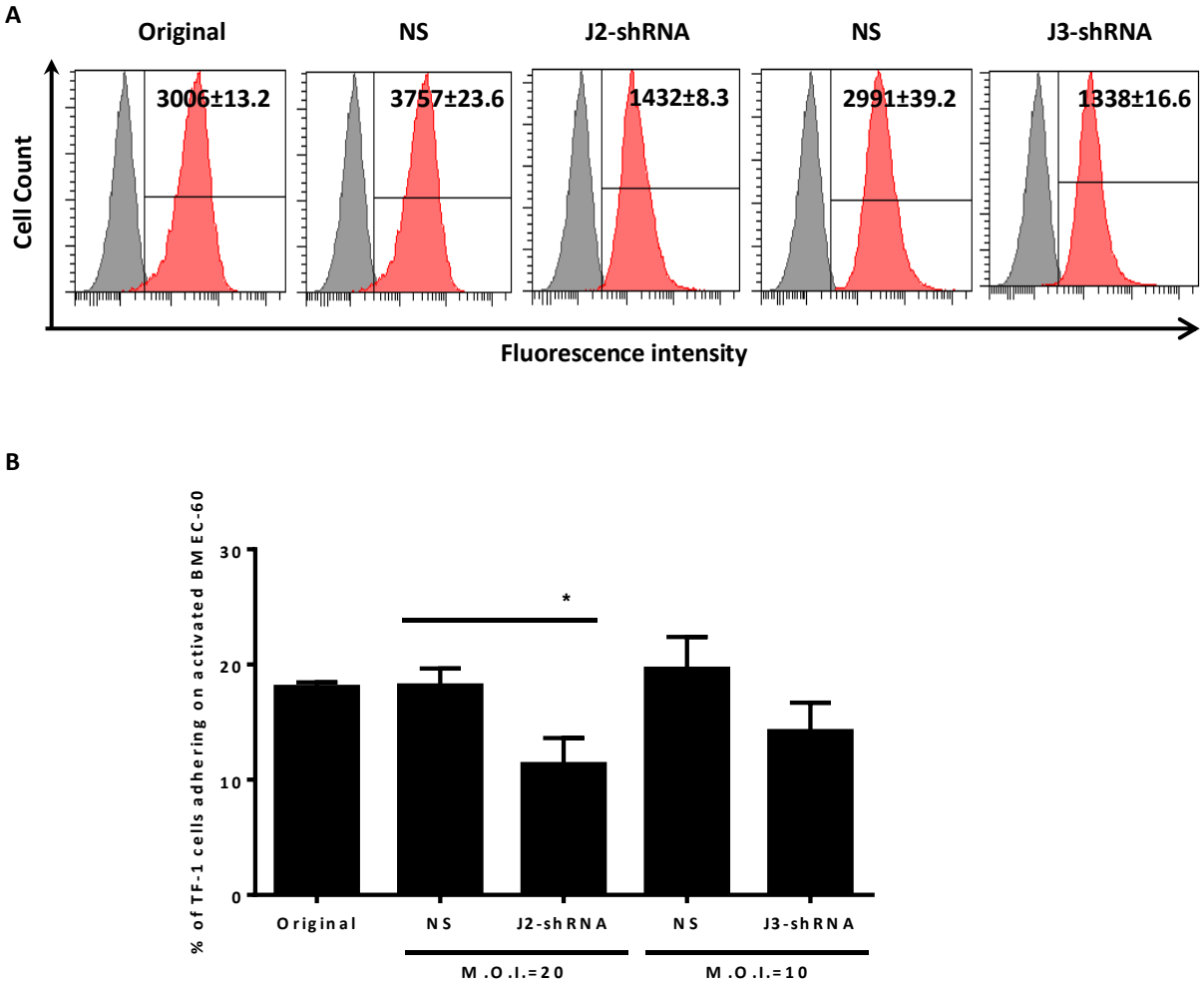

Figure 4.4. JAM-A silencing in TF-1 cells reduced their cell adhesion on BMEC-60 cells.
TF-1 cells were infected by lentiviral particles containing either JAM-A shRNAs (J2 at the M.O.I. of 20 or J3 at the M.O.I. of 10) or their non-silencing controls (NS) at the same M.O.I. respectively and selected in 2mg/ml puromycin were provided by Drs Hale and Zhang. (A) Representative FACS histograms of non-transduced TF-1 cells (Original), non-silencing (NS) and JAM-A shRNAs (J2 and J3-shRNA) transduced TF-1 cells stained with the JAM-A-PE antibodies (red) and their isotype controls (gray). M.F.I.± S.E.M. for n=3 shown in the top right corner. (B) Non-transduced TF-1 cells (Original) and the transduced cells were allowed to adhere to IL-1β-pretreated BMEC-60 cells at 37°C for 1 hour. Values are means ± S.E.M. for n=4 independent experiments. The statistical analysis was done using Student's *t*-test and values < 0.05 (*) or < 0.01 are considered significant or very significant respectively.

These same cells were also tested for their adhesion to fibronectin. Interestingly, TF-1 cells expressing lower levels of JAM-A adhered significantly less to fibronectin. This is illustrated in Figure 4.5, where adhesion was reduced from 27.9±0.3% to 20.4±1.7% with J2 shRNA TF-1 cells and from 25.1±1.6% to 14.6±1.7% with J3 shRNA TF-1 cells (p<0.05 for both) compared to the non-silencing control TF-1 cells.

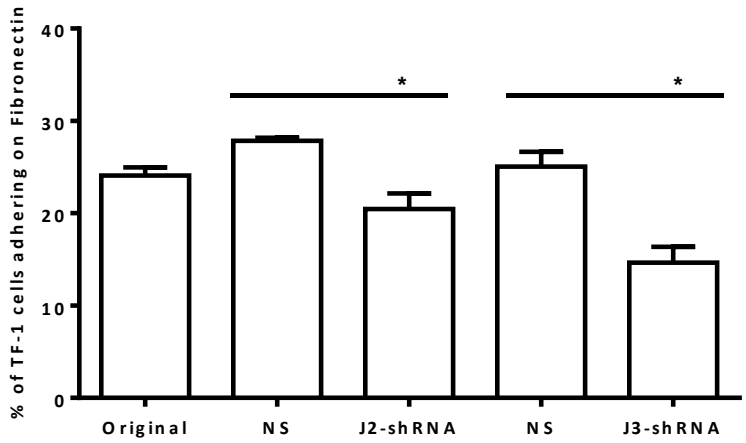

Figure 4.5. TF-1 cells expressing lower levels of JAM-A have reduced adhesion to fibronectin.
TF-1 cells transduced by lentiviral particles containing either JAM-A shRNAs (J2 at the M.O.I. of 20 or J3 at the M.O.I. of 10) or their non-silencing controls (NS) at the same M.O.I. respectively and selected in 2 mg/ml puromycin were provided by Drs Hale and Zhang. Non-transduced TF-1 cells (Original) and the transduced cells were allowed to adhere to fibronectin at 37°C for 1 hour. Values are means ± S.E.M. for n=3 independent experiments. The statistical analysis was done using Student's *t*-test and values < 0.05 (*) or < 0.01 are considered significant or very significant respectively.

In summary, these studies show that

i) TF-1 cells expressing JAM-A adhered to IL-1β stimulated BMEC-60 cells and the ECM molecule, fibronectin, but not to collagen I when compared to the BSA control.

ii) The soluble chimaeric protein, JAM-A Fc, significantly inhibited adhesion of TF-1 cells to BMEC-60 cells, but not to fibronectin.

iii) TF-1 cell lines with reduced JAM-A surface expression showed reduced adhesion to both BMEC-60 cells and fibronectin.

4.3.1.2. The adhesion of the acute myeloid leukaemic cell line, HL-60

HL-60 cells represent another acute myeloid leukaemic cell line which expresses JAM-A (Chapter 3). Cell adhesion studies similar to those described for TF-1 cells were carried out and demonstrated that 30.3±2.0% of HL-60 cells adhered on IL-1β pretreated BMEC-60 cells (p<0.01 compared to BSA), 5.5±3.2% adhered to fibronectin and 4.0±2.1% adhered to collagen I in comparison to 1.9±0.8% of BSA which was used as the negative control (Figure 4.6).

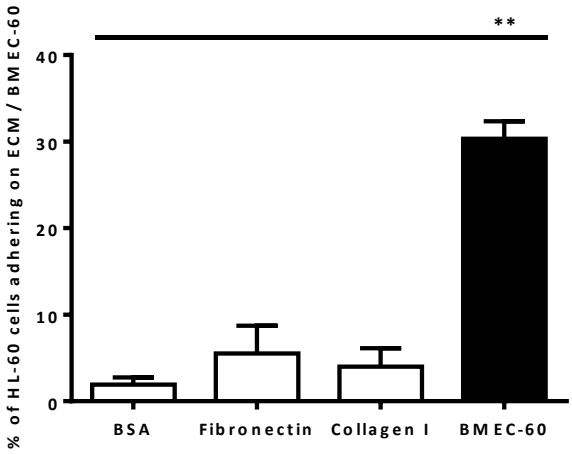

Figure 4.6. HL-60 cell adhesion to fibronectin, collagen I and IL-1β-pretreated BMEC-60 cells.
HL-60 cells were allowed to adhere to BSA, as the negative control, or to extracellular matrix molecules, fibronectin or collagen I, or IL-1β-pretreated BMEC-60 cells (BMEC-60) at 37°C for 1 hour. Values are means ± S.E.M. for n=3 independent experiments. The statistical analysis was done using Student's *t*-test and values < 0.05 or < 0.01 (**) are considered significant or very significant respectively.

As fibronectin adhesion was low, blocking studies were conducted using the BMEC-60 adhesion assay only. To test whether JAM-A was involved in HL-60 cell adhesion, the HL-60 cells were firstly incubated with JAM-A-Fc chimaeric protein or anti-JAM-A antibody before allowing them to adhere to IL-1β stimulated BMEC-60 cells. In these experiments, 31.5± 5.1% of cells in blocking control (Fc) and 29.2±3.9% of cells in antibody negative control

(goat IgG) adhered on BMEC-60 cells, showing no statistical difference to the untreated HL-60 cells (28.6±4.3%, p=0.68 and 0.92 respectively; Figure 4.7). For JAM-A-Fc or antibody blockade of HL-60 cells, HL-60 cell adhesion to IL-1β-pre-stimulated BMEC-60 was reduced to 12.4±4.1% (p<0.05 compared to Fc control) in the presence of the JAM-A-Fc protein and to 14.5±2.0% (p<0.05 compared to antibody negative control) in the presence of the anti-JAM-A antibody (Figure 4.7).

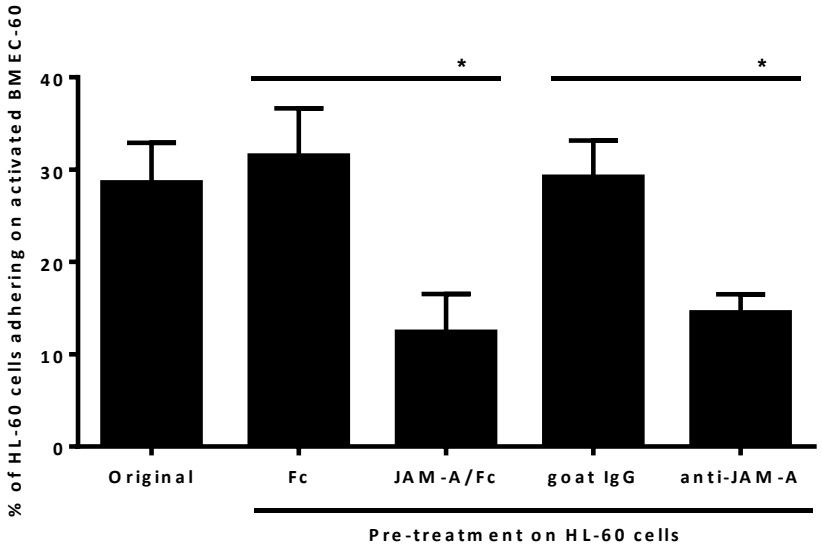

Figure 4.7. HL-60 cell adhesion on IL-1β-pretreated BMEC-60 cells.
HL-60 cells were incubated without (Untreated) of with the indicated chimaeric proteins (10 μg/ml) or antibodies (10 μg/ml, AF1103, R&D systems) and allowed to adhere to IL-1β-pretreated BMEC-60 at 37°C for 1 hour. Values are means ± S.E.M. for n=3 independent experiments. The statistical analysis was done using Student's *t*-test and values < 0.05 (*) or < 0.01 are considered significant or very significant respectively.

To analyse this further, JAM-A was knocked down in HL-60 cells using siRNAs as described below and the adhesion of the knocked down cells to BMEC-60 cells examined.

4.3.1.3.JAM-A siRNA optimisation and the effects of JAM-A knock down on HL-60 cell adhesion to BMEC-60 cells

To further analyse the function of JAM-A on HL-60 cell adhesion, three JAM-A siRNAs together with non-silencing controls were purchased from Ambion (Materials and Methods, section 2.7). To first optimise nucleofection conditions, HL-60 cells were nucleofected with a TexRed labelled non-targeting siRNA (SR30002, OriGene Technologies, Inc.) at different concentrations. Figure 4.8.A shows the nucleofection efficiencies using flow cytometry. Up to 94 to 95% of cells were nucleofected with the TexRed labelled siRNA at concentrations of 100 nM and 200 nM when measured 24 hours post nucleofection. The transfection process affected cell viability to some extent as shown in Figure 4.8.B, with cell mortality ranging between 18.2% and 31.5%, and being observed even with low nucleofection efficiencies (20nM siRNA). As the TexRed labelled siRNA concentration was increased, more entered the cells during the transfection process as demonstrated both by flow cytometry and microscopic analysis (Figures 4.8.A and 4.8.C).

From these results, 100 nM concentrations of JAM-A siRNAs were used in subsequent experiments. The knockdown efficiency of JAM-A siRNA in HL-60 cells was then analysed over 24 to 72 hours. JAM-A knockdown was optimal at 24 hour post nucleofection, with the M.F.I.s for JAM-A cell surface staining being 56.3±12.3% with siRNA 150 ($p<0.05$), 72.6±8.5% with siRNA 151 ($p<0.05$), 92.2±9.0% with siRNA 152 ($p=0.43$) and 43.4±5.6% with the combination of siRNA 150 and 151 ($p<0.01$), when compared to the non-silencing siRNA control (NS; Figure 4.9). Representative FACS histograms at 24 hours post nucleofection are shown in Figure 4.10.A. By 72 hours, JAM-A expression had almost returned to the non-silencing control level (Figure 4.9). There was no difference in cell viability among NS and siRNAs at each time point, but the percentage of viable cells increased by from just over

A. Nucleofection efficiency

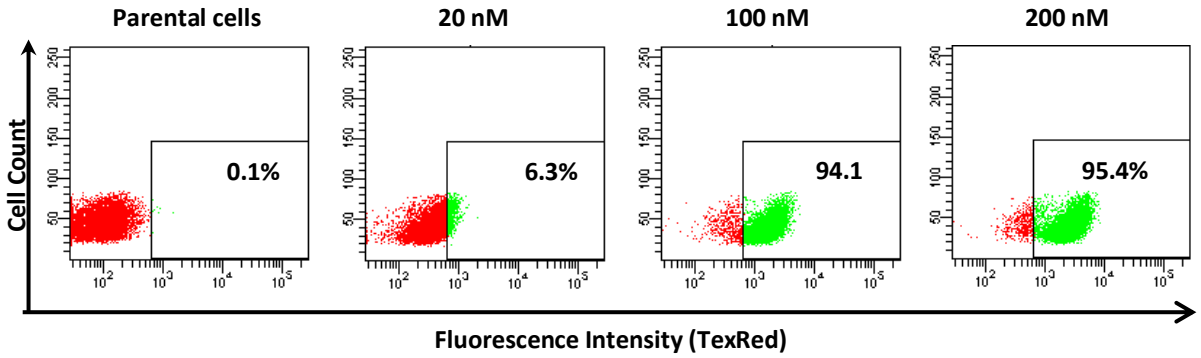

B. Cell mortality

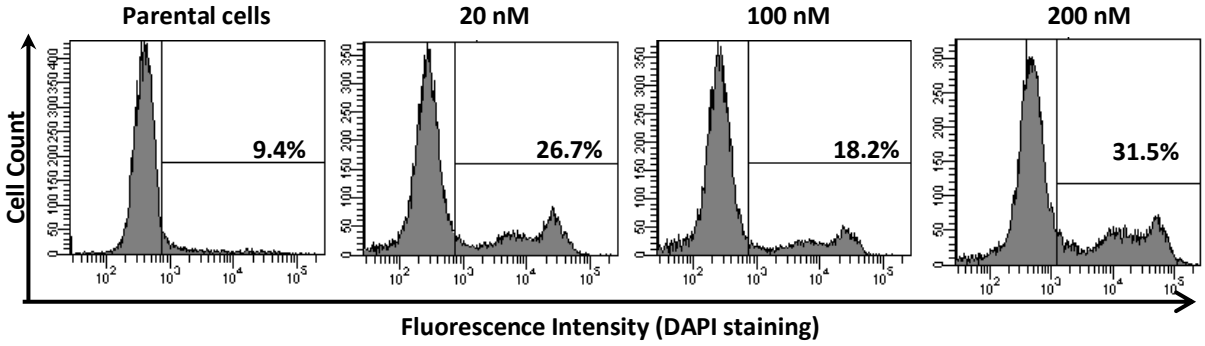

C. Images of nucleofected cells with TexRed labelled siRNA

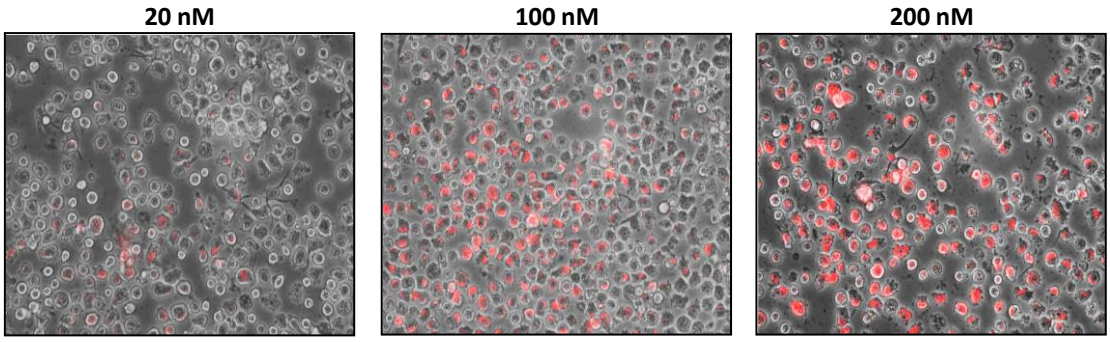

Figure 4.8. Optimisation of nucleofection with TexRed labelled-siRNA in HL-60 cells.
HL-60 cells were nucleofected with 2 nM, 100 nM and 200 nM of TexRed-siRNA and incubated at 37°C for 24 hours. The cells were harvested at 24 hours post nucleofection and tested for (A) nucleofection efficiency and for (B) cell mortality by flow cytometry. The efficiency was assessed by the number of TexRed positive cells and the cell mortality was examined using DAPI staining. (C) Images of HL-60 cells nucleofected with 20nM, 100nM or 200nM of TexRed siRNA were taken 24 hours post nucleofection by fluorescence microscopy at X10 magnification.

60% to over 80% over the 72 hour period post nucleofection (Table 4.1). As shown, the best knock-down efficiency was at 24 hours post nucleofection, and hence the nucleofected HL-60 cells were used at this time point for functional studies. Considering JAM-A expression among nucleofected cells, it declined significantly with siRNA 150, 151 and 150+151 only (p<0.05), while with siRNA 152 it remained similar to the NS control (p=0.74; Figure 4.10.A), when each was compared to the NS control. Cell viability among these five conditions showed no statistical significant difference (p >0.05 at each time; Figure 4.10.B; Table 4.1).

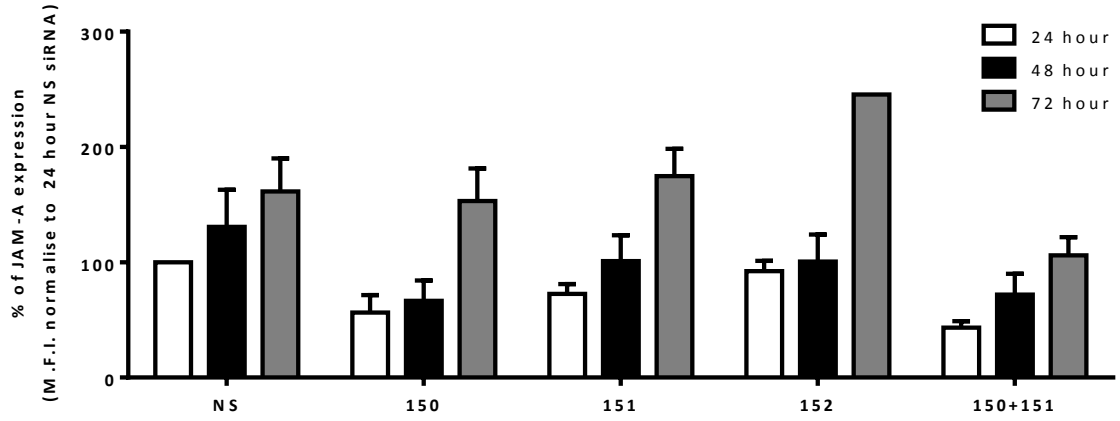

Figure 4.9. JAM-A siRNAs knockdown efficiency in HL-60 cells.
HL-60 cells were nucleofected with JAM-A siRNA (150, 151, 152 or a combination of 150+151 at 100nM in total or the non-silencing control (NS). The cells were harvested from 24 to 72 hours and tested for knockdown of cell surface JAM-A by flow cytometry. Values are M.F.I ± S.E.M. for n=3-9 independent experiments normalised to NS siRNA treated HL-60 cells at 24 hours post nucleofection. N=9 for NS, N=8 for 150 and 151, n=6 for 152 and n=4 for 150+151 at 24 hour; n=3 for all groups at 48 hour; n=4 for all groups at 72 hour.

Table 4.1. HL-60 cell viability post JAM-A siRNA nucleofection.

Hours post nucleofection	Non-silencing (NS)	siRNA 150 (150)	siRNA 151 (151)	siRNA 152 (152)	siRNA mixed (150+151)
24	63.7±2.1%	64.9±2.4%	64.3±2.2%	60.8±1.5%	63.7±4.7%
48	74.4±6.7%	73.6±6.2%	75.9±6.3%	71.5±10.0%	73.0±5.4%
72	85.4±1.8%	82.1±3.3%	86.7±1.9%	90.0±0.0%	82.1±0.2%

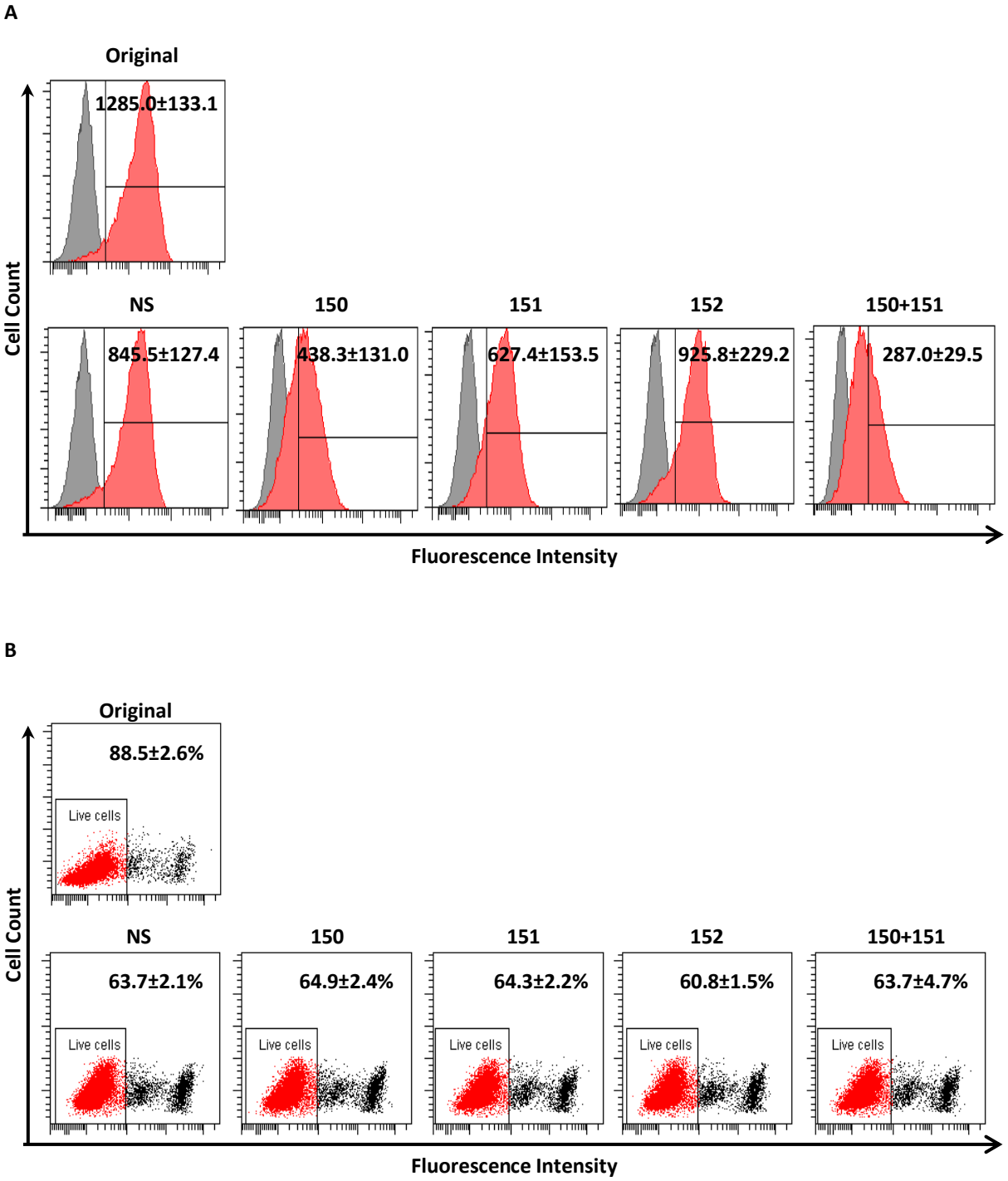

Figure 4.10. JAM-A silencing efficiency and cell viability of HL-60 cells at 24 hour post nucleofection.
Non-nucleofected HL-60 cells (Original) and those nucleofected with 100nM of JAM-A siRNA (150, 151, 152 or a combination of 150+151 at 100nM in total) and the non-silencing control (NS) were harvested at 24 hours. Knockdown efficiency and cell viability were checked before assessing these cells in the adhesion assay. (A) Representative FACS histograms of non-silencing and JAM-A siRNAs (red) in HL-60 cells stained with the JAM-A-PE antibodies and their isotype controls (gray). M.F.I.± S.E.M. for N=4-8 independent experiments shown in the top right corner. (B) Their cell viability was tested by DAPI staining and the DAPI-negative cells were gated as live cells. The mean % of live cells± S.E.M. for N=4-8 independent experiments is shown in the top right corner.

Knocking down JAM-A expression in HL-60 cells reduced their cell adhesion to IL-1β activated BMEC-60 cells from 34.8±3.2% for the NS control to 16.0±2.3% (p<0.01), 20.1±4.8% (p<0.05) and 26.4± 11.4% (p=0.42) with three individual siRNAs (150, 151 and 152 respectively), and to 22.1±3.3% with a combination of 150+151 siRNAs (p<0.05; Figure 4.11).

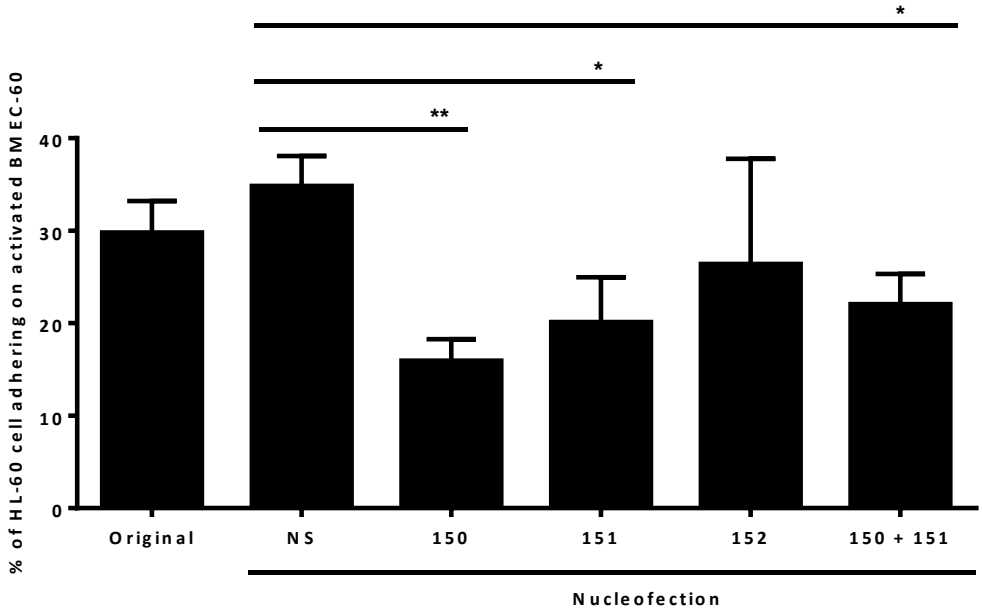

Figure 4.11. JAM-A silencing in HL-60 cells reduced their cell adhesion onto BMEC-60 cells.
HL-60 cells were nucleofected with 100nM of JAM-A siRNA (150, 151, 152 (n=4) or a combination of 150+151 (n=3) at 100nM in total) and the non-silencing control (NS; n=6). The non-nucleofected HL-60 cells (Original; n=5) and the nucleofected cells were harvested at 24 hours for adhesion assays to IL-1β-pretreated BMEC-60 cells. Values are means ± S.E.M. for n=3-6 independent experiments. The statistical analysis was done using Student's *t*-test and values < 0.05 (*) or < 0.01 (**) are considered significant or very significant respectively.

In summary, these studies show that

i) More HL-60 cells expressing JAM-A adhered to IL-1β stimulated BMEC-60 cells than to the ECM molecules, fibronectin and collagen I.

ii) The siRNAs to JAM-A, 150 and 151, effectively knocked down JAM-A in HL-60 cells, most significantly at 24 hours post nucleofection

iii) HL-60 cell lines with reduced JAM-A surface expression showed reduced adhesion to both BMEC-60 cells.

4.3.1.4. The adhesion of umbilical cord blood $CD34^+$ cells

To investigate whether JAM-A is involved in modulating normal haematopoietic cell adhesion to bone marrow niche elements, their ability to adhere to fibronectin, collagen I and BMEC-60 cells was first examined. UCB $CD34^+$ cells were isolated and then cultured for overnight in Flt-3 ligand, TPO, SCF and IL-6. As shown in Figure 4.12.A, 33.7±3.2% UCB $CD34^+$ cells adhered to IL-1β stimulated BMEC-60 cells (p<0.01 compared to BSA). The adhesion to fibronectin and collagen I was lower than to BMEC-60 cells, with 16.6±3.1% of cells adhering to fibronectin and 7.5±6.5% adhering to collagen I. While the adhesion to fibronectin was significantly different from adhesion to the BSA control (p<0.05), this was not the case for collagen I. It was found that 5.4±0.5% of $CD34^+$ cells adhered to BSA. Addition of JAM-A antibody reduced UCB $CD34^+$ cell adhesion onto IL-1β-pre-treated BMEC-60 cells from 25.1±1.3% to 17.9±1.7% (p<0.01; Figure 4.12.B).

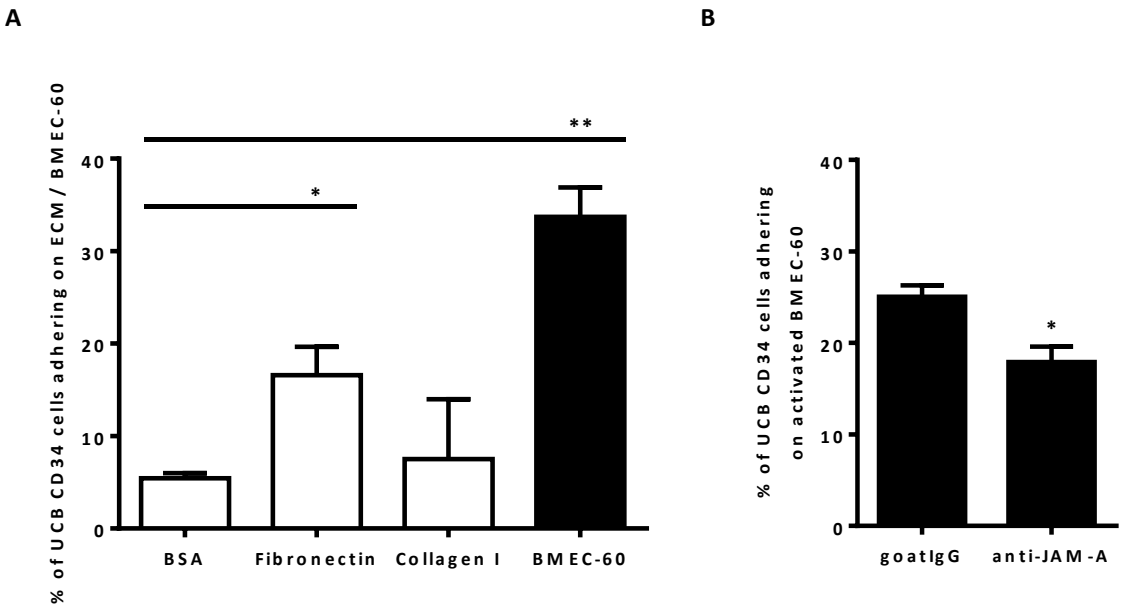

Figure 4.12. JAM-A blockade in UCB CD34$^+$ cells reduced their cell adhesion on BMEC-60 cells.
(A) UCB CD34$^+$ cells were allowed to adhere to BSA as a protein control, fibronectin, collagen I or IL-1β-pretreated BMEC-60 cells (BMEC-60) at 37°C for 1 hour (n=4). (B) UCB CD34$^+$ cells were blocked with JAM-A antibody (10 μg/ml, AF1103, R&D systems) prior to the adhesion assay on IL-1β-pre-treated BMEC-60 cells (n=6). Values are means ± S.E.M. for n=4-6 independent experiments and the statistical analysis was done using paired *t*-test and values < 0.05 (*) or < 0.01 (**) are considered significant or very significant respectively.

Next, JAM-A was knocked down in UCB CD34$^+$ cells using a combination of JAM-A siRNAs 150 and 151. At 100nM concentration, JAM-A expression on UCB CD34$^+$ cells decreased by 67.5%, from an M.F.I. of 992.8±172.9 in NS control cells to an M.F.I. of 372.5±51.6 in the JAM-A siRNA nucleofected cells 24 hours after nucleofection (p<0.05, Figure 4.13.A). The cell viabilities with the two treatments were 67.3±5.8% and 64.9±8.5% (p=0.50) respectively. JAM-A silencing in UCB CD34$^+$ cells also reduced their cell adhesion from 33.7±3.2% to 19.2±1.9% to BMEC-60 cells (p<0.01 for JAM-A siRNA vs. NS siRNA treated cells, Figure 4.13.B).

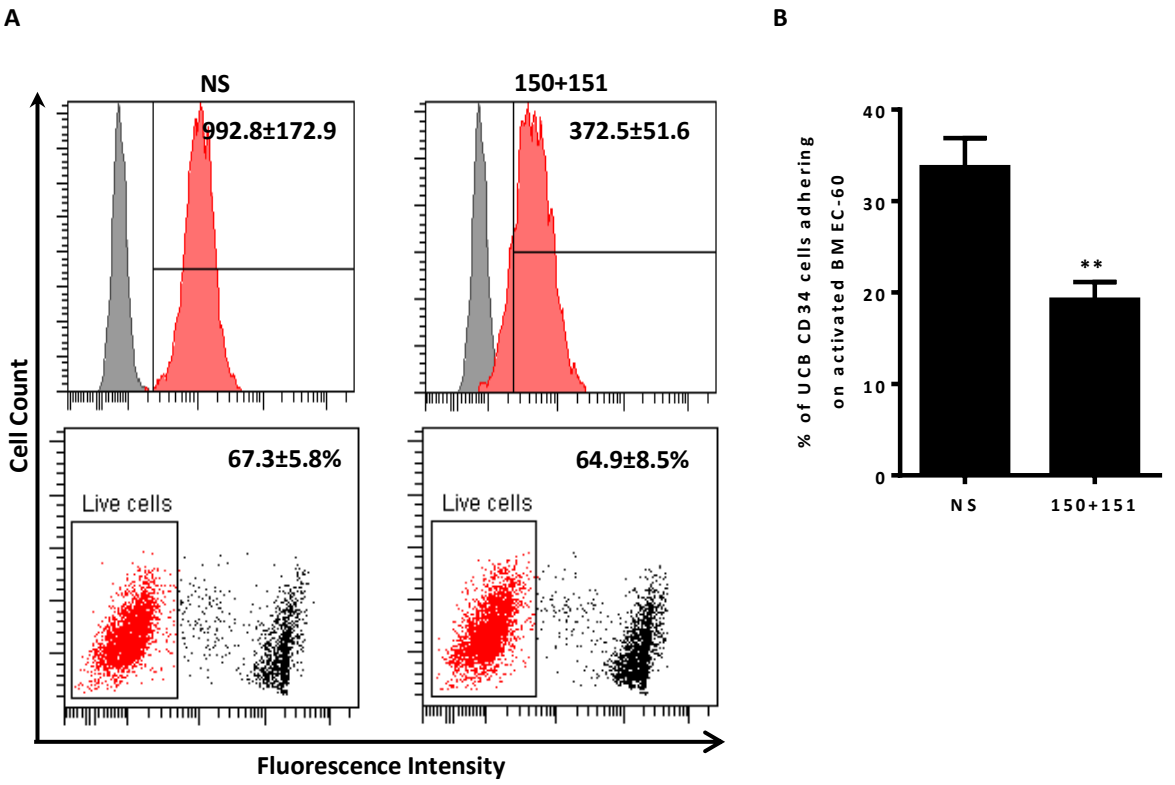

Figure 4.13. JAM-A silencing in UCB CD34$^+$ cells reduced their cell adhesion onto BMEC-60 cells.
(A) Representative FACS histograms of cell surface staining for JAM-A for non-silencing (NS) and JAM-A siRNA (150+151) knocked down UCB CD34$^+$ cells 24 hours after nucleofection with 100nM in total. The cells were then stained with the JAM-A-PE antibody (red; M.Ab.F11 clone) and the isotype control (gray) as shown in the upperhistograms after gating of live cells following DAPI staining (lower histograms). The values of M.F.I. ± S.E.M. and % non-DAPI staining ± S.E.M. are shown for each stain in the top right corner of the plot. (B) Nucleofected UCB CD34$^+$ cells were allowed to adhere onto IL-1β-pre-treated BMEC-60 cells at 37°C for 1 hour. Values are means ± S.E.M. for n=4 independent experiments and the statistical analysis was done using paired *t*-test and values < 0.05 or < 0.01 (**) are considered significant or very significant respectively.

JAM-A blockade and knockdown in UCB CD34$^+$ cells was also examined for their effects on cell adhesion to fibronectin. Figure 4.14 shows that, in independent experiments, UCB CD34$^+$ cell adhesion to fibronectin declined from 9.0±1.6% to 4.7±1.5% in the presence of JAM-A antibody (by 52%; p=0.11 compared to control antibody) and from 16.6±3.1% to 10.5±1.5% with JAM-A silencing (by 63%; p<0.05 compared to the NS control).

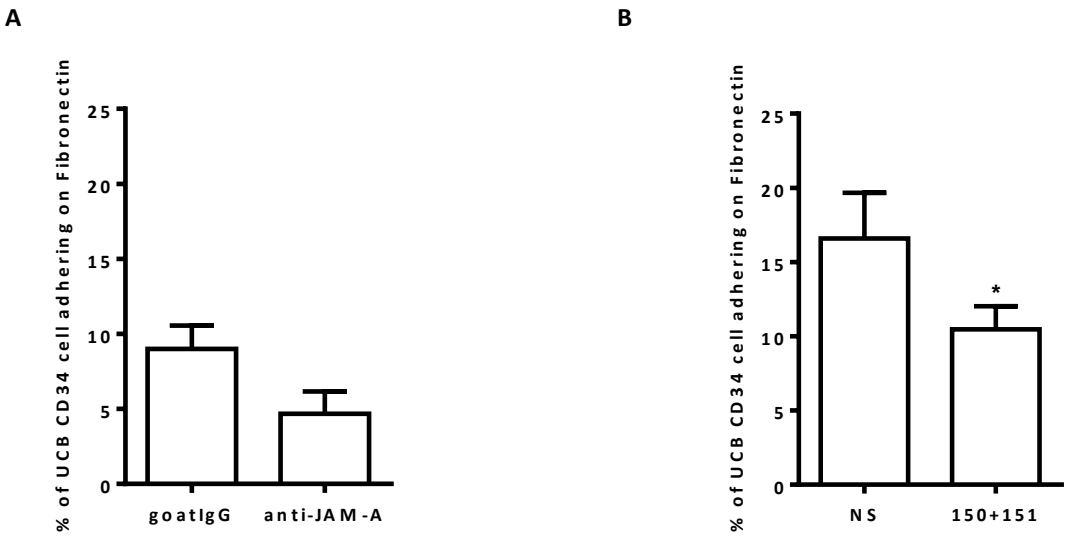

Figure 4.14. JAM-A blockade and silencing in UCB CD34$^+$ cells reduced their cell adhesion onto fibronectin. UCB CD34$^+$ cells were treated with (A) JAM-A blocking antibody (10 μg/ml, AF1103, R&D systems) for 30 minutes or control antibody (n=6) or (B) JAM-A siRNAs at 100nM for the total siRNAs (n=4) for 24 hours and allowed to adhere to fibronectin at 37°C for 1 hour. Values are means ± S.E.M. for n=4-6 independent experiments and the statistical analysis was done using paired *t*-test and values < 0.05 (*) or < 0.01 are considered significant or very significant respectively.

In summary, these studies show that

i) More human UCB CD34$^+$ cells adhered to IL-1β stimulated BMEC-60 cells than to the ECM molecules, fibronectin and collagen I, and more adhered to fibronectin than to collagen I.

ii) The siRNAs to JAM-A, 150 and 151, knocked down cell surface JAM-A on UCB CD34$^+$ cells at 24 hours post nucleofection.

iii) Both JAM-A blocking antibody and the JAM-A silencing led to significantly reduced adhesion of UCB CD34$^+$ cells to BMEC-60 cells.

iv) JAM-A knockdown significantly reduced adhesion of UCB CD34$^+$ cells to fibronectin.

4.3.1.5.JAM-A overexpression in a JAM-A negative cell line using lentiviral vector constructs

An alternative way to validate the function of JAM-A is to overexpress JAM-A in a JAM-A negative cell line and then examine the effects of this over-expression on cell adhesion to fibronectin, collagen I and BMEC-60 cells. As Jurkat cells did not express JAM-A (Chapter 3), a lentiviral vector was developed in house to over-express JAM-A in Jurkat cells.

The JAM-A sequence, which was purchased as an I.M.A.G.E. clone (Clone #100066761, EU831732) from Geneservice, was first cloned into the pENTR211 vector (see Materials and Methods, section 2.5.2), and the purified plasmid restriction enzyme digested with different combinations of restriction enzymes and analysed by electrophoresis (Materials and Methods, section 2.5.5 and 2.5.6). Based on the predicted enzyme restriction map of the JAM-A plasmid (Figure 2.3.B), two sizes of restriction fragments, 2885 bp and 599 bp, were expected with *Hpa* I enzyme digestion, two of 2762 bp and 752 bp with *Eco* RI enzyme digestion, four of 2428 bp, 457 bp, 304 bp and 295 bp with the combination of *Hpa* I and *Eco* RI enzyme digestion, one of 3484 with *Eco* RV or *Hind* III enzyme digestion, and two of 3348 bp and 136 bp with the combination of *Eco* RV and *Hind* III enzyme digestion. These were confirmed as shown in Figure 4.15.

Forward and reverse primers were designed based on the JAM-A EU831648 sequence when adding additional restriction enzyme sites and the Kozak sequence (5'- GCCACC-3') at the 5' end of the construct (described in Materials and Methods, section 2.5.7). The optimal annealing temperature was determined using a 2-step PCR programme (Materials and Methods, section 2.5.8), and it was shown to be in the range of 62 to 69°C for amplifying the JAM-A full-length sequence of 922 bp (Figure 4.16).

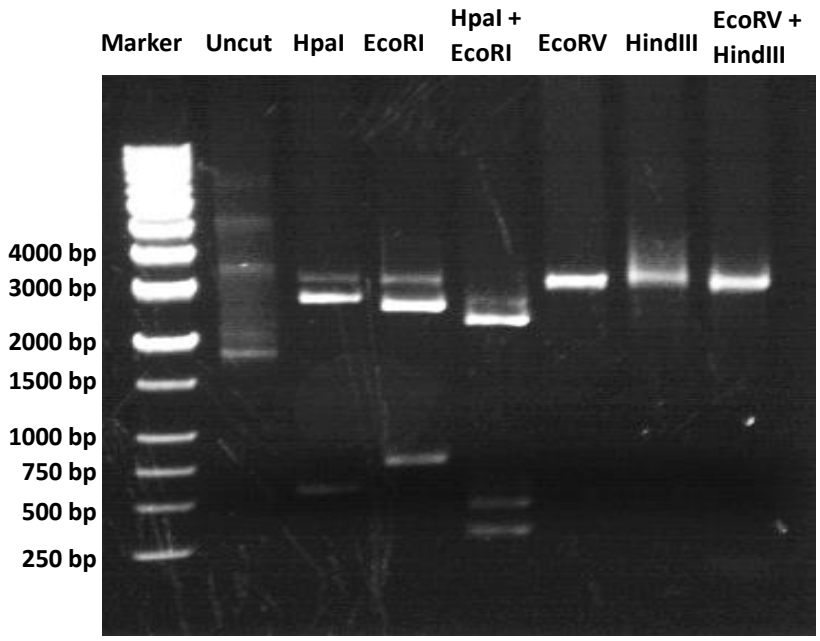

Figure 4.15. JAM-A I.M.A.G.E. clone restriction enzyme digestion.
The JAM-A image DNA clone was restriction digested using the restriction enzymes shown prior to gel electrophoresis. Fragments of approximately 2885 bp and 599 bp were observed with *Hpa* I digestion,of approximately 2762 bp and 752 bp with *Eco* RI digestion, of approximately 2428 bp, 457 bp, 304 bp and 295 bp with the combination of *Hpa* I and *Eco* RI digestion, of approximately 3484 with *Eco* RV or *Hind* III digestion, and of approximately 3348 bp and 136 bp with the combination of *Eco* RV and *Hind* III digestion. On the left are DNA markers.

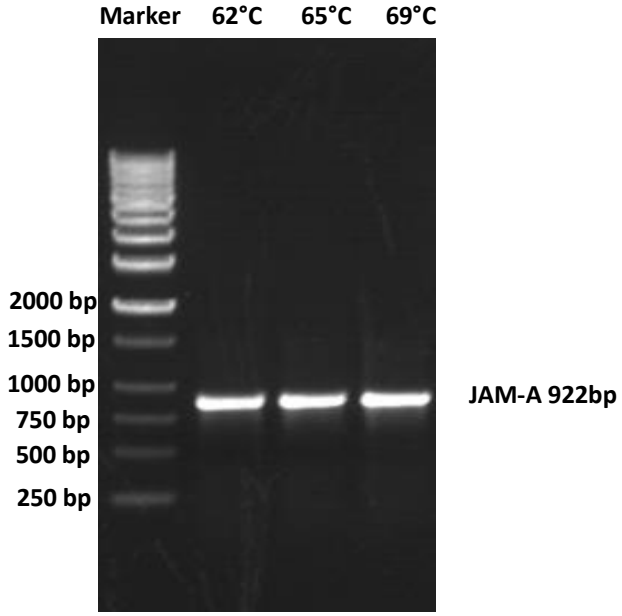

Figure 4.16. JAM-A cDNA fragments generated at different primer annealing temperatures.
DNA gel electrophoresis of full length JAM-A DNA fragments produced with primers described in Chapter 2 section 2.5.7 at three annealing temperatures, 62°C, 65°C and 69°C. DNA markers are shown on the left of the figure.

The amplified PCR product was cloned into the pCR® II-TOPO® TA vector after adding an additional dATP to the ends of the PCR products, amplified using One shot® TOP10 competent cells and clones selected in Ampicillin (Materials and Methods, section 2.5.). The numbers of colonies generated after different ligation conditions are shown in Table 4.2.

Table 4.2. The numbers of colonies forming using different ligation conditions.

Conditions (Vector: Insert)	Colonies per plate
Vector self-ligation (1:0)	28
1:0.5	117
1:1	136
1:2	>200

The JAM-A PCR cDNA fragment was cloned into the pCR® II-TOPO® TA vector at different cDNA to vector ratios. The numbers of colony generated are shown.

Ten colonies from the 1:1 ratio were randomly selected and tested for the presence of the JAM-A inserts by *Eco*RI restriction enzyme digestion (Figure 4.17). Clones numbered 3, 4 and 8 were selected for sequencing. The sequencing result for clone #8 (JAM-A-pCRII (8)) is shown in Figure 4.17 as this was used for further cloning into the lentiviral vector, pLNT-sffv MCS.

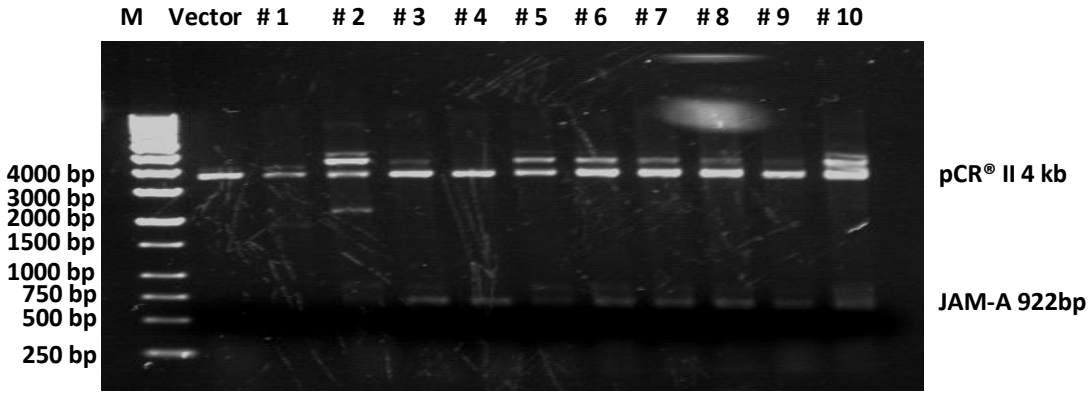

Figure 4.17. The results of JAM-A cloning into the pCR® II-TOPO® TA vector.
Ten colonies were selected as described and the isolated JAM-A cDNA plasmids subjected to *Eco* RI restriction enzyme digestion prior to gel electrophoresis. The JAM-A fragment of 922bp is shown. M: DNA 1kb ladder marker.

The JAM-A sequence was released from the #8 JAM-A-pCR® II clone using a combination of restriction enzyme digestion, *Bam* HI and *Xho* I, while the pLNT-sffv MSC lentiviral expressing vector was digested under the same conditions to limearise it and this was followed by DNA dephosphorylation (Materials and Methods, section 2.6.5). The result of JAM-A DNA sequencing (Figure 4.18) and the treated pLNT-sffv MSC lentiviral expressing vector were then isolated using DNA electrophoresis shown in Figure 4.19 for gel extraction (Materials and Methods, section 2.6.4, respectively).

The #8 JAM-A-pCR® II clone and the pLNT-sffv MSC lentiviral vector were digested using the restriction enzymes, *Bam* HI and *Xho* I (Materials and Methods, section 2.5.5). The JAM-A DNA sequence and the treated pLNT-sffv MSC lentiviral expressing vector were then isolated using DNA electrophoresis as shown in Figure 4.19 and the DNA extracted (Materials and Methods, section 2.5.4). The purified pLNT-sffv MSC lentiviral vector was dephosphorylated before ligating with the isolated JAM-A sequence at different ratios of vector to insert and the ligation products were transformed into TOP10 competent cells and selected for ampicillin resistance as described in Chapter 2 section 2.5.

A

```
Query 85   AGCTACACCAGGAATGACGAGGTCTGTTTGAATTCTCCTTCACTTCGGGCACTAGGCTGG 144
           ||||  ||||||||||||||||||||||||||||||||||||||||||||||||||||||
Sbjct 924  AGCTTCACCAGGAATGACGAGGTCTGTTTGAATTCTCCTTCACTTCGGGCACTAGGCTGG 865

Query 145  CTGTAAATCACCTTCTTACTCGAAGTCCCTTTCTTTGTTCTGTCAAAGTGGCCTCGGCTA 204
           ||||||||||||||||||||||||||||||||||||||||||||||||||||||||||||
Sbjct 864  CTGTAAATCACCTTCTTACTCGAAGTCCCTTTCTTTGTTCTGTCAAAGTGGCCTCGGCTA 805

Query 205  TAGGCAAACCAGATGCCAAAAACCAAGATTCCCAGGAGAATCAGGGTTACAAGGACGGCT 264
           ||||||||||||||||||||||||||||||||||||||||||||||||||||||||||||
Sbjct 804  TAGGCAAACCAGATGCCAAAAACCAAGATTCCCAGGAGAATCAGGGTTACAAGGACGGCT 745

Query 265  GCCACGATGACCCCCACACTCCGCTCCACAGCTTCCATGCGCACAGCATTTGAAGTCATG 324
           ||||||||||||||||||||||||||||||||||||||||||||||||||||||||||||
Sbjct 744  GCCACGATGACCCCCACACTCCGCTCCACAGCTTCCATGCGCACAGCATTTGAAGTCATG 685

Query 325  GGTGTCCCATACCCATTCCGTGCCTCACAGCTGTATTCTCCAGTATCAGAGGCTGACAGG 384
           ||||||||||||||||||||||||||||||||||||||||||||||||||||||||||||
Sbjct 684  GGTGTCCCATACCCATTCCGTGCCTCACAGCTGTATTCTCCAGTATCAGAGGCTGACAGG 625

Query 385  GGATCAAAGACCAGCTCTCCTGTTGTGGGATTCAGGACATAGGAAGAGTTGCTGAAGGCA 444
           ||||||||||||||||||||||||||||||||||||||||||||||||||||||||||||
Sbjct 624  GGATCAAAGACCAGCTCTCCTGTTGTGGGATTCAGGACATAGGAAGAGTTGCTGAAGGCA 565

Query 445  CGGGTGCTTTTGGGATTCGTAGGCATCACTATCCCATCTTTGAACCAGGTGTATTCAGAA 504
           ||||||||||||||||||||||||||||||||||||||||||||||||||||||||||||
Sbjct 564  CGGGTGCTTTTGGGATTCGTAGGCATCACTATCCCATCTTTGAACCAGGTGTATTCAGAA 505

Query 505  GGTGGGGAACCATCTTGTTCTGAGCATGTCAGCACTGCCCGGTTCCCAATGGTGGCAGAG 564
           ||||||||||||||||||||||||||||||||||||||||||||||||||||||||||||
Sbjct 504  GGTGGGGAACCATCTTGTTCTGAGCATGTCAGCACTGCCCGGTTCCCAATGGTGGCAGAG 445

Query 565  GAGGGGATGTTAACTGTAGGCTTGGATGGAGGCACAAGCACGATGAGCTTGACCTTGACC 624
           ||||||||||||||||||||||||||||||||||||||||||||||||||||||||||||
Sbjct 444  GAGGGGATGTTAACTGTAGGCTTGGATGGAGGCACAAGCACGATGAGCTTGACCTTGACC 385

Query 625  TCCCCATAGCTGTTGCCGCCTTCCTCAGAGACCATACAAGTGTATGTCCCAGTGTCTTCC 684
           ||||||||||||||||||||||||||||||||||||||||||||||||||||||||||||
Sbjct 384  TCCCCATAGCTGTTGCCGCCTTCCTCAGAGACCATACAAGTGTATGTCCCAGTGTCTTCC 325

Query 685  CGTGTCACGGACTTGAAGGTGATACCAGTTGGCAAGAAGGTCACCCGGTCCTCATAGGAA 744
           ||||||||||||||||||||||||||||||||||||||||||||||||||||||||||||
Sbjct 324  CGTGTCACGGACTTGAAGGTGATACCAGTTGGCAAGAAGGTCACCCGGTCCTCATAGGAA 265

Query 745  GCTGTGATCTTGTTATTATAGCAAACGAGTCTGGTGGTGTCTCCTTGGTCAAACTTCCAC 804
           ||||||||||||||||||||||||||||||||||||||||||||||||||||||||||||
Sbjct 264  GCTGTGATCTTGTTATTATAGCAAACGAGTCTGGTGGTGTCTCCTTGGTCAAACTTCCAC 205

Query 805  TCCACACGGGGAGAAGAAAAGCCCGAGTAGGCACAGGACAACTTCACAGGATTATTCTCA 864
           ||||||||||||||||||||||||||||||||||||||||||||||||||||||||||||
Sbjct 204  TCCACACGGGGAGAAGAAAAGCCCGAGTAGGCACAGGACAACTTCACAGGATTATTCTCA 145

Query 865  GGAATTCTGACTTCAGGTTCANAAGAGTGCACTGTAACACTGCCCAATGCCAGGGAGCAC 924
           |||||||||||||||||||| ||||||||||||||||||||||||||||||||||||||
Sbjct 144  GGAATTCTGACTTCAGGTTCAGAAGAGTGCACTGTAACACTGCCCAATGCCAGGGAGCAC 85

Query 925  AACAGGATCGCCAATATGAAGANGCACAACAGTTTNCNTCTCGACTTGCGCCTTTGTCCC 984
           |||||||||||||||||||| |||||||||||| | ||||||||||||||||||||||||
Sbjct 84   AACAGGATCGCCAATATGAAGAGGCACAACAGTTTCC-TCTCGACTTGCGCCTTTGTCCC 26

Query 985  CATGGTGG 992
           ||||||||
Sbjct 25   CATGGTGG 18
```

Figure 4.18. The sequence of JAM-A - pCR® II (8) cDNA. (Continued on next page)

B

```
Query 65   CCACCATGGGGACAAAGGCGCAAGTCGAGAGGAAACTGTTGTGCCTCTTCATATTGGCGA 124
           ||||||||||||||||||||||||||||||||||||||||||||||||||||||||||||
Sbjct 18   CCACCATGGGGACAAAGGCGCAAGTCGAGAGGAAACTGTTGTGCCTCTTCATATTGGCGA 77

Query 125  TCCTGTTGTGCTCCCTGGCATTGGGCAGTGTTACAGTGCACTCTTCTGAACCTGAAGTCA 184
           ||||||||||||||||||||||||||||||||||||||||||||||||||||||||||||
Sbjct 78   TCCTGTTGTGCTCCCTGGCATTGGGCAGTGTTACAGTGCACTCTTCTGAACCTGAAGTCA 137

Query 185  GAATTCCTGAGAATAATCCTGTGAAGTTGTCCTGTGCCTACTCGGGCTTTTCTTCTCCCC 244
           ||||||||||||||||||||||||||||||||||||||||||||||||||||||||||||
Sbjct 138  GAATTCCTGAGAATAATCCTGTGAAGTTGTCCTGTGCCTACTCGGGCTTTTCTTCTCCCC 197

Query 245  GTGTGGAGTGGAAGTTTGACCAAGGAGACACCACCAGACTCGTTTGCTATAATAACAAGA 304
           ||||||||||||||||||||||||||||||||||||||||||||||||||||||||||||
Sbjct 198  GTGTGGAGTGGAAGTTTGACCAAGGAGACACCACCAGACTCGTTTGCTATAATAACAAGA 257

Query 305  TCACAGCTTCCTATGAGGACCGGGTGACCTTCTTGCCAACTGGTATCACCTTCAAGTCCG 364
           ||||||||||||||||||||||||||||||||||||||||||||||||||||||||||||
Sbjct 258  TCACAGCTTCCTATGAGGACCGGGTGACCTTCTTGCCAACTGGTATCACCTTCAAGTCCG 317

Query 365  TGACACGGGAAGACACTGGGACATACACTTGTATGGTCTCTGAGGAAGGCGGCAACAGCT 424
           ||||||||||||||||||||||||||||||||||||||||||||||||||||||||||||
Sbjct 318  TGACACGGGAAGACACTGGGACATACACTTGTATGGTCTCTGAGGAAGGCGGCAACAGCT 377

Query 425  ATGGGGAGGTCAAGGTCAAGCTCATCGTGCTTGTGCCTCCATCCAAGCCTACAGTTAACA 484
           ||||||||||||||||||||||||||||||||||||||||||||||||||||||||||||
Sbjct 378  ATGGGGAGGTCAAGGTCAAGCTCATCGTGCTTGTGCCTCCATCCAAGCCTACAGTTAACA 437

Query 485  TCCCCTCCTCTGCCACCATTGGGAACCGGGCAGTGCTGACATGCTCAGAACAAGATGGTT 544
           ||||||||||||||||||||||||||||||||||||||||||||||||||||||||||||
Sbjct 438  TCCCCTCCTCTGCCACCATTGGGAACCGGGCAGTGCTGACATGCTCAGAACAAGATGGTT 497

Query 545  CCCCACCTTCTGAATACACCTGGTTCAAAGATGGGATAGTGATGCCTACGAATCCCAAAA 604
           ||||||||||||||||||||||||||||||||||||||||||||||||||||||||||||
Sbjct 498  CCCCACCTTCTGAATACACCTGGTTCAAAGATGGGATAGTGATGCCTACGAATCCCAAAA 557

Query 605  GCACCCGTGCCTTCAGCAACTCTTCCTATGTCCTGAATCCCACAACAGGAGAGCTGGTCT 664
           ||||||||||||||||||||||||||||||||||||||||||||||||||||||||||||
Sbjct 558  GCACCCGTGCCTTCAGCAACTCTTCCTATGTCCTGAATCCCACAACAGGAGAGCTGGTCT 617

Query 665  TTGATCCCCTGTCAGCCTCTGATACTGGAGAATACAGCTGTGAGGCACGGAATGGGTATG 724
           ||||||||||||||||||||||||||||||||||||||||||||||||||||||||||||
Sbjct 618  TTGATCCCCTGTCAGCCTCTGATACTGGAGAATACAGCTGTGAGGCACGGAATGGGTATG 677

Query 725  GGACACCCATGACTTCAAATGCTGTGCGCATGGAAGCTGTGGAGCGGAGTGTGGGGGTCA 784
           ||||||||||||||||||||||||||||||||||||||||||||||||||||||||||||
Sbjct 678  GGACACCCATGACTTCAAATGCTGTGCGCATGGAAGCTGTGGAGCGGAGTGTGGGGGTCA 737

Query 785  TCGTGNCAGCCGTCCTTGTAACCCTGATTCTCCTGNGAATCTTGNTTTTTGGCATCTGGT 844
           |||||  |||||||||||||||||||||||||||||  ||||||||  ||||||||||||||
Sbjct 738  TCGTGGCAGCCGTCCTTGTAACCCTGATTCTCCTGGGAATCTTGGTTTTTGGCATCTGGT 797

Query 845  TTGCCTATAGCCGAGGCCACTTTGACAGAACAAAGAAAGGGACTTCNAGTAAGANNNTGA 904
           |||||||||||||||||||||||||||||||||||||||||||||||  |||||||  |||
Sbjct 798  TTGCCTATAGCCGAGGCCACTTTGACAGAACAAAGAAAGGGACTTCGAGTAAGAAGGTGA 857

Query 905  NTTACAGCCAGCCTANTGCCCGAANTGAANGAGAATTCAAACAGACCTCGTCATTCCTG 963
           ||||||||||||||  ||||||||  ||||  ||||||||||||||||||||||||||||
Sbjct 858  TTTACAGCCAGCCTAGTGCCCGAAGTGAAGGAGAATTCAAACAGACCTCGTCATTCCTG 916
```

Figure 4.18. The sequence of JAM-A - pCR® II (8) cDNA. (Continued from previous page)
The JAM-A-pCR II (8) DNA was sequenced using (A) M13 forward and (B) reverse primers. The sequence *algorithms* were done using NBCI Standard Nucleotide BLAST® online software (http://blast.ncbi.nlm.nih.gov/Blast.cgi). Query: Sequencing results; Sbjct: Reference sequence (EU831732).

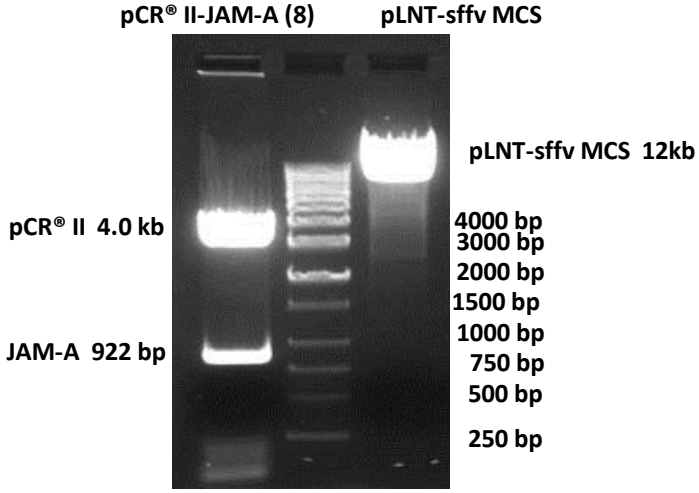

Figure 4.19. The restriction enzyme digestion of JAM-A - pCR® II (8) and the pLNT-sffv MCS vector using *Bam* HI and *Xho* I.
The JAM-A-pCR II (8) cDNA clone and the pLNT-sffv MCS vector were double digested with *Bam* HI and *Xho* I restriction enzymes to release the JAM-A sequence (922 bp) and to generate a linear form of the pLNT-sffv MCS vector (12 kb). The two DNA fragments were electrophoresed and isolated from the gel before being purified using gel extraction kit. The DNA ladder is in the centre lane of the gel.

Table 4.3 shows the numbers of colonies generated after ligation with different ratios of vector to insert. The DNA from ten colonies from the ratio 1:0.5 was subjected to *Bam* HI and *Xho* I restriction enzyme digestion. Figure 4.20 shows that clones #2, #3, #5, #6, #8, #9 and #10 contained both pLNT-sffv MSC lentiviral vector with JAM-A cDNA with bands of approximately 12 kilobase pairs (kb) and 922 basepairs (bp) respectively.

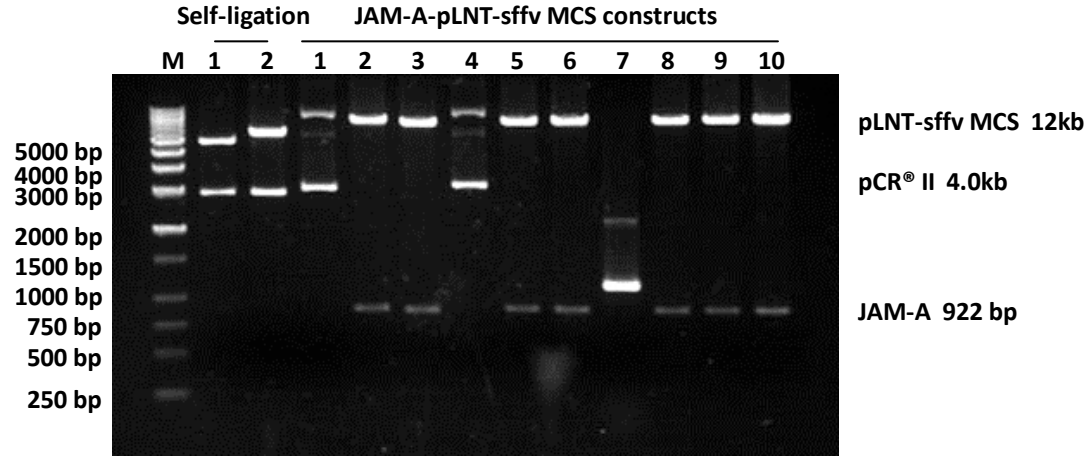

Figure 4.20. The results of JAM-A cloning into the pLNT-sffv MCS lentiviral vector.
Ten colonies, generated after vector to insert ligation ratios of 1:1 were used, were selected and the DNA isolated and digested with the *Eco* RI restriction enzyme prior to gel electrophoresis. M is the DNA ladder.

Table 4.3. The numbers of colonies formed using different ligation ratios for pLNT-sffv MCS vector and JAM-A PCR cDNA.

Conditions (Vector: Insert)	Colonies per plate
Vector self-ligation (1:0)	49
1:0.5	166
1:1	151
1:2	99

Variable numbers of colonies were generated with after ligation of different ratios of vector and JAM-A cDNA.

In order to confirm that the seven constructs could be expressed in mammalian cells, the plasmids were transfected into HEK 293T cells and the proteins in the lysate analysed by Western Blotting 24 hour post-transfection (Materials and Methods, section 2.10). Five of these were further analysed by flow cytometry for JAM-A cell suface expression (Materials and Methods, section 2.9). The results show that JAM-A was expressed in HEK 293T cells at low amounts (original, eGFP and vector only lanes in Figure 4.20.A) prior to introducing the JAM-A construct (Figure 4.21) and highly expressed after the lentiviral construct containing JAM-A was introduced. A ~30 kD band was observed among overexpressing clones and this was consistent with a previous finding related to the digestion of JAM-A by disintegrin metalloproteinases (ADAM10 and 17) in HEK293T cells (353). As clone #3 (JAM-A-pLNT-sffv MCS) showed a higher M.F.I. (Figure 4.21.B), it was then selected for the production of JAM-A lentiviral vector particles in packaging cell lines (Materials and Methods, section 2.6).

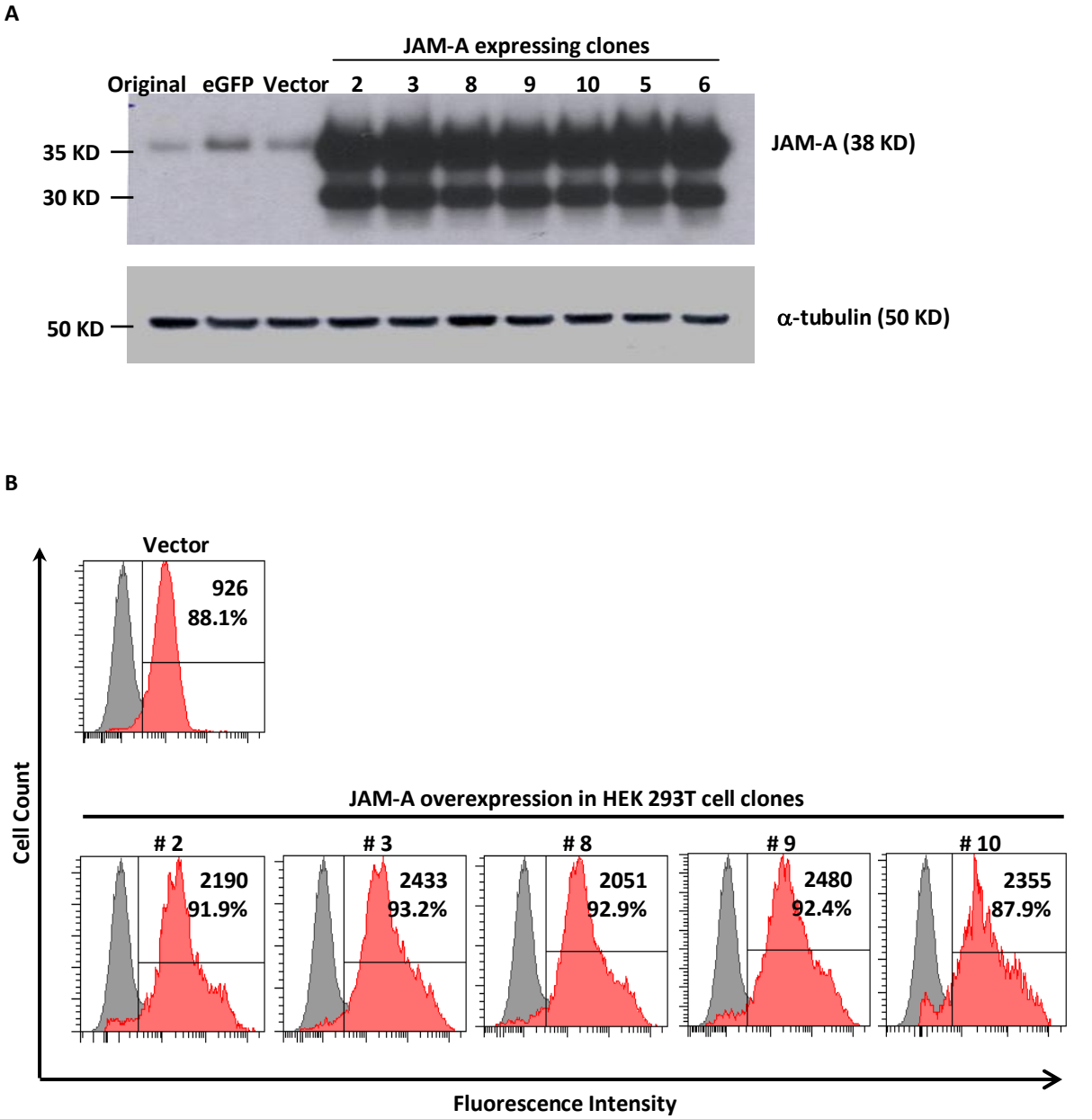

Figure 4.21. Transient expression of JAM-A in HEK 293T cells.
HEK293T cells were mock transfected or transfected with eGFP, lentiviral vector alone or lentiviral constructs containing JAM-A using Lipofectamine™ 2000. (A) The total JAM-A protein expression in HEK 293T cells in the original mock transfected, or in cells transduced with eGFP, empty lentiviral vector (Vector) or JAM-A containing lentiviral vector (#2, #3, #5, #6, and #8-#10) constructs was analysed by Western blotting of whole lysates using the JAM-A antibody (M.Ab.F11 clone). α-tubulin detection was used as the loading control. (B) Representative histograms showing cell surface JAM-A expression in HEK 293T cells transfected with an empty vector (Vector) or after transfection with JAM-A containing lentiviral constructs (#2, #3, and #8-#10). The cells were stained with an isotype control (gray) or the JAM-A antibody (clone M.Ab.F11; red) followed by goat anti-mouse IgG-APC antibody. M.F.I. and the % positive are shown in the top right corners of each plot (n=1).

For the lentiviral transduction of JAM-A negative Jurkat cells, a similar eGFP lentivial construct was first compared with the JAM-A lentiviral construct. Figure 4.22 shows the titration first of LV-eGFP viral particles into the Jurkat cell line (see Materials and Methods section 2.6.11) using M.O.I.s ranging from 1 to 40 and determining the efficiency of transduction under a fluorescence microscope and by flow cytometric analysis. As shown in Figure 4.22, approximately 75% of Jurkat cells expressed eGFP protein at an M.O.I. of 1, and this increased to over 97% with M.O.I.s of 10 to 40.

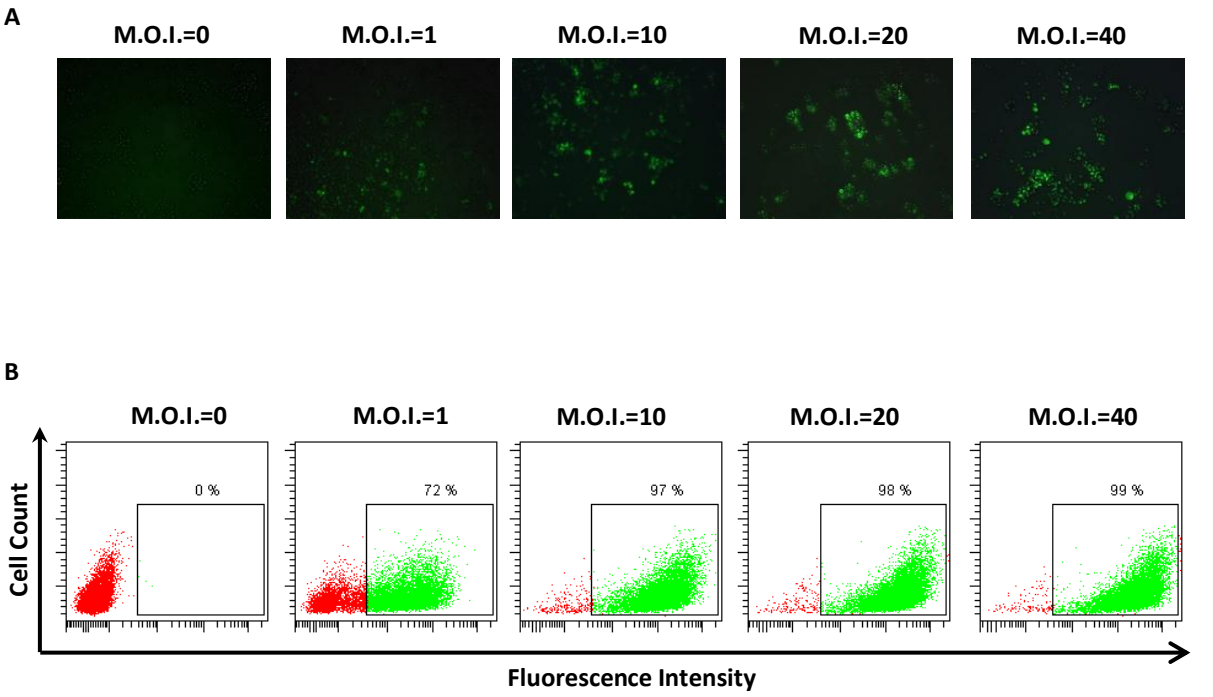

Figure 4.22. Jurkat cells were transduced with LV-eGFP viral particles at different multiplicities of infection (M.O.I.s).
LV-eGFP lentiviral particles were transduced into Jurkat cells using different M.O.I.s ranging from 1 to 40 (n=1). (A) The cells were observed under a fluorescence microscope 48 hours post transduction. (B) The percentage of eGFP positive cells (shown in green) was assessed by flow cytometry (n=1). Negative staining is shown in red.

Jurkat cells were next transduced with JAM-A containing lentiviral particles at M.O.I.s of 10 or 20 and the expression of cell surface JAM-A analysed by flow cytometry 48 hours after

transduction. Figure 4.23 shows that 53.4±3.5% and 70.6±3.6% of Jurkat cells expressed cell surface JAM-A at 48 hours after they were transduced with the JAM-A containing lentiviral particles at M.O.I. of 10 or 20 respectively.

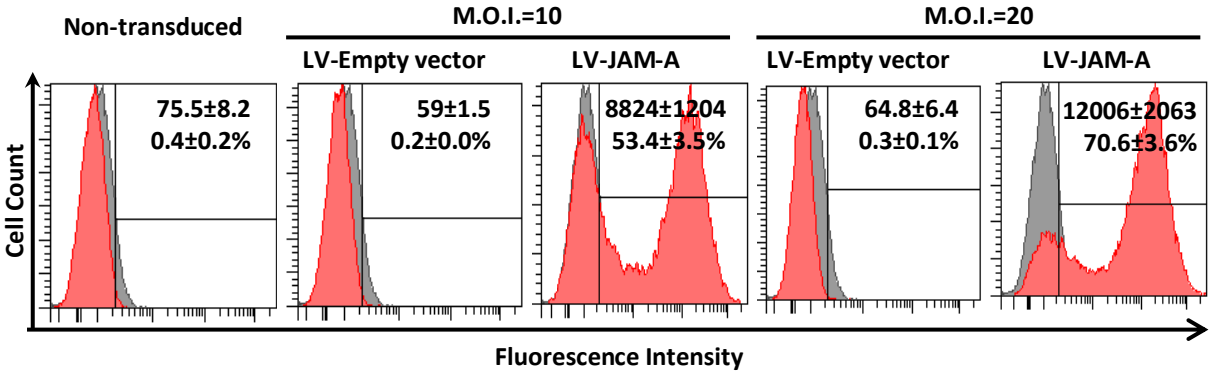

Figure 4.23. JAM-A expression on Jurkat cells after lentiviral transduction.
Non-transduced Jurkat cells and Jurkat cells transduced with LV-empty vector and LV-JAM-A vector were analysed for their surface expression of JAM-A (red) by flow cytometry at 48 hour after transduction. The isotype control is shown in gray. The values of M.F.I. ± S.E.M. and % positive ± S.E.M. of n=4 independent experiments are shown for each group in the top right corner of the plot.

The adhesion of these JAM-A expressing or non-expressing Jurkat cells 48 hours after lentiviral transduction was next examined. Figure 4.24.A demonstrates that 25.4±3.5% of non-transduced Jurkat cells adhered to fibronectin and 42.2±3.0% adhered to IL-1β-pre-treated BMEC-60 cells, in comparison to the BSA control (4.8±1.0%, both with $p<0.01$). However, their adhesion to collagen I (6.0±2.0%) was similar to that of the BSA protein control. For the transduced cells, JAM-A expression resulted in an increase of cell adhesion to both IL-1β pre-treated BMEC-60 cells and fibronectin. Figure 4.24.B shows that 48.2±6.2% of LV-JAM-A transduced cells and 35.3±3.2% of LV-empty vector transduced cells at an M.O.I. of 10 adhered to IL-1β stimulated BMEC-60 cells, while 40.1±4.6% of LV-JAM-A transduced

cells and 27.3±3.5% % of LV-empty vector transduced cells at an M.O.I. of 20 adhered to IL-1β stimulated BMEC-60 cells (p<0.05 for all JAM-A expressing vs. non-expressing cells).

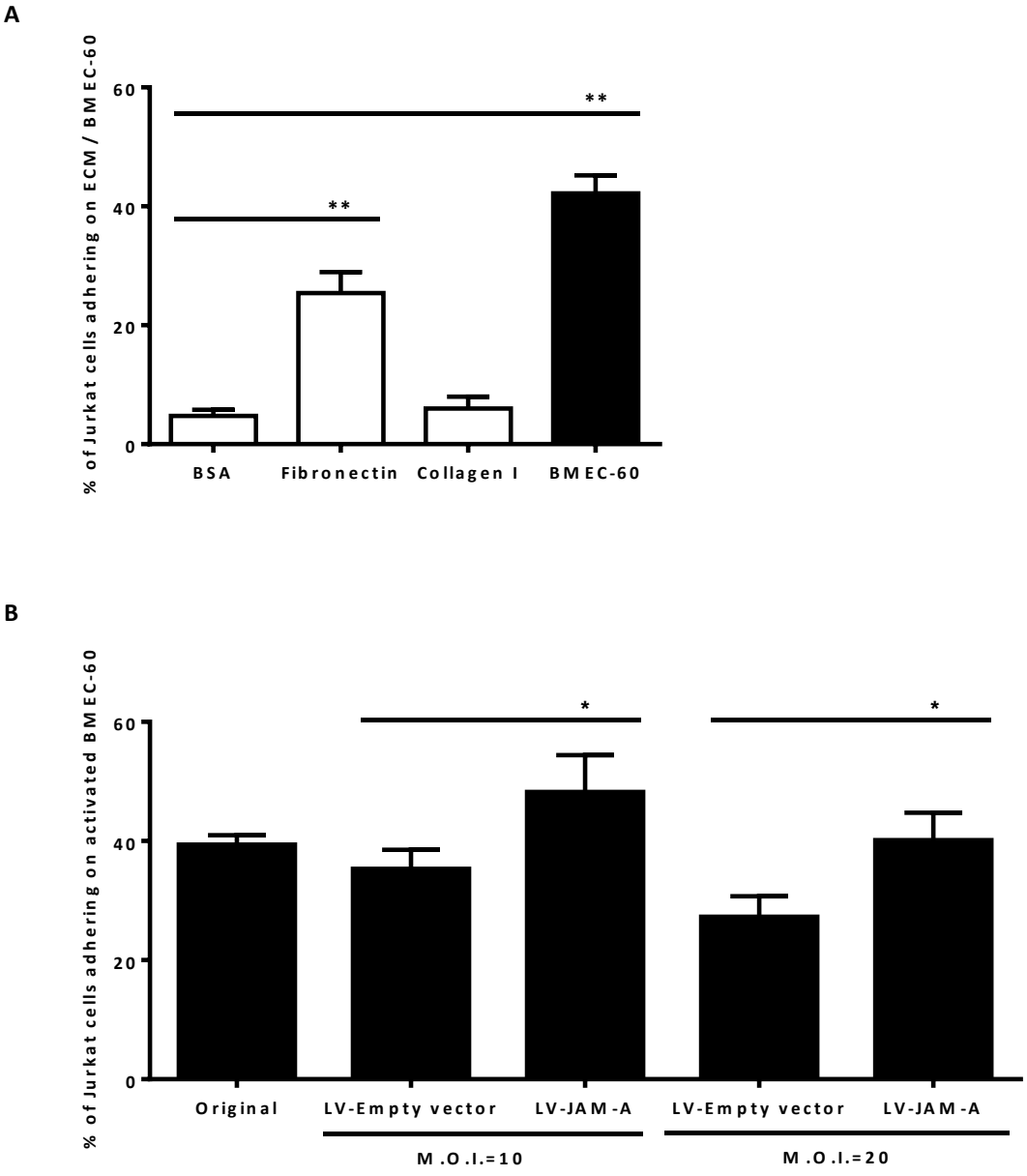

Figure 4.24. Expression of JAM-A in Jurkat cells enhanced cell adhesion on BMEC-60 cells.
(A) The non-transduced Jurkat cells were analysed for their adhesion to extracellular matrix (ECM) and IL-1β pretreated BMEC-60 cells (BMEC-60) at 37°C for 1 hour. (B) The Jurkat cells that were transduced with the JAM-A expressing vector (LV-JAM-A) or the control vector (LV-Empty vector) (48 hours after transduction) and the non-transduced Jurkat cells (Original) were allowed to adhere onto IL-1β activated BMEC-60 at 37°C for 1 hour. Values are means ± S.E.M. for n=5 independent experiments. The statistical analysis was done using Student's *t*-test and values < 0.05 (*) or < 0.01 (**) are considered significant or very significant respectively.

Jurkat cell adhesion onto fibronectin was also examined. Figure 4.24 shows a significant increase in the adhesion of JAM-A expressing Jurkat cells when transduced at the M.O.I. of 10, from 17.6±0.6% for the LV-Empty vector to 25.7±2.3% for the LV-JAM-A vector (p<0.05; Figure 4.25). A similar but not statistically significant trend was observed at an M.O.I. of 20, with a average increase from 23.1±5.8% to 29.5±5.8% (p=0.47; Figure 4.25).

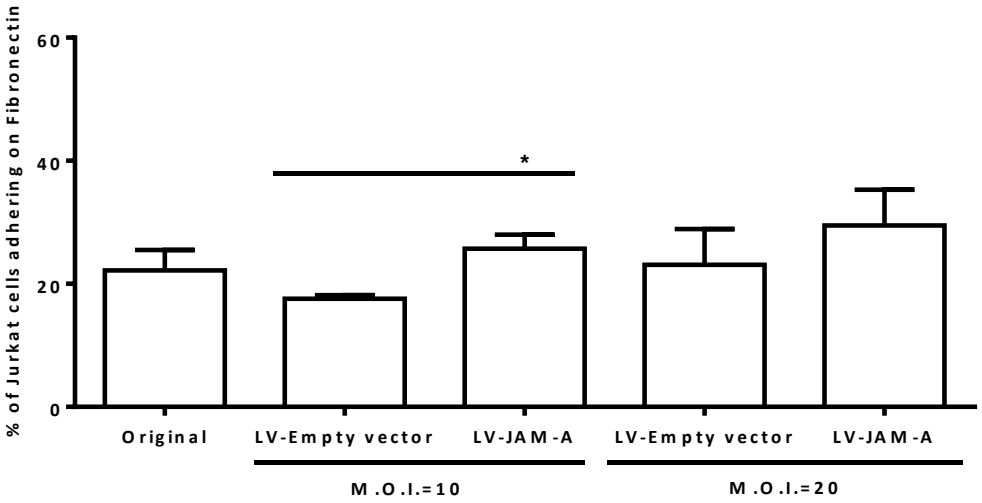

Figure 4.25. Expression of JAM-A in Jurkat cells enhanced cell adhesion onto fibronectin.
The non-transduced Jurkat cells (Original) and cells that were transduced with the JAM-A expressing vector (LV-JAM-A) or the control vector (LV-Empty vector) (48 hours after transduction) were analysed for their adhesion onto fibronectin at 37°C for 1 hour. Values are means ± S.E.M. for n=4 independent experiments. The statistical analysis was done using Student's *t*-test and values < 0.05 (*) or < 0.01 are considered significant or very significant respectively.

In summary, these studies show that

i) Jurkat cells which do not express JAM-A adhered to IL-1β stimulated BMEC-60 cells, and to fibronectin, and to a lesser extent to collagen I.

ii) Jurkat cells can be transduced with lentiviral JAM-A constructs and express JAM-A on their cell surface.

iii) Significantly more JAM-A expressing Jurkat cells adhered to IL-1β stimulated BMEC-60 cells than did JAM-A negative cells.

iv) JAM-A expression in Jurkat cells increased cell adhesion to fibronectin.

4.3.2. Does JAM-A regulate cell migration to CXCL12?

Since the CXCR4/CXCL12 axis plays a crucial role in both normal and malignant haematopoietic stem/progenitor cell homing to bone marrow, the ability of JAM-A to modulate this homing was examined *in vitro.*

To begin with, the expression of CXCR4, a receptor of CXCL12, and its co-receptor, CD164, was examined on a panel of myeloid and lymphoid leukaemic cell lines. Figure 4.26 shows that CXCR4 as assessed with the 12G5 clone antibody was present on the surface of all the tested cell lines, except for KG-1 and TF-1 cells, while CD164 when measured with the N6B6 antibody was present on the surface of all the cell lines tested except for NALM-1 and Reh cells.

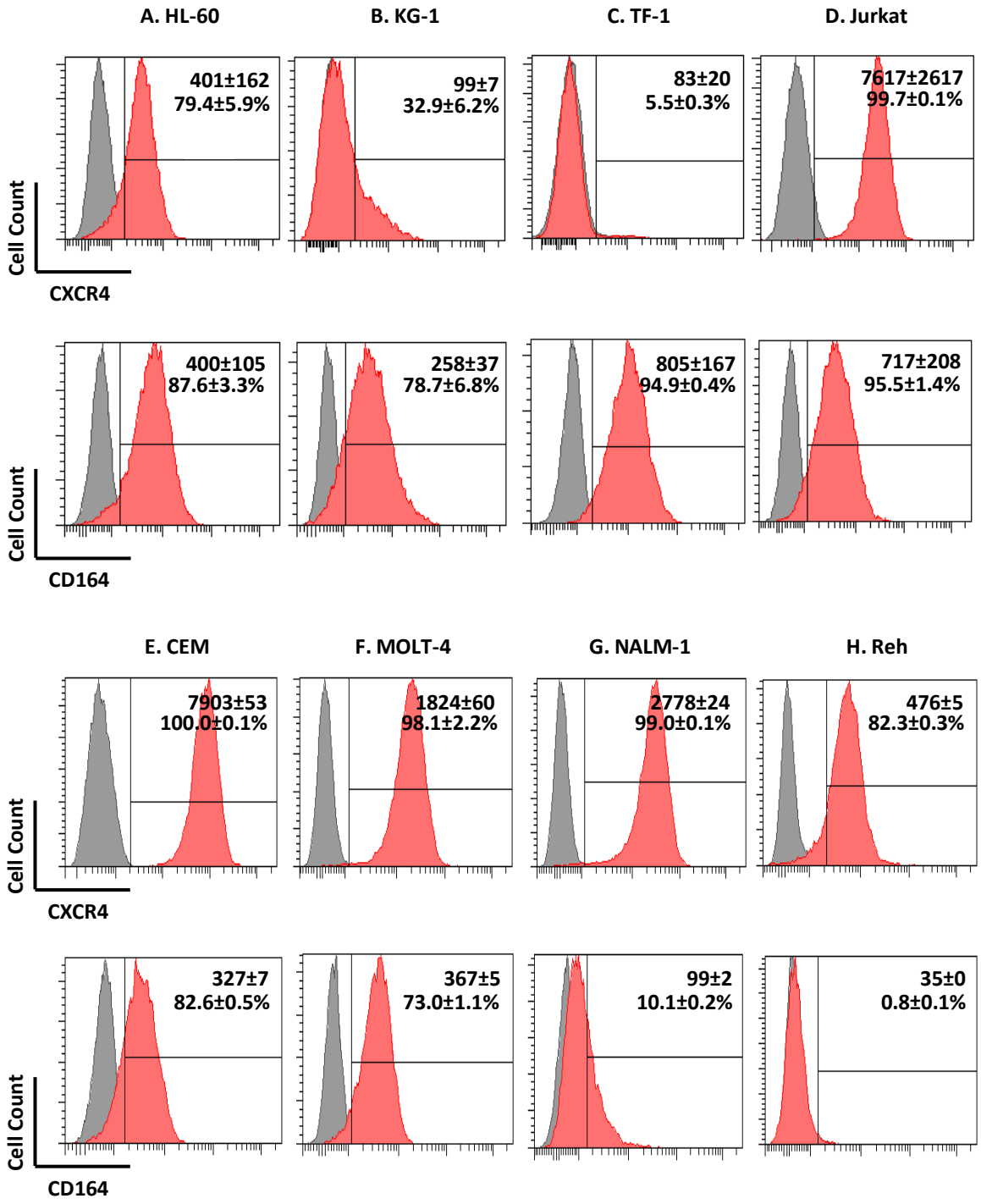

Figure 4.26. Expression of CXCR4 and CD164 on leukaemic cell lines.
Representative FACS histograms of acute leukaemic cell lines, including acute myeloid leukaemia cell lines: (A) HL-60, (B) KG-1 and (C) TF-1 cells, and T lymphoid leukaemia cell lines (D) Jurkat cells, and (E) CEM and (F) MOLT-4 cells, andB-lymphoid leukaemia cell lines (G) NALM-1 and (H) Reh cells ,stained with CXCR4-APC (12G5 clone, red, top plots) and CD164-PE antibodies (N6B6 clone, red, for A-D bottom plots) or CD164-FITC antibodies (N6B6 clone, red, for E-H bottom plots) and their isotype controls (gray). M.F.I.± S.E.M. and the % positive± S.E.M for n=3 independent experiments.

4.3.2.1. JAM-A and HL-60 cell migration

HL-60 cells were first allowed to migrate across transwells coated with 10 μg/ml fibronectin or $5x10^4$ BMEC-60 cells pre-treated with 10ng/ml IL-1β for 4 hours towards different concentrations of CXCL12 so as to optimise the conditions for their cell migration (Materials and Methods section 2.12.2). Figure 4.27 shows that HL-60 cell chemotaxis was optimal at 100ng/ml across BMEC-60 cells, but was continuing to increase across fibronectin even with CXCL12 concentrations as high as 1600ng/ml. At all concentrations of CXCL12, the migration of HL-60 cells was statistically significant compared to no CXCL12 (p<0.05 or p<0.01 as indicated in Figure 4.27). At 100ng/ml CXCL12, 5.4±0.7 % of HL-60 cells migrated across fibronectin and 5.8±0.5 % of HL-60 cells migrated across BMEC-60 cells. This increased to 16.7±1.3% of HL-60 cells migrating across fibronectin towards 1600 ng/ml of CXCL12. Thus, in further experiments with HL-60 cells, 100ng/ml of CXCL12 was used with BMEC-60 cells as substrate, while 1600ng/ml of CXCL12 was used when cells were migrating across fibronectin.

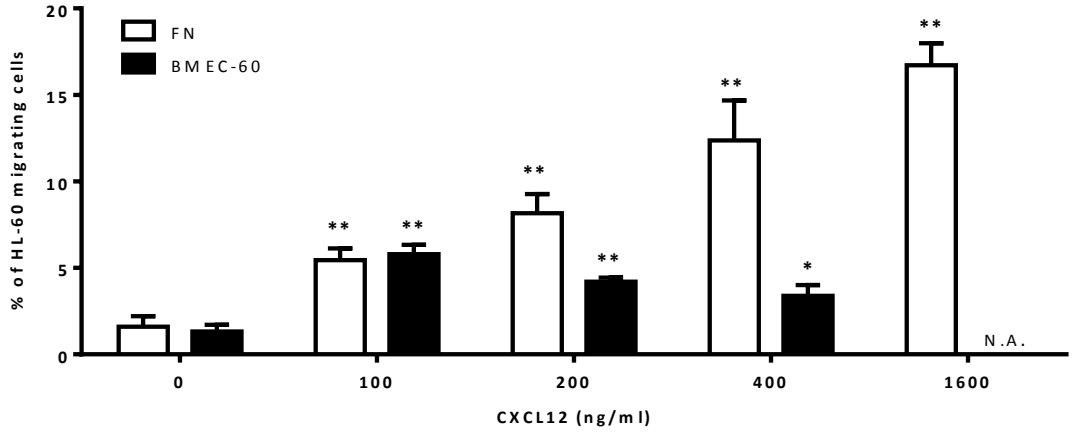

Figure 4.27. HL-60 cell migration across fibronectin and IL-1β activated BMEC-60 cells towards CXCL12.
HL-60 cells were added to the top of fibronectin (empty, n=4) or IL-1β stimulated BMEC-60 cell-coated transwells (black, n=3) with CXCL12 at varying concentrations ranging from 0 to 1600 ng/ml placed in the bottom chambers. The cells were allowed to migrate for 5 hours before being harvested from bottom chambers and counted by flow cytometry. Values are means ± S.E.M. for n=3-4 independent experiments and the statistical analysis was done using Student's *t*-test and all values were <0.05 (*) or < 0.01 (**) considered significant or very significant respectively. N.A.: not assayed.

Figure 4.28.A shows that JAM-A blockade reduced chemotactic migration towards CXCL12. On fibronectin, 18.8±2.8% of Fc-blocked HL-60 cells migrated towards CXCL12 and this decreased to 15.3±2.8% (p=0.39) with the JAM-A/Fc peptide pre-incubated HL-60 cells. A similar, and again non-significant, trend was observed with JAM-A antibody blockade (from 13.3±3.2% to 10.7±2.5%; p=0.53).

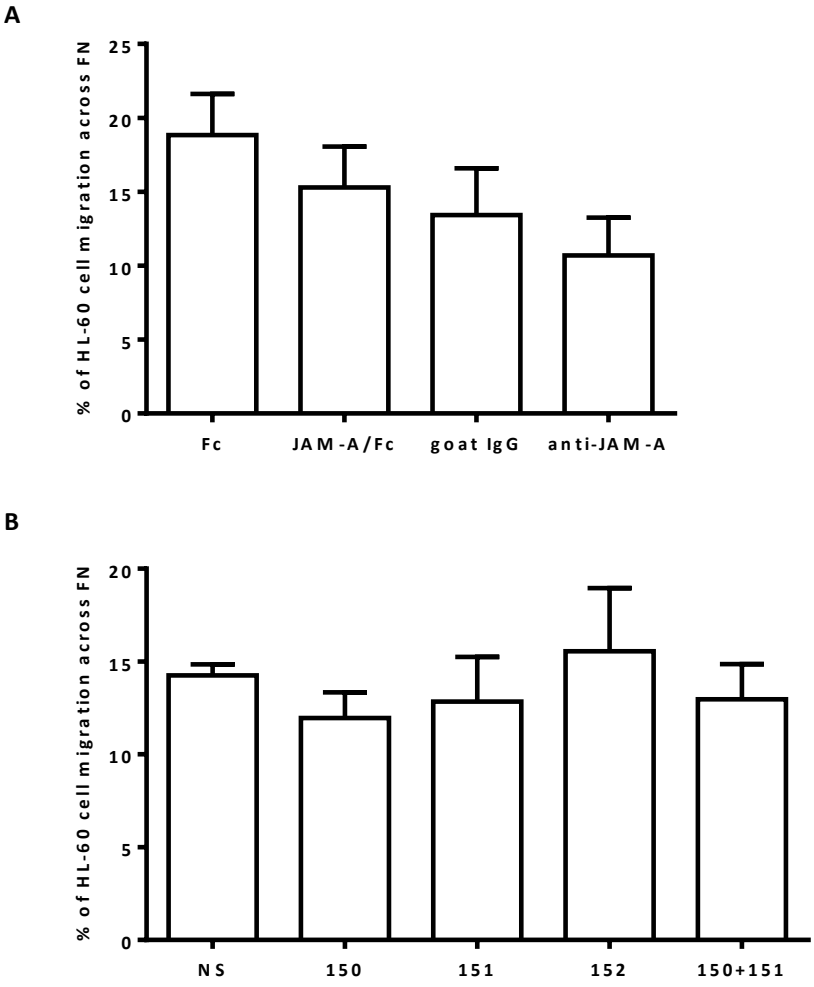

Figure 4.28. Blocking or knocking down JAM-A did not significantly reduce HL-60 cell migration across fibronectin towards CXCL12.
The figure shows the absolute cell number migrating across fibronectin (n=4-5 in A and 3-6 in B) towards CXCL12. (A) HL-60 cells were pre-incubated with JAM-A blocking peptide (JAM-A Fc) or JAM-A antibody (anti-JAM-A, 10 μg/ml, AF1103, R&D systems) in parallel to their controls, Fc and goat IgG for 30 minutes at 37°C, before performing the transwell assay. (B) HL-60 cells 24 hours post nucleofection with non-silencing (NS) or JAM-A siRNA (150, 151, 150+151) were analysed in the transwell migration assay. Values are means ± S.E.M. for n=3-6 independent experiments and the statistical analysis was done using Student's *t*-test and all values were <0.05 or < 0.01 considered significant or very significant respectively.

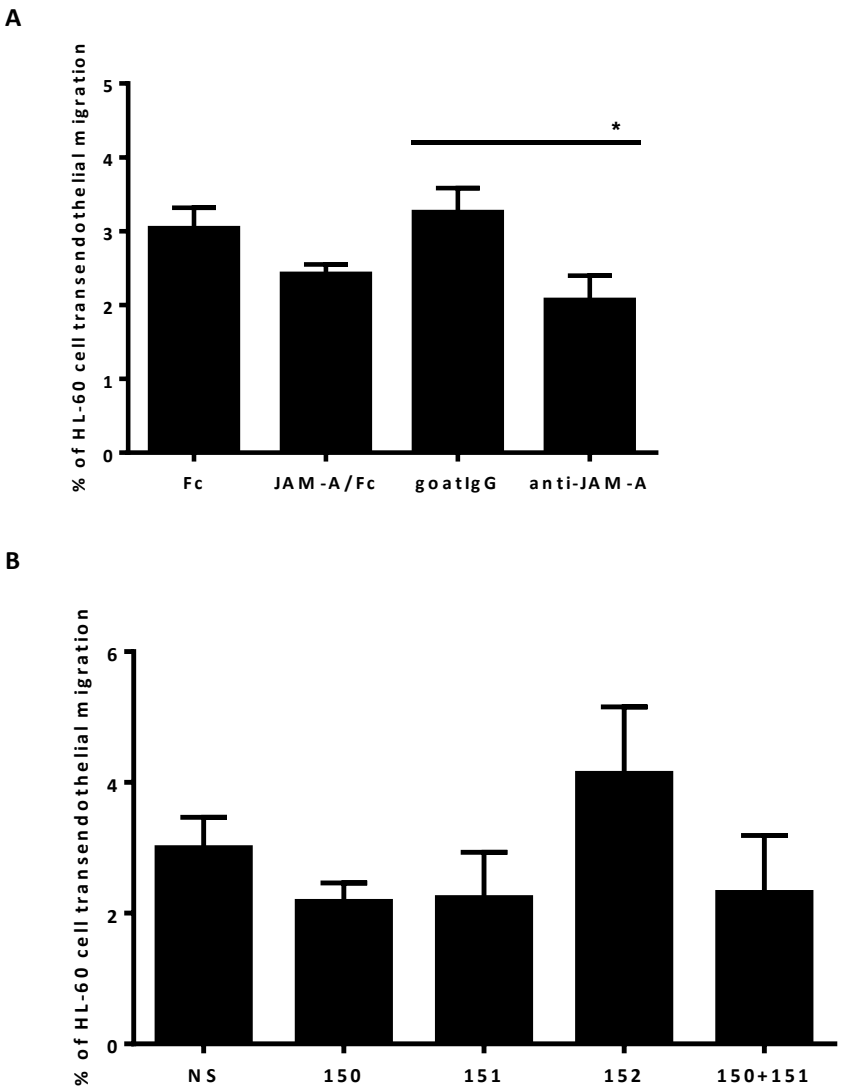

Figure 4.29. Effect of blocking or knocking down JAM-A on HL-60 cell migration across BMEC-60 cells towards CXCL12.

The figure shows the absolute cell number migrating across IL-1β stimulated BMEC-60 cells (n=3-4) towards CXCL12. (A) HL-60 cells were pre-incubated with JAM-A blocking peptide (JAM-A Fc) or JAM-A antibody (anti-JAM-A, 10 μg/ml, AF1103, R&D systems) in parallel to their controls, Fc and goat IgG for 30 minutes at 37°C before performing the transwell assay. (B) HL-60 cells 24 hours after nucleofection of non-silencing (NS) or JAM-A siRNAs (150, 151, 150+151) were analysed in the transwell assay (n=3-6). Values are means ± S.E.M. for n=3-6 independent experiments and the statistical analysis was done using Student's *t*-test and all values were <0.05 (*) or < 0.01 considered significant or very significant respectively.

JAM-A knocked down HL-60 cells were applied to the transwell assay to futher assess its role in cell migration (Figure 4.28.B). When JAM-A expression was reduced in HL-60 cells with JAM-A specific siRNAs, 150, 151 or the combination of both, HL-60 cell migration across fibronectin was slightly, but not significantly, reduced from 14.3±0.6% in the NS control cells

to 12.0±1.4%, 12.9±2.4% and 13.0±1.9% in the 150, 151 and 150+151 siRNA knocked down cells respectively. With BMEC-60 cells, only 3.0±0.3% of Fc-blocked HL-60 cells migrated across BMEC-60 cells towards CXCL12 and this was reduced to 2.4±0.1% (p=0.13) in the presence of JAM-A/Fc peptide (Figure 4.29.A). A similar trend was observed using JAM-A antibody (3.3±0.3% vs. 2.1±0.3%; p<0.05; Figure 4.29.A). JAM-A siRNA knocked down HL-60 cells were applied to the transwell assay (Figure 4.29.B). The average percentage of NS migrating cells was 3.0±0.5% on BMEC-60 cells. 150, 151 siRNAs or the combination of both siRNAs reduced HL-60 cell migration to 2.2±0.3%, 2.2±0.7% and 2.3±0.9% respectively (Figure 4.29.B).

In summary, these studies show that

i) A proportion of HL-60 cells can migrate towards CXCL12 across IL-1β stimulated BMEC-60 cells, and fibronectin.

ii) Less HL-60 cell migrated across BMEC-60 cells compared to fibronectin over the timeframe of these experiments and these represented only a minor fraction of HL-60 cells.

iii) Overall the experiments did not identify a significant role for JAM-A in modulating CXCL12 induced migration across fibronectin, while it seems likely from these and earlier experiments that HL-60 adhesion to BMEC-60 cells may have prevented their migration towards CXCL12 under the conditions used.

4.3.2.2.JAM-A and Jurkat cell migration

The JAM-A expressing Jurkat cells were also tested in these transwell assays. To begin with, non-transduced Jurkat cells were allowed to migrate across fibronectin or BMEC-60 cells towards a series of concentrations of CXCL12. Figure 4.30 demonstrates CXCL12 dose-dependent chemotactic migration across fibronectin, which was continuing to increase at 1600ng/ml of CXCL12 with 13.2±3.3% of Jurkat cells migrating. In contrast, the optimal Jurkat cell transendothelial migration occurred at 100ng/ml of CXCL12, where only 4.4±0.3% of cells migrated. Jurkat cell migration on fibronectin and BMEC-60 cells at 0 ng/ml of CXCL12 was 0.3±0.1% and 0.2±0.1%, respectively.

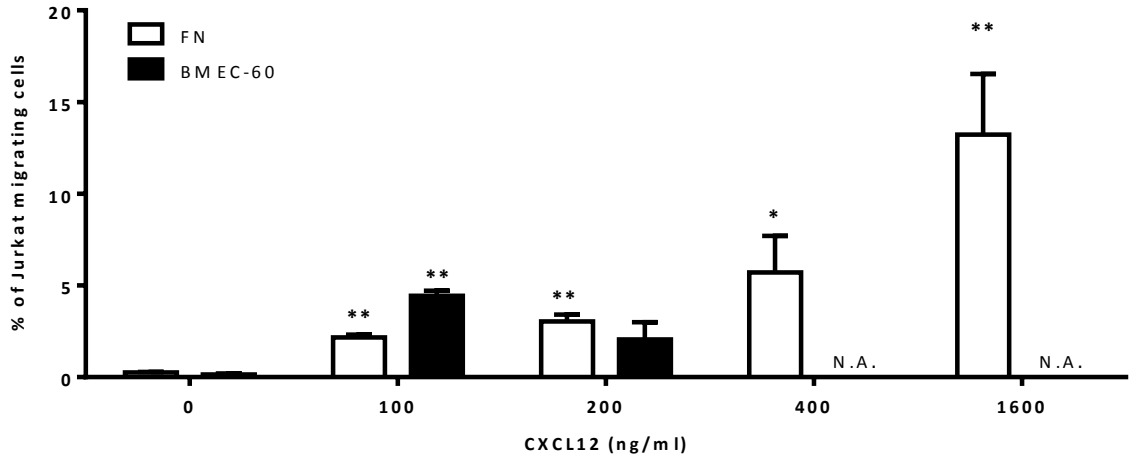

Figure 4.30. Jurkat cell migration across fibronectin and BMEC-60 cells towards CXCL12.
Jurkat cells were placed in the chamber with fibronectin (n=3-4) or IL-1β stimulated for 4 hours BMEC-60 cell-coated transwells (black, n=2) with CXCL12 concentrations varying from from 0 to 1600 ng/ml added in the bottom chambers. The cells were allowed to migrate for 5 hours before being harvested from bottom chambers and counted by flow cytometry. Values are means ± S.E.M. for n=2-4 independent experiments. The statistical analysis was done using Student's *t*-test. P values of < 0.05 (*) or < 0.01 (**) are considered significant or very significant respectively. N.A.: not assayed.

The expression of CXCR4, a receptor of CXCL12, and its co-receptor, CD164, was examined on the transduced Jurkat cell lines in comparison to the non-transduced cell line. The levels

of surface CXCR4 and CD164 expression were not significantly changed on JAM-A expressing in Jurkat cells in culture compared to their corresponding empty vector controls (p>0.05; Figure 4.31).

When the transduced Jurkat cells were tested in these migration assays, there was a slight, but non-significant increase in cell migration across on fibronectin from 18.8±3.9% to 22.2±4.0% at an M.O.I. of 10, and from 12.9±2.7% to 17.0±3.1% at an M.O.I. of 20 (p=0.55 and p=0.34, respectively; Figure 4.32.A). For BMEC-60 cells, JAM-A expression reduced Jurkat cell chemotaxis and transendothelial migration towards CXCL12 from 4.1±0.2% to 2.5±0.2% (M.O.I. of 10; p<0.05) and from 4.2±1.0% to 3.0±0.3% (M.O.I. of 20; p=0.29), respectively when compared to the non-silencing control (Figure 4.32.B).

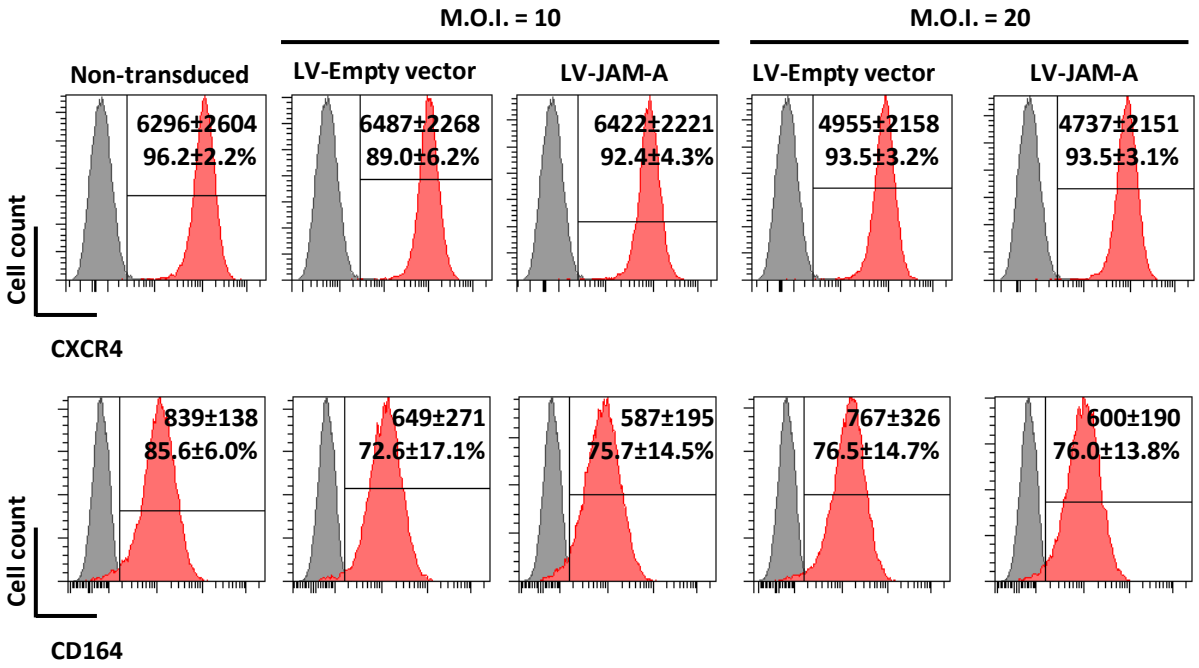

Figure 4.31. Expression of CXCR4 and CD164 on transduced Jurkat cell lines.
Representative FACS histograms of non-transduced and transduced Jurkat cell lines stained with CXCR4-APC (12G5 clone, red, top plots, n=3-4) and CD164-PE antibodies (N6B6 clone, red, bottom plots, n=3) and their isotype controls (gray). The gating was set up based on 1% of isotype controls. M.F.I.± S.E.M. and the % positive± S.E.M for n=3-4 independent experiments.

A

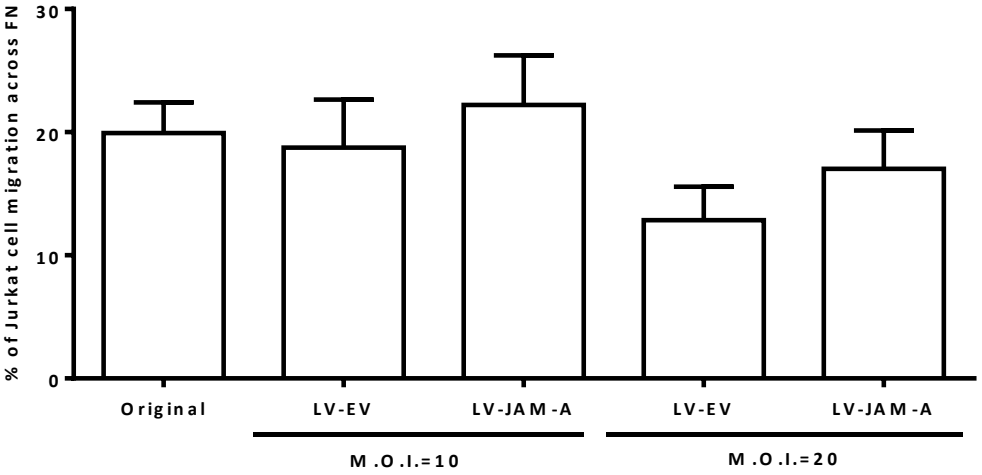

B

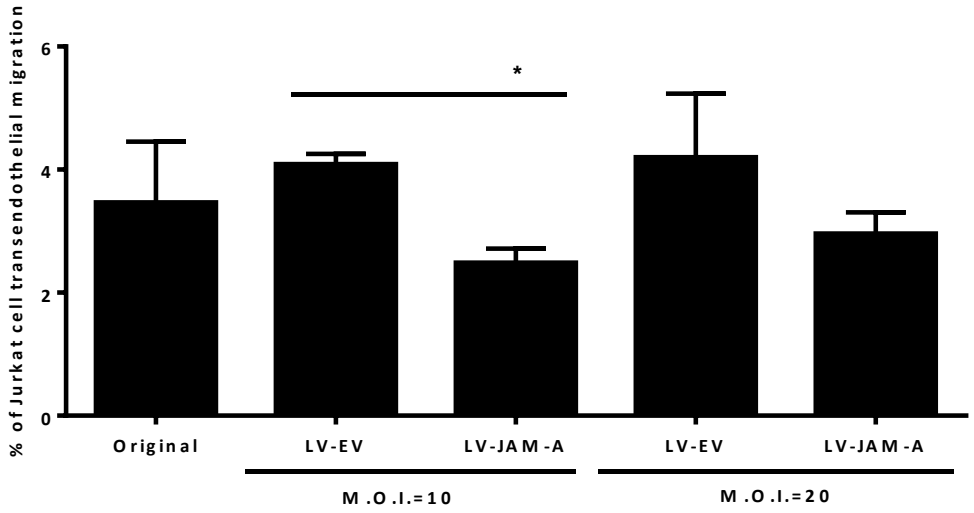

Figure 4.32. JAM-A expressing Jurkat cells and their chemotactic migration across fibronectin oor BMEC-60 cells towards CXCL12.
The non-transduced (Original) and the JAM-A transduced Jurkat cells were allowed to migrate acros (A)s fibronectin or (B) IL-1β stimulated BMEC-60 cells towards CXCL12. The figure shows the absolute Jurkat cell number migrating (A) on fibronectin (n=6) and (B) on activated BMEC-60 cells (n=3) towards CXCL12. Values are means ± S.E.M. for n=3-6 independent experiments and the statistical analysis was done using Student's *t*-test and the values < 0.05 (*) or < 0.01 are considered significant or very significant respectively.

In summary, these studies show that

i) A proportion of Jurkat cells can migrate towards CXCL12 across IL-1β stimulated BMEC-60 cells and fibronectin.

ii) Substantially less Jurkat cell migrated across BMEC-60 cells compared to fibronectin over the timeframe of these experiments.

iii) Overall the experiments did not identify a significant role for JAM-A in modulating CXCL12 induced migration across fibronectin, while it seems likely from these and earlier experiments that JAM-A expressing Jurkat cell adhesion to BMEC-60 cells may have slightly reduced their migration towards CXCL12 under the conditions used.

4.3.2.3.JAM-A and umbilical cord blood CD34$^+$ cell migration

Significantly more UCB CD34$^+$ cells migrated across BMEC-60 cells towards CXCL12 than was observed with the leukaemic cell lines used (Figure 4.33). JAM-A blockade with specifc antibody and knock down with specific siRNAs were used to assess if JAM-A functioned in UCB CD34$^+$ cell migration towards CXCL12. JAM-A blockade with specific antibody slightly and significantly increased CD34$^+$ cell chemotaxis across fibronectin to CXCL12 (goat IgG: 47.5±3.3% and anti-JAM-A: 52.1±4.0% of cells migrating respectively, $p<0.05$; Figure 4.33.A). In contrast, the JAM-A blockade with the same antibody slightly reduced CD34$^+$ cell transendothelial migration towards CXCL12 (goat IgG: 23.1±2.6% and anti-JAM-A: 20.7±1.6%, of the cells migrating respectively, $p=0.21$; Figure 4.33.B).

The combination of JAM-A siRNA 150 + 151 reduced slightly but not significantly UCB CD34$^+$ cell chemotaxis across fibronectin (30.8±4.5% v.s. 26.0±3.3%, $p=0.379$; Figure 4.34.A) and reduced their transendothelial migration towards CXCL12 (NS: 28.5±2.7% and siRNA: 19.3±2.2% of the cells migrating respectively, $p=0.076$; Figure 4.34.B). The knockdown efficiency and cell viability were shown previously in Figure 4.13.A.

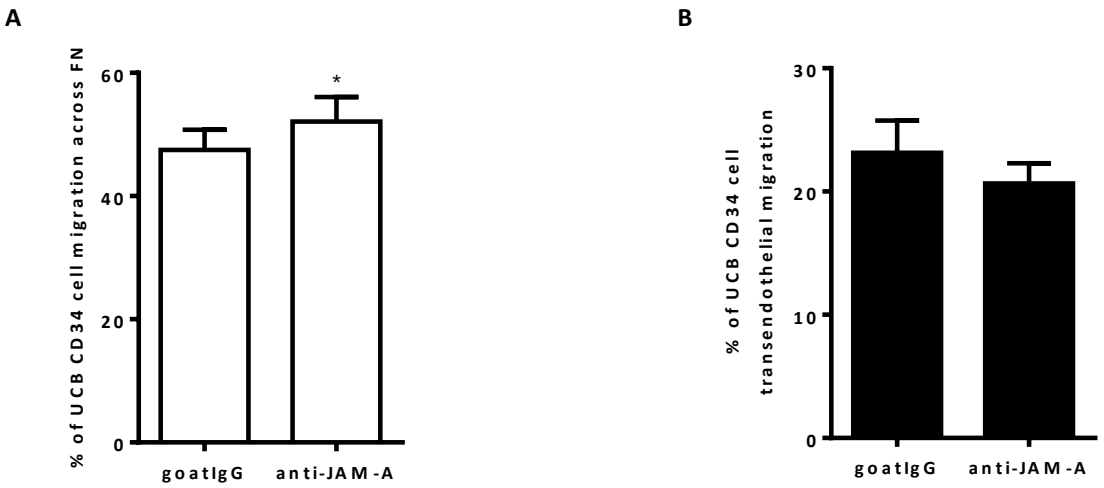

Figure 4.33. JAM-A blockade of UCB CD34$^+$ cell chemotaxis towards CXCL12 across fibronectin or BMEC-60 cells.

The figure shows the absolute percentage of UCB CD34$^+$ cell migrating across (A) fibronectin and (B) IL-1β stimulated BMEC-60 cells towards CXCL12. UCB CD34$^+$ cells were pre-incubated with JAM-A antibody (anti-JAM-A, 10 μg/ml, AF1103, R&D systems) in parallel to goat IgG for 30 minutes at 37°C before performing in transwell assay. Values are means ± S.E.M. for n=6 independent experiments and the statistical analysis was done using paired *t*-test and all values <0.05 (*) or < 0.01 are considered significant or very significant respectively.

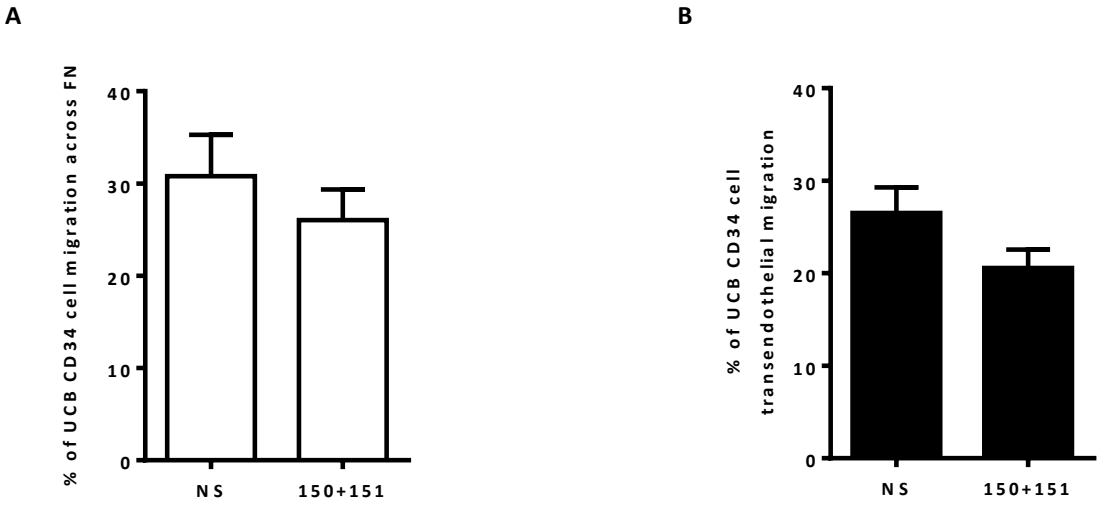

Figure 4.34. JAM-A silencing of UCB CD34$^+$ cell chemotaxis towards CXCL12 across fibronectin or BMEC-60 cells.

The figure shows the absolute percentage of UCB CD34$^+$ cell migrating across (A) fibronectin (n=3) and (B) IL-1β stimulated BMEC-60 cells (n=4) towards CXCL12. UCB CD34$^+$ cells were nucleofected with a combination of JAM-A siRNAs (150+151) and non-silencing control siRNA (NS). Values are means ± S.E.M. for n=3-4 independent experiments. The statistical analysis was done using paired *t*-test and values < 0.05 or < 0.01 are considered significant or very significant respectively.

In summary, these studies show that

i) A higher proportion of UCB $CD34^+$ cells can migrate towards CXCL12 across IL-1β stimulated BMEC-60 cells, and fibronectin than HL-60 or Jurkat cells.

ii) Less UCB $CD34^+$ cell migrated across BMEC-60 cells compared to fibronectin over the timeframe of these experiments.

iii) Overall the experiments did not identify a consistent role for JAM-A in modulating CXCL12 induced migration across fibronectin, while it seems likely from these and earlier experiments that UCB $CD34^+$ cell adhesion to BMEC-60 cells may have prevented their migration towards CXCL12 under the conditions used.

iv) Blocking JAM-A or knocking down JAM-A on UCB $CD34^+$ cells may have reduced their adhesion to BMEC-60 cells and this may have resulted in slightly fewer cells migrating across BMEC-60 cells towards CXCL12.

4.4. Discussion

The roles of JAM-A in cell adhesion and transmigration were examined in this chapter and discussed separately in this section. Several cell lines were chosen as models to determine if JAM-A had a function in cell adhesion and migration, before testing the rare human $CD34^+$ cell subset from UCB. TF-1 cells were selected as the first model as it expressed JAM-A and lacked the known JAM-A binding partner, LFA-1. Both JAM-A blockade and silencing decreased TF-1 cell adhesion onto activated BMEC-60 cells and fibronectin. Not surprisingly, this JAM-A-mediated cell adhesion to BMEC-60 cells was not restricted to this cell line, as similar effects were observed in HL-60 cells, and the adhesion of HL-60 cells declined when JAM-A was either blocked using the same JAM-A antibody or knocked down using specific

siRNAs. HL-60 did not adhere well to fibronectin. The different adhesion abilities of the two cell lines to fibronectin may be due to their dissimilar VLA4 expression, a fibronectin receptor, since another fibronectin receptor, VLA5, was not detectable on these cell lines (Figure 4.35). In addition, JAM-A-null Jurkat cells showed increased adhesion to BMEC-60 cells and fibronectin when JAM-A was overexpressed in them. When UCB $CD34^+$ cells were tested, JAM-A antibody blockade and siRNA knockdown reduced their adhesion onto activated BMEC-60 cells, and to a lesser extent to fibronectin.

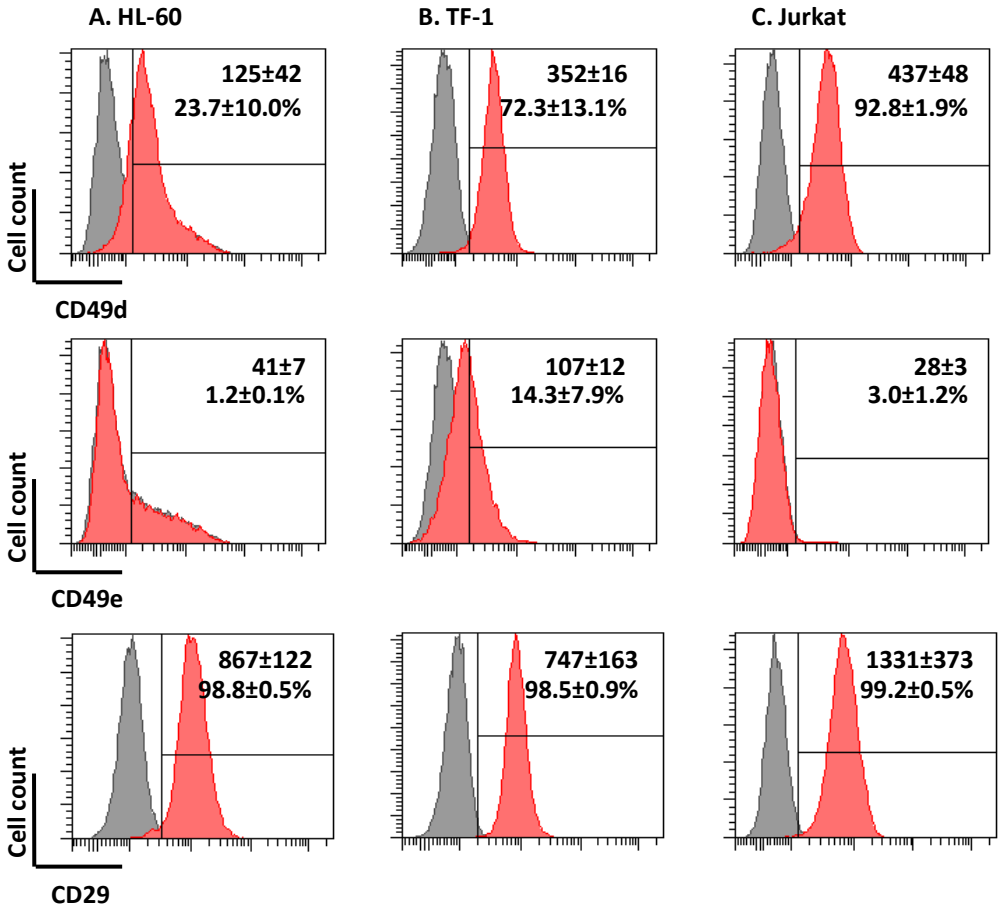

Figure 4.35. Expression of VLA4 integrin (CD49d) and VLA5 integrin (CD49e) on selected acute leukaemic cell lines.
Representative FACS histograms of acute leukaemic cell lines, including two acute myeloid leukaemia cell lines (A) HL-60 (n=4), (B) TF-1 cells (n=3), and one T lymphoid leukaemia cell line (C) Jurkat cells (n=3), stained with CD49d-APC (FAB1345A clone, red, top plots) and CD49e-APC antibodies (FAB1644A clone, red, middle plots) or CD29-FITC antibodies (red, bottom plots) and their isotype controls (gray). M.F.I.± S.E.M. and the % positive± S.E.M for n=3-4 independent experiments.

In all these experiments, the blockade or knockdown of JAM-A reduced adhesion to BMEC-60 cells by around 20-30%. This suggested that JAM-A was not acting alone in mediating this adhesion, but contributed significantly to it. Indeed, numerous studies have shown that selectins, addressins, sialomucins and integrins can co-ordinately regulate the adhesion of HS/PCs to endothelia as shown in Figure 4.36. Transendothelial migration is known to be a complicated process involving initial cell rolling or tethering onto endothelial cells, followed by firm adhesion when the CXCR4 chemokine receptor and VLA-4 integrin signalling are activated, cell transmigration through the endothelial cells and finally detachment from the endothelial cells (354).

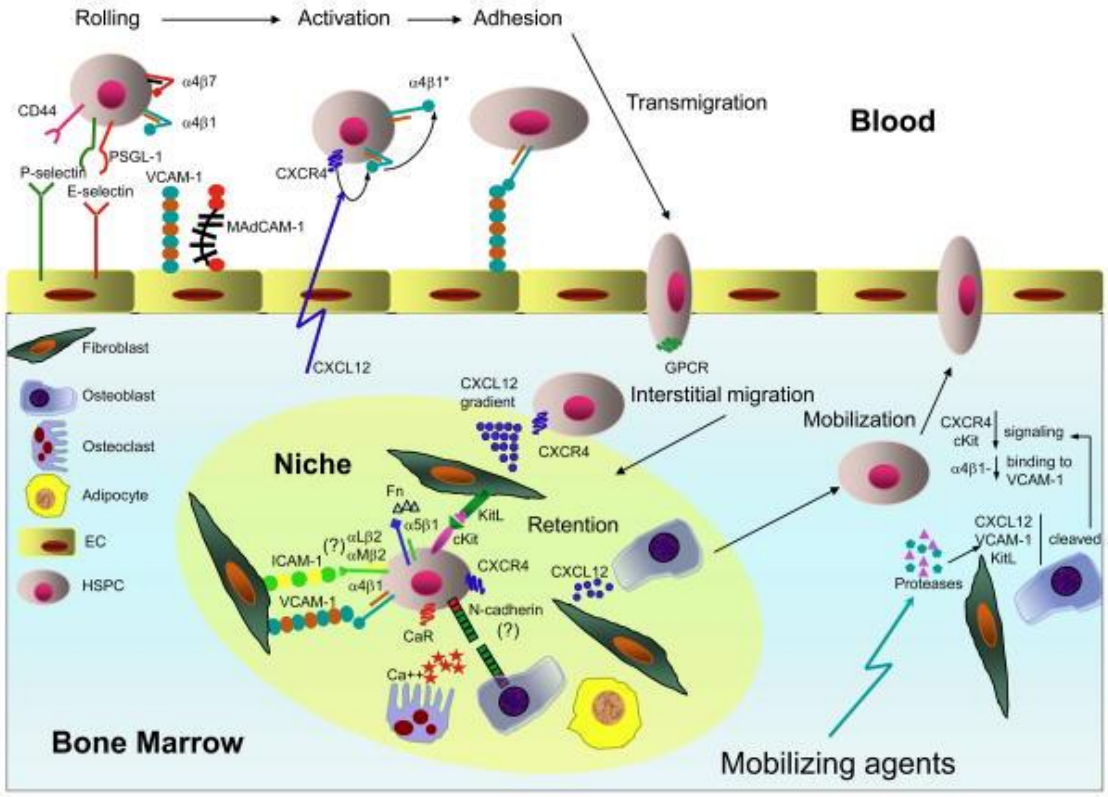

Figure 4.36. HS/PC migration into the bone marrow.
HS/PCs first bind to selectins on sinusoidal endothelium in the bone marrow via the selectin ligand PSGL-1 or the addressin (CD44) and possibly MadCAM-1 via $\alpha4\beta7$ interactions, before interacting firmly via VLA4 (integrin $\alpha4\beta1$) with VCAM-1. The latter process is activated by CXCL12, which induces VLA-4 to undergo a conformational change and this adhesion is followed by transmigration across the endothelium in response to CXCL12. The HS/PCs then lodge in niches, by interacting with VCAM-1, fibronectin and other molecules. Taken from Mazo *et. al.* (354). Reprinted from Trends in Immunology 32, Mazo IB, Massberg S, von Andrian UH., Hematopoietic stem and progenitor cell trafficking, 493-503, Copyright (2011), with permission from Elsevier.

To determine whether JAM-A influenced UCB $CD34^+$ cell migration, the roles of JAM-A in chemotaxis towards CXCL12 across fibronectin, an extracellular matrix molecule rich in bone marrow, and BMEC-60 cells, a representative of bone marrow endothelium, were examined. Interestingly, antibody blockade slightly but significantly promoted UCB $CD34^+$ cell chemotaxis on fibronectin towards CXCL12, but inhibited transendothelial migration on BMEC-60 cells. With JAM-A siRNA knockdown, both types of chemotaxis were reduced slightly, although not significantly. This might be explained by a close association of fibronectin binding integrins with JAM-A where the JAM-A antibody interfered non-specifically with integrin binding to fibronectin and promoted migration rather than firm adhesion, an effect not likely to be observed with JAM-A siRNA knockdown. In the BMEC-60 transmigration studies, JAM-A may be promoting UCB $CD34^+$ cell adhesion to homophilic or heterophilic ligands on BMEC-60 cells and thus its knockdown or blockade may prevent some initial adhesion and thus reduce subsequent cell migration. The lack of significance in this latter case suggests that JAM-A is more likely to act as an adhesion molecule or a regulator of adhesion rather than as a migratory molecule in HS/PCs.

The mechanism whereby JAM-A promotes UCB $CD34^+$ cell adhesion to BMEC-60 cells is not understood. The functions of JAM-A are different on different cell types. JAM-A is known to be able to form homophilic dimers with another JAM-A unit and to form heterophilic dimers with integrins LFA-1 ($\alpha L\beta 2$) on leucocytes (232, 233, 239, 245, 355), integrin GPIIIa on platelets (330) and integrin $\alpha V\beta 3$ (CD51/CD61) on endothelial cells (333). These dimers could be either cis-interactions or trans-interactions. LFA-1-JAM-A interactions between leucocytes and endothelial cells have been proposed to disrupt JAM-A-JAM-A intercellular interaction at endothelial junctions and consequently facilitate leucocyte transendothelial migration (268). Interestingly, studies by Woodfin *et. al.* indicate that ICAM-1, JAM-A and

PECAM-1 on endothelial cells sequentially mediate leucocyte transmigration (258, 259). Recent studies have also demonstrated that JAM-A redistributes to the apical region of inflamed endothelium prior to cells passing through endothelial cells (262). Notably, the bone marrow sinusoidal endothelium acts in a similar way to inflamed endothelium with constitutive expression of E-selectin, VCAM-1 and ICAM-1 (175-178). One might envisage that JAM-A might under these conditions be located with these molecules on the endothelia and enhance either selectin mediated rolling or VLA4 firm adhesion. In this respect, JAM-A could modulate integrin recycling, a process shown to occur in neutrophils (251). Alternatively, JAM-A on HS/PCs might interact with JAM-A on endothelial cells. Indeed, JAM-A-JAM-A interactions in trans have been reported between platelets or PB $CD34^+$ endothelial progenitor cells and inflamed endothelium (239, 355), while it was predicted between leucocyte and endothelia (reviewed in (243)).

CHAPTER 5

TO DETERMINE THE MECHANISM OF ACTION OF JAM-A ON HUMAN UCB CD34$^+$ CELLS

5.1. Introduction

The chemokine CXCL12 is known to play a key role in haematopoietic stem/progenitor cells (HS/PCs) homing to and lodgement in the bone marrow niche (reviewed in (314)). This chemokine is secreted by CXCL12 abundant stromal adventitial reticular cells (CAR cells) or in the mouse by nestin$^+$mesenchymal stromal cells (nestin$^+$MSCs), which are located in the endosteal region and in a perivascular location (reviewed in (93)). Recent studies from our laboratory, to which the author contributed have shown that the clonogenic nestin$^+$MS-5 murine bone marrow stromal cell (BM MSC) line not only regulates HSC/HPC fate (115) but can also regulate vasculogenesis and angiogenesis by endothelial progenitor cells via CXCL12 (338). Hence, these stromal cells and CXCL12 have a dual role in the vascular niche to maintain the vasculature and to support haematopoiesis (338). Since bone marrow endothelial cells (BMECs) act as the gate keepers controlling HS/PCs trafficking, they provide the first point of contact with HS/PCs and secrete or present cytokines or chemokines that promote HS/PC migration towards the bone marrow niche (356). Both mouse and human BMECs have been reported to present CXCL12 (187, 195, 196), with Netelenbos *et al.* further demonstrating that CXCL12 is presented on proteoglycans on BMECs and that this is involved in promoting HS/PC adhesion (188). van Buul *et al.* provided functional evidence by showing an endothelial CXCL12-dependent redistribution of CXCR4 on human HS/PCs during the interaction of these two cell types *in vitro*, and subsequently showed that this mediated their cell migration (189). Studies from our laboratory have shown the expression of CXCL12

in normal and leukaemic human bone marrow sections and particularly on the vasculature (Figure 5.1). As an immortalised bone marrow endothelial cell line, BMEC-60, was used throughout these studies, CXCL12 expression was also examined on BMEC-60 using immunofluorescence staining and its expression by these cells confirmed (Figure 5.2).

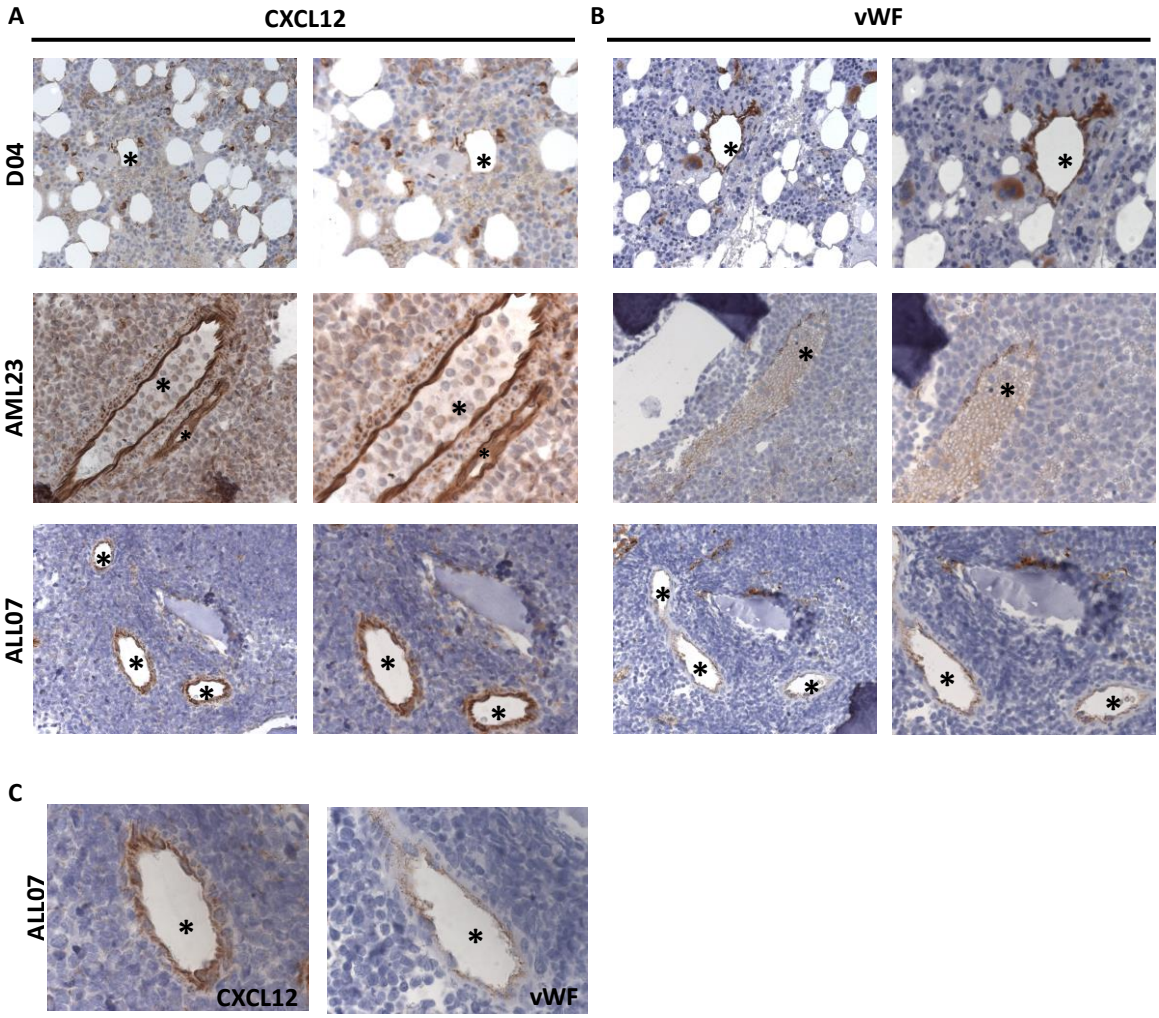

Figure 5.1. CXCL12 staining in human normal bone marrow section.
Three representative paraffin embedded sections of human bone marrow trephines obtained from a healthy donor (D04; upper), one AML patient (AML23; middle) and one ALL patient (ALL07; lower) which were stained for (A) CXCL12 (79018, R&D systems) or (B) vWF (36B11, Novocastra Laboratories) and developed using immunohistochemical techniques before being examined by light microscopy. Stars in (A) show strong CXCL12 staining on blood vessel endothelial cells, which correlate with vWF staining in (B). Magnification X40 (on the left of pairs) and X60 (on the right of pairs) or (C) at X100 magnification of ALL07 are shown. (Kindly provided by Dr. Youyi Zhang).

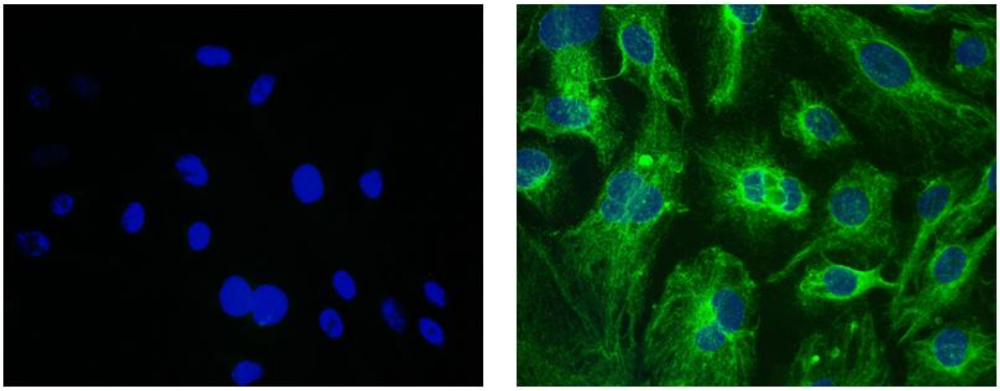

Figure 5.2. CXCL12 expression in BMEC-60 cells.
Immortalised bone marrow endothelial cells (BMEC-60) were seeded on fibronectin pre-coated 4 well-chamber slides at 37°C overnight and stained for isotype negative control (left) or for CXCL12 (Clone 79018, R&D systems, green; right) followed by Alexa Fluor®488 goat anti-mouse IgG antibody (A-11001, Invitrogen) using immunofluorescent techniques described in Chapter 2, Section 2.8. Images represent one from n=3 independent experiment and nuclei were counterstained with DAPI (blue). Magnification X60.

CXCR4, the cognate receptor for CXCL12, is expressed on endothelial cells (357). On human $CD133^+/CD34^+$ HS/PCs, CXCL12 interacts with CXCR4 in a complex with such other molecules as the sialomucin CD164 (140), integrins (21, 195, 358) and the tetraspanin CD82 (359), all of which are involved in HSC/HPC adhesion to BM MSCs and/or endothelia. CXCL12 has at least two proposed roles in the homing of HS/PCs to their bone marrow niches. It changes the conformation of VLA-4 ($\alpha4\beta1$ integrin) on HS/PCs, allowing this molecule to adhere firmly to VCAM-1 on bone marrow sinusoidal endothelia, a process that then allows CXCR4 on HS/PCs to promote the migration of HS/PCs across the endothelial barrier (354). The CXCL12 and CXCR4 axis is thus critical for both HS/PC engraftment, and also subsequently its retention in the bone marrow as reviewed in (114, 158, 213). Despite this, the detailed biological processes are still not fully elucidated, particularly in terms of the co-receptors that modulate this response.

The results in Chapter 4 demonstrate that JAM-A on human UCB $CD34^+$ HS/PCs is involved in the adhesion of human HS/PCs to bone marrow vascular niche cells *in vitro*, and may play a

role in the migration of these cells across fibronectin towards CXCL12. Other studies from this laboratory (140) have shown that CXCR4, when presented with CXCL12, interacts with both VLA-4 and VLA-5 integrins as well as the sialomucin CD164. The interaction with CD164 has been shown to be required for CXCR4 signalling (140). Thus, our hypothesis was that JAM-A might also act as a co-receptor for CXCR4 on HS/PCs to regulate its signalling and the subsequent activation of VLA-4 or VLA-5 integrins thereby enhancing HS/PC adhesion and/or migration towards CXCL12.

There are several potential signalling pathways that may be co-regulated by CXCR4 and JAM-A. CXCR4 is a G-protein-coupled receptor that activates several signal transduction pathways upon CXCL12 binding. The most important biological effects of CXCL12/CXCR4 interactions include activation of calcium flux and focal adhesion components, through PLC/PKC, FAK/Pyk2/Crk/Paxillin complex or Rap1 signalling pathways for cell adhesion and chemotaxis or migration, activation of the PI3K/AKT pathway for cell survival, and activation of the Ras/ERK1/2 pathway for cell proliferation with both having a role in cell adhesion and migration as reviewed in (198, 201, 299, 360, 361). JAM-A has been shown to physically interact with PDZ-GEF2 through its intracellular domain and hence to activate Rap1-mediated cell migration in other cell types (255, 362). On neutrophils, the mechanism has been shown to involve the modulation by JAM-A of Rap1 activation which promotes β1 intergrin internalisation and regulates the function of this integrin on these cells (251).

The studies in this Chapter were designed to determine whether JAM-A on human UCB $CD34^+$ HS/PCs interacts with CXCR4, β1 integrins or the CXCR4 co-receptors, CD164 and CD82, and modulates CXCR4 signalling on HS/PCs through the activation of ERK1/2, AKT, PKCζ or Rap1 in the presence of CXCL12.

5.2. Aims and Objectives

The main aims for this chapter are twofold, (i) to investigate whether CXCR4, CD164, CD29 or CD82 co-localise or interact with JAM-A, and (ii) if so, to define potential mechanisms that may affect the function of these molecules on HS/PCs.

5.3. Results

5.3.1. JAM-A co-localises and interacts with CXCR4 at the leading edges of HL-60 cells in response to CXCL12.

Studies by Forde *et al.* (140) showed that CXCR4 interacted with the VLA-4 and VLA-5, on Jurkat and human UCB $CD133^+$ cells and that this co-localisation to the leading edge of the cell was then associated with CD164 interaction when CXCL12 was presented to the cells on fibronectin. ICAM-3 was found not to associate in this complex over short time frames of 0 to 10 minutes. The latter was generally confirmed in the studies presented here, although some interaction appeared to occur at longer time periods (Figures 5.3 and 5.4).

In the studies presented here, these associations were first confirmed on HL-60 cells for CXCR4, CD29 integrin and CD164 interactions, using ICAM-3 as a control, and then extended to JAM-A. HL-60 cells served as a model for human UCB $CD34^+$ cells, which are much rarer cell subsets, with $CD34^+$ cells being used to confirm the interactions. As shown in Figure 5.3, CXCR4 and CD164 co-localised at the leading edge of HL-60 cells within 5-10 minutes in the presence of CXCL12 on fibronectin as assessed microscopically. This CXCR4 and CD164 co-localisation gradually increased over time (from 3.8±1.0% at 0 minutes to 20.3±3.9%, 24.1±2.1% and 37.5±4.0% of cells showing co-localisation over 5, 10 and 30 minutes respectively). In contrast, JAM-A had co-localised with CD164 by 5 minutes (30.6±5.1% of cells co-localising at 5 minutes vs. 10.4±4.9% at 0 minutes) and then this co-localisation

gradually declined over 10 to 30 minutes (Figure 5.3). JAM-A co-localised with CXCR4 by 5 minutes, but this peaked at 10 minutes (30.2±3.1% of cells co-localising at 10 minutes vs. 7.3±1.7% at 0 minutes) before beginning to decline. ICAM-3, in contrast, did not co-localise with CXCR4 or with JAM-A (remaining between 9.8±3.0% at 0 minutes and 9.3±3.2% at 30 minutes).

To confirm this co-association of molecules, a PLA (proximity ligation assay) was performed to investigate their physical interaction *in situ*. In this assay, the interactions between JAM-A, CXCR4 and CD164 occurred within 5 minutes after CXCL12 was presented to HL-60 cells on fibronectin (Figure 5.4). For comparison, the numbers of cells on which these molecules interacted at 5 minutes compared to 0 minutes was respectively for CXCR4 and CD164: 36.7±3.9% vs. 11.5±4.5%; for CXCR4 and JAM-A: 52.6±7.3% vs. 11.2±3.2%; and for JAM-A and CD164: 31.3±5.4% vs. 9.1±4.7% (Figure 5.4.B). While the interactions between CXCR4 and JAM-A and CD164 and JAM-A were maintained over 30 minutes, the CXCR4-JAM-A interaction had begun to decline by 10 minutes (Figure 5.4).

The PLA assay is more robust than co-location assays using microscopy at assessing molecular interactions and hence it can be concluded that CXCR4 and JAM-A interactions along with CD164 had essentially occurred rapidly and within 5 minutes.

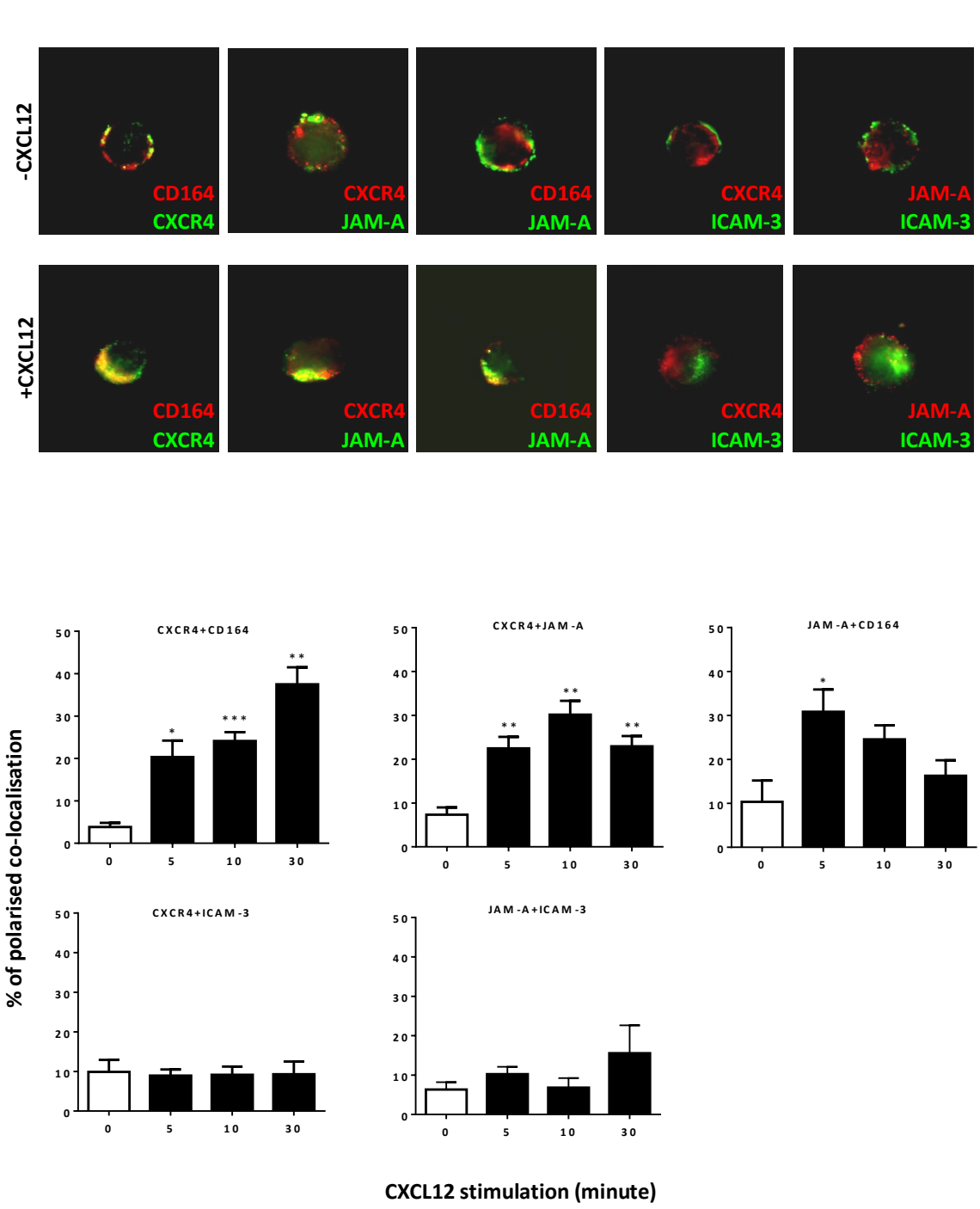

Figure 5.3. Co-localisation of JAM-A with CXCR4 and CD164 on HL-60 cells over time when presented with CXCL12 on fibronectin.

HL-60 cells were presented with CXCL12 on fibronectin from 0 to 30 minutes and at each time point cells were stained with JAM-A (M.Ab.F11 or 36-1700 from Invitrogen), CXCR4 (Ab2074), CD164 (N6B6) and ICAM-3 (ICAM-3.3) in different combinations. (A) shows the co-localisation of pairs of molecules after CXCL12 stimulation for 10 minutes. (B) depicts the percentage of each pair of proteins co-localising at the indicated time. The images are at X80 magnification. Values are means ± S.E.M. of 3 independent experiments where 100 cells were counted. The statistical analysis was done using Student's *t*-test and values of < 0.05 (*) or 0.01 (**) are considered significant or very significant respectively compared to 0 minutes.

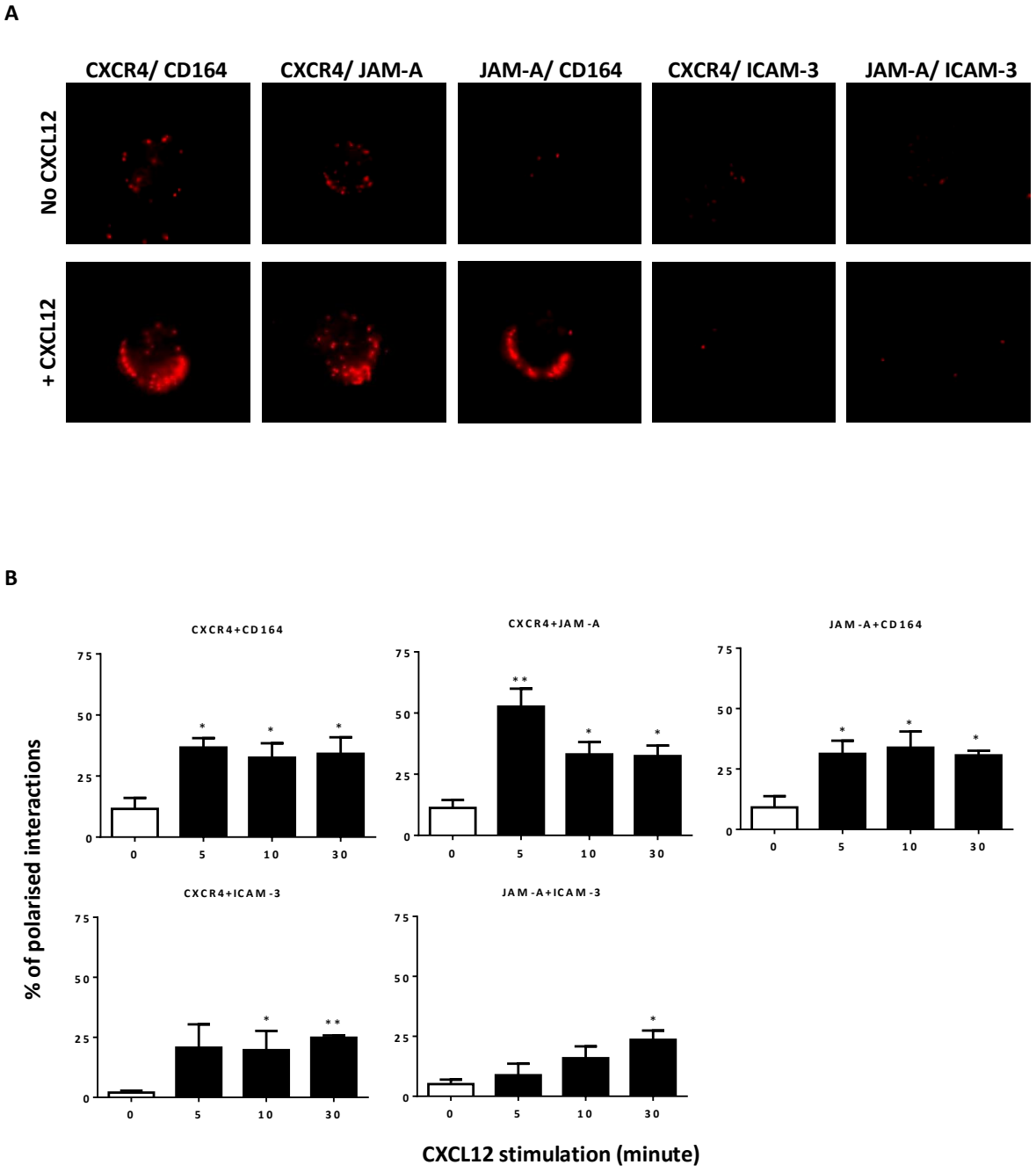

Figure 5.4. Interaction of JAM-A with CXCR4 and CD164 on HL-60 cells when presented with CXCL12 on fibronectin.

HL-60 cells were presented with CXCL12 on fibronectin from 0 to 30 minutes and the interactions of JAM-A (M.Ab.F11 or 36-1700 from Invitrogen), CXCR4 (Ab2074), CD164 (N6B6) and ICAM-3 (ICAM-3.3) examined using the PLA assay. (A) The red dots in the images show the interactions of pairs of molecules. (B) shows the quantitative data over time. The images are at X80 magnification. Values are means ± S.E.M. of 3 independent experiments where 100 cells were counted. The statistical analysis was done using Student's *t*-test and values of < 0.05 (*) or < 0.01 (**) are considered significant or very significant respectively compared to 0 minutes.

Next, using immunofluoresecence and then the PLA assay, which determines molecular proximity and interactions, integrin β1/CD29, was shown to increase its co-localisation with CXCR4 significantly within 5 minutes, with 25.4±3.9% of cells co-localising at 5 minutes (vs. 8.4±1.6% at 0 minutes before decreasing over 10 to 30 minutes on HL-60 cells (Figure 5.5). JAM-A had also co-localised with CD29 within 5 minutes and this was maintained over the next 10 to 30 minutes (15.4±0.8% and 16.9±2.4% at 10 and 30 minutes respectively vs. 8.2±0.6% at 0 minutes).

With the PLA assay, integrin β1/CD29, had increased its molecular interaction with CXCR4 significantly within 5 minutes, with 28.9±4.9% of cells showing such interactions at 5 minutes vs. 11.1±2.8% at 0 minute before decreasing over 10 to 30 minutes (Figures 5.6.B). JAM-A had also interacted with CD29 within 5 minutes and this was increased over the next 10 and was then maintained up to at least 30 minutes on HL-60 cells.

During this thesis research, the CD82 tetraspanin molecule was found to interact with CXCR4 (359), and this molecule was also examined for its interaction with JAM-A. Figures 5.7 and 5.8 showed that CD82 co-localised and interacted with JAM-A in the presence of CXCL12. The co-localisation of JAM-A and CD82 increased from 3.8±0.4% at 0 minutes to 12.1±1.8%, 17.0±3.4% and 17.2±1.1% at 5 to 30 minutes respectively (Figure 5.7.B). The interaction between CD82 and JAM-A as defined by the PLA assay increased from 24.4±3.2% at 0 minutes to 50.5±2.0% at 5 minutes, and then began to decline (41.9±8.8% at 10 minutes and 36.3±2.4% at 30 minutes; Figure 5.8.B). In summary, these results suggest that there is significant interaction of JAM-A with CD82 within 5 minutes of CXCL12 being presented to HL-60 cells on fibronectin and that these interactions are more robustly defined with the PLA assay than by microscopic co-localisation studies.

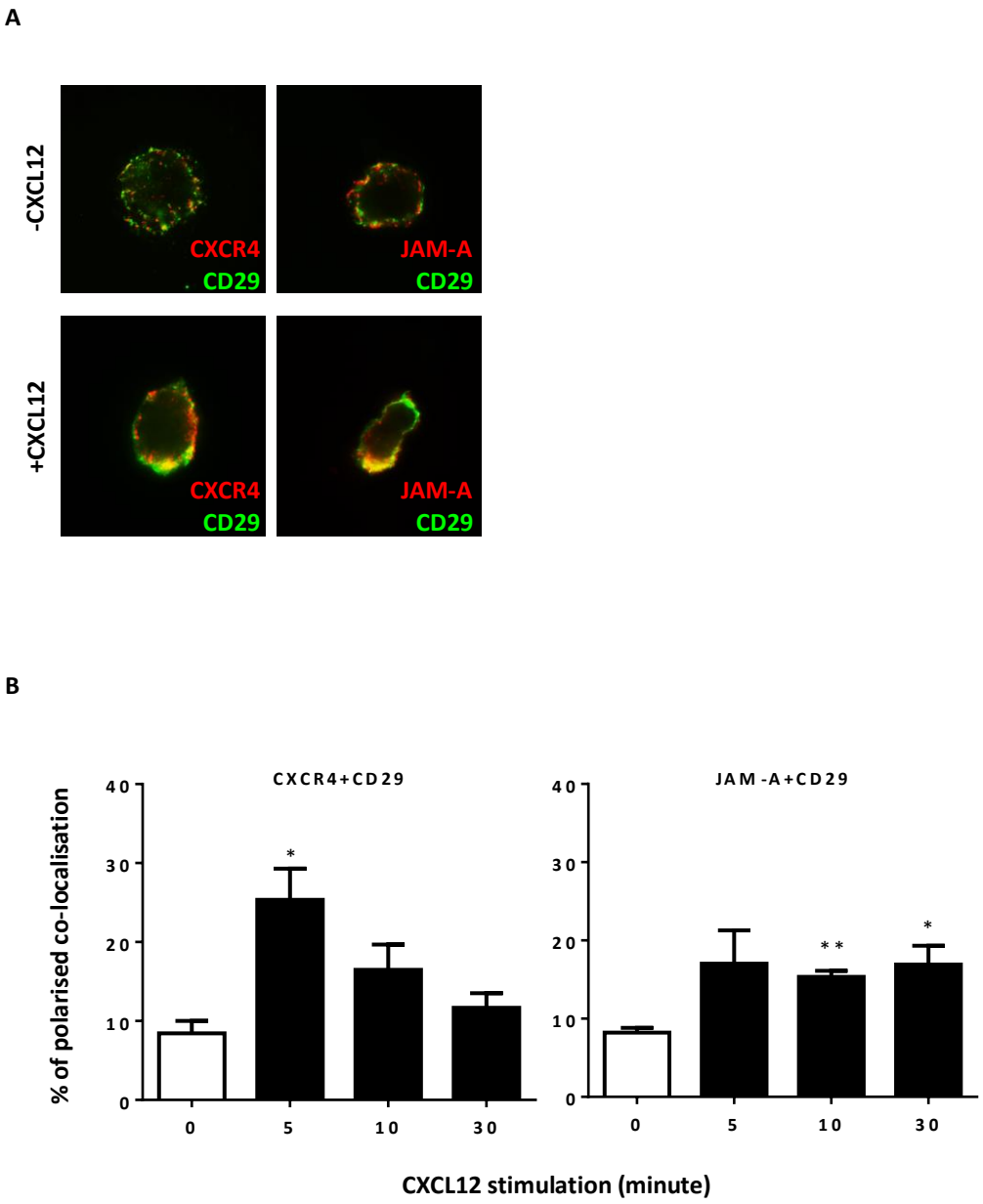

Figure 5.5. Co-localisation of JAM-A, CXCR4 and CD29 on HL-60 cells over time when presented with CXCL12 on fibronectin.

HL-60 cells were presented with CXCL12 on fibronectin from 0 to 30 minutes and at each time point cells were stained with JAM-A (M.Ab.F11), CXCR4 (Ab2074) and CD29 (Mab13). (A) shows the co-localisation of pairs of molecules after CXCL12 stimulation for 10 minutes. (B) depicts the percentage of each pair of proteins co-localising at the indicated time. The images are at X80 magnification. Values are means ± S.E.M. of 3 independent experiments where 100 cells were counted. The statistical analysis was done using Student's *t*-test and values of < 0.05 (*) or 0.01 (**) are considered significant or very significant respectively compared to 0 minutes.

A

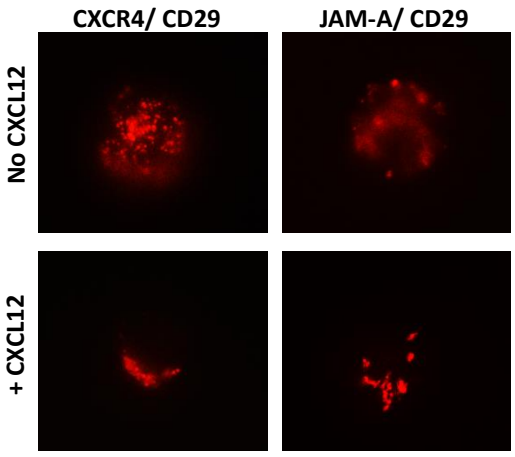

B

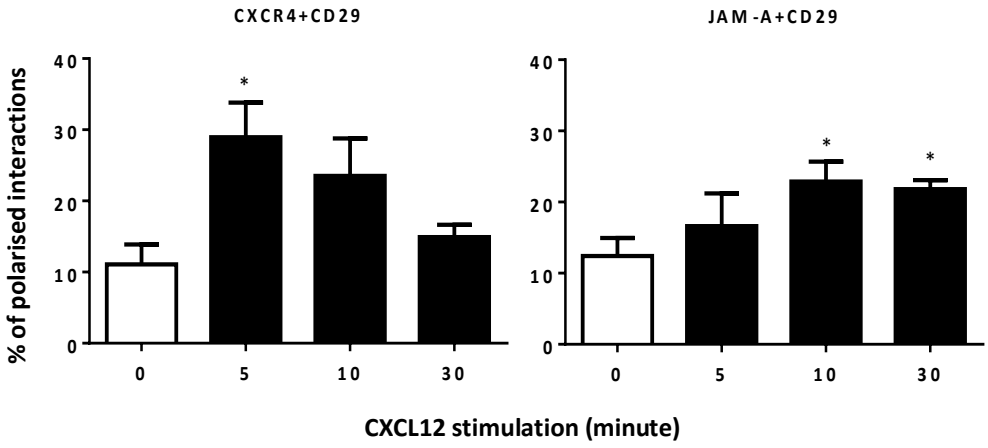

Figure 5.6. Interaction of JAM-A and CXCR4 with CD29 on HL-60 cells when presented with CXCL12 on fibronectin.

HL-60 cells were presented with CXCL12 on fibronectin from 0 to 30 minutes and the interactions of JAM-A (36-1700), CXCR4 (Ab2074) and CD29 (Mab13) examined using the PLA assay. (A) The red dots in the images show the interactions of pairs of molecules. (B) shows the quantitative data over time. The images are at X80 magnification. Values are means ± S.E.M. of 3 independent experiments where 100 cells were counted. The statistical analysis was done using Student's *t*-test and values of < 0.05 (*) are considered significant compared to 0 minutes.

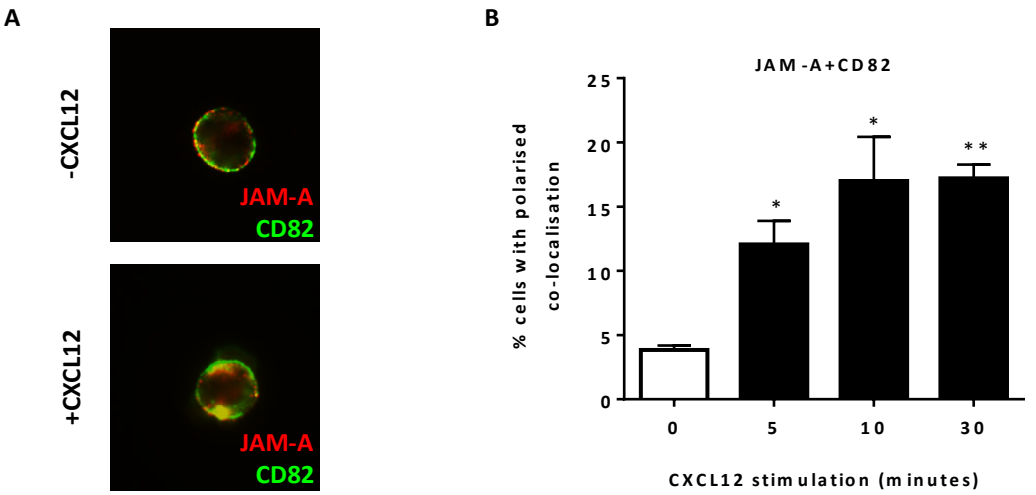

Figure 5.7. Co-localisation of JAM-A and CD82 on HL-60 cells over time when presented with CXCL12 on fibronectin.
HL-60 cells were presented with CXCL12 on fibronectin from 0 to 30 minutes and at each time point cells were stained with JAM-A (M.Ab.F11) and CD82 (B-L2) in different combinations. (A) shows the co-localisation of pairs of molecules after CXCL12 stimulation for 10 minutes. (B) depicts the percentage of each pair of proteins co-localising at the indicated time. The images were at X80 magnification. Values are means ± S.E.M. of 3 independent experiments where 100 cells were counted. The statistical analysis was done using Student's *t*-test and values of < 0.05 (*) or 0.01 (**) are considered significant or very significant respectively compared to 0 minutes.

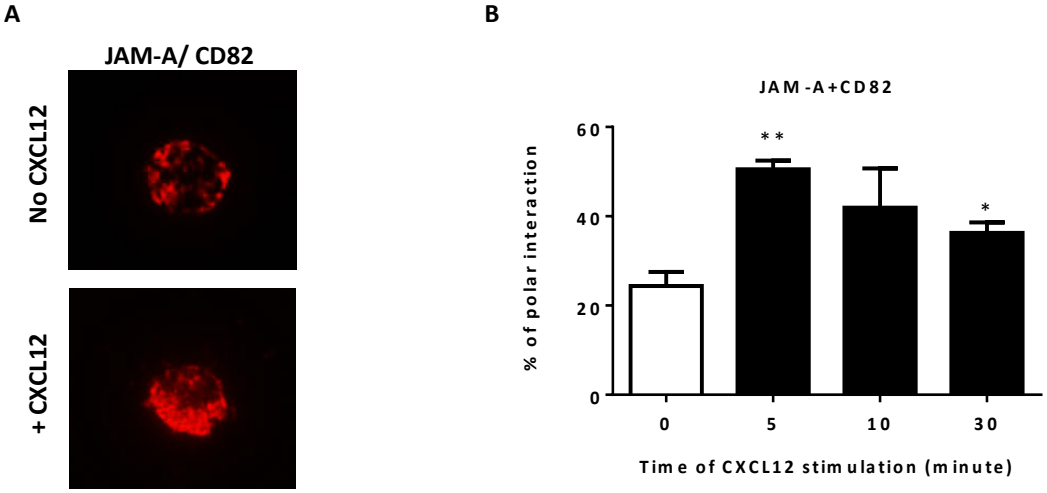

Figure 5.8. Interaction of JAM-A with CD82 on HL-60 cells when presented with CXCL12 on fibronectin.
HL-60 cells were presented with CXCL12 on fibronectin from 0 to 30 minutes and the interactions of JAM-A (36-1700) and CD82 (B-L2) examined using the PLA assay. (A) The red dots in the images show the interactions of pairs of molecules. (B) shows the quantitative data over time. The images are at X80 magnification. Values are means ± S.E.M. of 3 independent experiments where 100 cells were counted. The statistical analysis was done using Student's *t*-test and values of < 0.05 (*) or < 0.01 (**) are considered significant or very significant compared to 0 minutes.

5.3.2. JAM-A co-localises and interacts with CXCR4 at the leading edges of UCB CD34+ cells in response to CXCL12.

To investigate potential role of JAM-A on haematopoietic stem/progenitor cell (HS/PCs), the co-localisation and PLA assays were carried out on UCB CD34$^+$ cells based on molecules tested on HL-60 cells and, because of the difficulty in isolating large numbers of UCB CD34$^+$ cells, for the 10 minute timepoint only. As the PLA assay was more robust, the data generated with this assay was used for quantitation. Using immunofluorescence, JAM-A co-localised with CXCR4, but not to ICAM-3, on the leading edge of the cell (Figure 5.9). JAM-A also physically interacted with CXCR4 and CD164 (Figure 5.10) at the leading edge of UCB CD34$^+$ cells at the 10 minutes post CXCL12 simulation. In these experiments, the number of human UCB CD34$^+$ cells demonstrating these interactions in the presence of CXCL12 varied from 42 to 48 %.

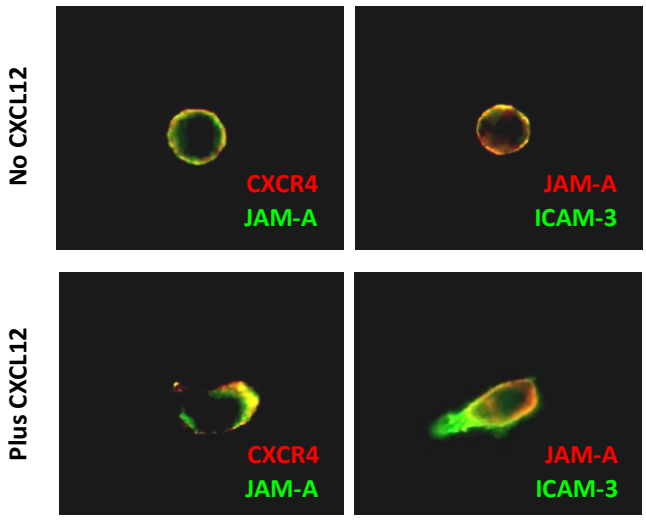

Figure 5.9. Co-localisation of JAM-A with CXCR4 on human UCB CD34$^+$ cells over time when presented with CXCL12 on fibronectin.
UCB CD34$^+$ cells were presented with or without CXCL12 on fibronectin for 10 minutes and stained with JAM-A (M.Ab.F11 or 36-1700), CXCR4 (Ab2074) and ICAM-3 (ICAM-3.3) in different combinations. The images represent one from 3 independent experiments at X80 magnification.

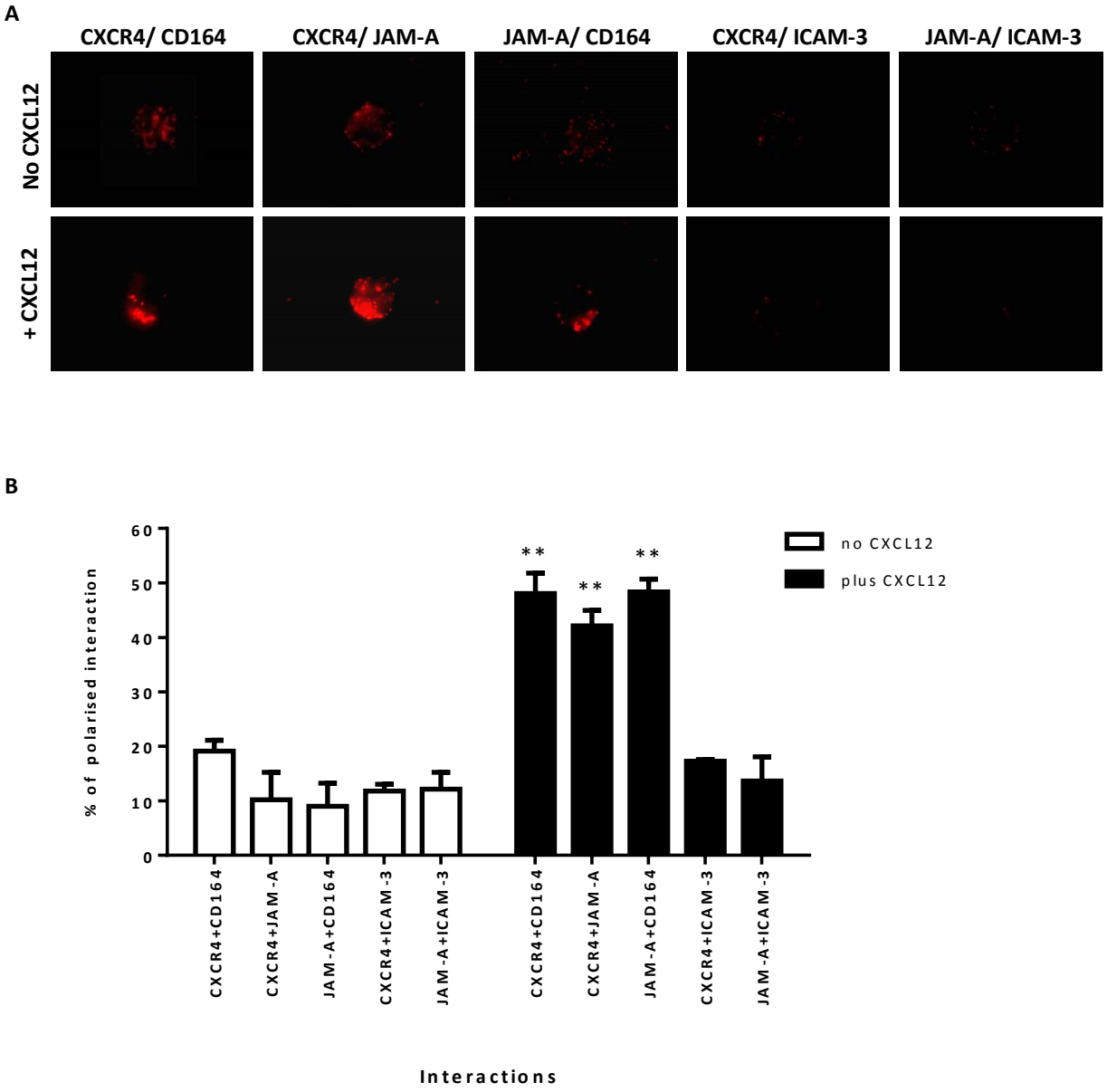

Figure 5.10. Interaction of JAM-A with CXCR4 and CD164 on human UCB CD34$^+$ cells when presented with CXCL12 on fibronectin.
UCB CD34$^+$ cells were presented with CXCL12 on fibronectin for 10 minutes. The interactions of JAM-A (M.Ab.F11 or 36-1700 from Invitrogen), CXCR4 (Ab2074), CD164 (N6B6) and ICAM-3 (ICAM-3.3) were examined using the PLA assay. (A) The red dots in the images show the interactions of pairs of molecules. (B) shows the quantitative data. The images are at X80 magnification. Values are means ± S.E.M. of 3 independent experiments where 100 cells were counted. The statistical analysis was done using Student's *t*-test and values of < 0.01 (**) are considered very significant compared to no CXCL12.

The associations of JAM-A and CXCR4 with CD29 or CD82 were also examined on different isolates of human UCB CD34$^+$ cells. The numbers of cells involved in the interactions of CD29 with CXCR4 were 8.1±2.1% without CXCL12 and 21.3±3.3% with CXCL12 (p<0.05) and of

CD29 with JAM-A were 6.8±1.4% without CXCL12 and 19.5±3.7% with CXCL12 (p<0.05) (Figures 5.11 and 5.12).

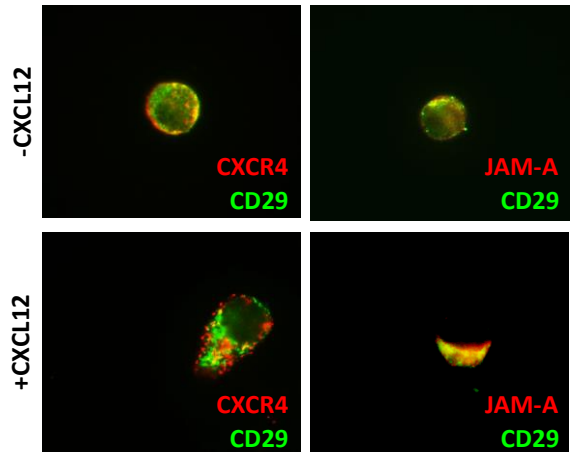

Figure 5.11. Co-localisation of CXCR4 and JAM-A with CD29 on human UCB CD34$^+$ cells over time when presented with CXCL12 on fibronectin.
UCB CD34$^+$ cells were presented with or without CXCL12 on fibronectin for 10 minutes and stained with JAM-A (M.Ab.F11), CXCR4 (Ab2074) and CD29 (Mab13) in different combinations. The images represent one from 3 independent experiments at X80 magnification.

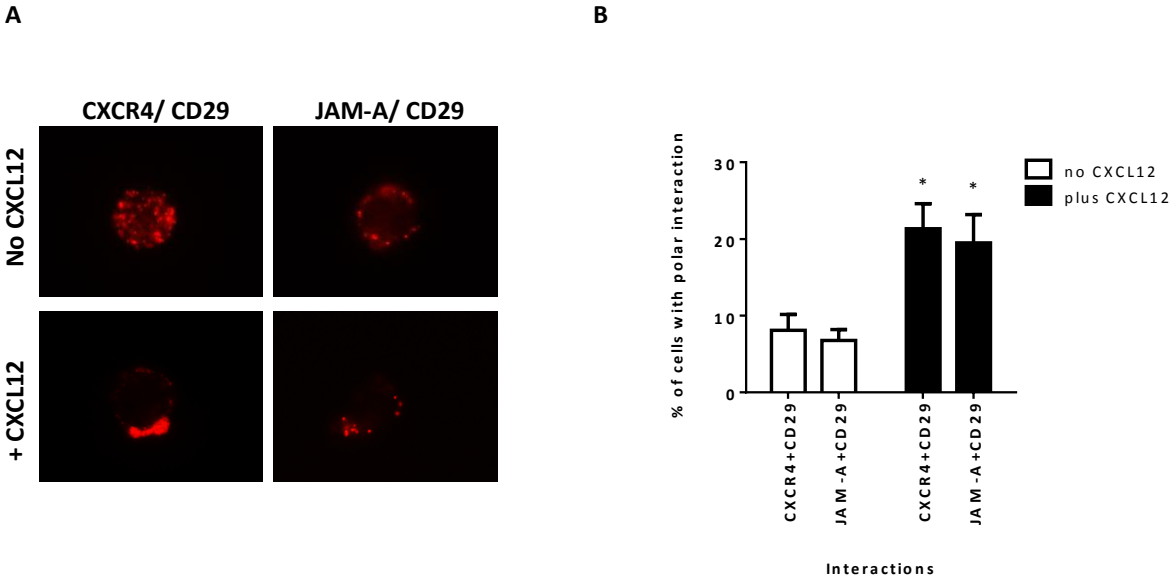

Figure 5.12. Interaction of JAM-A and CXCR4 with CD29 on human UCB CD34$^+$ cells when presented with CXCL12 on fibronectin.
Human UCB CD34$^+$ cells were presented with CXCL12 on fibronectin for 10 minutes. The interactions of JAM-A (36-1700), CXCR4 (Ab2074) and CD29 (18/CD29) examined using the PLA assay. (A) The red dots in the images show the interactions of pairs of molecules overtime. (B) shows the quantitative data. The images are at X80 magnification. Values are means ± S.E.M. of 3 independent experiments where 100 cells were counted. The statistical analysis was done using Student's t-test and values of < 0.05 (*) are considered significant compared to no CXCL12.

The association of CD82 and JAM-A on UCB CD34$^+$ cells appeared polarised and enhanced upon CXCL12 stimulation as shown in Figures 5.13 and 5.14. The percentage of cells with polarised interactions increased from 12.1±1.4% to 34.2±3.6% over 10 minutes in the presence of CXCL12 (p<0.01; Figure 5.14.B).

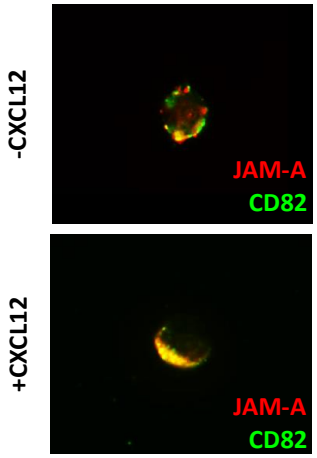

Figure 5.13. Co-localisation of JAM-A with CD82 on human UCB CD34$^+$ cells over time when presented with CXCL12 on fibronectin.
UCB CD34$^+$ cells were presented with or without CXCL12 on fibronectin for 10 minutes and stained with JAM-A (M.Ab.F11) and CD82 (B-L2) in different combinations. The images represent one from 3 independent experiments at X80 magnification.

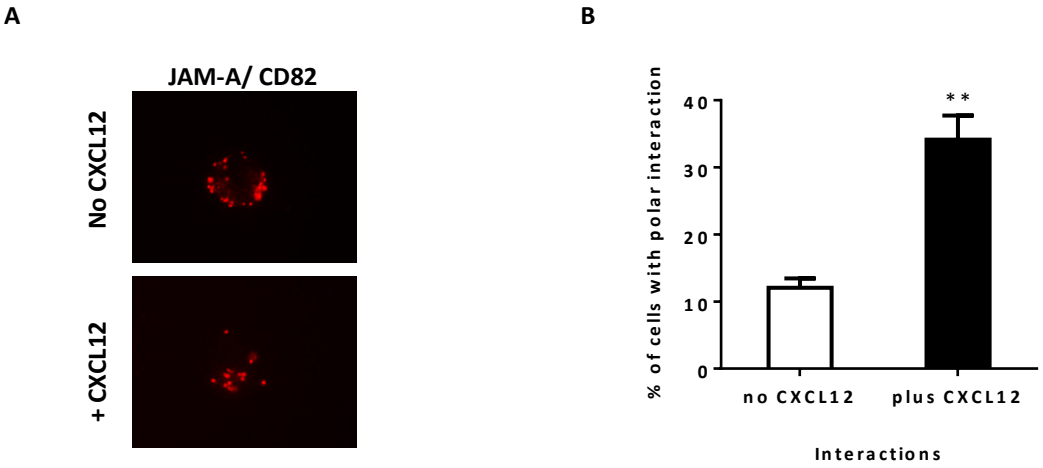

Figure 5.14. Interaction of JAM-A with CD82 on human UCB CD34$^+$ cells when presented with CXCL12 on fibronectin.
UCB CD34$^+$ cells were presented with or without CXCL12 on fibronectin for 10 minutes. The interactions of JAM-A (36-1700) and CD82 (B-L2) were examined using the PLA assay. (A) The red dots in the images show the interactions of pairs of molecules. (B) shows the quantitative data. The images were at X80 magnification. Values are means ± S.E.M. of 3 independent experiments where 100 cells were counted. The statistical analysis was done using Student's t-test and values of < 0.01 (**) are considered very significant compared to no CXCL12.

In summary, JAM-A was found to interact with CXCR4, CD164, CD29 and CD82, but not ICAM-3, on human UCB $CD34^+$ cells within 10 minutes of being presented with CXCL12 on fibronectin. The human UCB cells had been isolated and cryopreserved ahead of the assays and on the day of assays cultured for 16 hours in serum free Stemspan medium with Flt-3 ligand, SCF, TPO and IL-6 as specified in Chapter 2 section 2.3.2 of the Materials and Methods before the PLA and co-localisation studies was done. Notably, the number of cells where this interaction took place varied and this was most likely due to the use of different donor UCB pools or to the selection of a single timepoint of 10 minutes. A head to head comparison of different molecules with the same batches of pooled human UCB $CD34^+$ cells and the addition of further time points at 1 or 5 minutes would be beneficial. However, time constraints did not permit these studies to be carried out at this time. Nevertheless, this is the first time that JAM-A has been shown to interact with these molecules on human UCB $CD34^+$ cells and the first time that JAM-A has been shown to interact with CD164 and CD82.

5.3.3. The internalisation of JAM-A and CD29 in the presence of CXCL12.

Cera *et al.* have shown that JAM-A and CD29 can internalise in murine neutrophils within 30 minutes of stimulating these cells with chemotactic peptides, WKYMVm or fMLP, and that this was altered in the absence of jam-a in murine jam-a null neutrophils (251). To test if CXCL12 altered the surface expression levels of JAM-A and integrin β1 (CD29), HL-60 cells were firstly examined for the presence of these two molecules after incubation with CXCL12 or AMD3100 for 4 hours and 24 hours.

JAM-A surface expression was not altered by CXCL12 (p=0.50) nor by AMD3100 (p=0.24) treatment for 4 hours (Figure 5.15.A) but there was a slight drop in JAM-A expression in both treatments at 24 hours (p=0.04 and p=0.02; Figure 5.15.B). A slight change of CD29 on

these cells in the presence of CXCL12 was only witnessed at 24 hours (p<0.01; Figure 5.15.D), whereas more significant changes were observed with AMD3100 at the two time points (both p<0.01, Figure 5.15.C and D).

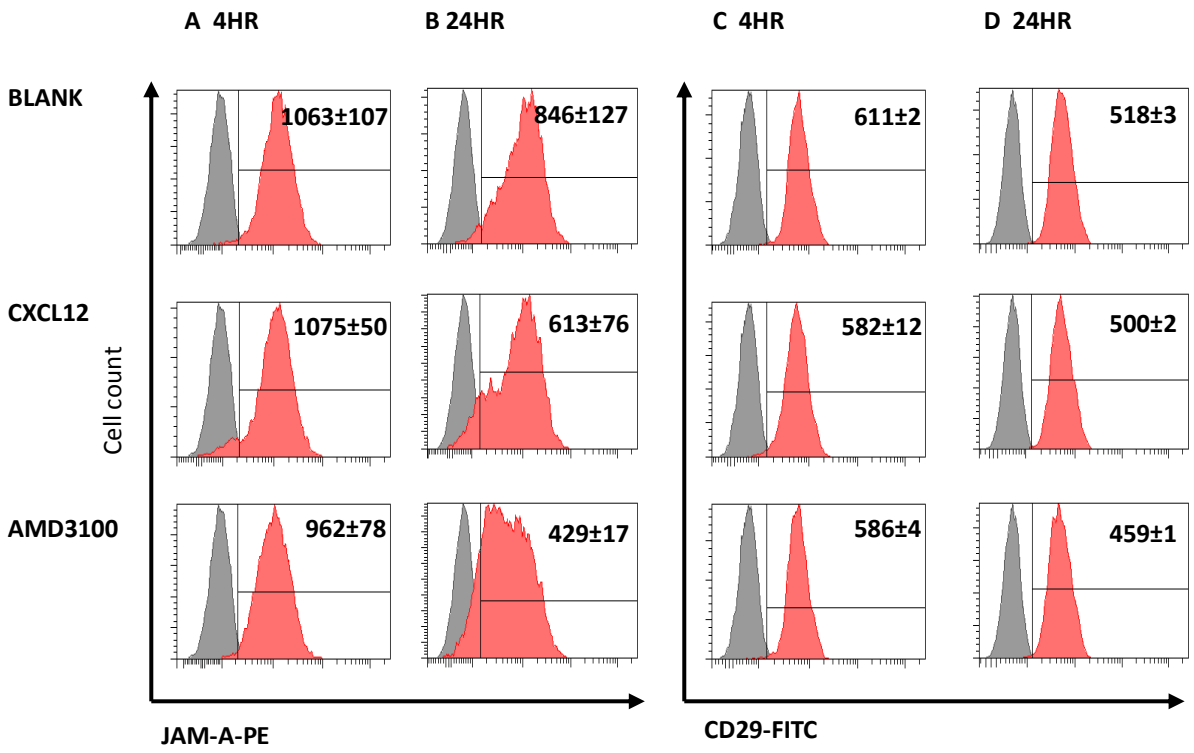

Figure 5.15. Phenotype of HL-60 cells with treatment of CXCL12 or AMD3100.
Representative FACS histograms of HL-60 cells incubated in IMDM medium with 0.5% BSA in the presence of 100ng/ml CXCL12, 5nM AMD3100 or medium along (Blank) for 4 hours (A,C) or for 24 hours (B,D), followed by staining with the (A,B) PE-JAM-A (M.Ab.F11), (C,D) FITC-CD29 (β1-integrin) antibodies (red) and their isotype controls (gray). M.F.I.± S.E.M. is shown in the top right corner of the plot. N=3 independent experiments.

To measure JAM-A and CD29 integrin internalisation, an immunofluorescence internalisation assay was applied. The protocol was published by Cera *et al.* (251) and was modified in order to measure JAM-A or integrin internalisation upon CXCL12 stimulation. In brief, HL-60 cells were pre-cooled and viable cells labelled with 10 μgs/ml JAM-A (M.Ab.F11) or CD29 (Mab 13) antibody on ice for 30 minutes. After unlabelled antibody was washed

away, the cells were seeded onto fibronectin-coated slides with or without CXCL12 and incubated at 37°C for the indicated time points (0 to 120 minutes). At each time point, the cells were washed in acid wash buffer, and this was followed by fixation, permeablisation and staining for microscopy analysis (Chapter 2 Section 2.15). Figure 5.16 shows JAM-A internalisation increased over time from 10 to 120 minutes and was statistically significant at 60 minutes and 120 minutes ($p<0.05$) when compared to 0 minutes.

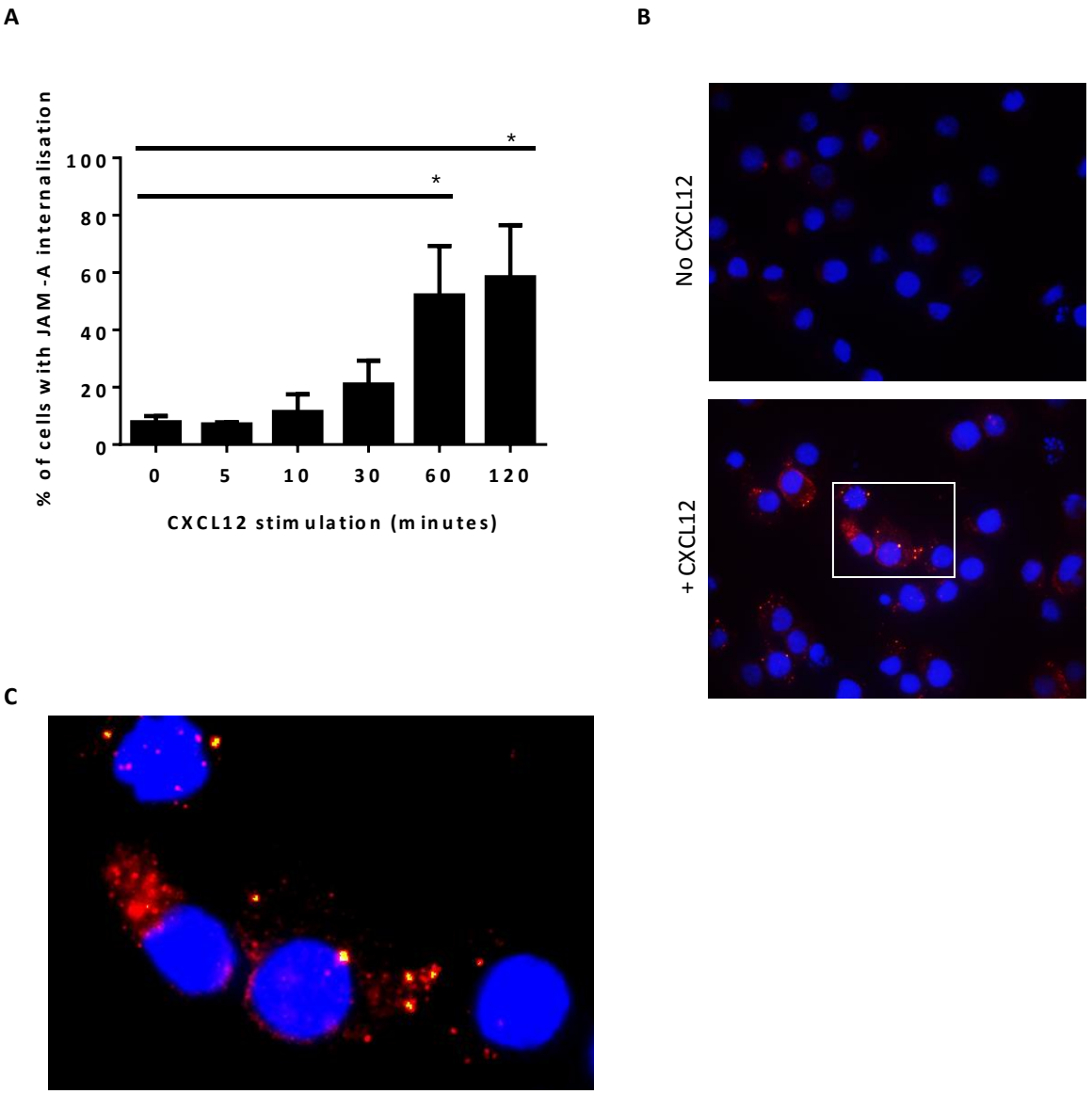

Figure 5.16. JAM-A internalised in HL-60 upon CXCL12 treatment.
Immunofluorescence internalisation analysis of JAM-A in HL-60 cells presented with 200 ng/ml CXCL12 on fibronectin from 0 to 120 minutes. The cells were stained with JAM-A (M.Ab.F11) and seeded on fibronectin-coated slides with or without CXCL12 for the indicated time, followed by acid washing to remove surface labelling. The cells were then fixed and labelled with Alexa fluor®555 goat anti-mouse IgG antibody. (A) depicts the percentage of JAM-A internalised at the indicated time. Values are means ± S.E.M. of 3 independent experiments where 100 cells were counted. The statistical analysis was done using Student's *t*-test and values < 0.05 (*) are considered significant. (B) shows the images at 0 and 120 minutes at X60 magnification and (C) shows an enlarged image from white square in (B).

The results of CD29 internalisation are shown in Figure 5.17. CD29 internalisation increased significantly at 60 and 120 minutes (Figure 5.17).

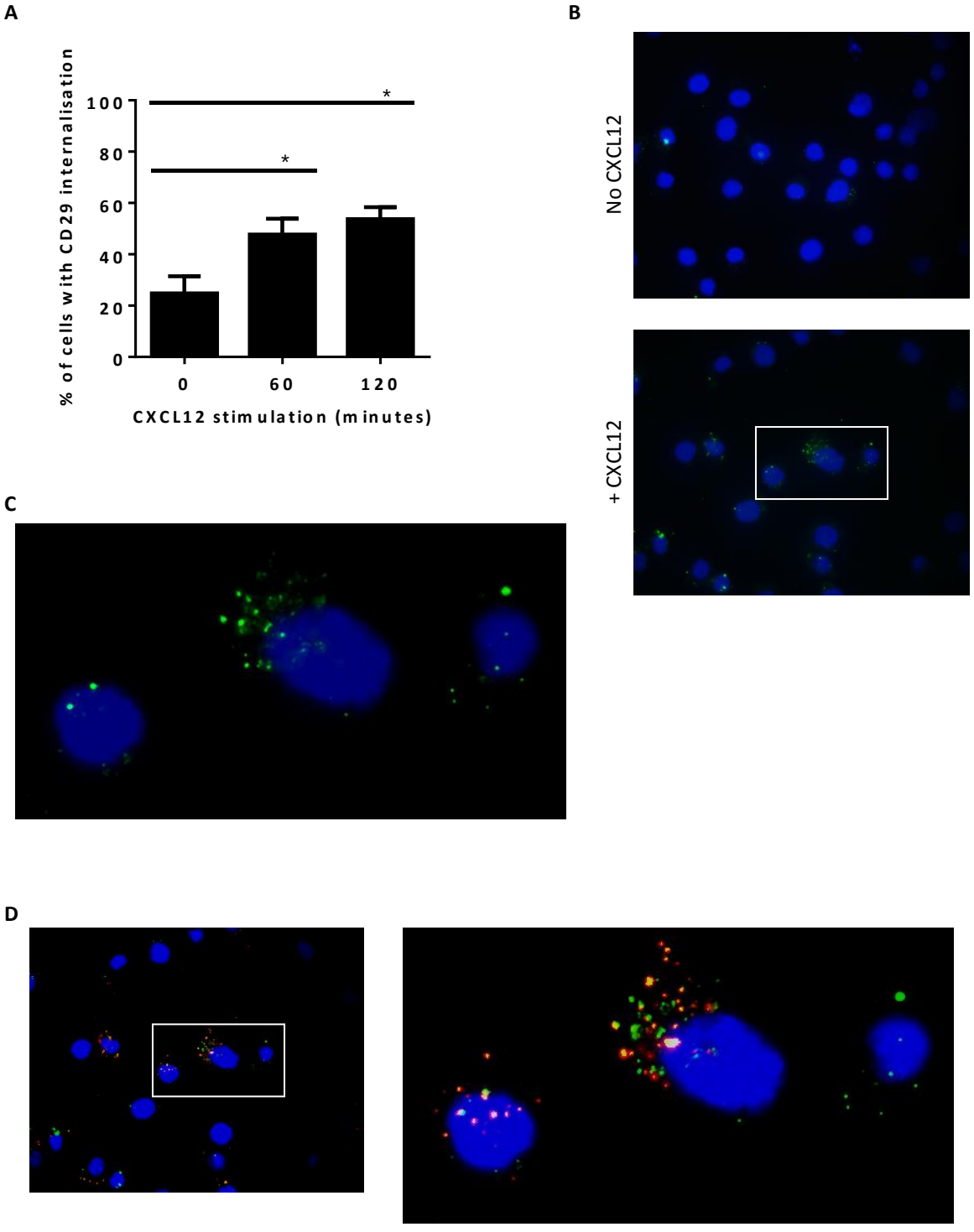

Figure 5.17. Integrin β1 (CD29) internalised in HL-60 upon CXCL12 treatment.
Immunofluorescence internalisation analysis of CD29 in HL-60 cells presented with 200 ng/ml CXCL12 on fibronectin from 0 to 120 minutes. The cells were stained with CD29 (Mab13) and seeded on fibronectin-coated slides with or without CXCL12 for the indicated time points, followed by acid washing to remove surface labelling. The cells were then fixed and labelled with Alexa fluor®488 goat anti-mouse IgG antibody. (A) depicts the percentage of JAM-A internalised at the indicated times. Values are means ± S.E.M. of 3 independent experiments for 0, 60 and 120 minutes where 100 cells were counted. The statistical analysis was done using Student's *t*-test and values < 0.05 (*) are considered significant. (B) shows the images at 120 minutes at X60 magnification and (C) shows an enlarged image from the white square in (B). (D) shows the merged staining of CD29 and JAM-A internalisation from the same field in (B) and (C).

To investigate whether JAM-A regulates β1-integrin internalisation, JAM-A was knocked down in HL-60 cells using previous validated siRNAs (150+151) and the internalisation assay performed as described previously. Figure 5.18 shows that β1-integrin internalisation was impaired in HL-60 cells with JAM-A knockdown at 60 minutes with the presence of CXCL12. Thus, from these initial studies, JAM-A appears to regulate CD29 internalisation on HL-60 cells in the presence of CXCL12. Further studies are required to determine if this also occurs in human UCB cells.

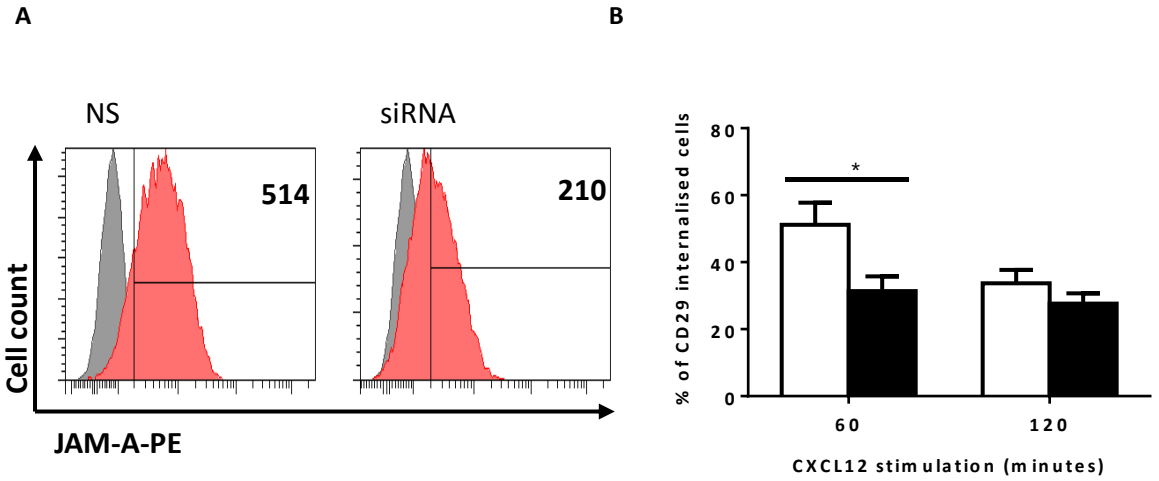

Figure 5.18. Impaired integrin β1 (CD29) internalisation in JAM-A-knock-down HL-60 cells upon CXCL12 treatment.
The cells were nucleofected with 100 nM non-silencing siRNA (NS; empty) or JAM-A siRNAs (150+151; black) followed by immunofluorescence internalisation analysis of CD29 in HL-60 cells presented with 200 ng/ml CXCL12 on fibronectin at 60 and 120 minutes. (A) The cells were stained with the PE-JAM-A antibodies (M.Ab.F11; red) and their isotype controls (gray) at 24 hours post nucleofection. Representative FACS histograms from one experiment are shown for the gates set for the isotype controls and the primary antibody stain in the top right corner of the plot. (B) The nucleofected cells were stained with CD29 (Mab13) and seeded on fibronectin-coated slides with or without CXCL12 for the indicated time points, followed by acid washing to remove surface labelling. The cells were then fixed, permeabilsed and stained. The percentage of internalisation at the indicated time is shown. Values are means ± S.E.M. of 3 independent experiments where 100 cells were counted. The statistical analysis was done using Student's *t*-test and values < 0.05 (*) are considered significant.

5.3.4. Does JAM-A regulate signalling pathways activated by CXCL12?

5.3.4.1. Phospho-kinase array analyses

One hypothesis from these studies is that JAM-A regulates downstream signalling mediated through CXCL12 and CXCR4 interactions. In order to obtain a global view of signalling activities occurring in response to CXCL12 stimulation and the influence of JAM-A on this signalling, because of the large numbers of cells needed to do these experiments and the cost implications, a pilot study was carried out by using HL-60 cell lysates with a Human Phospho-Kinase Antibody Array (R&D systems), which detects the relative site-specific phosphorylation of 40 kinases. The pilot experiment was designed as follows. HL-60 cells were first transfected with non-silencing (NS) or JAM-A siRNAs (Chapter 2 section 2.7). The cells were then cultured for 24 hours prior to exposure to CXCL12. HL-60 cells (NS or JAM-A siRNAs) were then cultured in the absence or presence of CXCL12 presented on fibronectin for 5 minutes, and the total protein lysates collected and applied to the array. The blotted filters were compared by first normalising the data to the positive control proteins and subtracting the normalised negative background controls, and then the fold differences determined with and without CXCL12 stimulation for each of the NS and siRNA samples. The results are shown Figure 5.19.B and the fold differences summarised in Table 5.1. There were 36 kinase phosphorylation sites detected that are listed as being potentially up-regulated and 10 as being potentially down-regulated (referred to as CXCL12 potentially up-regulated or CXCL12 potentially down-regulated in Table 5.1 respectively) in the non-silencing group upon CXCL12 stimulation (NS+CXCL12) in comparison to no CXCL12 treatment (NS no CXCL12).

A

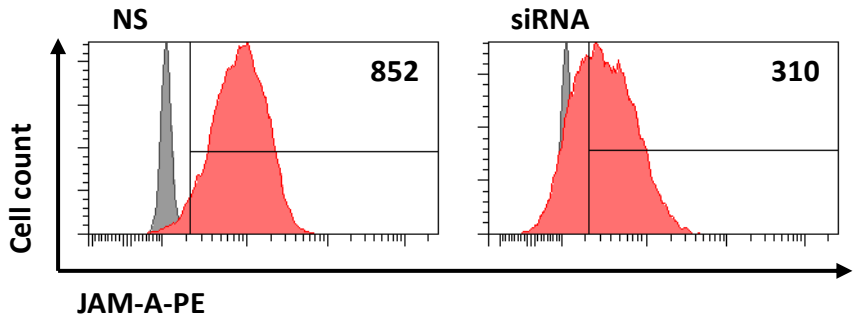

B

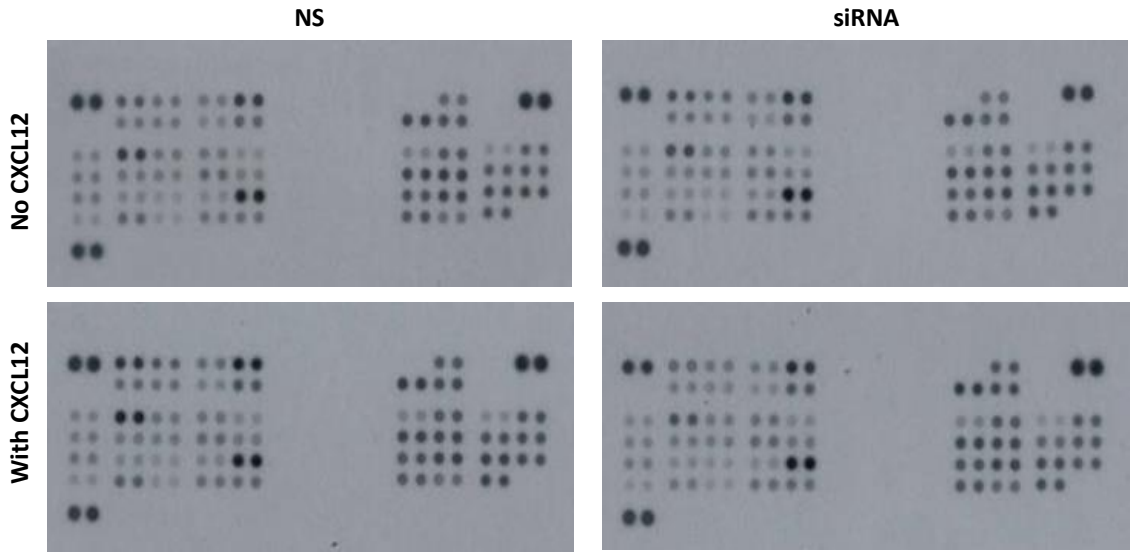

C

Positive control	p38a (T180/Y182)	ERK1/2 (T202/Y204, T185/Y187)	JNK pan (T183/Y185, T221/Y223)	GSK-3a/b (S21/S9)		p53 (S392)		Positive control
	MEK1/2 (S218/S222, S222/S226)	MSK1/2 (S376/S360)	AMPKa1 (T174)	Akt (S473)	Akt (T308)	p53 (S46)		
TOR (S2448)	CREB (S133)	HSP27 (S78/S82)	AMPKa2 (T172)	b-Catenin	p70 S6 Kinase (T389)	p53 (S15)	p27 (T198)	Paxillin (Y118)
Src (Y419)	Lyn (Y397)	Lck (Y394)	STAT2 (Y689)	STAT5a (Y699)	p70 S6 Kinase (T421/S424)	RSK1/2/3 (S380)	p27 (T157)	PLCg-1 (Y783)
Fyn (Y420)	Yes (Y426)	Fgr (Y412)	STAT3 (Y705)	STAT5b (Y699)	p70 S6 Kinase (T229)	RSK1/2 (S221)	c-Jun (S63)	Pyk2 (Y402)
Hck (Y411)	Chk-2 (T68)	FAK (Y397)	STAT6 (Y641)	STAT5a/b (Y699)	STAT1 (Y701)	STAT4 (Y693)	eNOS (S1177)	
Positive control		Negative control						Positive control

Figure 5.19. Global detection of phospho-kinases in HL-60 cells with JAM-A knockdown and following CXCL12 stimulation. Pilot study.

HL-60 cells at 24 hour post nucleofection of JAM-A siRNA (siRNA 150+151) or non-silencing control (NS) with or without 5-minute stimulation of 100 ng/ml CXCL12. (A) Representative FACS histograms of JAM-A expression on HL-60 cells at 24 hours post nucleofection. (B) The total cell lysates were performed on Human Phospho-Kinase Antibody Arrays (R&D Systems, Inc.) which recognise 46 specific phosphorylation sites on 40 kinases. (C) The distribution of detected phospho-kinases is shown.

In other published studies, an up regulation or down regulation of 1.5 fold or above compared to the negative control is considered to be significant (363). Based on such criteria and although there is the limitation that multiple independent analyses were not completed for either HL-60 cells or UCB $CD34^+$ cells in this thesis research, three of the proteins analysed were upregulated above 1.5 fold in the non-silencing group upon CXCL12 stimulation (NS+CXCL12) in comparison to no CXCL12 treatment (NS no CXCL12) and these are highlighted in Table 5.1 in bold and red. These upregulated phophokinases in HL-60 cells treated with CXCL12 were firstly ERK1/2 (extracellular-signal-regulated kinases 1/2; also known as MAPK3/1) that form part of the Ras-Raf-ERK signal transduction cascade (reviewed in (364)) with ERK1 here being phosphorylated on Threonine 202 and Tyrosine 204, and ERK2 being phosphorylated on Threonine 185 and Tyrosine 187. The known CXCL12/CXCR4 signalling cascade through ERK for adhesion and proliferation is shown in the Discussion in Figure 5.26. The second was p38 MAP kinase alpha, a serine/threonine kinase (reviewed in (365)), phosphorylated here on Threonine 180 and Tyrosine 182. p38 signalling has been reported previously to regulate ALL cell chemotaxis towards CXCL12 (217) and cell adhesion (366). The third was p53 where the post translational modification was observed with phosphorylated Serine 392, but Serine 15 and Serine 46 were not phosphorylated above 1.5 fold in the non-silencing group upon CXCL12 stimulation compared to no CXCL12. It is reported that p38 MAPK can phosphorylate Serine 392 on p53, whereas Erk1/2 can phosphorylate Threonine 55 on p53 (reviewed in (367)). p53 has been shown to have a role in haematopoietic stem cell biology where it regulates HS/PC proliferation and differentiation, while maintaining genetic stability (reviewed in (368)). When JAM-A was knocked down in HL-60 cells and the knockdown cells stimulated with CXCL12 (siRNA+CXCL12), the up-regulated phosphorylation of ERK1/2 (NS+CXCL12 vs.

siRNA+CXCL12: 2.01 vs. 1.18) and p38a (NS+CXCL12 vs. siRNA+CXCL12: 1.83 vs. 0.86) was substantially reduced (Table 5.1; red and bold highlighted figures). There appeared to be very little effect of JAM-A knockdown on p53 at any of the sites tested (Serine15, 46 or 392). Furthermore, when the data were compared to JAM-A knockdown without CXCL12 stimulation, it appeared that CXCL12 but not JAM-A was required for p53 (S392) phosphorylation, both JAM-A and CXCL12 were required for p38a (T180/Y182) phosphorylation and JAM-A and CXCL12 activated ERK1/2 by phosphorylating T202/Y204 and T185/Y187 independently or perhaps synergistically. Additionally, Chk2 (T68) (checkpoint kinase 2) and CREB (S133) (cyclic adenosine monophosphate response element binding protein), to a lesser extent, were down regulated with JAM-A knockdown after CXCL12 stimulation (Table 5.1; orange and bold highlighted figures), suggesting that JAM-A is positively regulating the response of these cells to CXCL12 through intermediates.

Two additional phospho-kinases, STAT5a (Y699) and β-catenin, showed enhanced phosphorylation in response to CXCL12 (almost 1.2 fold), and this was further increased (above 1.5 fold) with JAM-A knockdown in CXCL12 stimulated HL-60 cells (Table 5.1; blue and bold highlighted figures). AMPKa2 (T172) showed a similar pattern to the above two kinases. Thus, JAM-A appears to be negatively regulating the response of these cells to CXCL12.

When CXCL12 stimulation in the presence or absence of JAM-A was compared with the JAM-A knockdown without CXCL12 stimulation, p70 S6 kinases showed a >1.5 fold up-regulation of phosphorylation in JAM-A knockdown cells, at Threonine 229 and Threonine 421/Serine 424 (Table 5.1; green and bold highlight). These were not substantially altered by CXCL12 stimulation in NS control cells. Thus, JAM-A appears to negatively affect p70 S6 kinase phosphorylation in the absence of CXCL12 stimulation.

Table 5.1. Fold differences of 46 specific kinase phosphorylation sites on 40 kinases in HL-60 cells with JAM-A knockdown and in the presence of CXCL12.

Kinase (Phosphorylation sites)	NS + CXCL12	siRNA + CXCL12	siRNA no CXCL12
CXCL12 potentially up-regulated			
ERK1/2 (T202/Y204, T185/Y187)	**2.01**	**1.18**	**1.50**
p38a (T180/Y182)	**1.83**	**0.86**	**1.09**
p53 (S392)	**1.51**	**1.42**	**1.18**
JNK pan (T183/Y185, T221/Y223)	1.36	1.22	1.09
GSK-3a/b (S21/S9)	1.36	1.47	1.12
AKT (S473)	1.35	1.47	1.11
CREB (S133)	**1.32**	**0.76**	**0.82**
Paxillin (Y118)	1.30	1.02	1.35
p27 (T157)	1.28	0.75	1.25
MEK1/2 (S218/S222, S222/S226)	1.27	0.87	0.98
eNOS (S1177)	1.27	1.07	1.46
PLCγ-1 (Y783)	1.26	0.98	1.29
p70 S6 Kinase (T229)	**1.26**	**1.32**	**1.56**
c-Jun (S63)	1.25	0.97	1.33
p27 (T198)	1.24	0.93	1.21
p70 S6 Kinase (T421/S424)	**1.24**	**1.19**	**1.56**
MSK1/2 (S376/S360)	1.23	0.91	0.96
STAT5a/b (Y699)	1.21	1.37	1.17
Chk-2 (T68)	**1.20**	**0.58**	**0.77**
STAT4 (Y693)	1.19	1.23	1.36
STAT6 (Y641)	1.19	1.38	1.26
STAT5a (Y699)	**1.17**	**1.57**	**0.84**
RSK1/2 (S221)	1.16	1.10	1.40
β-Catenin	**1.16**	**1.71**	**0.83**
p70 S6 Kinase (T389)	1.15	1.16	1.17
FAK (Y397)	1.15	1.18	0.86
p53 (S15)	1.13	1.06	1.12
AKT (T308)	1.13	1.11	1.14
STAT3 (Y705)	1.13	1.25	1.05
STAT1 (Y701)	1.11	1.13	1.43
p53 (S46)	1.10	1.01	0.96
Lck (Y394)	1.09	1.19	0.97
Fgr (Y412)	1.08	1.15	0.97
HSP27 (S78/S82)	1.05	1.03	0.95
Fyn (Y420)	1.01	0.83	0.71
AMPKa2 (T172)	**1.01**	**1.46**	**0.90**

The pixel intensity of each phospho-kinase on the blots in Figure 5.19.B. was analysed using Quantity One 4.6.3 basic software (Bio-Rad Laboratories Inc.) as described in section 2.10.7. The average value of the duplicate of each kinase was normalised to their NS without CXCL12 control as 1.00. The kinases with values > 1.00 in NS with CXCL12 (NS + CXCL12) samples were defined as CXCL12 potentially up-regulated kinases, while the values < 1.00 were defined as CXCL12 potentially down-regulated kinases as shown. The kinases were then listed in the table in a descending order based on the values in NS + CXCL12 column 2.

Table 5.1 continued. Fold differences of 46 specific kinase phosphorylation sites on 40 kinases in HL-60 cells with JAM-A knockdown and in the presence of CXCL12 (continued).

Kinase (Phosphorylation sites)	NS + CXCL12	siRNA + CXCL12	siRNA no CXCL12
CXCL12 potentially down-regulated			
AMPKa1 (T174)	0.99	1.05	0.87
Lyn (Y397)	0.99	1.09	0.86
RSK1/2/3 (S380)	0.94	0.90	1.10
Yes (Y426)	0.94	0.98	0.82
Hck (Y411)	0.93	0.81	0.78
Pyk2 (Y402)	**0.92**	**0.67**	**1.09**
STAT2 (Y689)	0.92	1.09	0.74
STAT5b (Y699)	0.90	1.24	0.78
TOR (S2448)	0.87	0.72	0.81
Src (Y419)	**0.75**	**0.64**	**0.60**

The pixel intensity of each phospho-kinase on the blots in Figure 5.19.B. was analysed using Quantity One 4.6.3 basic software (Bio-Rad Laboratories Inc.) as described in section 2.10.7. The average value of the duplicate of each kinase was normalised to their NS without CXCL12 control as 1.00. The kinases with values > 1.00 in NS with CXCL12 (NS + CXCL12) samples were defined as CXCL12 potentially up-regulated kinases, while the values < 1.00 were defined as CXCL12potentially down-regulated kinases as shown. The kinases were then listed in the table in a descending order based on the values in NS + CXCL12 column 2.

Additionally, JAM-A appeared to positively regulate Src (Y419) and Pyk2 (Y402) phosphorylation in the absence or presence of CXCL12 respectively (Table 5.1; purple and bold highlighted figures). The former did not change with CXCL12, while the latter appeared additive with CXCL12. Thus, from these pilot studies, JAM-A knockdown appeared to affect different signalling pathways differently in the presence and absence of CXCL12. It would be ideal to repeat these studies on multiple batches of HL-60 cells and UCB $CD34^+$ cells to confirm these findings and pathways in more detail and to validate these results in other assays, as these were experiments that could not be finalised because of time constraints.

5.3.4.2. Potential signalling pathways affected by JAM-A

A working hypothesis was developed from the studies in section 5.3.4.2. This is illustrated in Figure 5.20. Further studies are required to validate this hypothesis and these signalling effects.

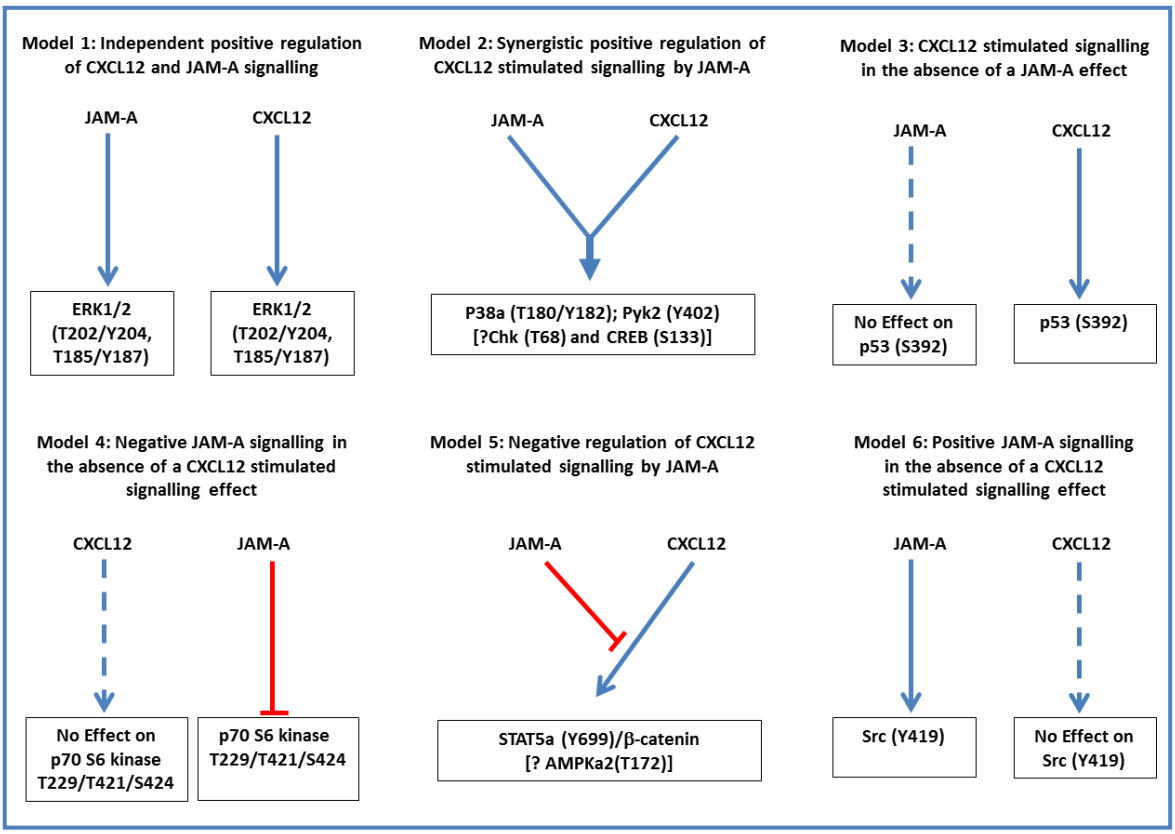

Figure 5.20. A hypothesis for crosstalk between JAM-A and CXCL12 stimulated signalling.
Six potential working models for the regulation of JAM-A and CXCL12 stimulated protein kinase phosphorylation. The blue filled lines and arrows show enhanced phosphorylation of intermediates, while the red lines show a negative effect on CXCL12 stimulated signalling via these phosphorylated intermediates. The dotted blue line demonstrates no effect.

5.3.4.3. Does JAM-A regulate the ERK1/2 signalling pathway independently of CXCL12?

The array results above, although preliminary, highlight ERK1/2 as one of the potentially important signalling molecules that is modulated by JAM-A and by CXCL12 stimulation of

HL-60 cells. As JAM-A expressing and non-expressing Jurkat cells had been made in this laboratory and during this D.Phil. thesis research, as sufficient UCB $CD34^+$ cells were difficult to source and as others have confirmed that Jurkat cells respond to CXCL12 by phosphorylating ERK1/2 (369), the first experiments were carried out using Jurkat cells. From literature reviews, two additional potential CXCR4 downstream signalling pathways were included with the ERK1/2 analysis in the initial screen. These were AKT (140), and PKCζ (140). In the pilot experiment, CXCL12 added to non-transduced Jurkat cells which did not express JAM-A led to ERK1/2 phosphorylation between 30 to 60 seconds after the addition of CXCL12 (Figure 5.21). AKT, but not PKCζ, showed slightly enhanced phosphorylation in Jurkat cells stimulated with CXCL12 at 60 minutes, although further repeats are required to confirm these findings and to test additional timepoints for CXCL12 stimulation (Figure 5.21). This initial experiment was taken further by examining whether JAM-A negative (but transduced with an empty vector) or JAM-A positive Jurkat cells signalled similarly when stimulated with 100 nM CXCL12 (Peprotech) at 0, 30 or 60 seconds. Three separate transductions were done and tested. Figure 5.22 confirms that all three JAM-A transduced Jurkat cells expressed JAM-A and that this JAM-A expression was slightly increased in three experiments with CXCL12 stimulation over 60 seconds. In three experiments, CXCL12 enhanced AKT phosphorylation slightly, while JAM-A expression plus CXCL12 stimulation reduced AKT phosphorylation slightly, but not significantly, at 60 seconds (Figure 5.22). PKCζ signalling was not significantly affected over the time period analysed. ERK phosphorylation was enhanced with JAM-A expression and upon CXCL12 stimulation in two of the transduced Jurkat cell groups (Figure 5.22). The levels of phosphorylated ERK1/2 in these Jurkat cells which had been transduced with an empty lentiviral vector appeared to be reduced when compared to the non-transduced Jurkat cells. Phosphorylated ERK1/2 was

not detected in the third clone either when transduced with empty vector or with the JAM-A containing vector alone. Unfortunately time constraints did not allow this to be analysed further.

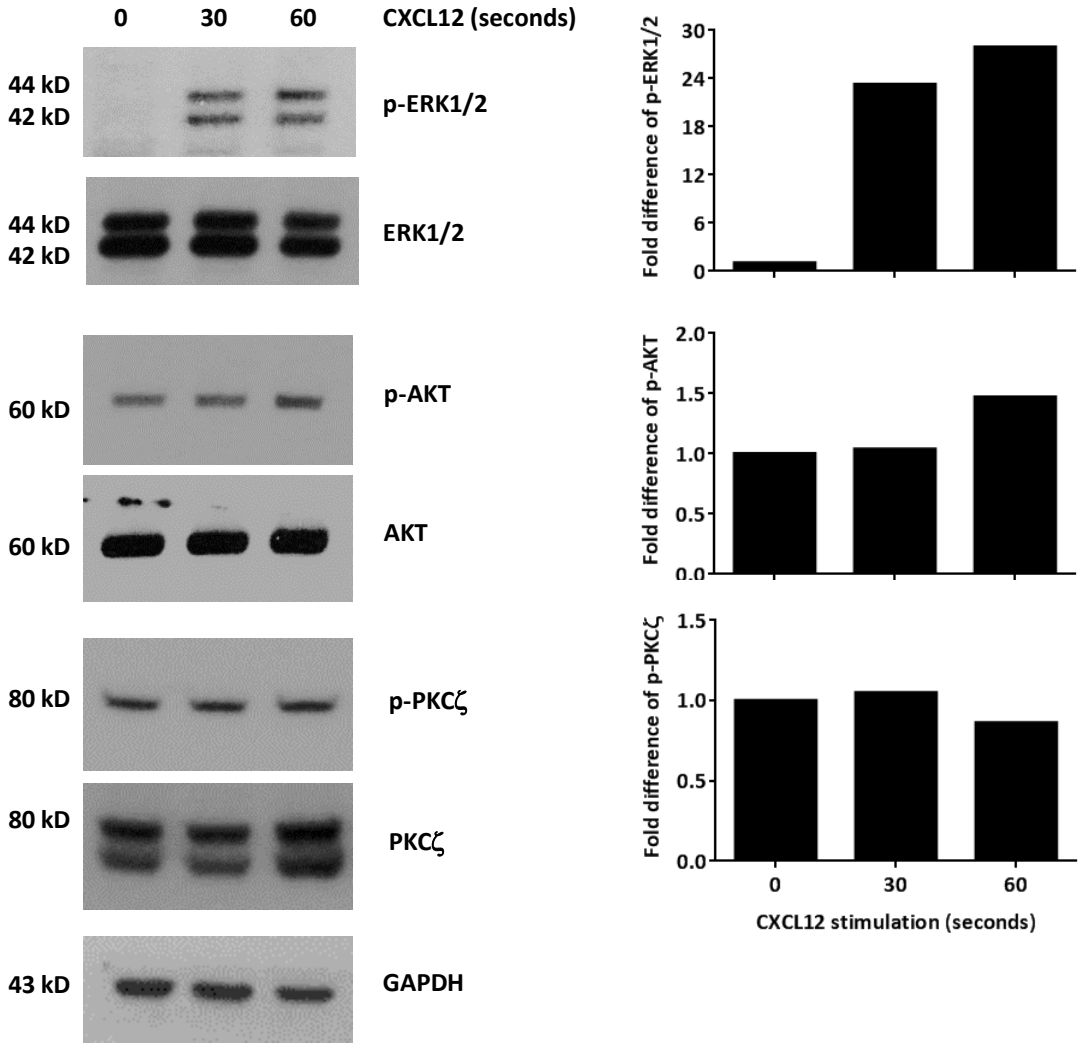

Figure 5.21. CXCR4 downstream signalling in Jurkat cell.
Phospho-ERK1/2 (p-ERK1/2), phospho-AKT and phospho-PKC-ζ signalling were examined in Jurkat cells upon stimulation with 100 nM CXCL12 for 0, 30 and 60 seconds. GAPDH was used as a loading control with phospho protein levels compared with their total protein signal after being normalised to the total at 0 seconds as 1.00 for an average of n=2 assays. The band sizes are shown to the left of the blots.

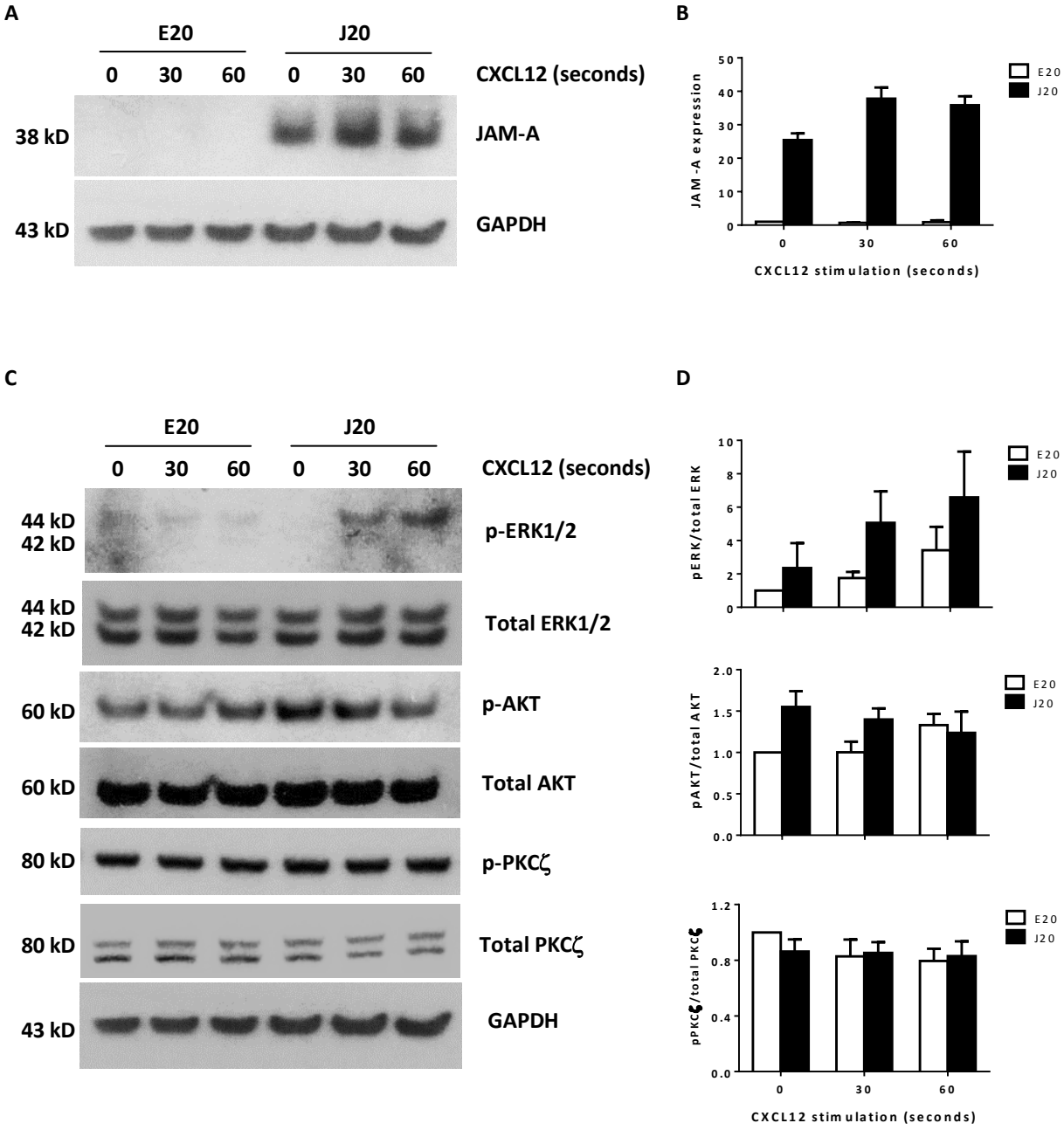

Figure 5.22. CXCR4 Signalling pathway detection in Jurkat cell with overexpression of JAM-A.
Jurkat cells were transduced with lentiviral vector particles containing JAM-A (J20) or empty vector (E20) as an experimental control. The cells were stimulated with 100 nM CXCL12 (Peprotech) for 0, 30 and 60 seconds. The total protein lysates were collected to test (A) JAM-A expression and (C) the phosphorylation of ERK1/2, AKT and PKCζ kinases by Western blotting. GAPDH was used as the loading control. The blots represent one from n=3 independent experiments. The band sizes are shown to the left of the blots. (B) and (D) Densitometry analysis of fold difference of the phosphorylated kinase normalised to the total amount of kinase protein is shown. Values are means ± S.E.M. of 3 independent experiments for 0, 30s and 60s.

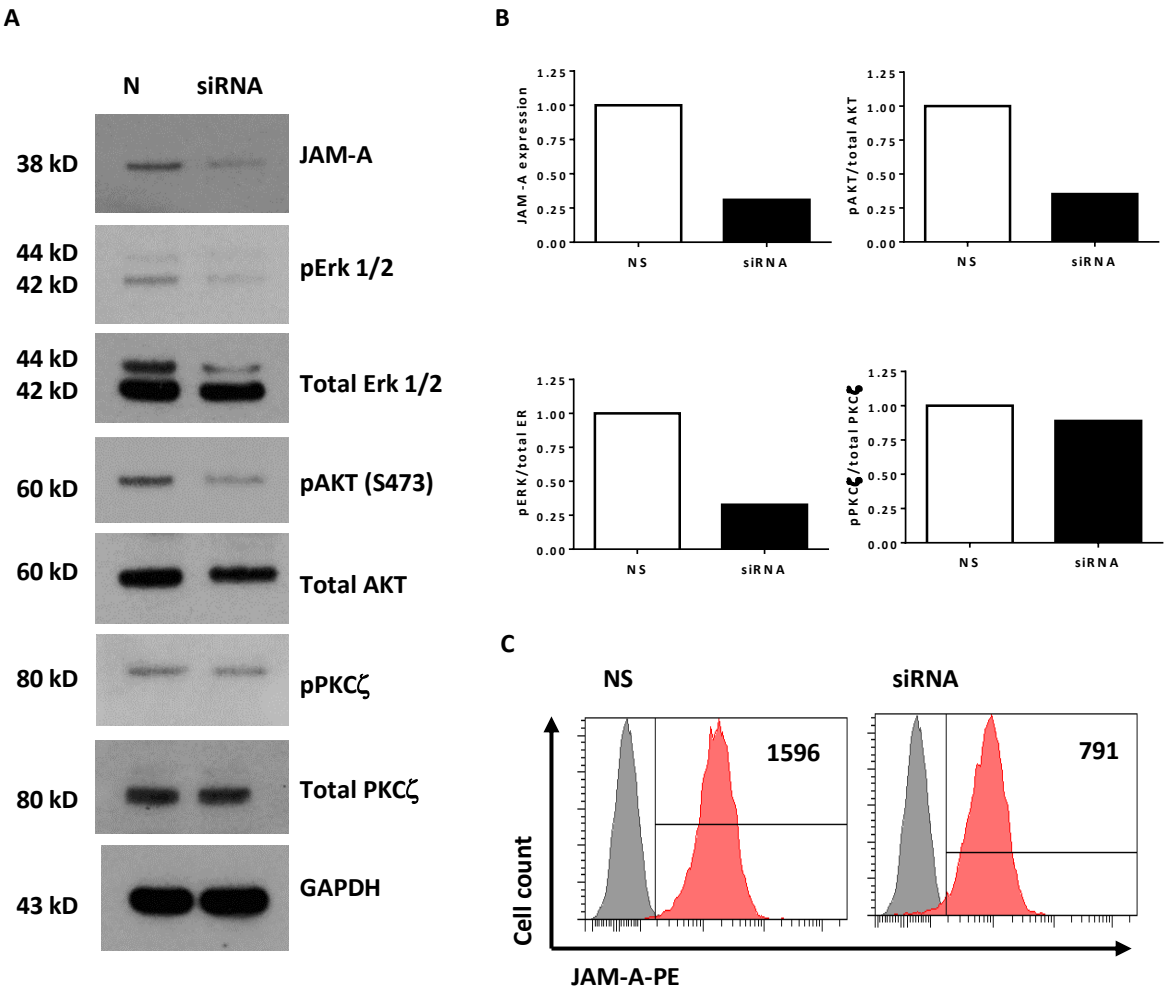

Figure 5.23. CXCR4 Signalling pathway detection in UCB CD34$^+$ cells with JAM-A silencing. Pilot study. 1x10^7 UCB CD34$^+$ cells were purified from frozen UCB MNCs and cultured overnight in Stemspan medium with SCF, IL-6, Flt-3 ligand and TPO (Chapter 2 Section 2.3) before being nucleofected with 100nM JAM-A siRNAs (150+151) or the non-silencing siRNA control (NS; Chapter 2 Section 2.7) and the cells cultured overnight. The cells were then stimulated with 100 nM CXCL12 (Peprotech) from 30 seconds. (A) The total protein lysates were collected for the JAM-A and phospho-kinase analysis by Western blotting and (B) densitometry analysis of phosphorylated kinase normalised to the total amount of kinase protein is shown. GAPDH here represented the loading control. The band sizes are shown to the left of the blots. (C) Representative FACS histograms of surface JAM-A expression on UCB CD34$^+$ cells at 24 hours post nucleofection (n=1).

To overcome potential effects of the lentiviral vector on the cells, a preliminary analysis was also carried out on human UCB CD34$^+$ cells with JAM-A knocked down using specific JAM-A siRNAs or NS siRNA. These cells had been grown in Stemspan medium with 4 cytokines for 2 days before being stimulated with CXCL12 (Chapter 2 section 2.11.2). JAM-A was knocked down in UCB CD34$^+$ cells by ~70% of total protein as defined by Western blotting and by

~50% of the cell surface level as defined by FACS analysis. In these pilot studies this affected both ERK1/2 and AKT phosphorylation more than PKCζ in these cells (Figure 5.23). Knockdown of JAM-A appeared to affect the levels of total ERK1/2 and AKT and this needs to be examined further as highlighted in the Discussion. Again, time constraints did not allow this to be investigated fiurther.

5.3.4.4. Does JAM-A regulate the Rap1 signalling pathway in the presence of CXCL12?

While the studies on ERK1/2 signalling were being conducted, experiments were also established with Rap1 signalling as Rap1 has been also shown separately to mediate the signalling of both CXCR4 (370) and JAM-A (251) in certain cell types such as neutrophils and lymphoid cells. A Rap1-GTP pull down kit (Thermo Fisher Scientific Inc.) was used first to study the effects of JAM-A overexpression in Jurkat cells on Rap1 phosphorylation in the presence of CXCL12. Jurkat cells that had been transduced with lentiviral particles containing JAM-A (J20) or empty vector (E20) were stimulated with 100 nM CXCL12 (Peprotech) from 0 to 60 seconds in RPMI-1640 medium without serum. The procedure used was modified from a published protocol (371), the details of which were described in Chapter 2, section 2.11. The protein lysates were extracted as recommended in the Rap1-GTP pull down kit (Thermo Fisher Scientific Inc.). Rap1 phosphorylation was examined first in non-transduced Jurkat cells and Rap1 was phosphorylated with CXCL12 stimulation from 30 to 60 seconds (Figure 5.24.A). Following on from this, Jurkat cells transduced with empty viral vector (E20) or JAM-A (J20) were examined. The results show that the phosphorylation of Rap1 was enhanced with overexpression of JAM-A with CXCL12 stimulation, but Rap1 phosphorylation was also found to increase with JAM-A and without CXCL12 albeit to a lesser extent (Figure 5.24.B). The effects resemble model 2, where CXCL12 and JAM-A act

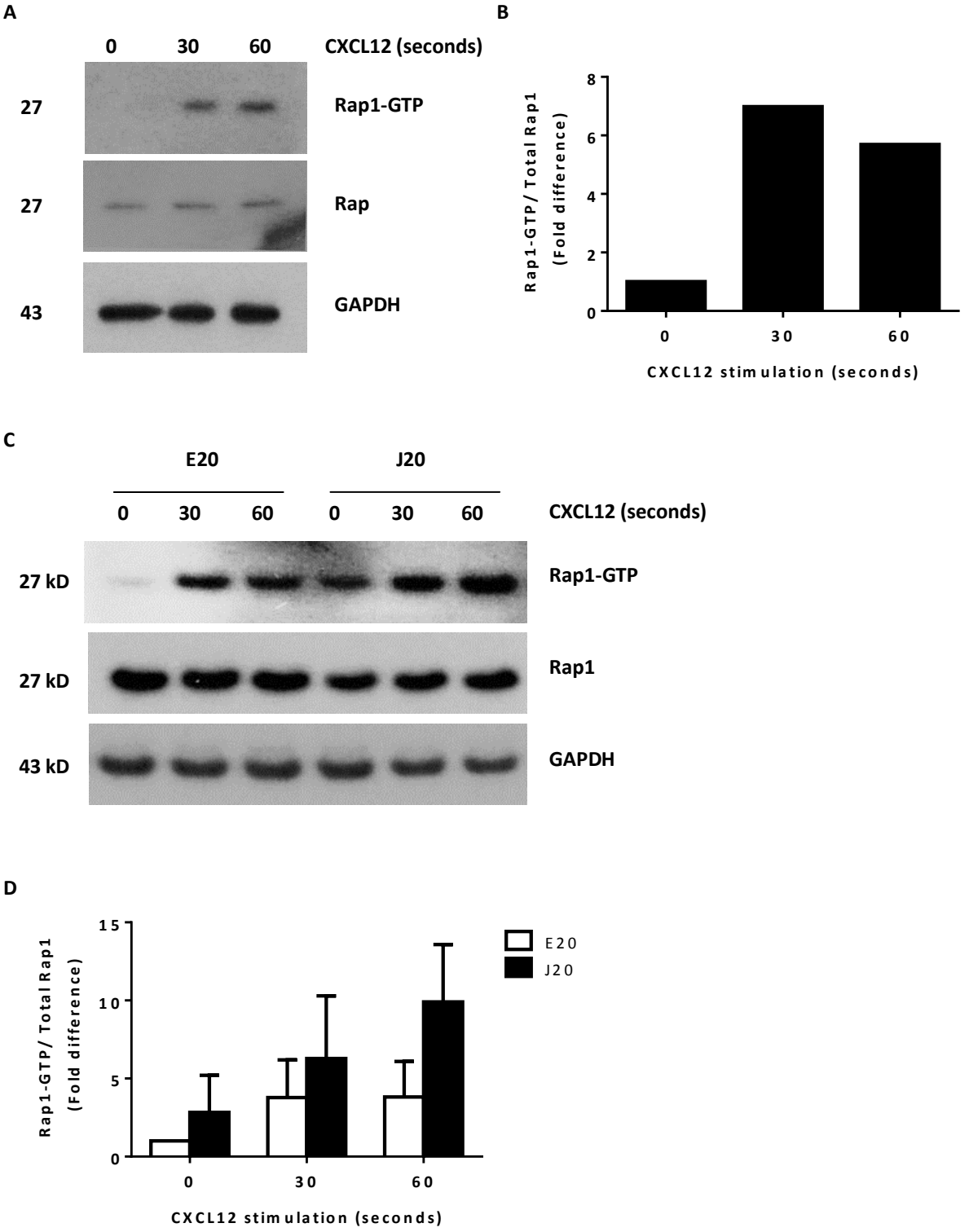

Figure 5.24. Rap1 phosphorylation by CXCL12 and JAM-A in Jurkat cells.
(A) Non-transduced Jurkat cells (N=2) and (C) the transduced Jurkat cells (N=3) with lentiviral vector particles containing JAM-A (J20) or empty vector (E20) as an experimental control were stimulated with 100 nM CXCL12 (Peprotech) for 0, 30 and 60 seconds. A pull-down assay was performed on cell lysates using RalGDS-RBD probe to isolate active Rap1 (Rap1-GTP) and the lysates then analysed by Western blotting using total Rap1 and GAPDH as loading controls. The band sizes are shown to the left of the blots. (B) and (D) depict densitometry analysis of active Rap1 normalised to the total amount of Rap1 protein. Values are means ± S.E.M. of 2-3 independent experiments for 0, 30s and 60s.

synergistically to stimulate this pathway (Figure 5.21). Rap1 phosphorylation analysis was performed on human UCB CD34$^+$ cells using similar conditions. However, since it was difficult to source sufficient numbers of cells similar to the numbers used for the Jurkat studies and even though total Rap1 protein was detectable in UCB CD34$^+$ cell lysate, the active form of Rap1 was not detected and no conclusions could be drawn (Figure 5.25). Again the JAM-A knockdown appeared to affect total Rap1 and again this needs to be investigated further.

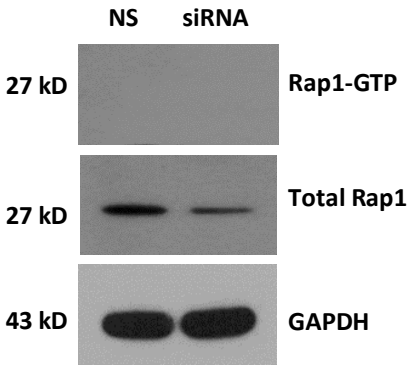

Figure 5.25. Rap1 phophorylation in UCB CD34$^+$ cells with JAM-A silencing.
5x10^6 UCB CD34$^+$ cells for each condition were purified from frozen UCB MNCs and cultured overnight in Stemspan medium with SCF, IL-6, Flt-3 ligand and TPO (Chapter 2 Section 2.3) before being nucleofected with 100nM JAM-A siRNA (150+151) or non-silencing control (NS; Chapter 2 Section 2.7) and cultured overnight in Stemspan medium with the 4 cytokines followed by stimulation with 100 nM CXCL12 (Peprotech) for 30 seconds. A pull-down assay was performed on cell lysates using RalGDS-RBD probe to isolate active Rap1 (Rap1-GTP) and Western blotting for Rap1 and GAPDH as a loading control. The band sizes are shown to the left of the blots. Representative of one of N=2 experiments.

5.4. Discussion

Many investigations have concentrated on the role of CXCL12 on HS/PC chemotaxis and show that CXCL12 regulates HS/PC homing to and engraftment in the bone marrow and the translocation of HS/PCs within the bone marrow niches. The role of CXCL12/CXCR4 in enhancing cell adhesion to endothelia has been relatively less well studied than its role in

chemotaxis, although CXCL12 is known to activate the integrin VLA-4 on HS/PCs allowing these cells to adhere firmly to VCAM-1 on sinusoidal endothelia in bone marrow (354). It has also been shown that presentation of CXCL12 on bone marrow endothelial cells facilitates leukaemic cell adhesion and the redistribution of homing molecules on the polarised target cells (189).

The studies presented here confirm the expression of CXCL12 by bone marrow endothelial cells, as well as by the bone marrow endothelial cell line, BMEC-60. This suggests but does not prove that CXCL12 originating from BMECs may play a role in activating VLA-4 integrin on HS/PCs and in subsequent interaction and the adhesion of HS/PCs to the sinusoidal endothelia. The results further indicate that, after CXCL12 exposure, JAM-A is likely to play an essential role in this process since both co-localisation and proximity ligation assays indicate that it rapidly interacts with the CXCL12 chemokine receptor, CXCR4, as well as with its co-receptor, CD164, plus β1-integrin and CD82 at the leading edge of human UCB $CD34^+$ cells and HL-60 cells. This confirms and extends earlier research by Forde *et al*. (140) who demonstrated that CXCR4 incorporates CD164 and the Integrin VLA-4 in a homing/adhesion complex in response to CXCL12 stimulation. A further method to confirm the interaction of these molecules with JAM-A would be to carry out co-immunoprecipitation experiments of JAM-A with each of its interacting partners.

This latter experiment and signalling studies described below were hindered by time constraints in completing the thesis research and only preliminary studies could be conducted as described below. To identify potential mechanisms through which JAM-A and CXCL12/CXCR4 co-regulate cell adhesion, a pilot phospho-kinase proteome array was performed in JAM-A knockdown cells in the presence or absence of CXCL12, and a 1.5-fold difference was used to identify potential changes in the phosphorylation of kinases. This

was a pilot experiment in a cell line where cell numbers are not restricted. This experiment needs to be repeated but preferably using human UCB $CD34^+$ cells without knockdown, or $CD34^+$ cells transfected with non-silencing or JAM-A siRNAs and then the cells treated with or without CXCL12. This would be a challenging experiment as $CD34^+$ cells are present in UCB in low amounts and substantial numbers of cells would be required to probe multiple membranes in such an assay. The feasibility of this is being reviewed. However, despite the limitations of this pilot experiment, this preliminary analysis suggested that JAM-A could have a number of different potential regulatory roles. The first was that it could act independently of CXCL12 stimulation, with both CXCL12 and JAM-A enhancing signalling through ERK1/2 (also known as p44/p42 MAPK or MAPK3/1) phosphorylation. Attempts were made to begin to confirm these effects by Western blotting studies using JAM-A non-expressing and expressing Jurkat cells with or without CXCL12 stimulation. First, phosphorylation of ERK1/2 in parental JAM-A^- Jurkat cells was only detected in the presence of CXCL12 when tested at 30 and 60 seconds, and this indicates that CXCL12 is a critical activator for this kinase phosphorylation. Second, when analysed in Jurkat cells which had been stably transduced with a non-silencing control gene, ERK1/2 phosphorylation was low compared to the original Jurkat cell line, although ERK phosphorylation increased with CXCL12 stimulation. JAM-A expression in Jurkat cells enhanced ERK activation upon CXCL12 stimulation, but only the upper phosphorylated band appeared to be detected. Further experiments are required to directly compare non transduced Jurkat cells with non-expressing empty vector and JAM-A transduced cells in the same experiment to ensure that ERK1/2 phosphorylation is not affected by the lentiviral transduction. A preliminary experiment was carried out in UCB $CD34^+$ cells to test the phosphorylation of ERK1/2, AKT and PKCζ after CXCL12 stimulation in cells transfected with a non-silencing siRNA and this

was successfully demonstrated. When this experiment was done with JAM-A siRNA knockdown, pERK1/2 and pAKT were reduced. However, there was also a slight reduction in total ERK1/2 and AKT, indicating that, while promising, further optimisation is necessary, using lower siRNA concentrations in the transfection or analysing each JAM-A siRNA independently.

The ERK signalling pathways have been widely studied and shown to regulate a range of cellular processes, such as cell proliferation, differentiation, adhesion and chemotaxis. ERK1/2 is a downstream effector of CXCL12/CXCR4 axis, regulating cell adhesion and proliferation (214). Previously in our laboratory, Forde *et al.* showed AKT and PKCζ were phosphorylated after a ≥1 minute stimulation with CXCL12 (140). The former, but not the latter, was observed in the parental Jurkat cells in the experiments carried out here where CXCL12 stimulation was for 30 to 60 seconds. Forde *et al.* also showed that CD164 was not required for ERK1/2 phosphorylation in HS/PC in response to CXCL12 (140). Here, our hypothesis is that CXCL12 from BMECs and JAM-A act synergistically to induce the phosphorylation of ERK1/2. This may be aided by the complex that JAM-A and CXCR4 forms in response to CXCL12. β1 integrin and the tetraspanin, CD82, are also found to be incorporated into this CXCR4-JAM-A complex. This might allow JAM-A to interact with its cognate ligand on BMECs, a process which might further enhance ERK1/2 phosphorylation in a CXCL12 independent manner and contribute to the firm adhesion of HS/PCs to the bone marrow sinusoidal endothelium.

There are other potential signalling pathways where JAM-A and CXCR4 may interact and which may be investigated further to validate the preliminary phosphokinase array results. For example, p38a appears to be phosphorylated through the synergistic action of CXCL12 and JAM-A, while phosphorylation of β-catenin and STAT5a by CXCL12 stimulation is

downregulated by JAM-A. In contrast, p70 S kinase appears to be downregulated by JAM-A in the absence of CXCL12 stimulation in HL-60 cells. The p38a MAPK is reported to be involved in chemotaxis towards CXCL12 (217), while β-catenin is a well-known downstream effector of WNT signalling that regulates HS/PC self-renewal vs. quiescence (128, 129), homeostasis (130) and maintenance (131). STAT5 modulates lymphocyte development and overexpression of its constitutively activate form is sufficient to cause chronic myeloid leukaemia (reviewed in (373)). Earlier studies have demonstrated that CXCL12 activates Janus kinase 2 (JAK2) and JAK3 but not JAK1 (374) through a G-protein independent manner, and that this subsequently leads to the activation of the STAT family of transcription factors. STAT5 activation by CXCL12 in ALL leukaemic cells supports their cell proliferation and survival (375). Thus, JAM-A may regulate or promote quiescence as opposed to proliferation of HS/PCs, with the former being required for effective homing to bone marrow. Additional studies by Joo *et al.* (376) have shown that CXCL12 regulates p70 S6 kinase phosphorylation and that this in turn promotes the survival of MO7e cells. The studies presented here suggest that this may not occur with HL-60 cells in response to CXCL12 but instead that JAM-A may directly affect p70 S kinase phosphorylation in these cells.

Rap1 is another interesting candidate that was not present in the proteome array. It is known to regulate integrin recycling and consequently regulates cell adhesion and migration. Rap1 is activated by CXCL12 in lymphocytes (370), and an impaired activation of Rap1 has been observed in JAM-A-deficient murine neutrophils (251). In this thesis, in JAM-A non-expressing Jurkat cells, the phosphorylation of Rap1 occurred when non transduced Jurkat cells were stimulated with CXCL12. In the non-silencing control transduced Jurkat cells, a similar effect was observed and there was no negative effect on total Rap1 expression. With JAM-A expression in Jurkat cells, Rap1 phosphorylation was enhanced without CXCL12 and

then enhanced further with CXCL12. This suggests that JAM-A alone is sufficient for Rap1 activation, but can act synergistically with CXCL12 to promote higher levels of Rap1 phosphorylation. Interestingly, JAM-A has been shown to physically interact with PDZ-GEF2, a Rap1 activator and to activate Rap1 at epithelial cell junctions (362). Recently, it has been demonstrated that the active form of Rap1 translocates to the polarised cell membrane in response to CXCL12-mediated chronic lymphoid leukaemic cell trafficking, suggesting that the redistribution of active Rap1 could be another factor affecting adhesion or trafficking (377). Unfortunately, in the studies in this thesis, Rap1 activation in UCB $CD34^+$ cells was inconclusive due to time constraints in collecting sufficient cells for analysis and similar optimisation is required as described for the ERK1/2 experiments. Whether JAM-A acts to retain active Rap1 at the membrane for HS/PC polarity and homing and adhesion to niches would be an interesting subject to investigate, as would the possibility that JAM-A affects β1-integrin recycling. Previously, Cera *et al.* have shown that CD29 remains high on the cell surface and less is internalised in JAM-A knockout murine neutrophils when exposed to fMLP or chemotactic peptide WKYMVm, suggesting that JAM-A regulates CD29 internalisation and recycling in neutrophils (251). Preliminary studies in this thesis suggest that JAM-A could promote CD29 internalisation in HL-60 cells post CXCL12 stimulation. These and the phosphorylation studies need to be confirmed especially with UCB $CD34^+$ cells.

CHAPTER 6

GENERAL DISCUSSION

6.1. Summary of Findings

The aim of this thesis was to understand the communication between the bone marrow endothelial or vascular niche and human stem/progenitor cells (HS/PCs) and/or human leukaemic initiating cells (LICs). The mechanisms by which such studies could provide insights into (i) improving engraftment of individual HS/PCs after transplantation and (ii) developing new combination therapies for leukaemia are of particular importance. As the populations of HS/PCs and LICs are rare and difficult to identify, the studies concentrated on human $CD34^+$ cells derived from umbilical cord blood (UCB) and on a number of leukaemic cell lines as assay models. Furthermore, based on a previous finding in our laboratory (324), the studies were mainly carried out by investigating the role of the junctional adhesion molecule, JAM-A, on HS/PCs and leukaemic cell lines.

A comprehensive analysis of the differential expression of JAM-A protein was firstly carried out on phenotypically defined UCB haematopoietic progenitor subsets, more mature UCB haematopoietic lineage cells, leukaemic cell lines, primary leukaemic cells and three types of bone marrow vascular niche cells. In Chapter 3, JAM-A was observed to be expressed on most UCB $CD34^+$ and all UCB $CD133^+$ cells. The expression remained at similar levels on phenotypically-defined progenitors, including common myeloid progenitors (CMP), common lymphoid progenitor cells (CLP), common granulocyte/monocyte progenitors (GMP) and megakaryocyte/erythroid progenitors (MEP), to that found on the $CD34^+$ single positive populations. With this broad expression on all $CD133^+$ cells, it was decided not to conduct *in*

vivo repopulating studies in NSG mice as $CD133^+$ cells have previously been shown contain the repopulating cells.

For the mature UCB cells, JAM-A was found to be more highly expressed on monocytes and megakaryocytes, and showed variable expression on myeloid and lymphoid cells. These studies indicate that JAM-A expression on UCB cells differs from that reported to occur in the mouse and where JAM-A was reported to be a marker for repopulating HSCs although it was not exclusively expressed on these cells (152). In malignant haematopoietic cells, JAM-A was present in most bone marrow sections, although the staining was variable. Nevertheless, there were consistently high levels of JAM-A expressed by megakaryocytes in both normal and leukaemic bone marrows and weak to strong expression on endothelium, and stronger staining was observed especially for the endothelium in leukaemic sections. It is thus possible that the leukaemic cells enhance JAM-A expression on these vascular niche cells. In fresh bone marrow (BM) samples, JAM-A expression on B cell acute lymphoid leukaemic (B-ALL) $CD34^+$ cells was tested because these were the easiest cells to access and JAM-A was consistently higher than on the $CD34^-$ cells or $CD34^-CD19^+$ cells. Previous findings from Cox *et al.* showed that these populations all have long-term proliferative capability and are responsible for B-ALL transformation (80). Preliminary data from Dr Blair's group suggest that the JAM-A^+ B-ALL subsets can all proliferate in NSG mice following transplantation (unpublished data). Furthermore, while initial studies showed that JAM-A^+ B-ALL cells proliferated *in vitro*, JAM-A^- cells could be detected several weeks after culture initiation. In this respect, it was noted that not all the cells within the bone marrow of B-ALL patients analysed were JAM-A^+. Whether this effect is a response to the culture conditions or implies that some LICs are JAM-A^- remains to be determined. Due to a smaller cohort of T-ALL patients tested in this study, the analysis on primary ALL cells was focused mainly on B-ALL. As JAM-A was

found to be highly expressed on monocytes and megakaryocytes from UCB and also present in monoblastic and megakaryoblastic and other acute leukaemic bone marrow sections, it would be of interest to repeat the B-ALL studies with these acute myeloid leukaemias.

Finally, JAM-A expression was detectable on the human bone marrow endothelial cell line, BMEC-60, but not on human bone marrow mesenchymal stem cells (BMSCs) or human mesenchymal stromal cells (MSCs), and hence had a more restricted expression on bone marrow niche cells. JAM-A has been shown in other cell types to bind homophillically to JAM-A and heterophilically to LFA-1 (234, 243). JAM-A-JAM-A interactions in trans are thus likely to play a role in the crosstalk between haematopoietic cells and BMECs specifically in the bone marrow endothelial niche. In terms of leukaemic cells, it will be interestingly to know if JAM-A$^-$ cells have a higher proliferative potential which is supported by their lower ability to be held within the bone marrow niche and more rapid disease progression.

Chapter 4 set out to investigate the role of JAM-A in cell adhesion and transmigration. Three methods, JAM-A blockade, silencing and overexpression, were used to manipulate JAM-A expression on haematopoietic cell lines as models for UCB HS/PCs, before testing UCB CD34$^+$ cells, and their cell adhesion and transendothelial migration towards CXCL12 were measured. Blockade and silencing of JAM-A decreased TF-1 cell adhesion onto activated BMEC-60 cells and fibronectin, an extracellular matrix molecule rich in bone marrow. Not surprisingly, this JAM-A-mediated cell adhesion to BMEC-60 cells was not cell line specific, as a drop in HL-60 cell adhesion was also observed when JAM-A was either blocked using the same JAM-A antibody or knocked down using JAM-A specific siRNAs. However, HL-60 cells did not adhere substantially to fibronectin. The different adhesion abilities of the two cell lines to fibronectin may be due to their dissimilar fibronectin receptor expression. In addition, JAM-A-null Jurkat cells showed increased adhesion to BMEC-60 cells and

fibronectin when JAM-A was expressed in them. Finally, JAM-A antibody blockade and siRNA knockdown reduced UCB $CD34^+$ cell adhesion onto activated BMEC-60 cells, and to a lesser extent to fibronectin. As the blockade or knockdown of JAM-A reduced adhesion to BMEC-60 cells by around 20-30% in all these experiments, it may suggest that JAM-A was not acting alone in mediating this adhesion, but contributed significantly to it. Many studies have shown that selectins, addressins, sialomucins and integrins can co-ordinately regulate the adhesion of HS/PCs to endothelia as shown in Figure 4.35, and this subsequently affects their transendothelial migration (354). Therefore, the second topic in Chapter 4 was to determine if JAM-A had a role in chemotaxis towards CXCL12 across fibronectin and BMEC-60 cells. Interestingly, antibody blockade slightly but significantly promoted UCB $CD34^+$ cell chemotaxis on fibronectin towards CXCL12, while, in the BMEC-60 transmigration studies, JAM-A blockade or knockdown reduced cell migration. The lack of significance in transendothelial migration indicates that it is more likely for JAM-A to act as an adhesion molecule or a regulator of adhesion rather than as a migratory molecule in HS/PCs.

Chapter 5 aimed to investigate potential downstream signalling by which JAM-A could modulate cell adhesion. As circulating cells normally adhere in response to a particular trigger, CXCL12, a known chemokine mediating cell adhesion on bone marrow endothelial cells, was chosen as the stimulus (187-189, 378). CXCL12 expression was confirmed on BMECs in normal and malignant human bone marrow sections as well as on the BMEC-60 cell line. Following this, CXCL12 triggered the redistribution and association of JAM-A with CXCR4 to the leading edge of HL-60 cells and UCB $CD34^+$ cells, suggesting that JAM-A modulates downstream signalling of CXCR4. These co-localisation and PLA studies could be further confirmed by co-immunopreciptation studies. Using JAM-A overexpressing Jurkat cells, activation by phosphorylation of ERK and Rap1 kinases was enhanced by JAM-A

without or after CXCL12 stimulation. PKC-ζ kinase did not change over the time period tested. Variability in the detection of signalling molecules following lentiviral transduction and after knockdown needs to be investigated further to confirm the effects of JAM-A on CXCL12 induced ERK signalling. To follow up on these experiment, the internalisation of JAM-A and integrin β1 upon CXCL12 stimulation was analysed in a pilot experiment. The latter was impaired when JAM-A was knocked down in HL-60 cells. Had time permitted, the next steps would have been to investigate whether JAM-A regulates integrin internalisation and recycling using identical signalling in HS/PCs and to further validate the signalling responses observed in the phospho-protein array to determine which of the models JAM-A might follow.

6.2. Future Work

The work presented here concentrated on the expression and *in vitro* function of JAM-A on human UCB $CD34^+$ cells. While these studies were being done, it was shown by others that the interaction between two other JAM members, JAM-B on BMSCs and JAM-C on HSCs, could regulate haematopoiesis by modulating CXCL12 secretion in the bone marrow stromal cells (148), agreeing with our hypothesis of a potential connection between JAMs and CXCL12. In the work presented here, expression of CXCL12 and JAM-A was confirmed on BMECs. CXCL12 presented on BMECs has been reported to mediate leucocyte polarity and redistribution of CXCR4 on the cell surface (189). On UCB $CD34^+$ cells, this is accompanied by JAM-A co-localisation as shown in the present work. Furthermore, JAM-A not only formed a complex with CXCR4 but also interacted with β1-integrin and CD82. Whether these molecules interact and regulate haematopoiesis *in vivo* would be the next interesting topic. Nevertheless, first further signalling studies need to be carried out to validate the potential

signalling pathways modulated by JAM-A. The regulation of HS/PCs or LICs by bone marrow endothelial niche cells is still not fully understood and loss of JAM-A on B-ALL cells may coincide with a worse prognosis in leukaemic progression. Studies by Rafii *et al.* indicate that human primary BMECs particularly support megakaryocytic progenitor differentiation (170, 356). In this present work, JAM-A was found to be highly expressed on megakaryocytic progenitors and at a lower level on BMECs. Lately, Pitchford *et al.* reported that CXCR4-dependent migration of megakaryocytes towards the endothelial niche is required for their maturation (379). Since JAM-A polarised with CXCR4 on UCB $CD34^+$ cells in response to CXCL12, and also mediated their cell adhesion onto BMEC-60 cells, one might speculate that JAM-A could be involved in the translocation of HS/PCs to the bone marrow vascular niche, a process that could possibly lead to their proliferation or maturation. Thus, one direction for this work would be to investigate whether JAM-A-mediated adhesion contributes to megakaryopoiesis and HS/PC proliferation in the bone marrow endothelial niche. To do this, JAM-A blockade or specific cellular knockdown could be applied to interrupt JAM-A mediated interaction on BMECs, followed by megakaryocyte colony formation measurements or *in vivo* repopulating studies. The potential ability of JAM-A to regulate or synergise with CXCL12 mediated signalling or to act independently of CXCL12 mediated signalling has been proposed in this thesis and would be of interest to fully validate and confirm that these proposed pathways regulate firm adhesion of HS/PCs to BMECs.

From the niche point of view, an unpublished study in our laboratory indicates that JAM-A expression by human umbilical vein endothelial cells (HUVEC) is regulated by CXCL12. CXCL12 has also been shown to regulate *in vitro* HUVEC tubule formation (338), indicating that CXCL12 in the BM niches not only regulates HS/PC fate, but also modulates vasculogenesis. Earlier studies have shown that JAM-A mediates fibroblast growth factor 2

(FGF2)-induced angiogenesis in mice. This failure of FGF2-induced angiogenesis in JAM-A$^{-/-}$ mice was due to impaired endothelial cell sprouting (248). Naik *et al.* showed that JAM-A on the endothelial cells was redistributed to the cell surface following FGF2 treatment, and its interaction with the integrin $\alpha v\beta 3$ was disrupted in order for FGF2-induced ERK1/2 activation to be initiated for new blood vessel formation (247). More recently, the tetraspanin, CD9, has been linked to JAM-A and integrin $\alpha v\beta 3$ on resting endothelia, with FGF2 promoting JAM-A release from the complex so that it can dimerise and function appropriately (257). It is hence hypothesised that JAM-A may also be involved in CXCL12-induced angiogenesis, which will need to be proven with further experiments. By applying the *in situ* proximate ligation assay (PLA) to this study, the mechanisms by which the components of this complex distribute and dissociate in response to the CXCL12 trigger would be revealed.

6.3. Conclusion

To date, approximately 30,000 umbilical cord blood units have been used for transplantation (UCBT) globally since the first successful case was reported 25 years ago (5). UCBT with a greater human leucocyte antigen (HLA) mismatch results in a lower rate of acute and chronic graft versus host disease (GVDH) than observed with mobilised peripheral blood (6, 7), while a low viable CD34^{+} haematopoietic stem cell (HS/PC) number in UCBT can result in decreased engraftment and delayed immune reconstitution (8-10). Many strategies have been examined in order to improve the success rate of UCBT. Pooling multiple donors for transplantation into a single recipient has been suggested (11). Expansion of the stem cells *ex vivo* is another method to obtain sufficient cell numbers for transplantation (13). Lately, intra-bone marrow injection was found to efficiently shorten haematopoietic

recovery in mice model (16-18), while in humans there was a slight improvement in neutrophil recovery and a better improvement in platelet recovery (380).

In our laboratory, we are concentrating on improvement of the interaction between HS/PCs and the bone marrow niches and several strategies are being examined in our laboratory. It has been suggested that the bone marrow vascular reconstruction is important for transplanted cell engraftment in the bone marrow (381). Increasing evidence suggests that the bone marrow endothelial niche is of major importance to HS/PCs and regulates their cell proliferation and differentiation (reviewed in (382)). On the other hand, LICs may be protected from chemotherapeutic drug or irradiation therapy by interacting with niche, and this may be a cause of relapse (reviewed in (121)). Since most signals provided by niche have an influence over short-distances, cell-cell contact is important to retain the target cells in the niche for this triggering. Gold *et al.* depicted that various adhesion molecules on $CD34^+$ cells were required for the recovery of neutrophil, platelet or red blood cell reconstitution (21). Previous work in our laboratory (324) and by another group (381) suggested that JAM-A could be a candidate that co-regulated CXCL12-mediated cellular functions.

In this present work, the expression of JAM-A on human haematopoietic cells was illustrated and JAM-A was shown in part to be responsible for their adhesion onto human bone marrow endothelial cells in a CXCL12-dependent manner. The results further suggest that JAM-A is a new candidate involved in the crosstalk between HS/PC or possibly LICs and niche cells. However, it is possible that JAM-A loss may also signal disease progression and this requires further testing. Furthermore, a functional link between JAM-A and CXCL12/CXCR4 and the downstream signalling cascades in modulating UCB HS/PC adhesion is suggested although this needs to be validated. The communication between niche cells and HS/PCs or

LICs has been shown to be involved in the regulation of HS/PC fates and can also provide protection for LICs or alter the niche. Disruptions of LIC interaction with the niche has been proposed as a potential therapy for leukaemia. Targeting CXCR4 or another adhesion molecule, CD44, is currently in clinical trials for AML (reviewed in (162)). Very recently, Bonardi *et al.* showed that JAM-A expression is upregulated in AML $CD34^+$ cells, a potential LIC-containing population, compared to AML $CD34^-$ cells (83). All three of these surface molecules are present on normal HSCs, and these normal HSCs can be replaced by transplanted normal HSCs from allogeneic donors. Whether JAM-A is lost from LICs with disease progression is important to know if LICs are to be eliminated using therapies that target JAM-A. Alternatively, preventing JAM-A^+ cell adhesion may assist in preventing interaction of AML LICs with the bone marrow niche so that the AML can be targeted more effectively with other chemotherapeutic drugs.

To our knowledge, this is the first demonstration of JAM-A expression profiling on a wide range of human haematopoietic lineage cells and on bone marrow sections, whether normal or leukaemic, and the first demonstration of JAM-A crosstalk with CXCR4, β1-integrin, CD164 and CD82 on UCB HS/PCs.

REFERENCES

1. Gyurkocza B, Rezvani A, Storb RF. 2010. Allogeneic hematopoietic cell transplantation: the state of the art. *Expert Rev Hematol* 3: 285-99
2. Li HW, Sykes M. 2012. Emerging concepts in haematopoietic cell transplantation. *Nat Rev Immunol* 12: 403-16
3. Cutler C, Ballen KK. 2012. Improving outcomes in umbilical cord blood transplantation: state of the art. *Blood Rev* 26: 241-6
4. Ballen KK, Gluckman E, Broxmeyer HE. 2013. Umbilical cord blood transplantation: the first 25 years and beyond. *Blood* 122: 491-8
5. Gluckman E, Broxmeyer HA, Auerbach AD, Friedman HS, Douglas GW, Devergie A, Esperou H, Thierry D, Socie G, Lehn P, et al. 1989. Hematopoietic reconstitution in a patient with Fanconi's anemia by means of umbilical-cord blood from an HLA-identical sibling. *N Engl J Med* 321: 1174-8
6. Stanevsky A, Shimoni A, Yerushalmi R, Nagler A. 2011. Cord blood stem cells for hematopoietic transplantation. *Stem Cell Rev* 7: 425-33
7. Gluckman E, Rocha V, Boyer-Chammard A, Locatelli F, Arcese W, Pasquini R, Ortega J, Souillet G, Ferreira E, Laporte JP, Fernandez M, Chastang C. 1997. Outcome of cord-blood transplantation from related and unrelated donors. Eurocord Transplant Group and the European Blood and Marrow Transplantation Group. *N Engl J Med* 337: 373-81
8. Isoyama K, Oda M, Kato K, Nagamura-Inoue T, Kai S, Kigasawa H, Kobayashi R, Mimaya J, Inoue M, Kikuchi A, Kato S, Japan Cord Blood Bank N. 2010. Long-term outcome of cord blood transplantation from unrelated donors as an initial transplantation procedure for children with AML in Japan. *Bone Marrow Transplant* 45: 69-77
9. Terakura S, Azuma E, Murata M, Kumamoto T, Hirayama M, Atsuta Y, Kodera Y, Yazaki M, Naoe T, Kato K. 2007. Hematopoietic engraftment in recipients of unrelated donor umbilical cord blood is affected by the CD34+ and CD8+ cell doses. *Biol Blood Marrow Transplant* 13: 822-30
10. Wagner JE, Barker JN, DeFor TE, Baker KS, Blazar BR, Eide C, Goldman A, Kersey J, Krivit W, MacMillan ML, Orchard PJ, Peters C, Weisdorf DJ, Ramsay NK, Davies SM. 2002. Transplantation of unrelated donor umbilical cord blood in 102 patients with malignant and nonmalignant diseases: influence of CD34 cell dose and HLA disparity on treatment-related mortality and survival. *Blood* 100: 1611-8
11. De Lima M, St John LS, Wieder ED, Lee MS, McMannis J, Karandish S, Giralt S, Beran M, Couriel D, Korbling M, Bibawi S, Champlin R, Komanduri KV. 2002. Double-chimaerism after transplantation of two human leucocyte antigen mismatched, unrelated cord blood units. *Br J Haematol* 119: 773-6
12. Kim DW, Chung YJ, Kim TG, Kim YL, Oh IH. 2004. Cotransplantation of third-party mesenchymal stromal cells can alleviate single-donor predominance and increase engraftment from double cord transplantation. *Blood* 103: 1941-8
13. Robinson SN, Simmons PJ, Yang H, Alousi AM, Marcos de Lima J, Shpall EJ. 2011. Mesenchymal stem cells in ex vivo cord blood expansion. *Best Pract Res Clin Haematol* 24: 83-92
14. Bernardo ME, Ball LM, Cometa AM, Roelofs H, Zecca M, Avanzini MA, Bertaina A, Vinti L, Lankester A, Maccario R, Ringden O, Le Blanc K, Egeler RM, Fibbe WE, Locatelli F. 2011. Co-infusion of ex vivo-expanded, parental MSCs prevents life-threatening acute GVHD, but does not reduce the risk of graft failure in pediatric patients undergoing allogeneic umbilical cord blood transplantation. *Bone Marrow Transplant* 46: 200-7
15. Macmillan ML, Blazar BR, DeFor TE, Wagner JE. 2009. Transplantation of ex-vivo culture-expanded parental haploidentical mesenchymal stem cells to promote engraftment in

pediatric recipients of unrelated donor umbilical cord blood: results of a phase I-II clinical trial. *Bone Marrow Transplant* 43: 447-54

16. Castello S, Podesta M, Menditto VG, Ibatici A, Pitto A, Figari O, Scarpati D, Magrassi L, Bacigalupo A, Piaggio G, Frassoni F. 2004. Intra-bone marrow injection of bone marrow and cord blood cells: an alternative way of transplantation associated with a higher seeding efficiency. *Exp Hematol* 32: 782-7
17. Kushida T, Inaba M, Hisha H, Ichioka N, Esumi T, Ogawa R, Iida H, Ikehara S. 2001. Intra-bone marrow injection of allogeneic bone marrow cells: a powerful new strategy for treatment of intractable autoimmune diseases in MRL/lpr mice. *Blood* 97: 3292-9
18. Frassoni F, Gualandi F, Podesta M, Raiola AM, Ibatici A, Piaggio G, Sessarego M, Sessarego N, Gobbi M, Sacchi N, Labopin M, Bacigalupo A. 2008. Direct intrabone transplant of unrelated cord-blood cells in acute leukaemia: a phase I/II study. *Lancet Oncol* 9: 831-9
19. Ahmadbeigi N, Soleimani M, Vasei M, Gheisari Y, Mortazavi Y, Azadmanesh K, Omidkhoda A, Janzamin E, Beyer Nardi N. 2013. Isolation, Characterization and Transplantation of Bone Marrow derived cell component with Hematopoietic Stem Cell Niche properties. *Stem Cells Dev*
20. Robinson SN, Simmons PJ, Thomas MW, Brouard N, Javni JA, Trilok S, Shim JS, Yang H, Steiner D, Decker WK, Xing D, Shultz LD, Savoldo B, Dotti G, Bollard CM, Miller L, Champlin RE, Shpall EJ, Zweidler-McKay PA. 2012. Ex vivo fucosylation improves human cord blood engraftment in NOD-SCID IL-2Rgamma(null) mice. *Exp Hematol* 40: 445-56
21. Gold J, Valinski HM, Hanks AN, Ballen KK, Hsieh CC, Becker PS. 2006. Adhesion receptor expression by CD34+ cells from peripheral blood or bone marrow grafts: correlation with time to engraftment. *Exp Hematol* 34: 680-7
22. Doulatov S, Notta F, Laurenti E, Dick JE. 2012. Hematopoiesis: a human perspective. *Cell Stem Cell* 10: 120-36
23. Lorenz E. 1951. Modification of irradiation injury in mice and guinea pigs by bone marrow injections. *Journal of the National Cancer Institute* 12: 197-201
24. Till JE, Mc CE. 1961. A direct measurement of the radiation sensitivity of normal mouse bone marrow cells. *Radiat Res* 14: 213-22
25. Becker AJ, Mc CE, Till JE. 1963. Cytological demonstration of the clonal nature of spleen colonies derived from transplanted mouse marrow cells. *Nature* 197: 452-4
26. Siminovitch L, McCulloch EA, Till JE. 1963. The Distribution of Colony-Forming Cells among Spleen Colonies. *J Cell Physiol* 62: 327-36
27. Knoblich JA. 2008. Mechanisms of asymmetric stem cell division. *Cell* 132: 583-97
28. Evans MJ, Kaufman MH. 1981. Establishment in culture of pluripotential cells from mouse embryos. *Nature* 292: 154-6
29. Martin GR. 1981. Isolation of a pluripotent cell line from early mouse embryos cultured in medium conditioned by teratocarcinoma stem cells. *Proc Natl Acad Sci U S A* 78: 7634-8
30. Mountford JC. 2008. Human embryonic stem cells: origins, characteristics and potential for regenerative therapy. *Transfus Med* 18: 1-12
31. Takahashi K, Yamanaka S. 2006. Induction of pluripotent stem cells from mouse embryonic and adult fibroblast cultures by defined factors. *Cell* 126: 663-76
32. Takahashi K, Tanabe K, Ohnuki M, Narita M, Ichisaka T, Tomoda K, Yamanaka S. 2007. Induction of pluripotent stem cells from adult human fibroblasts by defined factors. *Cell* 131: 861-72
33. Yu J, Vodyanik MA, Smuga-Otto K, Antosiewicz-Bourget J, Frane JL, Tian S, Nie J, Jonsdottir GA, Ruotti V, Stewart R, Slukvin, II, Thomson JA. 2007. Induced pluripotent stem cell lines derived from human somatic cells. *Science* 318: 1917-20
34. Yamanaka S. 2012. Induced pluripotent stem cells: past, present, and future. *Cell Stem Cell* 10: 678-84

35. Prindull G, Prindull B, Meulen N. 1978. Haematopoietic stem cells (CFUc) in human cord blood. *Acta Paediatr Scand* 67: 413-6
36. Luis TC, Killmann NM, Staal FJ. 2012. Signal transduction pathways regulating hematopoietic stem cell biology: introduction to a series of Spotlight Reviews. *Leukemia* 26: 86-90
37. Guo Y, Lubbert M, Engelhardt M. 2003. CD34- hematopoietic stem cells: current concepts and controversies. *Stem Cells* 21: 15-20
38. Civin CI, Strauss LC, Brovall C, Fackler MJ, Schwartz JF, Shaper JH. 1984. Antigenic analysis of hematopoiesis. III. A hematopoietic progenitor cell surface antigen defined by a monoclonal antibody raised against KG-1a cells. *J Immunol* 133: 157-65
39. Sutherland DR, Watt SM, Dowden G, Karhi K, Baker MA, Greaves MF, Smart JE. 1988. Structural and partial amino acid sequence analysis of the human hemopoietic progenitor cell antigen CD34. *Leukemia* 2: 793-803
40. Cardoso AA, Watt SM, Batard P, Li ML, Hatzfeld A, Genevier H, Hatzfeld J. 1995. An improved panning technique for the selection of CD34+ human bone marrow hematopoietic cells with high recovery of early progenitors. *Exp Hematol* 23: 407-12
41. Sutherland HJ, Lansdorp PM, Henkelman DH, Eaves AC, Eaves CJ. 1990. Functional characterization of individual human hematopoietic stem cells cultured at limiting dilution on supportive marrow stromal layers. *Proc Natl Acad Sci U S A* 87: 3584-8
42. Berenson RJ, Andrews RG, Bensinger WI, Kalamasz D, Knitter G, Buckner CD, Bernstein ID. 1988. Antigen CD34+ marrow cells engraft lethally irradiated baboons. *J Clin Invest* 81: 951-5
43. Gangenahalli GU, Singh VK, Verma YK, Gupta P, Sharma RK, Chandra R, Luthra PM. 2006. Hematopoietic stem cell antigen CD34: role in adhesion or homing. *Stem Cells Dev* 15: 305-13
44. Watt SM, Karhi K, Gatter K, Furley AJ, Katz FE, Healy LE, Altass LJ, Bradley NJ, Sutherland DR, Levinsky R, et al. 1987. Distribution and epitope analysis of the cell membrane glycoprotein (HPCA-1) associated with human hemopoietic progenitor cells. *Leukemia* 1: 417-26
45. Osawa M, Hanada K, Hamada H, Nakauchi H. 1996. Long-term lymphohematopoietic reconstitution by a single CD34-low/negative hematopoietic stem cell. *Science* 273: 242-5
46. Goodell MA, Rosenzweig M, Kim H, Marks DF, DeMaria M, Paradis G, Grupp SA, Sieff CA, Mulligan RC, Johnson RP. 1997. Dye efflux studies suggest that hematopoietic stem cells expressing low or undetectable levels of CD34 antigen exist in multiple species. *Nat Med* 3: 1337-45
47. Fina L, Molgaard HV, Robertson D, Bradley NJ, Monaghan P, Delia D, Sutherland DR, Baker MA, Greaves MF. 1990. Expression of the CD34 gene in vascular endothelial cells. *Blood* 75: 2417-26
48. Brown J, Greaves MF, Molgaard HV. 1991. The gene encoding the stem cell antigen, CD34, is conserved in mouse and expressed in haemopoietic progenitor cell lines, brain, and embryonic fibroblasts. *Int Immunol* 3: 175-84
49. Bonnet D. 2003. Hematopoietic stem cells. *Birth Defects Res C Embryo Today* 69: 219-29
50. Bhatia M, Bonnet D, Murdoch B, Gan OI, Dick JE. 1998. A newly discovered class of human hematopoietic cells with SCID-repopulating activity. *Nat Med* 4: 1038-45
51. McGuckin CP, Forraz N, Baradez MO, Lojo-Rial C, Wertheim D, Whiting K, Watt SM, Pettengell R. 2003. Colocalization analysis of sialomucins CD34 and CD164. *Stem Cells* 21: 162-70
52. Corbeil D, Karbanova J, Fargeas CA, Jaszai J. 2013. Prominin-1 (CD133): Molecular and Cellular Features Across Species. *Adv Exp Med Biol* 777: 3-24
53. Walker TL, Wierick A, Sykes AM, Waldau B, Corbeil D, Carmeliet P, Kempermann G. 2013. Prominin-1 allows prospective isolation of neural stem cells from the adult murine hippocampus. *J Neurosci* 33: 3010-24

54. Yin AH, Miraglia S, Zanjani ED, Almeida-Porada G, Ogawa M, Leary AG, Olweus J, Kearney J, Buck DW. 1997. AC133, a novel marker for human hematopoietic stem and progenitor cells. *Blood* 90: 5002-12
55. Miraglia S, Godfrey W, Yin AH, Atkins K, Warnke R, Holden JT, Bray RA, Waller EK, Buck DW. 1997. A novel five-transmembrane hematopoietic stem cell antigen: isolation, characterization, and molecular cloning. *Blood* 90: 5013-21
56. Corbeil D, Roper K, Hellwig A, Tavian M, Miraglia S, Watt SM, Simmons PJ, Peault B, Buck DW, Huttner WB. 2000. The human AC133 hematopoietic stem cell antigen is also expressed in epithelial cells and targeted to plasma membrane protrusions. *J Biol Chem* 275: 5512-20
57. Grosse-Gehling P, Fargeas CA, Dittfeld C, Garbe Y, Alison MR, Corbeil D, Kunz-Schughart LA. 2013. CD133 as a biomarker for putative cancer stem cells in solid tumours: limitations, problems and challenges. *J Pathol* 229: 355-78
58. de Wynter EA, Buck D, Hart C, Heywood R, Coutinho LH, Clayton A, Rafferty JA, Burt D, Guenechea G, Bueren JA, Gagen D, Fairbairn LJ, Lord BI, Testa NG. 1998. CD34+AC133+ cells isolated from cord blood are highly enriched in long-term culture-initiating cells, NOD/SCID-repopulating cells and dendritic cell progenitors. *Stem Cells* 16: 387-96
59. Bhatia M. 2001. AC133 expression in human stem cells. *Leukemia* 15: 1685-8
60. Gorgens A, Radtke S, Mollmann M, Cross M, Durig J, Horn PA, Giebel B. 2013. Revision of the human hematopoietic tree: granulocyte subtypes derive from distinct hematopoietic lineages. *Cell Rep* 3: 1539-52
61. Reya T, Morrison SJ, Clarke MF, Weissman IL. 2001. Stem cells, cancer, and cancer stem cells. *Nature* 414: 105-11
62. Adolfsson J, Mansson R, Buza-Vidas N, Hultquist A, Liuba K, Jensen CT, Bryder D, Yang L, Borge OJ, Thoren LA, Anderson K, Sitnicka E, Sasaki Y, Sigvardsson M, Jacobsen SE. 2005. Identification of Flt3+ lympho-myeloid stem cells lacking erythro-megakaryocytic potential a revised road map for adult blood lineage commitment. *Cell* 121: 295-306
63. Arndt K, Grinenko T, Mende N, Reichert D, Portz M, Ripich T, Carmeliet P, Corbeil D, Waskow C. 2013. CD133 is a modifier of hematopoietic progenitor frequencies but is dispensable for the maintenance of mouse hematopoietic stem cells. *Proc Natl Acad Sci U S A* 110: 5582-7
64. Majka M, Ratajczak J, Machalinski B, Carter A, Pizzini D, Wasik MA, Gewirtz AM, Ratajczak MZ. 2000. Expression, regulation and function of AC133, a putative cell surface marker of primitive human haematopoietic cells. *Folia Histochem Cytobiol* 38: 53-63
65. Fonseca AV, Corbeil D. 2011. The hematopoietic stem cell polarization and migration: A dynamic link between RhoA signaling pathway, microtubule network and ganglioside-based membrane microdomains. *Commun Integr Biol* 4: 201-4
66. Bauer N, Wilsch-Brauninger M, Karbanova J, Fonseca AV, Strauss D, Freund D, Thiele C, Huttner WB, Bornhauser M, Corbeil D. 2011. Haematopoietic stem cell differentiation promotes the release of prominin-1/CD133-containing membrane vesicles--a role of the endocytic-exocytic pathway. *EMBO Mol Med* 3: 398-409
67. Fargeas CA, Karbanova J, Jaszai J, Corbeil D. 2011. CD133 and membrane microdomains: old facets for future hypotheses. *World J Gastroenterol* 17: 4149-52
68. Larochelle A, Savona M, Wiggins M, Anderson S, Ichwan B, Keyvanfar K, Morrison SJ, Dunbar CE. 2011. Human and rhesus macaque hematopoietic stem cells cannot be purified based only on SLAM family markers. *Blood* 117: 1550-4
69. Kawamoto H, Ikawa T, Masuda K, Wada H, Katsura Y. 2010. A map for lineage restriction of progenitors during hematopoiesis: the essence of the myeloid-based model. *Immunol Rev* 238: 23-36
70. Ji H, Ehrlich LI, Seita J, Murakami P, Doi A, Lindau P, Lee H, Aryee MJ, Irizarry RA, Kim K, Rossi DJ, Inlay MA, Serwold T, Karsunky H, Ho L, Daley GQ, Weissman IL, Feinberg AP. 2010. Comprehensive methylome map of lineage commitment from haematopoietic progenitors. *Nature* 467: 338-42

71. Doulatov S, Notta F, Eppert K, Nguyen LT, Ohashi PS, Dick JE. 2010. Revised map of the human progenitor hierarchy shows the origin of macrophages and dendritic cells in early lymphoid development. *Nat Immunol* 11: 585-93
72. Houghton J, Morozov A, Smirnova I, Wang TC. 2007. Stem cells and cancer. *Semin Cancer Biol* 17: 191-203
73. Pierce GB. 1974. Neoplasms, differentiations and mutations. *Am J Pathol* 77: 103-18
74. Dick JE. 2008. Stem cell concepts renew cancer research. *Blood* 112: 4793-807
75. Hoang VT, Zepeda-Moreno A, Ho AD. 2012. Identification of leukemia stem cells in acute myeloid leukemia and their clinical relevance. *Biotechnol J* 7: 779-88
76. Bonnet D, Dick JE. 1997. Human acute myeloid leukemia is organized as a hierarchy that originates from a primitive hematopoietic cell. *Nat Med* 3: 730-7
77. Lapidot T, Sirard C, Vormoor J, Murdoch B, Hoang T, Caceres-Cortes J, Minden M, Paterson B, Caligiuri MA, Dick JE. 1994. A cell initiating human acute myeloid leukaemia after transplantation into SCID mice. *Nature* 367: 645-8
78. Goardon N, Marchi E, Atzberger A, Quek L, Schuh A, Soneji S, Woll P, Mead A, Alford KA, Rout R, Chaudhury S, Gilkes A, Knapper S, Beldjord K, Begum S, Rose S, Geddes N, Griffiths M, Standen G, Sternberg A, Cavenagh J, Hunter H, Bowen D, Killick S, Robinson L, Price A, Macintyre E, Virgo P, Burnett A, Craddock C, Enver T, Jacobsen SE, Porcher C, Vyas P. 2011. Coexistence of LMPP-like and GMP-like leukemia stem cells in acute myeloid leukemia. *Cancer Cell* 19: 138-52
79. Cox CV, Martin HM, Kearns PR, Virgo P, Evely RS, Blair A. 2007. Characterization of a progenitor cell population in childhood T-cell acute lymphoblastic leukemia. *Blood* 109: 674-82
80. Cox CV, Evely RS, Oakhill A, Pamphilon DH, Goulden NJ, Blair A. 2004. Characterization of acute lymphoblastic leukemia progenitor cells. *Blood* 104: 2919-25
81. Cox CV, Diamanti P, Evely RS, Kearns PR, Blair A. 2009. Expression of CD133 on leukemia-initiating cells in childhood ALL. *Blood* 113: 3287-96
82. Buzzai M, Licht JD. 2008. New molecular concepts and targets in acute myeloid leukemia. *Curr Opin Hematol* 15: 82-7
83. Bonardi F, Fusetti F, Deelen P, van Gosliga D, Vellenga E, Schuringa JJ. 2013. A proteomics and transcriptomics approach to identify leukemic stem cell (LSC) markers. *Mol Cell Proteomics* 12: 626-37
84. Schofield R. 1978. The relationship between the spleen colony-forming cell and the haemopoietic stem cell. *Blood Cells* 4: 7-25
85. Lord BI, Testa NG, Hendry JH. 1975. The relative spatial distributions of CFUs and CFUc in the normal mouse femur. *Blood* 46: 65-72
86. Shackney SE, Ford SS, Wittig AB. 1975. Kinetic-microarchitectural correlations in the bone marrow of the mouse. *Cell Tissue Kinet* 8: 505-16
87. Naito K, Tamahashi N, Chiba T, Kaneda K, Okuda M, Endo K, Yoshinaga K, Takahashi T. 1992. The microvasculature of the human bone marrow correlated with the distribution of hematopoietic cells. A computer-assisted three-dimensional reconstruction study. *Tohoku J Exp Med* 166: 439-50
88. Taichman RS, Emerson SG. 1994. Human osteoblasts support hematopoiesis through the production of granulocyte colony-stimulating factor. *J Exp Med* 179: 1677-82
89. Zhang J, Niu C, Ye L, Huang H, He X, Tong WG, Ross J, Haug J, Johnson T, Feng JQ, Harris S, Wiedemann LM, Mishina Y, Li L. 2003. Identification of the haematopoietic stem cell niche and control of the niche size. *Nature* 425: 836-41
90. Calvi LM, Adams GB, Weibrecht KW, Weber JM, Olson DP, Knight MC, Martin RP, Schipani E, Divieti P, Bringhurst FR, Milner LA, Kronenberg HM, Scadden DT. 2003. Osteoblastic cells regulate the haematopoietic stem cell niche. *Nature* 425: 841-6

91. Kiel MJ, Yilmaz OH, Iwashita T, Terhorst C, Morrison SJ. 2005. SLAM family receptors distinguish hematopoietic stem and progenitor cells and reveal endothelial niches for stem cells. *Cell* 121: 1109-21
92. Kopp HG, Avecilla ST, Hooper AT, Rafii S. 2005. The bone marrow vascular niche: home of HSC differentiation and mobilization. *Physiology (Bethesda)* 20: 349-56
93. Bianco P. 2011. Bone and the hematopoietic niche: a tale of two stem cells. *Blood* 117: 5281-8
94. Bianco P. 2011. Minireview: The stem cell next door: skeletal and hematopoietic stem cell "niches" in bone. *Endocrinology* 152: 2957-62
95. Lo Celso C, Scadden DT. 2011. The haematopoietic stem cell niche at a glance. *J Cell Sci* 124: 3529-35
96. Levesque JP, Winkler IG, Hendy J, Williams B, Helwani F, Barbier V, Nowlan B, Nilsson SK. 2007. Hematopoietic progenitor cell mobilization results in hypoxia with increased hypoxia-inducible transcription factor-1 alpha and vascular endothelial growth factor A in bone marrow. *Stem Cells* 25: 1954-65
97. Levesque JP, Helwani FM, Winkler IG. 2010. The endosteal 'osteoblastic' niche and its role in hematopoietic stem cell homing and mobilization. *Leukemia* 24: 1979-92
98. Stier S, Ko Y, Forkert R, Lutz C, Neuhaus T, Grunewald E, Cheng T, Dombkowski D, Calvi LM, Rittling SR, Scadden DT. 2005. Osteopontin is a hematopoietic stem cell niche component that negatively regulates stem cell pool size. *J Exp Med* 201: 1781-91
99. Nilsson SK, Johnston HM, Whitty GA, Williams B, Webb RJ, Denhardt DT, Bertoncello I, Bendall LJ, Simmons PJ, Haylock DN. 2005. Osteopontin, a key component of the hematopoietic stem cell niche and regulator of primitive hematopoietic progenitor cells. *Blood* 106: 1232-9
100. Nakamura Y, Arai F, Iwasaki H, Hosokawa K, Kobayashi I, Gomei Y, Matsumoto Y, Yoshihara H, Suda T. 2010. Isolation and characterization of endosteal niche cell populations that regulate hematopoietic stem cells. *Blood* 116: 1422-32
101. Chitteti BR, Cheng YH, Kacena MA, Srour EF. 2013. Hierarchical organization of osteoblasts reveals the significant role of CD166 in hematopoietic stem cell maintenance and function. *Bone* 54: 58-67
102. Arai F, Hirao A, Ohmura M, Sato H, Matsuoka S, Takubo K, Ito K, Koh GY, Suda T. 2004. Tie2/angiopoietin-1 signaling regulates hematopoietic stem cell quiescence in the bone marrow niche. *Cell* 118: 149-61
103. Gillette JM, Larochelle A, Dunbar CE, Lippincott-Schwartz J. 2009. Intercellular transfer to signalling endosomes regulates an ex vivo bone marrow niche. *Nat Cell Biol* 11: 303-11
104. Lo Celso C, Fleming HE, Wu JW, Zhao CX, Miake-Lye S, Fujisaki J, Cote D, Rowe DW, Lin CP, Scadden DT. 2009. Live-animal tracking of individual haematopoietic stem/progenitor cells in their niche. *Nature* 457: 92-6
105. Xie Y, Yin T, Wiegraebe W, He XC, Miller D, Stark D, Perko K, Alexander R, Schwartz J, Grindley JC, Park J, Haug JS, Wunderlich JP, Li H, Zhang S, Johnson T, Feldman RA, Li L. 2009. Detection of functional haematopoietic stem cell niche using real-time imaging. *Nature* 457: 97-101
106. Woodward J. 2010. Regulation of haematopoietic progenitor cell proliferation and survival: The involvement of the osteoblast. *Cell Adh Migr* 4: 4-6
107. Wilson A, Trumpp A. 2006. Bone-marrow haematopoietic-stem-cell niches. *Nat Rev Immunol* 6: 93-106
108. Nolan DJ, Ginsberg M, Israely E, Palikuqi B, Poulos MG, James D, Ding BS, Schachterle W, Liu Y, Rosenwaks Z, Butler JM, Xiang J, Rafii A, Shido K, Rabbany SY, Elemento O, Rafii S. 2013. Molecular signatures of tissue-specific microvascular endothelial cell heterogeneity in organ maintenance and regeneration. *Dev Cell* 26: 204-19

109. Schweitzer KM, Drager AM, van der Valk P, Thijsen SF, Zevenbergen A, Theijsmeijer AP, van der Schoot CE, Langenhuijsen MM. 1996. Constitutive expression of E-selectin and vascular cell adhesion molecule-1 on endothelial cells of hematopoietic tissues. *Am J Pathol* 148: 165-75
110. Mazo IB, Gutierrez-Ramos JC, Frenette PS, Hynes RO, Wagner DD, von Andrian UH. 1998. Hematopoietic progenitor cell rolling in bone marrow microvessels: parallel contributions by endothelial selectins and vascular cell adhesion molecule 1. *J Exp Med* 188: 465-74
111. Li Z, Li L. 2006. Understanding hematopoietic stem-cell microenvironments. *Trends Biochem Sci* 31: 589-95
112. Winkler IG, Barbier V, Nowlan B, Jacobsen RN, Forristal CE, Patton JT, Magnani JL, Levesque JP. 2012. Vascular niche E-selectin regulates hematopoietic stem cell dormancy, self renewal and chemoresistance. *Nat Med* 18: 1651-7
113. Ding L, Saunders TL, Enikolopov G, Morrison SJ. 2012. Endothelial and perivascular cells maintain haematopoietic stem cells. *Nature* 481: 457-62
114. Sugiyama T, Kohara H, Noda M, Nagasawa T. 2006. Maintenance of the hematopoietic stem cell pool by CXCL12-CXCR4 chemokine signaling in bone marrow stromal cell niches. *Immunity* 25: 977-88
115. Mendez-Ferrer S, Michurina TV, Ferraro F, Mazloom AR, Macarthur BD, Lira SA, Scadden DT, Ma'ayan A, Enikolopov GN, Frenette PS. 2010. Mesenchymal and haematopoietic stem cells form a unique bone marrow niche. *Nature* 466: 829-34
116. Sacchetti B, Funari A, Michienzi S, Di Cesare S, Piersanti S, Saggio I, Tagliafico E, Ferrari S, Robey PG, Riminucci M, Bianco P. 2007. Self-renewing osteoprogenitors in bone marrow sinusoids can organize a hematopoietic microenvironment. *Cell* 131: 324-36
117. Naveiras O, Nardi V, Wenzel PL, Hauschka PV, Fahey F, Daley GQ. 2009. Bone-marrow adipocytes as negative regulators of the haematopoietic microenvironment. *Nature* 460: 259-63
118. Katayama Y, Battista M, Kao WM, Hidalgo A, Peired AJ, Thomas SA, Frenette PS. 2006. Signals from the sympathetic nervous system regulate hematopoietic stem cell egress from bone marrow. *Cell* 124: 407-21
119. Winkler IG, Sims NA, Pettit AR, Barbier V, Nowlan B, Helwani F, Poulton IJ, van Rooijen N, Alexander KA, Raggatt LJ, Levesque JP. 2010. Bone marrow macrophages maintain hematopoietic stem cell (HSC) niches and their depletion mobilizes HSCs. *Blood* 116: 4815-28
120. Fujisaki J, Wu J, Carlson AL, Silberstein L, Putheti P, Larocca R, Gao W, Saito TI, Lo Celso C, Tsuyuzaki H, Sato T, Cote D, Sykes M, Strom TB, Scadden DT, Lin CP. 2011. In vivo imaging of Treg cells providing immune privilege to the haematopoietic stem-cell niche. *Nature* 474: 216-9
121. Lane SW, Scadden DT, Gilliland DG. 2009. The leukemic stem cell niche: current concepts and therapeutic opportunities. *Blood* 114: 1150-7
122. Adams GB, Chabner KT, Alley IR, Olson DP, Szczepiorkowski ZM, Poznansky MC, Kos CH, Pollak MR, Brown EM, Scadden DT. 2006. Stem cell engraftment at the endosteal niche is specified by the calcium-sensing receptor. *Nature* 439: 599-603
123. Greenbaum A, Hsu YM, Day RB, Schuettpelz LG, Christopher MJ, Borgerding JN, Nagasawa T, Link DC. 2013. CXCL12 in early mesenchymal progenitors is required for haematopoietic stem-cell maintenance. *Nature* 495: 227-30
124. Ding L, Morrison SJ. 2013. Haematopoietic stem cells and early lymphoid progenitors occupy distinct bone marrow niches. *Nature* 495: 231-5
125. Duncan AW, Rattis FM, DiMascio LN, Congdon KL, Pazianos G, Zhao C, Yoon K, Cook JM, Willert K, Gaiano N, Reya T. 2005. Integration of Notch and Wnt signaling in hematopoietic stem cell maintenance. *Nat Immunol* 6: 314-22

126. Bhardwaj G, Murdoch B, Wu D, Baker DP, Williams KP, Chadwick K, Ling LE, Karanu FN, Bhatia M. 2001. Sonic hedgehog induces the proliferation of primitive human hematopoietic cells via BMP regulation. *Nat Immunol* 2: 172-80
127. Goldman DC, Bailey AS, Pfaffle DL, Al Masri A, Christian JL, Fleming WH. 2009. BMP4 regulates the hematopoietic stem cell niche. *Blood* 114: 4393-401
128. Fleming HE, Janzen V, Lo Celso C, Guo J, Leahy KM, Kronenberg HM, Scadden DT. 2008. Wnt signaling in the niche enforces hematopoietic stem cell quiescence and is necessary to preserve self-renewal in vivo. *Cell Stem Cell* 2: 274-83
129. Schaniel C, Sirabella D, Qiu J, Niu X, Lemischka IR, Moore KA. 2011. Wnt-inhibitory factor 1 dysregulation of the bone marrow niche exhausts hematopoietic stem cells. *Blood* 118: 2420-9
130. Renstrom J, Istvanffy R, Gauthier K, Shimono A, Mages J, Jardon-Alvarez A, Kroger M, Schiemann M, Busch DH, Esposito I, Lang R, Peschel C, Oostendorp RA. 2009. Secreted frizzled-related protein 1 extrinsically regulates cycling activity and maintenance of hematopoietic stem cells. *Cell Stem Cell* 5: 157-67
131. Kieslinger M, Hiechinger S, Dobreva G, Consalez GG, Grosschedl R. 2010. Early B cell factor 2 regulates hematopoietic stem cell homeostasis in a cell-nonautonomous manner. *Cell Stem Cell* 7: 496-507
132. Zheng J, Huynh H, Umikawa M, Silvany R, Zhang CC. 2011. Angiopoietin-like protein 3 supports the activity of hematopoietic stem cells in the bone marrow niche. *Blood* 117: 470-9
133. Akhter S, Rahman MM, Lee HS, Kim HJ, Hong ST. 2013. Dynamic roles of angiopoietin-like proteins 1, 2, 3, 4, 6 and 7 in the survival and enhancement of ex vivo expansion of bone-marrow hematopoietic stem cells. *Protein Cell* 4: 220-30
134. Yoshihara H, Arai F, Hosokawa K, Hagiwara T, Takubo K, Nakamura Y, Gomei Y, Iwasaki H, Matsuoka S, Miyamoto K, Miyazaki H, Takahashi T, Suda T. 2007. Thrombopoietin/MPL signaling regulates hematopoietic stem cell quiescence and interaction with the osteoblastic niche. *Cell Stem Cell* 1: 685-97
135. Heissig B, Hattori K, Dias S, Friedrich M, Ferris B, Hackett NR, Crystal RG, Besmer P, Lyden D, Moore MA, Werb Z, Rafii S. 2002. Recruitment of stem and progenitor cells from the bone marrow niche requires MMP-9 mediated release of kit-ligand. *Cell* 109: 625-37
136. Kollet O, Dar A, Shivtiel S, Kalinkovich A, Lapid K, Sztainberg Y, Tesio M, Samstein RM, Goichberg P, Spiegel A, Elson A, Lapidot T. 2006. Osteoclasts degrade endosteal components and promote mobilization of hematopoietic progenitor cells. *Nat Med* 12: 657-64
137. Caselli A, Olson TS, Otsuru S, Chen X, Hofmann TJ, Nah HD, Grisendi G, Paolucci P, Dominici M, Horwitz EM. 2013. IGF-1-Mediated Osteoblastic Niche Expansion Enhances Long-Term Hematopoietic Stem Cell Engraftment after Murine Bone Marrow Transplantation. *Stem Cells*
138. Williams DA, Rios M, Stephens C, Patel VP. 1991. Fibronectin and VLA-4 in haematopoietic stem cell-microenvironment interactions. *Nature* 352: 438-41
139. Stucki A, Rivier AS, Gikic M, Monai N, Schapira M, Spertini O. 2001. Endothelial cell activation by myeloblasts: molecular mechanisms of leukostasis and leukemic cell dissemination. *Blood* 97: 2121-9
140. Forde S, Tye BJ, Newey SE, Roubelakis M, Smythe J, McGuckin CP, Pettengell R, Watt SM. 2007. Endolyn (CD164) modulates the CXCL12-mediated migration of umbilical cord blood CD133+ cells. *Blood* 109: 1825-33
141. Avigdor A, Goichberg P, Shivtiel S, Dar A, Peled A, Samira S, Kollet O, Hershkoviz R, Alon R, Hardan I, Ben-Hur H, Naor D, Nagler A, Lapidot T. 2004. CD44 and hyaluronic acid cooperate with SDF-1 in the trafficking of human CD34+ stem/progenitor cells to bone marrow. *Blood* 103: 2981-9

142. Krause DS, Lazarides K, von Andrian UH, Van Etten RA. 2006. Requirement for CD44 in homing and engraftment of BCR-ABL-expressing leukemic stem cells. *Nat Med* 12: 1175-80
143. Arai F, Hosokawa K, Toyama H, Matsumoto Y, Suda T. 2012. Role of N-cadherin in the regulation of hematopoietic stem cells in the bone marrow niche. *Ann N Y Acad Sci* 1266: 72-7
144. Kiel MJ, Acar M, Radice GL, Morrison SJ. 2009. Hematopoietic stem cells do not depend on N-cadherin to regulate their maintenance. *Cell Stem Cell* 4: 170-9
145. Yang FC, Atkinson SJ, Gu Y, Borneo JB, Roberts AW, Zheng Y, Pennington J, Williams DA. 2001. Rac and Cdc42 GTPases control hematopoietic stem cell shape, adhesion, migration, and mobilization. *Proc Natl Acad Sci U S A* 98: 5614-8
146. Florian MC, Dorr K, Niebel A, Daria D, Schrezenmeier H, Rojewski M, Filippi MD, Hasenberg A, Gunzer M, Scharffetter-Kochanek K, Zheng Y, Geiger H. 2012. Cdc42 activity regulates hematopoietic stem cell aging and rejuvenation. *Cell Stem Cell* 10: 520-30
147. Carrillo-Garcia C, Janzen V. 2012. Restoring cell polarity: an HSC fountain of youth. *Cell Stem Cell* 10: 481-2
148. Arcangeli ML, Frontera V, Bardin F, Obrados E, Adams S, Chabannon C, Schiff C, Mancini SJ, Adams RH, Aurrand-Lions M. 2011. JAM-B regulates maintenance of hematopoietic stem cells in the bone marrow. *Blood* 118: 4609-19
149. Sudo T, Yokota T, Oritani K, Satoh Y, Sugiyama T, Ishida T, Shibayama H, Ezoe S, Fujita N, Tanaka H, Maeda T, Nagasawa T, Kanakura Y. 2012. The endothelial antigen ESAM monitors hematopoietic stem cell status between quiescence and self-renewal. *J Immunol* 189: 200-10
150. Bigas A, D'Altri T, Espinosa L. 2012. The Notch pathway in hematopoietic stem cells. *Curr Top Microbiol Immunol* 360: 1-18
151. Kobayashi H, Butler JM, O'Donnell R, Kobayashi M, Ding BS, Bonner B, Chiu VK, Nolan DJ, Shido K, Benjamin L, Rafii S. 2010. Angiocrine factors from Akt-activated endothelial cells balance self-renewal and differentiation of haematopoietic stem cells. *Nat Cell Biol* 12: 1046-56
152. Sugano Y, Takeuchi M, Hirata A, Matsushita H, Kitamura T, Tanaka M, Miyajima A. 2008. Junctional adhesion molecule-A, JAM-A, is a novel cell-surface marker for long-term repopulating hematopoietic stem cells. *Blood* 111: 1167-72
153. Frontera V, Arcangeli ML, Zimmerli C, Bardin F, Obrados E, Audebert S, Bajenoff M, Borg JP, Aurrand-Lions M. 2011. Cutting edge: JAM-C controls homeostatic chemokine secretion in lymph node fibroblastic reticular cells expressing thrombomodulin. *J Immunol* 187: 603-7
154. Yokota T, Oritani K, Butz S, Kokame K, Kincade PW, Miyata T, Vestweber D, Kanakura Y. 2009. The endothelial antigen ESAM marks primitive hematopoietic progenitors throughout life in mice. *Blood* 113: 2914-23
155. Ooi AG, Karsunky H, Majeti R, Butz S, Vestweber D, Ishida T, Quertermous T, Weissman IL, Forsberg EC. 2009. The adhesion molecule esam1 is a novel hematopoietic stem cell marker. *Stem Cells* 27: 653-61
156. Ninomiya M, Abe A, Katsumi A, Xu J, Ito M, Arai F, Suda T, Kiyoi H, Kinoshita T, Naoe T. 2007. Homing, proliferation and survival sites of human leukemia cells in vivo in immunodeficient mice. *Leukemia* 21: 136-42
157. Colmone A, Amorim M, Pontier AL, Wang S, Jablonski E, Sipkins DA. 2008. Leukemic cells create bone marrow niches that disrupt the behavior of normal hematopoietic progenitor cells. *Science* 322: 1861-5
158. Sipkins DA, Wei X, Wu JW, Runnels JM, Cote D, Means TK, Luster AD, Scadden DT, Lin CP. 2005. In vivo imaging of specialized bone marrow endothelial microdomains for tumour engraftment. *Nature* 435: 969-73
159. Konopleva MY, Jordan CT. 2011. Leukemia stem cells and microenvironment: biology and therapeutic targeting. *J Clin Oncol* 29: 591-9

160. Wellmann S, Guschmann M, Griethe W, Eckert C, von Stackelberg A, Lottaz C, Moderegger E, Einsiedel HG, Eckardt KU, Henze G, Seeger K. 2004. Activation of the HIF pathway in childhood ALL, prognostic implications of VEGF. *Leukemia* 18: 926-33
161. Deeb G, Vaughan MM, McInnis I, Ford LA, Sait SN, Starostik P, Wetzler M, Mashtare T, Wang ES. 2011. Hypoxia-inducible factor-1alpha protein expression is associated with poor survival in normal karyotype adult acute myeloid leukemia. *Leuk Res* 35: 579-84
162. Van Etten RA. 2013. New insights into the normal and leukemic stem cell niche: a timely review. *Cytometry B Clin Cytom* 84: 5-6
163. ten Cate B, de Bruyn M, Wei Y, Bremer E, Helfrich W. 2010. Targeted elimination of leukemia stem cells; a new therapeutic approach in hemato-oncology. *Curr Drug Targets* 11: 95-110
164. Freund D, Bauer N, Boxberger S, Feldmann S, Streller U, Ehninger G, Werner C, Bornhauser M, Oswald J, Corbeil D. 2006. Polarization of human hematopoietic progenitors during contact with multipotent mesenchymal stromal cells: effects on proliferation and clonogenicity. *Stem Cells Dev* 15: 815-29
165. Zhang Y, Chai C, Jiang XS, Teoh SH, Leong KW. 2006. Co-culture of umbilical cord blood CD34+ cells with human mesenchymal stem cells. *Tissue Eng* 12: 2161-70
166. Li N, Feugier P, Serrurrier B, Latger-Cannard V, Lesesve JF, Stoltz JF, Eljaafari A. 2007. Human mesenchymal stem cells improve ex vivo expansion of adult human CD34+ peripheral blood progenitor cells and decrease their allostimulatory capacity. *Exp Hematol* 35: 507-15
167. Wagner W, Wein F, Roderburg C, Saffrich R, Faber A, Krause U, Schubert M, Benes V, Eckstein V, Maul H, Ho AD. 2007. Adhesion of hematopoietic progenitor cells to human mesenchymal stem cells as a model for cell-cell interaction. *Exp Hematol* 35: 314-25
168. da Silva CL, Goncalves R, dos Santos F, Andrade PZ, Almeida-Porada G, Cabral JM. 2010. Dynamic cell-cell interactions between cord blood haematopoietic progenitors and the cellular niche are essential for the expansion of CD34+, CD34+CD38- and early lymphoid CD7+ cells. *J Tissue Eng Regen Med* 4: 149-58
169. Flores-Figueroa E VS, Montgomery K, Greenberg PL, Gratzinger D. 2012. Distinctive contact between CD34+ hematopoietic progenitors and CXCL12+ CD271+ mesenchymal stromal cells in benign and myelodysplastic bone marrow. *Laboratory Investigation*: 12
170. Rafii S, Shapiro F, Pettengell R, Ferris B, Nachman RL, Moore MA, Asch AS. 1995. Human bone marrow microvascular endothelial cells support long-term proliferation and differentiation of myeloid and megakaryocytic progenitors. *Blood* 86: 3353-63
171. Cheng X, Macvittie T, Meisenberg B, Welty E, Farese A, Tadaki D, Takebe N. 2007. Human brain endothelial cells (HUBEC) promote SCID repopulating cell expansion through direct contact. *Growth Factors* 25: 141-50
172. Prosper F, Verfaillie CM. 2001. Regulation of hematopoiesis through adhesion receptors. *J Leukoc Biol* 69: 307-16
173. Li W, Johnson SA, Shelley WC, Yoder MC. 2004. Hematopoietic stem cell repopulating ability can be maintained in vitro by some primary endothelial cells. *Exp Hematol* 32: 1226-37
174. Kiel MJ, Yilmaz OH, Iwashita T, Yilmaz OH, Terhorst C, Morrison SJ. 2005. SLAM family receptors distinguish hematopoietic stem and progenitor cells and reveal endothelial niches for stem cells. *Cell* 121: 1109-21
175. Rafii S, Shapiro F, Rimarachin J, Nachman RL, Ferris B, Weksler B, Moore MA, Asch AS. 1994. Isolation and characterization of human bone marrow microvascular endothelial cells: hematopoietic progenitor cell adhesion. *Blood* 84: 10-9
176. Schweitzer CM, van der Schoot CE, Drager AM, van der Valk P, Zevenbergen A, Hooibrink B, Westra AH, Langenhuijsen MM. 1995. Isolation and culture of human bone marrow endothelial cells. *Exp Hematol* 23: 41-8
177. Candal FJ, Rafii S, Parker JT, Ades EW, Ferris B, Nachman RL, Kellar KL. 1996. BMEC-1: a human bone marrow microvascular endothelial cell line with primary cell characteristics. *Microvasc Res* 52: 221-34

178. Rood PM, Calafat J, von dem Borne AE, Gerritsen WR, van der Schoot CE. 2000. Immortalisation of human bone marrow endothelial cells: characterisation of new cell lines. *Eur J Clin Invest* 30: 618-29
179. Seandel M, Butler JM, Kobayashi H, Hooper AT, White IA, Zhang F, Vertes EL, Kobayashi M, Zhang Y, Shmelkov SV, Hackett NR, Rabbany S, Boyer JL, Rafii S. 2008. Generation of a functional and durable vascular niche by the adenoviral E4ORF1 gene. *Proc Natl Acad Sci U S A* 105: 19288-93
180. Feugier P, Jo DY, Shieh JH, MacKenzie KL, Rafii S, Crystal RG, Moore MA. 2002. Ex vivo expansion of stem and progenitor cells in co-culture of mobilized peripheral blood CD34+ cells on human endothelium transfected with adenovectors expressing thrombopoietin, c-kit ligand, and Flt-3 ligand. *J Hematother Stem Cell Res* 11: 127-38
181. Mohle R, Moore MA, Nachman RL, Rafii S. 1997. Transendothelial migration of CD34+ and mature hematopoietic cells: an in vitro study using a human bone marrow endothelial cell line. *Blood* 89: 72-80
182. Hamada T, Mohle R, Hesselgesser J, Hoxie J, Nachman RL, Moore MA, Rafii S. 1998. Transendothelial migration of megakaryocytes in response to stromal cell-derived factor 1 (SDF-1) enhances platelet formation. *J Exp Med* 188: 539-48
183. Naiyer AJ, Jo DY, Ahn J, Mohle R, Peichev M, Lam G, Silverstein RL, Moore MA, Rafii S. 1999. Stromal derived factor-1-induced chemokinesis of cord blood CD34(+) cells (long-term culture-initiating cells) through endothelial cells is mediated by E-selectin. *Blood* 94: 4011-9
184. Carlos TM, Harlan JM. 1994. Leukocyte-endothelial adhesion molecules. *Blood* 84: 2068-101
185. Springer TA. 1994. Traffic signals for lymphocyte recirculation and leukocyte emigration: the multistep paradigm. *Cell* 76: 301-14
186. Kolaczkowska E, Kubes P. 2013. Neutrophil recruitment and function in health and inflammation. *Nat Rev Immunol* 13: 159-75
187. Imai K, Kobayashi M, Wang J, Shinobu N, Yoshida H, Hamada J, Shindo M, Higashino F, Tanaka J, Asaka M, Hosokawa M. 1999. Selective secretion of chemoattractants for haemopoietic progenitor cells by bone marrow endothelial cells: a possible role in homing of haemopoietic progenitor cells to bone marrow. *Br J Haematol* 106: 905-11
188. Netelenbos T, van den Born J, Kessler FL, Zweegman S, Merle PA, van Oostveen JW, Zwaginga JJ, Huijgens PC, Drager AM. 2003. Proteoglycans on bone marrow endothelial cells bind and present SDF-1 towards hematopoietic progenitor cells. *Leukemia* 17: 175-84
189. van Buul JD, Voermans C, van Gelderen J, Anthony EC, van der Schoot CE, Hordijk PL. 2003. Leukocyte-endothelium interaction promotes SDF-1-dependent polarization of CXCR4. *J Biol Chem* 278: 30302-10
190. Ross EA, Freeman S, Zhao Y, Dhanjal TS, Ross EJ, Lax S, Ahmed Z, Hou TZ, Kalia N, Egginton S, Nash G, Watson SP, Frampton J, Buckley CD. 2008. A novel role for PECAM-1 (CD31) in regulating haematopoietic progenitor cell compartmentalization between the peripheral blood and bone marrow. *PLoS One* 3: e2338
191. Becker PS. 2012. Dependence of acute myeloid leukemia on adhesion within the bone marrow microenvironment. *ScientificWorldJournal* 2012: 856467
192. Nagasawa T, Nakajima T, Tachibana K, Iizasa H, Bleul CC, Yoshie O, Matsushima K, Yoshida N, Springer TA, Kishimoto T. 1996. Molecular cloning and characterization of a murine pre-B-cell growth-stimulating factor/stromal cell-derived factor 1 receptor, a murine homolog of the human immunodeficiency virus 1 entry coreceptor fusin. *Proc Natl Acad Sci U S A* 93: 14726-9
193. Zlotnik A, Yoshie O. 2012. The chemokine superfamily revisited. *Immunity* 36: 705-16
194. Nagasawa T, Kikutani H, Kishimoto T. 1994. Molecular cloning and structure of a pre-B-cell growth-stimulating factor. *Proc Natl Acad Sci U S A* 91: 2305-9

195. Peled A, Grabovsky V, Habler L, Sandbank J, Arenzana-Seisdedos F, Petit I, Ben-Hur H, Lapidot T, Alon R. 1999. The chemokine SDF-1 stimulates integrin-mediated arrest of CD34(+) cells on vascular endothelium under shear flow. *J Clin Invest* 104: 1199-211
196. Dar A, Goichberg P, Shinder V, Kalinkovich A, Kollet O, Netzer N, Margalit R, Zsak M, Nagler A, Hardan I, Resnick I, Rot A, Lapidot T. 2005. Chemokine receptor CXCR4-dependent internalization and resecretion of functional chemokine SDF-1 by bone marrow endothelial and stromal cells. *Nat Immunol* 6: 1038-46
197. Ponomaryov T, Peled A, Petit I, Taichman RS, Habler L, Sandbank J, Arenzana-Seisdedos F, Magerus A, Caruz A, Fujii N, Nagler A, Lahav M, Szyper-Kravitz M, Zipori D, Lapidot T. 2000. Induction of the chemokine stromal-derived factor-1 following DNA damage improves human stem cell function. *J Clin Invest* 106: 1331-9
198. Rankin SM. 2012. Chemokines and adult bone marrow stem cells. *Immunol Lett* 145: 47-54
199. Bleul CC, Farzan M, Choe H, Parolin C, Clark-Lewis I, Sodroski J, Springer TA. 1996. The lymphocyte chemoattractant SDF-1 is a ligand for LESTR/fusin and blocks HIV-1 entry. *Nature* 382: 829-33
200. Aiuti A, Webb IJ, Bleul C, Springer T, Gutierrez-Ramos JC. 1997. The chemokine SDF-1 is a chemoattractant for human CD34+ hematopoietic progenitor cells and provides a new mechanism to explain the mobilization of CD34+ progenitors to peripheral blood. *J Exp Med* 185: 111-20
201. Kucia M, Jankowski K, Reca R, Wysoczynski M, Bandura L, Allendorf DJ, Zhang J, Ratajczak J, Ratajczak MZ. 2004. CXCR4-SDF-1 signalling, locomotion, chemotaxis and adhesion. *J Mol Histol* 35: 233-45
202. Balabanian K, Lagane B, Infantino S, Chow KY, Harriague J, Moepps B, Arenzana-Seisdedos F, Thelen M, Bachelerie F. 2005. The chemokine SDF-1/CXCL12 binds to and signals through the orphan receptor RDC1 in T lymphocytes. *J Biol Chem* 280: 35760-6
203. Feng Y, Broder CC, Kennedy PE, Berger EA. 1996. HIV-1 entry cofactor: functional cDNA cloning of a seven-transmembrane, G protein-coupled receptor. *Science* 272: 872-7
204. Mendez-Ferrer S, Lucas D, Battista M, Frenette PS. 2008. Haematopoietic stem cell release is regulated by circadian oscillations. *Nature* 452: 442-7
205. Nagasawa T, Hirota S, Tachibana K, Takakura N, Nishikawa S, Kitamura Y, Yoshida N, Kikutani H, Kishimoto T. 1996. Defects of B-cell lymphopoiesis and bone-marrow myelopoiesis in mice lacking the CXC chemokine PBSF/SDF-1. *Nature* 382: 635-8
206. Ma Q, Jones D, Borghesani PR, Segal RA, Nagasawa T, Kishimoto T, Bronson RT, Springer TA. 1998. Impaired B-lymphopoiesis, myelopoiesis, and derailed cerebellar neuron migration in CXCR4- and SDF-1-deficient mice. *Proc Natl Acad Sci U S A* 95: 9448-53
207. Zou YR, Kottmann AH, Kuroda M, Taniuchi I, Littman DR. 1998. Function of the chemokine receptor CXCR4 in haematopoiesis and in cerebellar development. *Nature* 393: 595-9
208. Bae GU, Gaio U, Yang YJ, Lee HJ, Kang JS, Krauss RS. 2008. Regulation of myoblast motility and fusion by the CXCR4-associated sialomucin, CD164. *J Biol Chem* 283: 8301-9
209. Sanchez-Martin L, Sanchez-Mateos P, Cabanas C. 2013. CXCR7 impact on CXCL12 biology and disease. *Trends Mol Med* 19: 12-22
210. Tarnowski M, Liu R, Wysoczynski M, Ratajczak J, Kucia M, Ratajczak MZ. 2010. CXCR7: a new SDF-1-binding receptor in contrast to normal CD34(+) progenitors is functional and is expressed at higher level in human malignant hematopoietic cells. *Eur J Haematol* 85: 472-83
211. Berahovich RD, Zabel BA, Penfold ME, Lewen S, Wang Y, Miao Z, Gan L, Pereda J, Dias J, Slukvin, II, McGrath KE, Jaen JC, Schall TJ. 2010. CXCR7 protein is not expressed on human or mouse leukocytes. *J Immunol* 185: 5130-9
212. Schall TJ, Proudfoot AE. 2011. Overcoming hurdles in developing successful drugs targeting chemokine receptors. *Nat Rev Immunol* 11: 355-63

213. Tavor S, Petit I. 2010. Can inhibition of the SDF-1/CXCR4 axis eradicate acute leukemia? *Semin Cancer Biol* 20: 178-85
214. Sharma M, Afrin F, Satija N, Tripathi RP, Gangenahalli GU. 2011. Stromal-derived factor-1/CXCR4 signaling: indispensable role in homing and engraftment of hematopoietic stem cells in bone marrow. *Stem Cells Dev* 20: 933-46
215. Zepeda-Moreno A, Saffrich R, Walenda T, Hoang VT, Wuchter P, Sanchez-Enriquez S, Corona-Rivera A, Wagner W, Ho AD. 2012. Modeling SDF-1-induced mobilization in leukemia cell lines. *Exp Hematol* 40: 666-74
216. Mohle R, Bautz F, Rafii S, Moore MA, Brugger W, Kanz L. 1998. The chemokine receptor CXCR-4 is expressed on CD34+ hematopoietic progenitors and leukemic cells and mediates transendothelial migration induced by stromal cell-derived factor-1. *Blood* 91: 4523-30
217. Bendall LJ, Baraz R, Juarez J, Shen W, Bradstock KF. 2005. Defective p38 mitogen-activated protein kinase signaling impairs chemotaxic but not proliferative responses to stromal-derived factor-1alpha in acute lymphoblastic leukemia. *Cancer Res* 65: 3290-8
218. Mohle R, Schittenhelm M, Failenschmid C, Bautz F, Kratz-Albers K, Serve H, Brugger W, Kanz L. 2000. Functional response of leukaemic blasts to stromal cell-derived factor-1 correlates with preferential expression of the chemokine receptor CXCR4 in acute myelomonocytic and lymphoblastic leukaemia. *Br J Haematol* 110: 563-72
219. Hatse S, Princen K, Bridger G, De Clercq E, Schols D. 2002. Chemokine receptor inhibition by AMD3100 is strictly confined to CXCR4. *FEBS Lett* 527: 255-62
220. Hendrix CW, Flexner C, MacFarland RT, Giandomenico C, Fuchs EJ, Redpath E, Bridger G, Henson GW. 2000. Pharmacokinetics and safety of AMD-3100, a novel antagonist of the CXCR-4 chemokine receptor, in human volunteers. *Antimicrob Agents Chemother* 44: 1667-73
221. Domanska UM, Kruizinga RC, Nagengast WB, Timmer-Bosscha H, Huls G, de Vries EG, Walenkamp AM. 2013. A review on CXCR4/CXCL12 axis in oncology: no place to hide. *Eur J Cancer* 49: 219-30
222. Broxmeyer HE, Orschell CM, Clapp DW, Hangoc G, Cooper S, Plett PA, Liles WC, Li X, Graham-Evans B, Campbell TB, Calandra G, Bridger G, Dale DC, Srour EF. 2005. Rapid mobilization of murine and human hematopoietic stem and progenitor cells with AMD3100, a CXCR4 antagonist. *J Exp Med* 201: 1307-18
223. De Clercq E. 2009. The AMD3100 story: the path to the discovery of a stem cell mobilizer (Mozobil). *Biochem Pharmacol* 77: 1655-64
224. Kalatskaya I, Berchiche YA, Gravel S, Limberg BJ, Rosenbaum JS, Heveker N. 2009. AMD3100 is a CXCR7 ligand with allosteric agonist properties. *Mol Pharmacol* 75: 1240-7
225. Uy GL, Rettig MP, Motabi IH, McFarland K, Trinkaus KM, Hladnik LM, Kulkarni S, Abboud CN, Cashen AF, Stockerl-Goldstein KE, Vij R, Westervelt P, DiPersio JF. 2012. A phase 1/2 study of chemosensitization with the CXCR4 antagonist plerixafor in relapsed or refractory acute myeloid leukemia. *Blood* 119: 3917-24
226. Shen W, Bendall LJ, Gottlieb DJ, Bradstock KF. 2001. The chemokine receptor CXCR4 enhances integrin-mediated in vitro adhesion and facilitates engraftment of leukemic precursor-B cells in the bone marrow. *Exp Hematol* 29: 1439-47
227. Murakami T, Nakajima T, Koyanagi Y, Tachibana K, Fujii N, Tamamura H, Yoshida N, Waki M, Matsumoto A, Yoshie O, Kishimoto T, Yamamoto N, Nagasawa T. 1997. A small molecule CXCR4 inhibitor that blocks T cell line-tropic HIV-1 infection. *J Exp Med* 186: 1389-93
228. Sehgal A, Keener C, Boynton AL, Warrick J, Murphy GP. 1998. CXCR-4, a chemokine receptor, is overexpressed in and required for proliferation of glioblastoma tumor cells. *J Surg Oncol* 69: 99-104
229. Muller A, Homey B, Soto H, Ge N, Catron D, Buchanan ME, McClanahan T, Murphy E, Yuan W, Wagner SN, Barrera JL, Mohar A, Verastegui E, Zlotnik A. 2001. Involvement of chemokine receptors in breast cancer metastasis. *Nature* 410: 50-6

230. Naik UP, Ehrlich YH, Kornecki E. 1995. Mechanisms of platelet activation by a stimulatory antibody: cross-linking of a novel platelet receptor for monoclonal antibody F11 with the Fc gamma RII receptor. *Biochem J* 310 (Pt 1): 155-62
231. Kornecki E, Walkowiak B, Naik UP, Ehrlich YH. 1990. Activation of human platelets by a stimulatory monoclonal antibody. *J Biol Chem* 265: 10042-8
232. Martin-Padura I, Lostaglio S, Schneemann M, Williams L, Romano M, Fruscella P, Panzeri C, Stoppacciaro A, Ruco L, Villa A, Simmons D, Dejana E. 1998. Junctional adhesion molecule, a novel member of the immunoglobulin superfamily that distributes at intercellular junctions and modulates monocyte transmigration. *J Cell Biol* 142: 117-27
233. Williams LA, Martin-Padura I, Dejana E, Hogg N, Simmons DL. 1999. Identification and characterisation of human Junctional Adhesion Molecule (JAM). *Mol Immunol* 36: 1175-88
234. Arcangeli ML, Frontera V, Aurrand-Lions M. 2012. Function of Junctional Adhesion Molecules (JAMs) in Leukocyte Migration and Homeostasis. *Arch Immunol Ther Exp (Warsz)*
235. Parris JJ, Cooke VG, Skarnes WC, Duncan MK, Naik UP. 2005. JAM-A expression during embryonic development. *Dev Dyn* 233: 1517-24
236. Sobocki T, Sobocka MB, Babinska A, Ehrlich YH, Banerjee P, Kornecki E. 2006. Genomic structure, organization and promoter analysis of the human F11R/F11 receptor/junctional adhesion molecule-1/JAM-A. *Gene* 366: 128-44
237. Gupta SK, Pillarisetti K, Ohlstein EH. 2000. Platelet agonist F11 receptor is a member of the immunoglobulin superfamily and identical with junctional adhesion molecule (JAM): regulation of expression in human endothelial cells and macrophages. *IUBMB Life* 50: 51-6
238. Murakami M, Francavilla C, Torselli I, Corada M, Maddaluno L, Sica A, Matteoli G, Iliev ID, Mantovani A, Rescigno M, Cavallaro U, Dejana E. 2010. Inactivation of junctional adhesion molecule-A enhances antitumoral immune response by promoting dendritic cell and T lymphocyte infiltration. *Cancer Res* 70: 1759-65
239. Stellos K, Langer H, Gnerlich S, Panagiota V, Paul A, Schonberger T, Ninci E, Menzel D, Mueller I, Bigalke B, Geisler T, Bultmann A, Lindemann S, Gawaz M. 2010. Junctional adhesion molecule A expressed on human CD34+ cells promotes adhesion on vascular wall and differentiation into endothelial progenitor cells. *Arterioscler Thromb Vasc Biol* 30: 1127-36
240. Moog-Lutz C, Cave-Riant F, Guibal FC, Breau MA, Di Gioia Y, Couraud PO, Cayre YE, Bourdoulous S, Lutz PG. 2003. JAML, a novel protein with characteristics of a junctional adhesion molecule, is induced during differentiation of myeloid leukemia cells. *Blood* 102: 3371-8
241. Nagamatsu G, Ohmura M, Mizukami T, Hamaguchi I, Hirabayashi S, Yoshida S, Hata Y, Suda T, Ohbo K. 2006. A CTX family cell adhesion molecule, JAM4, is expressed in stem cell and progenitor cell populations of both male germ cell and hematopoietic cell lineages. *Mol Cell Biol* 26: 8498-506
242. Sobocka MB, Sobocki T, Banerjee P, Weiss C, Rushbrook JI, Norin AJ, Hartwig J, Salifu MO, Markell MS, Babinska A, Ehrlich YH, Kornecki E. 2000. Cloning of the human platelet F11 receptor: a cell adhesion molecule member of the immunoglobulin superfamily involved in platelet aggregation. *Blood* 95: 2600-9
243. Weber C, Fraemohs L, Dejana E. 2007. The role of junctional adhesion molecules in vascular inflammation. *Nat Rev Immunol* 7: 467-77
244. Kostrewa D, Brockhaus M, D'Arcy A, Dale GE, Nelboeck P, Schmid G, Mueller F, Bazzoni G, Dejana E, Bartfai T, Winkler FK, Hennig M. 2001. X-ray structure of junctional adhesion molecule: structural basis for homophilic adhesion via a novel dimerization motif. *EMBO J* 20: 4391-8
245. Ostermann G, Weber KS, Zernecke A, Schroder A, Weber C. 2002. JAM-1 is a ligand of the beta(2) integrin LFA-1 involved in transendothelial migration of leukocytes. *Nat Immunol* 3: 151-8

246. Shaw SK, Ma S, Kim MB, Rao RM, Hartman CU, Froio RM, Yang L, Jones T, Liu Y, Nusrat A, Parkos CA, Luscinskas FW. 2004. Coordinated redistribution of leukocyte LFA-1 and endothelial cell ICAM-1 accompany neutrophil transmigration. *J Exp Med* 200: 1571-80
247. Naik MU, Mousa SA, Parkos CA, Naik UP. 2003. Signaling through JAM-1 and alphavbeta3 is required for the angiogenic action of bFGF: dissociation of the JAM-1 and alphavbeta3 complex. *Blood* 102: 2108-14
248. Cooke VG, Naik MU, Naik UP. 2006. Fibroblast growth factor-2 failed to induce angiogenesis in junctional adhesion molecule-A-deficient mice. *Arterioscler Thromb Vasc Biol* 26: 2005-11
249. Arrate MP, Rodriguez JM, Tran TM, Brock TA, Cunningham SA. 2001. Cloning of human junctional adhesion molecule 3 (JAM3) and its identification as the JAM2 counter-receptor. *J Biol Chem* 276: 45826-32
250. Lamagna C, Meda P, Mandicourt G, Brown J, Gilbert RJ, Jones EY, Kiefer F, Ruga P, Imhof BA, Aurrand-Lions M. 2005. Dual interaction of JAM-C with JAM-B and alpha(M)beta2 integrin: function in junctional complexes and leukocyte adhesion. *Mol Biol Cell* 16: 4992-5003
251. Cera MR, Fabbri M, Molendini C, Corada M, Orsenigo F, Rehberg M, Reichel CA, Krombach F, Pardi R, Dejana E. 2009. JAM-A promotes neutrophil chemotaxis by controlling integrin internalization and recycling. *J Cell Sci* 122: 268-77
252. Bazzoni G, Tonetti P, Manzi L, Cera MR, Balconi G, Dejana E. 2005. Expression of junctional adhesion molecule-A prevents spontaneous and random motility. *J Cell Sci* 118: 623-32
253. Azari BM, Marmur JD, Salifu MO, Cavusoglu E, Ehrlich YH, Kornecki E, Babinska A. 2010. Silencing of the F11R gene reveals a role for F11R/JAM-A in the migration of inflamed vascular smooth muscle cells and in atherosclerosis. *Atherosclerosis* 212: 197-205
254. Naik MU, Naik TU, Suckow AT, Duncan MK, Naik UP. 2008. Attenuation of junctional adhesion molecule-A is a contributing factor for breast cancer cell invasion. *Cancer Res* 68: 2194-203
255. McSherry EA, Brennan K, Hudson L, Hill AD, Hopkins AM. 2011. Breast cancer cell migration is regulated through junctional adhesion molecule-A-mediated activation of Rap1 GTPase. *Breast Cancer Res* 13: R31
256. Ghislin S, Obino D, Middendorp S, Boggetto N, Alcaide-Loridan C, Deshayes F. 2011. Junctional adhesion molecules are required for melanoma cell lines transendothelial migration in vitro. *Pigment Cell Melanoma Res* 24: 504-11
257. Peddibhotla SS, Brinkmann BF, Kummer D, Tuncay H, Nakayama M, Adams RH, Gerke V, Ebnet K. 2013. Tetraspanin CD9 links JAM-A to alphavbeta3 integrin to mediate bFGF-specific angiogenic signaling. *Mol Biol Cell*
258. Woodfin A, Reichel CA, Khandoga A, Corada M, Voisin MB, Scheiermann C, Haskard DO, Dejana E, Krombach F, Nourshargh S. 2007. JAM-A mediates neutrophil transmigration in a stimulus-specific manner in vivo: evidence for sequential roles for JAM-A and PECAM-1 in neutrophil transmigration. *Blood* 110: 1848-56
259. Woodfin A, Voisin MB, Imhof BA, Dejana E, Engelhardt B, Nourshargh S. 2009. Endothelial cell activation leads to neutrophil transmigration as supported by the sequential roles of ICAM-2, JAM-A, and PECAM-1. *Blood* 113: 6246-57
260. Khandoga A, Kessler JS, Meissner H, Hanschen M, Corada M, Motoike T, Enders G, Dejana E, Krombach F. 2005. Junctional adhesion molecule-A deficiency increases hepatic ischemia-reperfusion injury despite reduction of neutrophil transendothelial migration. *Blood* 106: 725-33
261. Ostermann G, Fraemohs L, Baltus T, Schober A, Lietz M, Zernecke A, Liehn EA, Weber C. 2005. Involvement of JAM-A in mononuclear cell recruitment on inflamed or atherosclerotic endothelium: inhibition by soluble JAM-A. *Arterioscler Thromb Vasc Biol* 25: 729-35
262. Stamatovic SM, Sladojevic N, Keep RF, Andjelkovic AV. 2012. Relocalization of junctional adhesion molecule-A during inflammatory stimulation of brain endothelial cells. *Mol Cell Biol*

263. Severson EA, Parkos CA. 2009. Mechanisms of outside-in signaling at the tight junction by junctional adhesion molecule A. *Ann N Y Acad Sci* 1165: 10-8
264. Severson EA, Jiang L, Ivanov AI, Mandell KJ, Nusrat A, Parkos CA. 2008. Cis-dimerization mediates function of junctional adhesion molecule A. *Mol Biol Cell* 19: 1862-72
265. Mandell KJ, Babbin BA, Nusrat A, Parkos CA. 2005. Junctional adhesion molecule 1 regulates epithelial cell morphology through effects on beta1 integrins and Rap1 activity. *J Biol Chem* 280: 11665-74
266. Naik UP, Naik MU. 2008. Putting the brakes on cancer cell migration: JAM-A restrains integrin activation. *Cell Adh Migr* 2: 249-51
267. Nava P, Capaldo CT, Koch S, Kolegraff K, Rankin CR, Farkas AE, Feasel ME, Li L, Addis C, Parkos CA, Nusrat A. 2011. JAM-A regulates epithelial proliferation through Akt/beta-catenin signalling. *EMBO Rep* 12: 314-20
268. Wojcikiewicz EP, Koenen RR, Fraemohs L, Minkiewicz J, Azad H, Weber C, Moy VT. 2009. LFA-1 binding destabilizes the JAM-A homophilic interaction during leukocyte transmigration. *Biophys J* 96: 285-93
269. Sakaguchi T, Nishimoto M, Miyagi S, Iwama A, Morita Y, Iwamori N, Nakauchi H, Kiyonari H, Muramatsu M, Okuda A. 2006. Putative "stemness" gene jam-B is not required for maintenance of stem cell state in embryonic, neural, or hematopoietic stem cells. *Mol Cell Biol* 26: 6557-70
270. Praetor A, McBride JM, Chiu H, Rangell L, Cabote L, Lee WP, Cupp J, Danilenko DM, Fong S. 2009. Genetic deletion of JAM-C reveals a role in myeloid progenitor generation. *Blood* 113: 1919-28
271. Immenschuh S, Naidu S, Chavakis T, Beschmann H, Ludwig RJ, Santoso S. 2009. Transcriptional induction of junctional adhesion molecule-C gene expression in activated T cells. *J Leukoc Biol* 85: 796-803
272. Zimmerli C, Lee BP, Palmer G, Gabay C, Adams R, Aurrand-Lions M, Imhof BA. 2009. Adaptive immune response in JAM-C-deficient mice: normal initiation but reduced IgG memory. *J Immunol* 182: 4728-36
273. Bradfield PF, Scheiermann C, Nourshargh S, Ody C, Luscinskas FW, Rainger GE, Nash GB, Miljkovic-Licina M, Aurrand-Lions M, Imhof BA. 2007. JAM-C regulates unidirectional monocyte transendothelial migration in inflammation. *Blood* 110: 2545-55
274. Woodfin A, Voisin MB, Beyrau M, Colom B, Caille D, Diapouli FM, Nash GB, Chavakis T, Albelda SM, Rainger GE, Meda P, Imhof BA, Nourshargh S. 2011. The junctional adhesion molecule JAM-C regulates polarized transendothelial migration of neutrophils in vivo. *Nat Immunol* 12: 761-9
275. Scheiermann C, Colom B, Meda P, Patel NS, Voisin MB, Marrelli A, Woodfin A, Pitzalis C, Thiemermann C, Aurrand-Lions M, Imhof BA, Nourshargh S. 2009. Junctional adhesion molecule-C mediates leukocyte infiltration in response to ischemia reperfusion injury. *Arterioscler Thromb Vasc Biol* 29: 1509-15
276. Sircar M, Bradfield PF, Aurrand-Lions M, Fish RJ, Alcaide P, Yang L, Newton G, Lamont D, Sehrawat S, Mayadas T, Liang TW, Parkos CA, Imhof BA, Luscinskas FW. 2007. Neutrophil transmigration under shear flow conditions in vitro is junctional adhesion molecule-C independent. *J Immunol* 178: 5879-87
277. Chavakis T, Keiper T, Matz-Westphal R, Hersemeyer K, Sachs UJ, Nawroth PP, Preissner KT, Santoso S. 2004. The junctional adhesion molecule-C promotes neutrophil transendothelial migration in vitro and in vivo. *J Biol Chem* 279: 55602-8
278. Aurrand-Lions M, Lamagna C, Dangerfield JP, Wang S, Herrera P, Nourshargh S, Imhof BA. 2005. Junctional adhesion molecule-C regulates the early influx of leukocytes into tissues during inflammation. *J Immunol* 174: 6406-15

279. Zen K, Babbin BA, Liu Y, Whelan JB, Nusrat A, Parkos CA. 2004. JAM-C is a component of desmosomes and a ligand for CD11b/CD18-mediated neutrophil transepithelial migration. *Mol Biol Cell* 15: 3926-37
280. Zen K, Liu Y, McCall IC, Wu T, Lee W, Babbin BA, Nusrat A, Parkos CA. 2005. Neutrophil migration across tight junctions is mediated by adhesive interactions between epithelial coxsackie and adenovirus receptor and a junctional adhesion molecule-like protein on neutrophils. *Mol Biol Cell* 16: 2694-703
281. Stellos K, Panagiota V, Gnerlich S, Borst O, Bigalke B, Gawaz M. 2012. Expression of junctional adhesion molecule-C on the surface of platelets supports adhesion, but not differentiation, of human CD34 cells in vitro. *Cell Physiol Biochem* 29: 153-62
282. Li X, Stankovic M, Lee BP, Aurrand-Lions M, Hahn CN, Lu Y, Imhof BA, Vadas MA, Gamble JR. 2009. JAM-C induces endothelial cell permeability through its association and regulation of {beta}3 integrins. *Arterioscler Thromb Vasc Biol* 29: 1200-6
283. Rabquer BJ, Amin MA, Teegala N, Shaheen MK, Tsou PS, Ruth JH, Lesch CA, Imhof BA, Koch AE. 2010. Junctional adhesion molecule-C is a soluble mediator of angiogenesis. *J Immunol* 185: 1777-85
284. Santoso S, Orlova VV, Song K, Sachs UJ, Andrei-Selmer CL, Chavakis T. 2005. The homophilic binding of junctional adhesion molecule-C mediates tumor cell-endothelial cell interactions. *J Biol Chem* 280: 36326-33
285. Arcangeli ML, Frontera V, Bardin F, Thomassin J, Chetaille B, Adams S, Adams RH, Aurrand-Lions M. 2012. The Junctional Adhesion Molecule-B regulates JAM-C-dependent melanoma cell metastasis. *FEBS Lett* 586: 4046-51
286. Mandicourt G, Iden S, Ebnet K, Aurrand-Lions M, Imhof BA. 2007. JAM-C regulates tight junctions and integrin-mediated cell adhesion and migration. *J Biol Chem* 282: 1830-7
287. Kitayama H, Sugimoto Y, Matsuzaki T, Ikawa Y, Noda M. 1989. A ras-related gene with transformation suppressor activity. *Cell* 56: 77-84
288. Gloerich M, Bos JL. 2011. Regulating Rap small G-proteins in time and space. *Trends Cell Biol* 21: 615-23
289. Boettner B, Van Aelst L. 2009. Control of cell adhesion dynamics by Rap1 signaling. *Curr Opin Cell Biol* 21: 684-93
290. Hattori M, Minato N. 2003. Rap1 GTPase: functions, regulation, and malignancy. *J Biochem* 134: 479-84
291. Gotoh T, Hattori S, Nakamura S, Kitayama H, Noda M, Takai Y, Kaibuchi K, Matsui H, Hatase O, Takahashi H, et al. 1995. Identification of Rap1 as a target for the Crk SH3 domain-binding guanine nucleotide-releasing factor C3G. *Mol Cell Biol* 15: 6746-53
292. Wang H, Singh SR, Zheng Z, Oh SW, Chen X, Edwards K, Hou SX. 2006. Rap-GEF signaling controls stem cell anchoring to their niche through regulating DE-cadherin-mediated cell adhesion in the Drosophila testis. *Dev Cell* 10: 117-26
293. Rubinfeld B, Munemitsu S, Clark R, Conroy L, Watt K, Crosier WJ, McCormick F, Polakis P. 1991. Molecular cloning of a GTPase activating protein specific for the Krev-1 protein p21rap1. *Cell* 65: 1033-42
294. Kurachi H, Wada Y, Tsukamoto N, Maeda M, Kubota H, Hattori M, Iwai K, Minato N. 1997. Human SPA-1 gene product selectively expressed in lymphoid tissues is a specific GTPase-activating protein for Rap1 and Rap2. Segregate expression profiles from a rap1GAP gene product. *J Biol Chem* 272: 28081-8
295. Polakis PG, Rubinfeld B, Evans T, McCormick F. 1991. Purification of a plasma membrane-associated GTPase-activating protein specific for rap1/Krev-1 from HL60 cells. *Proc Natl Acad Sci U S A* 88: 239-43
296. Hattori M, Tsukamoto N, Nur-e-Kamal MS, Rubinfeld B, Iwai K, Kubota H, Maruta H, Minato N. 1995. Molecular cloning of a novel mitogen-inducible nuclear protein with a Ran GTPase-activating domain that affects cell cycle progression. *Mol Cell Biol* 15: 552-60

297. Ishida D, Kometani K, Yang H, Kakugawa K, Masuda K, Iwai K, Suzuki M, Itohara S, Nakahata T, Hiai H, Kawamoto H, Hattori M, Minato N. 2003. Myeloproliferative stem cell disorders by deregulated Rap1 activation in SPA-1-deficient mice. *Cancer Cell* 4: 55-65
298. Bos JL, de Rooij J, Reedquist KA. 2001. Rap1 signalling: adhering to new models. *Nat Rev Mol Cell Biol* 2: 369-77
299. Stork PJ, Dillon TJ. 2005. Multiple roles of Rap1 in hematopoietic cells: complementary versus antagonistic functions. *Blood* 106: 2952-61
300. Gallagher R, Collins S, Trujillo J, McCredie K, Ahearn M, Tsai S, Metzgar R, Aulakh G, Ting R, Ruscetti F, Gallo R. 1979. Characterization of the continuous, differentiating myeloid cell line (HL-60) from a patient with acute promyelocytic leukemia. *Blood* 54: 713-33
301. Koeffler HP, Golde DW. 1978. Acute myelogenous leukemia: a human cell line responsive to colony-stimulating activity. *Science* 200: 1153-4
302. Kitamura T, Tange T, Terasawa T, Chiba S, Kuwaki T, Miyagawa K, Piao YF, Miyazono K, Urabe A, Takaku F. 1989. Establishment and characterization of a unique human cell line that proliferates dependently on GM-CSF, IL-3, or erythropoietin. *J Cell Physiol* 140: 323-34
303. Schneider U, Schwenk HU, Bornkamm G. 1977. Characterization of EBV-genome negative "null" and "T" cell lines derived from children with acute lymphoblastic leukemia and leukemic transformed non-Hodgkin lymphoma. *Int J Cancer* 19: 621-6
304. Foley GE, Lazarus H, Farber S, Uzman BG, Boone BA, McCarthy RE. 1965. Continuous Culture of Human Lymphoblasts from Peripheral Blood of a Child with Acute Leukemia. *Cancer* 18: 522-9
305. Minowada J, Onuma T, Moore GE. 1972. Rosette-forming human lymphoid cell lines. I. Establishment and evidence for origin of thymus-derived lymphocytes. *J Natl Cancer Inst* 49: 891-5
306. Rosenfeld C, Goutner A, Choquet C, Venuat AM, Kayibanda B, Pico JL, Greaves MF. 1977. Phenotypic characterisation of a unique non-T, non-B acute lymphoblastic leukaemia cell line. *Nature* 267: 841-3
307. Minowada J, Tsubota T, Greaves MF, Walters TR. 1977. A non-T, non-B human leukemia cell line (NALM-1): establishment of the cell line and presence of leukemia-associated antigens. *J Natl Cancer Inst* 59: 83-7
308. Schweitzer KM, Vicart P, Delouis C, Paulin D, Drager AM, Langenhuijsen MM, Weksler BB. 1997. Characterization of a newly established human bone marrow endothelial cell line: distinct adhesive properties for hematopoietic progenitors compared with human umbilical vein endothelial cells. *Lab Invest* 76: 25-36
309. Kozak M. 1999. Initiation of translation in prokaryotes and eukaryotes. *Gene* 234: 187-208
310. Kozak M. 1991. Effects of long 5' leader sequences on initiation by eukaryotic ribosomes in vitro. *Gene Expr* 1: 117-25
311. Kozak M. 1981. Possible role of flanking nucleotides in recognition of the AUG initiator codon by eukaryotic ribosomes. *Nucleic Acids Res* 9: 5233-52
312. Voermans C, Gerritsen WR, von dem Borne AE, van der Schoot CE. 1999. Increased migration of cord blood-derived CD34+ cells, as compared to bone marrow and mobilized peripheral blood CD34+ cells across uncoated or fibronectin-coated filters. *Exp Hematol* 27: 1806-14
313. Allalou A, Wahlby C. 2009. BlobFinder, a tool for fluorescence microscopy image cytometry. *Comput Methods Programs Biomed* 94: 58-65
314. Sahin AO, Buitenhuis M. 2012. Molecular mechanisms underlying adhesion and migration of hematopoietic stem cells. *Cell Adh Migr* 6: 39-48
315. Hamon M, Mbemba E, Charnaux N, Slimani H, Brule S, Saffar L, Vassy R, Prost C, Lievre N, Starzec A, Gattegno L. 2004. A syndecan-4/CXCR4 complex expressed on human primary lymphocytes and macrophages and HeLa cell line binds the CXC chemokine stromal cell-derived factor-1 (SDF-1). *Glycobiology* 14: 311-23

316. Leung KT, Chan KY, Ng PC, Lau TK, Chiu WM, Tsang KS, Li CK, Kong CK, Li K. 2011. The tetraspanin CD9 regulates migration, adhesion, and homing of human cord blood CD34+ hematopoietic stem and progenitor cells. *Blood* 117: 1840-50
317. O'Leary H, Ou X, Broxmeyer HE. 2013. The role of dipeptidyl peptidase 4 in hematopoiesis and transplantation. *Curr Opin Hematol*
318. Sangeetha VM, Kadekar D, Kale VP, Limaye LS. 2012. Pharmacological inhibition of caspase and calpain proteases: a novel strategy to enhance the homing responses of cord blood HSPCs during expansion. *PLoS One* 7: e29383
319. Hoggatt J, Singh P, Sampath J, Pelus LM. 2009. Prostaglandin E2 enhances hematopoietic stem cell homing, survival, and proliferation. *Blood* 113: 5444-55
320. Durand EM, Zon LI. 2010. Newly emerging roles for prostaglandin E2 regulation of hematopoiesis and hematopoietic stem cell engraftment. *Curr Opin Hematol* 17: 308-12
321. Rossi L, Manfredini R, Bertolini F, Ferrari D, Fogli M, Zini R, Salati S, Salvestrini V, Gulinelli S, Adinolfi E, Ferrari S, Di Virgilio F, Baccarani M, Lemoli RM. 2007. The extracellular nucleotide UTP is a potent inducer of hematopoietic stem cell migration. *Blood* 109: 533-42
322. Schioppa T, Uranchimeg B, Saccani A, Biswas SK, Doni A, Rapisarda A, Bernasconi S, Saccani S, Nebuloni M, Vago L, Mantovani A, Melillo G, Sica A. 2003. Regulation of the chemokine receptor CXCR4 by hypoxia. *J Exp Med* 198: 1391-402
323. Ceradini DJ, Kulkarni AR, Callaghan MJ, Tepper OM, Bastidas N, Kleinman ME, Capla JM, Galiano RD, Levine JP, Gurtner GC. 2004. Progenitor cell trafficking is regulated by hypoxic gradients through HIF-1 induction of SDF-1. *Nat Med* 10: 858-64
324. Martin-Rendon E, Hale SJ, Ryan D, Baban D, Forde SP, Roubelakis M, Sweeney D, Moukayed M, Harris AL, Davies K, Watt SM. 2007. Transcriptional profiling of human cord blood CD133+ and cultured bone marrow mesenchymal stem cells in response to hypoxia. *Stem Cells* 25: 1003-12
325. Parmar K, Mauch P, Vergilio JA, Sackstein R, Down JD. 2007. Distribution of hematopoietic stem cells in the bone marrow according to regional hypoxia. *Proc Natl Acad Sci U S A* 104: 5431-6
326. Colla S, Storti P, Donofrio G, Todoerti K, Bolzoni M, Lazzaretti M, Abeltino M, Ippolito L, Neri A, Ribatti D, Rizzoli V, Martella E, Giuliani N. 2010. Low bone marrow oxygen tension and hypoxia-inducible factor-1alpha overexpression characterize patients with multiple myeloma: role on the transcriptional and proangiogenic profiles of CD138(+) cells. *Leukemia* 24: 1967-70
327. Arai A, Nosaka Y, Kohsaka H, Miyasaka N, Miura O. 1999. CrkL activates integrin-mediated hematopoietic cell adhesion through the guanine nucleotide exchange factor C3G. *Blood* 93: 3713-22
328. Marks PW, Arai M, Bandura JL, Kwiatkowski DJ. 1998. Advillin (p92): a new member of the gelsolin/villin family of actin regulatory proteins. *J Cell Sci* 111 (Pt 15): 2129-36
329. Walzer T, Galibert L, Comeau MR, De Smedt T. 2005. Plexin C1 engagement on mouse dendritic cells by viral semaphorin A39R induces actin cytoskeleton rearrangement and inhibits integrin-mediated adhesion and chemokine-induced migration. *J Immunol* 174: 51-9
330. Sobocka MB, Sobocki T, Babinska A, Hartwig JH, Li M, Ehrlich YH, Kornecki E. 2004. Signaling pathways of the F11 receptor (F11R; a.k.a. JAM-1, JAM-A) in human platelets: F11R dimerization, phosphorylation and complex formation with the integrin GPIIIa. *J Recept Signal Transduct Res* 24: 85-105
331. Cera MR, Del Prete A, Vecchi A, Corada M, Martin-Padura I, Motoike T, Tonetti P, Bazzoni G, Vermi W, Gentili F, Bernasconi S, Sato TN, Mantovani A, Dejana E. 2004. Increased DC trafficking to lymph nodes and contact hypersensitivity in junctional adhesion molecule-A-deficient mice. *J Clin Invest* 114: 729-38

332. Ogasawara N, Kojima T, Go M, Fuchimoto J, Kamekura R, Koizumi J, Ohkuni T, Masaki T, Murata M, Tanaka S, Ichimiya S, Himi T, Sawada N. 2009. Induction of JAM-A during differentiation of human THP-1 dendritic cells. *Biochem Biophys Res Commun* 389: 543-9
333. Naik MU, Naik UP. 2006. Junctional adhesion molecule-A-induced endothelial cell migration on vitronectin is integrin alpha v beta 3 specific. *J Cell Sci* 119: 490-9
334. Hoebeke I, De Smedt M, Stolz F, Pike-Overzet K, Staal FJ, Plum J, Leclercq G. 2007. T-, B- and NK-lymphoid, but not myeloid cells arise from human CD34(+)CD38(-)CD7(+) common lymphoid progenitors expressing lymphoid-specific genes. *Leukemia* 21: 311-9
335. Hao QL, Zhu J, Price MA, Payne KJ, Barsky LW, Crooks GM. 2001. Identification of a novel, human multilymphoid progenitor in cord blood. *Blood* 97: 3683-90
336. Blair A, Pamphilon DH. 2003. Leukaemic stem cells. *Transfus Med* 13: 363-75
337. McCarthy JM, Capullari T, Thompson Z, Zhu Y, Spellacy WN. 2006. Umbilical cord nucleated red blood cell counts: normal values and the effect of labor. *J Perinatol* 26: 89-92
338. Zhou B, Tsaknakis G, Coldwell KE, Khoo CP, Roubelakis MG, Chang CH, Pepperell E, Watt SM. 2012. A novel function for the haemopoietic supportive murine bone marrow MS-5 mesenchymal stromal cell line in promoting human vasculogenesis and angiogenesis. *Br J Haematol* 157: 299-311
339. Ebnet K, Suzuki A, Horikoshi Y, Hirose T, Meyer Zu Brickwedde MK, Ohno S, Vestweber D. 2001. The cell polarity protein ASIP/PAR-3 directly associates with junctional adhesion molecule (JAM). *EMBO J* 20: 3738-48
340. Sabattini E, Bacci F, Sagramoso C, Pileri SA. 2010. WHO classification of tumours of haematopoietic and lymphoid tissues in 2008: an overview. *Pathologica* 102: 83-7
341. Gallacher L, Murdoch B, Wu DM, Karanu FN, Keeney M, Bhatia M. 2000. Isolation and characterization of human CD34(-)Lin(-) and CD34(+)Lin(-) hematopoietic stem cells using cell surface markers AC133 and CD7. *Blood* 95: 2813-20
342. Diamanti P, Cox CV, Blair A. 2012. Comparison of childhood leukemia initiating cell populations in NOD/SCID and NSG mice. *Leukemia* 26: 376-80
343. Wang JC, Doedens M, Dick JE. 1997. Primitive human hematopoietic cells are enriched in cord blood compared with adult bone marrow or mobilized peripheral blood as measured by the quantitative in vivo SCID-repopulating cell assay. *Blood* 89: 3919-24
344. Laurenti E, Doulatov S, Zandi S, Plumb I, Chen J, April C, Fan JB, Dick JE. 2013. The transcriptional architecture of early human hematopoiesis identifies multilevel control of lymphoid commitment. *Nat Immunol* 14: 756-63
345. Notta F, Doulatov S, Laurenti E, Poeppl A, Jurisica I, Dick JE. 2011. Isolation of single human hematopoietic stem cells capable of long-term multilineage engraftment. *Science* 333: 218-21
346. Ozaki H, Ishii K, Horiuchi H, Arai H, Kawamoto T, Okawa K, Iwamatsu A, Kita T. 1999. Cutting edge: combined treatment of TNF-alpha and IFN-gamma causes redistribution of junctional adhesion molecule in human endothelial cells. *J Immunol* 163: 553-7
347. Levesque JP, Winkler IG. 2011. Hierarchy of immature hematopoietic cells related to blood flow and niche. *Curr Opin Hematol*
348. Scadden DT. 2006. The stem-cell niche as an entity of action. *Nature* 441: 1075-9
349. Papayannopoulou T. 2000. Mechanisms of stem-/progenitor-cell mobilization: the anti-VLA-4 paradigm. *Semin Hematol* 37: 11-8
350. McEver RP, Martin MN. 1984. A monoclonal antibody to a membrane glycoprotein binds only to activated platelets. *J Biol Chem* 259: 9799-804
351. Corada M, Chimenti S, Cera MR, Vinci M, Salio M, Fiordaliso F, De Angelis N, Villa A, Bossi M, Staszewsky LI, Vecchi A, Parazzoli D, Motoike T, Latini R, Dejana E. 2005. Junctional adhesion molecule-A-deficient polymorphonuclear cells show reduced diapedesis in peritonitis and heart ischemia-reperfusion injury. *Proc Natl Acad Sci U S A* 102: 10634-9

352. Lam BS, Adams GB. 2010. Hematopoietic stem cell lodgment in the adult bone marrow stem cell niche. *Int J Lab Hematol* 32: 551-8
353. Koenen RR, Pruessmeyer J, Soehnlein O, Fraemohs L, Zernecke A, Schwarz N, Reiss K, Sarabi A, Lindbom L, Hackeng TM, Weber C, Ludwig A. 2009. Regulated release and functional modulation of junctional adhesion molecule A by disintegrin metalloproteinases. *Blood* 113: 4799-809
354. Mazo IB, Massberg S, von Andrian UH. 2011. Hematopoietic stem and progenitor cell trafficking. *Trends Immunol* 32: 493-503
355. Babinska A, Kedees MH, Athar H, Ahmed T, Batuman O, Ehrlich YH, Hussain MM, Kornecki E. 2002. F11-receptor (F11R/JAM) mediates platelet adhesion to endothelial cells: role in inflammatory thrombosis. *Thromb Haemost* 88: 843-50
356. Rafii S, Mohle R, Shapiro F, Frey BM, Moore MA. 1997. Regulation of hematopoiesis by microvascular endothelium. *Leuk Lymphoma* 27: 375-86
357. Volin MV, Joseph L, Shockley MS, Davies PF. 1998. Chemokine receptor CXCR4 expression in endothelium. *Biochem Biophys Res Commun* 242: 46-53
358. Peled A, Kollet O, Ponomaryov T, Petit I, Franitza S, Grabovsky V, Slav MM, Nagler A, Lider O, Alon R, Zipori D, Lapidot T. 2000. The chemokine SDF-1 activates the integrins LFA-1, VLA-4, and VLA-5 on immature human CD34(+) cells: role in transendothelial/stromal migration and engraftment of NOD/SCID mice. *Blood* 95: 3289-96
359. Larochelle A, Gillette JM, Desmond R, Ichwan B, Cantilena A, Cerf A, Barrett AJ, Wayne AS, Lippincott-Schwartz J, Dunbar CE. 2012. Bone marrow homing and engraftment of human hematopoietic stem and progenitor cells is mediated by a polarized membrane domain. *Blood* 119: 1848-55
360. Teicher BA, Fricker SP. 2010. CXCL12 (SDF-1)/CXCR4 pathway in cancer. *Clin Cancer Res* 16: 2927-31
361. Glodek AM, Le Y, Dykxhoorn DM, Park SY, Mostoslavsky G, Mulligan R, Lieberman J, Beggs HE, Honczarenko M, Silberstein LE. 2007. Focal adhesion kinase is required for CXCL12-induced chemotactic and pro-adhesive responses in hematopoietic precursor cells. *Leukemia* 21: 1723-32
362. Severson EA, Lee WY, Capaldo CT, Nusrat A, Parkos CA. 2009. Junctional adhesion molecule A interacts with Afadin and PDZ-GEF2 to activate Rap1A, regulate beta1 integrin levels, and enhance cell migration. *Mol Biol Cell* 20: 1916-25
363. Zach S, Felk S, Gillardon F. 2010. Signal transduction protein array analysis links LRRK2 to Ste20 kinases and PKC zeta that modulate neuronal plasticity. *PLoS One* 5: e13191
364. Chang F, Steelman LS, Lee JT, Shelton JG, Navolanic PM, Blalock WL, Franklin RA, McCubrey JA. 2003. Signal transduction mediated by the Ras/Raf/MEK/ERK pathway from cytokine receptors to transcription factors: potential targeting for therapeutic intervention. *Leukemia* 17: 1263-93
365. Cuadrado A, Nebreda AR. 2010. Mechanisms and functions of p38 MAPK signalling. *Biochem J* 429: 403-17
366. Yi L, Chandrasekaran P, Venkatesan S. 2012. TLR signaling paralyzes monocyte chemotaxis through synergized effects of p38 MAPK and global Rap-1 activation. *PLoS One* 7: e30404
367. Meek JLaD. 2013. Switching on p53: an essential role for protein phosphorylation? *BioDiscovery*: 20
368. Solozobova V, Blattner C. 2011. p53 in stem cells. *World J Biol Chem* 2: 202-14
369. O'Callaghan K, Lee L, Nguyen N, Hsieh MY, Kaneider NC, Klein AK, Sprague K, Van Etten RA, Kuliopulos A, Covic L. 2012. Targeting CXCR4 with cell-penetrating pepducins in lymphoma and lymphocytic leukemia. *Blood* 119: 1717-25
370. Katagiri K, Shimonaka M, Kinashi T. 2004. Rap1-mediated lymphocyte function-associated antigen-1 activation by the T cell antigen receptor is dependent on phospholipase C-gamma1. *J Biol Chem* 279: 11875-81

371. Katagiri K, Kinashi T. 2012. Rap1 and integrin inside-out signaling. *Methods Mol Biol* 757: 279-96
372. Morrison DK. 2012. MAP kinase pathways. *Cold Spring Harb Perspect Biol* 4
373. Warsch W, Walz C, Sexl V. 2013. JAK of all trades: JAK2-STAT5 as novel therapeutic targets in BCR-ABL1+ chronic myeloid leukemia. *Blood*
374. Vila-Coro AJ, Rodriguez-Frade JM, Martin De Ana A, Moreno-Ortiz MC, Martinez AC, Mellado M. 1999. The chemokine SDF-1alpha triggers CXCR4 receptor dimerization and activates the JAK/STAT pathway. *FASEB J* 13: 1699-710
375. Mowafi F, Cagigi A, Matskova L, Bjork O, Chiodi F, Nilsson A. 2008. Chemokine CXCL12 enhances proliferation in pre-B-ALL via STAT5 activation. *Pediatr Blood Cancer* 50: 812-7
376. Joo EK, Broxmeyer HE, Kwon HJ, Kang HB, Kim JS, Lim JS, Choe YK, Choe IS, Myung PK, Lee Y. 2004. Enhancement of cell survival by stromal cell-derived factor-1/CXCL12 involves activation of CREB and induction of Mcl-1 and c-Fos in factor-dependent human cell line MO7e. *Stem Cells Dev* 13: 563-70
377. Pye DS, Rubio I, Pusch R, Lin K, Pettitt AR, Till KJ. 2013. Chemokine unresponsiveness of chronic lymphocytic leukemia cells results from impaired endosomal recycling of rap1 and is associated with a distinctive type of immunological anergy. *J Immunol* 191: 1496-504
378. Rood PM, Gerritsen WR, Kramer D, Ranzijn C, von dem Borne AE, van der Schoot CE. 1999. Adhesion of hematopoietic progenitor cells to human bone marrow or umbilical vein derived endothelial cell lines: a comparison. *Exp Hematol* 27: 1306-14
379. Pitchford SC, Lodie T, Rankin SM. 2012. VEGFR1 stimulates a CXCR4-dependent translocation of megakaryocytes to the vascular niche, enhancing platelet production in mice. *Blood* 120: 2787-95
380. Rocha V, Labopin M, Ruggeri A, Podesta M, Gallamini A, Bonifazi F, Sanchez-Guijo FM, Rovira M, Socie G, Baltadakis I, Michallet M, Deconinck E, Bacigalupo A, Mohty M, Gluckman E, Frassoni F. 2013. Unrelated cord blood transplantation: outcomes after single-unit intrabone injection compared with double-unit intravenous injection in patients with hematological malignancies. *Transplantation* 95: 1284-91
381. Chute JP, Muramoto GG, Salter AB, Meadows SK, Rickman DW, Chen B, Himburg HA, Chao NJ. 2007. Transplantation of vascular endothelial cells mediates the hematopoietic recovery and survival of lethally irradiated mice. *Blood* 109: 2365-72
382. Doan PL, Chute JP. 2012. The vascular niche: home for normal and malignant hematopoietic stem cells. *Leukemia* 26: 54-62